НАУЧНО-ПРАКТИЧЕСКИЙ ЖУРНАЛ

ISSN 1682-0363 (print)
ISSN 1819-3684 (online)

БЮЛЛЕТЕНЬ СИБИРСКОЙ МЕДИЦИНЫ

BULLETIN OF SIBERIAN MEDICINE

Том 23
№ 4. 2024

Издательский дом Сибирского государственного медицинского университета представляет серию книг

«Наследие томской медицины»

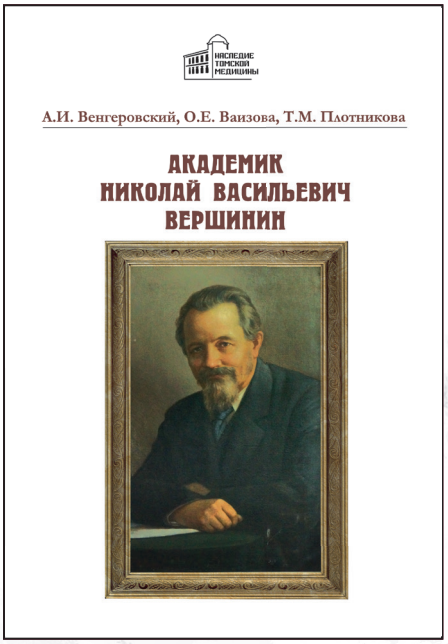

В книге представлены биография и обзор научной, педагогической и общественной деятельности выдающегося фармаколога, академика АМН СССР, заслуженного деятеля науки РСФСР, лауреата Сталинской (Государственной) премии Николая Васильевича Вершинина (1867–1951).

Для врачей, студентов, ученых, всех интересующихся историей медицины.

Книга посвящена памяти доктора медицинских наук, профессора Владимира Демьяновича Суходоло (1919–2000), участника обороны Ленинграда, инвалида Великой Отечественной войны, работавшего в Сибирском государственном медицинском университете (СибГМУ, Томском медицинском институте) в 1948–2000 гг. С уважением, восхищением и любовью профессора В.Д. Суходоло вспоминают ученики, коллеги, друзья, члены семьи, родные.

Для тех, кто интересуется историей медицины, Сибирского государственного медицинского университета, Томска.

В книге представлены биография и обзор научной, педагогической и общественной деятельности выдающегося микробиолога, вирусолога и эпидемиолога, академика АМН СССР, заслуженного деятеля науки РСФСР Сергея Петровича Карпова (1903–1976).

Для врачей, студентов, ученых, всех интересующихся историей медицины.

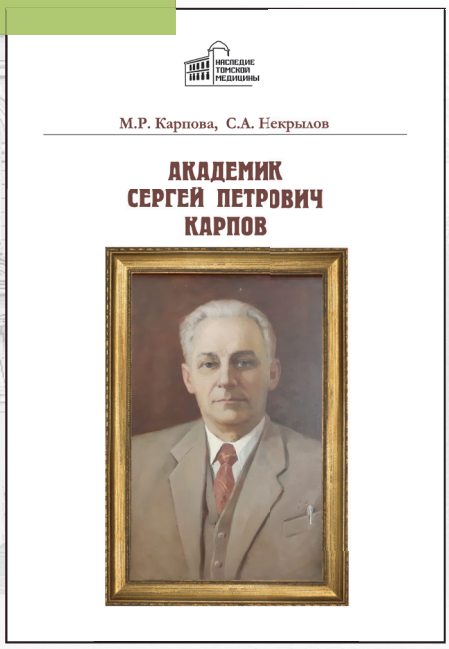

BULLETIN OF SIBERIAN MEDICINE

Peer-reviewed scientific-practical journal
Issued quarterly

Volume 23, No. 4, 2024

ISSN 1682-0363 (print)
ISSN 1819-3684 (online)

FOUNDER AND PUBLISHER:
Siberian State Medical University, Ministry of Healthcare of the Russian Federation

Registered by the Ministry of Mass Media and Communications of the Russian Federation
Certificate of registration
No. 77-7366 of 26.03.2001

The journal "Bulletin of Siberian Medicine" is included in the list of peer-reviewed scientific journals and publications issued in the Russian Federation, which should publish main scientific results of doctoral and Candidate of Sciences theses

Bulletin of Siberian Medicine is indexed in:
Scopus
Web of Science (WoS (ESCI))
Science Index
RSCI
Ulrich's International Periodicals Directory
Cyberleninka
DOAS

Editorial Board Office:
107, Lenina Av., Tomsk, 634050, Russian Federation
Telephone: +7-(382-2)-51-41-53.
http://bulletin.ssmu.ru
E-mail: bulletin.tomsk@mail.ru

Publisher: Siberian State Medical University.
2, Moscow Trakt, Tomsk, 634050,
Russian Federation.
Editors: E.E. Stepanova, Yu.P. Gotfrid
Translators: M.E. Orlova, K.Yu.Skvortsova
Electronic makeup, cover design
L.D. Krivtsova

Printed in Litburo LLC,
4, Koroleva Str., Tomsk, 634055, Russian Federation

Signed to print on 27.12.2024
Format 60 × 84/8. Offset print.
Coated paper. Times font.
P.s. 5,5. C.p.s. 5,0.
500 copies. Order No. 501.

The price – free.
Date of publication 28.12.2024.

БЮЛЛЕТЕНЬ СИБИРСКОЙ МЕДИЦИНЫ

Научно-практический журнал
Выходит 4 раза в год

Том 23, № 4, 2024

ISSN 1682-0363 (print)
ISSN 1819-3684 (online)

УЧРЕДИТЕЛЬ И ИЗДАТЕЛЬ:
ФГБОУ ВО «Сибирский государственный медицинский университет» Минздрава России

Журнал основан в 2001 году
Зарегистрирован в Министерстве РФ по делам печати, телерадиовещания и средств массовых коммуникаций
Свидетельство регистрации ПИ № 77-7366 от 26.03.2001 г.

Журнал входит в Перечень ведущих рецензируемых научных журналов и изданий, выпускаемых в РФ, в которых должны быть опубликованы основные научные результаты диссертаций на соискание ученой степени доктора и кандидата наук

Индексация:
Scopus
Web of Science (WoS (ESCI))
РИНЦ (Science Index)
RSCI
Ulrich's International Periodicals Directory
Cyberleninka
DOAS

Редакция:
634050, г. Томск, пр. Ленина, 107.
Тел.: (382-2)-51-41-53.
http://bulletin.ssmu.ru
E-mail: bulletin.tomsk@mail.ru

Оригинал-макет:
Издательство СибГМУ.
634050, г. Томск, Московский тракт, 2.
Редакторы: Е.Е. Степанова, Ю.П. Готфрид
Перевод: М.Е. Орлова, Дж. Палацца
Электронная верстка, дизайн обложки Л.Д. Кривцова

Отпечатано в ООО «Литбюро»,
634055, г. Томск, ул. Королёва, 4.

Подписано в печать 27.12.2024 г.
Формат 60 × 84/8. Печать офсетная.
Бумага мелованная. Гарнитура «Times».
Печ. л. 5,5. Усл. печ. л. 5,0.
Тираж 500 экз. Заказ 501.

Цена – свободная.
Дата выхода в свет 28.12.2024.

СОДЕРЖАНИЕ

CONTENTS

ОРИГИНАЛЬНЫЕ СТАТЬИ

ORIGINAL ARTICLES

УДК 577.21:616-018]-092.9-091.1
https://doi.org/10.20538/1682-0363-2024-4-5-14

Dynamic changes in RNA integrity, gene expression, and tissue pathomorphology of experimental mice in the postmortem period

Buyko E.E., Perina E.A., Vasilchenko D.V., Tsydenova I.A., Khmelevskaya E.S., Ufandeev A.A., Kaidash O.A., Ivanov V.V., Vtorushin S.V., Udut E.V.

Siberian State Medical University
2, Moscow Trakt, Tomsk, 634050, Russian Federation

ABSTRACT

Aim. To examine the pattern of morphological changes, RNA quality number, and gene expression in mouse tissues sampled at autopsy under controlled experimental conditions.

Materials and methods. Balb/c mice were euthanized and subsequently subjected to necropsy at 0, 3, 12, 24, 48, and 72 hours of the postmortem period. During the first three hours following euthanasia, the mice were maintained at room temperature, after which they were transferred to a refrigerator (4 °C). Total RNA was extracted from tissue samples taken from the kidney, liver, and brain; the integrity of the RNA samples was assessed by capillary electrophoresis, and the RNA quality number (RQN) was calculated. The expression levels of *Actb*, *Epas1*, and *Rps18* housekeeping genes were evaluated by real-time quantitative reverse transcription polymerase chain reaction (RT-qPCR) with original primers and probes using the TaqMan assay. The histologic examination was performed according to standard techniques.

Results. Degradation of RNA extracted from mouse kidney tissues appeared to be greater than that of RNA taken from the liver. In the meantime, a negative linear correlation was observed between RQN and the duration of the postmortem interval for liver and kidney samples. In contrast, no significant changes in the RQN score were observed for brain RNA samples at any of the time points. The expression of the *Epas1* and *Rps18* genes was significantly decreased in mouse kidney and liver tissues. However, the level of *Epas1* and *Rps18* gene expression in the brain remained stable at all time points and did not exhibit a significant decrease at 72 hours after euthanasia. No obvious morphological changes were detected by the histologic examination, which does not exclude the presence of ultrastructural pathological changes.

Conclusion. RQN in autopsy tissues serves as a crucial predictor of sample quality for molecular biology studies, including gene expression analysis.

Keywords: postmortem interval, autopsy, RNA integrity, PCR, gene expression

Conflict of interest. The authors declare the absence of obvious or potential conflict of interest related to the publication of this article.

Source of financing. The study was supported by the Russian Science Foundation project No. 23-69-10035 “New approaches to validating the results of molecular profiling of pathological tissue changes based on molecular profiling data obtained from biopsy and autopsy studies”.

For citation: Buyko E.E., Perina E.A., Vasilchenko D.V., Tsydenova I.A., Khmelevskaya E.S., Ufandeev A.A., Kaidash O.A., Ivanov V.V., Vtorushin S.V., Udut E.V. Dynamic changes in rna integrity, gene expression, and tissue pathomorphology of experimental mice in the postmortem period. *Bulletin of Siberian Medicine.* 2024;23(4):5–14. https://doi.org/10.20538/1682-0363-2024-4-5-14.

✉ *Buyko Evgeny E.,* buykoevgen@yandex.ru

Динамические изменения целостности РНК, экспрессии генов и патоморфология тканей экспериментальных мышей в посмертном периоде

Буйко Е.Е., Перина Е.А., Васильченко Д.В., Цыденова И.А., Хмелевская Е.С., Уфандеев А.А., Кайдаш О.А., Иванов В.В., Вторушин С.В., Удут Е.В.

Сибирский государственный медицинский университет (СибГМУ)
Россия, 634050, г. Томск, Московский тракт, 2

РЕЗЮМЕ

Цель. Изучение закономерности морфологических изменений, величины целостности РНК и паттернов экспрессии генов тканей мышей, отобранных при аутопсии в контролируемых условиях.

Материалы и методы. Мышей линии Balb/c подвергали эвтаназии с последующей некропсией через 0, 3, 12, 24, 48, 72 ч. Первые 3 ч после эвтаназии мыши находились при комнатной температуре, а затем были перемещены в холодильник (4 °C). Общую РНК выделяли из образцов тканей почек, печени, головного мозга, целостность образцов РНК измеряли при помощи капиллярного электрофореза с расчетом значений RQN (RNA Quality Number). Уровень экспрессии генов домашнего хозяйства Actb, Epas1, Rps18 оценивали при помощи обратно-транскриптазной количественной полимеразной цепной реакции в режиме реального времени (RT-qPCR) с оригинальными праймерами и зондами по технологии TaqMan. Гистологическое исследование выполнено по стандартной методике.

Результаты. Выделенная из тканей почек мышей РНК подвержена деградации в большей степени с увеличением посмертного интервала, чем РНК печени. При этом обнаружена отрицательная линейная зависимость между показателем RQN и длительностью посмертного интервала для образцов печени и почек животных. В то же время образцы РНК головного мозга не демонстрировали существенного изменения показателя RQN во всех временных точках. В тканях почек и печени мышей значительно снижается экспрессия генов *Epas1* и *Rps18*. Однако величина экспрессии генов *Epas1* и *Rps18* в головном мозге животных остается стабильной во всех временных точках и не демонстрирует значительного снижения через 72 ч после проведения эвтаназии. При гистологическом исследовании не обнаружено явных морфологических изменений, что не исключает наличия ультраструктурных патологических изменений.

Заключение. Величина целостности РНК (RQN) в аутопсийных тканях является важным предиктором качества образца для молекулярно-биологических исследований, включая анализ экспрессии генов.

Ключевые слова: посмертный интервал, аутопсия, целостность РНК, ПЦР, экспрессия генов

Конфликт интересов. Авторы декларируют отсутствие явных и потенциальных конфликтов интересов, связанных с содержанием настоящей статьи.

Источник финансирования. Исследование выполнено при финансовой поддержке Российского научного фонда в рамках научного проекта № 23-69-10035 «Новые подходы валидации результатов молекулярного профилирования патологических изменений тканей на основе данных молекулярного профилирования, полученных при исследовании биопсии и аутопсии».

Соответствие принципам этики. Исследование одобрено комиссией IACUC СибГМУ (заключение № 1 от 05.06.2023).

Для цитирования: Буйко Е.Е., Перина Е.А., Васильченко Д.В., Цыденова И.А., Хмелевская Е.С., Уфандеев А.А., Кайдаш О.А., Иванов В.В., Вторушин С.В., Удут Е.В. Динамические изменения целостности РНК, экспрессии генов и патоморфология тканей экспериментальных мышей в посмертном периоде. *Бюллетень сибирской медицины.* 2024;23(4):5–14. https://doi.org/10.20538/1682-0363-2024-4-5-14.

INTRODUCTION

Postmortem tissue studies have fundamental importance for forensic medicine and biological research in the study of the etiology and pathogenesis of many diseases [1, 2], especially in oncology [3].

Biological materials of cancer patients obtained at autopsy are of great interest for research since they provide an adequate assessment of the quality of clinical diagnosis and allow to develop optimized treatment strategies [4]. The main approach to identifying pathological changes occurring in the

body at the tissue level is morphological research, which is an interpretation of the tissue structure based on findings of the microscopy analysis, including the use of immunohistochemistry methods. In the meantime, implementation of advanced methods for assessing protein expression into clinical practice and translational multi-omics studies provide the most comprehensive understanding of cancer-related pathogenetic processes associated with changes in the molecular, metabolic, and genetic landscapes [5].

However, the use of postmortem tissues is invariably accompanied by a time delay, since samples cannot be immediately stored under conditions, which prevent biological molecules from degradation. Cell autolysis and tissue degradation threaten the reliability of gene expression data and multi-omics studies [2].

Therefore, the time interval between death and sample collection is an important factor in the accuracy and reliability of molecular biology research data, and we can consider postmortem RNA degradation as one of the markers of autopsy tissue integrity [2].

Traditionally, RNA integrity has been assessed qualitatively by comparing the intensities of 28S and 18S ribosomal RNA (rRNA) bands during agarose gel electrophoresis. More recently, automated electrophoresis systems employing microfluidic technologies have been developed that are capable of quantitatively assessing RNA quality based on the analysis of digital electropherograms [6].

Indeed, RNA molecules in cells are extremely vulnerable to degradation, and measuring the RNA Quality Number (RQN) is a standard method for assessing RNA degradation [7].

The literature data on the influence of RNA integrity on the reliability and validity of the results of molecular biology studies of autopsy tissues are contradictory [8–10]. Several studies have attempted to investigate the relationship between RNA integrity in postmortem human brain tissue and the results of gene expression analysis [11] or transcriptome profiling [7].

However, a significant limitation in the design of the presented studies is that they do not assess the influence of such factors as the duration of the postmortem interval and standardization of tissue sample preparation. Therefore, the study of the influence of these factors on dynamic changes in RNA integrity under strictly controlled experimental conditions has a great practical significance; these conditions can only be created using animal models.

The aim of this study was to investigate the patterns of morphological changes, RNA quality number, and gene expression patterns in mouse tissues, selected and sampled at autopsy under controlled experimental conditions.

MATERIALS AND METHODS

The experiments were carried out on 30 female Balb/c mice (aged 7 weeks at the beginning of the study) obtained from the specific pathogen-free facility of the Research Institute of Cytology and Genetics of the Siberian Branch of the Russian Academy of Sciences (Novosibirsk).

The use of animals in this study was approved by the IACUC commission at Siberian State Medical University (Protocol No. 1 of 05.06.2023).

The animals of all groups were euthanized by cervical dislocation following Forane anesthesia (AESICA QUEENBOROUGH Limited, United Kingdom).

The animals of group 1 were subjected to necropsy immediately after euthanasia as a control (n = 5). The animals of the remaining experimental groups were subjected to necropsy at 3, 12, 24, 48, and 72 hours after euthanasia (n = 5 for all groups). In the meantime, in the first hours after euthanasia, the mice were kept at room temperature and then were placed in the refrigerator (+4 °C). This allowed to simulate conditions that were as close as possible to the routine autopsy protocol for patients who died in specialized medical facilities [4].

Total RNA was extracted from tissue samples using the HiPure Total RNA Kit (Guangzhou Magen Biotechnology, China) in accordance with the manufacturer's instructions. The concentration and quality of the isolated RNA were assessed by measuring the optical density at 260 and 280 nm using the Nanodrop 2000 UV-VIS spectrophotometer (Thermo Scientific, USA). The integrity of the RNA samples was assessed using capillary electrophoresis on the Bio-Fragment Analyzer (Bioptic Inc., China).

The isolated RNA was used to synthesize cDNA using the MMLV RT kit (Evrogen, Russia) in accordance with the manufacturer's instructions. Primers and probes (FAM-BHQ1) were designed using the Vector NTI Advance 11.5, Oligo 7,5 software and the NCBI Nucleotide Database (http://www.ncbi.nlm.nih.gov/nuccore). The expression level of *Epas1 (Endothelial PAS Domain Protein 1)* and *Rps18 (Ribosomal Protein S18)* genes was assessed using TaqMan RT-qPCR on the Rotor-Gene-6000 amplifier

(Corbett Research, Australia) (with original primers and probes (*ACTB: F* 5' TGGCAACGAGCGGTTC 3'; *R* 5' CATAGAGGTCTTTACGGATGTCA 3'; *Probe* FAM-5'-tggcaacgagcggttc-3'- BHQ1; amplicon of 134 bp; *EPAS1: F* 5' ATGTGTGAGCCAATCCAGC 3'; *R* 5' TCCAAGATTCTGTCGTCACAG 3'; *Probe* FAM-5'-atgtgtgagccaatccagc-3'- BHQ1; amplicon of 116 bp; *Rps18: F* 5' CCGCCATGTCTCTAGTGATC 3'; *R* 5' GTGATGGCGAAGGCTATTT 3'; *Probe* FAM-5'- ccgccatgtctctagtgatc-3'- BHQ1; amplicon of 97 bp). PCR was performed in three replicates in a volume of 15 µl containing 250 µM dNTPs (SibEnzyme, Russia), 300 nM forward and reverse primers, 200 nM probe, 2.5 mM $MgCl_2$, 19 x SE buffer (67 mM Tris–HCl, pH 8.8 at 25 ºC, 16.6 mM $(NH_4)_2SO_4$, 0.01 % Tween-20), 2.5 U Hot Start Taq DNA polymerase (SibEnzyme, Russia), and 50 ng cDNA. The two-step amplification program included 1 cycle of initial denaturation for 10 min at 94 ºC; 40 cycles – step 1 for 10 sec at 94 ºC and step 2 for 20 sec at 60 ºC. The *Actb* (actin beta) gene was used as a reference gene. Relative gene expression was calculated using the Pfaffl method [12] and expressed in units. Calibrator values were averaged values obtained from the RNA samples extracted from mouse tissues immediately after euthanasia.

For the histologic examination, the mouse tissue samples were placed in 10% neutral buffered formalin with subsequent fixation of the material for 24 hours. The histologic processing of the material was carried out according to the standard method in the ASP 6025 automated vacuum tissue processor (Leica Microsystems, Germany) with the preparation of paraffin blocks. Histologic sections with 4–5 µm thickness were obtained from the paraffin blocks using the HM 430 sliding microtome (Thermo Fisher Scientific, Germany). Microslides were stained with a ready-made solution of hematoxylin and eosin in the Varistain™ Gemini automated slide staining (Thermo Fisher Scientific, United Kingdom). Morphological examination and photography of the histologic microslides were carried out using the Eclipse Ni upright microscope (Nikon, Japan) and Nikon digital camera (Japan) with the NIS-Elements D 5.20.00 image analysis tool (Nikon, Japan). The morphological study included an assessment of changes in organs and tissues for signs of autolysis.

Experimental data were processed using the GraphPad Prism 8 software (GraphPad Software, USA). All results were presented as the mean and the standard deviation ($M \pm SD$). The normality of distribution was checked using the Shapiro – Wilk test. The significance of differences between the study groups was tested by the analysis of variance adjusted by the Benjamini – Hochberg correction. The relationship between the features was assessed using the Pearson's correlation coefficient. The differences were considered statistically significant at $p < 0.05$.

RESULTS

In the present study, the quality of RNA isolated from the mouse kidney, liver, and brain was assessed under conditions similar to those used in human autopsy, and RQN was used as an indicator of RNA integrity.

It was found that in the mouse tissues taken from the kidneys, liver, and brain immediately after euthanasia, the RQN values were 8.86 ± 0.49, 8.48 ± 0.44, and 8.36 ± 0.61, respectively (Fig. 1A, 1C, 1E). When calculating RQN, we considered the fractions of the areas in the 18S and 28S peaks on the electropherogram compared to the total area under the curve, the proportion of large molecules compared to smaller ones, and the height of the 18S and 28S peaks, which allowed to obtain comprehensive information about the degree of degradation in RNA molecules [13]. RQN values range from 1 to 10, where 10 corresponds to the highest integrity of the isolated RNA. The obtained results indicate high integrity of RNA molecules in the selected samples and are consistent with literature data [14].

Keeping mice after euthanasia at room temperature for 3 hours did not result in a decrease in RNA integrity in any of the organs studied (Fig. 1A, 1C, 1E). The integrity of RNA isolated from the mouse kidneys after further storage at +4 °C for 12 hours was reduced by 34.9% ($p < 0.0001$), the integrity of liver RNA decreased by 15.8% ($p = 0.0443$) (Fig. 1A and 1C). A further increase in the postmortem interval to 24, 48, and 72 hours at +4 °C was accompanied by a consistent decrease in the RNA integrity for the tissues of both organs; the end RQN values for them were 4.00 ± 0.86 and 4.81 ± 0.35, respectively.

Thus, RNA isolated from mouse kidney tissue was more susceptible to degradation with increasing postmortem interval. At the same time, brain RNA samples did not show a significant change in RQN at all time points (Fig. 1E). It is important to note that the 260 / 280 ratio, which characterizes the purity of the isolated total RNA, was in the range from 2.0 to 2.3 for all RNA samples, and no significant changes in this parameter were observed immediately after

euthanasia of the animals and at different time points of the postmortem interval.

A negative linear relationship was found between RQN and the duration of the postmortem interval for mouse liver and kidney samples (Fig. 1B and 1D). In the meantime, such a correlation was not identified for mouse brain tissue (Fig. 1F). The obtained results indicate that the degree of RNA degradation depends on the type of tissue and the duration of the postmortem interval.

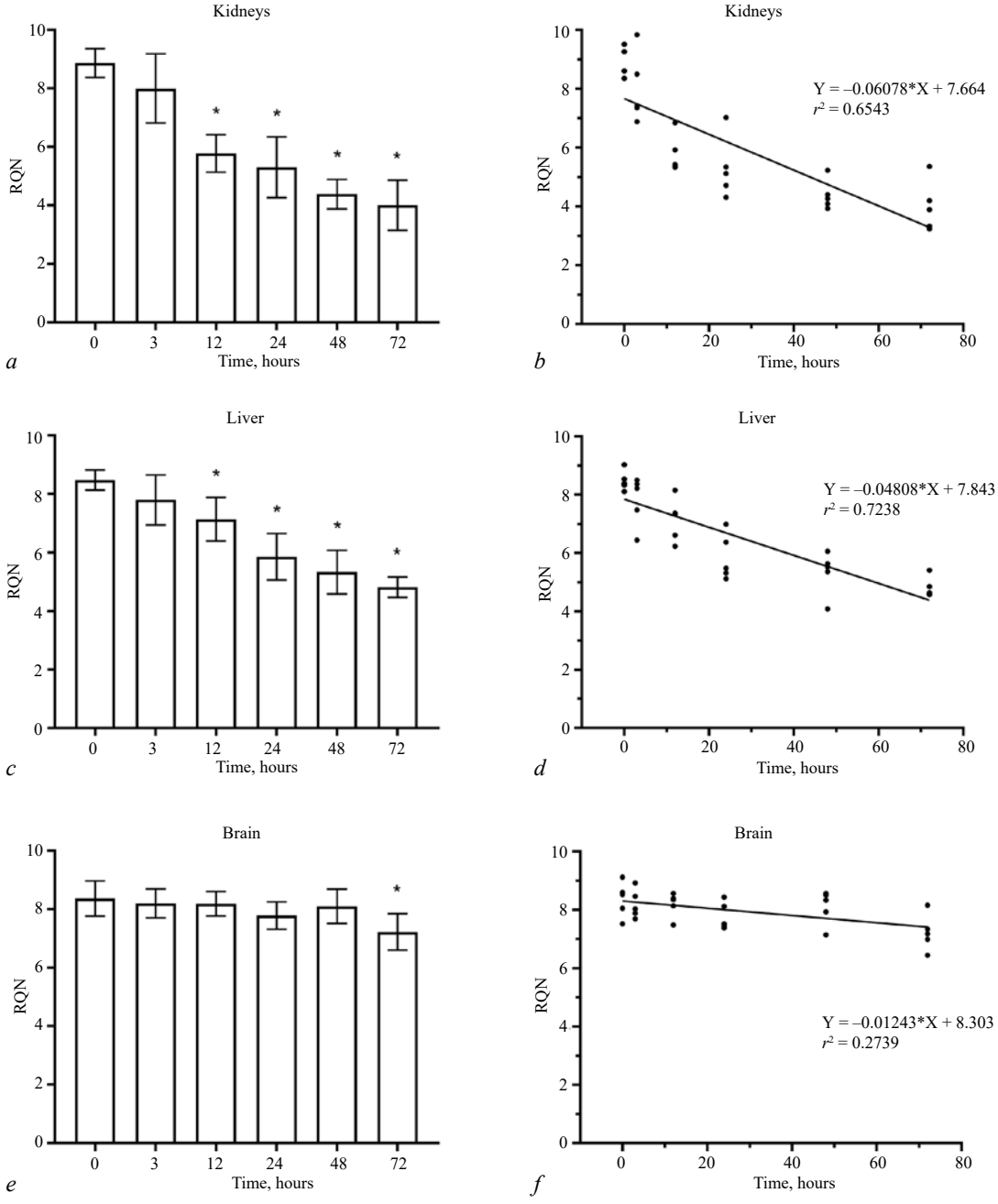

Fig. 1 – RQN and its relationship with time after euthanasia in the kidneys (A and B), liver (C and D), and brain (E and F) of mice. Mouse cadavers were kept at room temperature for the first three hours after euthanasia; then they were moved to the refrigerator (+4 ˚C). The number of animals in each group was $n = 5$. * – the differences were statistically significant ($p < 0.05$) compared to the group of animals subjected to necropsy immediately after euthanasia (0 h)

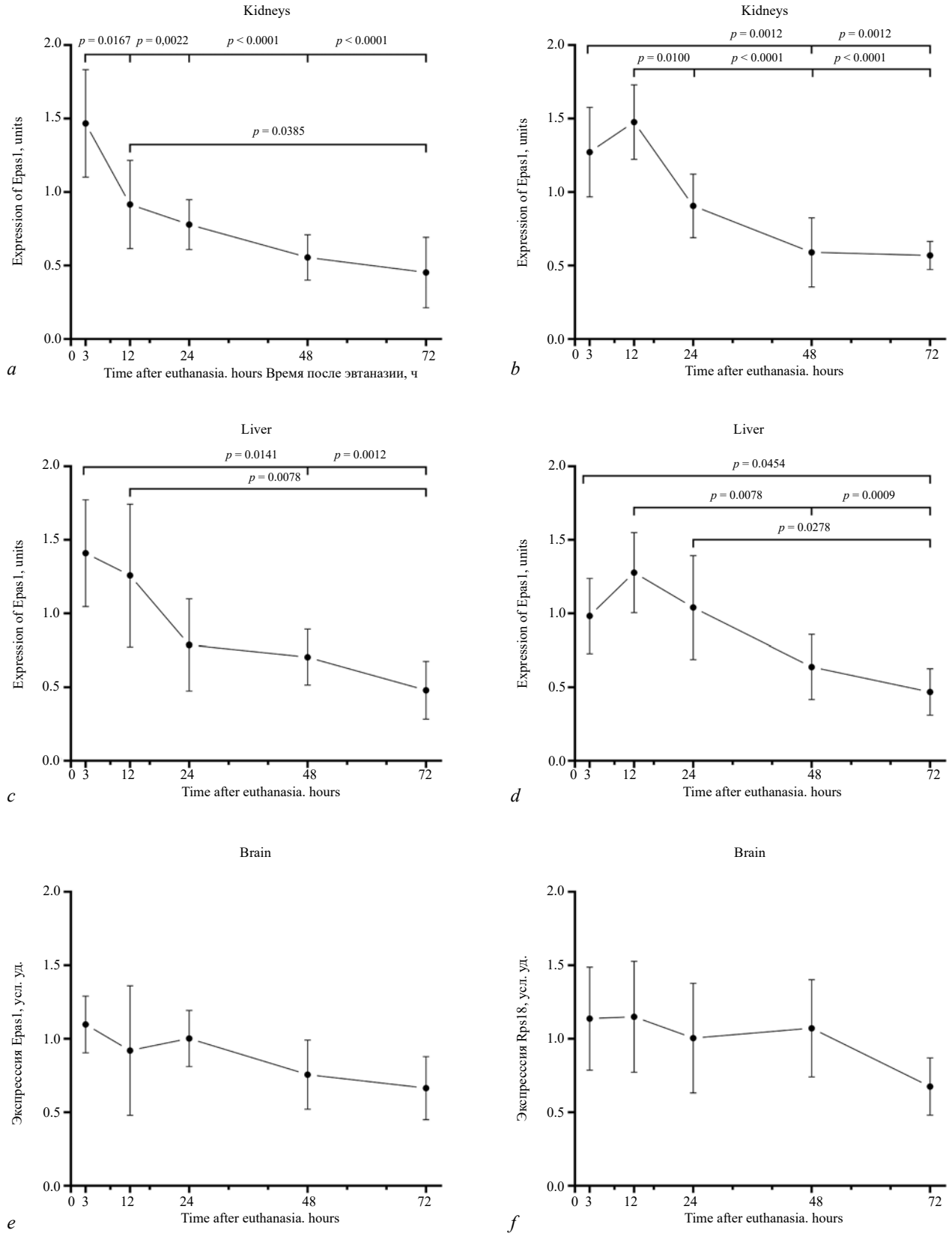

Fig. 2 – Expression of *Epas1* and *Rps18* genes in the kidneys, liver, and brain of mice at different time points after euthanasia, assessed with respect to the *Actb* (actin beta) reference gene. Mouse cadavers were kept at room temperature for the first three hours after euthanasia; then they were moved to the refrigerator (+4 ˚C). The number of animals in each group was $n = 5$. * – the differences were statistically significant ($p < 0.05$) compared to the group of animals subjected to necropsy immediately after euthanasia (0 h)

It is known that the integrity of RNA molecules is important in experiments aimed at assessing gene expression [14]. To assess the relationship between RNA integrity in mouse tissue and the results of molecular biology studies in selected samples of kidneys, liver, and brain using RT-PCR, the expression of housekeeping genes *Actb*, *Epas1,* and *Rps18* was assessed. *Actb* was chosen as a reference gene due to its high stability in the postmortem tissue samples [15].

Following the experiments, it was established that in the kidney tissues of mice after storing for 12 hours (3 hours at room temperature and 9 hours at +4 °C), the expression of the *Epas1* gene significantly decreased from 1.5 ± 0.4 units to 0.9 ± 0.3 units (p = 0.0167). In the liver, the expression of this gene decreased only 48 hours after euthanasia (1.4 ± 0.4 units after 3 hours and 0.7 ± 0.2 units after 48 hours, respectively, p = 0.0141). Increasing the postmortem interval resulted in a further decrease in *Epas1* gene expression in the kidneys and liver (Fig. 2A and 2C).

It is worth noting that the kidney and liver tissues showed a slight increase in *Rps18* gene expression 12 hours after euthanasia (by 15.4% in the kidneys and by 30.0% in the liver compared to autopsy material collected 3 hours later) (Fig. 2B and 2D). Subsequently, the expression of this gene decreased, and after 72 hours of tissue storage, it was 0.6 ± 0.1 units in the kidneys (1.3 ± 0.3 units after 3 hours, p = 0.0012) and 0.5 ± 0.2 units in the liver (1.0 ± 0.3 units after 3 hours, p = 0.0454).

At the same time, the expression level of the *Epas1* and *Rps18* genes in the brain of the animals remained stable at all time points and did not show a significant decrease 72 hours after euthanasia (Fig. 1E and 1F).

Therefore, the demonstrated dynamic changes in gene expression patterns in mice are consistent with the above results of RNA integrity assessment and depend on the organ studied and the duration of the postmortem interval.

To characterize postmortem changes in autopsy samples (kidneys, liver, and brain) of mice, pathomorphological and histologic studies were carried out (Fig. 3).

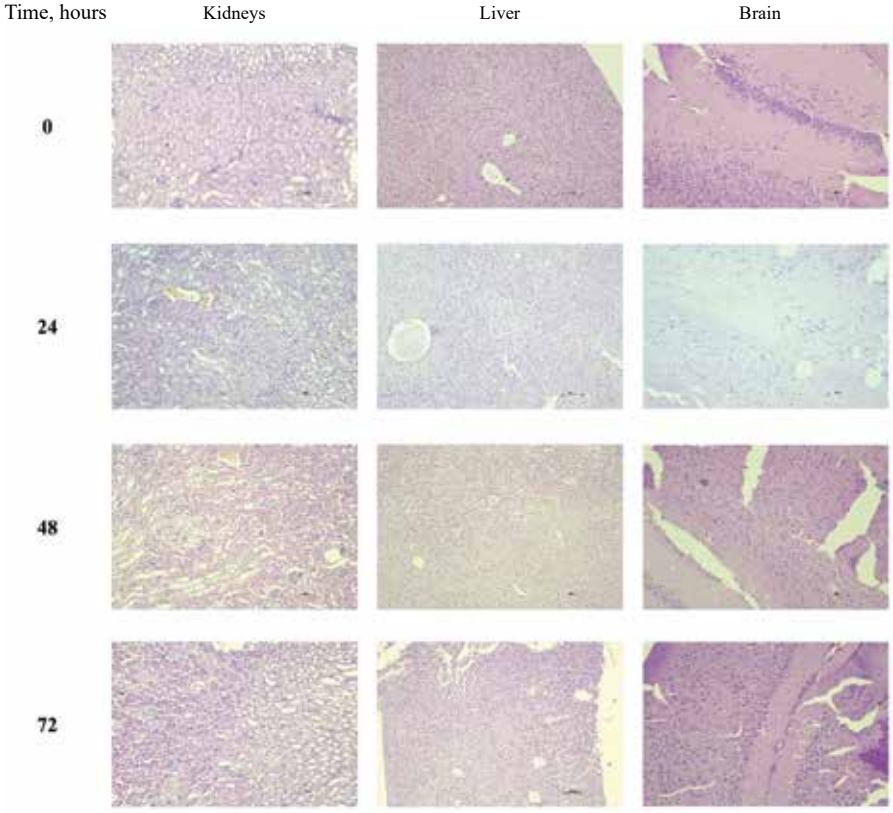

Fig. 3. Microscopic image of the kidneys, liver, and brain of mice at different time points after euthanasia. For the first three hours after euthanasia, mouse cadavers were kept at room temperature; then they were moved to the refrigerator (+4 °C). Staining with hematoxylin and eosin, ×10

In tissue samples obtained from the experimental animals at different time points (at 0, 3, 12, 24, 48, and 72 hours after euthanasia), the histologic structure of organs was preserved. In the kidneys at all stages of the experiment, the cortex and medulla were clearly differentiated, the renal tubules appeared normal, and no autolysis phenomena were detected at the optical level (Fig. 3). When examining the liver samples, the histologic structure of the organ was also preserved; some of the specimens contained cytoplasmic lipid inclusions in hepatocytes and showed signs of granular dystrophy. No signs of autolysis were detected in any of the samples studied (Fig. 3). Mild pericellular edema was observed in the brain, macro- and microglia were preserved, and no autolysis was detected in any of the samples studied (Fig. 3).

Thus, at the microscopic level, no obvious morphological changes, such as autolysis and degenerative changes, were detected, which does not exclude the presence of ultrastructural pathological changes [16].

DISCUSSION

The integrity of RNA molecules is of paramount importance in experiments aimed at assessing gene expression of isolated RNA, especially in modern high-tech studies using microarrays and multi-omics technologies [13, 17]. Indeed, one of the main problems in working with autopsy tissues is pronounced heterogeneity of samples, since the factors determining molecular parameters before and after death cannot be fully controlled [18, 19].

Understanding the relationship of changes occurring at different times in the postmortem interval when working with autopsy samples with sample quality and the correctness of interpretation of the results of molecular biology studies, including RNA integrity and gene expression profile, is of great importance [20].

Therefore, in the present study, we investigated the patterns of morphological changes, RNA integrity, and gene expression patterns in mouse tissues taken at autopsy under controlled experimental conditions.

The analysis showed the presence of tissue specificity with low RQN at different times in the postmortem interval. In this case, the kidneys and liver demonstrated a negative correlation of RQN with increasing time before sampling. In contrast, brain tissue samples were much less susceptible to postmortem changes resulting in a decrease in the RQN score. Similar results were obtained earlier in experiments studying the effect of the postmortem interval on the quality of total RNA isolated from the brain of Balb/c mice [21]. Assessing RNA integrity is essential to obtain reliable results about gene expression levels [22]. RQN ranged from 1 to 10 [13], where RQN above 8.0 indicated high integrity of RNA samples, RQN of 5.0 to 8.0 indicated moderately degraded samples, and RQN below 5.0 indicated significant degradation [23]. RQN of 5 is often used as a criterion for inclusion of biological samples in a study, although there is no consensus in the literature on this matter [23].

The kidney and liver tissues of mice at the endpoint of the study (72 hours after euthanasia) demonstrated a decrease in the RQN score by more than 50% to 4.0 ± 0.86 and 4.81 ± 0.35, respectively, which is consistent with a significant decrease in the amount of mRNA of stably expressed genes *Epas1* and *Rps18*.

Indeed, some studies have shown that the integrity of ribosomal RNA, expressed in RQN, can be used as an alternative parameter of the quality of messenger RNA (mRNA) [9, 22].

In the meantime, the results of the histologic examination using routine staining did not reflect dynamic tissue degradation in the postmortem period at the molecular level. To identify patterns in the development of ultrastructural changes, studies using electron microscopy methods are required [16].

Therefore, RQN in autopsy tissues serves as a crucial predictor of sample quality for molecular biology studies, including gene expression analysis. Further research will help identify patterns describing the relationship of molecular profiles of tissues obtained from the deceased with biopsy material and standardize protocols for handling autopsy material to obtain valuable results in multi-omics studies.

CONCLUSION

Following the study, it was established that RNA degradation in the postmortem period occurs tissue-specifically and is most pronounced in the kidneys and liver of experimental animals, in contrast to the brain. In mouse kidney and liver tissues, expression of stably expressed *Epas1* and *Rps18* genes was significantly reduced. The expression levels of the *Epas1* and *Rps18* genes in the brain of the animals remained stable at all time points and did not show a significant decrease at 72 hours after euthanasia. The observed dynamic changes in gene expression patterns in mice are consistent with the results of RNA integrity

assessment and depend on the organ studied and the duration of the postmortem interval. Thus, RQN in autopsy tissues serves as a crucial predictor of sample quality for molecular biology studies, including gene expression analysis.

REFERENCES

1. Mackenzie I. R., Neumann M. Molecular neuropathology of frontotemporal dementia: insights into disease mechanisms from postmortem studies. *Journal of neurochemistry.* 2016; *138*: 54-70. DOI: 10.1111/jnc.13588
2. Zhu Y., Wang L., Yin Y., Yang E. Systematic analysis of gene expression patterns associated with postmortem interval in human tissues. *Scientific reports*. 2017; 7(1): 5435. DOI: 10.1038/s41598-017-05882-0
3. Strand C., Enell J., Hedenfalk I., Fernö M. RNA quality in frozen breast cancer samples and the influence on gene expression analysis–a comparison of three evaluation methods using microcapillary electrophoresis traces. BMC molecular biology. 2007; 8: 1-9. DOI: 10.1186/1471-2199-8-38
4. Kocsmár É., Schmid M., Cosenza-Contreras M., Kocsmár I., Föll M., Krey L. et al. Proteome alterations in human autopsy tissues in relation to time after death. Cellular and Molecular Life Sciences. 2023; 80(5): 117. DOI: 10.1007/s00018-023-04754-3.
5. Cao L., Huang C., Zhou D. C., Hu Y., Lih T. M., Savage S. R. et al. Proteogenomic characterization of pancreatic ductal adenocarcinoma. *Cell.* 2021; 184(19): 5031-5052. DOI: 10.1016/j.cell.2021.08.023
6. Sidova M., Tomankova S., Abaffy P., Kubista M., Sindelka, R. Effects of post-mortem and physical degradation on RNA integrity and quality. *Biomolecular detection and quantification.* 2015; 5: 3-9. DOI: 10.1016/j.bdq.2015.08.002
7. Johnson E. S., Stenzel K. E., Lee S., Blalock E. M. Declining RNA integrity in control autopsy brain tissue is robustly and asymmetrically associated with selective neuronal mRNA signal loss. *bioRxiv.* 2021; 2021.09. 07.459326. DOI: 10.1101/2021.09.07.459326
8. Fan J., Khani R., Sakamot H., Zhon Y., Michae C., Pen D. et al. Quantification of nucleic acid quality in postmortem tissues from a cancer research autopsy program. *Oncotarget.* 2016; 7(41): 66906. DOI: 10.18632/oncotarget.11836
9. White K., Yang P., Li L., Farshori A., Medina A. E., Zielke H.R. Effect of postmortem interval and years in storage on RNA quality of tissue at a repository of the NIH NeuroBioBank. *Biopreservation and biobanking.* 2018; 16(2): 148-157. DOI: 10.1089/bio.2017.0099
10. Van der Linden A., Blokker B. M., Kap M., Weustink A. C., Riegman P. H., Oosterhuis J. W. Post-mortem tissue biopsies obtained at minimally invasive autopsy: an RNA-quality analysis. PLoS One. 2014; 9(12): e115675. DOI: 10.1371/journal.pone.0115675
11. Miyahara K., Hino M., Yu Z., Ono C., Nagaoka A., Hatano M., Shishido R., Yabe H., Tomita H., Kunii Y. The influence of tissue pH and RNA integrity number on gene expression of human postmortem brain. Frontiers in Psychiatry. 2023; 14: 1156524. DOI: 10.3389/fpsyt.2023.1156524.
12. Pfaffl M.W. A new mathematical model for relative quantification in real-time RT-PCR. *Nucleic Acids Research*. 2001;29(9):e45–45. DOI: 10.1093/nar/29.9.e45/
13. Schroeder A., Mueller O., Stocker S., Salowsky R., Leiber M., Gassmann M. et al. The RIN: an RNA integrity number for assigning integrity values to RNA measurements. *BMC Molecular Biology*. 2006;7:1–14. DOI: 10.1186/1471-2199-7-3.
14. Thompson K.L., Pine P.S., Rosenzweig B.A., Turpaz Y., Retief J. Characterization of the effect of sample quality on high density oligonucleotide microarray data using progressively degraded rat liver RNA. *BMC Biotechnology.* 2007:7:1–12. DOI: 10.1186/1472-6750-7-57.
15. Weickert C.S., Sheedy D., Rothmond D.A., Dedova I., Fung S., Garrick T. et al. Selection of reference gene expression in a schizophrenia brain cohort. *Australian & New Zealand Journal of Psychiatry.* 2010;44(1):59–70. DOI: 10.3109/00048670903393662.
16. Hostiuc S., Rusu M.C., Mănoiu V.S., Vrapciu A.D., Negoi I., Popescu M.V. Usefulness of ultrastructure studies for the estimation of the postmortem interval. A systematic review. *Rom. J. Morphol. Embryol*. 2017;58(2):377–384.
17. Kvastad L., Carlberg K., Larsson L., Villacampa E.G., Stuckey A., Stenbeck L. et al. The spatial RNA integrity number assay for in situ evaluation of transcriptome quality. *Communications Biology*. 2021;4(1):57. DOI: 10.1038/s42003-020-01573-1.
18. Vennemann M., Koppelkamm A. mRNA profiling in forensic genetics I: possibilities and limitations. *Forensic Science International.* 2010;203(1-3):71–75. DOI: 10.1016/j.forsciint.2010.07.006.
19. Stan A.D., Ghose S., Gao X.M., Roberts R.C., Lewis-Amezcua K., Hatanpaa K.J. et al. Human postmortem tissue: what quality markers matter? *Brain Research*. 2006;1123(1):1–11. DOI: 10.1016/j.brainres.2006.09.025.
20. Sobue S., Sakata K., Sekijima Y., Qiao S., Murate T., Ichihara M. Characterization of gene expression profiling of mouse tissues obtained during the postmortem interval. *Experimental and Molecular Pathology.* 2016; 100(3): 482-492. DOI: 10.1016/j.yexmp.2016.05.007
21. Heimberger A.B., Crotty L.E., Archer G.E., McLendon R.E., Friedman A., Dranoff G. et al. Bone marrow-derived dendritic cells pulsed with tumor homogenate induce immunity against syngeneic intracerebral glioma. *Journal of Neuroimmunology.* 2020;103(1):16–25. DOI: 10.1016/s0165-5728(99)00172-1.
22. Padhi B.K., Singh M., Rosales M., Pelletier G., Cakmak S. A PCR-based quantitative assay for the evaluation of mRNA integrity in rat samples. *Biomolecular Detection and Quantification.* 2018;15:18–23. DOI: 10.1016/j.bdq.2018.02.001.
23. Fleige S., Pfaffl M.W. RNA integrity and the effect on the real-time qRT-PCR performance. *Molecular Aspects of Medicine*. 2006;27(2-3):126–139. DOI: 10.1016/j.mam.2005. 12.003.

Authors' contribution

Buyko E.E. – review of literature, acquisition and interpretation of experimental data, drafting of the article. Perina E.A. – identification of dynamic changes in RNA integrity, drafting of the article. Vasilchenko D.V. – carrying out of histologic studies. Tsydenova I.A. – carrying out of molecular biology studies. Khmelevskaya E.S. – collection of biological material. Ufandeev A.A. – statistical processing of the data. Kaidash O.A. – coordination of sample collection for the comprehensive assessment of parameters of the molecular biology study. Ivanov V.V. – conception and design, coordination of the study, drafting of the article, final approval of the manuscript for publication. Vtorushin S.V. – carrying out of the experiment, analysis and interpretation of the data. Udut E.V. – coordination of the study, final approval of the manuscript for publication.

Authors' information

Buyko Evgeny E. – Junior Researcher, Central Research Laboratory, Siberian State Medical University, Tomsk, buykoevgen@yandex.ru, ORCID: 0000-0002-6714-1938

Perina Ekaterina A. – Junior Researcher, Center for Preclinical Trials, Central Research Laboratory, Siberian State Medical University, Tomsk, catherineperina@gmail.com, ORCID: 0000-0002-4273-8228, +7-923-410-91-53

Vasilchenko Dmitry V. – Cand. Sci. (Med.), Leading Researcher, Central Research Laboratory, Siberian State Medical University, Tomsk, vasilchenkodmitry1991@gmail.com, ORCID:0000-0002-9780-0770

Tsydenova Irina A. – Laboratory Assistant, Center for Preclinical Trials, Central Research Laboratory, Siberian State Medical University, Tomsk, tsydenova422@gmail.com, ORCID: 0000-0002-2716-3075

Khmelevskaya Ekaterina S. – Cand. Sci. (Med.), Researcher, Center for Biological Research and Bioengineering, Central Research Laboratory, Siberian State Medical University, Tomsk, kat.hmelevsk@gmail.com, ORCID: 0000-0003-1776-4149

Ufandeev Alexander A. – Junior Researcher, Center for Preclinical Trials, Central Research Laboratory, Siberian State Medical University, Tomsk, ufandeev@gmail.com, ORCID: 0000-0002-3837-1179

Kaidash Olga A.– Senior Researcher, Center for Preclinical Trials, Central Research Laboratory, Siberian State Medical University, Tomsk, kaidash_2011@mail.ru, ORCID: 0000-0001-8761-7537

Ivanov Vladimir V. – Cand. Sci. (Biology), Associate Professor, Head of the Center for Preclinical Trials, Central Research Laboratory, Siberian State Medical University, Tomsk, ivanovvv1953@gmail.com, ORCID: 0000-0003-3326-729X

Vtorushin Sergey V. – Dr. Sci. (Med.), Professor, Professor of the Pathological Anatomy Division, Siberian State Medical University, Tomsk, vtorushin.sv@ssmu.ru, ORCID:0000-0002-1195-4008

Udut Elena V. – Dr. Sci. (Med.), Professor of the Russian Academy of Sciences, Head of Central Research Laboratory, Siberian State Medical University, Tomsk, udut.ev@ssmu.ru, ORCID: 0000-0002-6104-4782.

(✉) **Buyko Evgeny E.,** buykoevgen@yandex.ru

Received 30.05.2024;
approved after peer review 19.08.2024;
accepted 12.09.2024

УДК 616.895.8–07–08–02:616.89–008.45/.48
https://doi.org/10.20538/1682-0363-2024-4-15-21

Features of structural and functional changes of the brain in patients with schizophrenia

Galkin S.A.[1], Kornetova E.G.[1], Kornetov A.N.[2], Petkun D.A.[1], Bokhan N.A.[1, 2]

[1] Mental Health Research Institute, Tomsk National Research Medical Center (NRMC), the Russian Academy of Sciences
4, Aleutskaya Str., Tomsk, 634014, Russian Federation

[2] Siberian State Medical University
2, Moscow Trakt, Tomsk, 634050, Russian Federation

ABSTRACT

Aim. To establish the features of structural and functional changes in the brain in patients with schizophrenia.

Materials and methods. A morphometric analysis of the brain using MRI scans was performed, along with a clinical assessment of the electroencephalogram (EEG) of 35 patients with schizophrenia (20 men and 15 women). The control group included 18 healthy sex- and age-matched individuals (10 men and 8 women). Statistical processing was carried out using the $\chi 2$ test, the Fisher's exact test, and the Spearman's rank correlation coefficient.

Results. Compared to the control group, patients with schizophrenia were significantly more likely to show signs of ventricular dilation ($p = 0.039$), asymmetry of the lateral ventricles ($p = 0.041$), periventricular edema ($p < 0.001$), and enlargement of the subarachnoid space of the cerebellum ($p = 0.004$). Changes (class >1A) in the functional activity of the brain in the group of patients with schizophrenia were detected in 65.7% of the cases. In more than half of the cases, patients with schizophrenia showed decreased bioelectric activity of the brain (class 2 in 48.6% and class 3 in 11.4%); at the same time, EEG signs of paroxysmal activity were detected in a few patients (class B in 11.4% and class C in 5.7%) ($p < 0.001$). A statistically significant direct correlation was found between the enlargement of the subarachnoid space of the cerebellum and paroxysmal EEG activity in patients with schizophrenia ($r = 0.377$; $p = 0.044$).

Conclusion. The findings of our study highlight that the combined use of MRI and EEG can provide important information about brain pathology in schizophrenia. The data obtained are also important for testing the hypothesis on the association between vascular and functional disorders of the brain in patients with schizophrenia.

Keywords: schizophrenia, brain pathology, magnetic resonance imaging, electroencephalography, paroxysmal activity

Conflict of interest. The authors declare the absence of obvious or potential conflicts of interest related to the publication of this article.

Source of financing. The study was conducted as part of the state assignment No. 075-01392-23-00 "Personalized diagnosis and therapy of patients with polymorbid disorders of the schizophrenic and affective spectrum", registration number 123041900006-4.

Conformity with the principles of ethics. All study participants signed an informed consent to participate in the study. The study was approved by the local Ethics Committee at the Mental Health Research Institute of Tomsk NRMC (Protocol No. 157 of 18.11.2022).

For citation: Galkin S.A., Kornetova E.G., Kornetov A.N., Petkun D.A., Bokhan N.A. Features of structural and functional changes of the brain in patients with schizophrenia. *Bulletin of Siberian Medicine.* 2024;23(4):15–21. https://doi.org/10.20538/1682-0363-2024-4-15-21.

✉ *Galkin Stanislav A.,* s01091994@yandex.ru

Особенности структурных и функциональных изменений головного мозга у больных шизофренией

Галкин С.А.[1], Корнетова Е.Г.[1], Корнетов А.Н.[2], Петкун Д.А.[1], Бохан Н.А.[1, 2]

[1] Научно-исследовательский институт (НИИ) психического здоровья, Томский национальный исследовательский медицинский центр (НИМЦ)
Россия, 634014, г. Томск, ул. Алеутская, 4

[2] Сибирский государственный медицинский университет (СибГМУ)
Россия, 634050, г. Томск, Московский тракт, 2

РЕЗЮМЕ

Цель. Установить особенности структурных и функциональных изменений головного мозга у больных шизофренией.

Материалы и методы. Проведен морфометрический анализ магнитно-резонансных изображений головного мозга, а также клиническая оценка электроэнцефалограммы (ЭЭГ) 35 больных шизофренией (20 мужчин и 15 женщин). В контрольную группу вошли 18 здоровых лиц (10 мужчин и 8 женщин), которые были подобраны по возрасту и полу основной группе пациентов. Статистическая обработка проводилась с помощью критерия $\chi 2$ и точного критерия Фишера, а также корреляционного анализа Спирмена.

Результаты. По сравнению с группой контроля у больных шизофренией статистически значимо чаще обнаруживаются признаки расширения желудочков ($p = 0{,}039$), асимметрии боковых желудочков ($p = 0{,}041$), отека перивентрикулярных зон ($p < 0{,}001$) и расширения субарахноидального пространства мозжечка ($p = 0{,}004$). Модификации (класс >1А) функциональной активности мозга в группе больных шизофренией были выявлены в 65,7% случаев. Более чем в половине случаев у больных шизофренией обнаруживалось замедление биоэлектрической активности мозга (класс 2 – 48,6% и класс 3 – 11,4%), одновременно с этим у небольшой части пациентов выявлялись ЭЭГ-признаки пароксизмальной активности (класс В – 11,4% и класс С – 5,7%) ($p < 0{,}001$). Выявлена статистически значимая прямая корреляция между расширением субарахноидального пространства мозжечка и пароксизмальной активностью у больных шизофренией ($r_s = 0{,}377$; $p = 0{,}044$).

Заключение. Полученные данные в нашем исследовании подчеркивают, что совместное использование магнитно-резонансной томографии и ЭЭГ может предоставить важную информацию о мозговой патологии при шизофрении. Полученные нами результаты имеют значение для проверки гипотезы о связи дисциркуляторных и функциональных нарушений головного мозга у больных шизофренией.

Ключевые слова: шизофрения, мозговая патология, магнитно-резонансная томография, электроэнцефалография, пароксизмальная активность

Конфликт интересов. Авторы декларируют отсутствие явных и потенциальных конфликтов интересов, связанных с публикацией настоящей статьи.

Источник финансирования. Исследование проведено в рамках выполнения госзадания № 075-01392-23-00 «Персонализированная диагностика и терапия больных полиморбидными расстройствами шизофренического и аффективного спектра», регистрационный номер 123041900006-4.

Соответствие принципам этики. Все участники исследования подписали информированное согласие на участие в исследовании. Исследование одобрено локальным этическим комитетом НИИ психического здоровья Томского НИМЦ (протокол № 157 от 18.11.2022).

Для цитирования: Галкин С.А., Корнетова Е.Г., Корнетов А.Н., Петкун Д.А., Бохан Н.А. Особенности структурных и функциональных изменений головного мозга у больных шизофренией. *Бюллетень сибирской медицины.* 2024;23(4):15–21. https://doi.org/10.20538/1682-0363-2024-4-15-21.

INTRODUCTION

The study of the structural and functional features of the brain in patients with schizophrenia remains one of the most actively developed areas in psychiatry [1, 2]. Many previous studies have clearly shown that in schizophrenia, gray matter atrophy is observed in various parts of the brain [1–4]. Even at early stages of the disease, patients with the first episode of schizophrenia have a decrease in gray matter content in regions, such as the temporal gyrus, dorsolateral prefrontal cortex, inferior frontal gyrus, thalamus, hippocampus, amygdala, etc. [4, 5]. In addition, the presence of dyscirculatory foci and multiple cysts, as well as dilation and asymmetry of the lateral ventricles were found [6, 7].

The literature devoted to neurophysiological (electroencephalographic) testing has extensively described flattening of the amplitude of the negative wave – N100 auditory evoked potentials (EP) in schizophrenia, although there is contrary information [10] indicating that the amplitude of N100 does not change significantly in patients with schizophrenia compared to the control group. On the other hand, a relatively high percentage of individuals with this disorder show changes in the EEG in the form of generalized slow wave activity (delta and theta waves), asymmetry, the presence of sharp waves and/or spike–and–wave complexes (paroxysmal patterns) [11–13].

Summarizing the above data, we can say that, despite the large number of original research conducted earlier, the results of studying structural and functional changes in the brain in patients with schizophrenia are quite debatable, which causes a lot of discussion regarding the variety of mechanisms (pathogenesis) of the disease and its diagnostic instability.

On the other hand, despite the widespread use of new high-tech methods (positron emission tomography, single-photon emission computed tomography, magnetoencephalography, functional magnetic resonance imaging (MRI), etc.), studies of structural and functional features in the research of brain diseases, electroencephalography (EEG) and magnetic resonance imaging (MRI) methods remain the most adequate in displaying pathological processes in the brain. Electroencephalography has almost a hundred-year history and is one of the first physiological methods used to study the functional activity of the brain in patients with schizophrenia. Today it remains a fairly popular way to examine the brain. In general, bioelectric signals arise as a result of the combined dendritic inhibitory and excitatory postsynaptic activity of billions of neurons, primarily pyramidal cells in the neocortex of the brain [14]. One of the main limitations of the method is the difficulty in determining the source of recorded activity, since pulse activity generators in different parts of the brain can reproduce the same EEG pattern recorded distally on the scalp [15]. EEG has high temporal and low spatial resolution, which is compensated by structural MRI, which, instead, is characterized by high spatial and low temporal resolution [16]. Structural MRI provides detailed information about the regions of the brain that have pathological changes in many diseases, including schizophrenia [17].

The aim of the study was to establish the features of structural and functional changes in the brain in patients with schizophrenia.

MATERIALS AND METHODS

The study was approved by the local Ethics Committee at the Mental Health Research Institute of Tomsk NRMC (Protocol No. 157 of 18.11.2022). All study participants signed an informed consent to participate in the study.

In total, 35 patients with schizophrenia (20 men and 15 women) who underwent treatment in the Endogenous Disorders Department of the Mental Health Research Institute Clinic of Tomsk NRMC were selected for this study. Inclusion criteria were as follows: patients aged 18–55 years old; they were diagnosed with schizophrenia according to the criteria of ICD–10 (F20); the duration of the disease is at least 1 year; and patients signed a written consent to participate in the study. Exclusion criteria were the following: psychoactive substance dependence (except tobacco), dementia, no significant neurological history (brain injury, stroke), refusal to participate in the study.

The age of the patients included in the study was 37 [32; 44] years. The duration of the disease was 15 [11; 21] years. At the time of inclusion in the study, patients received basic therapy with second-generation atypical antipsychotic medications (CPZeq – 400 [200; 600] mg / day), the duration of basic therapy was 4 [3; 8] years. The severity of psychopathological symptoms was assessed using the PANSS (Positive and Negative Syndrome Scale) [18] in the adapted Russian version – SCI–PANSS [19]. The overall PANSS score of the patients was 81 [68; 101]. The severity of positive symptoms was 12 [9; 27] points

versus 23 [20; 26] points for negative ones, while the severity of general psychopathological symptoms was 44 [39; 53] points.

The control group included 18 healthy individuals (10 men and 8 women) who matched the main group of patients in terms of age and gender ($p > 0.05$) with similar exclusion criteria.

The methodology of the clinical examination (MRI and EEG) is presented in detail in our previous articles [6, 11].

The statistical analysis was carried out using the R 4.2.2 software. Compliance with the law of normal distribution was checked using the Shapiro – Wilk test. The data did not follow the normal distribution. Quantitative data were presented as the median and the interquartile range Me [Q_1; Q_3]. Qualitative data were presented by frequency parameters in absolute and relative units – n (%). The chi-squared test and the Fisher's exact test were used to compare frequencies (in the case of frequencies less than 5). The Spearman's rank correlation coefficient (r_s) was used to identify the relationships between the studied parameters. The threshold level of statistical significance of p was assumed to be 0.05.

RESULTS

According to the analysis of brain morphometry using MRI, the following pathological changes were found in the studied groups of patients and controls: dilation and / or asymmetry of the lateral ventricles, periventricular edema, enlargement of the subarachnoid space of the large hemispheres and / or cerebellum, the presence of cysts in the brain (Table 1).

Table 1

Analysis of brain morphometry using MRI in the studied groups of patients and controls, *n* (%)

MR parameter	Patients with schizophrenia, $n = 35$	Control, $n = 18$	p
Ventricular dilation	12 (34.3%)	1 (5.6%)	0.039*
Asymmetry of the lateral ventricles	11 (31.4%)	1 (5.6%)	0.041*
Periventricular edema	31 (88.6%)	6 (33.3%)	<0.001*
Enlargement of the subarachnoid space of the large hemispheres	13 (37.1%)	4 (22.2%)	0.358
Enlargement of the subarachnoid space of the cerebellum	30 (85.7%)	8 (44.4%)	0.004*
Cysts	8 (22.8%)	2 (11.1%)	0.463

* Statistically significant differences here and in Tables 2, 3.

Compared to the control group, patients with schizophrenia were significantly more likely to show signs of ventricular dilation ($p = 0.039$), asymmetry of the lateral ventricles ($p = 0.041$), periventricular edema ($p < 0.001$), and enlargement of the subarachnoid space of the cerebellum ($p = 0.004$).

When summarizing the obtained EEG data, changes (class > 1A) in the functional activity of the brain were detected in 65.7% of cases in the group of patients with schizophrenia (Table 2).

Table 2

EEG modifications in the studied patient and control groups, *n* (%)

EEG modifications		Patients with schizophrenia, $n = 35$	Control, $n = 18$
Slowing on EEG (class)	1	14 (40%)	18 (100%)
	2	17 (48.6%)	–
	3	4 (11.4%)	–
	4	–	–
Paroxysmal activity (class) (class)	A	29 (82.9%)	18 (100%)
	8	4 (11.4%)	–
	C	2 (5.7%)	–
	D	–	–-

* $p < 0.001$.

In more than half of the cases, patients with schizophrenia showed slowing of the bioelectric activity of the brain (class 2 in 48.6% and class 3 in 11.4% of cases). At the same time, EEG signs of paroxysmal activity were detected in a few patients (class B in 11.4% and class C in 5.7% of cases).

Table 3 shows the correlation analysis data on EEG changes depending on the detected pathological changes according to the analysis of brain morphometry using MRI in patients with schizophrenia.

Table 3

The relationship between the parameters of brain MRI and EEG in patients with schizophrenia

MR parameter	Slowing on EEG	Paroxysmal activity
Ventricular dilation	$r_s = 0.022$ $p = 0.923$	$r_s = 0.189$ $p = 0.409$
Asymmetry of the lateral ventricles	$r_s = 0.092$ $p = 0.691$	$r_s = 0.148$ $p = 0.521$
Periventricular edema	$r_s = 0.099$ $p = 0.666$	$r_s = 0.116$ $p = 0.613$
Enlargement of the subarachnoid space of the large hemispheres	$r_s = 0.144$ $p = 0.531$	$r_s = 0.152$ $p = 0.509$

End of table 3

The relationship between the parameters of brain MRI and EEG in patients with schizophrenia

MR parameter	Slowing on EEG	Paroxysmal activity
Enlargement of the subarachnoid space of the cerebellum	$r_s = 0.025$ $p = 0.326$	$r_s = 0.377$ $p = 0.044$*
Cysts	$r_s = 0.111$ $p = 0.632$	$r_s = 0.146$ $p = 0.527$

A statistically significant correlation was found between paroxysmal activity on EEG and the enlargement of the subarachnoid space of the cerebellum in patients with schizophrenia ($r_s = 0.377$; $p = 0.044$). We could not find statistically significant correlations with the clinical parameters of patients (age, duration of the disease, duration of basic therapy, severity of psychopathological symptoms according to PANSS) ($p > 0.05$ for all).

DISCUSSION

The data presented in our original study indicate the presence of extensive structural and functional changes in the brain in patients with schizophrenia. The dyscirculatory disorders detected using MRI in schizophrenia are consistent with the results of earlier studies [4, 5, 20, 21]. As is known, the detected MRI parameters are not independent diseases, but arise in response to pathological processes occurring in the brain. Nevertheless, unlike a number of previous studies [4, 5], we were unable to establish significant correlations of brain abnormalities with the clinical and dynamic features of schizophrenia, which may be due to the innate nature of pathological changes in the brain. For example, parents of newborn children often learn about the enlargement of the subarachnoid space after examination. These phenotypic features reflect disorders of embryonic morphogenesis resulting from the constellation of hereditary factors and perinatal effects, the clinical assessment of which is important for the identification of abnormalities in the development of the nervous system [22].

We also identified significant changes in the functional activity of the brain in patients with schizophrenia in the form of a slowdown in biopotentials and emergence of paroxysmal activity on EEG. It is assumed that these changes are associated with inhibitory deficit of GABAergic projections of the cortex to pyramidal neurons. This can lead to uncontrolled excitation (hyperexcitation) of pyramidal neurons, which, in turn, affect their targets, causing excitotoxic changes leading to regression of neural networks due to loss of dendrites and synapses. This model is confirmed by data on soma volume deficit in the primary and secondary cortex (soma volume of pyramidal cells correlates with the degree of dendritic branching [23]. It should also be noted that impaired GABAergic-glutamatergic interaction in the pyramidal neurons of the brain is one of the main mechanisms of epileptogenesis [24].

In addition, we found a significant relationship between MRI and EEG data, namely a direct correlation between the enlargement of the subarachnoid space of the cerebellum and the presence of paroxysmal activity in patients with schizophrenia, which is consistent with clinical cases of patients with epilepsy [25, 26]. As is known, the detection of paroxysmal activity on EEG indicates a trend toward convulsive states. Paroxysmal activity reflects a change in the functioning of basic neurophysiological processes with an increase in the activity of subcortical synchronizing regulators that contribute to the occurrence of seizures. In clinical practice, information about brain structures that can cause paroxysmal activity on EEG is of great value, especially for patients with schizophrenia receiving long-term therapy with antipsychotics and, in some cases, antidepressants.

CONCLUSION

Thus, the data obtained in our study emphasize that the combined use of MRI and EEG can offer key insights into brain pathology in schizophrenia. Our findings also contribute to the search for specific structural and functional neurobiomarkers of schizophrenia.

REFERENCES

1. Lebedeva I.S. The search of the “intact” structural and functional brain systems as a paradigm shift in schizophrenia research. *S.S. Korsakov Journal of Neurology and Psychiatry*. 2015;115(2):37–41 (in Russ.). DOI: 10.17116/jnevro20151152137-41.
2. McCarley R.W., Nakamura M., Shenton M.E., Salisbury D.F. Combining ERP and structural MRI information in first episode schizophrenia and bipolar disorder. *Clin. EEG Neurosci*. 2008;39(2):57–60. DOI: 10.1177/155005940803900206.
3. Shamrey V.K., Puchkov N.A., Tarumov D.A., Trufanov A.G., Markin K.V., Prochik Ya.E., Bogdanovskaya A.S. Microstructural brain pathology in paranoid schizophrenia (according to magnetic resonance tractography). *Psychiatry*. 2023;21(2):38–49 (in Russ.). DOI: 10.30629/2618-6667-2023-21-2-38-49.
4. Mørch-Johnsen L., Agartz I., Jensen J. The neural correlates of negative symptoms in schizophrenia: examples from MRI

literature. *Clin. EEG Neurosci*. 2018;49(1):12–17. DOI: 10.1177/1550059417746214.
5. Ellison-Wright I., Glahn D.C., Laird A.R., Thelen S.M., Bullmore E. The anatomy of first-episode and chronic schizophrenia: an anatomical likelihood estimation meta-analysis. *Am. J. Psychiatry.* 2008;165(8):1015–1023. DOI: 10.1176/appi.ajp.2008.07101562.
6. Kornetova E.G., Koval S.D., Kornetov A.N., Parshukova D.A., Ivanova S.A., Semke A.V., et al. Brain pathology in schizophrenia: association with clinical and constitutional factors. *Yakut Medical Journal*. 2019;65(1):17–21 (in Russ.). DOI: 10.25789/YMJ.2019.65.05.
7. Del Re E.C., Bouix S., Fitzsimmons J., Blokland G.A.M., Mesholam-Gately R., Wojcik J. et al. Diffusion abnormalities in the corpus callosum in first episode schizophrenia: Associated with enlarged lateral ventricles and symptomatology. *Psychiatry Res.* 2019;277:45–51. DOI: 10.1016/j.psychres.2019.02.038.
8. Kropotov J.D., Pronina M.V., Ponomarev V.A., Poliakov Y.I., Plotnikova I.V., Mueller A. Latent ERP components of cognitive dysfunctions in ADHD and schizophrenia. *Clin. Neurophysiol*. 2019;130(4):445–453. DOI: 10.1016/j.clinph.2019.01.015.
9. Rosburg T. Auditory N100 gating in patients with schizophrenia: A systematic meta-analysis. *Clin. Neurophysiol*. 2018;129(10):2099–2111. DOI: 10.1016/j.clinph.2018.07.012.
10. Lijffijt M., Cox B., Acas M.D., Lane S.D., Moeller F.G., Swann A.C. Differential relationships of impulsivity or antisocial symptoms on P50, N100, or P200 auditory sensory gating in controls and antisocial personality disorder. *J. Psychiatr. Res.* 2012;46(6):743–750. DOI: 10.1016/j.jpsychires.2012.03.001.
11. Galkin S.A., Kornetova E.G., Ivanova S.A. Comparative analysis of EEG in patients with schizophrenia receiving various atypical antipsychotics. *Bulletin of Siberian Medicine*. 2024;23(1):15–22 (in Russ.). DOI: 10.20538/1682-0363-2024-1-15-22.
12. Gashkarimov V.R., Sultanova R.I., Efremov I.S., Asadullin A.R. Machine learning techniques in diagnostics and prediction of the clinical features of schizophrenia: a narrative review *Consortium Psychiatricum.* 2023;4(3):43–53 (in Russ.). DOI: 10.17816/CP11030.
13. Arora M., Knott V.J., Labelle A., Fisher D.J. Alterations of resting EEG in hallucinating and nonhallucinating schizophrenia patients. *Clin. EEG Neurosci*. 2021;52(3):159-–67. DOI: 10.1177/1550059420965385.
14. Müller-Putz G.R. Electroencephalography. *Handb. Clin. Neurol*. 2020;168:249–262. DOI: 10.1016/B978-0-444-63934-9.00018-4.
15. Mari-Acevedo J., Yelvington K., Tatum W.O. Normal EEG variants. *Handb. Clin. Neurol*. 2019;160:143–160. DOI: 10.1016/B978-0-444-64032-1.00009-6.
16. Liu Z., Ding L., He B. Integration of EEG/MEG with MRI and fMRI. *IEEE Eng. Med. Biol. Mag*. 2006;25(4):46–53. DOI: 10.1109/memb.2006.1657787.
17. Lancaster T.M., Dimitriadis S.I., Perry G., Zammit S., O'Donovan M.C., Linden D.E. Morphometric Analysis of Structural MRI Using Schizophrenia Meta-analytic Priors Distinguish Patients from Controls in Two Independent Samples and in a Sample of Individuals With High Polygenic Risk. *Schizophr. Bull*. 2022;48(2):524–532. DOI: 10.1093/schbul/sbab125.
18. Kay S.R., Fiszbein A., Opler L.A. The positive and negative syndrome scale (PANSS) for schizophrenia. *Schizophrenia Bulletin*. 1987;13(2):261–276. DOI: 10.1093/schbul/13.2.261.
19. Mosolov S.N. Scales of psychometric assessment of schizophrenia symptoms and the concept of positive and negative disorders. Moscow, 2001:238 (in Russ.).
20. Micoulaud-Franchi J.A., Balzani C., Faugere M. Neurophysiologie clinique en psychiatrie: 1 – Techniques, vocabulaires et indications de l'électroencéphalographie conventionnelle. *Annales Médico-psychologiques Revue Psychiatrique.* 2013;171:334–341. DOI: 10.1016/j.amp.2013.04.005.
21. Chiapponi C., Piras F., Fagioli S., Piras F., Caltagirone C., Spalletta G. Age-related brain trajectories in schizophrenia: a systematic review of structural MRI studies. *Psychiatry Res*. 2013;214(2):83–93. DOI: 10.1016/j.pscychresns.2013.05.003.
22. Nikityuk B.A., Kornetov N.A. Integrative biomedical anthropology. Tomsk: Tomsk State University, 1998:82 (in Russ.).
23. Sweet R.A., Bergen S.E., Sun Z., Marcsisin M.J., Sampson A.R., Lewis D.A. Anatomical evidence of impaired feedforward auditory processing in schizophrenia. *Biol. Psychiatry*. 2007;61(7):854–864. DOI: 10.1016/j.biopsych.2006.07.033.
24. Evstigneev V.V., Kisten O.V. The basic mechanisms of epileptogenesis and epilepsy. *Proceedings of the National Academy of Sciences of Belarus. Medical Series.* 2011;(3):106–114 (in Russ.).
25. Rhodes R.H., Lehman R.M., Wu B.Y., Roychowdhury S. Focal chronic inflammatory epileptic encephalopathy in a patient with malformations of cortical development, with a review of the spectrum of chronic inflammatory epileptic encephalopathy. *Epilepsia*. 2007;48(6):1184–1202. DOI: 10.1111/j.1528-1167.2007.01034.x.
26. Boling W., Kore L. Subarachnoid Hemorrhage-Related Epilepsy. *Acta Neurochir. Suppl.* 2020;127:21–25. DOI: 10.1007/978-3-030-04615-6_4.

Authors' contribution

Galkin S.A. – neurophysiological examination of patients, analysis of data, drafting of the manuscript. Kornetova E.G. – conception and design, clinical, psychopathological, and psychometric examination of the sample, critical revision of the manuscript for important intellectual content. Kornetov A.N. – conception and design, review of publications on the topic of the manuscript, drafting and editing of the manuscript. Petkun D.A. – psychometric examination of patients. Bokhan N.A. – final approval of the manuscript for publication.

Authors' information

Galkin Stanislav A. – Cand. Sci. (Med.), Researcher, Mental Health Research Institute, Tomsk NRMC, Tomsk, s01091994@yandex.ru, http://orcid.org/0000-0002-7709-3917

Kornetova Elena G. – Dr. Sci. (Med.), Head of the Endogenous Disorders Department, Mental Health Research Institute, Tomsk NRMC, Tomsk, ekornetova@outlook.com, http://orcid.org/0000-0002-5179-9727

Kornetov Alexander N. – Dr. Sci. (Med.), Professor, Head of the Fundamental Psychology and Behavioral Medicine Division, Siberian State Medical University, Tomsk, alkornetov@gmail.com, http://orcid.org/0000-0002-2342-7504

Petkun Dmitry A. – Junior Researcher, Mental Health Research Institute, Tomsk NRMC, Tomsk, substantia_p@mail.ru, http://orcid.org/0000-0002-6587-6347

Bokhan Nikolay A. – Dr. Sci. (Med.), Professor, Distinguished Scientist of the Russian Federation, Academician of the Russian Academy of Sciences, Director of the Mental Health Research Institute, Tomsk NRMC, Head of the Psychiatry, Narcology and Psychotherapy Division, Siberian State Medical University, Tomsk, bna909@gmail.com, http://orcid.org/0000-0002-1052-855X

(✉) **Galkin Stanislav A.,** s01091994@yandex.ru

Received 02.07.2024;
approved after peer review 30.08.2024;
accepted 12.09.2024

УДК 616-002.1-092:612.112.91.085.2
https://doi.org/10.20538/1682-0363-2024-4-22-30

Transformation of NETs under the effect of pathogens and IgG

Kazimirskii A.N., Salmasi J.M., Poryadin G.V., Panina M.I., Kim A.E., Rogozhina L.S.

Pirogov Russian National Research Medical University
1, Ostrovityanova Str., Moscow, 117997, Russian Federation

ABSTRACT

Background. Many studies have shown that neutrophil extracellular traps (NETs) in the form of web-like structures are present in the peripheral blood of patients with inflammatory diseases. In our research, in addition to traditional web-like NET structures, several anomalous forms were identified, including NETs with cloud-like appearance.

Aim. To investigate morphological and functional transformation of NETs under the influence of *Klebsiella pneumoniae* and immunoglobulin G (IgG).

Materials and methods. The study included 42 patients of Moscow City Clinical Hospital No. 51: 28 patients with acute inflammation in the abdominal cavity (appendicitis, cholecystitis, pancreatitis, peritonitis), 6 patients diagnosed with ulcerative colitis, and 8 patients with hernias. Neutrophils were isolated using gradient-density centrifugation. To calculate NETs, we used SYBR Green I-induced fluorescence microscopy (Evrogen, Russia), with the dye specifically interacting with double-stranded DNA. The functional activity of NETs was determined in the *Klebsiella pneumoniae* (ATCC 700603) capture test.

Results. In patients with inflammatory diseases of the abdominal cavity in the postoperative period, the functional activity of NETs was several times lower than in healthy individuals. NETs in these patients capture and bind no more than 20 cells of the microorganism. Under the effect of IgG, neutrophil networks transform into loose cloud-like structures, which can hardly capture and bind the pathogen, binding only 8.46 ± 0.44 cells of the microorganism. Spontaneous enzymatic degradation of cloud like NETs may be accompanied by the production of secondary alteration factors.

Conclusion. The results of the study provide the grounds for the development of new approaches to elaborating vaccination regimens and using immunobiologics that require preliminary monitoring of the state of innate immunity, in particular, neutrophil networks in the patient's body.

Keywords: neutrophil extracellular traps, neutrophil web-like structure, neutrophil cloud-like structures, inflammation, NET functional activity, vaccination, immunobiological therapy

Conflict of interest. The authors declare the absence of obvious or potential conflicts of interest related to the publication of this article.

Source of financing. The authors state that they received no funding for the study.

Conformity with the principles of ethics. All study participants signed an informed consent to participate in the study. The study was approved by the Ethics Committee at Pirogov Russian National Research Medical University (Protocol No. 203 of 21.12.2021).

For citation: Kazimirskii A.N., Salmasi J.M., Poryadin G.V., Panina M.I., Kim A.E., Rogozhina L.S. Transformation of NETs under the effect of pathogens and IgG. *Bulletin of Siberian Medicine.* 2024;23(4):22–30. https://doi.org/10.20538/1682-0363-2024-4-22-30.

✉ *Kazimirskii Alexander N.,* alnica10@mail.ru

Трансформация нейтрофильных сетей под влиянием патогенов и иммуноглобулинов класса G

Казимирский А.Н., Салмаси Ж.М., Порядин Г.В., Панина М.И., Ким А.Э., Рогожина Л.С.

Российский национальный исследовательский медицинский университет (РНИМУ) им. Н.И. Пирогова Россия, 117997, г. Москва, ул. Островитянова, 1

РЕЗЮМЕ

Введение. Исследования многих авторов показали, что в периферической крови пациентов с воспалительными заболеваниями присутствуют нейтрофильные экстраклеточные ловушки (НЭЛ, NETs) в морфологической форме нейтрофильных сетей. В наших исследованиях помимо традиционной структуры НЭЛ в виде нейтрофильных сетей были выявлены некоторые аномальные формы, в том числе и вуалеобразные формы НЭЛ.

Цель. Исследование морфофункциональной трансформации НЭЛ под влиянием *Klebsiella pneumoniae* и иммуноглобулинов класса G (IgG).

Материалы и методы. В исследование включены 42 больных 51-й ГКБ г. Москвы: 28 – с острыми воспалительными процессами в брюшной полости (аппендицит, холецистит, панкреатит, перитонит), шесть – с диагнозом «язвенный колит», восемь – с грыжами. Нейтрофилы выделяли, используя градиентное центрифугирование. Для подсчета НЭЛ использовали флуоресцентную микроскопию с красителем SYBR Green (ЗАО «Евроген», Россия), специфично взаимодействующего с двухцепочечной ДНК. Функциональную активность НЭЛ определяли в тесте с захватом *Klebsiella pneumoniae* (ATCC 700603).

Результаты. У больных с воспалительными заболеваниями брюшной полости в послеоперационном периоде функциональная активность НЭЛ ослаблена по сравнению со здоровыми в несколько раз. Нейтрофильные экстраклеточные ловушки у этих больных захватывают и связывают не более 20 клеток микроорганизма. Под влиянием IgG нейтрофильные сети превращаются в рыхлые вуалеобразные структуры. Эти нейтрофильные структуры обладают очень слабой способностью к захвату и связыванию патогена, соединяя 8,46 ± 0,44 клеток микроорганизма. Спонтанная ферментативная деградация нейтрофильных «вуалей» может сопровождаться продукцией факторов вторичной альтерации.

Заключение. Результаты исследования создают предпосылки для формирования новых подходов к разработке режимов вакцинации и применения иммунобиологических препаратов, требующих предварительного контроля состояния врожденного иммунитета, в частности, нейтрофильных сетей в организме пациентов.

Ключевые слова: нейтрофильные экстраклеточные ловушки, нейтрофильные сети, нейтрофильные вуали, воспаление, функциональная активность НЭЛ, вакцинация, лечение иммунобиологическими препаратами

Конфликт интересов. Авторы декларируют отсутствие явных и потенциальных конфликтов интересов, связанных с публикацией настоящей статьи.

Источник финансирования. Авторы заявляют об отсутствии финансирования при проведении исследования.

Соответствие принципам этики. Все участники исследования подписали информированное согласие на участие в исследовании. Исследование одобрено этическим комитетом РНИМУ им. Н.И. Пирогова (протокол № 203 от 21.12.2021).

Для цитирования: Казимирский А.Н., Салмаси Ж.М., Порядин Г.В., Панина М.И., Ким А.Э., Рогожина Л.С. Трансформация нейтрофильных сетей под влиянием патогенов и иммуноглобулинов класса G. *Бюллетень сибирской медицины.* 2024;23(4):22–30. https://doi.org/10.20538/1682-0363-2024-4-22-30.

INTRODUCTION

Components of innate immunity and, in particular, neutrophils form the first line of defense against various foreign agents (viral, bacterial, etc.) invading the human body. Numerous studies have shown that the protective function of neutrophils is implemented through the formation of neutrophil extracellular traps (NETs). The NET formation is an effective mechanism for combating invading microorganisms, and the lack of NET formation or hydrolysis of the main NET nucleotide chain by

bacterial DNases makes the human body susceptible to infections [1].

NETs are a form of reaction of pre-activated neutrophils to interactions with host cells in a state of apoptosis, as well as various microorganisms, including viruses [2]. Neutrophils receive signals to release NETs through various innate immunity receptors (TLRs).

Many authors in their studies have shown that NETs are present in the peripheral blood of patients with inflammatory diseases in the form of neutrophil web-like structures. However, in our research, in addition to traditional web-like NET structures, some anomalous forms were identified, including NETs with cloud-like appearance [3].

These cloud-like NETs can be formed under the effect of immunoglobulin G (IgG) [4]. Some reports also mention cloud-like NETs that were found in the blood of patients with inflammatory diseases and in some healthy persons [5, 6]. However, the causes underlying the formation of various forms of NETs are still unclear. The functional role of web-like and cloud-like NETs is also unclear.

The aim of the study was to investigate morphological and functional transformation of NETs under the influence of *Klebsiella pneumoniae* and IgG.

MATERIALS AND METHODS

The study included 42 patients treated at Moscow City Clinical Hospital No. 51: 28 patients who underwent surgery for acute inflammatory processes in the abdominal cavity (acute appendicitis, acute cholecystitis, acute pancreatitis / necrotizing pancreatitis, peritonitis), 6 patients with ulcerative colitis undergoing non-surgical treatment, and 8 patients with umbilical and inguinal hernias (5 patients did not undergo surgery, while 3 patients underwent surgery).

The study of blood samples was carried out in the laboratory at the Department of Pathological Physiology and Clinical Pathological Physiology of the Institute of Human Biology and Pathology (Pirogov Russian National Research Medical University). All procedures were performed in accordance with the ethical principles of the WMA Declaration of Helsinki. Patients signed an informed consent to participate in the study. The study was approved by the Ethics Committee at Pirogov Russian National Research Medical University (Protocol No. 203 of 21.12.2021).

Determining the composition of NETs

Obtaining neutrophil cell fractions. Vacutainer EDTA blood collection tubes were used for blood sampling. Neutrophils were isolated from venous blood treated with EDTA by the traditional method using gradient density centrifugation. The purity of the isolated neutrophil fraction was 98–100%. Neutrophils were washed twice from Ficoll impurities with a sodium phosphate buffer solution (50 mM, pH 7.4). Blood cells were precipitated by centrifugation (600 g, 15 min). Isolated neutrophils were resuspended in the RPMI-1640 medium and used in short-term culture experiments. The viability of isolated neutrophils was at least 95% (test with 0.1% trypan blue solution).

Immunofluorescence detection of NETs. We developed a method using fluorescence microscopy, the main stages of which were described earlier, and used it to register NETs [7]. NETs were detected using a fluorescent SYBR Green-I dye (Evrogen; Russia), which specifically interacts with double-stranded DNA. Microscopy, counting, and photo registration of cells and extracellular structures were performed at x 1,000 magnification. The results were expressed as a percentage, the ratio of the number of extracellular traps to the total number of cells in the field of view.

Culture of neutrophils with IgG. Human IgG preparation (Sorbent, Russia) was added to the sterile isolated cells and incubated with the cells in an atmosphere of 5% CO_2 at 37 °C for 1 hour. A 100 µl sample prepared in the RPMI-1640 medium contained neutrophils and IgG preparation (5 µg / ml). The final concentration of cells in the culture medium was 2×10^5 / ml.

Capturing a test microorganism. The functional activity of web-like NETs was determined using the *Klebsiella pneumoniae* capture test (ATCC 700603). To do this, a microbial culture of *Klebsiella pneumoniae* in the RPMI-1640 medium at a concentration of 10^3 / µl was added to neutrophils immobilized on poly-L-lysine coated glass slides. Web-like NETs capture the test microorganism in accordance with their potential functional activity. After staining (SYBR Green-I, 15 min) and washing off the excess dye, the morphological structure of NETs and the number of *Klebsiella pneumoniae* cells associated with each extracellular structure were determined by microscopy.

Statistical processing

The results obtained were processed using the Statistica 12.0 (StatSoft Inc., USA). NET parameters obtained in the study of blood samples obtained from

patients were processed using nonparametric statistics and presented as the median and the interquartile range *Me* [Q_{25}–Q_{75}]. Quantitative variables were compared using the Mann – Whitney *U* test and the Kruskal – Wallis analysis of variance. The results of experiments on short-term neutrophil culture, characterized by normal data distribution, were presented as the mean and the standard error of the mean ($M \pm m$). Quantitative variables were compared using the Student's *t*-test. The differences were considered statistically significant at $p < 0.05$.

RESULTS

Morphological characteristics of NETs in patients with inflammatory diseases of the abdominal cavity. Web-like NETs were present in the peripheral blood in all patients with inflammatory diseases of the abdominal cavity in the postoperative period. The number of neutrophil web-like structures was registered in the range from 14.2 % [7.7–17.9%] in acute appendicitis to 17.6% [10.3–26.6%] in the development of peritonitis. Uncomplicated abdominal inflammation in the postoperative period was characterized by a similar number of NETs in the peripheral blood. Thus, in local acute inflammation, the relative count of NETs corresponded to the range of *Me* 14.2–15.1%. Diffuse peritonitis was accompanied by an increase in the number of NETs up to the level of *Me* 17.6% (Fig.1). Thus, when inflammation spread to other organs and serous membranes of the abdominal cavity (in the case of peritonitis), the number of web-like NETs increased ($p = 0.668$).

Determination of the size of NETs in microns showed a statistically significant ($p = 0.0189$) increase in the size of NETs in patients with acute cholecystitis and pancreatitis. The size of NETs increased up to 53.65 [43.9–88.45] microns in acute cholecystitis and up to 91.9 [62.0–120.0] microns in acute pancreatitis compared to the group of patients with acute appendicitis, where it was 44.65 [35.6–57.6] microns (Fig. 2). In addition to web-like NETs, neutrophilic structures in the form of single strands, fibers, and clouds were found in patients. The increase in the size of NETs in patients with cholecystitis and pancreatitis was associated with the presence of these unusual extracellular structures in the blood that previously were not thoroughly described and studied. The smallest size of NETs was found in patients with ulcerative colitis (comparison group) who received non-surgical treatment (32.2 (6.3–57.4) microns).

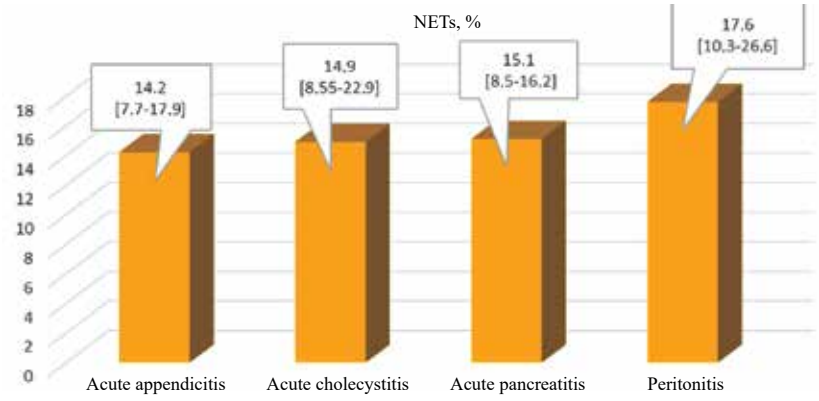

Fig. 1. The number of NETs in inflammatory diseases of the abdominal cavity (postoperative period), *Me* [Q_{25}–Q_{75}], %

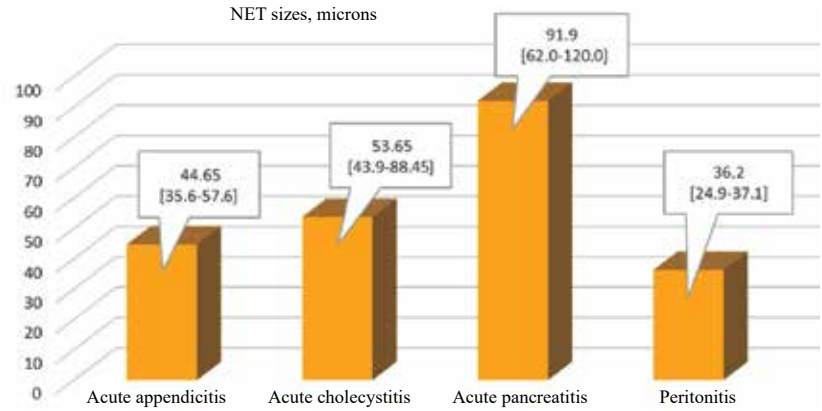

Fig. 2. Sizes of NETs in various inflammatory diseases of the abdominal cavity, *Me* [Q_{25}–Q_{75}], microns

The study of the morphological characteristics of NETs in patients with inflammatory diseases (Fig. 3, 4) raised a number of important questions related to understanding the process of functional transformation of neutrophil extracellular structures. Solving the issues of morphological and functional transformation of web-like NETs might be the key to understanding the role of various forms of NETs in the defense against infections and will allow to draw conclusions regarding their functional activity.

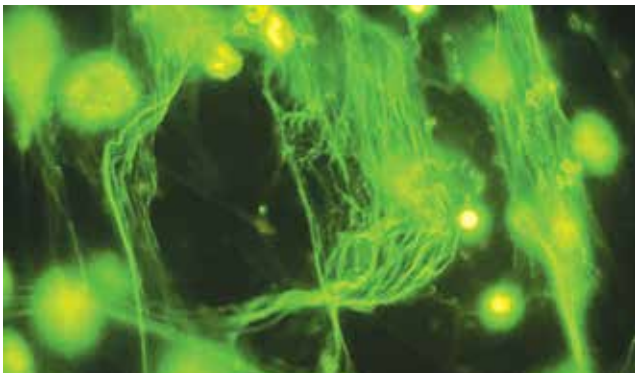

Fig. 3. Web-like NETs. Large structures. Uncomplicated appendicitis after surgery. An example of an uncomplicated inflammatory process with a favorable course. Here and in Fig. 4, 5, 7, incubation time is 1 h. Staining with CYBR Green I. x1,000

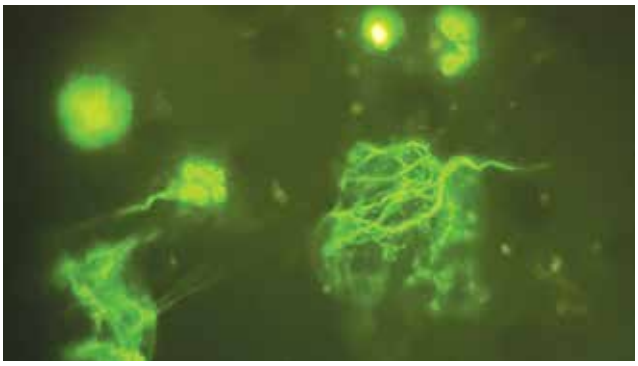

Fig. 4. Web-like NETs. Ulcerative colitis (non-surgical treatment). Small structures

Functional characteristics of NETs in healthy persons and patients with inflammatory diseases of the abdominal cavity. To study the role of NETs in the immune defense of the body and their functional activity, we developed a methodological approach in which NETs obtained from patients interacted *in vitro* with cells of the test microorganism *Klebsiella pneumoniae* (ATCC 700603). During the interaction of neutrophils with pathogen cells, the protective potential of innate immunity cells was realized.

Healthy donors. Neutrophils obtained from healthy donors have high functional activity [3]. Contact interactions with *Klebsiella pneumoniae* cells cause the formation of web-like NETs, as well as capture and binding of a large number of cells of the test microorganism (Fig. 5). During this process, web-like NET fibers are retracted and transformed into a cloud-like structure. The range of binding pathogen cells by NETs obtained from healthy donors is 70–90 cells per cloud. Each NET under our experimental conditions captured and retained an average of 78.05 ± 10.58 *Klebsiella pneumoniae* cells. Moreover, almost all cells of the test microorganism were localized inside NETs.

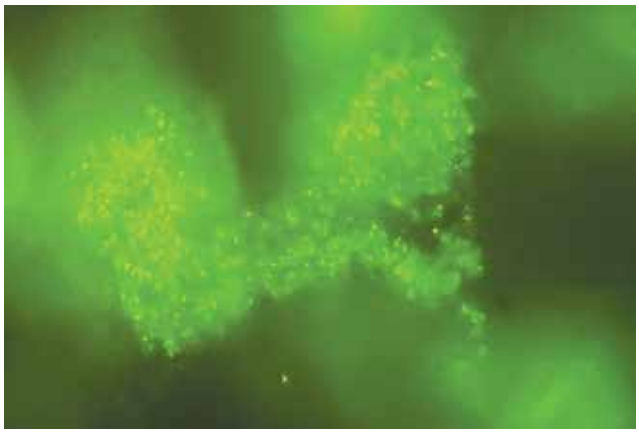

Fig. 5. Web-like NETs of healthy donors capture and bind a large number of *Klebsiella pneumoniae* (ATCC 700603) cells and acquire a cloud-like appearance

Patients with inflammatory diseases of the abdominal cavity. In patients with inflammatory diseases of the abdominal cavity (appendicitis, cholecystitis, pancreatitis) in the postoperative period, the functional activity of NETs is much more weakened compared to healthy donors. NETs in these patients capture and bind on average no more than 20 cells of the test microorganism. Some of the cells of the test microorganism remain unbound by NETs, which may contribute to the development of a postoperative infectious complication in these patients [8].

Dynamics of changes in the functional activity of web-like NETs. The dynamics of changes in the functional activity of NETs (pathogen capture and binding) in patients during web-like NET formation was studied in a group of patients with umbilical and inguinal hernias. In patients with non-strangulated

hernias who did not undergo surgery, the number of pathogen cells captured *in vitro* by a single NET varied from 4.62 ± 0.36 to 26.56 ± 3.45 after 1 and 2 hours of culture, respectively, which means it increased during culture by 5.8 times.

In patients who underwent surgery for strangulated hernias, pathogen capture reached 38.17 ± 3.74 *Klebsiella pneumoniae* cells per NET after 1 hour of culture and 25.85 ± 3.20 pathogen cells per one NET after 2 hours of culture. The sharp increase in the capture and binding of the pathogen by NETs in operated patients after 1 hour of culture may be explained by the involvement of *in vivo* pre-activated neutrophils in *in vitro* interaction between neutrophils in the operated patients and pathogen cells.

The subsequent decrease in the functional activity of NETs in operated patients during the second hour of culture may be due to the fact that part of the initially formed web-like NETs together with pathogen cells after 1 hour of culture turn into cloud-like structures that are absorbed by neutrophils capable of developing phagocytic activity.

A decrease in the number of NETs after their formation was investigated *in vivo* and *in vitro* and described in detail in the works of other researchers [9]. The conducted studies revealed the dependence of the elimination of formed NETs on both the phagocytic activity of neutrophils and macrophages [10, 11] and the enzymatic activity of pancreatic DNase I [12, 13]. Proinflammatory cytokines have been shown to stimulate phagocytosis and accelerate the destruction of NETs by macrophages and dendritic cells [14]. In patients with severe bacterial infections, vascular occlusions were caused by impaired elimination of NETs *ex vivo*, which was accompanied by the formation of intravascular blood clots containing NETs [15].

Functional characteristics of NETs in patients with inflammatory diseases of the abdominal cavity under the influence of IgG. Web-like NETs are very sensitive to IgG. Under the influence of IgG they turn into loose cloud-like structures (Fig. 6), while their size increases [4], and the ability to capture and bind the pathogen sharply deteriorates (Fig. 8).

In addition to the fact that cloud-like NETs formed under the IgG influence have a very weak ability to capture and bind the pathogen, they also bind cells of the test microorganism only on the periphery of the cloud-like structure (Fig. 7). This type of binding, apparently, makes it possible for the pathogen to avoid the influence of damaging factors produced in activated neutrophils.

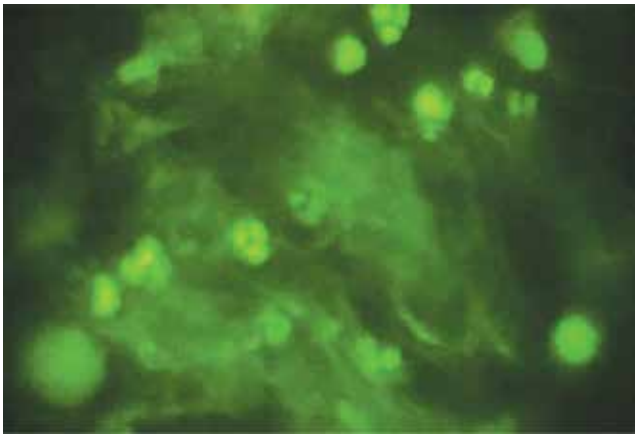

Fig. 6. Cloud-like NETs. Cloud-like forms of NETs were obtained from web-like neutrophil structures during their incubation with IgG (5 mcg / ml). Incubation time was 30 min. Coloring with CYBR Green-I. x1,000

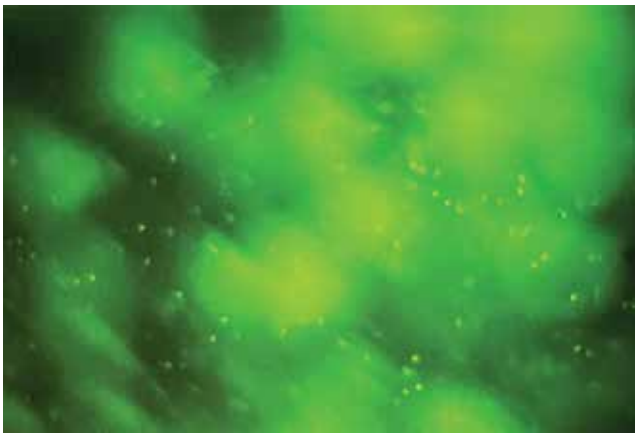

Fig. 7. Attenuation of pathogen capture and binding (*Klebsiella pneumoniae*) by cloud-like NETs. Peripheral binding of the pathogen by cloud-like NETs

It should be noted that similar cloud-like extracellular structures were also found in some patients. They also had a low binding capacity in relation to *Klebsiella pneumoniae* and also bound them only on the periphery of the cloud-like structure.

The results of the study of the functional activity of cloud-like NETs in comparison with web-like structures are shown in Table.

Table

Effect of IgG on neutrophil trapping of *Klebsiella pneumoniae* in patients with acute inflammatory processes in the abdominal cavity

Morphological structure of NETs and incubation conditions	Number of microorganisms captured by neutrophil traps, $M \pm m$
Neutrophil web-like structures without IgG influence	20. ± 1.67

End of table

Morphological structure of NETs and incubation conditions	Number of microorganisms captured by neutrophil traps, $M \pm m$
Cloud-like structures formed under IgG influence	8.46 ± 0.44*

* $p < 0.001$ compared to parameters without IgG influence.

In addition to the weakening of functional activity, cloud-like NETs are more susceptible to spontaneous enzymatic degradation of DNA fibers that form the basis of this morphological structure of NETs in comparison with web-like NETs, which carries an obvious risk of developing subsequent long-term complications in these patients. As a result of DNA fiber degradation in the extracellular space, the content of extracellular purine bases, which are factors of secondary alteration, can significantly increase. This effect was previously found and described in patients with post-COVID syndrome. NETs in the form of single DNA strands of considerable size were found in patients with post-COVID syndrome. Spontaneous enzymatic degradation of these strands causes an increase in the concentration of extracellular purine nitrogenous bases and is an additional factor in tissue damage and inhibition of T lymphocyte activity.

RESULTS AND DISCUSSION

The results of the study of NETs in patients with acute inflammation in the abdominal cavity revealed the dependence of the quantitative parameters of NETs (their number and size) on the type of inflammation, the size and degree of delimitation of the inflammatory lesion.

A comprehensive analysis of NETs, including not only the quantitative determination of NET parameters, but also the assessment of the morphological and functional transformation of neutrophil structures, will allow to fully identify the pathophysiological patterns of the inflammatory process, will become the key to understanding the role of certain NET forms in the fight against infections, and will allow to determine the functional activity of neutrophil extracellular structures.

The functional activity of NETs, understood as pathogen capture and binding, in healthy donors and in patients with acute infectious inflammation in the abdominal cavity has some similarities, but there are also differences.

In both healthy donors and patients, the interactions of the pathogen and neutrophils cause the formation of web-like NETs, and then the formed web-like structures capture and bind the pathogen. During this process, the DNA fibers are shortened (retracted), the size of this neutrophil structure becomes more compact, and the web-like NET is transformed into a cloud-like one. The pathogen cells are localized in the central part of this cloud-like structure.

The differences relate to the number of pathogen cells captured by cloud-like NETs. Cloud-like neutrophil structures originating from web-like ones in healthy donors capture and bind a significant number of cells of the test pathogen, several times more than similar cloud-like structures in patients. Some pathogen cells remain unbound in the study of the functional activity of NETs in patients with inflammatory diseases.

A morphological and functional restructuring of the NETs is observed under the influence of IgG. The results of the study demonstrate changes in the structure of NETs under the influence of IgG. Neutrophil web-like structures turn into loose cloud-like ones that have a weakened ability to bind the pathogen, which means they acquire low functional activity. A feature of the functional activity of IgG-induced NETs is peripheral binding of the pathogen.

The study demonstrates two types of cloud-like structures: functionally active clouds, which are formed from neutrophil web-like structures after pathogen capture, and ineffective clouds, which are formed from neutrophil web-like structures under the influence of IgG. In our opinion, these ineffective cloud-like structures pose a certain danger to the human body due to the possible generation of secondary alteration factors in the form of extracellular purine bases. The content of these extracellular purine nitrogenous bases can significantly increase as a result of spontaneous enzymatic hydrolysis of DNA in neutrophil cloud-like structures and induce a decrease in immune resistance as a result of inhibition of the activity of T cells in the immunity.

In addition, extracellular purine nitrogenous bases can cause damage to the structures of the nervous system and cells of internal organs. Their long-term effect on the body can cause long-term adverse effects.

CONCLUSION

From a practical perspective, the study and its results create prerequisites for new approaches to the development of vaccination regimens and the use of immunobiologic drugs, in particular, monoclonal antibody drugs, especially considering the fact that at present new medical technologies are sought to improve the effectiveness of patient treatment.

The lack of knowledge about the mechanisms of interaction between innate immunity and adaptive immune responses in the human body can significantly limit the use of vaccines and monoclonal antibody preparations. It also contributes to certain distrust of this type of therapy in patients [16]. Cases of thrombosis in combination with thrombocytopenia after vaccination [17] and progressive multifocal leukoencephalopathy caused by polyomavirus during treatment with monoclonal antibodies [18] have been described.

As the indications for the use of monoclonal antibody drugs expand, there are reports of complications and even deaths after the use of these drugs [19, 20] due to the development of multiple organ dysfunction syndrome. The causes of adverse effects after monoclonal antibody therapy are still insufficiently studied, but it can be assumed with a high degree of probability that the formation of ineffective neutrophil cloud-like structures can become a mechanism for inducing hemocoagulation and producing secondary alteration factors. Therefore, it is important to correlate the vaccination and treatment regimen with immunobiologic drugs with control of the state of innate immunity, in particular, with detection of spontaneous neutrophil web-like structures in the blood of patients.

REFERENCES

1. Chakraborty S., Tabrizi Z., Bhatt N.N., Franciosa S.A., Bracko O. A brief overview of neutrophils in neurological diseases. *Biomolecules*. 2023;13(5):743. DOI: 10.3390/biom13050743.
2. Kazimirskii A.N., Salmasi Zh.M., Poryadin G.V. Antiviral system of innate immunity: COVID-19 pathogenesis and treatment. *Bulletin of RSMU*. 2020;(5):5–14 (in Russ.). DOI: 10.24075/vrgmu.2020.054.
3. Kazimirskii A.N., Salmasi Zh.M., Poryadin G.V., Panina M.I., Rogozhina L.S., Stupin V.A., et al. Neutrophil extracellular traps in inflammatory diseases of the abdominal cavity. *Pathological Physiology and Experimental Therapy*. 2024;68(1):15–25 (in Russ). DOI: 10.25557/0031-2991.2024.01.15-25.
4. Kazimirskii A.N., Salmasi Zh.M., Poryadin G.V., Panina M.I., Larina V.N., Stupin V.A. et al. IgG activates neutrophil extracellular trap formation and modifies their structure. *Bulletin of Experimental Biology*. 2022;174(12):786–789 (in Russ.). DOI: 10.47056/0365-9615-2022-174-12-786-789.
5. Novikov D.G., Zolotov A.N., Kirichenko N.A., Mordyk A.V. A method for detecting neutrophilic extracellular traps in a supravitally stained blood sample. Patent RU 2768 152 C1, 2022.03.23. https://yandex.ru/patents/doc/RU2768152C1_20220323 (in Russ.).
6. Novikov D.G., Zolotov A.N., Bikbavova G.R., Livzan M.A., Telyatnikova L.I. Neutrophil extracellular traps in a patient with ulcerative colitis. *Russian Journal of Evidence-Based Gastroenterology*. 2022;11(2):31–38 (in Russ.). DOI: 10.17116/dokgastro20221102131.
7. Kazimirskii A.N., Salmasi Zh.M., Poryadin G.V., Panina M.I. New opportunities for diagnosis and investigation of the pathogenesis of various types of inflammation. *Pathological Physiology and Experimental Therapy*. 2022;66(2):34–42 (in Russ.). DOI: 10.25557/0031-2991.2022.02.34-42.
8. Kazimirskii A.N., Salmasi Zh.M., Poryadin G.V., Panina M.I., Stupin V.A., Kim A.E. et al. Neutrophil extracellular traps in the anti-infectious defense of human organism. *Bulletin of Siberian Medicine*. 2024;23(1):56–63 (in Russ.). DOI: 10.20538/1682-0363-2024-1-56-63.
9. Demkow U. Molecular mechanisms of neutrophil extracellular trap (NETs) degradation. *Int. J. Mol. Sci*. 2023;24(5):4896. DOI: 10.3390/ijms24054896.
10. Farrera C., Fadeel B. macrophage clearance of neutrophil extracellular traps is a silent process. *J. Immunol.* 2013;191:2647–2656. DOI: 10.4049/jimmunol.1300436.
11. Chen L., Zhao Y., Lai D., Zhang P., Yang Y., Li,Y. et al. Neutrophil extracellular traps promote macrophage pyroptosis in sepsis. *Cell Death Dis*. 2018;9(6):597. DOI: 10.1038/s41419-018-0538-5.
12. Zhou Y., Xu Z., Liu Z. Impact of neutrophil extracellular traps on thrombosis formation: new findings and future perspective. *Front. Cell. Infect. Microbiol.* 2022;12:910908. DOI: 10.3389/fcimb.2022.910908.
13. Lauková L., Konečná B., Janovičová Ľ., Vlková B., Celec P. Deoxyribonucleases and their applications in biomedicine. *Biomolecules* 2020;10:1036. DOI: 10.3390/biom10071036.
14. Nakazawa D., Shida H., Kusunoki Y., Miyoshi A., Nishio S., Tomaru U. et al. The responses of macrophages in interaction with neutrophils that undergo NETosis. *J. Autoimmun*. 2016;67:19–28. DOI: 10.1016/j.jaut.2015.08.018.
15. Szturmowicz M., Barańska I., Skoczylas A., Jędrych M.E., Demkow U. Correlation of bronchoalveolar lavage lymphocyte count with the extent of lung fibrosis and with plethysmographic lung volumes in patients with newly recognized hypersensitivity pneumonitis. *Cent. Eur. J. Immunol*. 2020;45(3):276–282. DOI: 10.5114/ceji.2020.101246.
16. Connors J., Cusimano G., Mege N., Woloszczuk K., Konopka E., Bell M. et al. Using the power of innate immunoprofiling to understand vaccine design, infection, and immunity. *Hum. Vaccin Immunother*. 2023;19(3):2267295. DOI: 10.1080/21645515.2023.2267295.
17. De Michele M., Kahan J., Berto I., Schiavo O.G., Iacobucci M., Toni D. et al. Cerebrovascular complications of COVID-19 and COVID-19 vaccination. *Circ. Res*. 2022;130(8):1187–1203. DOI: 10.1161/CIRCRESAHA.122.319954.
18. Sharma K., Tolaymat S., Yu H., Elkhooly M., Jaiswal S., Jena A. et al. Progressive multifocal leukoencephalopathy in anti-CD20 and other monoclonal antibody (mAb) therapies used in multiple sclerosis: A review. *J. Neurol. Sci.* 2022;443:120459. DOI: 10.1016/j.jns.2022.120459.
19. Faccini T., Dhesi Z., Shah S. Death by antibody. *BMJ Case Rep*. 2019;12(5):e225519. DOI: 10.1136/bcr-2018-225519.
20. Kirby C., Herlihy D., Clarke L., Mullan R. Sarcoidosis manifesting during treatment with secukinumab for psoriatic arthritis. *BMJ Case Rep*. 2021;14(2):e240615. DOI: 10.1136/bcr-2020-240615.

Authors' contribution

Kazimirskii A.N. – experimental research, preparation of illustrative material, drafting of the manuscript. Salmasi J.M. – editing of the article. Poryadin G.V. – conception and design. Panina M.I. – editing of the article, statistical processing of the data. Kim A.E. – experimental research. Rogozhina L.S. – collection and processing of the data.

Author's information

Kazimirskii Alexander N. – Dr. Sci. (Biology), Associate Professor, Leading Researcher, Department of Molecular Technologies, Research Institute of Translational Medicine, Professor of the Department of Pathophysiology and Clinical Pathophysiology, Institute of Biology and Human Pathology, Pirogov Russian National Research Medical University, Moscow, alnica10@mail.ru, https://orcid.org/0000-0002-3079-4089

Salmasi Jean M. – Dr. Sci. (Med.), Professor, Head of the Department of Pathophysiology and Clinical Pathophysiology, Institute of Biology and Human Pathology, Pirogov Russian National Research Medical University, Moscow, profjms@yandex.ru, https://orcid.org/0000-0001-8524-0019

Poryadin Gennady V. – Dr. Sci. (Med.), Professor of the Department of Pathophysiology and Clinical Pathophysiology, Corresponding Member of RAS, Institute of Biology and Human Pathology, Pirogov Russian National Research Medical University, Moscow, poryadin_GV@rsmu.ru, https://orcid.org/0000-0003-2010-3296

Panina Marina I. – Dr. Sci. (Med.), Professor, Professor of the Department of Pathophysiology and Clinical Pathophysiology, Institute of Biology and Human Pathology, Pirogov Russian National Research Medical University, Moscow, pan-mar@list.ru, https://orcid.org/0000-0002-7651-0037

Kim Anna E. – Teaching Assistant, Department of Pathophysiology and Clinical Pathophysiology, Institute of Biology and Human Pathology, Pirogov Russian National Research Medical University, Moscow, infoany@mail.ru, https://orcid.org/0000-0001-8119-772X

Rogozhina Lyudmila S. – Teaching Assistant, Department of Advanced-Level Surgery No. 1, Pirogov Russian National Research Medical University, Moscow, lusy-090909@yandex.ru, https://orcid.org/0000-0002-3983-7890

(✉) **Kazimirskii Alexander N.,** alnica10@mail.ru

Received 06.05.2024;
approved after peer review 23.05.2024;
accepted 13.06.2024

УДК 616.131-008.331.1-005.755-0221.6
https://doi.org/10.20538/1682-0363-2024-4-31-37

A model of chronic thromboembolic pulmonary hypertension with the use of microencapsulated fibrin particles

Karpov A.A.[1, 2], Shilenko L.A.[1], Vaulina D.D.[1], Sidorova E.E.[1], Akhmetova A.A.[1], Bunenkov N.S.[1], Vorotilov A.V.[1], Ivkin D.Yu.[2], Karpenko V.V.[1], Galagudza M.M.[1]

[1] *Almazov National Medical Research Center*
2, Akkuratova Str., Saint Petersburg, 197341, Russian Federation

[2] *Saint Petersburg State Chemical and Pharmaceutical University*
14a, Professora Popova Str., Saint Petersburg, 197022, Russian Federation

ABSTRACT

Aim. To develop a model of chronic thromboembolic pulmonary hypertension (CTEPH) in rats by embolization of the pulmonary vascular bed with microencapsulated fibrin (MF).

Materials and methods. Microencapsulated fibrin (MF) was prepared by encapsulating fibrin particles smaller than 71 μm in sodium alginate. Non-encapsulated fibrin with a particle size of 71–200 μm was used as an alternative embolic particle. Modeling was performed on male Wistar rats. The animals were divided into 4 groups. Intact (INT) animals ($n = 7$) were administered normal saline intravenously. In the NF8 group ($n = 14$), non-encapsulated fibrin was injected as embolic particles 8 times every 4 days. In the MF5 group ($n = 14$), 0.5 ml MF (9,047 ± 430 particles) was administered intravenously 5 times every 5 days. In the MF8 group ($n = 14$), MF was administered 8 times every 4 days. Six weeks after the last injection of embolic particles, cardiac catheterization with manometry and histologic examination of the lungs were performed.

Results. According to cardiac catheterization, right ventricular systolic pressure (RVSP) in the MF8 group was significantly higher compared to rats from the INT and NF8 groups ($p < 0.05$). The hypertrophy index and the percentage of collagen fibers in the structure of the vascular wall of the pulmonary artery branches were significantly higher in the MF5 and MF8 groups than in the INT and NF8 groups ($p < 0.01$). There were no significant differences between the MF5 and MF8 groups.

Conclusion. A representative CTEPH model in rats was developed, characterized by a stable increase in RVSP and pronounced structural changes in the branches of the pulmonary artery.

Keywords: chronic thromboembolic pulmonary hypertension, pulmonary embolism, experimental model, rats, microencapsulated fibrin, sodium alginate

Conflict of interest. The authors declare the absence of obvious or potential conflicts of interest related to the publication of this article.

Source of financing. The research was funded by the Russian Science Foundation grant No. 23-75-10122, https://rscf.ru/project/23-75-10122/

Conformity with the principles of ethics. The study was approved by the Bioethics Committee at Saint Petersburg State Chemical and Pharmaceutical University (Protocol Rats-02.2019-5 of 12.02.2019).

For citation: Karpov A.A., Shilenko L.A., Vaulina D.D., Sidorova E.E., Akhmetova A.A., Bunenkov N.S., Vorotilov A.V., Ivkin D.Yu., Karpenko V.V., Galagudza M.M. A model of chronic thromboembolic pulmonary hypertension with the use of microencapsulated fibrin particles. *Bulletin of Siberian Medicine.* 2024;23(4):31–37. https://doi.org/10.20538/1682-0363-2024-4-31-37.

✉ *Karpov Andrey A.,* karpov_aa@almazovcentre.ru

Экспериментальная модель хронической тромбоэмболической легочной гипертензии с применением микроинкапсулированных частиц фибрина

Карпов А.А.[1, 2], Шиленко Л.А.[1], Ваулина Д.Д.[1], Сидорова Е.Е.[1], Ахметова А.А.[1], Буненков Н.С.[1], Воротилов А.В.[1], Ивкин Д.Ю.[2], Карпенко В.В.[1], Галагудза М.М.[1]

[1] *Национальный медицинский исследовательский центр (НИМЦ) им. В.А. Алмазова Россия, 197341, г. Санкт-Петербург, ул. Аккуратова, 2*

[2] *Санкт-Петербургский государственный химико-фармацевтический университет (СПХФУ) Россия, 197022, г. Санкт-Петербург, ул. Профессора Попова, 14а*

РЕЗЮМЕ

Цель. Разработать экспериментальную модель хронической тромбоэмболической легочной гипертензии (ХТЭЛГ) у крыс с помощью эмболизации сосудистого русла легких микроинкапсулированным фибрином (МФ).

Материалы и методы. Микроинкапсулированный фибрин изготавливался путем заключения в альгинат натрия частиц фибрина размером меньше 71 мкм. В качестве альтернативных эмболизирующих частиц использовался неинкапсулированный фибрин с размером частиц 71–200 мкм. Экспериментальное моделирование проведено на самцах крыс линии Вистар. Животные были разделены на четыре группы. Контроль (КОН) (n = 7) – внутривенно вводился физиологический раствор. НФ8 (n = 14) – в качестве эмболизирующих частиц вводился неинкапсулированный фибрин 8 раз с интервалами в 4 дня. МФ5 (n = 14) – МФ в объеме 0,5 мл (9 047 ± 430 частиц) вводился внутривенно 5 раз с интервалами в 5 дней. МФ8 (n = 14) – МФ вводился 8 раз с интервалами в 4 дня. Через 6 нед после последнего введения эмболизирующих частиц выполнялись катетеризация сердца с манометрией и гистологическое исследование легких.

Результаты. По данным катетеризации сердца, систолическое давление в правом желудочке (СДПЖ) в группе МФ8 было значимо выше по сравнению с крысами из группы КОН и НФ8 (p < 0,05). Индекс гипертрофии и процент коллагеновых волокон в структуре сосудистой стенки ветвей легочной артерии были значимо выше в группах МФ5 и МФ8, чем в группах КОН и НФ8 (p < 0,01). Значимых различий между группами МФ5 и МФ8 выявлено не было.

Заключение. Разработана репрезентативная модель ХТЭЛГ на крысах, характеризующаяся стабильным повышением СДПЖ и выраженными структурными изменениями ветвей легочной артерии.

Ключевые слова: хроническая тромбоэмболическая легочная гипертензия, тромбоэмболия легочной артерии, экспериментальная модель, крысы, микроинкапсулированный фибрин, альгинат натрия

Конфликт интересов. Авторы декларируют отсутствие явных и потенциальных конфликтов интересов, связанных с публикацией настоящей статьи.

Источник финансирования. Исследование выполнено за счет гранта Российского научного фонда № 23-75-10122, https://rscf.ru/project/23-75-10122/

Соответствие принципам этики. Исследование одобрено биоэтической комиссией СПХФУ (протокол Rats-02.2019-5 от 12.02.2019).

Для цитирования: Карпов А.А., Шиленко Л.А., Ваулина Д.Д., Сидорова Е.Е., Ахметова А.А., Буненков Н.С., Воротилов А.В., Ивкин Д.Ю., Карпенко В.В., Галагудза М.М. Экспериментальная модель хронической тромбоэмболической легочной гипертензии с применением микроинкапсулированных частиц фибрина. *Бюллетень сибирской медицины.* 2024;23(4):31–37. https://doi.org/10.20538/1682-0363-2024-4-31-37.

INTRODUCTION

Chronic thromboembolic pulmonary hypertension (CTEPH) is a complication of pulmonary embolism (PE) [1]. This form of pulmonary hypertension is characterized by impaired thromboembolic lysis, microvascular damage, and, as a consequence, a stable increase in pulmonary artery pressure and pulmonary vascular resistance [2].

The above changes lead to right ventricular (RV) hypertrophy, which ultimately leads to RV dilatation and failure. Ten-year survival of patients with CTEPH

who do not receive specific therapy with an average pulmonary artery pressure of more than 50 mm Hg is 5%, while in patients who underwent PE without a significant increase in pulmonary artery pressure, the survival rate exceeds 50% [3]. Despite the active development of surgical and medical approaches to the treatment of CTEPH, the effect of the therapy remains insufficient [1]. At the same time, preclinical trials on new therapeutic approaches are challenging due to the lack of an experimental model that can sufficiently reflect the pathophysiological and structural changes in the vascular bed of the lungs in CTEPH.

Currently, there are two main approaches to modeling CTEPH: the use of natural thromboemboli and artificial embolic particles [4]. The use of natural thromboemboli is usually combined with the use of fibrinolysis inhibitors, such as tranexamic acid [5–8]. However, this modeling approach is labor intensive due to the need for *in vitro* production of autologous thromboemboli for each animal [9]. In addition, even with the use of tranexamic acid, an increase in the pulmonary artery pressure is unstable due to the pronounced fibrinolytic activity of blood plasma in rats [7]. On the other hand, the use of artificial particles, primarily polystyrene microspheres, in previously published works was characterized by a stable increase in the pulmonary artery pressure [10–13], which did not lead to complete reproduction of CTEPH pathogenesis, since polystyrene microspheres and similar particles were uncapable of degrading and did not contain biologically active thrombus molecules, such as fibrin degradation products (FDP) and fibrin itself.

In our previous study, we modeled CTEPH using partially biodegradable microspheres based on sodium alginate, which did not contain additional inclusions [14]. The study demonstrated a persistent increase in the pulmonary artery pressure, a decrease in exercise tolerance, and the appearance of histologic changes in the vascular bed characteristics of CTEPH. However, this model did not take into account the important role of FDPs, which have significant biological functions, including anticoagulation and proinflammatory ones [15]. Taking these data into account, it is advisable to develop a model that combines the advantages of natural thromboemboli, such as the biological effects of fibrin itself and the release of FDP, and artificial particles that have the required size and a given rate of biodegradation.

The aim of this study was to develop an experimental model of CTEPH in rats using embolization of the pulmonary vascular bed with microencapsulated fibrin.

MATERIALS AND METHODS

We used 62 male Wistar rats in this study. The average weight was 230 ± 27 g. All animals were kept in standardized conditions and had free access to complete granulated pet food and water in agreement with the requirements according to the GOST (Russian National Standard) 33216-2014.

Production of embolic particles. At the first stage, fibrin powder from human blood plasma (Sigma-Aldrich, USA) was mechanically degraded, sifted through a sieve with a mesh size of 71 μm, and mixed with a solution of ultrapure sodium alginate (Sigma-Aldrich, USA) in a ratio of 1:7. The resulting suspension was homogenized using a submersible laboratory ultrasonic disperser with a stand (SpetsmashSonic, Russia). To obtain microencapsulated fibrin (MF), the suspension was supplied to the input of the Encapsulator B-390 system (BUCHI, Switzerland), and a 2% barium chloride solution was used as a stabilizing agent. Fibrin powder was mechanically ground, and then 71–200 μm particle fractions were separated using laboratory sieves to obtain non-encapsulated fibrin. All procedures were carried out under sterile conditions.

To model CTEPH, all animals were randomly divided into 4 groups. Intact (INT) animals (n = 8) were injected 1.5 ml of normal saline in the caudal vein 8 times every 4 days. In the NF8 group (n = 14), non-encapsulated fibrin was injected as embolic particles in a volume equivalent to that in the MF5 and MF8 groups, suspended in 1.5 ml of normal saline, 8 times every 4 days. In the MF5 group (n = 14), 0.5 ml MF (9,047 ± 430 particles) was administered in the caudal vein 5 times every 5 days. Before the injection, barium chloride solution was completely removed, and MF was suspended in 1.5 ml of normal saline. In the MF8 group (n = 14), the same volume of MF was injected in the caudal vein 8 times every 4 days. Six weeks after the last injection of embolic particles, right ventricular systolic pressure (RVSP) was measured, and a histologic examination of the lungs was performed to determine the percentage of collagen fibers in the structure of the vascular wall of the branches of the pulmonary artery and the hypertrophy index.

Study of in vivo biodegradation of embolic particles. In a separate experimental series, CTEPH was modeled in rats using the NF8 (n = 6) and MF8 (n = 6) protocols to determine the rate of embolic particle biodegradation at different time intervals.

To assess the dynamics of biodegradation of embolic particles on day 1, 2, 4, and 6 weeks after the final administration, the animals were euthanized using an isoflurane overdose. A histologic examination of the lower lobe of the right lung was performed. At each time point, embolic particles were counted in the lumen of the pulmonary artery branches along the entire cross-section of the distal third of the lung lobe using the Eclipse Ni-U light microscope (Nikon, Japan) and Nis Elements Br4 software (Nikon, Japan).

Invasive hemodynamic monitoring. The rats were anesthetized using isoflurane inhalation via the SomnoSuite Low-Flow Anesthesia System (Kent Scientific, Torrington, CT, USA). The animals were placed on a heating pad combined with the TCAT-2LV Animal Temperature Controller (Physitemp Instruments Inc., USA). Mechanical ventilation was performed using the SAR-830/AP device (CWE Inc., USA). A puncture of the heart apex was performed to measure RVSP. Pressure was recorded using the Mindray ePM 10 monitor (Mindray, China).

Histologic examination. The animals were euthanized using an isoflurane overdose. For the histologic examination, the lower lobe of the right lung was divided into 4 equal transverse levels. Micropreparations were stained according to the Picro Mallory staining method (BioVitrum, Russia) to identify collagen fibers. Quantitative analysis was carried out in two distal sections of the lung using the Eclipse Ni-U microscope (Nikon, Japan) at ×10 to ×40, as well as Nis Elements Br4 (Nikon, Japan) and ImageJ (Wayne Rasband, USA) software. For all found vessels belonging to the branches of the pulmonary artery, the following parameters were determined: the percentage of collagen fibers in the structure of the vascular wall [16], as well as the hypertrophy index, calculated as the ratio of the area of the vascular wall to the area of the entire vessel expressed as a percentage [17].

Data analysis was performed using the R 4.2.2 software. The Newman – Keuls test was used to assess the statistically significant difference between the groups. Results were presented as the median and the interquartile range Me [Q_1; Q_3]. The differences were considered significant at $p < 0.05$.

RESULTS

Characteristics of embolic particles. The size of MF particles was 205 ± 38 μm (Fig. 1, *a*), particles of non-encapsulated fibrin were 155 ± 60 μm in diameter after suspension in normal saline and ultrasonic treatment.

The study of embolic particle biodegradation revealed a consistent decrease in the number of detected MF particles. By the time CTEPH simulation was completed, the number of these particles was 6% of the baseline. When assessing the biodegradation of non-encapsulated fibrin after 2 weeks, only 2% of particles were detected, and no embolic particles were detected further on (Fig. 1, *b*).

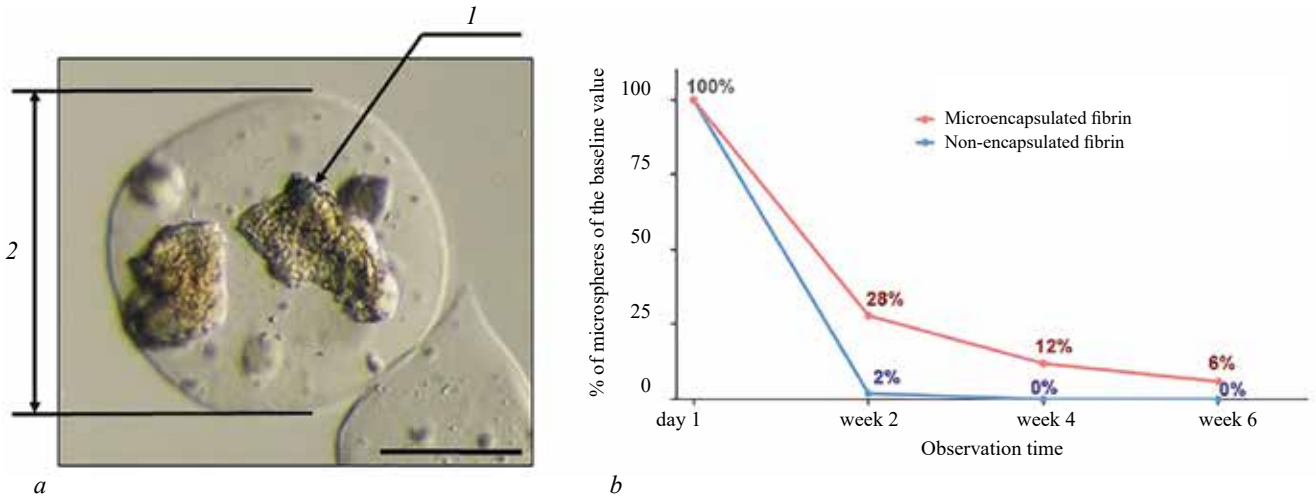

Fig. 1. Embolic particles: *a* – representative fibrin micrograph (bar = 100 μm), *1* – fibrin particles, *2* – microcapsule with fibrin; *b* – embolic particle biodegradation in the vascular bed

During embolic particle administration, mortality in the main series of experiments was 4 animals in the NF8 group, and 2 and 4 animals in the MF5 and MF8 groups, respectively. The cause of death was the development of acute right heart failure or paradoxical embolism with stroke.

According to cardiac catheterization data, RVSP in the MF8 group was significantly higher than in the INT and NF8 groups ($p < 0.05$). There were no significant differences in the RVSP levels between the INT, NF8, and MF5 groups (Fig. 2).

According to the results of the histologic examination, the hypertrophy index and the percentage of collagen fibers in the vascular wall structure in the MF5 and MF8 groups were significantly higher than in the INT and NF8 groups ($p < 0.01$). There were no significant differences between the MF5 and MF8 groups (Fig.3).

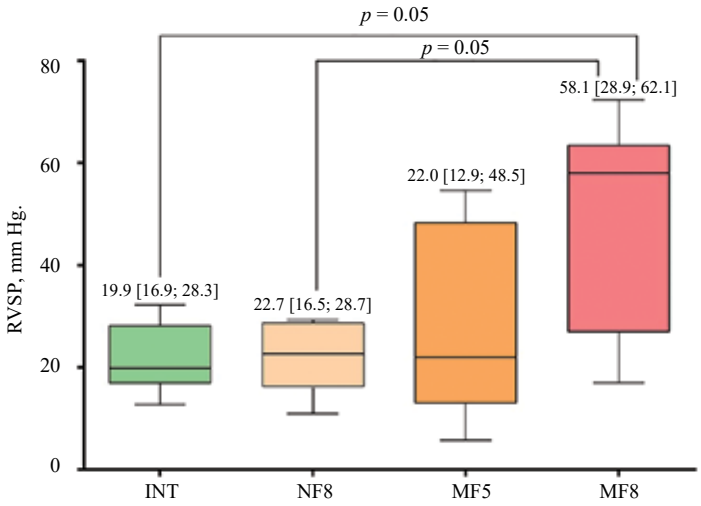

Fig. 2. Right ventricular systolic pressure 6 weeks after the last embolic particle administration according to cardiac catheterization data

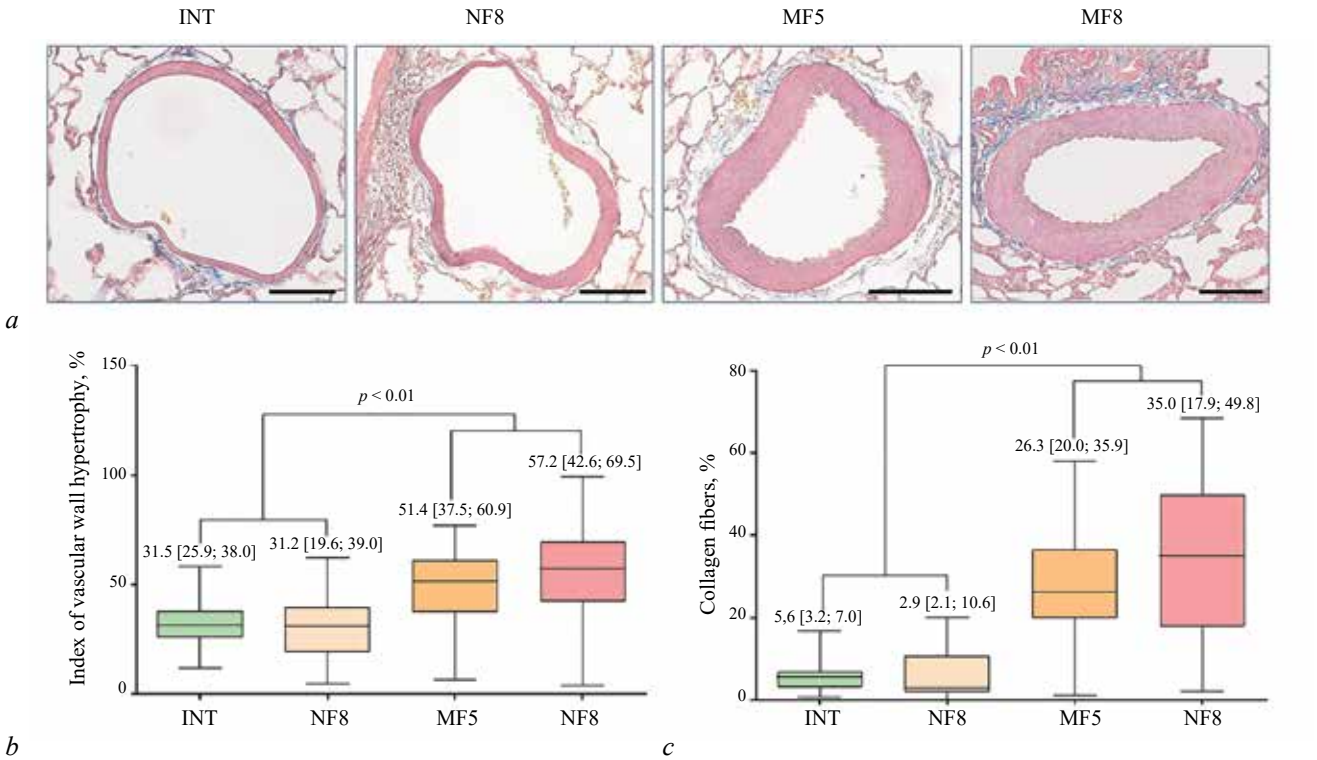

Fig. 3. Results of the histologic examination of pulmonary artery branches: *a* – representative micrograph (bar = 100 μm); *b* – index of vascular wall hypertrophy; *c* – collagen fibers in vascular wall structure, %

DISCUSSION

As a result of the study, a new experimental CTEPH model was developed, characterized by a stable increase in RV pressure and significant remodeling of the pulmonary circulation vessels. This was achieved by repeated intravenous administration of MF, which, as shown in [18, 19], is capable of stimulating the migration of leukocytes directly, being a chemoattractant, and through enhancing the secretion of cytokines by leukocytes and endothelial cells. The use of this type of embolic particles made it possible to combine the advantages of both natural thromboemboli – partial biodegradation and release of biologically active substances (fibrin and FDP), and artificial ones – a controlled rate of particle biodegradation and convenient dosing. In addition, in contrast to autologous thrombi, the use of fibrin has significantly reduced efforts to produce thromboemboli.

When modeling CTEPH in this study, the MF8 group was characterized by a persistent increase in RVSP. In the MF5 group, the dose of embolic particles administered was insufficient to reproduce stable pulmonary hypertension. According to epy histologic examination, a significant increase in the index of vascular wall hypertrophy and the percentage of fibrosis in its structure was noted in both groups where MF was used and did not differ significantly between them. The use of non-encapsulated fibrin did not lead to significant changes in either the RVSP level or the remodeling of the pulmonary artery branches.

Similar results were achieved in our previous study, where microencapsulated autologous thrombi were used as embolic particles [9]. However, this model was characterized by significant efforts, which made its practical application difficult. In addition, in contrast to previously published articles on artificial particles based on polystyrene [10–13], the developed embolic particles were capable of partial and controlled biodegradation and release of biologically active substances. These properties contributed to greater pathophysiological accuracy of the presented model.

CONCLUSION

The developed model could be used both to study the CTEPH pathogenesis and to test new therapeutic approaches to the treatment of this disease. In the future, it is planned to conduct a comparative study of empty alginate microspheres with microencapsulated fibrin to most clearly demonstrate the role of biologically active substances released during the biodegradation of thromboemboli during the CTEPH development.

REFERENCES

1. Konstantinides S.V., Meyer G., Becattini C., Bueno H., Geersing G.J., Harjola V.P. et al. 2019 ESC guidelines for the diagnosis and management of acute pulmonary embolism developed in collaboration with the European Respiratory Society (ERS). *Eur. Heart J.* 2020;41(4):543–603. DOI: 10.1093/eurheartj/ehz405.
2. Simonneau G., Dorfmüller P., Guignabert C., Mercier O., Humbert M. Chronic thromboembolic pulmonary hypertension: the magic of pathophysiology. *Ann. Cardiothorac. Surg*. 2022;11(2):106–119. DOI: 10.21037/acs-2021-pte-10.
3. Riedel M., Stanek V., Widimsky J., Prerovsky I. Longterm follow-up of patients with pulmonary thromboembolism. Late prognosis and evolution of hemodynamic and respiratory data. *Chest*. 1982;81(2):151–158. DOI: 10.1378/chest.81.2.151.
4. Karpov A.A., Vaulina D.D., Smirnov S.S., Moiseeva O.M., Galagudza M.M. Rodent models of pulmonary embolism and chronic thromboembolic pulmonary hypertension. *Heliyon*. 2022;8(3):e09014. DOI: 10.1016/j.heliyon.2022.e09014.
5. Deng C., Wu D., Yang M., Chen Y., Wang C., Zhong Z. et al. Expression of tissue factor and forkhead box transcription factor O-1 in a rat model for chronic thromboembolic pulmonary hypertension. *J. Thromb. Thrombolysis*. 2016;42(4):520–528. DOI: 10.1007/s11239-016-1413-9.
6. Deng C., Zhong Z., Wu D., Chen Y., Lian N., Ding H. et al. Role of FoxO1 and apoptosis in pulmonary vascular remolding in a rat model of chronic thromboembolic pulmonary hypertension. *Sci. Rep*. 2017;7(1):2270. DOI: 10.1038/s41598-017-02007-5.
7. Runyon M.S., Gellar M.A., Sanapareddy N., Kline J.A., Watts J.A. Development and comparison of a minimally-invasive model of autologous clot pulmonary embolism in Sprague-Dawley and Copenhagen rats. *Thromb. J*. 2010;8:3. DOI: 10.1186/1477-9560-8-3.
8. Wu D., Chen Y., Wang W., Li H., Yang M., Ding H. et al. The role of inflammation in a rat model of chronic thromboembolic pulmonary hypertension induced by carrageenan. *Ann. Transl. Med*. 2020;8(7):492. DOI: 10.21037/atm.2020.02.86.
9. Karpov A.A., Mihailova A.M., Cherepanov D.E., Chefu S.G., Shilenko L.A., Vaulina D.D. et al. The use of microencapsulated autologous thrombi for modelling chronic thromboembolic pulmonary hypertension in rats. *Bull. Exp. Biol. Med*. 2023;175(5):616–619. DOI: 10.1007/s10517-023-05912-0.
10. Zagorski J., Neto-Neves E., Alves N.J., Fisher A.J., Kline J.A. Modulation of soluble guanylate cyclase ameliorates pulmonary hypertension in a rat model of chronic thromboembolic pulmonary hypertension by stimulating angiogenesis. *Physiol. Rep*. 2022;10(1):e15156. DOI: 10.14814/phy2.15156.
11. Toba M., Nagaoka T., Morio Y., Sato K., Uchida K., Homma N. et al. Involvement of Rho kinase in the pathogenesis of acute pulmonary embolism-induced polystyrene microspheres in rats. *Am. J. Physiol. Lung Cell Mol. Physiol*. 2010;298(3):L297–303. DOI: 10.1152/ajplung.90237.2008.

12. Watts J.A., Marchick M.R., Gellar M.A., Kline J.A. Up-regulation of arginase II contributes to pulmonary vascular endothelial cell dysfunction during experimental pulmonary embolism. *Pulm. Pharmacol. Ther*. 2011;24(4):407–413. DOI: 10.1016/j.pupt.2011.01.009.
13. Arias-Loza P.A., Jung P., Abeßer M., Umbenhauer S., Williams T., Frantz S. et al. Development and characterization of an inducible rat model of chronic thromboembolic pulmonary hypertension. *Hypertension*. 2016;67(5):1000–1005. DOI: 10.1161/HYPERTENSIONAHA.116.07247.
14. Karpov A.A., Anikin N.A., Mihailova A.M., Smirnov S.S., Vaulina D.D., Shilenko L.A. et al. Model of chronic thromboembolic pulmonary hypertension in rats caused by repeated intravenous administration of partially biodegradable sodium alginate microspheres. *Int. J. Mol. Sci*. 2021;22(3):1149. DOI: 10.3390/ijms22031149.
15. Jennewein C., Tran N., Paulus P., Ellinghaus P., Eble J.A., Zacharowski K. Novel aspects of fibrin(ogen) fragments during inflammation. *Mol. Med*. 2011;17(5-6):568–573. DOI: 10.2119/molmed.2010.00146.
16. Ippolito C., Colucci R., Segnani C., Errede M., Girolamo F., Virgintino D. et al. Fibrotic and vascular remodelling of colonic wall in patients with active ulcerative colitis. *J. Crohns Colitis*. 2016;10(10):1194–1204. DOI: 10.1093/ecco-jcc/jjw076.
17. Kitagawa M.G., Reynolds J.O., Wehrens X.H.T., Bryan R.M. Jr., Pandit L.M. Hemodynamic and pathologic characterization of the TASK-1-/- mouse does not demonstrate pulmonary hypertension. *Front. Med. (Lausanne)*. 2017;4:177. DOI: 10.3389/fmed.2017.00177.
18. Barnhart M.I., Riddle J.M., Bluhm G.B., Quintana C. Fibrin promotion and lysis in arthritic joints. *Ann. Rheum. Dis*. 1967;26(3):206–218. DOI: 10.1136/ard.26.3.206.
19. Colvin R.B., Johnson R.A., Mihm M.C. Jr., Dvorak H.F. Role of the clotting system in cell-mediated hypersensitivity. I. Fibrin deposition in delayed skin reactions in man. *J. Exp. Med*. 1973 138(3):686–698. DOI: 10.1084/jem.138.3.686.

Authors' contribution

Karpov A.A. – conception and design, analysis and interpretation of the data, critical revision of the manuscript for important intellectual content, drafting of the manuscript. Shilenko L.A. – conception and design, production of embolic particles, invasive hemodynamic monitoring, drafting of the manuscript. Vaulina D.D. – production of embolic particles, analysis and interpretation of the data, drafting of the manuscript. Sidorova E.E., Akhmetova A.A., Karpenko V.V. – intravenous administration of embolic particles, histologic examination, analysis and interpretation of the data. Bunenkov N.S. – analysis and interpretation of the data, drafting of the manuscript. Vorotilov A.V. – production of embolic particles, invasive hemodynamic monitoring. Ivkin D.Yu. – critical revision of the manuscript for important intellectual content, drafting of the manuscript. Galagudza M.M. – project leader; conception and design, critical revision of the manuscript for important intellectual content, final approval of the manuscript for publication.

Authors' information

Karpov Andrey A. – Cand. Sci. (Med.), Head of the Research Department of Pulmonary Circulation Disorders, Almazov NRMC; Senior Researcher, Center for Experimental Pharmacology, Saint Petersburg State Chemical and Pharmaceutical University, Saint Petersburg, karpov_aa@almazovcentre.ru, https://orcid.org/0000-0003-0114-5896

Shilenko Leonid A. – 1st-year Resident, Department of Intermediate-Level Therapy with Clinic, Laboratory Assistant, Research Department of Pulmonary Circulation Disorders, Almazov NRMC, Saint Petersburg, Shilenko.leo@yandex.ru, https://orcid.org/0000-0002-1002-9419

Vaulina Daria D. – Junior Researcher, Research Department of Pulmonary Circulation Disorders, Almazov NRMC, Saint Petersburg, uplavice@gmail.com, https://orcid.org/0000-0003-1088-2396

Sidorova Elizaveta E. – Student, Almazov NRMC, Saint Petersburg, sidorova.elev@gmail.com, https://orcid.org/0009-0001-6878-3764

Akhmetova Anna A. – Student, Almazov NRMC, Saint Petersburg, ahmetova.anna.askarovna@gmail.com, https://orcid.org/0009-0006-0317-7241

Bunenkov Nikolay S. – Cand. Sci. (Med.), Laboratory Assistant, Research Department of Pulmonary Circulation Disorders, Almazov NRMC, Saint Petersburg, bunenkov_ns@almazovcentre.ru, https://orcid.org/0000-0003-4331-028X

Vorotilov Alexander V. – Laboratory Assistant, Research Department of Pulmonary Circulation Disorders, Almazov NRMC, Saint Petersburg, allegoriarus@gmail.com, https://orcid.org/0000-0002-2772-6579

Ivkin Dmitry Yu. – Cand. Sci. (Biology), Director of the Center for Experimental Pharmacology, Saint Petersburg State Chemical and Pharmaceutical University, Saint Petersburg, dmitry.ivkin@pharminnotech.com, https://orcid.org/0000-0001-9273-6864

Karpenko Vladislava V. – Laboratory Assistant, Research Department of Pulmonary Circulation Disorders, Almazov NRMC, Saint Petersburg, vladislavavk26@gmail.com, https://orcid.org/0009-0003-2207-1918

Galagudza Mikhail M. – Dr. Sci. (Med.), Professor, Corresponding Member of the RAS, Director of the Institute of Experimental Medicine, Almazov NRMC, Saint Petersburg, galagudza@almazovcentre.ru, https://orcid.org/0000-0001-5129-9944

(✉) **Karpov Andrey A.,** karpov_aa@almazovcentre.ru

Received 11.05.2024;
approved after peer review 01.08.2024;
accepted 12.09.2024

УДК 616.12-008.46-36.12-06:616.24-005.3-07
https://doi.org/10.20538/1682-0363-2024-4-38-46

Assessing pulmonary congestion in patients hospitalized with decompensated chronic heart failure according to lung ultrasound and remote dielectric sensing (ReDS)

Kobalava Zh.D.[1], Safarova A.F.[1,2], Tolkacheva V.V.[1], Zorya O.T.[1], Cabello Montoya F.E.[1], Nazarov I.S.[1], Lapshin A.A.[1,2], Smirnov I.P.[1], Khutsishvili N.I.[1], Galochkin S.A.[1,2], Vatsik-Gorodetskaya M.V.[2]

[1] *Peoples' Friendship University of Russia (RUDN University)*
8, Mikluho-Maklaya Str., Moscow, 117198, Russian Federation

[2] *Vinogradov City Clinical Hospital*
61, Vavilova Str., Moscow, 117292, Russian Federation

ABSTRACT

Aim. To conduct a comparative assessment of parameters and dynamics of pulmonary congestion according to lung ultrasound and remote dielectric sensing (ReDS) in patients hospitalized with decompensated chronic heart failure (CHF)

Materials and methods. The pilot single-center study included patients hospitalized with decompensated CHF. Lung ultrasound and ReDS were simultaneously performed within 24 hours from the moment of hospitalization and at discharge. Eight-zone lung ultrasound was performed with the calculation of the sum of B-lines. Pulmonary congestion was confirmed with the sum of B-lines ≥ 5. ReDS was performed according to the manufacturer's protocol. Congestion was confirmed at the value of more than 35%. To determine ReDS interoperator variability, each patient was examined by two operators who were blind to each other's findings with a 20–30-minute interval.

Results. Thirty-five patients were included in the study: 40% (n = 14) men, the average age was 71 (65.5; 78.5) years, the median NT-proBNP was 1,379 (470; 4,277) pg / l. Hydrothorax at admission was observed in 31,4% (n = 11) of patients. The incidence of pulmonary congestion according to lung ultrasound was 57.1% (n = 20): 31.4% (n = 11) of patients had mild congestion, 22.9% (n = 8) – moderate, and 2.9% (n = 1) – severe congestion. ReDS data revealed pulmonary congestion in 62.9% (n = 22) of cases, of which 37,1% (n = 13) of cases were characterized by mild, 22.9% (n = 8) – by moderate, and 2.9% (n = 1) – by severe congestion. A moderate correlation was found between ReDS (%) and lung ultrasound (sum of B-lines) findings at admission (Spearman's rank correlation coefficient = 0.402; p = 0.017). No correlation between the two methods was found at discharge (p = 0.613). The frequency of agreement between lung ultrasound and ReDS on signs of congestion at admission was 77.1% (p = 0.004) with an average Cohen's Kappa coefficient (κ = 0.53). The average interoperator variability in ReDS was 9.9%.

Conclusion. A moderate correlation was revealed between ReDS (%) and lung ultrasound (sum of B-lines) in detecting pulmonary congestion (Spearman's rank correlation coefficient = 0.402; p = 0.017). No correlation between the two methods was found at discharge (p = 0.613).

Keywords: heart failure, pulmonary congestion, lung ultrasound, remote dielectric sensing (ReDS)

Conflict of interest. The authors declare the absence of obvious or potential conflicts of interest related to the publication of this article.

Source of financing. The authors state that they received no funding for the study.

Conformity with the principles of ethics. All patients signed an informed consent to participate in the study. The study was approved by the Ethics Committee at RUDN University.

✉ *Tolkacheva Veronika V.,* tolkachevav@mail.ru

For citation: Kobalava Zh.D., Safarova A.F., Tolkacheva V.V., Zorya O.T., Cabello Montoya F.E., Nazarov I.S., Lapshin A.A., Smirnov I.P., Khutsishvili N.I., Galochkin S.A., Vatsik-Gorodetskaya M.V. Assessing pulmonary congestion in patients hospitalized with decompensated chronic heart failure according to lung ultrasound and remote dielectric sensing (ReDS). *Bulletin of Siberian Medicine.* 2024;23(4):38–46. https://doi.org/10.20538/1682-0363-2024-4-38-46.

Оценка наличия и динамики легочного застоя по данным ультразвукового и дистанционного диэлектрического исследования (REDS) у пациентов, госпитализированных с декомпенсацией хронической сердечной недостаточности

Кобалава Ж.Д.[1], Сафарова А.Ф.[1,2], Толкачева В.В.[1], Зоря О.Т.[1], Кабельо Монтойа Ф.Э.[1], Назаров И.С.[1], Лапшин А.А.[1,2], Смирнов И.П.[1], Хуцишвили Н.И.[1], Галочкин С.А.[1,2], Вацик-Городецкая М.В.[2]

[1] Российский университет дружбы народов (РУДН)
Россия, 117198, г. Москва, ул. Миклухо-Маклая, 8

[2] Городская клиническая больница (ГКБ) им. В.В. Виноградова
Россия, 117292, г. Москва, ул. Вавилова, 61

РЕЗЮМЕ

Цель: провести сравнительную оценку наличия и динамики легочного застоя по данным ультразвукового (УЗИ) и дистанционного диэлектрического (ReDS) исследования у пациентов, госпитализированных с декомпенсацией хронической сердечной недостаточности (ХСН).

Материалы и методы. В пилотное одноцентровое исследование включались пациенты, госпитализированные с декомпенсацией ХСН. В течение 24 ч от момента госпитализации и при выписке одномоментно проводились УЗИ легких и исследование с применением технологии ReDS. Ультразвуковое исследование легких выполнялось по протоколу с оценкой восьми зон и подсчетом суммы В-линий. Легочный застой подтверждался при сумме В-линий ≥5. Исследование ReDS выполнялось по протоколу производителя, застой подтверждался при получении значения более 35%. Для определения межоператорской вариабельности ReDS каждому пациенту исследование проводили два заслепленных оператора с интервалом 20–30 мин независимо друг от друга.

Результаты. В исследование были включены 35 пациентов: 40% (n = 14) мужчин, средний возраст 71 (65,5; 78,5) год, медиана NT-proBNP составила 1 379 (470; 4 277) пг/л. Гидроторакс при поступлении наблюдался у 31,4% (n = 11) пациентов. Частота легочного застоя, по данным УЗИ, составила 57,1% (n = 20), из них легкая степень застоя наблюдалась у 31,4% (n = 11), средняя – у 22,9% (n = 8), тяжелая – у 2,9% (n = 1) пациентов. Легочный застой, по данным ReDS, наблюдался у 62,9% (n = 22), из них легкий у 37.1% (n = 13), средний у 22,9% (n = 8), тяжелый у 2.9% (n = 1). Выявлена умеренная корреляционная связь между показателями ReDS (%) и УЗИ легких (сумма В-линий) при поступлении (r = 0,402; p = 0,017). При выписке корреляционной взаимосвязи между двумя методами выявлено не было (p = 0,613). Частота согласия по наличию или отсутствию признаков застоя, по данным обоих методов, на момент поступления составила 77,1% (p = 0,004) со средним значением коэффициента согласия каппа Коэна (к = 0,53). Наблюдалась средняя межоператорская вариабельность для исследования ReDS (коэффициент вариабельности 9,9%).

Заключение. Отмечена умеренная корреляционная связь между показателями ReDS (%) и УЗИ легких (сумма В-линий) в отношении выявления легочного застоя при поступлении (r = 0,402; p = 0,017). При выписке корреляционной взаимосвязи между двумя методами выявлено не было (p = 0,613).

Ключевые слова: сердечная недостаточность, легочный застой, УЗИ легких, дистанционное диэлектрическое исследование (ReDS)

Конфликт интересов. Авторы декларируют отсутствие явных и потенциальных конфликтов интересов, связанных с публикацией настоящей статьи.

Источник финансирования. Авторы заявляют об отсутствии финансирования при проведении исследования.

Соответствие принципам этики. Все пациенты подписали информированное согласие на участие в исследовании. Исследование одобрено локальным этическим комитетом РУДН.

Для цитирования: Кобалава Ж.Д., Сафарова А.Ф., Толкачева В.В., Зоря О.Т., Кабельо Монтойа Ф.Э., Назаров И.С., Лапшин А.А., Смирнов И.П., Хуцишвили Н.И., Галочкин С.А., Вацик-Городецкая М.В. Оценка наличия и динамики легочного застоя по данным ультразвукового и дистанционного диэлектрического исследования (REDS) у пациентов, госпитализированных с декомпенсацией хронической сердечной недостаточности. *Бюллетень сибирской медицины.* 2024;23(4):38–46. https://doi.org/10.20538/1682-0363-2024-4-38-46.

INTRODUCTION

Determining the hydration status, including a quantitative assessment of congestion severity, is one of the urgent tasks in the treatment of decompensated heart failure in hospital and outpatient settings. Hemodynamic overload and subsequent venous congestion are links of pathophysiological reactions included in the formation of this condition.

Discharge from hospital before congestion is fully resolved increases the risk of death and re-hospitalization [1–3]. In addition, patients may experience subclinical congestion at discharge, which is detected only by laboratory and instrumental methods, and clinical manifestations may develop even before the end of the first week after the discharge [2, 3].

More than 90% of heart failure-related hospitalizations are due to pulmonary congestion (CHAMPION trial) [4]. Early detection of pulmonary congestion is extremely important, as it allows to prevent the development of a decompensation episode, start proper treatment, and improve the disease prognosis.

According to current European guidelines, chest X-ray and lung ultrasound are recommended as instrumental methods to detect pulmonary congestion in patients with acute heart failure (HF) [5, 6].

According to previously published studies, including randomized clinical trials and large foreign registries, lung ultrasound demonstrated significantly higher sensitivity and specificity in detecting pulmonary congestion and had independent prognostic value [7–9]. However, due to the limitations of these methods, a search for new methods to assess the degree of pulmonary congestion remains relevant.

A non-invasive remote dielectric sensing (ReDS) technology makes it possible to quantify the total volume of fluid in the lungs by determining the dielectric properties of the tissue. As a result of the measurement, the operator quickly and safely receives a numerical value corresponding to the percentage of fluid in the lung tissue. According to the meta-analysis, which included works published from 2017 to 2021 with the analysis of a sample of 985 patients, management of patients using the ReDS technology reduced the frequency of readmission for HF [10].

Still, studies on the comparative assessment of lung ultrasound and ReDS in patients with HF are few [11], and there are no studies involving Russian patient population.

Therefore, the aim of this study was to compare the incidence and dynamics of pulmonary congestion according to lung ultrasound and ReDS in patients hospitalized with acute decompensated heart failure (ADHF).

MATERIALS AND METHODS

The study included 35 patients hospitalized with ADHF, regardless of left ventricular ejection fraction, in the emergency hospital of V.V. Vinogradov City Clinical Hospital (Moscow). ADHF was diagnosed based on current clinical guidelines [12, 13].

The study did not include patients with severe liver diseases, immobilization, terminal somatic symptom disorders and malignant diseases, acute coronary syndrome, edema of another etiology, an electrical pacemaker, severe chest deformity, and acute infectious diseases (including COVID-19-assicuated pneumonia).

The research protocol was approved by the local Ethics Committee at RUDN University. All patients signed an informed consent to the examination procedures. The study was performed in accordance with the standards of Good Clinical Practice and the principles of the Declaration of Helsinki.

All patients included in the study underwent a standard physical, laboratory, and instrumental examination upon hospitalization and discharge, which included lung ultrasound, determination of NT-proBNP, a study using the ReDS technology, liver FibroScan, bioimpedance vector analysis of the body composition, and assessment of venous congestion according to the VExUS score. The design of the study is shown in Fig.1. The characteristics and main laboratory and instrumental parameters of the patients are presented in Table.

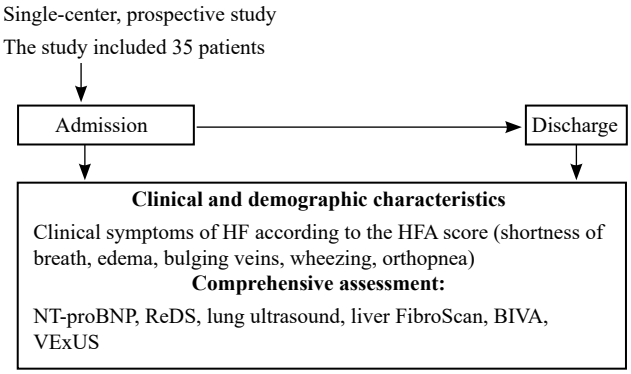

Fig. 1. Design of the study

Table

Clinical and demographic characteristics and laboratory and instrumental findings of patients included in the study, *n* = 35

Parameter	Value
Clinical and demographic characteristics	
Gender (male / female), *n* (%)	14 (40%)/21 (60%)
Age, years, *Me* (*IQR*)	71 [65.5; 78.5]
BMI, kg / m^2, *Me* (*IQR*)	34.5 [27.0; 38.6]
Smoking, *n* (%)	8 (22.9%)
LVEF, % *Me* (*IQR*)	52 [40; 55]
Arterial hypertension, *n* (%)	34 (97.2%)
Previous stroke, *n* (%)	5 (14.3%)
Coronary artery disease, *n* (%)	14 (40.0%)
Previous myocardial infarction, *n* (%)	6 (17.2%)
Atrial fibrillation / flutter, *n* (%)	22 (62.9%)
Type 2 diabetes mellitus, *n* (%)	9 (25.7%)
Chronic kidney disease, *n* (%)	22 (62.9%)
COPD / BA, *n* (%)	5 (14.3%)
SBP, mm Hg., *Me* (*IQR*)	133 [120.5; 146]
DBP, mm Hg., *Me* (*IQR*)	80 [70; 84.5]
Heart rate, beats per min, *Me* (*IQR*)	85 [74; 120]
Laboratory and instrumental characteristics at admission	
Liver stiffness, kPa, *Me* (*IQR*)	13 [6; 21]
Sum of B-lines in lung ultrasound, *Me* (*IQR*)	8 [4; 16]
BIVA, resistance, Om / m, *M* ± *SD*	394 ± 99
BIVA, reactance, Om / m, *Me* (*IQR*)	38 [31; 45]
Size of the inferior vena cava, mm, *M* ± *SD*	22 ± 5
Congestion grade according to VExUS, *n* (%)	GRADE 0: 14 (40%) GRADE 1: 3 (8.6%) GRADE 2: 6 (17.1%) GRADE 3: 12 (34.3%)
NT-proBNP, pg / ml, *Me* (*IQR*)	1,379 (470; 4,277)
ReDS findings, *M* ± *SD*	37 ± 6

Note. BMI – body mass index, LVEF – left ventricular ejection fraction, SBP – systolic blood pressure, DBP – diastolic blood pressure, BIVA – bioimpedance vector analysis.

To identify and assess the severity of pulmonary congestion, lung ultrasound was performed according to the protocol with the calculation of the number of B-lines in 8 zones along the anterior and lateral surfaces of the chest using the GE Vivid iq ultrasound system. The sum of B-lines of 6–15 was considered as mild, of 16–30 – as moderate, of more than 30 – as severe congestion.

The ReDS technology is based on the estimation of dielectric properties of the tissue. Low-power electromagnetic radiation passes through tissues from the emitter to the receiver. Since water has a very high dielectric constant, and dielectric constants of tissues are determined mainly by liquid contained in it, the assessment of changes in the parameters of radio waves makes it possible to accurately measure the total volume of liquid in the tissue. Thus, the ReDS system calculates the air-to--liquid volumetric ratio and shows the percentage of pulmonary fluid [10, 11, 14].

The study was conducted according to the manufacturer's protocol. A sensor was placed on the right side of the patient`s chest in a sitting position. The measurement took about 45 seconds (Fig.2). The manufacturer's recommended range of normal values was 20–35%. More than 35% indicated pulmonary congestion. The severity of congestion was determined by the following values: 36-40% – grade 1 (increased fluid content in the lungs), 41–50% – grade 2 (high fluid content in the lungs), more than 50% – grade 3 (extremely high fluid content in the lungs).

To determine ReDS interoperator variability, each patient was examined by two operators who were blind to each other's findings with a 20–30-minute interval.

Statistical processing of the results was performed using the MedCalc version 19.0 and SPSS (version 22.0) software. Quantitative variables were described as the arithmetic mean (*M*) and the standard deviation (*SD*) (with a normal distribution) or as the median and the interquartile range *Me (IQR)* (with a non-normal distribution).

Fig. 2. Remote dielectric sensing (ReDS) technology**.** The device consists of two sensors (front and rear), a computing unit, and a monitor

The nature of data distribution was determined using the Kolmogorov – Smirnov test. For normally distributed data, the significance of differences was assessed by the Student's *t*-test for dependent and independent samples. For non-normally distributed data, the significance of differences between the groups was assessed using the Mann– Whitney test for independent samples and the Wilcoxon's test for dependent samples. The differences were considered statistically significant at $p < 0.05$ (with the Bonferroni correction). The direction and strength of the correlation between the two quantitative variables were estimated by the Spearman's rank correlation coefficient (with non-normally distributed data).

To assess interoperator variability for qualitative parameters, the coefficient of agreement, or Cohen's kappa (κ) was determined, which was calculated using the formula: $\kappa = (po - pe) / (1 - pe)$, where po is actually observed agreement between operators, pe is expected agreement that would be observed by chance alone (with complete agreement, $\kappa = 1$, and in the absence of agreement, $\kappa = 0$). In the meantime, $\kappa = 0–0.2$ indicates slight agreement, $\kappa = 0.21–0.4$ – fair agreement, $\kappa = 0.41–0.6$ – moderate agreement, $\kappa = 0.61–0.8$ – substantial agreement, and $\kappa = 0.81$-1 – almost perfect agreement.

RESULTS

Pulmonary congestion at admission according to ReDS data was diagnosed in 62.9% ($n = 22$) of patients, of which 37.1% ($n = 13$) of patients had mild, 22.9% ($n = 8$) of patients – moderate, and 2.9% ($n = 1$) of patients – severe congestion. Pulmonary congestion at discharge was detected in 44% ($n = 15$) of patients. Lung ultrasound revealed pulmonary congestion at admission in 57.2% ($n = 20$) of cases, of which mild congestion was detected in 31.4% ($n = 11$) of patients, moderate – in 22.9% ($n = 8$) of patients, and severe – in 2.9% ($n = 1$) of cases. At discharge, it was detected in 16% cases ($n = 5$) (Fig.3). Hydrothorax at admission was observed in 31.4% ($n = 11$) of patients.

A moderate correlation was found between ReDS (%) and lung ultrasound (sum of B-lines) findings at admission ($r = 0.402$; $p = 0.017$). At discharge, no correlation was found between the two methods ($p = 0.613$) (Fig.4).

The frequency of agreement between the two methods on the presence or absence of signs of congestion at admission was 77.1% ($p = 0.004$) with a moderate Cohen's kappa value ($\kappa = 0.53$). At discharge, the frequency of agreement between the methods was 41.7% ($p = 0.223$), and the Cohen's kappa value was negative. Taking into account hydrothorax as a sign of congestion along with the sum of B-lines on lung ultrasound at admission, the agreement between the methods was 71.4% ($p = 0.033$), and Cohen's kappa was $\kappa = 0.388$. At discharge, taking into account hydrothorax did not change the frequency of agreement between the two methods in detecting pulmonary congestion.

The average interoperator variability for the ReDS study was revealed (the variability coefficient was

9.9%). At the same time, ReDS showed that variability between operators was 12.7% at admission and 6.6% at discharge. For the ReDS study, Cohen's kappa between operators in detecting pulmonary congestion was κ = 0.82 (κ = 0.908 at admission and κ = 0.657 at discharge).

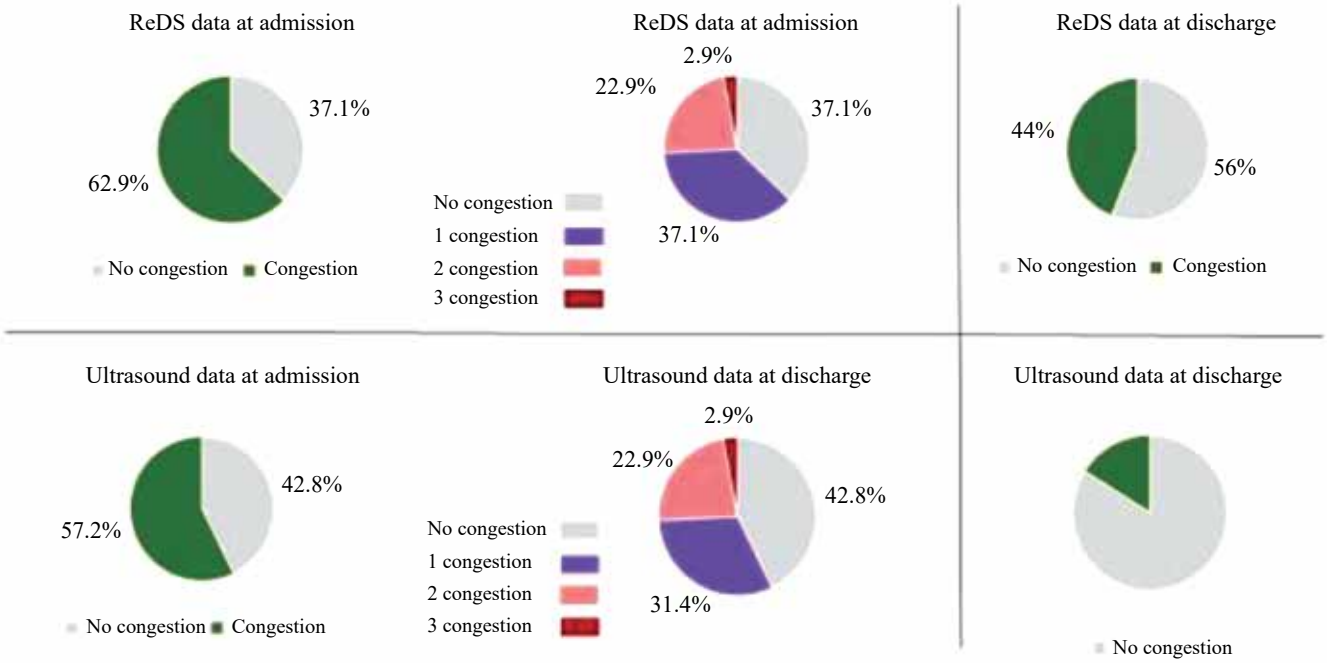

Fig. 3. The incidence of pulmonary congestion in patients with ADHF at admission and at discharge according to ReDS and lung ultrasound findings (n = 35)

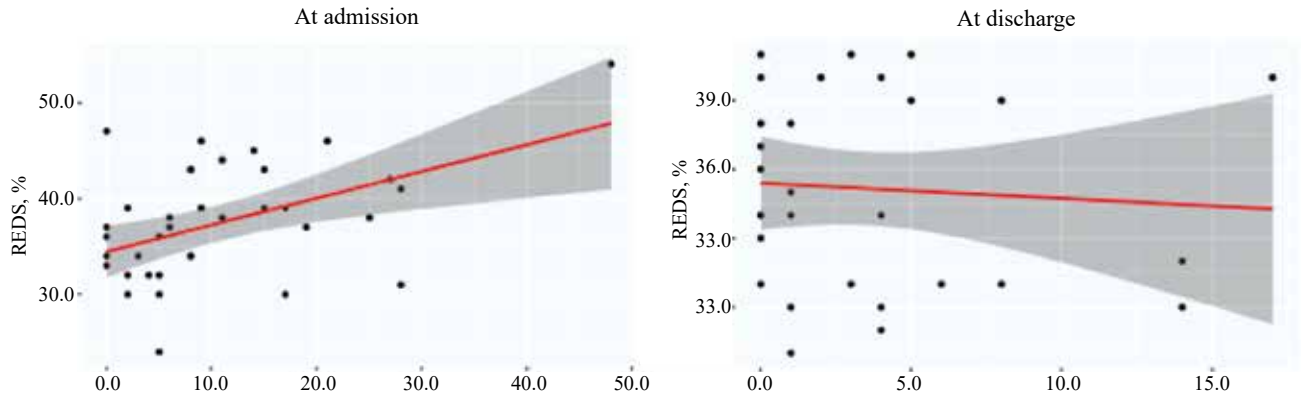

Correlation between ReDS and lung ultrasound (r = 0.402, p = 0.017)

Correlation between ReDS and lung ultrasound (p = 0.613)

Fig. 4. Correlation between ReDS (%) and lung ultrasound (sum of B-lines) findings

DISCUSSION

The accuracy of the diagnosis of pulmonary congestion by lung ultrasound is high, the sensitivity and specificity of this method exceed 95%. The consensus of experts recommends lung ultrasound for the diagnosis of pulmonary congestion [15]. Therefore, lung ultrasound in this study was considered as the gold standard for assessing pulmonary congestion. However, this study is a semi-quantitative method and requires appropriate equipment and highly qualified specialists.

As an alternative method for quantifying the degree of congestion in the lungs and displaying the percentage of pulmonary fluid in 45 seconds, the ReDS technology can be used. This is a non-invasive method that does not require expertise.

A strong correlation was demonstrated between ReDS findings and clinical signs of pulmonary congestion in patients with ADHF during hospital stay [16]. It was shown that ReDS values were strongly correlated with other assessment methods, including high-resolution computed tomography (0.90 (95% confidence interval (CI) 0.85–0.95) [17] and right heart catheterization [18]. In a study conducted in Japan, a moderate correlation between ReDS values and high-resolution computed tomography was revealed (r = 0.65, p < 0.001). In addition, it was shown that the ReDS value is an independent predictor of pulmonary congestion after adjustment for N-terminal pro b-type natriuretic peptide (NT-proBNP) and patient's body weight [19].

The gold standard for quantifying the severity of pulmonary congestion is catheterization of the right heart with measurement of pulmonary capillary wedge pressure (PCWP). However, given a number of limitations, such as the invasive nature of the procedure, the risk of complications, including exacerbation of HF, especially in patients with unstable hemodynamics and those receiving anticoagulants, catheterization of the right heart is not widely used in routine clinical practice.

In a study conducted in Israel including 139 patients with HF, a positive correlation was found between the ReDS values and pulmonary artery pressure (r = 0.492, p < 0.001), as well as between the values of ReDS and central venous pressure (r = 0.406, p < 0.001). It was shown that the ReDS value (threshold value of 34%) had high sensitivity (90.7%), high specificity (77.1%), and a negative prognostic value (94.9%) in determining PCWP of 18 mm Hg [20]. In another study, a moderate correlation was found between the values of ReDS and PCWP (r = 0.698, p < 0.001); the ReDS value of 28% was a threshold value for predicting PCWP > 15 mm Hg with sufficiently high sensitivity (0.70) and specificity (0.75) [17].

It was shown that the ReDS technology is comparable to lung ultrasound in detecting subclinical pulmonary congestion, since ReDS values of > 35% had sensitivity of 66.7%, specificity of 87.5%, and a negative prognostic value of 93.3% compared to the sum of B-lines in lung ultrasound [11].

In our study, pulmonary congestion at admission according to ReDS data was diagnosed in 62.9% of cases, according to lung ultrasound – in 57.2% of patients. A moderate correlation was found between ReDS (%) and lung ultrasound (sum of B-lines) findings at admission (r = 0.402; p = 0.017). The interoperator variability of ReDS was also studied. The Cohen's kappa for the ReDS study in detecting pulmonary congestion was κ =0.82 (κ = 0.908 at admission and κ = 0.657 at discharge), which indicated almost complete agreement in values between the two operators. This is confirmed by the literature data. A study in Japan involving 10 healthy volunteers also demonstrated very high reliability of ReDS measurements between three operators (0.966, 95% CI: 0.952–0.976). This allows to suggest that a single ReDS measurement is reliable [21].

CONCLUSION

The remote dielectric sensing (ReDS) technology has a moderate correlation with lung ultrasound in terms of assessing pulmonary congestion in patients hospitalized with ADHF. However, it is worth noting that currently these methods can be considered as complementary, and the use of the ReDS technology in patients with HF requires further study.

REFERENCES

1. Chioncel O., Mebazaa A., Harjola V.P., Coats A.J., Piepoli M.F., Crespo-Leiro M.G. et al. On behalf of the ESC heart failure long-term registry investigators. Clinical phenotypes and outcome of patients hospitalized for acute heart failure: the ESC Heart Failure Long-Term Registry. *Eur. J. Heart Fail.* 2017;19:1242e1254. DOI: 10.1002/ejhf.890.
2. Rattarasarn I., Yingchoncharoen T., Assavapokee T. Prediction of rehospitalization in patients with acute heart failure using point-of-care lung ultrasound. *BMC Cardiovasc. Disord.* 2022;22:330. DOI: 10.1186/s12872-022-02781-9.
3. Rivas-Lasarte M., Maestro A., Fernández-Martínez J., López-López L., Solé-González E., Vives-Borrás M. et al. Prevalence and prognostic impact of subclinical pulmonary congestion at discharge in patients with acute heart failure. *ESC Heart Fail.* 2020;7:2621e2628. DOI: 10.1002/ehf2.12842.

4. Adamson P.B., Abraham W.T., Aaron M., Aranda J.M., Bourge R.C., Smith A. et al. CHAMPION trial rationale and design: the long-term safety and clinical efficacy of a wireless pulmonary artery pressure monitoring system. *J. Card. Fail.* 2011;17:3e10. DOI: 10.1016/j.cardfail.2010.08.002.
5. 2022 AHA/ACC/HFSA guideline for the management of heart failure: a report of the American college of Cardiology/American heart association joint committee on clinical practice guidelines. *Circulation.* 2022;145:e895–e1032. DOI: 10.1161/CIR.0000000000001063.
6. 2021 ESC guidelines for the diagnosis and treatment of acute and chronic heart failure. *Eur. Heart J.* 2021;42:3599e3726. DOI: 10.1002/ejhf.2333.
7. Platz E., Merz A., Jhund P., Vazir A., Campbell R., McMurray J.J. Dynamic changes and prognostic value of pulmonary congestion by lung ultrasound in acute and chronic heart failure: a systematic review. *European Journal of Heart Failure.* 2017;19(9):1154–1163. DOI: 10.1002/ejhf.839.
8. Picano E., Scali M.C., Ciampi Q., Lichtenstein D. Lung ultrasound for the cardiologist. *JACC Cardiovasc Imaging.* 2018;11(11):1692–1705. DOI: 10.1016/j.jcmg.2018.06.023.
9. Pivetta E., Goffi A., Nazerian P., Castagno D., Tozzetti C., Tizzani P. et al. Lung ultrasound integrated with clinical assessment for the diagnosis of acute decompensated heart failure in the emergency department: a randomized controlled trial. *European Journal of Heart Failure.* 2019;21:754–766. DOI: 10.1002/ejhf.1379.
10. Sattar Y., Zghouzi M., Suleiman A., Sheikh A., Kupferman J., Sarfraz A. et al. Efficacy of remote dielectric sensing (ReDS) in the prevention of heart failure rehospitalizations: a metaanalysis. *Journal of Community Hospital Internal Medicine Perspectives*. 2021;11(5):646–652. DOI: 10.1080/20009666.2021.1955451.
11. Izumida T., Imamura T., Kinugawa K. Remote dielectric sensing and lung ultrasound to assess pulmonary congestion. *Heart and Vessels.* 2023;38:517–522. DOI: 10.1007/s00380-022-02190-0.
12. 2021 ESC guidelines for the diagnosis and treatment of acute and chronic heart failure. *European Heart Journal.* 2021;42(36):3599–3726. DOI: 10.1093/eurheartj/ehab368.
13. Gheorghiade M., Follath F., Ponikowski P. et al. European Society of Cardiology; European Society of Intensive Care Medicine. Assessing and grading congestion in acute heart failure: a scientific statement from the acute heart failure committee of the heart failure association of the European Society of Cardiology and endorsed by the European Society of Intensive Care Medicine. *Eur. J. Heart Fail*. 2010;12(5):423–433. DOI: 10.1093/eurjhf/hfq045.
14. Yuriditsky E., Horowitz J.M., Panebianco N.L., Sauthoff H., Saric M. Lung ultrasound imaging: a primer for echocardiographers. *J. Am. Soc. Echocardiogr.* 2021;34(12):1231–1241. DOI: 10.1016/j.echo.2021.08.009.
15. Volpicelli G., Elbarbary M., Blaivas M., Lichtenstein D.A., Mathis G., Kirkpatrick A.W. et al. International liaison committee on lung ultrasound (ILC-LUS) for international consensus conference on lung ultrasound (ICC-LUS) international evidence based recommendations for point-of-care lung ultrasound. *Intensive Care Med.* 2012;38(4):577–591. DOI: 10.1007/s00134-012-2513-4.
16. Uriel N., Sayer G., Imamura T., Rodgers D., Kim G., Raikhelkar J. et al. Relationship between noninvasive assessment of lung fluid volume and invasively measured cardiac hemodynamics. *J. Am. Heart Assoc*. 2018;7:e009175. DOI: 10.1161/jaha.118.009175.
17. Imamura T., Hori M., Ueno Y., Narang N., Onoda H., Tanaka S. et al. Association between lung fluid levels estimated by remote dielectric sensing values and invasive hemodynamic measurements. *J. Clin. Med.* 2022;11(5):1208. DOI: 10.3390/jcm11051208.
18. Amir O., Rappaport D., Zafrir B., Abraham W.T. A novel approach to monitoring pulmonary congestion in heart failure: initial animal and clinical experiences using remote dielectric sensing technology, Congest. *Heart Fail.* 2013;19(3):149–155. DOI: 10.1111/chf.12021.
19. Amir O., Azzam Z.S., Gaspar T., Faranesh-Abboud S., Andria N., Burkhoff D. et al. Validation of remote dielectric sensing (ReDS™) technology for quantification of lung fluid status: comparison to high resolution chest computed tomography in patients with and without acute heart failure. *Int. J. Cardiol.* 2016;221:841–846. DOI: 10.1016/j.ijcard.2016.06.323.
20. Imamura T., Gonoi W., Hori M., Ueno Y., Narang N., Onoda H. et al. Validation of noninvasive remote dielectric sensing system to quantify lung fluid levels. *J. Clin. Med.* 2021;11(1):164. DOI: 10.3390/jcm11010164.
21. Hori M., Imamura T., Fukuo A., Fukui T., Koi T., Ueno Y. et al. Validation of inter-rater and intra-rater reliability of remote dielectric sensing measurement. *Int. Heart J.* 2022;63:73e76. DOI: 10.1536/ihj.21-663.

Authors' contribution

Kobalava Zh.D., Safarova A.F., Vatsik-Gorodetskaya M.V. – conception and design. Tolkacheva V.V. Zorya O.T., Cabello Montoya F.E. – analysis of the acquired data, drafting of the article. Nazarov I.S., Lapshin A.A, Smirnov I.P., Khutsishvili N.I., Galochkin S.A. – collection and processing of the materials.

Authors' information

Kobalava Zhanna D. – Dr. Sci. (Med.), Professor, Head of the Department of Internal Medicine with a Course in Cardiology and Functional Diagnostics named after academician V.S. Moiseev, RUDN University, Moscow, zkobalava@mail.ru, https://orcid.org/0000-0002-5873-1768

Safarova Ayten F. –, Dr. Sci. (Med.), Professor of the Department of Internal Medicine with a Course in Cardiology and Functional Diagnostics named after academician V.S. Moiseev, RUDN University, Moscow, aytensaf@mail.ru, https://orcid.org/0000-0003-2412-5986

Tolkacheva Veronika V. – Dr. Sci. (Med.), Associate Professor, Department of Internal Medicine with a Course in Cardiology and Functional Diagnostics named after academician V.S. Moiseev, RUDN University, Moscow, tolkachevav@mail.ru, https://orcid.org/0000-0001-6847-8797

Zorya Olga T. – Cand. Sci. (Med.), Teaching Assistant, Department of Internal Medicine with a Course in Cardiology and Functional Diagnostics named after academician V.S. Moiseev, RUDN University, Moscow, olyazorya2020@outlook.com, https://orcid.org/0000-0002-8855-0079

Cabello Montoya Flora Elisa – Cand. Sci. (Med.), Teaching Assistant, Department of Internal Medicine with a Course in Cardiology and Functional Diagnostics named after academician V.S. Moiseev, RUDN University, Moscow, flora.cabello@mail.ru, https://orcid.org/0000-0002-2334-6675

Nazarov Ivan S. – Post-Graduate Student, Department of Internal Medicine with a Course in Cardiology and Functional Diagnostics named after academician V.S. Moiseev, RUDN University, Moscow, nazarovradomla@mail.ru, https://orcid.org/0000–0002–0950–7487

Lapshin Artem A. – Cand. Sci. (Med.), Teaching Assistant, Department of Internal Medicine with a Course in Cardiology and Functional Diagnostics named after academician V.S. Moiseev, RUDN University, Moscow, lapshin_aa@pfur.ru, https://orcid.org/0000-0002-4308-4764

Smirnov Ilya P. – Resident, Department of Internal Medicine with a Course in Cardiology and Functional Diagnostics named after academician V.S. Moiseev, RUDN University, Moscow, zzevor@mail.ru, https://orcid.org/0009-0001-0285-1752

Khutsishvili Nutsiko I. – Post-Graduate Student, Department of Internal Medicine with a Course in Cardiology and Functional Diagnostics named after academician V.S. Moiseev, RUDN University, Moscow, nutsiko.khutsishvili@gmail.com, https://orcid.org/0009-0009-2669-8092

Galochkin Svyatoslav A. – Cand. Sci. (Med.), Associate Professor, Department of Internal Medicine with a Course in Cardiology and Functional Diagnostics named after academician V.S. Moiseev, RUDN University, Moscow, galochkin-sa@rudn.ru, https://orcid.org/0000-0001-7370-8606

Vatsik-Gorodetskaya Maria V. – Cand. Sci. (Med.), Deputy Chief Physician for Anesthesiology and Resuscitation, V. V. Vinogradov City Clinical Hospital, Moscow, m.vatsyk@gmail.com, https://orcid.org/0000-0002-6874-8213

(✉) **Tolkacheva Veronika V.,** tolkachevav@mail.ru

Received 20.02.2024;
approved after peer review 15.04.2024;
accepted 13.06.2024

УДК 616.894-053.8-021.6:577.218
https://doi.org/10.20538/1682-0363-2024-4-47-54

Changes in VEGFR1 and VEGFR2 expression and endothelial cell maturity in laboratory animals with a model of Alzheimer's disease

Kukla M.V., Averchuk A.S., Stavrovskaya A.V., Rozanova N.A., Berdnikov A.K., Kolotyeva N.A., Salmina A.B.

Research Center of Neurology
80, Volokolamskoye Highway, Moscow, 125367, Russian Federation

ABSTRACT

Aim. To evaluate the expression of VEGFR1 and VEGFR2 and the maturity of endothelial cells in neurogenic niches in the model of Alzheimer's disease.

Materials and methods. The study was carried out on 6-month-old male C57BL/6 mice. The experimental group (n = 15) received 2 µl of 1 mM Aβ25-35 solution in the CA1 hippocampal region, while the control group (n = 15) received normal saline. Brain plasticity was assessed at day 10, 17, and 38 after surgery by the passive avoidance test. The expression of VEGFR1, VEGFR2, and CLDN5 was assessed by immunohistochemistry and the Image ExFluorer imaging system.

Results. In the control group, cognitive training stimulated angiogenesis in the neurogenic niches of the brain, which was accompanied by the formation of microvasculature with fully mature endothelium. In the experimental group, an early and pronounced increase in the VEGFR1 expression was observed by day 7 after cognitive training, which was followed by impaired barrier formation and high VEGFR2 expression by day 28 after cognitive training. These changes were associated with the formation of small vessels with structural incompetence of endothelial cells.

Conclusion. Angiogenesis in neurogenic niches of the animals with the model of Alzheimer's disease is characterized by incompetent mechanisms regulating the subpopulation composition of endothelial cells, impaired stabilization of the endothelial layer, and a decrease in the maturation rate of endothelial cells in newly formed microvessels by the time of cognitive deficit manifestation. This may contribute to microcirculatory dysfunction and impaired neurogenesis in neurogenic niches as well as to the development of pathological permeability and neuroinflammation. On the whole, the disruption of angiogenesis in neurogenic niches observed in the animal model of Alzheimer's disease suggests a potential contribution of this mechanism to the development of aberrant brain plasticity.

Keywords: VEGFR1, VEGFR2, CLDN5, neurogenesis, angiogenesis, neurogenic niches

Conflict of interest. The authors declare the absence of obvious or potential conflicts of interest related to the publication of this article.

Source of financing. The study was funded by the Russian Science Foundation grant No. 22-15-00126, https://rscf.ru/project/22-15-00126.

Conformity with the principles of ethics. The study was approved by the local ethics Committee at the Research Center of Neurology (Protocol No. 5-3/22 of 01.06.2022).

For citation: Kukla M.V., Averchuk A.S., Stavrovskaya A.V., Rozanova N.A., Berdnikov A.K., Kolotyeva N.A., Salmina A.B. Changes in VEGFR1 and VEGFR2 expression and endothelial cell maturity in laboratory animals with a model of Alzheimer's disease. *Bulletin of Siberian Medicine.* 2024;23(4):47–54. https://doi.org/10.20538/1682-0363-2024-4-47-54.

✉ *Kukla Mariya V.,* mashenka.ryazanova@list.ru

Изменение экспрессии VEGFR1 и VEGFR2 и зрелости клеток эндотелия у экспериментальных животных с моделью болезни Альцгеймера

Кукла М.В., Аверчук А.С., Ставровская А.В., Розанова Н.А., Бердников А.К., Колотьева Н.А., Салмина А.Б.

Научный центр неврологии
Россия, 125367, г. Москва, Волоколамское шоссе, 80

РЕЗЮМЕ

Цель: оценить экспрессию VEGFR1 и VEGFR2 и зрелость клеток эндотелия в нейрогенных нишах при экспериментальной болезни Альцгеймера (БА).

Материалы и методы. Исследование проведено на самцах мышей линии C57BL/6 в возрасте 6 мес. Экспериментальной группе (n = 15) вводили 2 мкл 1 мМ раствора Аβ25-35 в поле CA1 гиппокампа, контрольной группе (n = 15) – физиологический раствор. Пластичность мозга оценивали на 10-е, 17- и 38-е сут после операции с использованием теста условной реакции пассивного избегания. Экспрессию маркеров (VEGFR1, VEGFR2, CLDN5) исследовали методом иммуногистохимии с помощью системы визуализации Image ExFluorer.

Результаты. У животных контрольной группы когнитивный тренинг стимулирует процессы неоангиогенеза в нейрогенных нишах головного мозга, что сопровождается формированием микрососудов со зрелым эндотелием. У животных с экспериментальной моделью БА регистрируется раннее и выраженное увеличение экспрессии VEGFR1 к 7-м сут после когнитивной нагрузки, сопровождаемое нарушением барьерогенеза и высоким уровнем экспрессии VEGFR2 к 28-м сут после когнитивной нагрузки. Эти изменения сопряжены с формированием мелких сосудов с недостаточной структурной компетентностью клеток эндотелия.

Заключение. Неоангиогенез в нейрогенных нишах животных с экспериментальной моделью БА характеризуется несостоятельностью механизмов регуляции субпопуляционного состава клеток эндотелия, нарушением стабилизации эндотелиального слоя и снижением скорости созревания клеток эндотелия во вновь образованных микрососудах к периоду манифестации когнитивного дефицита, что может способствовать нарушению микроциркуляции и нейрогенеза в нейрогенных нишах, а также развитию патологической проницаемости и нейровоспаления. В целом нарушение процессов неоангиогенеза в нейрогенных нишах, регистрируемое при когнитивной нагрузке животных с моделью БА, свидетельствует о возможном вкладе этого механизма в развитие аберрантной пластичности головного мозга.

Ключевые слова: VEGFR1, VEGFR2, CLDN5, нейрогенез, ангиогенез, нейрогенные ниши

Конфликт интересов. Авторы заявляют об отсутствии конфликта интересов при проведении исследования.

Источник финансирования. Исследование выполнено за счет гранта Российского научного фонда № 22-15-00126, https://rscf.ru/project/22-15-00126.

Соответствие принципам этики. Исследование утверждены решением локального этического комитета ФГБНУ «Научный центр неврологии» (протокол № 5-3/22 от 01.06.2022).

Для цитирования: Кукла М.В., Аверчук А.С., Ставровская А.В., Розанова Н.А., Бердников А.К., Колотьева Н.А., Салмина А.Б. Изменение экспрессии VEGFR1 и VEGFR2 и зрелости клеток эндотелия у экспериментальных животных с моделью болезни Альцгеймера. *Бюллетень сибирской медицины.* 2024;23(4):47–54. https://doi.org/10.20538/1682-0363-2024-4-47-54.

INTRODUCTION

Alzheimer's disease (AD) is characterized by neurodegenerative changes due to impaired synthesis and accumulation of amyloid beta (Aβ) in the extracellular space [1, 2]. Simultaneously, phosphorylated tau protein accumulates within neurons, leading to damage and death of brain cells.

The effect of Aβ on neurons results in cell membrane dysfunction, disruption of signaling pathways, and premature neuronal death. These changes are particularly significant in brain regions

responsible for memory and cognitive functions, such as the hippocampus [3]. The activation of microglia in response to Aβ accumulation provokes neuroinflammation, while the disruption of the blood – brain barrier (BBB) under the effect of Aβ further contributes to inflammation and tissue damage [4]. In addition to BBB damage, microvessels in AD undergo extensive remodeling accompanied by unproductive angiogenesis and aberrant barriergenesis [5]. These events may be especially significant in neurogenic niches. Studies have shown that during ischemic brain injury, new microvessels with increased BBB permeability play a crucial role not only in the development of neuroinflammation, but also in the formation of new areas of neurogenesis, promoting brain tissue recovery [6].

It is worth noting that the vascular scaffold plays a key role in regulating neurogenesis. In the subventricular zone (SVZ), increased BBB permeability facilitates the entry of regulatory molecules from the blood into the microenvironment of neural stem cells (NSCs) and neuronal progenitor cells (NPCs), whereas in the subgranular zone of the hippocampus (SGZ), the microvessel wall is less permeable, making locally produced factors more critical for regulating the processes that maintain the NSC and NPC pools [7]. Such changes in the local microenvironment during neuroinflammation and aberrant angiogenesis in AD, as well as in other neurodegenerative diseases or brain development disorders, reduce the intensity of neurogenesis, contributing to cognitive deficits [8–10]. Previously, we demonstrated [11] that in the period preceding the development of cognitive deficits in animals with experimental AD, mitochondrial fission and endothelial cell autophagy in microvessels intensify in the SGZ of the hippocampus, indicating microvessel remodeling.

The role of vascular endothelial growth factor (VEGF) has long been studied in the context of neurogenesis and cerebral angiogenesis. In the brain, VEGF receptors are expressed on neuronal and glial cells, macrophages, and endothelial cells, regulating various aspects of their activity under both normal and pathological conditions [12, 13]. Overall, they facilitate the transmission of signals that positively regulate cell proliferation, migration, and development. There are three types of receptors: VEGFR1 (Flt-1), VEGFR2 (KDR or Flk-1), and VEGFR3 (Flt-4). VEGFR1 and VEGFR2 play crucial roles in regulating angiogenesis and neurogenesis in the brain, while VEGFR3 is typically associated with lymphatic angiogenesis and regulation of endothelial cell proliferation in lymphatic vessels [14]. The primary producers of VEGF are neuronal and glial cells [15, 16]. Given that angiogenesis is accompanied by the acquisition of a specific endothelial cell phenotype – tip cells (migrating along the gradient of pro-angiogenic molecules), stalk cells (proliferating and following tip cells establishing the walls of newly formed microvessels), and phalanx cells (stabilizing the barrier function of the vascular wall) – it is important to mention that activation of different receptor types on these cells regulates this specialization. For instance, VEGFR2 activation on the membrane of tip cells increases Dll4 expression. This protein then interacts with Notch receptors on neighboring endothelial cells, causing a decrease in VEGFR2 and VEGFR3 expression in these cells. This process prevents the conversion of stalk cells into tip cells (lateral inhibition mechanism). VEGFR1 activation on the membrane of phalanx cells promotes their migration [17, 18]. Notably, the expression of both types of receptors – VEGFR1 and VEGFR2 – in the brain tissue is exclusive to endothelial cells [19]. BBB stabilization in newly formed microvessels is ensured by the induction of expression of tight and adherens junction proteins (JAM, ZO1, CLDN5, etc.) in endothelial cells and the reduction of local VEGF production, which is important for maintaining the structural integrity of the barrier [16, 20]. When these mechanisms fail, barriergenesis becomes ineffective, potentially leading to the development of neuroinflammation.

The aim of this study was to evaluate the expression of VEGFR1 and VEGFR2 and the maturity of endothelial cells in neurogenic niches in the animal model of AD.

MATERIALS AND METHODS

Thirty male C57BL/6 mice were selected for the study. At the start of the experiments, the mice were 6 months old. The animals were kept under standard vivarium conditions with round-the-clock access to food and water. For anesthesia, Zoletil-100 (Virbac Sante Animale, France) diluted with saline in a 1:4 ratio was used. The mixture was administered intramuscularly at a dose of 15 mg of active substance per 25 g of body weight. Xyla (Interchemie werken "De Adelaar" B.V., the Netherlands) was also used, diluted in a 1:2 ratio and administered intramuscularly at a dose of 0.6 mg per 25 g of body weight.

A stereotactic surgery was performed using the coordinates AP – 2.0; ML – 1.9; DV – 1.3. The

experimental group of mice (n = 15) was bilaterally injected with 2 μl of 1 mM Aβ25-35 solution (Sigma-Aldrich Co., USA) directly into the hippocampus. The control group (n = 15) received identical injections of saline in the same volume.

All studies were conducted in accordance with ethical principles of animal use and were approved by the local Ethics Committee at the Research Center of Neurology (Protocol No. 5-3/22 of 01.06.2022).

Cognitive training. The full protocol and results of cognitive testing were presented earlier in [11]. The analysis used the passive avoidance response (PAR) test and the ShutAvoid 1.8.03 program on the Panlab Harvard Apparatus. The assessment was conducted on days 10, 17, and 38 after the surgery during daytime hours (corresponding to 1, 7, and 28 days after cognitive training of the animals).

At each time point, biological material was collected from 5 animals from each group one hour after cognitive testing.

Immunohistochemical study. To remove the animals from the experiment, they were anesthetized and decapitated. The extracted mouse brain was fixed in 4% paraformaldehyde (Wuhan Servicebio Co. Ltd, China). Histological sections of 10 μm thickness were prepared on the Tissue-Tek® Cryo3 cryostat (Sakura-Finetek, Japan). The biological material was stored at +4 ºC.

Immunohistochemical staining was performed using primary labeled antibodies: anti-VEGFR2 (1:250, AF6281-F488, Affinity, China); anti-CLDN5 (1:250, AF5216-F488, Affinity, China); anti-CD31 (1:250, AF6191-F555, Affinity, China), and primary anti-VEGFR1 (1:100, FNab09393, FineTest, China) with corresponding secondary goat anti-rabbit antibodies (1:100, E-AB-1060, Elabscience, China).

Prior to staining, the sections were washed in PBS (2.1.1. Rosmedbio, Russia) for 10 minutes and then in a 0.1% Triton X-100 solution for 20 minutes (Calbiochem Research Biochemicals, USA) with the addition of 5% BSA (1126GR100 BioFroxx, Germany). The sections were mounted under a coverslip using the Fluoroshield Mounting Medium with DAPI (Sigma Aldrich, F6057, USA). Visualization was performed using the Image ExFluorer visualization system (LCI, Korea), and the images were processed using the plugin for the ImageJ software [21]. The intensity of the specified marker expression was characterized by the number of cells expressing the corresponding marker, normalized to 100 DAPI-positive cells.

Western blotting protocol. Protein extraction from brain tissue homogenates was performed using RIPA Lysis Buffer (Servicebio, China) on ice. Protein separation was carried out by SDS-PAGE electrophoresis, loading 40 μg of protein into each well. Protein transfer to a nitrocellulose membrane (0.45 μm, Bio-Rad) was performed using the SVT-2 wet transfer system (Servicebio, China) at a constant current of 300 mA for 30 minutes. The membrane was incubated with primary antibodies VEGF (1:1000, AF5131, Affinity, China), BDNF (1:1000, DF6387, Affinity, China), and Actin (1:1500, AF7018, Affinity, China) for 12 hours at +4 ºC. After incubation, the membrane was washed in the Tris-Tween-20 solution. The next incubation of the membrane with secondary antibodies (1:1000, SAA544Rb59, Cloud-Clone, China) containing peroxidase was carried out for 60 minutes at +37 ºC. DAB stain was used for visualization. Protein detection was performed using the Geldoc Go system (Bio-Rad, USA). The Bio-Rad ImageLab software was used to analyze the obtained images.

PAR test results were analyzed using the one-way ANOVA and Fisher's exact test. Immunohistochemical data were evaluated using the Mann – Whitney U-test in the Statistica v. 12.0 software package (StatSoft Inc., USA). The results were considered significant at $p < 0.05$. The data were presented as the mean and the standard deviation ($M + \sigma$).

RESULTS AND DISCUSSION

As was previously shown, in animals with the model of AD-associated neurodegeneration, a statistically significant decline in cognitive functions was registered at day 28 after the first session in the PAR test [11]. This was accompanied by changes in Arg3.1/Arc expression in the neurogenic niches of the animals' brains [22], which allowed to consider the PAR protocol as an adequate method for implementing cognitive training in experiments.

We analyzed VEGFR1 expression in the neurogenic niches of animals in both groups (Fig. 1). In the control group, a statistically significant increase in the number of VEGFR1-expressing cells in the SGZ and SVZ was observed by day 28 compared to previous periods (p = 0.0450). We may suggest that it resembled induction of neoangiogenesis with a consistent progressive increase in the number of phalanx cells forming the endothelial layer in newly formed microvessels by day 28, likely related to the activation of neurogenesis following cognitive training [23]. This is indirectly supported by the fact that VEGFR1 activation stimulates the migration of

endothelial phalanx cells involved in the formation of new microvessels [15]. Notably, this effect was inverted in animals with AD, where an increase in the number of VEGFR1-positive cells was registered much earlier (on day 7 after training) and then almost disappears. This likely reflected the failure of training-stimulated neoangiogenesis mechanisms in animals with the AD model [11].

Next, we analyzed VEGFR2 expression in neurogenic niches (Fig. 2). A sign of increased angiogenesis stimulated by cognitive training in animals from both groups in the hippocampal SGZ was an increase in the number of VEGFR2-positive cells at day 7 ($p = 0.0495$). By day 28, the number of VEGFR2+ cells in the control group decreased, which may be associated with a decrease in the number of endothelial tip cells and an increase in the number of stalk cells (lateral inhibition mechanism). In the animals with AD, this mechanism appeared ineffective, as the number of VEGFR2-positive cells remained consistently high in both neurogenic niches until day 28, corresponding to the manifestation of cognitive dysfunction. Thus, neoangiogenesis in the neurogenic niches of animals with experimental AD was characterized by failed mechanisms regulating the subpopulation composition of endothelial cells and impaired stabilization of the endothelial layer in newly formed microvessels by the time of cognitive deficit manifestation (day 28 after training).

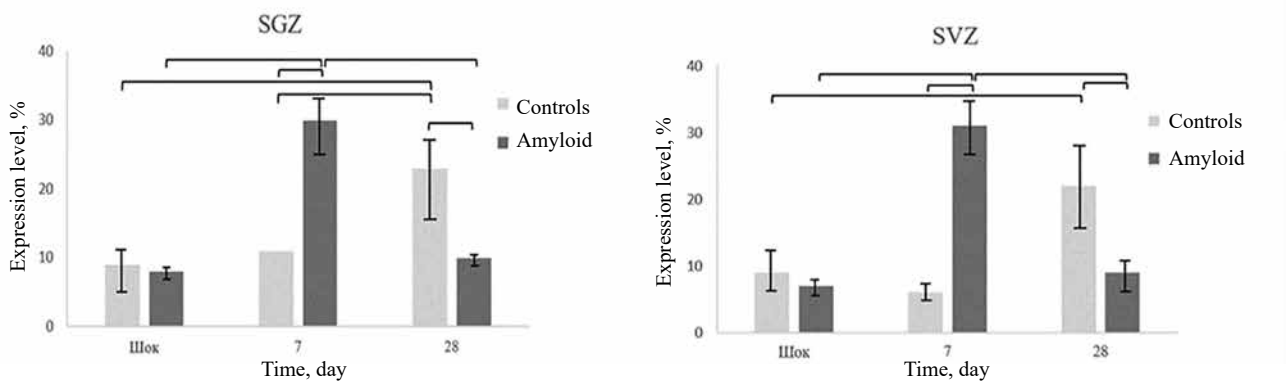

Fig. 1. The number of VEGFR1-positive cells in the SGZ and SVZ of control sham-operated animals (C) and animals with intrahippocampal injection of Aβ25-35 (A) at the time of cognitive training ("shock"), at day 7 and 28 after training, $M + \sigma$, $p < 0.05$

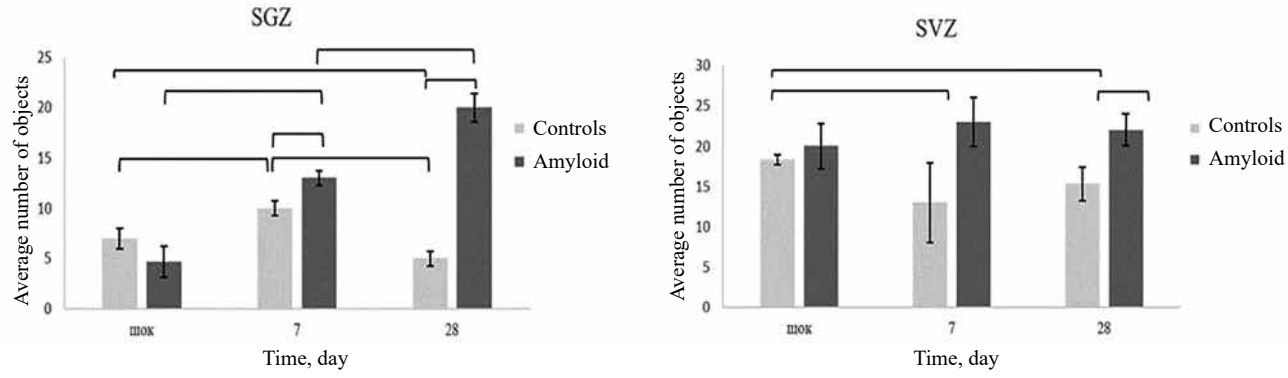

Fig. 2. Changes in the number of VEGFR2-positive cells in the SGZ and SVZ of control sham-operated animals (C) and animals with intrahippocampal injection of Aβ25-35 (A) at the time of training ("shock"), at 7 and 28 days after training. The number of VEGFR2-positive cells is normalized to 100 DAPI+ cells, $M + \sigma$, $p < 0.05$

When assessing VEGFA levels in the brain tissue (Fig. 3), we found that by day 28 after the training, the levels of this angiogenic factor progressively decreased in both control and Aβ-treated animals. However, no statistically significant differences in such changes were found in the control and experimental groups. Therefore, VEGF levels in the brain tissue were not associated with the observed inversion of VEGFR1

and VEGFR2 expression in neurogenic niches in animals of both groups. Apparently, local changes in training-stimulated VEGFA production in the SGZ and SVZ may be responsible for the observed effects, and this requires further study.

Given the findings that in experimental AD, angiogenesis in the neurogenic niches of the brain stimulated by learning might be associated with impaired endothelial layer formation, we further assessed how this related to the maturity of endothelial cells. To do this, we analyzed the ratio of CLDN5-expressing endothelial cells to the total number of CD31-positive cells in neurogenic niches (Fig. 4). Notably, in the SGZ of animals with experimental AD, in contrast to the control group, a significant decrease in the proportion of mature endothelial cells ($CLDN5^+$ $CD31^+$ cells) was registered at day 28, while in the SVZ, similar changes occurred earlier, at day 7, which corresponded to the period preceding the manifestation of cognitive deficit.

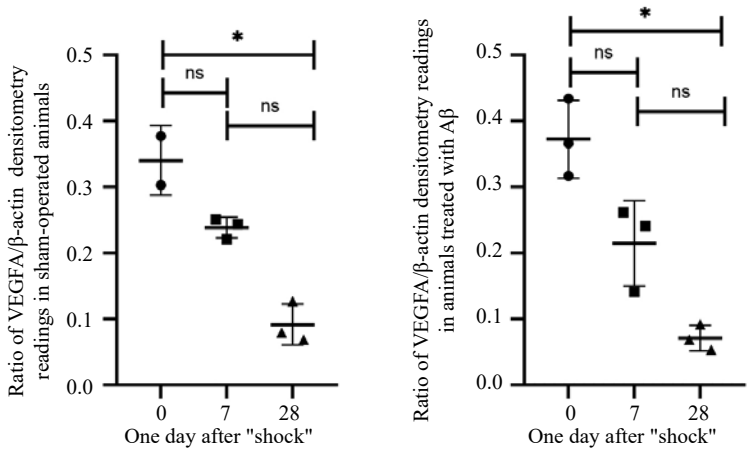

Fig. 3. Densitometry of Western blotting of brain tissue homogenate obtained from sham-operated animals (C) and animals with intrahippocampal injection of Aβ25-35 (A) for VEGFA expression normalized to β-actin expression: ns – no statistically significant differences between the groups, $M + \sigma$, $p < 0.05$

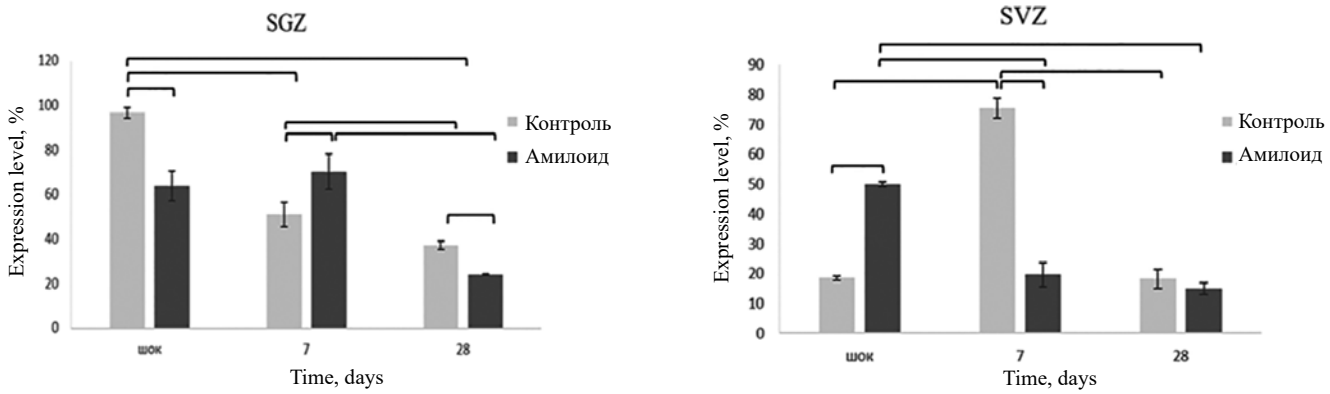

Fig. 4. Changes in the proportion of $CLDN5^+$ cells in the $CD31^+$ endothelial cell population in the SGZ and SVZ of control sham-operated animals (C) and animals with intrahippocampal injection of Aβ25-35 (A) at the time of training ("shock"), at day 7 and 28 after the training, $M + \sigma$, $p < 0.05$

CONCLUSION

When assessing the characteristics of expression of VEGF receptor subtypes and tight junction proteins in the endothelial cells of microvessels in the SGZ and SVZ, we established that cognitive training in the sham-operated animals resulted in intensified neoangiogenesis in the neurogenic niches of the brain, which is likely necessary to maintain effective neurogenesis. These events were accompanied by subpopulational changes in endothelial cells (suggesting lateral inhibition mechanism) and signs of their maturation (increased CLDN5 expression) during 28 days following the training, which was related to the period of emergence of new neurons in the neurogenic niche [24].

In animals with a model of AD, angiogenesis in neurogenic niches was also induced after cognitive training. However, at the time when cognitive deficits manifested (28 days after training), a statistically significant decrease in the number of VEGFR1-expressing cells and maintenance of high VEGFR2 expression were found in these brain regions, indicating failure of endothelial cells to form a stable endothelial layer, likely due to the disruption of lateral inhibition mechanisms. The changes in neoangiogenesis within neurogenic niches observed after the learning session in the animals with AD suggest a potential contribution of this mechanism to the development of neuroinflammation, local microcirculatory dysfunction, and the development of aberrant brain plasticity.

REFERENCES

1. Sehar U., Rawat P., Reddy A.P., Kopel J., Reddy P.H. Amyloid beta in aging and Alzheimer's disease. *International Journal of Molecular Sciences*. 2022;23(21):12924. DOI: 10.3390/ijms232112924.
2. Scopa C., Marrocco F., Latina V., Ruggeri F., Corvaglia V., La Regina. Impaired adult neurogenesis is an early event in Alzheimer's disease neurodegeneration, mediated by intracellular Aβ oligomers. *Cell Death & Differentiation*. 2020;27(3):934–948. DOI: 10.1038/s41418-019-0409-3.
3. Burnyasheva A.O., Stefanova N.A., Rudnitskaya E.A. Neurogenesis in the mature brain: changes in aging and the development of Alzheimer's disease. *Advances in Gerontology*. 2020;33(6):1080–1087. (In Russ.). DOI: 10.34922/AE.2020.33.6.008.
4. Komleva Y.K., Lopatina O.L., Gorina Y.V., Chernykh A.I., Trufanova L.V., Vais E.F. et al. Expression of NLRP3 inflammasomes in neurogenic niche contributes to the effect of spatial learning in physiological conditions but not in Alzheimer's type neurodegeneration. *Cellular and Molecular Neurobiology* 2022; 2(5):1355–1371. DOI: 10.1007/s10571-020-01021-y.
5. Alvarez-Vergara M.I., Rosales-Nieves A.E., March-Diaz R., Rodriguez-Perinan G., Lara-Ureña N., Ortega-de San Luis. Non-productive angiogenesis disassembles Aß plaque-associated blood vessels. *Nature Communications*. 2021;12(1):3098. DOI: 10.1038/s41467-021-23337-z.
6. Lin R., Cai J., Nathan C., Wei X., Schleidt S., Rosenwasser R. et al. Neurogenesis is enhanced by stroke in multiple new stem cell niches along the ventricular system at sites of high BBB permeability. *Neurobiology of Disease*. 2015;(74):229–239. DOI: 10.1016/j.nbd.2014.11.016.
7. Pozhilenkova E.A., Lopatina O.L., Komleva Y.K., Salmin V.V., Salmina A.B. Blood-brain barrier-supported neurogenesis in healthy and diseased brain. *Reviews in the Neurosciences*. 2017;28(4):397–415. DOI: 10.1515/revneuro-2016-0071.
8. Salmina A.B., Gorina Y.V., Komleva Y.K., Panina Y.A., Malinovskaya N.A. Early life stress and metabolic plasticity of brain cells: impact on neurogenesis and angiogenesis. *Biomedicines.* 2021;9(9):1092. DOI: 10.3390/biomedicines9091092.
9. Gorina Ya.V., Osipova E.D., Morgun A.V., Malinovskaya N.A., Komleva Yu.K., Lopatina O.L., et al. Aberrant angiogenesis in brain tissue in experimental Alzheimer's disease. *Bulletin of Siberian Medicine*. 2020;19(4):46–52. (In Russ.). DOI: 10.20538/1682-0363-2020-4-46-52.
10. Morgun A.V., Osipova E.D., Boitsova E.B., Lopatina O.L., Gorina Y.V., Pozhilenkova E.A. et al. Vascular component of neuroinflammation in experimental Alzheimer's disease in mice. *Cell and Tissue Biology.* 2020;(14):256–262. DOI: 10.1134/S1990519X20040057.
11. Averchuk A.S., Ryazanova M.V., Baranich T.I., Stavrovskaya A.V., Rozanova N.A., Novikova S.V., et al. Neurotoxic effect of β-amyloid is accompanied by changes in mitochondrial dynamics and autophagy of neurons and cerebral endothelial cells in an experimental model of Alzheimer's disease. *Bulletin of Experimental Biology and Medicine.* 2023;175(3):291–297. (In Russ.). DOI: 10.47056/0365-9615-2023-175-3-291-297.
12. Lei Y., Chen X., Mo J.L., Lv L.L., Kou Z.W., Sun F.Y. Vascular endothelial growth factor promotes transdifferentiation of astrocytes into neurons via activation of the MAPK/Erk-Pax6 signal pathway. *Glia.* 2023;71(7):1648–1666. DOI: 10.1002/glia.24361.
13. Okabe K., Fukada H., Tai-Nagara I., Ando T., Honda T., Nakajima K. Neuron-derived VEGF contributes to cortical and hippocampal development independently of VEGFR1/2-mediated neurotrophism. *Developmental Biology*. 2020;459(2):65–71. DOI: 10.1016/j.ydbio.2019.11.016.
14. Monaghan R.M., Page D.J., Ostergaard P., Keavney B.D. The physiological and pathological functions of VEGFR3 in cardiac and lymphatic development and related diseases. *Cardiovascular Research.* 2021;117(8):1877–1890. DOI: 10.1093/cvr/cvaa291.
15. Wittko-Schneider I.M., Schneider F.T., Plate K.H. Brain homeostasis: VEGF receptor 1 and 2—two unequal brothers in mind. *Cellular and Molecular Life Sciences*. 2013;70(10):1705–1725. DOI: 10.1007/s00018-013-1279-3.
16. Argaw A.T., Asp L., Zhang J., Navrazhina K., Pham T., Mariani J.N. et al. Astrocyte-derived VEGF-A drives blood-brain barrier disruption in CNS inflammatory disease. *The Journal of Clinical Investigation.* 2012;122(7):2454–2468. DOI: 10.1172/JCI60842.
17. De Smet F., Segura I., De Bock K., Hohensinner P.J., Carmeliet P. Mechanisms of vessel branching: filopodia on endothelial tip cells lead the way. *Arteriosclerosis, Thrombosis, and Vascular Biology*. 2009;29(5):639–649. DOI: 10.1161/ATVBAHA.109.185165.
18. Lacal P. M., Graziani G. Therapeutic implication of vascular endothelial growth factor receptor-1 (VEGFR-1) targeting in cancer cells and tumor microenvironment by competitive and non-competitive inhibitors. *Pharmacological Research*. 2018;136:97–107. DOI: 10.1016/j.phrs.2018.08.023.
19. Okabe K., Fukada H., Tai-Nagara I., Ando T., Honda T., Nakajima K. et al. Neuron-derived VEGF contributes to cortical and hippocampal development independently of VEGFR1/2-mediated neurotrophism. *Developmental Biology*. 2020;459(2):65–71. DOI: 10.1016/j.ydbio.2019.11.016.

20. Hashimoto Y., Greene C., Munnich A., Campbell M. The CLDN5 gene at the blood-brain barrier in health and disease. *Fluids and Barriers of the CNS*. 2023;20(1):22. DOI: 10.1186/s12987-023-00424-5.
21. Salmin V.V., Salmina A.B., Morgun A.V. RF Patent No. 2020612777. Plugin for ImageJ program for counting fluorescent labels on microphotographs. *Bulletin of Experimental Biology and Medicine.* 2020;(3). Published on 03.03.2020 (in Russ.).
22. Ryazanova M.V., Averchuk A.S., Stavrovskaya A.V., Rozanova N.A., Novikova S.V., Salmina A.B. Arc/Arg3.1 expression in the brain tissues during the learning process in Alzheimer's disease animal models. *Annals of Clinical and Experimental Neurology*. 2023;17(3):49–56. (In Russ.). DOI: 10.54101/ACEN.2023.3.6
23. Naito H., Iba T., Takakura N. Mechanisms of new blood-vessel formation and proliferative heterogeneity of endothelial cells. *International Immunology*. 2020;32(5):295305. DOI: 10.1093/intimm/dxaa008.
24. Niklison-Chirou M.V., Agostini M., Amelio I., Melino G. Regulation of adult neurogenesis in mammalian brain. *International Journal of Molecular Sciences*. 2020;21(14):4869. DOI: 10.3390/ijms21144869.

Authors' contribution

Kukla M.V. – design of the study, performing tests and immunohistochemical studies, drafting of the manuscript. Averchuk A.S. – performing immunohistochemical studies, processing of the data, drafting of the manuscript. Stavrovskaya A.V. – performing surgery, animal testing, processing of the data. Rozanova N.A. – preparing brain sections, performing immunohistochemistry. Berdnikov A.K., Kolotyeva N.A. – performing immunoblotting, analysis and interpretation of the data. Salmina A.B. – conception and design, processing of the obtained data, drafting of the manuscript, final approval of the manuscript for publication.

Acknowledgements

The authors would like to express their gratitude to the Laboratory of Experimental Pathology of the Nervous System and Neuropharmacology of the Research Center of Neurology for performing stereotactic surgery on animals, as well as to S.O. Yurchenko, Dr. Sci. (Physics and Mathematics), Head of the Research and Education Center "Soft Matter and Fluid Physics" of the Bauman Moscow State Technical University and A. Kopylova, Junior Researcher, for providing the opportunity to work and for providing assistance in conducting research on the Image ExFluorer visualization system.

Authors' information

Kukla Mariya V. – Post-Graduate Student, Researcher, Laboratory of Neurobiology and Tissue Engineering, Brain Science Institute, Research Center of Neurology, Moscow, mashenka.ryazanova@list.ru, https://orcid.org/0000-0003-0700-4912

Averchuk Anton S. – Cand. Sci. (Biology), Associate Professor, Senior Researcher, Laboratory of Neurobiology and Tissue Engineering, Brain Science Institute, Research Center of Neurology, Moscow, antonaverchuk@yandex.ru, https://orcid.org/0000-0002-1284-6711

Stavrovskaya Alla V. – Cand. Sci. (Biology), Leading Researcher, Laboratory of Experimental Pathology of the Nervous System and Neuropharmacology, Brain Science Institute, Research Center of Neurology, Moscow, alla_stav@mail.ru, https://orcid.org/0000-0002-8689-0934

Rozanova Nataliya A. – Post-Graduate Student, Researcher, Laboratory of Neurobiology and Tissue Engineering, Brain Science Institute, Research Center of Neurology, Moscow, nataliarozanovaa@gmail.com, https://orcid.org/0000-0001-9619-4679

Berdnikov Arseniy K. – Post-Graduate Student, Researcher, Laboratory of Neurobiology and Tissue Engineering, Brain Science Institute, Research Center of Neurology, Moscow, akberdnikov@gmail.com, https://orcid.org/0009-0007-4195-2533

Kolotyeva Nataliya A. – Dr. Sci. (Med.), Associate Professor, Senior Researcher, Laboratory of Neurobiology and Tissue Engineering, Brain Science Institute, Research Center of Neurology, Moscow, bortnikova.n@gmail.com, https://orcid.org/0000-0002-7853-6222

Salmina Alla B. – Dr. Sci. (Med.), Professor, Head of the Laboratory of Neurobiology and Tissue Engineering, Brain Science Institute, Research Center of Neurology, Moscow, allasalmina@mail.ru, https://orcid.org/0000-0003-4012-6348

(✉) **Kukla Mariya V.,** mashenka.ryazanova@list.ru

Received 30.05.2024;
approved after peer review 02.07.2024;
accepted 12.09.2024

УДК 616.345-006.6:575.117:616.155.33
https://doi.org/10.20538/1682-0363-2024-4-55-63

Phenotypic profile of blood monocytes and tumor-associated macrophages in relation to the expression of galectins 1 and 3 in colorectal cancer

Kurnosenko A.V.[1, 2], Reingardt G.V.[1, 2], Poletika V.S.[1], Kolobovnikova Yu.V.[1], Chumakova S.P.[1], Urazova O.I.[1], Grishchenko M.Yu.[1, 2], Churina E.G.[1], Gamirova K.A.[1, 2]

[1] *Siberian State Medical University*
2, Moscow Trakt, Tomsk, 634050, Russian Federation

[2] *Tomsk Regional Cancer Center*
115, Lenina Av., Tomsk, 634050, Russian Federation

ABSTRACT

Aim. To identify the features of the subpopulation composition of blood monocytes and tumor macrophages in relation to the plasma concentration and intratumoral expression of galectins 1 and 3 in patients with colorectal cancer.

Materials and methods. A total of 23 patients with colorectal cancer (ICD C18-20) were examined – 5 men and 18 women (average age 63.8 ± 9.4 years). The control group consisted of healthy volunteers; the comparison group encompassed age- and sex-matched patients with colon adenomas. The study materials included whole blood and tumor biopsies. The concentration of galectins 1 and 3 in the blood was determined by enzyme-linked immunosorbent assay, the content of tumor galectin-1^+ and galectin-3^+ cells – by immunohistochemistry. Subpopulations of blood monocytes were evaluated by flow cytometry; the macrophage immunophenotypes M1 ($CD68^+CD80^+$) and M2d ($CD68^+CD206^+$) in tumor tissues were determined using immunofluorescence staining. Statistical processing of the research results was performed by the Jamovi 2.3.21 software package for Windows.

Results. In patients with colorectal cancer (CRC), a positive relationship was identified between high plasma concentrations of galectins 1 and 3 and an imbalance of blood monocytes manifested by a decrease in the relative count of classical $CD14^{++}CD16^-$ monocytes and, conversely, an increase in the number of non-classical $CD14^+CD16^{++}$ and intermediate $CD14^+CD16^-$ cells. The relative numbers of M1 ($CD68^+CD80^+$) and M2d ($CD68^+CD206^+$) macrophages in CRC tissue samples turned out to be comparable and did not depend on the level of galectins 1 and 3 in the blood and tumor. In patients with colon adenomas, the M2d subpopulation of tumor-associated macrophages was predominant ($p = 0.031$).

Conclusion. In patients with CRC, galectins 1 and 3 have a modulating effect on the ratio of non-classical $CD14^+CD16^{++}$, intermediate $CD14^+CD16^-$, and classical $CD14^{++}CD16^-$ monocytes in the blood and do not affect the M1/M2d expression profile of tumor-associated macrophages.

Keywords: galectins, monocytes, macrophages, colorectal cancer, immunophenotype

Conflict of interest. The authors declare the absence of obvious or potential conflicts of interest related to the publication of this article.

Source of financing. The authors state that they received no funding for the study.

Conformity with the principles of ethics. All patients signed an informed consent to participate in the study. The study was approved by the Ethics Committee at Siberian State Medical University (Protocol No. 8881 of 29.11.2021).

For citation: Kurnosenko A.V., Reingardt G.V., Poletika V.S., Kolobovnikova Yu.V., Chumakova S.P., Urazova O.I., Grishchenko M.Yu., Churina E.G., Gamirova K.A. Phenotypic profile of blood monocytes and tumor-

✉ *Kurnosenko Anna V.,* kurnosenko.av@ssmu.ru

associated macrophages in relation to the expression of galectins 1 and 3 in colorectal cancer. *Bulletin of Siberian Medicine.* 2024;23(4):55–63. https://doi.org/10.20538/1682-0363-2024-4-55-63.

Фенотипический профиль моноцитов крови и опухоль-ассоциированных макрофагов во взаимосвязи с экспрессией галектинов 1 и 3 при раке толстой кишки

Курносенко А.В.[1,2], Рейнгардт Г.В.[1,2], Полетика В.С.[1], Колобовникова Ю.В.[1], Чумакова С.П.[1], Уразова О.И.[1], Грищенко М.Ю.[1,2], Чурина Е.Г.[1], Гамирова К.А.[1,2]

[1] *Сибирский государственный медицинский университет (СибГМУ)*
Россия, 634055, г. Томск, Московский тракт, 2

[2] *Томский областной онкологический диспансер (ТООД)*
Россия, 634040, г. Томск, пр. Ленина, 115

РЕЗЮМЕ

Цель. Выявить особенности субпопуляционного состава моноцитов крови и макрофагов опухоли во взаимосвязи с плазменной концентрацией и внутриопухолевой экспрессией галектинов 1 и 3 у больных раком толстой кишки.

Материалы и методы. Обследованы 23 больных колоректальным раком (МКБ С18–20) – 5 мужчин и 18 женщин, средний возраст (63,8 ± 9,4) лет. Группу контроля составили здоровые добровольцы, группу сравнения – пациенты с аденомами толстой кишки, сопоставимые по полу и возрасту. Материалом исследования являлись цельная кровь и биоптаты опухоли. Концентрацию галектинов 1 и 3 в крови определяли методом иммуноферментного анализа, содержание опухолевых галектин-1^+ и галектин-3^+ клеток – методом иммуногистохимии. Подсчет субпопуляций моноцитов крови выполняли методом проточной цитофлуориметрии, определение иммунофенотипов M1 ($CD68^+CD80^+$) и M2d ($CD68^+CD206^+$) макрофагов в опухолевой ткани – методом иммунофлуоресценции. Результаты исследования обрабатывали статистическими методами с применением программного пакета Jamovi 2.3.21 для Windows.

Результаты. У больных раком толстой кишки (РТК) установлена положительная связь между высокой плазменной концентрацией галектинов 1 и 3 и нарушением баланса моноцитов крови в виде снижения относительного содержания классических $CD14^{++}CD16^-$ моноцитов и, напротив, увеличения численности неклассических $CD14^+CD16^{++}$ и переходных $CD14^+CD16^-$ клеток. Относительное количество M1 ($CD68^+CD80^+$) и M2d ($CD68^+CD206^+$) макрофагов в образцах тканей РТК оказалось сопоставимым и не зависело от уровня галектинов 1 и 3 в крови и опухоли. У пациентов с аденомами толстой кишки преобладала M2d-субпопуляция опухоль-ассоциированных макрофагов ($p = 0{,}031$).

Заключение. У больных РТК галектины 1 и 3 оказывают модулирующее влияние на соотношение неклассических CD14+$CD16^{++}$, переходных $CD14^+CD16^-$ и классических $CD14^{++}CD16^-$ моноцитов в крови и не влияют на формирование M1/M2d-экспрессионного профиля опухоль-ассоциированных макрофагов.

Ключевые слова: галектины, моноциты, макрофаги, рак толстой кишки, иммунофенотип

Конфликт интересов. Авторы декларируют отсутствие явных и потенциальных конфликтов интересов, связанных с публикацией настоящей статьи.

Источник финансирования. Авторы заявляют об отсутствии финансирования при проведении исследования.

Соответствие принципам этики. Все пациенты подписали информированное согласие на участие в исследовании. Исследование одобрено этическим комитетом СибГМУ (протокол № 8881 от 29.11.2021).

Для цитирования: Курносенко А.В., Рейнгардт Г.В., Полетика В.С., Колобовникова Ю.В., Чумакова С.П., Уразова О.И., Грищенко М.Ю., Чурина Е.Г., Гамирова К.А. Фенотипический профиль моноцитов крови и опухоль-ассоциированных макрофагов во взаимосвязи с экспрессией галектинов 1 и 3 при раке толстой кишки. *Бюллетень сибирской медицины.* 2024;23(4):55–63. https://doi.org/10.20538/1682-0363-2024-4-55-63.

INTRODUCTION

Colorectal cancer (CRC) is one of the top malignancies in terms of morbidity and mortality both in Russia and worldwide [1, 2]. Despite significant efforts aimed at early detection of CRC and improvement of treatment methods, in half of cases, the disease is diagnosed at stage III–IV. One-year mortality amounts to 19.2%, and five-year survival is 57%. There is also an increase in the CRC incidence among young people [3].

The pathogenesis of CRC is based on the interaction of tumor cells with the tumor microenvironment (macrophages, endothelial and mesenchymal progenitor cells, fibroblasts, etc.). These interactions are mediated by many regulatory molecules, including galectins – proteins that bind to β-galactosides. Molecules of this family are characterized by a common carbohydrate-recognition domain and exert a variety of functions both extra- and intracellularly [4–7]. It has been shown that the pool of tumor-associated macrophages, myeloid-derived suppressor cells, and individual dendritic cells is replenished by blood monocytes [8].

The aim of the study was to identify the features of the subpopulation composition of blood monocytes and tumor-associated macrophages in relation to the plasma concentration and intratumoral expression of galectins 1 and 3 in patients with CRC.

MATERIALS AND METHODS

The study included 23 patients with verified CRC (ICD C18-20) – 5 men and 18 women (mean age 63.8 ± 9.4 years), who were registered at Tomsk Regional Cancer Center (chief physician – Maksim Yu. Grishchenko, Cand. Sci. (Med.), Associate Professor). The patients were divided into groups according to the stage of the disease: the group with stage I CRC included 4 people, with stage II – 9 patients, with stage III – 5 patients, and with stage IV – 5 patients. The comparison group encompassed patients with colon adenomas – 8 men and 7 women (mean age 60.7 ± 10.4 years). The control group included 11 healthy volunteers (6 men and 5 women aged 61.5 ± 9.7 years) from those who visited the institution for a regular health checkup.

The exclusion criteria were: chronic inflammatory non-infectious or infectious (in the acute phase) and autoimmune or allergic (without achieving control) diseases, purulent processes, other malignant neoplasms, antitumor therapy (at the time of the study and in medical history), as well as refusal to participate in the study. Each subject signed an informed consent. The study was approved by the Ethics Committee at Siberian State Medical University (Protocol No. 8881 of 29.11.2021). Information about the patient's age, diagnosis, tumor localization, and cancer stage was obtained from medical records.

The study material was whole venous blood and tumor biopsy samples (malignant and benign) obtained from the colon. The concentration of galectin 1 and galectin 3 in blood plasma was measured by enzyme-linked immunosorbent assay using the Boster Bio ELISA kits (USA). The expression of galectins in tumor biopsy samples was determined by immunohistochemistry using a standard technique. The number of monocyte subpopulations was counted by flow cytometry on the BD Accuri flow cytometer (USA) using antibodies to CD14 labeled with R-Phycoerythrin and antibodies to CD16 labeled with FITC.

Sample preparation involved lysis of erythrocytes, washing of leukocytes, addition of fluorochrome-labeled antibodies to the cell suspension according to the manufacturer's instructions, incubation of the solution, and addition of the staining buffer. The number of each monocyte subpopulation was evaluated according to the expression of CD14 and CD16 on the cell membranes. Monocytes expressing $CD14^{+}CD16^{++}$ were classified as non-classical, $CD14^{+}CD16^{-}$ – as classical, and $CD14^{++}CD16^{+}$ – as intermediate cells.

To assess the colocalization of CD68, CD206, and CD80 molecules on the surface of macrophages, triple immunofluorescence staining of paraffin sections (according to the standard technique) was performed, followed by confocal microscopy. For immunofluorescence staining, the following primary antibodies were used: mouse monoclonal anti-CD68 (Novus Biologicals, NBP2 445-39, clone KP1, 1:200 working dilution, USA), rabbit polyclonal anti-CD80 (Abcam, ab64116, 1:70 working dilution, USA), goat polyclonal anti-CD206 (R&D Systems, AF2634, 1:40 working dilution, USA). Additionally, the following combinations of secondary antibodies were utilized: anti-mouse Alexa Fluor 488-labeled, anti-rabbit Alexa Fluor 555-labeled, anti-goat Alexa Fluor 647-labeled (working dilution of all secondary antibodies was 1:400). When staining cell nuclei, DAPI fluorescent stain (ab104135, Abcam, USA) was used for their subsequent visualization on the Carl Zeiss LSM 780 NLO confocal microscope (Germany). The results were analyzed using the Black Zen and Qupath 0.4.4 software (Fig.1).

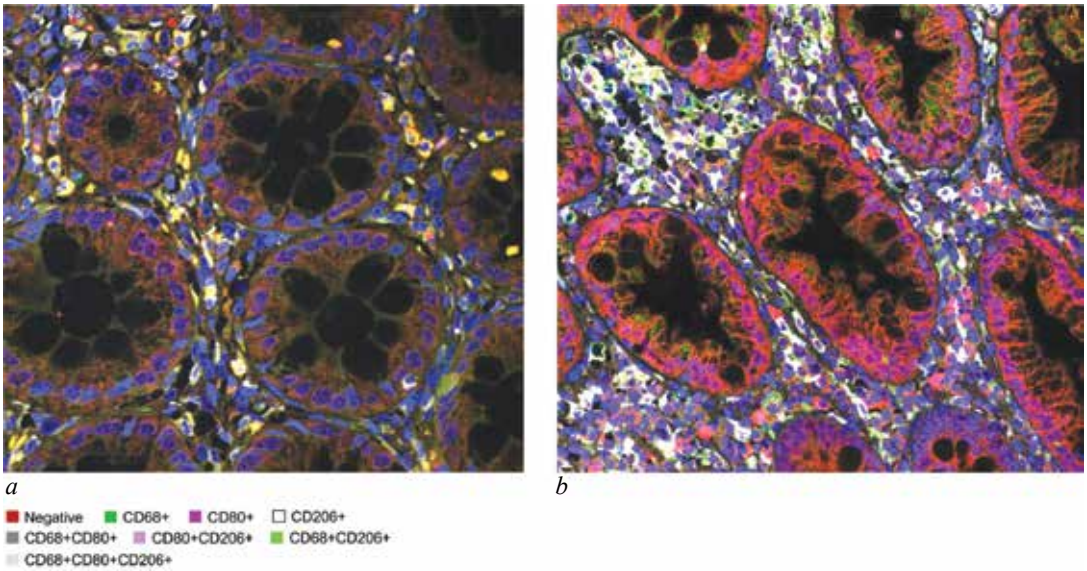

Fig. 1. Immunofluorescence staining of paraffin sections: *a* – colorectal cancer, *b* – colon adenoma

Based on the expression of the CD68/CD206/CD80 markers, $CD68^+CD80^+$ macrophages were considered as cells with M1 immunophenotype, and $CD68^+CD206^+$ – as cells with M2d immunophenotype. Since CD68 is a common marker for macrophages [9], the number of $CD68^+$ cells was initially assessed as a percentage of all stromal cells, and then the relative number of $CD68^+CD206^+$ and $CD68^+CD80^+$ cells was determined.

Statistical analysis of the results was performed using the Jamovi 2.3.21 software package for Windows. The Kolmogorov – Smirnov and the Shapiro – Wilk tests were used to check the normality of distribution of the studied variables. The Mann – Whitney *U*-test was used to assess the statistical significance of differences in quantitative variables between the samples. The Spearman's rank correlation coefficient (r_s) was calculated to identify relationships between paired quantitative variables. The results were considered statistically significant at $p < 0.05$.

RESULTS

According to our previous study [10], the content of galectin 1-expressing cells in the tumor tissue of patients with CRC was higher than in the comparison group: 33.5 (27.0; 55.0) % in CRC and 11.0 (5.0; 21.0) % in colon adenomas ($p < 0.001$). Similarly, the concentration of galectins 1 and 3 in the peripheral blood of individuals with CRC was higher than in patients with colon adenoma and healthy donors by 2.5 and 6.6 times, respectively ($p < 0.001$). A positive correlation was found between the concentration of galectin 1 and galectin 3 in peripheral blood plasma ($rs = 0.843$, $p < 0.01$).

Statistically significant differences in the number of classical, intermediate, and non-classical blood monocytes were found between the studied groups (Table 1). At the same time, the total number of leukocytes ($p = 0.201$) and monocytes ($p = 0.673$) in the blood was comparable.

Table 1

Subpopulation composition of blood monocytes in patients with colorectal cancer, *Me* (Q_1; Q_3)

Subpopulations of monocytes, %	Patients with CRC	Healthy donors
Classical $CD14^+CD16^-$	75.53 (71.41; 78.12)	88.66 (86.06; 93.29)
	$p < 0.001$	
Intermediate $CD14^{++}CD16^+$	8.76 (6.19; 10.53)	1.87 (0.93; 2.6)
	$p < 0.001$	
Non-classical $CD14^+CD16^{++}$	15.08 (11.80; 19.91)	4.09 (1.26; 5.51)
	$p < 0.001$	

The increase in the number of non-classical $CD14^+CD16^{++}$ monocytes had a direct strong correlation with the level of galectin 1 ($rs = 0.557$) and galectin 3 ($rs = 0.780$) in blood plasma. A similar relationship was observed for the number of intermediate $CD14^{++}CD16^+$ monocytes: a direct strong correlation was identified with the concentration of galectin 1 ($rs = 0.618$) and galectin 3 ($rs = 0.617$) in blood plasma.

Therefore, in patients with CRC, an increase in the number of $CD16^+$ monocytes in the blood was revealed compared to the group of healthy volunteers.

A direct strong correlation was determined between the number of non-classical monocytes and low tumor differentiation grade (G3), i.e. a high malignant potential of the tumor. On the other hand, an inverse strong relationship was identified between the number of classical monocytes ($CD14^{++}CD16^{-}$) in the blood and tumor differentiation grade ($rs = –0.469$, $p < 0.01$), the level of galectin 1 ($rs = –0.663$, $p < 001$) and galectin 3 ($rs = –0.804$, $p < 0.001$) in the blood plasma.

Following the analysis of the subpopulation composition of macrophages in tumor biopsy samples in patients with CRC and colon adenomas, no differences in the content of tumor-associated $CD68^{+}CD80^{+}$ macrophages (with the M1 phenotype) were found between the groups. The number of $CD68^{+}CD206^{+-}$ cells (macrophages with the M2d phenotype) in patients with CRC was 1.9 times smaller than in patients with colon adenomas (Table 2). At the same time, in patients with colon adenomas, relative predominance of the M2d macrophages in the tumor tissue was discovered ($p = 0.030$), while in CRC, the ratio of tumor-associated M1- and M2d macrophages was comparable.

Table 2

Subpopulation composition of tumor-associated macrophages in patients with colorectal cancer, *Me* (Q_1; Q_3)

Immunophenotype of macrophages, %	Colorectal cancer	Colon adenoma
M1 ($CD68^{+}CD80^{+}$)	4.34 (1.80; 6.74)	4.26 (1.19; 6.53)
	$p = 0.454$	
M2d ($CD68^{+}CD206^{+}$)	3.21 (2.01; 4.79)	6.10 (3.97; 7.71)
	$p = 0.031$	

The example of stained tumor tissue samples is shown in Fig. 2.

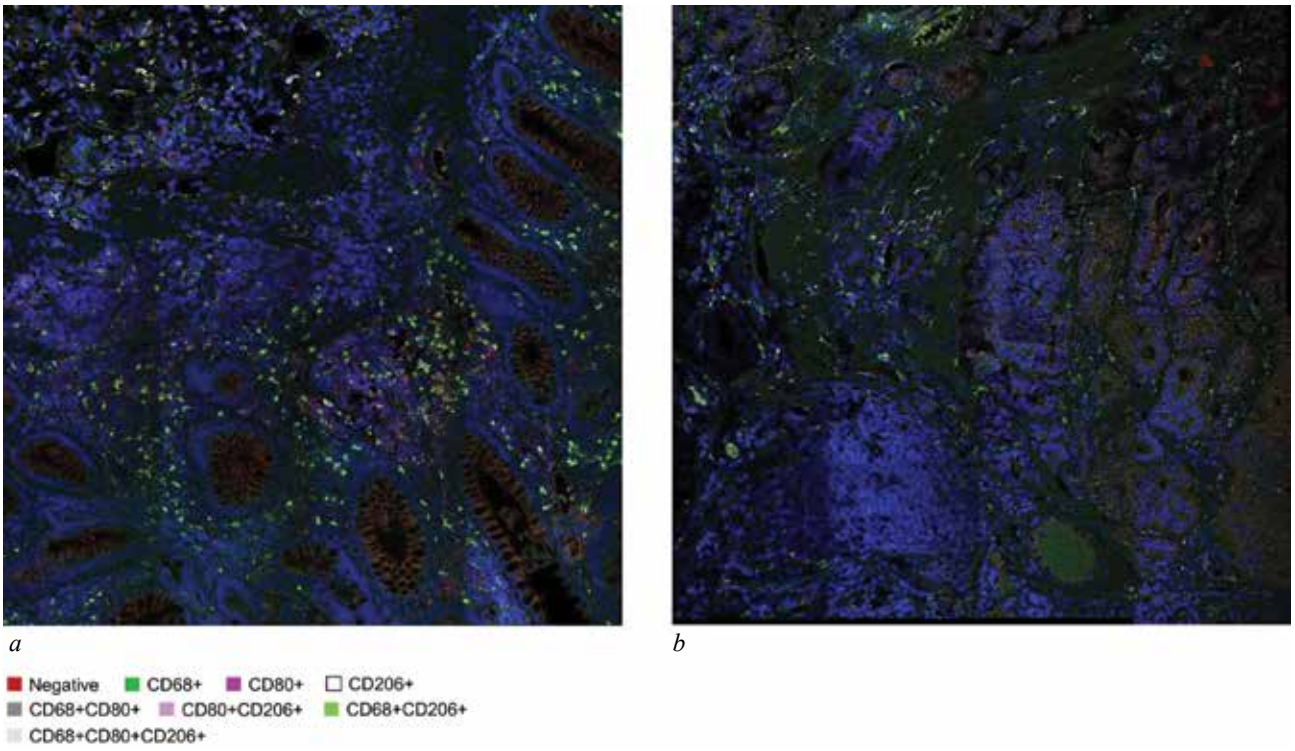

Fig. 2. Staining of tumor tissue specimens

The correlation analysis of the M1 / M2 expression profile of tumor-associated macrophages and the content of galectins 1 and 3 in peripheral blood and tumor tissue found no statistically significant relationships.

DISCUSSION

Galectins are a family of proteins expressed by a variety of cells, including cells in a tumor [11]. Among the lectins involved in the pathogenesis of cancer, galectin 1 and galectin 3 are of particular importance [12, 13]. These molecules not only affect the properties of tumor cells, such as the ability to proliferate and metastasize (detachment from the primary tumor, aggregation, adhesion, intra- and extravasation, migration, and invasion) and susceptibility to programmed cell death [14], but also participate in the interaction of the tumor with immunocompetent

cells having immunosuppressive properties, which contributes to tumor escape from immune surveillance [4]. The mechanism underlying this effect is based on binding of galectins to CD receptors on leukocytes, which regulates maturation of polarization, activation, and apoptosis of these cells [15, 16]. Galectins-1 and 3 also exhibit predominantly anti-inflammatory and tolerogenic (suppressive) effects toward macrophages, directing their polarization along the alternative M2 pathway [17, 18]. Macrophages differentiated in this way, in turn, actively synthesize galectin 1 and galectin 3 themselves, while classical M1 macrophages, on the contrary, are characterized by low expression of these lectins [19].

According to N.N. Sarbaeva (2016), the identification of two distinct macrophage subpopulations (M1 and M2) does not fully characterize the diversity of macrophage immunophenotypes due to their plasticity [20]. Macrophages with the anti-inflammatory M2 phenotype are classified into M2a, M2b, M2c, and M2d subpopulations. Such differences between the cells are due to the set of intracellular and membrane molecules expressed by them (transcription factors, differentiation clusters, receptors for cytokines and chemokines, etc.), secreted cytokines (mainly interleukin (IL) 10 and transforming growth factor β (TGFβ)), and functions (phagocytosis, activation of cell growth and regeneration processes, maintenance of tissue homeostasis, polarization of the immune response toward the Th2 (humoral) or Th17 (autoimmune) pathway, or Treg-mediated immunosuppression, etc.). According to the literature, macrophages expressing CD68 and CD206 markers (i.e. with the M2d phenotype) promote tumor growth, angiogenesis (including tumor vascularization through production of proangiogenic mediators), and extracellular matrix remodeling [21, 22].

Galectins 1 and 3 act as chemoattractants for monocytes newly recruited to the tumor site, thereby forming a vicious circle that promotes tumor progression [23, 17]. There is evidence that galectin 1 promotes M2 polarization of macrophages by regulating arginine metabolism and reducing nitric oxide production [24].

According to the results of the present study, patients with colitis showed a slight trend toward an increase in the proportion of M1 macrophages compared to patients with colon adenomas. This could be attributed to the involvement of inflammation in the mechanisms of malignant tumor growth. Inflammation can both precede the development of colitis-associated CRC and accompany the formation and progression of a tumor not associated with colitis. A colon tumor formed in the context of chronic inflammation is morphologically characterized by pronounced infiltration with immunocompetent cells, which in turn are a source of pro- and anti-tumorigenic and proinflammatory cytokines [25].

In a benign tumor (adenoma) of the colon, we found an imbalance in the ratio of M1 / M2 macrophages with the predominance of the M2d subpopulation, which, according to many authors, is more characteristic of malignant tumors [26–28]. Interpreting the obtained results, it should be noted that in most studies, the authors evaluate the immunophenotype of tumor-associated macrophages in comparison to healthy tissue samples. In our study, we assessed the ratio of M1 / M2 macrophages in CRC compared to their content in patients with colon adenoma.

Division of macrophages into polarized subpopulations (M1 and M2) is more consistent with *in vitro* conditions and does not fully reflect the heterogeneity of these cells *in vivo*. Markers that determine the M1 and M2 immunophenotypes can be simultaneously expressed on a single cell. For example, macrophages of human skin wounds, along with cytokines characteristic of M1 cells, synthesize IL-10 and express CD206, CD163, CD36, and the receptor for IL-4 on their membranes [29]. The possibility of direct and reverse transformation of M1 and M2 immunophenotypes accompanied by changes in the spectrum of secreted cytokines and efferocytosis (the process of burying dead cells – removal of apoptotic cells by phagocytosis) has been described [30, 31].

At the same time, there are no standardized methods for the quantitative assessment of macrophages, and significant differences in the protocols for their immunofluorescence typing exist [32]. To assess the subpopulation composition of macrophages, researchers use various combinations of surface molecules [33–35] due to the lack of highly specific markers. In our study, to level out the subjective component of the assessment, we used the QuPath software, which allows to automate cell counting or exclude the "tumor" component from the analysis and assess only the cells of the tumor microenvironment.

The pool of tumor-associated macrophages, immunosuppressive cells of myeloid origin, and immunogenic and tolerogenic dendritic cells is replenished via migration of monocytes originated from the bone marrow into tissues. The influence of the tumor on monocytes can manifest itself not only

within the tumor site, but also directly at the level of their precursors in the bone marrow or spleen. In turn, monocytes themselves produce cytokines and chemokines, thereby participating in the recruitment of new immune cells into the tumor site and maintaining inflammation [8].

According to some authors, the properties of tissue-associated macrophages are determined by the status of blood monocytes, while others claim that the role of monocytes in the formation of macrophage immunophenotypes is ambiguous [8, 30], and their differentiation depends on the interaction of cells with elements of the microenvironment and is mediated by growth factors, extracellular matrix components, etc. [23]. Galectin 1 is an inducer of monocyte chemotaxis and can modulate the expression of major histocompatibility antigens and FcγRI receptors, which mediate phagocytosis [28].

In the present study, we hypothesized that galectins 1 and 3 are capable of influencing the direction of polarization of monocytes as precursors of tumor-associated macrophages. According to our results, patients with CRC were characterized by a decrease in the content of classical monocytes in the blood, while the number of cells with alternative immunophenotypes – non-classical and intermediate monocytes – was increased.

According to the literature, an increase in the number of circulating non-classical $CD14^{+}CD16^{++}$ monocytes may be associated with their specific function of synthetizing growth factors, and an increase in the intermediate $CD14^{++}CD16^{+}$ monocyte count – with the production of tumor necrosis factor alpha (TNFα), which acts as a mediator of tumor-associated inflammation [29]. The positive relationship between high content of galectin 1 and galectin 3 and the increase in the number of non-classical $CD14^{+}CD16^{++}$ and intermediate $CD14^{++}CD16^{+}$ monocytes in the blood identified in our study indicates the possible effect of these lectins on the polarization of monocyte subpopulations toward CD16-positive cells.

The obtained quantitative data were not associated with the clinical and morphological parameters of the tumor, gender, and age of patients. We believe that this can be attributed to the variability of the clinical course of the underlying disease and the diversity of its symptoms, which depend on the location of the primary tumor node, the features of tumor growth, the presence of complications, the severity of inflammation-related manifestations of alteration accompanying cancer, etc.

The absence of a relationship between the content of galectins 1 and 3 in the blood and in the tumor with the M1 / M2 expression profile of tumor-associated macrophages in patients with CRC, on the one hand, indicates that galactoside-binding proteins do not have a significant distant and local effect on the maturation and functional specialization of tissue macrophages. On the other hand, this might be due to an insufficient sample size, which requires further, more detailed studies with an increase in sample data and expansion of the spectrum of tested regulatory biomolecules capable of polarizing the differentiation of myeloid cells within the tumor microenvironment.

CONCLUSION

We revealed galectin-1, 3-dependent changes in the subpopulation composition of monocytes: a decrease in the number of classical $CD14^{++}CD16^{-}$ cells and an increase in the number of non-classical $CD14^{+}CD16^{++}$ and intermediate $CD14^{+}CD16^{-}$ cells in the peripheral blood of patients with CRC. Elevated content of galectin 1-expressing tumor cells and high concentration of galectins 1 and 3 in the blood plasma did not influence the ratio of M1 ($CD68^{+}CD80^{+}$) and M2d ($CD68^{+}CD206^{+}$) tumor-associated macrophages.

A detailed study of the immunoregulatory effect of galectins on individual subpopulations of blood monocytes and tissue macrophages opens up prospects for the use of these lectins as new biomarkers for CRC and molecular targets for innovative methods of targeted and immune (via reprogramming of the tumor microenvironment) therapy for colon cancer.

REFERENCES

1. Sung H., Ferlay J., Siegel R.L., Laversanne M., Soerjomataram I., Jemal A. et al. Global cancer statistics 2020: GLOBOCAN estimates of incidence and mortality worldwide for 36 cancers in 185 countries. *CA Cancer J. Clin*. 2021;71(3):209–249. DOI: 10.3322/caac.21660.
2. Siegel R.L., Wagle N.S., Cercek A., Smith R.A., Jemal A. Colorectal cancer statistics, 2023. *CA Cancer J. Clin.* 2023;73(3):233–254. DOI: 10.3322/caac.21772.
3. Kaprin A.D., Starinsky V.V., Shakhzadova A.O. The state of cancer care for the Russian population in 2021. M: P.A.Hertsen Moscow Oncology Research Institute (MORI) – branch of the National Medical Research Center of Radiology of the Ministry of Health of the Russian Federation. 2022:239 (in Russ.).
4. Cherdyntseva N.V., Mitrofanova I.V., Buldakov M.A., Stakheeva M.N., Patysheva M.R., Zavjalova M.V., et al. Macrophages and tumor progression: on the way to macrophage-specific therapy. *Bulletin of Siberian Medicine*. 2017;16(4):61–74 (in Russ.).
5. Chou F.C., Chen H.Y., Kuo C.C., Sytwu H.K. Role of galectins in tumors and in clinical immunotherapy. *Int. J. Mol. Sci.* 2018;19(2):430. DOI: 10.3390/ijms19020430.

6. Orozco C.A., Martinez-Bosch N., Guerrero P.E., Vinaixa J., Dalotto-Moreno T., Iglesias M. et al. Targeting galectin-1 inhibits pancreatic cancer progression by modulating tumor-stroma crosstalk. *Proc. Natl. Acad. Scio USA.* 2018;115(16):e3769–778. DOI: 10.1073/pnas.1722434115.
7. Lin Y.H., Qiu D.C., Chang W.H., Yeh Y.Q., Jeng U.S., Liu F.T. et al. The intrinsically disordered N-terminal domain of galectin-3 dynamically mediates multisite self-association of the protein through fuzzy interactions. *J. Biol. Chem*. 2017;292(43):17845–17856. DOI: 10.1074/jbc.M117.802793.
8. Patysheva M.R., Stakheeva M.N., Larionova I.V., Tarabanovskaya N.A., Grigorieva E.S., Slonimskaya E.M., et al. Monocytes and cancer: promising role as a diagnostic marker and application in therapy. *Bulletin of Siberian Medicine.* 2019;18(1):60–75 (in Russ.). DOI: 10.20538/1682-0363-2019-1-60-75.
9. Zwager M.C., Bense R., Waaijer S., Qiu S.Q., Timmer-Bosscha H., de Vries E.G.E., et al. Assessing the role of tumour-associated macrophage subsets in breast cancer subtypes using digital image analysis. *Breast Cancer Res. Treat.* 2023;198(1):11–22. DOI: 10.1007/s10549-022-06859-y.
10. Kolobovnikova Yu.V., Urazova O.I., Poletika V.S., Reyngardt G.V., Romanova E.V., Kurnosenko A.V., et al. Galectin-1 and galectin-3 expression in colon cancer and its correlation with tumor invasion, differentiation, and metastatic spread. *Fundamental and Clinical Medicine.* 2021;6(4):45–53 (in Russ.).
11. Ge X.N., Ha S.G., Liu F.T., Rao S.P., Sriramarao P. Eosinophil-expressed galectin-3 regulates cell trafficking and migration. *Front. Pharmacol.* 2013;4:37. DOI: 10.3389/fphar.2013.00037.
12. Cornejo-García J.A., Romano A., Guéant-Rodríguez R.M., Oussalah A., Blanca-López N., Gaeta F., et al. A non-synonymous polymorphism in galectin-3 lectin domain is associated with allergic reactions to beta-lactam antibiotics. *Pharmacogenomics J.* 2016;16(1):79–82. DOI: 10.1038/tpj.2015.24.
13. Chetry M., Thapa S., Hu X., Song Y., Zhang J., Zhu H. et al. The role of galectins in tumor progression, treatment and prognosis of gynecological cancers. *J. Cancer.* 2018;9(24):4742–4755. DOI: 10.7150/jca.23628.
14. Ito K., Stannard K., Gabutero E., Clark A.M., Neo S.Y., Onturk S. et al. Galectin-1 as a potent target for cancer therapy: role in the tumor microenvironment. *Cancer Metastasis Rev.* 2012;31(3–4):763–778. DOI: 10.1007/s10555-012-9388-2.
15. Iqbal A.J., Sampaio A.L.F., Maione F., Greco K.V., Niki T., Hirashima M. et al. Endogenous galectin-1 and acute inflammation: emerging notion of a galectin-9 pro-resolving effect. *Am. J. Pathol.* 2011;178(3):1201–1209. DOI: 10.1016/j.ajpath.2010.11.073.
16. Rabinovich G.A., Conejo-García J.R.. Shaping the immune landscape in cancer by galectin-driven regulatory pathways. *J. Mol. Biol*. 2016;428(16):3266–3281. DOI: 10.1016/j.jmb.2016.03.021.
17. Yakushina V.D., Vasilyeva O.A., Ryazantseva N.V., Novitsky V.V., Savelyeva O.E., Prokhorenko T.S., et al. Galectin-1 and its role in development of innate and adaptive immunity. *Medical Immunology*. 2012;14(1-2):21–32 (in Russ.). DOI: 10.15789/1563-0625-2012-1-2-21-32.
18. Kianoush F., Nematollahi M., Waterfield J.D., Brunette D.M. Regulation of RAW264.7 macrophage polarization on smooth and rough surface topographies by galectin-3. *J. Biomed. Mater. Res. A*. 2017;105(9):2499–2509. DOI: 10.1002/jbm.a.36107.
19. Novak R., Dabelic S., Dumic J. Galectin-1 and galectin-3 expression profiles in classically and alternatively activated human macrophages. *Biochim. Biophys. Acta*. 2012;1820(9):1383–1390. DOI: 10.1016/j.bbagen.2011.11.014.
20. Dragomir A.C.D., Sun R., Choi H., Laskin J.D., Laskin D.L. Role of galectin-3 in classical and alternative macrophage activation in the liver following acetaminophen intoxication. *J. Immunol*. 2012;189(12):5934–5941. DOI: 10.4049/jimmunol.1201851.
21. Sarbaeva N.N., Ponomareva J.V., Milyakova M.N. Macrophages: diversity of phenotypes and functions, interaction with foreign materials. *Genes & Cells*. 2016;11(1):9–17 (in Russ.). DOI: 10.23868/gc120550.
22. Kapitanova K.S., Naumenko V.A., Garanina A.S., Mel'nikov P.A., Abakumov M.A., Alieva I.B. Prospects of applying nanoparticles to reprogram tumor-associate macrophages in immunotherapy of cancer. *Biochemistry*. 2019;84(7):934–952 (in Russ.). DOI: 10.1134/S0320972519070054.
23. Zhguleva A.S., Zementova M.S., Selkov S.A., Sokolov D.I. M1/M2 macrophages: origin, phenotype, methods of production, interaction with natural killer cells and trophoblast. *Medical Immunology*. 2024;26(3):425–448 (in Russ.). DOI: 10.15789/1563-0625-MMO-2877.
24. Correa S.G., Sotomayor C.E., Aoki M.P., Maldonado C.A., Rabinovich G.A. Opposite effects of galectin-1 on alternative metabolic pathways of L-arginine in resident, inflammatory, and activated macrophages. *Glycobiology*. 2003;13(2):119–128. DOI: 10.1093/glycob/cwg010.
25. Grachev A.N., Samoylova D.V., Rashidova M.A., Petrenko A.A., Kovaleva O.V. Tumor-associated macrophages: current research and perspectives of clinical use. *Advances in Molecular Oncology*. 2018;5(4):20–28 (in Russ.).
26. Barrionuevo P., Beigier-Bompadre M., Ilarregui J.M., Toscano M.A., Bianco G.A., Isturiz M.A. et al. A novel function for galectin-1 at the crossroad of innate and adaptive immunity: galectin-1 regulates monocyte/macrophage physiology through a nonapoptotic ERK-dependent pathway. *J. Immunol.* 2007;178(1):436–445. DOI: 10.4049/jimmunol.178.1.436.
27. Baran B., Bechyne I., Siedlar M., Szpak K., Mytar B., Sroka J. et al. Blood monocytes stimulate migration of human pancreatic carcinoma cells in vitro: the role of tumour necrosis factor- alpha. *Eur. J. Cell Biol*. 2009;88(12):743–752. DOI: 10.1016/j.ejcb.2009.08.002.
28. Wu K., Lin K., Li X., Yuan X., Xu P., Ni P. et al. Redefining tumor-associated macrophage subpopulations and functions in the tumor microenvironment. *Front. Immunol.* 2020;11:1731. DOI: 10.3389/fimmu.2020.01731.
29. Sindrilaru A., Peters T., Wieschalka S., Baican C., Baican A., Peter H. et al. An unrestrained proinflammatory M1 macrophage population induced by iron impairs wound healing in humans and mice. *J. Clin. Invest.* 2011;121(3):985–997. DOI: 10.1172/JCI44490.
30. Gong D., Shi W., Yi S., Chen H., Groffen J., Heisterkamp N. TGFβ signaling plays a critical role in promoting alternative macrophage activation. *BMC Immunol*. 2012;13:31. DOI: 10.1186/1471-2172-13-31.

31. Bill R., Wirapati P., Messemaker M., Roh W., Zitti B., Duval F., et al. CXCL9:SPP1 macrophage polarity identifies a network of cellular programs that control human cancers. *Science.* 2023;381(6657):515–524. DOI: 10.1126/science.ade2292.
32. Jayasingam S.D., Citartan M., Thang T.H., Mat Zin A.A., Ang K.C., Ch'ng E.S. Evaluating the polarization of tumor-associated macrophages into M1 and M2 phenotypes in human cancer tissue: technicalities and challenges in routine clinical practice. *Front. Oncol*. 2020;24(9):1512. DOI: 10.3389/fonc.2019.01512.
33. Dunstan R.W., Wharton K.A., Quigley C., Lowe A. The use of immunohistochemistry for biomarker assessment--can it compete with other technologies? *Toxicol. Pathol*. 2011;39(6):988–1002. DOI: 10.1177/0192623311419163.
34. Da C., Mc K., Va M., An O., Yv B. CD68/macrosialin: not just a histochemical marker. *Lab Invest*. 2017;97(1):4–13. DOI: 10.1038/labinvest.2016.116.
35. Fan W., Yang X., Huang F., Tong X., Zhu L. The Second Clinical Medical College ZCMU. Identification of CD206 as a potential biomarker of cancer stem-like cells and therapeutic agent in liver cancer. *Oncology Letters.* 2019;18(3):3218–3226. DOI: 10.3892/ol.2019.10673.

Authors' contribution

Kurnosenko A.V., Reingardt G.V., Gamirova K.A. – carrying out of the research, analysis and interpretation of the data. Poletika V.S., Grishchenko M.Yu., Churina E.G. – conception and design, justification of the research aim, main provisions, and conclusion of the manuscript. Kolobovnikova Yu.V., Chumakova S.P., Urazova O.I. – critical revision of the manuscript for important intellectual content and final approval of the manuscript for publication. All members of the research team meet the criteria and requirements for authorship.

Authors' information

Kurnosenko Anna V. – Post-Graduate Student, Pathophysiology Division, Siberian State Medical University, Tomsk; Oncologist, Tomsk Regional Cancer Center, Tomsk, kurnosenko.av@ssmu.ru, http://orcid.org/0000-0002-3210-0298

Reingardt Gleb V. – Teaching Assistant, Pathophysiology Division, Siberian State Medical University, Tomsk; Oncologist, Tomsk Regional Cancer Center, Tomsk, glebreyngardt@gmail.com, http://orcid.org/0000-0003-3148-0900

Poletika Vadim S. – Cand. Sci. (Med.), Associate Professor, Pathophysiology Division, Siberian State Medical University, Tomsk, vpoletika@yandex.ru, http://orcid.org/0000-0002-2005-305X

Kolobovnikova Yulia V. – Dr. Sci. (Med.), Associate Professor, Head of Normal Physiology Division, Professor of the Pathophysiology Division, Siberian State Medical University, Tomsk, kolobovnikova.julia@mail.ru, http://orcid.org/0000-0001-7156-2471

Chumakova Svetlana P. – Dr. Sci. (Med.), Associate Professor, Pathophysiology Division, Siberian State Medical University, Tomsk, chumakova_s@mail.ru, http://orcid.org/0000-0003-3468-6154

Urazova Olga I. – Dr. Sci. (Med.), Professor, Corresponding Member of the RAS, Head of the Pathophysiology Division, Siberian State Medical University, Tomsk, urazova.oi@ssmu.ru, http://orcid.org/0000-0002-9457-8879

Grishchenko Maksim Yu. – Cand. Sci. (Med.), Associate Professor, Head of the Surgery Division with a Course in Mobilization Training and Disaster Medicine, Siberian State Medical University; Chief Physician, Tomsk Regional Cancer Center, Tomsk, grischenko.mj@ssmu.ru, http://orcid.org/0000-0002-0961-7336

Churina Elena G. – Dr. Sci. (Med.), Professor, Pathophysiology Division, Siberian State Medical University, Tomsk, lena1236@yandex.ru, http://orcid.org/0000-0002-8509-9921

Gamirova Kristina A. – Post-Graduate Student, Division of Health Organization and Public Health, Siberian State Medical University; Oncologist, Tomsk Regional Cancer Center, Tomsk, k.a.gamirova@tomonco.ru, http://orcid.org/0009-0007-7947-360X

(✉) **Kurnosenko Anna V.,** kurnosenko.av@ssmu.ru

Received 19.07.2024;
approved after peer review 09.08.2024;
accepted 12.09.2024

УДК 616.98:578.834.1]-082.4-037-036.88
https://doi.org/10.20538/1682-0363-2024-4-64-73

Predictors of mortality in hospitalized patients with COVID-19

Malinovskiy V.A., Fedosenko S.V., Semakin A.V., Dirks I.I., Arzhanik M.B., Semenova O.L., Vinokurova D.A., Starovoitova E.A., Agaeva S.A., Nesterovich S.V., Kalyuzhin V.V.

Siberian State Medical University
2, Moscow Trakt, 634050, Tomsk, Russian Federation

ABSTRACT

Aim. To determine clinical and laboratory factors associated with a severe course and lethality in hospitalized patients with COVID-19.

Materials and methods. A retrospective comparative study included data of 745 adult patients hospitalized with COVID-19 from 16.05.2020 to 30.09.2020 (Tomsk, Russia). The intergroup comparison of indices, ROC analysis, and determination of odds ratio to assess the association between risk factors and the outcome were performed.

Results. Age > 62 years, pneumonia within a year before COVID-19, and the presence of ≥3 comorbidities were associated with a fatal outcome (FO). Negative predictors of the outcome at the time of hospitalization included dyspnea, diastolic blood pressure ≤ 80 and pulse pressure > 48 mmHg, SpO_2 < 94% (and/or a decrease to ≤ 89% throughout hospitalization). Laboratory predictors of FO at admission were platelets ≤ 183 × 10^9 / l, neutrophils > 4.57 × 10^9 / l, lymphocytes ≤ 1.08 × 10^9 / l, neutrophil-to-lymphocyte ratio > 4.8, aspartate aminotransferase > 39 U / l, urea > 6.75 mmol / l, lactate dehydrogenase > 219 U / l, blood albumin ≤ 38 g / l, C-reactive protein (CRP) > 47 mg / l. When threshold values were reached during any of the hospitalization periods, FO was associated with CRP > 38 mg / l, ferritin > 648.6 μg / l, D-dimer > 731.11 ng / ml, white blood cells > 14.27 × 10^9 / l, lymphocytes ≤ 0.73× 10^9 / l, duration of oxygen therapy > 3 days, need for non-invasive and invasive ventilation ≥ 1 day, need for glucocorticoid administration > 1 day, reaching a total course dose > 6 mg for dexamethasone.

Conclusion. The factors associated with FO in hospitalized patients with COVID-19 were identified.

Keywords: novel coronavirus infection, COVID-19, biomarkers, predictors of severe disease, predictors of mortality

Conflict of interest. The authors declare the absence of obvious or potential conflicts of interest related to the publication of this article.

Source of financing. The authors state that they received no funding for the study.

Conformity with the principles of ethics. All patients signed an informed consent to participate in the study. The study was approved by the Ethics Committee at Siberian State Medical University (Protocol No. 8511 of 21.12.2020).

For citation: Malinovskiy V.A., Fedosenko S.V., Semakin A.V., Dirks I.I., Arzhanik M.B., Semenova O.L., Vinokurova D.A., Starovoitova E.A., Agaeva S.A., Nesterovich S.V., Kalyuzhin V.V. Predictors of mortality in hospitalized patients with COVID-19. *Bulletin of Siberian Medicine.* 2024;23(4):64–73. https://doi.org/10.20538/1682-0363-2024-4-64-73.

✉ *Agaeva Sofiya A.,* agaeva.sofiyaa@gmail.com

Предикторы летального исхода у госпитализированных пациентов с COVID-19

Малиновский В.А., Федосенко С.В., Семакин А.В., Диркс И.И., Аржаник М.Б., Семенова О.Л., Винокурова Д.А., Старовойтова Е.А., Агаева С.А., Нестерович С.В., Калюжин В.В.

Сибирский государственный медицинский университет (СибГМУ)
Россия, 634050, г. Томск, Московский тракт, 2

РЕЗЮМЕ

Цель. Установить клинико-лабораторные факторы, ассоциированные с тяжелым течением и летальностью у госпитализированных пациентов с новой коронавирусной инфекцией (COVID-19).

Материалы и методы. Проведено ретроспективное сравнительное исследование по данным 745 взрослых пациентов, госпитализированных с COVID-19 с 16.05.2020 по 30.09.2020 (Томск, Россия). Выполнено межгрупповое сравнение показателей, ROC-анализ, определение отношения шансов для оценки связи между факторами риска и исходом.

Результаты. С летальным исходом (ЛИ) ассоциированы возраст старше 62 лет, пневмония в течение года до COVID-19, наличие ≥3 сопутствующих патологий. Негативные предикторы исхода на момент госпитализации: одышка, диастолическое давление ≤80 и пульсовое давление более 48 мм рт. ст., SpO_2 менее 94% (и (или) снижение за госпитализацию до ≤89%). Лабораторные предикторы ЛИ при госпитализации: тромбоциты ≤ 183 × 10^9/л, нейтрофилы более 4,57 × 10^9/л, лимфоциты ≤1,08 × 10^9/л, нейтрофильно-лимфоцитарное отношение более 4,8, аспартатаминотрансфераза более 39 ЕД/л, мочевина более 6,75 ммоль/л, лактатдегидрогеназа более 219 ЕД/л, альбумин крови ≤38 г/л, С-реактивный белок (СРБ) более 47 мг/л. При достижении пороговых значений в любой из периодов госпитализации с ЛИ ассоциировались: уровень СРБ в крови более 38 мг/л, ферритина более 648,6 мкг/л, D-димера более 731,11 нг/мл, лейкоцитов более 14,27 × 10^9/л, лимфоцитов ≤0,73 × 10^9/л, продолжительность оксигенотерапии более 3 сут, необходимость неинвазивной и инвазивной вентиляции легких ≥1 сут, потребность назначения глюкокортикостероидов более 1 сут, достижение общей курсовой дозы более 6 г по дексаметазону.

Заключение. Выявлены факторы, ассоциированные с ЛИ у госпитализированных пациентов с COVID-19.

Ключевые слова: новая коронавирусная инфекция, COVID-19, биомаркеры, предикторы тяжелого течения, предикторы летального исхода

Конфликт интересов. Авторы декларируют отсутствие явных и потенциальных конфликтов интересов, связанных с публикацией настоящей статьи.

Источник финансирования. Авторы заявляют об отсутствии финансирования при проведении исследования.

Соответствие принципам этики. Все пациенты подписали информированное согласие на участие в исследовании. Исследование одобрено локальным этическим комитетом СибГМУ (протокол № 8511 от 21.12.2020).

Для цитирования: Малиновский В.А., Федосенко С.В., Семакин А.В., Диркс И.И., Аржаник М.Б., Семенова О.Л., Винокурова Д.А., Старовойтова Е.А., Агаева С.А., Нестерович С.В., Калюжин В.В. Предикторы летального исхода у госпитализированных пациентов с COVID-19. *Бюллетень сибирской медицины.* 2024;23(4):64–73. https://doi.org/10.20538/1682-0363-2024-4-64-73.

INTRODUCTION

The outbreak of novel coronavirus infection (COVID-19) in late 2019 in the People's Republic of China triggered the pandemic that caused enormous socioeconomic damage and lasted for more than three years. The first waves of the pandemic were characterized by a lack of preparedness and unprecedented collapse of healthcare systems worldwide, as well as by the use of drugs with insufficient evidence-based efficacy.

As of December 2023, there were more than 772 million confirmed cases and more than 6.9 million deaths worldwide. According to the 2022 meta-

analysis, the highest rates of excess mortality from COVID-19 were registered in India (4.07 million deaths), USA (1.13 million deaths), and Russia (1.07 million deaths) [1].

Despite the existing vaccination programs, the emergence of modified variants of the virus with a less dangerous course of the disease and the spread of new strains around the world make the problem of COVID-19 control relevant. As more data become available, an analysis is being conducted to identify unique biomarkers that may correlate with COVID-19 severity and adverse outcomes in order to provide appropriate medical care and reduce the burden on healthcare.

The aim of this study was to determine clinical and laboratory factors associated with a severe course and lethality in hospitalized patients with COVID-19.

MATERIALS AND METHODS

A retrospective comparative study was carried out using a continuous sampling method. The study included medical records of 745 adult patients (343 men (46.0%) and 402 women (54.0%)) with COVID-19 confirmed by polymerase chain reaction (PCR), who were treated at the respiratory hospital (RH) in Siberian State Medical University clinics (Tomsk) from 16.05.2020 to 30.09.2020 (period of circulation of the wild-type SARS-CoV-2 strain in Russia). The study protocol was approved by the local Ethics Committee at Siberian State Medical University (Protocol No.8511 of 21.12.2020).

For all patients of the RH, anamnestic data and results of objective examination and laboratory and instrumental investigations were collected according to the approved algorithm in the first 48 hours from the moment of hospitalization for a dynamic assessment and determination of the relationship with the outcome of hospitalization. Two comparison groups were formed retrospectively, depending on the outcome of hospitalization. The main group consisted of patients whose hospitalization ended in discharge from hospital (survivors, $n = 683$), the comparison group consisted of patients with a fatal outcome (FO, deceased, $n = 62$).

Statistical analysis of the obtained data was performed using the Statistica 12 (StatSoft.Inc, USA), MedCalc 22.009 (Copy©MedCalc SoftWare Ltd., Belgium), and Microsoft® Excel® 2016 MSO (version 2309 16.0.16827.20166, USA) software packages. Quantitative variables were described as the median and the interquartile range Me (Q_{25}; Q_{75}). Qualitative variables were described as absolute and relative frequencies (n (%)). Intergroup comparison of quantitative variables was performed using the nonparametric Mann – Whitney U-test. Qualitative variables were compared using the Pearson's $\chi 2$ test.

The quantitative assessment of the association between the disease outcome and the presence of a risk factor in the sample was performed using odds ratio (OR). Results were presented using the odds ratio and 95% confidence interval (CI). The results were considered statistically significant if CI did not contain 1. In addition, the impact of factors on the odds of FO was assessed using the ROC analysis. The area under the curve (AUC) with 95% CI, the cut-off point according to the Youden index, and sensitivity and specificity for this point were evaluated. The results were considered significant at $p < 0.05$.

RESULTS

Demographic and anamnestic characteristics of the patients. Age of the patients in the group of survivors was 57 (43; 67) years, in the group of the deceased patients – 73 (66; 81) years ($p < 0.001$). Age of more than 62 years (AUC 0.804 (0.774; 0.832), $p < 0.001$) was a risk factor for an adverse outcome with sensitivity of 85.5% and specificity of 65.6%.

The compared patient groups did not differ significantly in gender distribution: the main group consisted of 316 men (46.3%) and 367 women (53.7%), the comparison group consisted of 27 men (43.5%) and 35 women (56.5%), $p = 0.681$. Patients' gender also did not significantly affect the outcome of hospitalization (OR 1.1 (0.7;1.9)). The duration of illness before hospitalization was 6 (3; 9) days in the main group and 5 (1.5; 7.0) days in the comparison group ($p = 0.011$). The analysis showed that pneumonia experienced by patients in the year preceding COVID-19 increased the odds of FO by almost 15 times (OR 14.9 (3.6; 61.6)).

In the outpatient setting, patients with COVID-19 were treated by a variety of medication groups. The analysis included only records of the patients whose data on pre-hospital drug intake could be clarified. Thus, antibacterial drugs (ABD) were taken in the outpatient setting by 117 (17.1% of 683) patients of the main group and 10 (16.1% of 62) patients of the deceased group ($p = 0.840$). Antiviral drugs were taken by 8 (36.4% of 22) patients from the deceased group and 146 (90.1% of 162) patients from the main group ($p < 0.001$). Non-steroidal anti-inflammatory drugs (NSAIDs) were received by 8 (34.8% of 23)

patients from the deceased group and 82 (82% of 100) survivors. Administration of antiviral drugs (umifenovir, interferon alfa-2b, interferon beta-1b, imidazolyl ethanamide pentandioic acid, ritonavir + lopinavir, tilorone, rimantadine, oseltamivir, meglumine acridone acetate, and kagocel) and NSAIDs at the prehospital stage was associated with a reduction of the odds for mortality by approximately 16 (OR 0.06 (0.02; 0.17)) and 9 (OR 0.11 (0.04; 0.32)) times, respectively ($p < 0.050$).

Following the analysis of patients' comorbidities, we formed groups of diseases that increased the odds of FO and did not affect it. Thus, the diseases that increased the risk of FO included coronary heart disease (by 8 times), essential hypertension (by 5 times), diabetes mellitus (by 2 times), chronic heart failure (by 5 times), anemia (by 4 times), liver cirrhosis (by 11 times), decreased glomerular filtration rate (GFR) of less than 60 ml / min / 1.73 m² according to the CKD-EPI equation (by 11 times), previous stroke (by 9 times), alcoholism (by 9 times), bedsores (by 9 times), cooccurring cancer (by 6 times), and neurological disorders (by 5 times). Group 2 encompassed diseases that did not increase the odds of FO: bronchial asthma, chronic obstructive pulmonary disease, liver diseases, except for cirrhosis, kidney diseases without decreased GFR, drug addiction (Table 1).

The presence of at least three comorbidities was associated with FO (AUC 0.821 (0.792; 0.848), $p < 0.001$) with sensitivity of 83.9% and specificity of 64.3%.

Table 1

Characteristics of comorbidities in the patients

Parameter	Main group (survivors), *n* (%)	Comparison group (deceased), *n* (%)	*p*	OR (95% CI), *Me* (Q_{25}; Q_{75})
CHD	160 (23.4%)	44 (71.0%)	<0.001	7.99 (4.49; 14.28)
Hypertension	386 (56.5%)	54 (87.1%)	<0.001	5.19 (2.43; 11.08)
Diabetes mellitus	107 (15.7%)	16 (25.8%)	0.039	1.87 (1.02; 3.43)
Chronic heart failure	147 (21.5%)	36 (58.1%)	<0.001	5.05 (2.95; 8.63)
Bronchial asthma	29 (4.3%)	3 (4.8%)	0.830	1.15 (0.34; 3.88)
COPD	27 (4.0%)	5 (8.1%)	0.127	2.13 (0.79; 5.74)
Anemia	37 (5.4%)	11 (17.8%)	0.001	3.76 (1.81; 7.81)
Liver cirrhosis	2 (0.3%)	2 (3.2%)	0.003	11.35 (1.57; 82.02)
Other liver diseases	30 (4.4%)	5 (8.1%)	0.191	1.91 (0.71; 5.11)
HIV infection	5 (0.7%)	2 (3.2%)	0.051	4.52 (0.86; 23.80)
Kidney diseases	223 (32.7%)	26 (41.9%)	0.138	1.49 (0.88; 2.53)
GFR < 60 ml / min / 1.73 m²	50 (7.3%)	29 (46.8%)	<0.001	11.13 (6.25; 19.79)
Injection drug abuse	1 (0.2%)	1 (1.6%)	0.328	11.16 (0.70; 180.71)
Previous stroke	20 (2.9%)	13 (21.0%)	<0.001	8.78 (4.12; 18.71)
Alcoholism	4 (0.6%)	3 (4.8%)	0.001	8.61(1.88; 39.37)
Bedsores	5 (0.7%)	4 (6.5%)	0.001	9.34 (2.44; 35.73)
Cancer	30 (4.4%)	14 (22.6%)	<0.001	6.34 (3.15; 12.75)
Neurological disorders	132 (19.3%)	35 (56.5%)	<0.001	5.41 (3.16; 9.26)

Note. CHD – coronary heart disease, COPD – chronic obstructive pulmonary disease, GFR – glomerular filtration rate. OR – odds ratio
p – statistical significance of intergroup differences. 95% CI –95% confidence interval.

Patient complaints and objective examination data on admission to the RH. Symptoms of patients on admission to the RH that affected the odds of FO were identified. Thus, dyspnea, which was present in 28.4% of survivors and 62.0% of the deceased ($p < 0.001$), was associated with higher odds of mortality. In contrast, the presence of anosmia and headache was associated with lower odds of mortality – OR 4.11 (2.30;7.50), OR 0.08 (0.01;0.57), and OR 0.51 (0.26;0.99), respectively. The proportion of patients with headache was 37.6 and 23.5% among survivors and deceased patients, respectively ($p = 0.044$). Anosmia was almost 10.5 times less common in the group of deceased patients (2%) compared to survivors (20.5%, $p = 0.001$). Such symptoms as cough, purulent sputum production, fever, chest pain, general weakness, chills, myalgia, and diarrhea were not significantly associated with mortality in the compared groups ($p > 0.05$).

Among the objective examination findings at admission to the RH, FO was also associated with diastolic blood pressure ≤ 80 mm Hg (AUC

0.603 (0.567; 0.639), p = 0.005, sensitivity 78.7%, specificity 38.3%), pulse pressure value > 48 mm Hg (AUC 0.581 (0.544; 0.616), p = 0.048, sensitivity 64.5%, specificity 56.4%), respiratory rate >19 breaths per minute (AUC 0.704 (0.670; 0.737), p < 0.001, sensitivity 44.3%, specificity 91.9%), blood oxygen saturation (SpO_2) measured by pulse oximetry < 94% (AUC 0.751 (0.718; 0.782), p < 0.001, sensitivity 64.5%, specificity 73.0%). A decrease in SpO_2 to ≤ 89% during hospital stay was also associated with FO (AUC 0.859 (0.831; 0.884), p < 0.0001, sensitivity 77.8%, specificity 84.6%). The odds of FO were increased if auscultatory signs, such as diminished breath sounds (OR 2.06 (1.15; 3.70)) and moist rales (OR 3.96 (1.51; 10.37)), were registered on admission in patients with COVID-19.

Laboratory parameters during hospital stay. Among hemogram parameters on admission to the RH, statistically significant predictors associated with FO included:

1) platelet count ≤ 183 × 10^9 / l (AUC 0.673 (0.638; 0.708), p = 0.001, sensitivity 61.7%, specificity 71.8%);

2) neutrophil count > 4.57 × 10^9 / l (AUC 0.696 (0.660; 0.730), p < 0.001, sensitivity 63.8%, specificity 72.4%);

3) lymphocyte count ≤ 1.08 × 10^9 / l (AUC 0.768 (0.735; 0.798), p < 0.001, sensitivity 70.2%, specificity 70.3%);

4) neutrophil-to-lymphocyte ratio > 4.8 (AUC 0.774 (0.741; 0.804), p < 0.001, sensitivity 66.0%, specificity 80.7%).

The analysis of changes in the hematologic parameters throughout hospitalization showed that increased leukocyte count > 14.27 × 10^9 (AUC 0.855 (0.827; 0.880), p < 0.001, sensitivity 70.0%, specificity 90.0%) and decreased lymphocyte count ≤ 0.73 × 10^9 / l (AUC 0.878 (0.852; 0.901), p < 0.001, sensitivity 85.0%, specificity 82.3%) were also predictors of FO of the disease (Table 2).

Table 2

Hematologic parameters					
Parameter	AUC, *Me* (Q_{25}; Q_{75})	p	Cut-off point	Sensitivity, %	Specificity, %
Thrombocytes, thousands / μl	0.673 (0.638; 0.708)	0.001	≤183	61.7	71.8
Leukocytes, ×10^9 / l	0.615 (0.578; 0.650)	0.028	>7.71	48.0	81.1
Neutrophils, ×10^9 / l	0.696 (0.660; 0.730)	<0.001	>4.57	63.8	72.4
Lymphocytes, ×10^9 / l	0.768 (0.735; 0.798)	<0.001	≤1.08	70.2	70.3
Neutrophil-to-lymphocyte ratio	0..774 (0.741; 0.804)	<0.001	>4.80	66.0	80.7
Leukocytes (maximum level)	0.855 (0.827; 0.880)	<0.001	>14.27	70.0	90.0
Lymphocytes (minimum level)	0.878 (0.852; 0.901)	<0.001	≤0.73	85.0	82.3

Note. Here and in Table 3, AUC – area under the curve.

p – significance of differences

Among the blood biochemistry parameters on admission, statistically significant predictors associated with FO were registered:

1) aspartate aminotransferase level > 39 U / l (AUC 0.647 (0.610; 0.682), p = 0.001, sensitivity 68.5%, specificity 58.8%);

2) urea level > 6.75 mmol / l (AUC 0.796 (0.764; 0.824), p < 0.001, sensitivity 75.9%, specificity 74.1%);

3) lactate dehydrogenase level > 219 U / l (AUC 0.777 (0.718; 0.828), p < 0.001, sensitivity 95.2%, specificity 51.8%);

4) blood albumin level ≤ 38 g / l (AUC 0.792 (0.731; 0.844), p < 0.001, sensitivity 89.5%, specificity 62%);

5) C-reactive protein (CRP) level > 47 mg / l (AUC 0.782 (0.744; 0.816), p < 0.001, sensitivity 66.7%, specificity 81%).

The analysis of blood biochemistry parameters demonstrated that CRP concentration > 38 mg / l (AUC 0.862 (0.833; 0.887), p < 0.001, sensitivity 89.4%, specificity 71.0%), ferritin level > 648.6 μg / l (AUC 0.715 (0.666; 0.761), p = 0.001, sensitivity 52.4%, specificity 86.0%), and serum D-dimer level > 731.11 ng / ml (AUC 0.792 (0.723; 0.850), p < 0.001, sensitivity 90.0%, specificity 61.%), registered as the highest at any of the hospitalization periods, were significantly associated with FO in COVID-19 (Table 3).

Table 3

Blood biochemistry parameters					
Parameter	AUC, *Me* (Q_{25}; Q_{75})	p	Cut-off point	Sensitivity, %	Specificity, %
Total protein, g / l	0.687 (0.650; 0.722)	<0.001	≤60	51.0	78.6
Glucose, mmol / l	0.637 (0.599; 0.674)	0.003	>6.13	55.0	76.3
Aspartate aminotransferase, U / l	0.647 (0.610; 0.682)	0.001	>39	68.5	58.8
Urea, mmol / l	0.796 (0.764; 0.824)	<0.001	>6.75	76.0	74.1
Creatinine, μmol / l	0.592 (0.555; 0.629)	0.057	>116	31.5	94.1
Sodium, mmol / l	0.637 (0.599; 0.674)	0.005	≤139.5	56.0	73.9
C-reactive protein, mg / l	0.782 (0.744; 0.816)	<0.001	>47	66.7	81.0
Lactate dehydrogenase, U / l	0.777 (0.718; 0.828)	<0.001	>219	95.2	51.8
Albumin, g / l	0.792 (0.731; 0.844)	<0.001	≤38	89.5	62.0
D-dimer, ng / ml	0.746 (0.655; 0.823)	0.002	>731	85.7	61.2
C-reactive protein	0.862 (0.833; 0.887)	<0.001	>38	89.4	71.0
Ferritin (maximum level), μg / l	0.715 (0.666; 0.761)	0.001	>648.6	52.4	86.0
D-dimer (maximum level), ng / ml	0.792 (0.723; 0.850)	<0.001	>731.11	90.0	61.1

Risks associated with therapeutic interventions. According to the ROC analysis, duration of oxygen therapy > 3 days (AUC 0.809 (0.779; 0.837), $p < 0.001$, sensitivity 88.7%, specificity 59.7%), the need for noninvasive ventilation (NIV) for ≥ 1 day (AUC 0.700 (0.666; 0.733), $p < 0.001$, sensitivity 43.6%, specificity 96.5%), and the need for invasive mechanical ventilation (IMV) for at least 1 day (AUC 0.699 (0.665; 0.732), $p < 0.001$, sensitivity 40.3%, specificity 99.6%) were associated with FO in hospitalized patients with COVID-19. It is important to note that the need for oxygen therapy via a face mask (OR 14.97 (5.38; 41.71)), the use of NIV (OR 22.61 (11.86; 43.10)), and the use of IMV (OR 384.35 (110.59; 1335.72), $p < 0.001$) increased the odds of FO.

The use of antiviral drugs (favipiravir, umifenovir, interferon alpha-2b, interferon beta-1b, ritonavir + lopinavir) and anticoagulants during hospitalization did not demonstrate a significant effect on the outcome of COVID-19 ($p > 0.05$).

According to the ROC analysis, the need for in-hospital glucocorticoid (GCS) administration for > 1 day (AUC 0.803 (0.772; 0.831), $p < 0.0001$, sensitivity 90.3%, specificity 62.1%) and reaching a total course dose of > 6 mg for dexamethasone (AUC 0.834 (0.806; 0.860), $p < 0.0001$, sensitivity 91.9%, specificity 60.9%) were predictors of mortality. The study also found that the odds of mortality in patients with COVID-19 who required the use of GCS (OR 29 (9.00; 93.45), $p < 0.001$), interleukin-6 inhibitors (OR 7.08 (2.99; 16.78), $p < 0.001$), and Janus kinase inhibitors (OR 7.78 (2.14; 28.36), $p = 0.001$) were significantly higher than in patients who did not receive these drugs.

DISCUSSION

The age of COVID-19 patients is considered as one of the key factors associated with mortality. Thus, according to the data of a multicenter study by F. Zhou et al. [2], increased odds of in-hospital mortality were associated with older age (a median age in the deceased group was 69.0 (63.0; 76.0) years, in the survivor group –52.0 (45.0; 58.0) years ($p < 0.0001$) OR 1.10 (1.03; 1.17), $p = 0.0043$). In a study by L. Kubiliute et al. (2023), older age was an independent predictor of in-hospital mortality, associated with a 4% increase in the odds of FO per year. This has been associated with a large number of comorbidities and immunosenescence characterized by age-related defects in T- and B-cell function, which attenuate the immune response to most viruses, including SARS-CoV-2 [3, 4].

In the performed study, no significant differences were revealed in the incidence of FO in hospitalized patients with COVID-19 depending on gender. It is worth noting that previously published clinical trial data cite different results on the effect of gender on mortality rates in COVID-19. Thus, in the studies by A.C. Jain et al. (2020) and N.Ç. Başaran et al. (2022), the mortality rate in men was higher than in women [5, 6]. In contrast, other studies have found no significant effect of gender on a hospitalization outcome [7–9] and patient survival [10].

According to a systematic review by L.J. Quinton et al. (2018), pneumonia has a significant impact on the physiological processes that maintain pulmonary homeostasis, with the development of long-term negative consequences that impair health and

accelerate mortality after the end of the acute disease phase [11]. In our study, the fact of developing pneumonia in the year preceding COVID-19 increased the odds of mortality almost by 15 times.

According to published data, the risk of FO is associated with the presence of comorbid pathology in the patient [12, 13]. In this study, not only the total number of comorbidities, but also the presence of a certain pathology or groups of diseases in patients, including CHD, essential hypertension, CHF, stroke, diabetes mellitus, anemia, alcoholism, liver cirrhosis, neurological diseases, decreased GFR of < 60 ml / min / 1.73m² according to CKD-EPI, and cancer, at the time of hospitalization or in the medical history had a significant impact on the outcome of COVID-19. Our results on the role of concomitant and comorbid pathology in predicting the severity of the course and outcome of COVID-19 generally correlate with the data of other authors [14–18].

In our study, the use of antiviral drugs at the outpatient stage was associated with decreased odds of mortality from COVID-19, which did not contradict the results of several other studies [19, 20].

The analysis of patient complaints demonstrated that anosmia and headache on admission to the hospital were associated with a favorable disease outcome in patients with COVID-19. Interestingly, similar results were obtained in the study by B. Talavera et al. (2020) [21].

The development of respiratory failure and its severity in COVID-19 reflects the severity of pulmonary parenchyma damage and is associated with a disease outcome according to studies [22]. Our study demonstrated that a decrease in SpO_2 to < 94% on admission and / or to ≤ 89% throughout hospital stay was associated with FO.

To date, multiple studies have been published that consider various laboratory values as predictors of an adverse outcome. At the same time, there is a noticeable variation in the threshold values of the studied parameters. According to the results of the study by B. Cheng et al. (2019), NLR value > 3.19 (AUC 0.810 (0.732; 0.878), $p < 0.001$) and CRP > 33.4 mg / l (AUC 0.890 (0.825; 0.946), $p < 0.001$) on admission were associated with FO [23]. In the performed study neutrophil-to-lymphocyte ratio > 4.8 (AUC 0.774 (0.741; 0.804), $p < 0.0001$, sensitivity 66%, specificity 80.7%) and CRP level > 47 mg / l (AUC 0.782 (0.744; 0.816), $p < 0.001$, sensitivity 66.7%, specificity 81.0%) measured early during hospital stay were associated with an adverse outcome in COVID-19.

According to H. Ghobadi et al. (2022), who studied the role of systemic inflammatory markers, leukocyte levels > 9.05×10^9/ l (AUC 0.969 (0.960; 0.977), $p < 0.0001$, sensitivity 89.0%, specificity 95.9%), neutrophil count > 8.79×10^9 / l (AUC 0.971 (0.962; 0.978), $p < 0.0001$, sensitivity 89.8%, specificity 94.3%), and lymphocyte count < 0.91×10^9 / l (AUC 0.566 (0.543; 0.589), $p < 0.0001$, sensitivity 50.4%, specificity 61.2%) were threshold values in predicting FO in patients with COVID-19 [24]. In our study, neutrophil level > 4.57×10^9 / l (AUC 0.696 (0.660; 0.730), $p < 0.001$, sensitivity 63.8%, specificity 72.4%), lymphocyte level ≤ 1.08×10^9 / l (AUC 0.768 (0.735; 0.798), $p < 0.001$, sensitivity 70.2%, specificity 70.3%), an increase in the leukocyte count > 14.27×10^9 / l (AUC 0.855 (0.827; 0.880), $p < 0.001$, sensitivity 70.0%, specificity 90.0%), and a decrease in the lymphocyte count ≤ 0.73×10^9 / l (AUC 0.878 (0.852; 0.901), $p < 0.001$, sensitivity 85.0%, specificity 82.3%) throughout hospital stay were associated with an adverse disease outcome.

Many researchers have considered platelet count as an available biomarker associated with disease severity and a risk of mortality in COVID-19. Thus, in a study by J. Duan et al. (2020), platelet level ≤ 174×10^9 / l (AUC 0.810 (0.760; 0.850, sensitivity 100.0%, specificity 56.0%) allowed to predict progression to severe disease [25]. In our study, the platelet count ≤ 183×10^9 / l (AUC 0.673 (0.638; 0.708), $p = 0.001$, sensitivity 61.7%, specificity 71.8%) was associated with an adverse outcome.

In a study by Z. Mohammadi et al. (2022), AST elevation > than 36.5 U / l (AUC 0.374 (0.328; 0.403, sensitivity 61.9%, specificity 57.6%) was a significant predictor of in-hospital COVID-19 mortality [26]. According to A. Pitamberwale et al (2022), a serum urea concentration of ≥ 52 mg / dl (sensitivity 73.6%, specificity 60.5%) was associated with FO. Maintaining a serum albumin concentration ≥ 3.25 g / dl demonstrated significance as a predictor of survival with 76.7% sensitivity and 59.3% specificity [27]. In our study, AST level > 39 U / l (AUC 0.647 (0.610; 0.682), $p = 0.001$, sensitivity 68.5%, specificity 58.8%), blood albumin ≤ 38 g / l (AUC 0.792 (0.731; 0.844), $p < 0.001$, sensitivity 89.5%, specificity 62.0%), and urea level > 6.75 mmol / l (AUC 0.796 (0.764; 0.824), $p < 0.001$, sensitivity 76.0%, specificity 74.1%) were predictors of FO in COVID-19 patients. It is worth noting that creatinine level did not significantly affect the outcome of the disease ($p = 0.057$) according to the performed study.

In the study by E. Poggiali et al. (2020), lactate dehydrogenase (LDH) level was considered as a marker of tissue damage and a predictor of severity of acute respiratory failure in patients with fatal acute respiratory distress syndrome (ARDS). In the meantime, LDH level > 450 U / l (AUC 0.760, $p < 0.0001$) with sensitivity of 75.0% and specificity of 70.0% allowed to predict moderate and severe ARDS [28]. In our study, the predictor of an adverse outcome was LDH level on admission > 219 U / l (AUC 0.777 (0.718; 0.828), $p < 0.001$, sensitivity 95.2%, specificity 51.8%).

In the study by A. Bastug et al., D-dimer on admission ≥ 0.565 mg / l (AUC 0.896 (0.810; 0.970), $p < 0.001$, sensitivity 85.7%, specificity 80.6%) allowed to predict an unfavorable course of the disease [8]. In our study, we demonstrated that the D-dimer level (throughout hospitalization) > 731.11 ng / ml (AUC 0.792 (0.723; 0.850), $p < 0.001$, sensitivity 90.0%, specificity 61.1%) was significantly associated with FO.

The analysis of prescribed therapy for COVID-19 during the hospitalization period draws attention to the fact that using GCS > 1 day and reaching a total course dose > 6 mg for dexamethasone were associated with an adverse hospitalization outcome. The odds of FO in patients who required the use of GCS, interleukin-6 inhibitors, and Janus kinase inhibitors were significantly higher than in patients who were not prescribed these drugs. Our findings should be interpreted with caution, as these groups of drugs have been used with a limited evidence base for efficacy and safety in COVID-19 and more often in a more severe progressive course of the disease [23, 29].

In addition, according to our study, duration of oxygen therapy for more than 3 days (AUC 0.809 (0.779; 0.837), $p < 0.001$, sensitivity 88.7%, specificity 59.7%), the need for NIV for ≥ 1 day (AUC 0.700 (0.666; 0.733), $p < 0.001$, sensitivity 43.6%, specificity 96.5%), and the need for IMV for ≥ 1 day (AUC 0.699 (0.665; 0.732), $p < 0.001$, sensitivity 40.3%, specificity 99.6%) were associated with FO in hospitalized patients with COVID-19. The obtained results do not contradict the data of other authors. Thus, in a study by V.N. Gorodin et al. (2022), the duration of oxygen therapy via nasal cannulas or a face mask for more than 4.5 days significantly increased the odds of FO (length between two successive R waves (RR) 1.919 (1.308; 2.817), $p < 0.05$, sensitivity 35.7%, specificity 95.2%). The fact of using NIV as a second step of respiratory support and the duration of its use > 2 days significantly increased the risk of an adverse outcome (RR 2.276 (1.202; 4.311), $p < 0.05$, sensitivity 75.9%, specificity 66.7% and RR 2.0 (1.184; 3.377), $p < 0.05$, sensitivity 68.2%, specificity 100.0%, respectively) [30].

CONCLUSION

The results of the study allowed us to identify a number of factors and their quantitative values that were predictors of FO already at the early stage of hospitalization for COVID-19. Thus, older age, presence of comorbidities, and pneumonia in the year preceding COVID-19 played a key role among anamnestic factors. In contrast, outpatient antiviral medication reduced the risk of an adverse outcome.

When assessing physical status, severe dyspnea, diastolic and pulse pressure levels, decreased oxygen saturation on admission and throughout hospitalization, as well as the presence of moist rales and diminished breathing may be considered as potential risk factors for COVID-19.

Decreased levels of platelets, lymphocytes, and serum albumin, increased levels of leukocytes, neutrophils, neutrophil-to-lymphocyte ratio, AST, urea, LDH, CRP, D-dimer, and ferritin should be identified among the laboratory markers associated with the risk of FO.

REFERENCES

1. Wang H., Paulson K.R., Pease S.A., Watson S., Comfort H., Zheng P. et al. Estimating excess mortality due to the COVID-19 pandemic: a systematic analysis of COVID-19-related mortality, 2020–21. *The Lancet.* 2022;399(10334):1513–1536. DOI: 10.1016/S0140-6736(21)02796-3.
2. Zhou F., Yu T., Du R., Fan G., Liu Y., Liu Z. et al. Clinical course and risk factors for mortality of adult inpatients with COVID-19 in Wuhan, China: a retrospective cohort study. *The Lancet*. 2020;395(10229):1054–1062. DOI: 10.1016/S0140-6736(20)30566-3.
3. Kubiliute I., Vitkauskaite M., Urboniene J., Svetikas L., Zablockiene B., Jancoriene L. Clinical characteristics and predictors for in-hospital mortality in adult COVID-19 patients: A retrospective single center cohort study in Vilnius, Lithuania. *PLoS One*. 2023;18(8):e0290656. DOI: 10.1371/journal.pone.0290656.
4. Bartleson J.M., Radenkovic D., Covarrubias A.J., Furman D., Winer D.A., Verdin E. SARS-CoV-2, COVID-19 and the Aging Immune System. *Nat. Aging*. 2021;1(9):769-782. DOI: 10.1038/s43587-021-00114-7.
5. Jain A.C., Kansal S., Sardana R., Bali R.K., Kar S., Chawla R. A retrospective observational study to determine the early predictors of in-hospital mortality at admission with COVID-19. *Indian J. Crit. Care Med*. 2020;24(12):1174–1179. DOI: 10.5005/jp-journals-10071-23683.
6. Başaran N.Ç., Özdede M., Uyaroğlu O.A., Şahin T.K., Özcan B., Oral H. et al. Independent predictors of in-hospi-

tal mortality and the need for intensive care in hospitalized non-critical COVID-19 patients: a prospective cohort study. *Intern. Emerg. Med*. 2022;17(5):1413–1424. DOI: 10.1007/s11739-022-02962-6.
7. Shi S., Liu X., Xiao J., Wang H., Chen L., Li J. et al. Prediction of adverse clinical outcomes in patients with coronavirus disease 2019. *J. Clin. Lab. Anal*. 2021;35(1):e23598. DOI: 10.1002/jcla.23598.
8. Bastug A., Bodur H., Erdogan S., Gokcinar D., Kazancioglu S., Kosovali B.D. et al. Clinical and laboratory features of COVID-19: Predictors of severe prognosis. *Int. Immunopharmacol*. 2020;88:106950. DOI: 10.1016/j.intimp.2020.106950.
9. Korkhmazov V.T., Alekseenko S.N., Perkhov V.I. Gender and age profile of mortality caused by COVID-19. *Innovative Medicine of Kuban*. 2022;4(28):39–46 (in Russ.). DOI: 10.35401/2541-9897-2022-25-4-39-46.
10. Raimondi F., Novelli L., Ghirardi A., Russo F.M., Pellegrini D. et al. Covid-19 and gender: lower rate but same mortality of severe disease in women-an observational study. *BMC Pulm. Med*. 2021;21(1):96. DOI: 10.1186/s12890-021-01455-0.
11. Quinton L.J., Walkey A.J., Mizgerd J.P. Integrative physiology of pneumonia. *Physiol. Rev.* 2018;98(3):1417–1464. DOI: 10.1152/physrev.00032.2017.
12. Arutyunov G.P., Tarlovskaya E.I., Arutyunov A.G., Belenkov Y.N., Konradi A.O., Lopatin Y.M. et al. International register "Analyzing the dynamics of comorbidities in SARS-CoV-2 survivors" (AKTIV SARS-CoV-2): analysis of predictors of short-term adverse outcomes in COVID-19. *Russian Journal of Cardiology*. 2021;26(4):116–131 (in Russ.). DOI: 10.15829/1560-4071-2021-4470.
13. Williamson E.J., Walker A.J., Bhaskaran K., Bacon S., Bates C. et al. Factors associated with COVID-19-related death using OpenSAFELY. *Nature*. 2020;584(7821):430–436. DOI: 10.1038/s41586-020-2521-4.
14. Hu K., Li B., Bae S., Kim S.R., Kim M.N., Shim W.J. et al. Impact of cardiovascular disease and risk factors on fatal outcomes in patients with COVID-19 according to age: a systematic review and meta-analysis. *Heart*. 2021;107(5):373–380. DOI: 10.1136/heartjnl-2020-317901.
15. Zhang J., Wang Z., Wang X., Hu Z., Yang C., Lei P. Risk Factors for Mortality of COVID-19 Patient Based on Clinical Course: A Single Center Retrospective Case-Control Study. *Front Immunol*. 2021;12:581469. DOI: 10.3389/fimmu.2021.581469.
16. Xiao Y., Wu D., Shi X., Liu S., Hu X., Zhou C., Tian X. et al. High Child-Pugh and CRUB65 scores predict mortality of decompensated cirrhosis patients with COVID-19: A 23-center, retrospective study. *Virulence*. 2021;12(1):1199–1208. DOI: 10.1080/21505594.2021.1909894.
17. Berenguer J., Borobia A.M., Ryan P., Rodríguez-Baño J., Bellón J.M., Jarrín I. et al. Development and validation of a prediction model for 30-day mortality in hospitalised patients with COVID-19: the COVID-19 SEIMC score. *Thorax*. 2021;76(9):920–929. DOI: 10.1136/thoraxjnl-2020-216001.
18. Cho S.I., Yoon S., Lee H.J. Impact of comorbidity burden on mortality in patients with COVID-19 using the Korean health insurance database. *Sci. Rep*. 2021;11(1):6375. DOI: 10.1038/s41598-021-85813-2.
19. Zhanibekov Zh.Zh., Chukhliaev P.V., Khavkina D.A., Akhmedova M.D., Ruzhentsova T.A. The importance of outpatient etiotropic therapy in patients hospitalized with COVID-19. *Journal of Infectology*. 2023;15(1):48–54 (in Russ.). DOI: 10.22625/2072-6732-2023-15-1-48-54.
20. Leneva I.A., Pshenichnaya N.Y., Bulgakova V.A. Umifenovir and coronavirus infections: a review of research results and clinical practice. *Therapy Archives*. 2020;92(11):91–97 (in Russ.). DOI: 10.26442/00403660.2020.11.000713.
21. Talavera B., García-Azorín D., Martínez-Pías E., Trigo J., Hernandez-Perez I., Valle-Penacoba G. et al. Anosmia is associated with lower in-hospital mortality in COVID. *J. Neurol. Sci*. 2020;419:117163. DOI: 10.1016/j.jns.2020.117163.
22. Yadaw A.S., Li Y.C., Bose S., Iyengar R., Bunyavanich S., Pandey G. Clinical features of COVID-19 mortality: development and validation of a clinical prediction model. *Lancet Digit Health*. 2020;2(10):516–525. DOI: 10.1016/S2589-7500(20)30217-X.
23. Cheng B., Hu J., Zuo X., Chen J., Li X., Chen Y., et al. Predictors of progression from moderate to severe coronavirus disease 2019: a retrospective cohort. *Clin. Microbiol. Infect*. 2020;26(10):1400–1405. DOI: 10.1016/j.cmi.2020.06.033.
24. Ghobadi H., Moham madshahi J., Javaheri N., Fouladi N., Mirzazadeh Y., Aslani M.R. Role of leukocytes and systemic inflammation indexes (NLR, PLR, MLP, dNLR, NLPR, AISI, SIR-I, and SII) on admission predicts in-hospital mortality in non-elderly and elderly COVID-19 patients. *Front. Med (Lausanne*). 2022;9:916453. DOI: 10.3389/fmed.2022.916453.
25. Duan J., Wang X., Chi J., Chen H., Bai L., Hu Q. et al. Correlation between the variables collected at admission and progression to severe cases during hospitalization among patients with COVID-19 in Chongqing. *J. Med. Virol*. 2020;92(11):2616–2622. DOI: 10.1002/jmv.26082.
26. Mohammadi Z., Faghih D.M., Vahed N., Ebrahimi B.H., Rahmani F. Clinical and Laboratory Predictors of COVID-19-Related In-hospital Mortality; a Cross-sectional Study of 1000 Cases. *Arch. Acad. Emerg. Med*. 2022;10(1):49. DOI: 10.22037/aaem.v10i1.1574.
27. Pitamberwale A., Mahmood T., Ansari A.K., Ansari S.A., Limgaokar K., Singh L. et al. Biochemical parameters as prognostic markers in severely Ill COVID-19 patients. *Cureus*. 2022;14(8):28594. DOI: 10.7759/cureus.28594.
28. Poggiali E., Zaino D., Immovilli P., Rovero L., Losi G., Dacrema A. et al. Lactate dehydrogenase and C-reactive protein as predictors of respiratory failure in COVID-19 patients. *Clin. Chim. Acta*. 2020;509:135–138. DOI: 10.1016/j.cca.2020.06.012.
29. Tomazini B.M., Maia I.S., Cavalcanti A.B., Berwanger O., Rosa R.G., Veiga V.C. et al. Effect of Dexamethasone on Days Alive and Ventilator-Free in Patients With Moderate or Severe Acute Respiratory Distress Syndrome and COVID-19: The CoDEX Randomized Clinical Trial. *JAMA*. 2020;324(13):1307–1316. DOI: 10.1001/jama.2020.17021.
30. Gorodin V.N., Moysova D.L., Pronin M.G., Zotov S.V., Mihayluk E.I., Tikhonenko Yu.V. Predictors of poor outcomes in patients with pandemic viral infections (influenza AH1N-1pdm09, COVID-19) on a ventilator. *Infectious Diseases3*

31. Gorodin V.N., Moysova D.L., Pronin M.G., Zotov S.V., Mihayluk E.I., Tikhonenko Yu.V. Predictors of poor outcomes in patients with pandemic viral infections (influenza AH1N-1pdm09, COVID-19) on a ventilator. *Infectious Diseases*. 2022;20(4):25–33 (in Russ.). DOI: 10.20953/1729-9225-2022-4-25-33.

Authors' contribution

Malinovskiy V.A.– conception and design, collection and processing of the material, drafting of the article. Fedosenko S.V. – conception and design, drafting and editing of the article. Semakin A.V. – collection and processing of the material, drafting of the article. Dirks I.I., Semenova O.L. – collection and processing of the material. Arzhanik M.B., Agaeva S.A. – collection and processing of the material, editing of the manuscript. Vinokurova D.A. – conception and design. Starovoitova E.A., Nesterovich S.V., Kalyuzhin V.V. – conception and design, editing of the manuscript.

Authors' information

Malinovskiy Vladislav A. – Post-Graduate Student, Division of General Medical Practice and Outpatient Therapy, Internal Medicine Physician, Siberian State Medical University, Tomsk, vladislav-9509@mail.ru, https://orcid.org/0009-0004-8099-3870

Fedosenko Sergey V. – Dr. Sci. (Med.), Associate Professor, Professor of the Division of General Medical Practice and Outpatient Therapy, Siberian State Medical University, Tomsk, s-fedosenko@mail.ru, https://orcid.org/0000-0001-6655-3300

Semakin Aleksey V. – Post-Graduate Student, Division of General Medical Practice and Polyclinic Therapy, Internal Medicine Physician, Siberian State Medical University, Tomsk, drsemakinav@gmail.com, https://orcid.org/0009-0008-4723-1494

Dirks Ivan I. – Student, Department of Medical Biology, Siberian State Medical University, Tomsk, i.dirks@yandex.ru, https://orcid.org/0009-0005-5560-0016

Arzhanik Marina B. – Cand. Sci. (Pedagogy), Associate Professor, Division of Medical and Biological Cybernetics, Siberian State Medical University, Tomsk, arzh_m@mail.ru, https://orcid.org/0000-0003-4844-9803

Semenova Oksana L. – Senior Lecturer, Division of Medical and Biological Cybernetics, Siberian State Medical University, Tomsk, oksleon@list.ru, https://orcid.org/0000-0002-6866-5020

Vinokurova Daria A. – Head of the Internal Medicine Clinic, Teaching Assistant, Division of Intermediate-Level Therapy with a Course in Pharmacology, Siberian State Medical University, Tomsk, vinokurovadarial@gmail.com, https://orcid.org/0000-0002-8422-8349

Starovoitova Elena A. – Dr. Sci. (Med.), Associate Professor, Head of the Division of General Medical Practice and Outpatient Therapy, Siberian State Medical University, Tomsk, elena-starovoytova@yandex.ru, https://orcid.org/0000-0002-4281-1157

Agaeva Sofiya A. – Student, Department of Pediatrics, Laboratory Assistant and Researcher, Division of Introduction into Internal Diseases with a Course in Therapy of the Pediatric Department, Siberian State Medical University, Tomsk, agaeva.sofiyaa@gmail.com, https://orcid.org/0009-0004-5619-5473

Nesterovich Sofia V. – Dr. Sci. (Med.), Chief Physician of Siberian State Medical University clinics, Tomsk, nesterovich.sv@ssmu.ru, https://orcid.org/0000-0003-2098-2964

Kalyuzhin Vadim V. – Dr. Sci. (Med.), Professor, Head of the Advanced Therapy Division with a Course in Rehabilitation, Physiotherapy and Sports Medicine, Siberian State Medical University, Tomsk, kalyuzhinvv@mail.ru, http://orcid.org/0000-0001-9640-2028

(✉) **Agaeva Sofiya A.,** agaeva.sofiyaa@gmail.com

Received 11.06.2024;
approved after peer review 25.06.2024;
accepted 27.06.2024

УДК 616.127-005.8-02:616.131-008.331.1]-055.1-053.81/.85
https://doi.org/10.20538/1682-0363-2024-4-74-81

Predictors of pulmonary hypertension in the subacute period of myocardial infarction in young and middle-aged males

Menshikova A.N., Gordienko A.V., Sotnikov A.V., Nosovich D.V.

S.M. Kirov Military Medical Academy
6, Akademika Lebedeva Str., Saint Petersburg, 194044, Russian Federation

ABSTRACT

Aim. To identify predictors of the development of pulmonary hypertension (PH) in the subacute period of myocardial infarction (MI) in young and middle-aged males to improve preventive measures.

Materials and methods. We studied the results of treatment of male patients aged 32–60 years with a verified diagnosis of MI. Based on echocardiography findings and detection of PH at the end of the third week of MI, the patients were divided into the study group (patients with PH) and the comparison group (patients with a normal pressure in the pulmonary artery). In the studied groups, a comparative assessment of various parameters was performed, and an analysis of the risks of developing PH using the Pearson's chi-squared test was conducted.

Results. We found that the risk of developing PH in the subacute period of MI was significantly affected by certain parameters of peripheral hemodynamics, the presence of bradycardia, and the calculated value of total pulmonary resistance. The main parameters of the lipid profile were found to be significant predictors of PH in the subacute period of MI, along with some parameters of electrolyte metabolism (sodium and magnesium in the first 48 hours of MI, potassium and calcium at the end of the third week of the disease). We established the presence of a reliable relationship between several parameters of the structural and functional state of the myocardium both in the first 48 hours of MI and the end of the third week of the disease with the risk of developing PH in the subacute period of MI.

Conclusion. The identified predictors make it possible to determine patients with MI who are at an increased risk of PH to timely diagnose and treat the disease and improve the prognosis.

Keywords: pulmonary hypertension, predictors, myocardial infarction, cardiovascular disease risk factors, pulmonary artery pressure, systolic dysfunction, echocardiography, men, young and middle age

Conflict of interest. The authors declare the absence of obvious or potential conflicts of interest related to the publication of this article.

Source of financing. The authors state that they received no funding for the study.

Conformity with the principles of ethics. The study was approved by the independent Ethics Committee at S.M. Kirov Military Medical Academy (Protocol No. 258 of 21.12.2021) and was carried out in accordance with the research plan of S.M. Kirov Military Medical Academy.

For citation: Menshikova A.N., Gordienko A.V., Sotnikov A.V., Nosovich D.V. Predictors of pulmonary hypertension in the subacute period of myocardial infarction in young and middle-aged males. *Bulletin of Siberian Medicine.* 2024;23(4):74–81. https://doi.org/10.20538/1682-0363-2024-4-74-81.

✉ *Menshikova Alexandra N.,* aleksandra12591@mail.ru

Предикторы легочной гипертензии в подостром периоде инфаркта миокарда у мужчин молодого и среднего возраста

Меньшикова А.Н., Гордиенко А.В., Сотников А.В., Носович Д.В.

Военно-медицинская академия (ВМА) им. С.М. Кирова
Россия, 194044, г. Санкт-Петербург, ул. Академика Лебедева, 6

РЕЗЮМЕ

Цель. Выявить предикторы развития легочной гипертензии (ЛГ) в подостром периоде инфаркта миокарда (ИМ) у мужчин молодого и среднего возраста для совершенствования профилактических мероприятий.

Материалы и методы. Изучены результаты лечения мужчин 32–60 лет с верифицированным диагнозом ИМ. По итогам выполнения эхокардиографии и выявления ЛГ в конце третьей недели ИМ пациентов разделяли на исследуемую группу (с ЛГ) и группу сравнения (с нормальным уровнем давления в легочной артерии). В изучаемых группах проведена сравнительная оценка различных параметров, а также выполнен анализ рисков развития ЛГ с помощью критерия $\chi 2$ Пирсона.

Результаты. На риск развития ЛГ в подостром периоде ИМ оказывают статистически значимое влияние некоторые параметры периферической гемодинамики, наличие брадикардии, расчетная величина общего легочного сопротивления. Значимыми предикторами ЛГ в подостром периоде ИМ оказались основные параметры липидограммы, а также некоторые показатели электролитного обмена (натрий и магний в первые 48 ч ИМ, калий и кальций в конце третьей недели заболевания). Установлено наличие статистически значимой взаимосвязи ряда показателей структурно-функционального состояния миокарда как первых 48 ч ИМ, так и конца третьей недели заболевания, с риском развития ЛГ в подостром периоде ИМ.

Заключение. Выявленные предикторы позволят формировать группы повышенного риска ЛГ среди пациентов с ИМ с целью своевременной диагностики и лечения для улучшения прогноза.

Ключевые слова: легочная гипертензия, предикторы, инфаркт миокарда, факторы риска кардиоваскулярных заболеваний, давление в легочной артерии, систолическая дисфункция, эхокардиография, мужчины, молодой и средний возраст

Конфликт интересов. Авторы декларируют отсутствие явных и потенциальных конфликтов интересов, связанных с публикацией настоящей статьи.

Источник финансирования. Авторы заявляют об отсутствии финансирования при проведении исследования.

Соответствие принципам этики. Исследование одобрено независимым этическим комитетом при Военно-медицинской академии им. С.М. Кирова (протокол № 258 от 21.12.2021) и выполнено в соответствии с планом научной работы ВМА им. С.М. Кирова.

Для цитирования: Меньшикова А.Н., Гордиенко А.В., Сотников А.В., Носович Д.В. Предикторы легочной гипертензии в подостром периоде инфаркта миокарда у мужчин молодого и среднего возраста. *Бюллетень сибирской медицины.* 2024;23(4):74–81. https://doi.org/10.20538/1682-0363-2024-4-74-81.

INTRODUCTION

Pulmonary hypertension (PH) is a pathological condition that is often a complication of a significant number of diseases, which underlies the modern classification of this pathology. PH is considered separately in diseases of the left chambers of the heart, especially in myocardial infarction (MI) [1, 2], since this complication significantly aggravates its course and worsens the prognosis [1, 3]. This statement has been proven to a greater extent in relation to elderly patients [4, 5]; however, there is currently a clear trend toward MI incidence in young individuals [6, 7].

Since young and middle-aged males are exposed to such common risk factors for the development of cardiovascular pathology as unhealthy diet, low physical activity, overweight, psychological stress, smoking, and arterial hypertension, the incidence of MI in this group of patients increases. In the long run, this will make PH a relevant problem in males of working age [6–8]. Echocardiography (ECHO) is the most accessible noninvasive method for detecting

increased pressure in the pulmonary artery, which, however, does not always allow for timely diagnosis of PH, despite its widespread use [1, 5, 8]. PH is characterized by a steadily progressive course. As a rule, it does not have clear clinical manifestations for a long time, which makes it difficult to diagnose and leads to disability of patients, as well as a decrease in the effectiveness of therapy [1, 2, 8].

The aim of the study was to identify predictors of the development of PH in the subacute period of MI in males under 60 years of age among the most accessible clinical and test parameters to improve its prevention.

MATERIALS AND METHODS

The main inclusion criteria were the following: male; age from 18 to 60 years; verified type 1 MI (Fourth Universal Definition of Myocardial Infarction, 2018) [9]. The exclusion criteria were as follows: female; age younger than 18 and older than 60 years; at baseline, reduced glomerular filtration rate (CKD-EPI, 2011) of less than 30 ml / min / 1.73 m^2; type 2, 3, 4, and 5 MI; presence of concomitant pathology capable of independently influencing the development of PH (viral hepatitis B and C, cirrhosis, other portal hypertension syndromes, HIV infection; systemic connective tissue diseases with constant immunosuppressive therapy; congenital heart disorders); verified cancers; endocrine pathology (except diabetes mellitus); pronounced deviations in the complete blood count (hemoglobin level of less than 130 g / l, platelet count of less than 100×10^9 / l, leukocyte count of less than 3.0×10^9 / l).

The study was approved by the Independent Ethics Committee at S.M. Kirov Military Medical Academy (Protocol No. 258 of 21.12.2021). All the examined persons or their relatives signed an informed consent to participate in this study before undergoing the procedures.

Thus, the study included 570 males aged 32–60 years, among whom Q-wave MI and the presence of complications were detected in 53.5% (305 patients) and 56.5% (322 patients) of cases, respectively. Reinfarction and recurrent MI were registered in 49.7% (283 patients) and 4.4% (25 patients) of cases, respectively. Depending on the location of MI, patients were distributed as follows: anterior MI in the left ventricle (LV) was detected in 47.0% (268 people) of cases, LV inferior wall MI – in 39.5% (225 people), and MI in other locations – in 13.5% (77 people). When divided into the study and the comparison group, the patients did not significantly differ in these characteristics. A fatal outcome was observed in 5.1% of cases (29 patients) – only among patients of the comparison group ($p = 0.012$).

In the first 48 hours (I) and at the end of the third week of MI (II), all patients underwent a set of clinical examinations and tests in accordance with approved clinical guidelines, including ECHO, during which the sizes of the heart chambers and the mean pulmonary artery pressure were recorded (mPAP) [1, 10], and LV systolic function was assessed (according to the Simpson method) [11–13]. The value of total pulmonary resistance (TPR) was calculated by the Shishmarev method [13–15]. ECHO was used to determine the following parameters in all patients: the dimensions of the left atrium (LA), the thickness of the LV posterior wall (PW), right ventricular end-diastolic volume (RVEDV), LV ejection fraction (EF), including cardiac index (CI), LV myocardial mass index (LVMMI), LV end-systolic (ESV/S) and end-diastolic (EDV/S) volumes. Indexing was estimated by body surface area (proposed by D. Du Bois and E.F. Du Bois) [10, 11]. Depending on the values of mPAP, the patients were divided into two groups: the study group, in which the level of $mPAP_I$ was within the normal range (less than 20 mm Hg) and elevated to 21 mm Hg and more – 102 patients (average age 51.0 ± 7.0 years); and the comparison group – patients with normal or elevated levels of $mPAP_I$ and normal levels of $mPAP_{II}$ – 468 patients (51.4 ± 6.0 years, $p = 0.978$).

In order to conduct early monitoring of manifestations of heart failure (HF), in the first 48 hours and at the end of the third week of MI, the severity of its symptoms (shortness of breath, palpitations, weakness, cough, fatigue) were assessed by calculating the index of subjective manifestations of HF (SMHFI) [15]. The main parameters of peripheral hemodynamics were used as parameters of the clinical examination: heart rate (HR) per minute, levels of systolic (systBP), diastolic (diastBP) and mean (meanBP) blood pressure (meanBP = diastBP + 1/3 × (systBP – diastBP)). Among the test parameters, the main parameters of the lipid profile were studied: the concentration of total cholesterol (TC) in the blood, lipoproteins ranked by density (high (HDL), very low (VLDL) and low (LDL)), their ratio (LDL/HDL and TC/HDL), and atherogenic coefficient (AC). In addition, parameters of electrolyte metabolism were determined, including the levels of potassium, sodium, total calcium, and magnesium.

All patients included in the study received drug therapy in accordance with clinical guidelines for the management of patients with MI, including anticoagulants, antiplatelets, and lipid-lowering agents, as well as renin – angiotensin – aldosterone system inhibitors, beta-blockers, and nitrates. Patients in the study group and the comparison group did not have significant differences in terms of drug therapy. The proportion of patients who underwent revascularization was 25.5% (26 people) and 21.8% (102 people, $p = 0.263$) in the study and comparison groups, respectively. The selected groups did not have significant differences in the number of arteries affected in coronary artery disease (CAD), the extent and severity of the identified CAD, as well as in the frequency and the volume of revascularization. The low proportion of patients who underwent coronary angiography and early myocardial revascularization is mainly due to their refusal to undergo the procedure and / or delayed hospitalization due to late presentation.

The obtained data of the clinical and test examinations were organized using a formalized medical history, presented in the form of an electronic database (Microsoft Excel 2016). The research results were statistically processed using the Microsoft Excel 2016, Statistica 10.0, and SAS JMP 11 software. The obtained parameters were compared between the selected groups using the Mann – Whitney test and the Pearson's chi-squared test. In addition, the latter was used to assess the statistical significance of the influence of factors on a binary target variable when calculating the risks of PH at the second time point (II) – absolute risk (AR, %) and relative risk with a 95% confidence interval (RR, abs. [95% CI]). The cut-off levels of these factors were determined by their maximum statistical significance. The value of $p < 0.05$ was considered to be statistically significant.

RESULTS

When assessing the influence of peripheral hemodynamic parameters on the risk of PH development at the second measurement point (II), it turned out that parameters determined during this period (II), such as $meanBP_{II}$ levels of 93.3 mm Hg or more (AR: 11.2%; RR: 1.98 [1.23; 3.19]; $p = 0.003$) and $diastBP_{II}$ of 75 mm Hg or more (AR: 10.9%; RR: 1.98 [1.19; 3.30]; $p = 0.005$), as well as $systBP_{I}$ level of 160 mm Hg or more (AR: 9.3%; RR: 1.58 [1.07, 2.33]; $p = 0.023$) and HR_{I} of less than 75 bpm (AR: 20.5%; RR: 3.71 [2 .19; 6.28]; $p < 0.001$) in the first hours (I) of MI had a significant relationship. It was revealed that the risk of developing PH after MI increases if the patient has bradycardia during ECG (AR: 17.3%; RR: 2.04 [1.33; 3.14]; $p = 0.020$) and decreases if sinus tachycardia is registered (AR: -17.9%; RR: 0.18 [0.06, 0.57]; $p < 0.001$). The risk of PH development in the subacute MI period increases in patients with a TPR_{I} value of less than 421 dyn. × s × cm^{-5} (AR: 20.1%; RR: 3.29 [2.03; 5.32]; $p < 0.001$) and TPR_{II} of 237.3 dyn. × s × cm^{-5} or more (AR: 17.6%; RR: 4.03 [1.81; 8.97]; $p < 0.001$). The risk of PH development after MI was associated with an estimated level of SMHFI of less than 19.3%, determined at the end of the third week of MI (AR: 12.1%; RR: 2.16 [1.02; 4.58]; $p = 0.033$).

Figures 1 and 2 present data on the relationship between lipid metabolism parameters and the risk of PH development after MI.

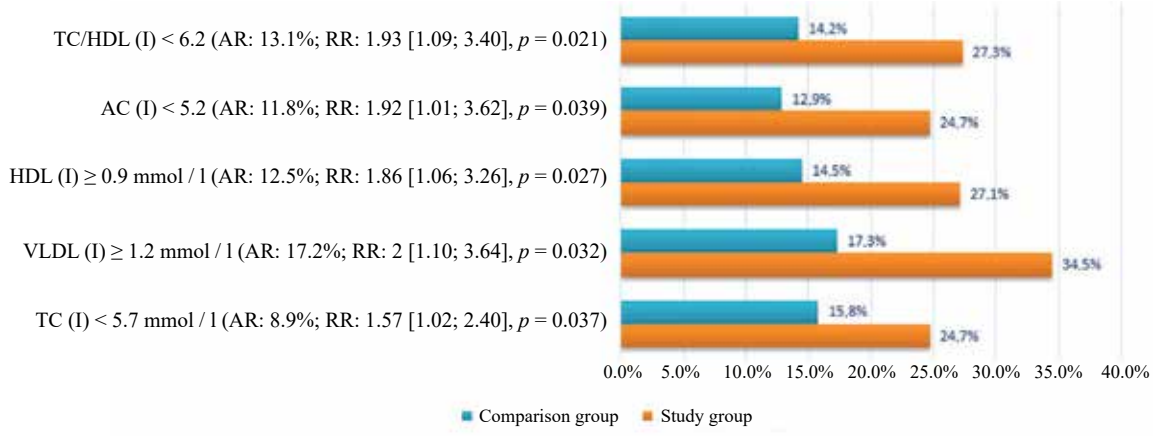

Fig. 1. Relationships between lipid metabolism parameters in the first hours of myocardial infarction and the risk of developing pulmonary hypertension in its subacute period: p – level of significance, the chi-squared test

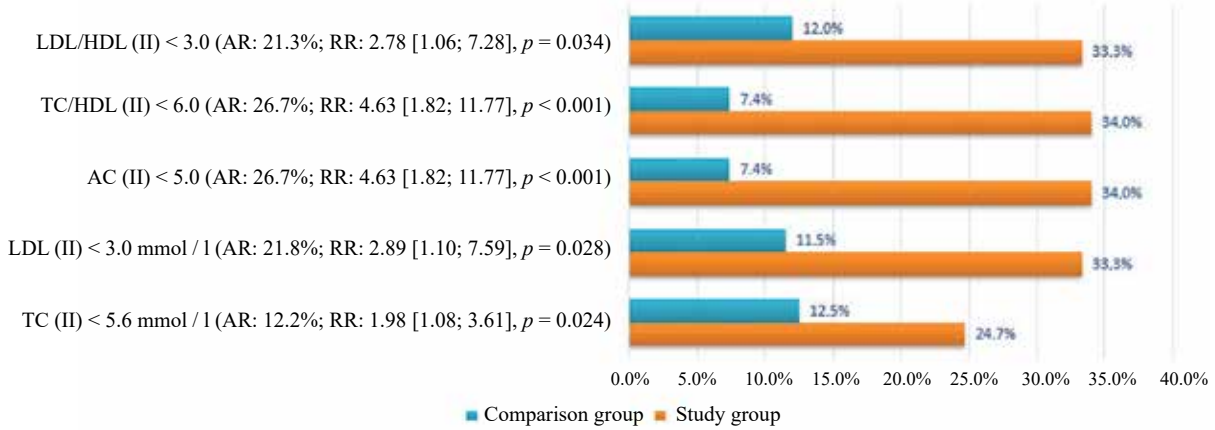

Fig. 2. Relationships between lipid metabolism parameters at the end of the third week of myocardial infarction and the risk of developing pulmonary hypertension during this period: *p* – level of significance, the chi-squared test

Significant patterns of changes in the risks of developing PH in the examined patients depending on the concentration of the main electrolytes in the blood plasma were obtained both during the first hours (Fig. 3) and at the end of the third week of the disease (Fig. 4).

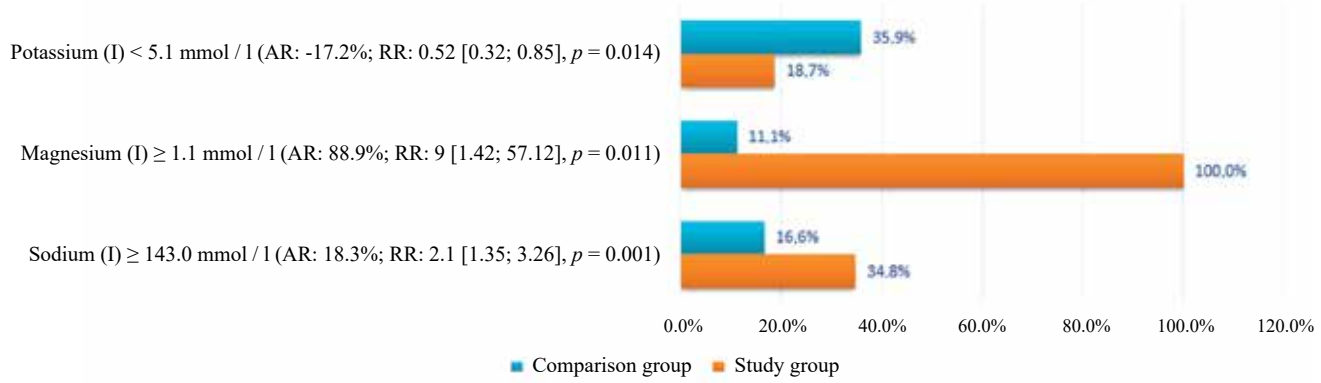

Fig. 3. Relationships between blood plasma electrolyte concentrations in the first hours of myocardial infarction and the risk of pulmonary hypertension at the second measurement point: *p* – level of significance, the chi-squared test

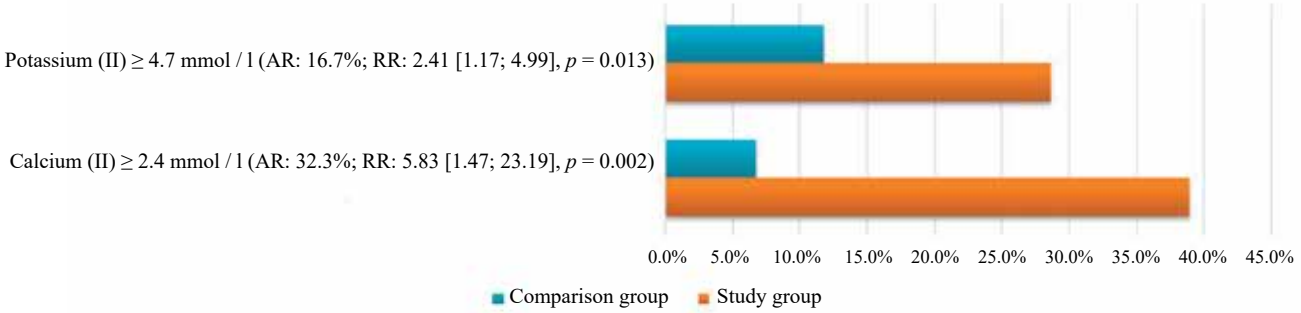

Fig. 4. Relationships between blood plasma electrolyte concentrations at the end of the third week of myocardial infarction and the risk of developing pulmonary hypertension in its subacute period: *p* – significance level, the chi-squared test

Of all the studied factors, the parameters of the structural and functional state of both the left and right heart chambers were found to have the largest number of relationships with the risk of PH development at the end of the subacute MI period (Fig. 5, 6). In the first 48 hours of the disease, the following parameters turned out to be significant: CI, LVMMI, LV ESV/S and LV EDV/S, LA sizes and LVPW thickness, LVEF, and RVEDV.

At the end of the third week of MI, a relationship with the risk of PH development was identified for the following parameters: right atrium (RA) size, LVMMI, LV PW thickness, and LA transverse size.

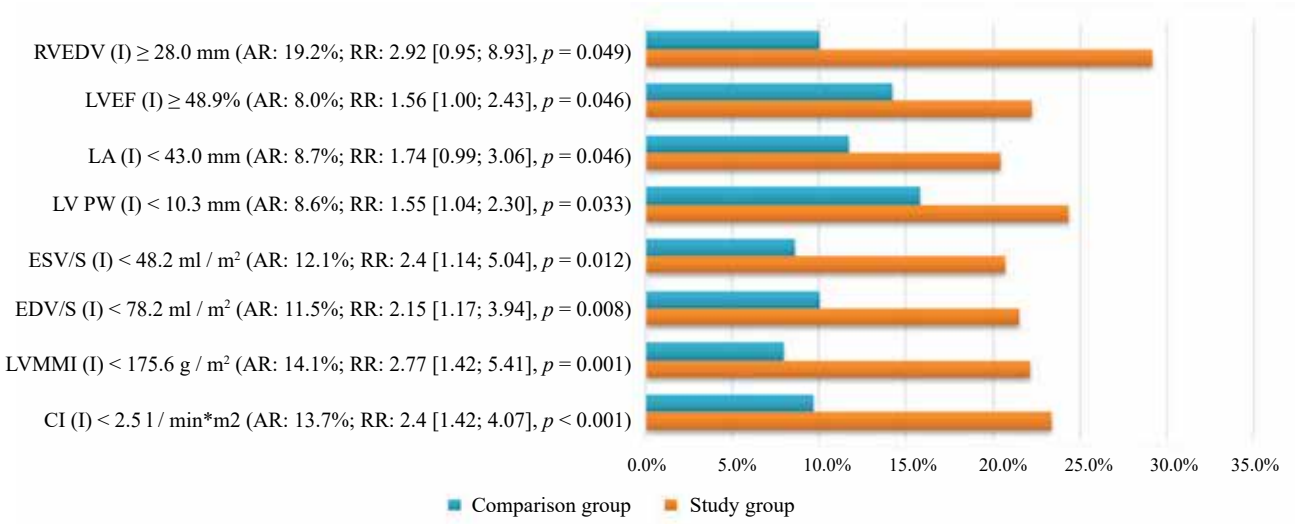

Fig. 5. Relationships between the parameters of the structural and functional state of the heart in the first hours of myocardial infarction and the risk of pulmonary hypertension development in the second period of the study: *p* – level of significance, the chi-squared test

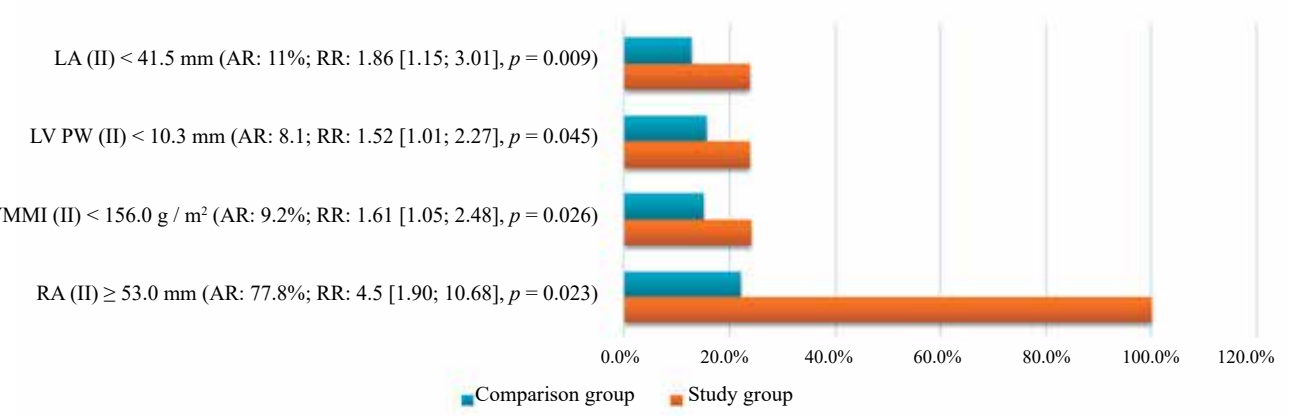

Fig. 6. Patterns of changes in parameters of the structural and functional state of the heart at the end of the third week of myocardial infarction and the risk of pulmonary hypertension development during this period: *p* – level of significance, the chi-squared test

DISCUSSION

Hemodynamic parameters, such as blood pressure and heart rate, as well as a significant increase in TPR in the patients of the study group, significantly affect the development of PH, which confirms that persistent narrowing of pulmonary vessels in addition to a passive retrograde increase in the pulmonary artery pressure participate in the pathogenesis of PH during MI [2, 8, 13]. It was found that the risk of PH development in the subacute MI period is higher in patients with bradycardia, which is most likely due to a long history of cardiovascular diseases accompanied by the development of atherosclerotic and/or postinfarction cardiosclerosis, leading to a decrease in the automaticity of the sinoatrial node [16]. The effect of the SMHFI value on the risk of developing the studied complication has no independent prognostic value; however, it indirectly reflects the degree of functional myocardial insufficiency. In the patients of the study group, the calculated SMHFI value was less than 19.3%, which corresponds to a minimal or moderate degree of myocardial insufficiency [16].

The identified relationship between the risk of developing PH in MI and lipid metabolism parameters is reflected in the literature. It has been shown that apolipoprotein AI- and E-dependent mechanisms employ the patterns of interrelated changes in pulmonary hemodynamics and lipid levels [17], with the involvement of specific regulatory elements, such as microRNA [18], protein associated with transforming growth factor beta [19], and exosomes [20]. Electrolyte changes found in the patients of the study group, in particular an increase in sodium concentration, indicate increased activity of hormones of the renin – angiotensin –aldosterone system, water

retention in the body, an increase in pre- and afterload on the myocardium, the occurrence and subsequent increase in diastolic dysfunction, and also hypertrophy of vascular smooth muscle cells and fibrosis of their walls [1, 14, 20]. An increase in the concentration of total calcium in the blood serum in the patients of the study group confirms the separate role of this ion and numerous calcium channels in the PH development due to the regulation of pulmonary vasoconstriction and remodeling of pulmonary vessels [21].

The parameters of the structural and functional state of the myocardium in the first hours of the disease significantly affect the risk of PH development, which indicates the presence of more pronounced LV systolic dysfunction in patients with PH, as well as dilatation and remodeling of the left heart [8, 14], which reflects the pathogenesis of PH in diseases of the left chambers of the heart [1]. The baseline increase in RVEDV in the patients of the study group indicates a smaller adaptive reserve of the right chambers of the heart and is a prerequisite for the PH development during the studied MI period and acts as a predictor of an unfavorable prognosis [22].

The result of the study confirms a statistically significant relationship between PH and LV dysfunction, and changes in electrolyte and lipid metabolism. However, we should not exclude the effect of other probable causes of PH, given their ability to additionally contribute to the development and progression of this pathology. In order to determine the presence of LV myocardial dysfunction as the main etiological factor of PH, as well as to conduct differential diagnosis with rare syndrome-like conditions as causes of increased pressure in the pulmonary arteries, it is recommended to determine the concentration of N-terminal pro–B-type natriuretic peptide [23]. It is important to establish the hemodynamic mechanisms of PH depending on the degree of pulmonary vascular resistance to initiate optimal therapy, which dictates the need for early diagnosis of increased pulmonary artery pressure [1, 8, 24]. When conducting the differential diagnosis of PH in MI, it is recommended to exclude right ventricular and atrial MI, ruptures of the interventricular septum, previously undiagnosed congenital heart disorders, as well as severe mitral regurgitation requiring surgical correction [3, 4, 25].

CONCLUSION

The study established the presence of a number of anamnestic, clinical, and test markers associated with the development of PH in the subacute period of MI. Their early detection at the stage of admission to hospital makes it possible to form a group of patients at high risk of developing this complication for timely and necessary diagnostic and therapeutic measures in accordance with the algorithm. ECHO is the most convenient, reliable, non-invasive, and currently available technique that allows to verify PH at early stages, as well as to predict the risk of its development. This explains the need to determine the level of mPAP over time in patients at high risk of developing PH in early phases of MI.

REFERENCES

1. Humbert M., Kovacs G., Hoeper M.M., Badagliacca R., Berger R.M.F., Brida M. et al. 2022 ESC/ERS Guidelines for the diagnosis and treatment of pulmonary hypertension. *Eur. Respir. J.* 2023;61(1):2200879. DOI: 10.1183/13993003.00879-2022.
2. Maeder M.T., Schoch O.D., Kleiner R., Joerg L., Weilenmann D., Swiss Society For Pulmonary Hypertension. Pulmonary hypertension associated with left-sided heart disease. *Swiss Med. Wkly*. 2017;147:w14395. DOI: 10.4414/smw.2017.14395.
3. Çetin M., Özer S., Çinier G., Yılmaz A.S., Erdoğan T., Şatıroğlu Ö. Left atrial volume index and pulmonary arterial pressure predicted MACE among patients with STEMI during 8-year follow-up: experience from a tertiary center. *Herz.* 2021;46(4):367–374. DOI: 10.1007/s00059-020-04966-4.
4. Sannino A., Smith R.L., Schiattarella G.G., Trimarco B., Esposito G., Grayburn P.A. Survival and cardiovascular outcomes of patients with secondary mitral regurgitation: a systematic review and meta-analysis. *JAMA Cardiol*. 2017;2(10):1130–1139. DOI: 10.1001/jamacardio.2017.2976.
5. Fan X.T., Wang S.J., Mujahid H., Ji X.P. Effect of elevated pulmonary artery systolic pressure on short-term prognosis in patients with acute myocardial infarction. *Angiology*. 2020;71(6):567–572. DOI: 10.1177/0003319720909056.
6. Benjamin E.J., Virani S.S., Callaway C.W., Chamberlain A.M., Chang A.R., Cheng S. et al. Heart Disease and Stroke Statistics-2018 Update: A Report From the American Heart Association. *Circulation*. 2018;137(12):e67–e492. DOI: 10.1161/CIR.0000000000000558.
7. Boitsov S.A., Pogosova N.V., Bubnova M.G., Drapkina O.M., Gavrilova N.E., Yeganyan R.A., et al. Cardiovascular prevention 2017. National guidelines. *Russian Journal of Cardiology*. 2018;23(6):7–122 (in Russ.). DOI: 10.15829/1560-4071-2018-6-7-122.
8. Chung K., Strange G., Codde J., Celermajer D., Scalia G.M., Playford D. Left heart disease and pulmonary hypertension: are we seeing the full picture? *Heart Lung Circ*. 2018;27(3):301–309. DOI: 10.1016/j.hlc.2017.09.015.
9. Thygesen K., Alpert J.S., Jaffe A.S., Chaitman B.R., Bax J.J., Morrow D.A. et al. Fourth universal definition of myocardial infarction (2018). *Eur. Heart J.* 2019;40(3):237–269. DOI: 10.1093/eurheartj/ehy462.
10. Kitabatake A., Iuone M., Asao M. Noninvasive evaluation of pulmonary hypertension by a pulsed Doppler technique. *Circulation.*1983;68(2):302–309. DOI: 10.1161/01.cir.68.2.302.

11. Vdovenko D.V., Libov I.A., Libis R.A. Assessment of function of the left heart myocardium by tissue doppler imaging and speckle tracking echocardiography in patients with chronic heart failure with preserved left ventricular ejection fraction. *Kardiologiia*.2019;59(2):17–23 (in Russ.). DOI:10.18087/cardio.2019.2.10227.
12. Galderisi M., Cosyns B., Edvardsen T., Cardim N., Delgado V., Di Salvo G. et al. 2016–2018 EACVI Scientific Documents Committee. Standardization of adult transthoracic echocardiography reporting in agreement with recent chamber quantification, diastolic function, and heart valve disease recommendations: an expert consensus document of the European Association of Cardiovascular Imaging. *Eur. Heart J. Cardiovasc. Imag.* 2017;18(12):1301–1310. DOI: 10.1093/ehjci/jex244.
13. Bartosh-Zelenaya S.Yu., Guseva O.A. The algorithm of echocardiography and the formation of the impression. St. Petersburg: SPbGPU, 2014: 65 (in Russ.).
14. Sotnikov A.V., Gordienko A.V., Nosovich D.V., Yakovlev V.V., Egorenkova E.V., Kovalev S.V. Noninvasive assessment of the effect of clinical parameters on hemodynamics of the small circle of blood circulation in men under 60 years of age with myocardial infarction in the initial periods of the disease. *Eurasian Heart Journal*. 2017;3:85 (in Russ.).
15. Gordienko A.V., Sotnikov A.V., Nosovich D.V. Clinical criteria for assessing the quality of life in young and middle-aged men in the initial periods of myocardial infarction. *Medical and pharmaceutical journal "Pulse"*. 2018;20(1):34–44 (in Russ.).
16. Sidhu S., Marine J.E. Evaluating and managing bradycardia. *Trends in Cardiovascular Medicine*. 2020;30(5):265–272. DOI: 10.1016/j.tcm.2019.07.001.
17. Yao X., Gordon E.M., Figueroa D.M., Barochia A.V., Levine S.J. Emerging roles of apolipoprotein E and apolipoprotein A-I in the pathogenesis and treatment of lung disease. *Am. J. Respir. Cell Mol. Biol*. 2016;55(2):159–169. DOI: 10.1165/rcmb.2016-0060TR.
18. Song Z., Gao R., Yan B. Potential roles of microRNA-1 and microRNA-133 in cardiovascular disease. *Rev. Cardiovasc. Med.* 2020;21(1):57–64. DOI: 10.31083/j.rcm.2020.01.577.
19. Boratkó A., Csortos C. PKC mediated phosphorylation of TIMAP regulates PP1c activity and endothelial barrier function. *Biochimica et Biophysica acta. Molecular Cell Research*. 2017;1864 (2):431–439. DOI: 10.1016/j.bbamcr.2016.12.001.
20. Yuan Y., Du W., Liu J., Ma W., Zhang L., Du Z., Cai B. Stem cell-derived exosome in cardiovascular diseases: macro roles of micro particles. *Front. Pharmacol*. 2018;*9*:547. DOI: 10.3389/fphar.2018.00547.
21. Liu G,. Fu D., Tian H., Dai A. The mechanism of ions in pulmonary hypertension. *Pulm. Circ.* 2021;11(1):1–20. DOI: 10.1177/2045894020987948.
22. Da Costa Junior A.A., Ota-Arakaki J.S., Ramos R.P., Uellendahl M., Mancuso F.J., Gil M.A. et al. Diagnostic and prognostic value of right ventricular strain in patients with pulmonary arterial hypertension and relatively preserved functional capacity studied with echocardiography and magnetic resonance. *Int. J. Cardiovasc. Imag*. 2017;33(1):39–46. DOI: 10.1007/s10554-016-0966-1.
23. McDonagh T.A., Metra M., Adamo M., Gardner R.S., Baumbach A., Böhm M. et al. 2021 ESC Guidelines for the diagnosis and treatment of acute and chronic heart failure. *Eur. Heart J*. 2021;42(36):3599–3726. DOI: 10.1093/eurheartj/ehab368.
24. Kabbach G., Mukherjee D. Pulmonary hypertension secondary to left heart disease. *Curr. Vasc. Pharmacol*. 2018;16(6):555–560. DOI: 10.2174/1570161115666170913105424.
25. Amorós-Figueras G., Roselló-Diez E., Sanchez-Quintana D., Casabella-Ramon S., Jorge E., Nevado-Medina J. et al. Changes in local atrial electrograms and surface ECG induced by acute atrial myocardial infarction. *Front. Physiol*. 2020;11:264. DOI: 10.3389/fphys.2020.00264.

Authors' information

Menshikova Alexandra N. – Associate Professor, Department of Advanced-level Therapy, S.M. Kirov Military Medical Academy, Saint Petersburg, aleksandra12591@mail.ru, https://orcid.org/0000-0001-9422-4969

Gordienko Alexander V. – Dr. Sci. (Med.), Professor, Professor of the Department of Advanced-level Therapy, S.M. Kirov Military Medical Academy, Saint Petersburg, gord503@mail.ru, https://orcid.org/0000-0002-6901-6436

Sotnikov Alexey V. – Dr. Sci. (Med.), Associate Professor, Professor of the Department of Advanced-level Therapy, S.M. Kirov Military Medical Academy, Saint Petersburg, alexey_vs@mail.ru, https://orcid.org/0000-0002-5913-9088

Nosovich Dmitry V. – Cand. Sci. (Med.), Senior Lecturer, Department of Advanced-level Therapy, S.M. Kirov Military Medical Academy, Saint Petersburg, nozovich@mail.ru, https://orcid.org/0000-0003-2891-4747

(✉) **Menshikova Alexandra N.,** aleksandra12591@mail.ru

Received 08.12.2024;
approved after peer review 02.05.2024;
accepted 13.06.2024

УДК 616.379-008.64-021.6-08:615.825.3:577.12
https://doi.org/10.20538/1682-0363-2024-4-82-94

Effects of forced treadmill exercise on lipid and carbohydrate metabolism parameters in a mouse model of type 2 diabetes mellitus

Milovanova K.G.[1], Zakharova A.N.[1], Orlova A.A.[1], Kollantay O.V.[1], Shuvalov I.Yu.[1], Popov S.A.[1], Medvedev M.A.[2], Kovalev I.V.[2], Yakimovich I.Yu.[2], Chibalin A.V.[1], Kapilevich L.V.[1, 2, 3]

[1] *National Research Tomsk State University*
36, Lenina Av., Tomsk, 634050, Russian Federation

[2] *Siberian State Medical University*
2, Moskovsky Tract, Tomsk, 634050, Russian Federation

[3] *National Research Tomsk Polytechnic University*
30, Lenina Av., Tomsk, 634050, Russian Federation

ABSTRACT

Aim. To study the effect of forced treadmill exercise on lipid and carbohydrate metabolism parameters in liver and skeletal muscle tissues of mice with a model of type 2 diabetes mellitus, taking into account age and biological rhythm characteristics.

Materials and methods. To create a model of type 2 diabetes mellitus (T2DM), a high-fat diet was used. Physical activity in the form of forced treadmill exercise was carried out for 4 weeks. Parameters of lipid and carbohydrate metabolism in muscle and liver tissues were determined by Western blotting.

Results. A decrease in glycogen content in the muscles in T2DM was associated with activation of its breakdown rather than with its reduced synthesis. Significant and multidirectional changes were recorded in the content of glycogen phosphorylase in the liver and skeletal muscle tissues. These changes were significantly influenced by both the nature of diet and physical activity. The development of T2DM in mice was accompanied by a decrease in high-density lipoprotein (HDL) content in the liver along with an increase in low-density lipoprotein (LDL) and very-low-density lipoprotein (VLDL) levels. It is worth noting that physical activity provided partial normalization of the ratio of lipid fractions, despite the fact that the exercises were performed in the context of a high-fat diet.

In the T2DM group, metabolic changes caused by both T2DM modeling and physical exercises were not only quantitative, but in some cases also qualitative. The effects of physical exercises performed at different times of the day on metabolic processes in the liver and muscle tissues varied significantly.

Conclusion. Physical activity can help prevent not only metabolic disorders (obesity and insulin resistance), but also associated complications on the part of the liver and cardiovascular system.

Keywords: liver, skeletal muscles, treadmill running, diabetes mellitus, obesity

Conflict of interest. The authors declare the absence of obvious or potential conflicts of interest related to the publication of this article.

Source of financing. The study was funded by the Russian Science Foundation grant No.19-15-00118, https://rscf.ru/project/19-15-00118-p

Conformity with the principles of ethics. The study was approved by the Bioethics Committee at the Biological Institute of National Research Tomsk State University (Protocol No. 32 of 02.12.2019).

✉ *Kapilevich Leonid V.,* kapil@yandex.ru

For citation: Milovanova K.G., Zakharova A.N., Orlova A.A., Kollantay O.V., Shuvalov I.Yu., Popov S.A., Medvedev M.A., Kovalev I.V., Yakimovich I.Yu., Kapilevich L.V. Effects of forced treadmill exercise on lipid and carbohydrate metabolism parameters in a mouse model of type 2 diabetes mellitus. *Bulletin of Siberian Medicine.* 2024;23(4):82–94. https://doi.org/10.20538/1682-0363-2024-4-82-94.

Эффекты принудительных беговых нагрузок на показатели липидного и углеводного обмена у мышей с моделью сахарного диабета типа 2

Милованова К.Г.[1], Захарова А.Н.[1], Орлова А.А.[1], Коллантай О.В.[1], Шувалов И.Ю.[1], Попов С.А.[1], Медведев М.А.[2], Ковалев И.В.[2], Якимович И.Ю.[2], Чибалин А.В.[1], Капилевич Л.В.[1, 2, 3]

[1] *Национальный исследовательский Томский государственный университет (НИ ТГУ)*
Россия, 634050, г. Томск, пр. Ленина, 36

[2] *Сибирский государственный медицинский университет (СибГМУ)*
Россия, 634050, г. Томск, Московский тракт, 2

[3] *Национальный исследовательский Томский политехнический университет (НИ ТПУ)*
Россия, 634050, г. Томск, пр. Ленина, 30

РЕЗЮМЕ

Цель: изучалось влияние принудительных физических нагрузок на показатели липидного и углеводного обмена в тканях печени и скелетных мышц у мышей с моделью сахарного диабета типа 2 (СД2) с учетом возрастных и биоритмологических особенностей.

Материалы и методы. Для формирования модели заболевания использовалась высокожировая диета, физические нагрузки в виде принудительного бега проводились в течение 4 нед. Показатели липидного и углеводного обмена в тканях мышц и печени определялись методом вестерн-блоттинга.

Результаты. Снижение содержания гликогена в мышцах при СД2 в большей степени связано с активацией процессов его распада, чем со снижением синтеза. Значительные и разнонаправленные изменения фиксировались в содержании гликогенфосфорилазы в тканях печени и скелетных мышц, на эти изменения существенное влияние оказывали и характер питания, и физические нагрузки. Развитие экспериментального СД2 у мышей сопровождалось снижением содержания липопротеинов высокой плотности в печени параллельно с возрастанием липопротеинов низкой и очень низкой плотности. Важно, что физические нагрузки обеспечивали частичную нормализацию соотношения липидных фракций, несмотря на то что выполнялись они на фоне продолжающейся жировой диеты.

В группе СД2 физические нагрузки носили не только количественный, но в некоторых случаях качественный характер. Эффекты физических нагрузок, применяемых в разное время суток, на метаболические процессы в печени и мышечной ткани значительно различаются.

Заключение. Физические нагрузки могут выступать средством профилактики не только непосредственно метаболических нарушений (ожирение и инсулинорезистентность), но и сопутствующих осложнений со стороны печени и в дальнейшем сердечно-сосудистой системы.

Ключевые слова: печень, скелетные мышцы, беговая нагрузка, сахарный диабет, ожирение

Конфликт интересов. Авторы декларируют отсутствие явных и потенциальных конфликтов интересов, связанных с публикацией настоящей статьи.

Источник финансирования. Исследование выполнено за счет гранта Российского научного фонда № 19-15-00118, https://rscf.ru/project/19-15-00118-p

Соответствие принципам этики. Исследование одобрено комиссией по биоэтике Биологического института НИ ТГУ (протокол № 32 от 02.12.2019).

Для цитирования: Милованова К.Г., Захарова А.Н., Орлова А.А., Коллантай О.В., Шувалов И.Ю., Попов С.А., Медведев М.А., Ковалев И.В., Якимович И.Ю., Чибалин А.В., Капилевич Л.В. Эффекты принудительных беговых нагрузок на показатели липидного и углеводного обмена у мышей с моделью сахарного диабета типа 2. *Бюллетень сибирской медицины.* 2024;23(4):82–94. https://doi.org/10.20538/1682-0363-2024-4-82-94.

INTRODUCTION

Type 2 diabetes mellitus (T2DM) is a serious metabolic disease characterized by insulin resistance and decreased insulin production, resulting in abnormally elevated blood glucose levels. It has been reported that T2DM can induce oxidative stress and inflammatory responses and promote various complications, including liver injury [1, 2].

Fatty liver disease associated with metabolic dysfunction and T2DM are two common metabolic disorders that often coexist and synergistically promote each other's progression [3]. Several pathophysiological pathways are involved in this relationship, including insulin resistance, inflammation, and lipotoxicity, contributing to understanding the complex relationships between these conditions [4]. Dyslipidemia has a significant impact on the risk of developing T2DM and micro- and macrovascular complications, and diabetes significantly contributes to an increased risk of liver fibrosis progression and hepatocellular carcinoma. Moreover, both pathologies have a synergistic effect on cardiovascular events and mortality [5].

The liver helps maintain normal fasting and postprandial blood glucose levels. Insulin loss affects the liver, leading to glycogenolysis and increased hepatic glucose production. Abnormalities in triglyceride storage and lipolysis in insulin-sensitive tissues, such as the liver, are early manifestations of disorders characterized by insulin resistance and are detected earlier than fasting hyperglycemia [2].

One of the models for the development of T2DM is feeding animals with a high-fat diet. High-fat diet can lead to obesity, hyperinsulinemia, and altered glucose homeostasis due to insufficient compensation by the islets of Langerhans. Since obesity in this case is caused by dietary manipulations rather than cytotoxic substances, such models are considered to be more similar to the human diseases [6–8].

Physical activity of varying intensity triggers a large number of biochemical, molecular, genetic, and epigenetic mechanisms underlying adaptive responses of the body to physiological stress [9]. In particular, it has been shown that physical activity has a positive effect on metabolic disorders [10]. Experiments with animals have shown that physical activity increases insulin sensitivity and improves glucose tolerance induced by a high-fat diet not only in the animals themselves but also in their offspring [10]. It has also been shown that circadian rhythms affect the effect of physical exercise. Glucose uptake by muscles and insulin tolerance also have a circadian nature and the effects of physical exercises are associated with the circadian rhythm of these parameters [11].

Therefore, the aim of this study was to investigate the effect of forced treadmill exercise on lipid and carbohydrate metabolism in liver and skeletal muscle tissue in a mouse model of T2DM, taking into account age and biological rhythm characteristics.

MATERIALS AND METHODS

Male mice of the C57bl/6 line were used in the study. The mice were obtained from the vivarium of the Tomsk National Research Medical Center of the Russian Academy of Sciences, Goldberg Research Institute of Pharmacology and Regenerative Medicine. Animal maintenance regime: 12 h /12 h light / dark cycle, with daylight starting at 6 am; free access to food and water; room temperature of 24 °C.

The study was conducted in accordance with the principles of the Basel Declaration and approved by the Bioethics Committee at the Biological Institute of Tomsk State University (Protocol No. 32 of 2.12.2019).

Two groups of mice were used in the experiment: young mice (112 mice aged 4 weeks at the beginning of the experiment) and aged mice (112 mice aged 32 weeks at the beginning of the experiment). The experiment lasted 16 weeks. Until week 12 of the experiment, the mice were divided into 2 subgroups: mice receiving a high-fat diet (56 mice) and mice receiving a standard chow diet (56 mice).

To model T2DM, a high-fat diet was used for 12 weeks, developed specifically for this experiment. The composition and energy value of the feed are described in detail in our previous work [12].

Starting from week 12 of the experiment, each group of animals was divided into two subgroups – animals exposed to (main – 21 animals) and not exposed to (control – 7 animals) forced treadmill exercises.

Different subgroups of mice in the main group performed forced treadmill exercise at different times of the day. Group A performed treadmill exercise in the morning (from 8:00 to 10:00) – 7 animals. Group B did treadmill exercise in the dark phase of the cycle (from 19:00 to 21:00) – 7 animals. In group C, the time of forced treadmill exercise alternated (shift training regime): in the first and third weeks, they performed the exercise in the dark (from 19:00 to 21:00), in the second and fourth weeks – in the morning (from 8:00 to 10:00) – 7 animals.

To normalize physical activity, the BMELAB SID-TM10 treadmill for mice was used [13]. Forced treadmill exercises were performed for 4 weeks. In the first six days, the duration of the exercise was gradually increased from 10 to 60 minutes (the increase by 10 minutes per day) 6 times a week and did not change during the subsequent three weeks. The angle of the treadmill (from 0 to 10°) and its rotation speed (from 15 to 18 m / min) were changed every week. Once a week (every seventh day), the exercise was not performed. Body weight was measured using laboratory scales. The weight of each animal was measured separately. Measurements were performed 11 times during 16 weeks.

The experimental animals were euthanized by decapitation 24 hours after the last exercise. We isolated m.gastrocnemius from both hind limbs and cleared the muscle tissue of connective and adipose tissue. The liver was extracted from the abdominal cavity and also cleared of surrounding tissue. Homogenization of skeletal muscle and liver tissue was performed as follows: before lysis, the tissue was first cut with a scalpel on a glass plate held on ice into small pieces of ~ 1 mm in size. They were then transferred to cold 1X RIPA Buffer (137 mM NaCl, 2.7 mM KCl, 1 mM MgCl2, 0.5 mM Na3VO4, 1% Triton X-100, 10% Glycerol, 20 mM Tris pH 7.8, 1 µg / ml Leupeptin, 0.2 mM PMSF, 10 mM NaF, 1 mM EDTA, 1 mM DTT, 5 mM Na pyrophosphate, 0.5 ml, 1 ml of 100 mM, 1 mM Benzamidine) in tubes with airtight caps and thick walls.

Fifty ml of the buffer was used per 20 mg of wet muscle tissue. The material was kept on ice during processing. Then, 5 mm stainless steel beads (Qiagen, Germany) were placed in the tubes. The tubes were placed in the Digital Vortex-Genie 2 laboratory mixer (Scientific Industries, Inc., USA) for 15 minutes at 4 °C. Then they were left on a mini-rotor shaker (MP-1, Biosan, Latvia) in the refrigerator for 1 hour. Next, they were centrifuged at 13,000 rpm for 5 minutes at 4 °C, after which the clear supernatant was transferred to new tubes with clear markings. Thirty µl were taken to determine the concentration of total protein in the sample (using the Bradford protein assay).

The following parameters were determined in the tissue homogenate. Muscle tissue – glycogen, lactate, glycogen synthase (GYS1), glycogen phosphorylase (PYGM). Liver tissue – liver glycogen synthase (GYS2), liver glycogen phosphorylase (PYGL), high-density lipoproteins (HDL), low-density lipoproteins (LDL), very-low-density lipoproteins (VLDL); alanine aminotransferase (ALT); aspartate aminotransferase (AST).

The analysis was performed using ready-made kits on the Anthos 2010 microplate photometer with software (Biochrom Ltd., UK). Sample preparation, colorimetric analysis, and calculations of the obtained data were carried out according to the manufacturer's protocol. Tissue homogenate was obtained according to the scheme for a sample weighing less than 100 mg. The concentration of total protein in the sample was determined using the modified Bradford protein assay.

PAGE electrophoresis was performed under denaturing conditions and according to the method described previously (Laemmli, 1970) with 5% stacking and 7% separating gels using the electrophoresis system (Mini-PROTEAN Tetra electrophoresis cell, USA) and the current source (PowerPacBasic, USA)). The concentration of total protein applied to each well was 7.5 µg. Using the blotting system (Trans-Blot Turbo, USA), proteins were transferred from the gel to a PVDF membrane (BioRad, USA) followed by blocking with 5% skim milk (BioRad, USA) in 1X TBSt (TBS with the addition of 0.1% Tween-20) for 1 h at room temperature. The target proteins were determined by incubation at 4 °C in 5% dry milk in TBSt overnight at a dilution of 1:1000 with rabbit polyclonal antibodies against citrate synthetase (cat. no. ab96600, abcam, UK) and with a cocktail of Total OXPHOS Rodent WB antibodies (cat. no. ab110413, abcam, UK), containing 5 mouse antibodies, each against the subunits of NDUFB8, SDHB, UQCRC2, MTCO1, ATP5A. The sample was then incubated with HRP-conjugated secondary antibodies (anti-mouse cat. #1706516, anti-rabbit cat. #1706515, BioRad, USA) for 1 h at room temperature in 3% dry

milk in TBSt. Antigen – antibody complexes were visualized using the ECL kit (SuperSigna West Dura, Thermo Scientific, USA) and the documentation system (ChemiDoc-It 2, UVP, UK). The densitometric analysis was performed using ImageJ software.

Immunoblotting. Proteins were transferred from the gel to the PVDF membrane (BioRad, USA) in transfer buffer (25 mM Tris – 192 mM glycine (pH 8.3), 20% ethanol) for 1.5 h at 400 mA. To check the quality of protein transfer to the membrane, the membrane was stained with Ponceau S dye. The dye reversibly binds to proteins, staining them red. To prepare the membrane for immunochemical staining, it was washed several times in a TBS solution (50 mM Tris, pH 7.4, 150 mM NaCl). Then, blocking was performed with 5% dry skim milk (Valio, Finland) prepared in PBST (PBS with the addition of 0.1% Tween-20). Blocking was carried out for one hour at room temperature and constant stirring. The membrane was then transferred into a TBST solution (50 mM Tris, pH 7.4, 150 mM NaCl, 0.1% Tween-20) containing 5% BSA and primary antibodies (1:1000 ratio by volume) and left for 14-17 hours at +4 °C and constant stirring. Next, the membrane was washed three times for 15 minutes with a TBST solution and then incubated at room temperature with constant stirring in a separate container for 1 hour in 10 ml of a TBST solution containing 5% dry skim milk and HRP-conjugated secondary antibodies in a ratio of 1:5000. Then the membrane was washed 3 times with a TBST solution for 15 min.

The bands of the formed protein complexes with primary and secondary antibodies on the membrane were visualized using the enhanced chemiluminescence (ECL) method, using the chemiluminescence kit (SuperSigna West Dura, Thermo Scientific, USA), developing the membranes on a documentation system (ChemiDoc-It 2, UVP, UK). The densitometric analysis was performed using ImageJ software.

Statistical data processing was performed using the GraphPad Prism package (academic license No. 1531155, valid until 21.12.2024). The significance level when testing the hypothesis of equality of two samples was estimated using the Kruskal – Wallis ANOVA test. All data had non-normal distribution of the variables. To compare the groups, two-way analysis of variance with Tukey's multiple comparison criterion and Holm – Sidak adjustment was used. The data were presented as the median and the interquartile range Me (Q_1; Q_3).

RESULTS

In the previous publication [14], we described changes in the body weight of mice during the experiment. Already starting from week 4 of the experiment, a significant increase in the body weight of mice fed with a high-fat diet was observed ($p < 0.05$). At week 12, the differences between the high-fat diet group and the standard chow diet group increased.

From week 12, both groups were divided into 4 subgroups, in which physical exercise was performed at different times of the day (light phase, dark phase, shift regimen). At week 16 (final week) of the experiment, we found that in the group of mice receiving a high-fat diet and in the standard chow diet group, the differences in body weight remained statistically significant ($p < 0.05$).

In the group receiving a high-fat diet, statistically significant differences ($p < 0.05$) in body weight compared to the control group were observed in all 3 subgroups that were exposed to physical activity. The most effective exercise was in the shift training regimen group. In this group, body weight was 1.2 times lower than in the control group.

In the first part of the work, we studied the level of glycogen, lactate, and carbohydrate metabolism enzymes in the tissues of skeletal muscles and the liver. The content of glycogen in the muscles of young animals receiving a high-fat diet decreased by 20%. Physical exercise led to an increase in the glycogen content in muscle tissue in mice receiving a standard chow diet and did not affect this parameter in the group of animals receiving a high-fat diet (Table 1). In aged mice, the content of glycogen in muscle tissue was lower than in young animals by 12%. Receiving a high-fat diet led to a decrease in this parameter by 17%. In both groups, physical activity performed in the morning or in the shift training regimen contributed to an increase in glycogen content, whereas exercise performed in the evening did not affect this parameter (Table 1).

The lactate content in the muscles of young animals fed with a high-fat diet decreased by 9%. Regular physical exercise led to a decrease in the lactate content in muscle tissue in both groups of young mice. In the group of animals fed with a high-fat diet, the decrease was pronounced to a greater extent and reached 50% in the shift training regimen group (Table 1). In aged animals, the lactate content in muscle tissue was lower by 25% than in young animals, while receiving a high-fat diet did not affect the lactate content. In the group of animals fed with

a standard chow diet, regular physical exercise led to a decrease in the lactate content in muscles by 1.5–2 times (the effect of exercises performed in the morning or in the alternating regimen was more pronounced). In aged mice fed with a high-fat diet, the shift training regimen reduced lactate levels by half, while morning or evening exercises had no effect on this parameter (Table 1).

Table 1

Carbohydrate metabolism parameters in skeletal muscle and liver tissues of mice, ng / ml, *Me* (Q_1; Q_3), $n = 6$

Diet	Age	Exercise	Skeletal muscles				Liver	
			GYS1	PYGM	Glycogen	Lactate	GYS2	PYGL
Standard	Young	Control	2172.36 (2137.53; 2364.49)	2.2 (1.6; 2.9)	1.5 (1.47; 1.53)	5.7 (5; 6.35)	4385.71 (4257.14; 4814.29)	18.7 (16.5; 22)
		Morning	2590.34 (2335.28; 2638.65) $p_3 \leq 0.05$	1.6 (1.2; 1.8) $p_3 \leq 0.05$	1.78 (1.78; 1.78) $p_3 \leq 0.05$	5 (4.6; 5.2) $p_3 \leq 0.05$	4700 (4528.57; 4957.14) $p_3 \leq 0.05$	18.7 (15.95; 20.35)
		Evening	2519.55 (2281.35; 2755.51) $p_4 \leq 0.05$	2 (1.8; 24) $p_6 \leq 0.05$	1.72 (1.69; 1.75) $p_4 \leq 0.05$	5.4 (5.1; 5.7)	4750 (4657.14; 4839.29) $p_4 \leq 0.05$	19.8 (18.84; 21.86)
		Shift	2574.61 (2518.43; 2668.99) $p_5 \leq 0.05$	1.4 (0.8; 1.9) $p_5 \leq 0.05$ $p_8 \leq 0.05$	1.78 (1.72; 1.83) $p_5 \leq 0.05$	5 (4.4; 5.6) $p_5 \leq 0.05$ $p_8 \leq 0.05$	4778.57 (4585.71; 4978.57) $p_5 \leq 0.05$	24.2 (23.1; 24.75) $p_5 \leq 0.05$ $p_7 \leq 0.05$ $p_8 \leq 0.05$
	Aged	Control	2184.72 (2063.37; 2270.11)	1.2 (1.2; 1.6) $p_2 \leq 0.001$	1.33 (1.28; 1.5) $p_2 \leq 0.05$	4.4 (4; 4.8) $p_2 \leq 0.05$	5185.71 (5071.43; 5328.57) $p_2 \leq 0.05$	17.33 (15.81; 19.94) $p_2 \leq 0.05$
		Morning	2652.13 (2595.96; 2747.08) $p_3 \leq 0.05$	2.4 (2.2; 3) $p_2 \leq 0.01$ $p_3 \leq 0.001$	1.72 (1.31; 2.11) $p_3 \leq 0.05$	2 (1.9; 2.1) $p_2 \leq 0.001$ $p_3 \leq 0.001$	5457.14 (4857.14; 5671.43) $p_2 \leq 0.05$	19.25 (19.25; 19.8) $p_2 \leq 0.05$ $p_3 \leq 0.05$
		Evening	2356.63 (2291.46; 2449.89) $p_2 \leq 0.05$ $p_4 \leq 0.05$	2.2 (2; 2.4) $p_4 \leq 0.05$	1.28 (1.19; 1.36) $p_2 \leq 0.05$ $p_6 \leq 0.05$	3 (2.8; 3.2) $p_2 \leq 0.05$ $p_4 \leq 0.05$ $p_6 \leq 0.05$	4900 (4757.14; 4914.29) $p_6 \leq 0.05$	17.6 (17.6; 19.8) $p_2 \leq 0.05$ $p_6 \leq 0.05$
		Shift	3155.51 (2974.04; 3194.27) $p_2 \leq 0.05$ $p_5 \leq 0.05$ $p_7 \leq 0.05$ $p_8 \leq 0.05$	2.8 (2.4; 3.2) $p_2 \leq 0.05$ $p_5 \leq 0.05$ $p_7 \leq 0.05$ $p_8 \leq 0.05$	1.78 (1.67; 2.03) $p_5 \leq 0.05$ $p_8 \leq 0.05$	2 (1.6; 2.8) $p_2 \leq 0.001$ $p_5 \leq 0.05$ $p_8 \leq 0.05$ $p_8 \leq 0.05$	5392.86 (5178.57; 5842.86) $p_2 \leq 0.05$ $p_8 \leq 0.05$	29.7 (29.15; 30.25) $p_2 \leq 0.05$ $p_5 \leq 0.01$ $p_7 \leq 0.01$ $p_8 \leq 0.01$
High-fat	Young	Control	2122.92 (2073.48; 2227.42)	4 (4; 5) $p_1 \leq 0.05$	1.22 (1.17; 1.28) $p_1 \leq 0.05$	5.2 (4.9; 5.53) $p_1 \leq 0.05$	4228.57 (3928.57; 4414.29)	22 (18.7; 23.24) $p_1 \leq 0.05$
		Morning	3100.45 (2761.12; 3165.62) $p_1 \leq 0.05$ $p_3 \leq 0.05$	2 (1.8; 2.8) $p_1 \leq 0.05$ $p_3 \leq 0.001$	1 (0.94; 1.06) $p_1 \leq 0.05$ $p_3 \leq 0.05$	3.2 (2.8; 3.7) $p_1 \leq 0.05$ $p_3 \leq 0.001$	4442.86 (4242.86; 4771.43) $p_1 \leq 0.05$	16.5 (16.5; 17.05) $p_1 \leq 0.05$ $p_3 \leq 0.05$
		Evening	2963.37 (1947.64; 3173.48) $p_4 \leq 0.05$	2.6 (1.3; 2.2) $p_1 \leq 0.05$ $p_4 \leq 0.05$ $p_6 \leq 0.05$	1.22 (1.11; 1.33) $p_1 \leq 0.05$	4.2 (3.7; 4.7) $p_1 \leq 0.05$ $p_4 \leq 0.05$ $p_6 \leq 0.05$	4464.29 (3925; 4589.29) $p_4 \leq 0.05$	16.5 (15.4; 16.91) $p_1 \leq 0.05$ $p_4 \leq 0.05$
		Shift	2644.27 (2606.07; 2670.11) $p_7 \leq 0.05$ $p_8 \leq 0.05$	1.8 (0.9; 2.7) $p_5 \leq 0.05$	1.11 (1.06; 1.17) $p_1 \leq 0.05$	2.8 (1.8; 3.8) $p_1 \leq 0.05$ $p_5 \leq 0.05$ $p_7 \leq 0.05$ $p_8 \leq 0.05$	4892.86 (4696.43; 5221.43) $p_5 \leq 0.05$ $p_7 \leq 0.05$ $p_8 \leq 0.05$	17.6 (17.05; 19.25) $p_1 \leq 0.05$ $p_5 \leq 0.05$
	Aged	Control	2365.62 (2181.35; 2431.91)	2.8 (2.6; 3) $p_1 \leq 0.05$ $p_2 \leq 0.05$	1.0 (0.74; 1.28) $p_1 \leq 0.05$	4.4 (4.1; 4.8) $p_2 \leq 0.05$	5145.71 (5117.14; 5321.43) $p_2 \leq 0.05$	15.75 (14.06; 16.58) $p_1 \leq 0.05$ $p_2 \leq 0.05$
		Morning	2489.21 (2448.76; 270 9.44) $p_2 \leq 0.05$	2.8 (2.2; 2.8) $p_2 \leq 0.05$	1.22 (0.89; 1.22) $p_1 \leq 0.05$	4.6 (3.9; 5.2) $p_1 \leq 0.05$ $p_2 \leq 0.05$	4985.71 (4707.14; 5250) $p_1 \leq 0.05$ $p_2 \leq 0.05$	15.4 (14.16; 15.95) $p_1 \leq 0.05$

End of table 1

Diet	Age	Exercise	Skeletal muscles				Liver	
			GYS1	PYGM	Glycogen	Lactate	GYS2	PYGL
		Evening	2442.02 (2398.2; 2515.06)	2.6 (2.5; 2.7) $p_1 \leq 0.05$ $p_2 \leq 0.05$ $p_4 \leq 0.05$ $p_6 \leq 0.05$	1.27 (1.17; 2.5)	5 (4.2; 5.3) $p_1 \leq 0.05$ $p_2 \leq 0.05$ $p_4 \leq 0.05$	4814.29 (4575; 5042.86) $p_2 \leq 0.05$	15.68 (13.61; 17.15) $p_1 \leq 0.05$
		Shift	2668.99 (2636.4; 2691.46) $p_1 \leq 0.05$	2.2 (2.1; 2.3) $p_1 \leq 0.05$ $p_2 \leq 0.05$ $p_5 \leq 0.05$ $p_7 \leq 0.05$ $p_8 \leq 0.05$	1.26 (1.04; 1.47) $p_1 \leq 0.05$ $p_5 \leq 0.05$	2.4 (2.4; 3.4) $p_1 \leq 0.05$ $p_2 \leq 0.05$ $p_5 \leq 0.01$ $p_7 \leq 0.001$ $p_8 \leq 0.001$	4771.43 (4621.43; 4957.14) $p_1 \leq 0.05$ $p_5 \leq 0.05$	19.8 (18.7; 23.65) $p_1 \leq 0.05$ $p_5 \leq 0.05$ $p_7 \leq 0.05$ $p_8 \leq 0.05$

Note. Here and in Table 2: p_1 – significant differences between the standard diet group and the high-fat diet group; p_2 – significant differences between the young and adult mice; p_3 – significant differences between the control group and the morning group; p_4 – significant differences between the control group and the evening group; p_5 – significant differences between the control group and the shift training group; p_6 – significant differences between the morning group and the evening group; p_7 – significant differences between the evening group and the shift training group.

The changes in glycogen synthase levels in muscle and liver tissues were generally similar (Table 1). In young animals fed with a high-fat diet, the levels of this enzyme did not change in either muscle or liver tissues. At the same time, exercise led to a significant increase in enzyme levels in both tissues, with the shift training regimen having the greatest effect. In aged animals, a high-fat diet also had no effect on glycogen synthase levels, but the effects of exercise differed.

In the group of animals receiving a standard chow diet, the levels of the enzyme increased significantly in both muscle and liver tissues. At the same time, in aged animals fed with a standard diet, the glycogen synthase content increased in the muscle tissues, but decreased in the liver tissue. In both cases, the greatest effect was produced by exercises performed in the alternating regimen.

The changes in glycogen phosphorylase levels in muscle and liver tissues, on the contrary, had a number of significant differences (Table 1). In young animals fed with a standard diet, physical exercise led to a significant increase in the enzyme content in the liver and a decrease in the muscle tissue, with the greatest effect produced by exercises performed in the shift training regimen. In young animals receiving a high-fat diet, the content of this enzyme doubled in the muscle tissue and increased only by 10% in the liver tissue. At the same time, physical exercise led to a significant increase in the enzyme content in muscles, while in the liver its content, on the contrary, decreased. In aged animals, a high-fat diet did not affect the glycogen phosphorylase content in the muscles, while in the liver, a decrease of 12% was noted. Regular exercise increased the enzyme levels in both tissue types, but the effect of exercise was greater in the standard diet group. Here, too, the greatest effect was seen with the shift training regimen.

In the second part of the work, we examined the content of HDL, LDL, and VLDL in the liver tissue of mice, as well as the content of aminotransferases (ALT, AST) (Table 2).

In young mice receiving a high-fat diet, the content of HDL in the liver decreased by 20%, while the content of LDL and VLDL increased by 15 and 10%, respectively. Physical exercise led to a reliable decrease in all three parameters in mice receiving a standard diet. In the animals receiving a high-fat diet, we observed a slight increase in the content of HDL in the liver under the influence of physical exercise along with a reliable decrease in LDL and VLDL (Table 2). In all cases, the greatest effect was produced by exercise performed in the morning hours and in the shift training regime.

In aged mice, the content of HDL in the liver was slightly lower, and the content of LDL and VLDL, on the contrary, was slightly higher than in young animals. The effects of physical exercise in the aged groups of animals were greater than in young mice.

The HDL content in the liver increased by 1.5 times, while the LDL and VLDL levels decreased, with the decrease in VLDL being more significant – in some cases, the parameter declined by two times (Table 2). Traditionally, exercises performed in the morning hours and in the shift training regimen were the most effective.

Table 2

Lipid metabolism parameters and the level of aminotransferases in the liver tissue of mice, ng / ml, *Me* (Q_1; Q_3), n = 6

Diet	Age	Exercise	HDL	LDL	VLDL	ALT	AST
Standard	Young	Control	2053 (1771.7; 2420)	1390.8 (1367.8; 1436.8)	6338.4 (5294.2; 7581)	101.6 (85.6; 108.4)	308.8 (306; 332.4)
		Morning	1800 (1540; 1020) $p_3 \leq 0.05$	1282.8 (1282.8; 1340.2) $p_3 \leq 0.05$	4330.8 (3691.2; 4893.2) $p_3 \leq 0.05$	126.2 (114.7; 140.7) $p_3 \leq 0.05$	378 (377.2; 398.2) $p_3 \leq 0.05$
		Evening	1673.8 (1554.3; 1877.9) $p_4 \leq 0.05$ $p_6 \leq 0.05$	1308.1 (1276.15; 1352.9)	5956 (4698.6; 6926.6) $p_6 \leq 0.05$	118 (103.5; 128.4) $p_4 \leq 0.05$	323.4 (296.6; 369.4) $p_6 \leq 0.05$
		Shift	968.8 (937.6; 1234.4) $p_5 \leq 0.05$ $p_7 \leq 0.05$ $p_8 \leq 0.05$	1298.9 (1273; 1344.85) $p_5 \leq 0.05$ $p_8 \leq 0.05$	4691.2 (4180.2; 5250) $p_5 \leq 0.05$ $p_8 \leq 0.05$	154.8 (128.4; 172.4) $p_5 \leq 0.05$ $p_7 \leq 0.05$ $p_8 \leq 0.05$	392.8 (342.8; 397.2) $p_5 \leq 0.05$ $p_8 \leq 0.05$
	Aged	Control	1674 (1586.8; 1739.2) $p_2 \leq 0.001$	2057.4 (2051.7; 2235.6) $p_2 \leq 0.001$	7544.2 (6672.8; 8099.4) $p_2 \leq 0.05$	72 (59.2; 82.8) $p_2 \leq 0.05$	188.8 (166.4; 192.8) $p_2 \leq 0.001$
		Morning	1858.6 (1755.4; 1907.5) $p_3 \leq 0.05$	1155.1 (1054.55; 1272.95) $p_2 \leq 0.05$ $p_3 \leq 0.05$	5985.2 (4930; 6014.7) $p_2 \leq 0.05$ $p_3 \leq 0.05$	63.6 (60.6; 67.8) $p_2 \leq 0.05$ $p_3 \leq 0.05$	160 (134.4; 187.6) $p_2 \leq 0.05$
		Evening	1674 (1608.8; 1717.2) $p_6 \leq 0.05$	1120.7 (1040.25; 1281.6) $p_2 \leq 0.05$ $p_4 \leq 0.05$	6058.8 (5573.6; 6110.2) $p_4 \leq 0.05$	84.4 (169.1; 199.4) $p_2 \leq 0.05$ $p_4 \leq 0.05$ $p_6 \leq 0.05$	168 (156.2; 180.4) $p_2 \leq 0.05$ $p_4 \leq 0.05$
		Shift	2120 (1932.4; 2140) $p_2 \leq 0.01$ $p_5 \leq 0.05$ $p_7 \leq 0.05$ $p_8 \leq 0.05$	1195.4 (1103.5; 1290.2) $p_5 \leq 0.05$	4279.4 (3558.7; 4853.1) $p_2 \leq 0.05$ $p_5 \leq 0.05$ $p_7 \leq 0.05$ $p_8 \leq 0.05$	93.6 (83.4; 97.6) $p_2 \leq 0.05$ $p_5 \leq 0.05$ $p_7 \leq 0.05$ $p_8 \leq 0.05$	192.2 (182.5; 236.2) $p_5 \leq 0.05$ $p_7 \leq 0.05$ $p_8 \leq 0.05$
High-fat	Young	Control	1630.6 (1540.3; 1699.1) $p_1 \leq 0.05$	1602.2 (1567.8; 1648.2) $p_1 \leq 0.05$	7029.6 (6956; 7382.4) $p_1 \leq 0.05$	133.8 (123.3; 159.8) $p_1 \leq 0.05$	324.4 (305.6; 347.2) $p_1 \leq 0.05$
		Morning	1708.8 (1632.6; 1774) $p_1 \leq 0.05$	1247.2 (1181.1; 1324.75) $p_3 \leq 0.01$	5073.6 (5029.4; 6308.8) $p_1 \leq 0.05$ $p_3 \leq 0.001$	100.4 (94.1; 103.3) $p_3 \leq 0.05$	243.2 (240.4; 257.2) $p_1 \leq 0.05$ $p_3 \leq 0.05$
		Evening	1741.2 (1681.5; 1789) $p_4 \leq 0.05$	1396.5 (1281.55; 1497.1) $p_4 \leq 0.05$	6647 (6022; 6988.9) $p_1 \leq 0.05$ $p_4 \leq 0.05$ $p_6 \leq 0.05$	119.2 (104.5; 129.9) $p_4 \leq 0.05$ $p_6 \leq 0.05$	316 (280.8; 332.4) $p_6 \leq 0.05$
		Shift	1752 (1710.8; 1795.3) $p_1 \leq 0.05$ $p_5 \leq 0.05$	1206.9 (1181.05; 1224.15) $p_5 \leq 0.05$ $p_8 \leq 0.05$	4926.4 (4625; 6213.2) $p_5 \leq 0.05$ $p_8 \leq 0.05$	99.2 (94.8; 108.4) $p_1 \leq 0.05$ $p_5 \leq 0.05$ $p_8 \leq 0.05$	231.2 (213.9; 243.1) $p_1 \leq 0.05$ $p_5 \leq 0.05$ $p_8 \leq 0.05$
	Aged	Control	1439.2 (1409.2; 1550) $p_1 \leq 0.05$ $p_2 \leq 0.05$	2811.4 (2711.4; 3083.25) $p_1 \leq 0.05$ $p_2 \leq 0.05$	8088.4 (7639.8; 9051.6) $p_2 \leq 0.05$	98.6 (92.9; 101.6) $p_1 \leq 0.05$ $p_2 \leq 0.05$	178.2 (156.3; 205.4) $p_2 \leq 0.05$
		Morning	1695.6 (1489.2; 1695.6) $p_1 \leq 0.05$ $p_3 \leq 0.05$	2195.4 (2091.9; 2264.35) $p_1 \leq 0.01$ $p_2 \leq 0.05$ $p_3 \leq 0.05$	6558.8 (6492.6; 6945.6) $p_2 \leq 0.05$ $p_3 \leq 0.05$	84.2 (69.8; 93.6) $p_1 \leq 0.05$ $p_2 \leq 0.05$ $p_3 \leq 0.05$	175.6 (174.6; 176.6) $p_2 \leq 0.05$

End of table 2

Diet	Age	Exercise	HDL	LDL	VLDL	ALT	AST
		Evening	1674 (1625.1; 1695.7) $p_4 \le 0.05$	2172.4 (2155.2; 2287.3) $p_1 \le 0.05$ $p_2 \le 0.05$ $p_4 \le 0.05$	7257.4 (7005.9; 7393.4) $p_1 \le 0.05$ $p_4 \le 0.05$ $p_6 \le 0.05$	77.2 (73.8; 86) $p_1 \le 0.05$ $p_2 \le 0.05$ $p_4 \le 0.05$ $p_6 \le 0.05$	185 (164.5; 207.7) $p_2 \le 0.05$
		Shift	2000 (1934.8; 2040) $p_2 \le 0.05$ $p_5 \le 0.05$ $p_7 \le 0.05$ $p_8 \le 0.05$	2092 (2063.2; 2155.2) $p_1 \le 0.05$ $p_2 \le 0.05$ $p_5 \le 0.05$	5132.4 (4500; 5577.2) $p_1 \le 0.05$ $p_5 \le 0.05$ $p_7 \le 0.05$ $p_8 \le 0.05$	77.2 (77.2; 80) $p_1 \le 0.05$ $p_2 \le 0.05$ $p_5 \le 0.05$ $p_7 \le 0.05$	188.4 (181; 198.9) $p_2 \le 0.05$

In young mice receiving a high-fat diet, the ALT and AST levels in the liver increased by 30 and 5%, respectively. Physical exercises led to a significant increase in the content of both enzymes in the liver of mice receiving a standard chow diet. When performing exercise in the shift regimen, the increase was 30–50%. In the meantime, in the high-fat diet group, we observed a decrease in the content of these enzymes in the liver tissue by 1.5 times. Here, too, the greatest effect was observed exercises performed in the shift regimen (Table 2).

In aged mice, we observed a significant decrease in the ALT and AST levels in the liver. In the animals receiving a high-fat diet, the ALT content in the liver slightly increased. Physical exercise in mice fed with a standard chow diet had opposite effects. Exercise performed in the morning hours contributed to a decrease in the content of both enzymes in the liver tissue, while exercise done in the shift regimen, on the contrary, led to a significant increase (Table 2). In aged animals fed with a high-fat diet, physical exercise led to a decrease in the content of ALT and an increase in the content of AST – the effects of exercise performed in the shift regimen were the most pronounced.

DISCUSSION

The obtained results show that the use of a high-fat diet in mice led to an increase in body weight and the development of obesity (body weight increased by 25% compared to the control group). Forced treadmill exercise had a pronounced effect on metabolism in mice with a model of T2DM. First of all, this was manifested by a decrease in the body weight of animals and depended on the time of the day when the exercise was performed.

As we have already mentioned above, the liver plays an important role in the regulation of carbohydrate and lipid metabolism, therefore, it becomes a target for pathological processes in metabolic disorders, primarily in T2DM [15]. Muscles contain the largest reservoir of glycogen, the depot of which is carefully regulated and affects insulin sensitivity. In our study, we recorded a decrease in glycogen content in the muscles with the development of metabolic disorders. It is important to note that physical exercise is unable to replenish glycogen depot in the context of a high-fat diet, whereas in animals receiving a standard diet, muscle glycogen depot increases significantly against the background of regular physical exercise. According to J. He, D.E. Kelley, a decrease in muscle glycogen correlates with a decrease in the oxidative capacity of mitochondria and the accumulation of lipids in the muscle tissue, and is also directly associated with the level of insulin resistance [16]. The disproportionality of these relationships may play a certain role in the pathogenesis of intracellular metabolic disorders in T2DM. In the meantime, the observed changes in lactate levels after regular physical exercise are most likely associated with the training effect on the cardiovascular system and are weakly associated with metabolic changes in the muscle tissue.

A decrease in the glycogen content is apparently associated with the activation of its breakdown processes rather than with a decrease in its synthesis. This is evidenced by the fact that the content of glycogen synthase in both muscles and liver did not change during the formation of metabolic disorders in mice, but increased during physical activity, primarily in healthy animals. Thus, the effects of this enzyme are more pronounced during physical activity than in the pathogenesis of metabolic disorders.

Yet, significant and multidirectional changes were recorded in the content of glycogen phosphorylase in the liver and skeletal muscle tissue. These changes were significantly influenced by both the nature of nutrition and physical activity. In all likelihood,

this enzyme is involved both in the mechanisms of development of pathological processes and in the mechanisms of adaptive effects of motor activity. This is evidenced by often oppositely directed changes in the content of glycogen phosphorylase in the muscle and liver tissue during physical activity.

The mechanisms of the identified differences in the reaction of carbohydrate metabolism to physical activity in healthy animals and animals with T2DM may be associated with the restructuring of gene expression mechanisms in metabolic disorders. Thus, pathway analysis of differentially regulated genes during exercise revealed upregulation of regulators of GLUT4 (SLC2A4RG, FL0T1, EXOC7, RAB13, RABGAP1, and CBLB), glycolysis (HK2, PFKFB1, PFKFB3, PFKM, FBP2, and LDHA), and insulin signaling mediators in individuals with T2DM compared to healthy controls [17]. It is worth noting that T2DM patients also demonstrated exercise-induced compensatory regulation of genes involved in amino acid biosynthesis and metabolism (PSPH, GATM, NOS1, and GLDC), which responded to differences in amino acid profile (consistently lower plasma glycine, cysteine, and arginine levels).

We have already mentioned above the close association between T2DM and lipid metabolism disorders in the liver. These disorders synergistically promote each other's progression. Several pathophysiological pathways are involved in this association, including insulin resistance, inflammation, and lipotoxicity [3]. Our results are in good agreement with this point of view: the development of experimental T2DM in mice is accompanied by a decrease in the HDL content in the liver in parallel with an increase in LDL and VLDL. It is important to stress that physical exercise provided partial normalization of the ratio of lipid fractions, despite the fact that it was performed in the context of a continuous high-fat diet. Thus, it can be argued that physical activity is able to partially neutralize the pathological effects of a high-fat diet even without dietary adjustments.

The mechanism of such an effect can be associated with increased production of anti-inflammatory myokines under the influence of physical exercise, which are capable of blocking chemotactic factors, such as monocyte chemoattractant protein-1, and/or proinflammatory mediators, such as IL-1β, TNFα, visfatin and plasminogen activator inhibitor-1, and/or increased synthesis of adipokines, such as adiponectin and apelin [17].

An important aspect of our results is the identified numerous differences in the age parameter – in the group of aged mice, metabolic changes caused by both the T2DM modeling and physical exercise were not only quantitative, but in some cases qualitative. In general, a completely expected correlation is observed – in the group of aged animals, disorders in carbohydrate and lipid metabolism were more pronounced, and the corrective effect of physical exercise was weaker in most cases [18]. However, we recorded a number of exceptions that distinguish aged animals from younger ones, such as a decrease in glycogen synthase and an increase in glycogen phosphorylase in the liver tissue. Qualitative differences were also found in liver aminotransferase levels.

It is worth noting that the effects of physical activity on the content of lipid fractions in the liver in aged animals were more pronounced than in young mice. In light of the above hypothesis about the role of myokines and adipokines in these processes, it can be assumed that this feature may be associated with a larger volume of adipose tissue in aged animals.

The explanation for the revealed differences may also be associated with the features of the transcription of muscle genes in response to physical activity. In the work by U. Raue et al., 661 genes were identified whose expression differed when performing exercises with weights in young and elderly people [19].

The results indicating a significant difference in the effects of physical activity performed at different times of the day on metabolic processes in the liver and muscle tissue are of great interest. In almost all cases, the least effective were exercises performed in the evening hours, that is, during the period of natural activity of the animals. The effects of exercises in the period of low activity (morning) were most often higher, but the greatest effect was produced by physical exercise performed in the shift training regimen – for one week in the morning and for another week in the evening. It should be noted that we have previously described similar patterns for the effects of physical activity on body weight and insulin tolerance [14].

There are few works in the literature devoted to the role of circadian rhythms on the effects of physical activity in general, and studies on the role of circadian rhythms in metabolic disorders are isolated. Therefore, there has been no consensus on the mechanisms of this effect yet. A number of authors associate this with the effect of stress, since a greater effect is inherent in exercises performed at an unusual time. This

hypothesis is partially consistent with our data on serum cortisol levels in mice [20].

At the same time, work [11] showed that circadian rhythmicity in insulin tolerance was also observed in the signaling pathways regulating insulin- and exercise-induced glucose uptake in skeletal muscles, including AKT, 5'-adenosine monophosphate-activated protein kinase (AMPK), and phosphorylation of the TBC1 4 domain family. Basal and insulin-stimulated glucose uptake by skeletal muscles and adipose tissues *in vivo* also differed during the day and at night. However, the rhythmicity of glucose uptake differed from the rhythm of insulin tolerance as a whole. Both insulin sensitivity and signaling of isolated skeletal muscles reached a maximum in the dark period. These results indicate that the mechanisms of circadian rhythmicity of carbohydrate metabolism cannot be limited to the stress factor alone.

CONCLUSION

The obtained results allow us to draw several important conclusions:

1. A decrease in the muscle glycogen content in T2DM is associated with the activation of its breakdown rather than with a decrease in its synthesis. This is evidenced by the fact that the content of glycogen synthase in both the muscles and the liver did not change during the formation of metabolic disorders in mice, but increased during physical activity, primarily in healthy animals.

2. Significant and multidirectional changes were recorded in the content of glycogen phosphorylase in the liver and skeletal muscle tissue; these changes were significantly influenced by both the type of diet and physical activity. In all likelihood, this enzyme is involved both in the mechanisms of pathological processes and in the mechanisms of adaptive effects of motor activity.

3. The development of experimental T2DM in mice is accompanied by a decrease in the content of HDL in the liver in parallel with an increase in LDL and VLDL. It is important that physical activity provided partial normalization of the lipid fraction ratio despite the fact that it was performed in the context of a continuous high-fat diet. Thus, it can be argued that physical activity is able to partially neutralize the pathological effects of a high-fat diet even without dietary adjustments.

4. In the group of aged mice, metabolic changes caused by both the T2DM modeling and physical activity were not only quantitative, but in some cases qualitative. In general, a completely expected correlation is observed – in the group of aged animals, carbohydrate and lipid metabolism disorders were more pronounced, and the corrective effect of physical activity was weaker in most cases. However, we recorded a number of exceptions that distinguish aged animals from young ones.

5. The effects of physical activity applied at different times of the day on metabolic processes in the liver and muscle tissue vary significantly. In almost all cases, the weakest effect was shown by exercises performed in the evening hours, that is, during the period of natural activity of rodents. The effects during the period of low activity (morning) were most often higher, but the greatest effect was produced by physical activity performed in the shift regimen – for one week in the morning and for one week in the evening.

The obtained results allow us to conclude that physical activity can act as a means of preventing not only metabolic disorders (obesity and insulin resistance), but also concomitant complications in the liver and, subsequently, the cardiovascular system. Due to the partial normalization of the parameters of carbohydrate and, most importantly, lipid metabolism, they are likely to reduce the risk of both fatty liver disease and vascular disorders.

REFERENCES

1. Ouyang G., Wang N., Tong J., Sun W., Yang J., Wu G. Alleviation of taurine on liver injury of type 2 diabetic rats by improving antioxidant and anti-inflammatory capacity. *Heliyon.* 2024;10(7):E28400. DOI: 10.1016/j.heliyon.2024.e28400.
2. Klyaritskaya I.L., Maksimova E.V. Liver damage in patients with diabetes mellitus. *Crimean Therapeutic Journal*. 2010;2(2):8–13 (in Russ.).
3. Fujimaki S., Kuwabara T. Diabetes-induced dysfunction of mitochondria and stem cells in skeletal muscle and the nervous system. *Int. J. Mol. Sci*. 2017; 18(10): 2147. DOI: 10.3390/ijms18102147.
4. Højlund K. Metabolism and insulin signaling in common metabolic disorders and inherited insulin resistance. *Dan. Med. J.* 2014;61(7):B4890.
5. Barrera F., Uribe J., Olvares N., Huerta P., Cabrera D., Romero-Gómez M. The Janus of a disease: Diabetes and metabolic dysfunction-associated fatty liver disease. *Ann. Hepatol.* 2024;9(4):101501. DOI: 10.1016/j.aohep.2024.101501.
6. Kapilevich L.V., Zakharova A.N., Dyakova E.Yu., Kironenko T.A., Milovanova K.G., Kalinnikova J.G., Chibalin A.V. Mouse experimental model of type II diabetes mellitus based on a high-fat diet. *Bulletin of Siberian Medicine*. 2019;18(3):53–61 (in Russ.). DOI: 10.20538/1682-0363-2019-3-53-61.
7. Nagy C., Einwallner E. Study of In vivo glucose metabolism in high-fat diet-fed mice using oral glucose tolerance

test (OGTT) and insulin tolerance test (ITT). *J. Vis. Exp*. 2018;7(131):1–12. DOI: 10.3791/56672.
8. Winzell M.S., Ahren B. The high-fat diet-fed mouse: a model for studying mechanisms and treatment of impaired glucose tolerance and type 2 diabetes. *Diabetes.* 2004;53(3):S215–S219. DOI: 10.2337/diabetes.53.suppl_3.s215.
9. Brinkmann C., Schwinger R.H., Brixius K. Physical activity and endothelial dysfunction in type 2 diabetic patients: the role of nitric oxide and oxidative stress. *Wien. Med. Wochenschr.* 2011;161(11-12): 305–314. DOI: 10.1007/s10354-011-0868-8.
10. Karstoft K., Pedersen B.K. Exercise and type 2 diabetes: focus on metabolism and inflammation. *Immunol. Cell Biol.* 2016;94:146–150. DOI: 10.1038/icb.2015.101.
11. Basse A.L., Dalbram E., Larsson L., Gerhart-Hines Z., Zierath J.R. Treebak J.T. Skeletal muscle insulin sensitivity show circadian rhythmicity which is independent of exercise training status. *Front. Physiol.* 2018;9:1198. DOI: 10.3389/fphys.2018.01198.
12. Zakharova A.N., Kalinnikova Y., Negodenko E.S., Orlova A.A., Kapilevich L.V. Experimental simulation of cyclic training loads. *Teor. Prakt. Fizich. Kult.* 2020;10:26–27.
13. Zakharova A.N., Milovanova K.G., Orlova A.A., Dyakova E.Y., Kalinnikova J.G., Kollantay O.V. et al. Effects of treadmill running at different light cycles in mice with metabolic disorders. *Int. J. Mol. Sci*. 2023;24:15132. DOI: 10.3390/ijms242015132.
14. Mokhort T.V. Dyslipidemia and diabetes mellitus: new data. *Medical News*. 2021;9: 9–55 (in Russ.).
15. He J., Kelley D.E. Muscle glycogen content in type 2 diabetes mellitus. *Am. J. Physiol. Endocrinol. Metab*. 2004;287(5): 1002-1007. DOI: 10.1152/ajpendo.00015.2004.
16. Hansen J.S., Zhao X., Irmler M., Liu X., Hoene M., Scheler M. et al. Type 2 diabetes alters metabolic and transcriptional signatures of glucose and amino acid metabolism during exercise and recovery. *Diabetologia*. 2015;58(8):1845–1854. DOI: 10.1007/s00125-015-3584-x.
17. Varra F.N., Varras M., Varra V.K., Theodosis-Nobelos P. Molecular and pathophysiological relationship between obesity and chronic inflammation in the manifestation of metabolic dysfunctions and their inflammation-mediating treatment options (Review). *Mol. Med. Rep.* 2024;29(6):95. DOI: 10.3892/mmr.2024.13219.
18. Meneilly G.S. Pathophysiology of diabetes in the elderly. In: Diabetes in old age. *John Wiley & Sons.* 2001;155–164. DOI: 10.1002/0470842326.ch2.
19. Raue U., Trappe T.A., Estrem S.T., Qian H-R., Helvering L.M., Smith R.C. et al. Transcriptomic signature of resistance exercise adaptations: mixed muscle and fiber type specific profiles in young and old adults. *J. Appl. Physiol* 2012;112:1625–1636. DOI: 10.1152/japplphysiol.00435.2011.
20. Zakharova A.N., Milovanova K.G., Orlova A.A., Kollantay O.V., Shuvalov I.Yu., Kapilevich L.V. Influence of light stress on the metabolic effects of runing loads in mice with a model of diabetes mellitus type II. *Journal of Stress Physiology & Biochemistry.* 2023;19(3):152–159. URL: https://sciup.org/143180562

Authors' contribution

Milovanova K.G., Zakharova A.N. – significant contribution to conception and design, analysis and interpretation of the data, drafting of the article. Kollantay O.V., Orlova A.A., Shuvalov I.Yu., Popov S.A. – collection of data, analysis of the data, processing and interpretation of the results. Kovalev I.V., Medvedev M.A., Yakimovich I.Yu., Chibalin A.V. – analysis of the data, processing and interpretation of the results, editing of the article. Kapilevich L.V. – research supervision, conception of the study, editing of the article, final approval of the article for publication.

Authors' information

Milovanova Ksenia G. – Cand. Sci. (Biology), Associate Professor, Department of Sports and Health Tourism, Sports Physiology and Medicine, National Research Tomsk State University, Tomsk, naffys@mail.ru, https://orcid.org/0000-0002-3038-3298

Zakharova Anna N. – Cand. Sci. (Biology), Associate Professor, Department of Sports and Health Tourism, Sports Physiology and Medicine, National Research Tomsk State University, Tomsk, azakharova91@gmail.com, https://orcid.org/0000-0003-1102-2830

Orlova Anna A. – Post-Graduate Student, Department of Sports and Health Tourism, Sports Physiology and Medicine, National Research Tomsk State University, Tomsk, anna.orlova.96@mail.ru, https://orcid.org/0000-0002-9886-9454

Kollantay Olesya V. – Post-Graduate Student, Department of Sports and Health Tourism, Sports Physiology and Medicine, National Research Tomsk State University, Tomsk, olesya.tay@mail.ru, https://orcid.org/0009-0001-2445-0124

Shuvalov Igor Yu. – Post-Graduate Student, Department of Sports and Health Tourism, Sports Physiology and Medicine, National Research Tomsk State University, Tomsk, oleg-100500-lol@mail.ru, https://orcid.org/0000-0002-1096-807X

Popov Sergey A. – Post-Graduate Student, Department of Sports and Health Tourism, Sports Physiology and Medicine, National Research Tomsk State University, Tomsk, sergeyup9@mail.ru, https://orcid.org/0009-0005-7820-4411

Medvedev Mikhail A. – Dr. Sci. (Med.), Professor, Academician of the RAS, Professor of the Normal Physiology Division, Siberian State Medical University, Tomsk, nphys@yandex.ru, https://orcid.org/0000-0002-5443-0271

Kovalev Igor V. – Dr. Sci. (Med.), Professor, Division of Biophysics and Functional Diagnostics, Siberian State Medical University, Tomsk, kovalew@mail.ru, https://orcid.org/0000-0002-9269-0170

Yakimovich Inessa Yu. – Dr. Sci. (Med.), Associate Professor, Head of the Division of Hygiene, Siberian State Medical University, Tomsk, yakimovich.ij@ssmu.ru, https://orcid.org/0000-0002-7485-5920

Chibalin Alexander V. – Cand. Sci. (Biology), Associate Professor, Department of Sports and Health Tourism, Sports Physiology and Medicine, National Research Tomsk State University, Tomsk, alexander.chibalin@ki.se https://orcid.org/0000-0002-6339-6271

Kapilevich Leonid V. – Dr. Sci. (Med.), Head of the Department of Sports and Health Tourism, Sports Physiology and Medicine, National Research Tomsk State University; Senior Researcher, Central Research Laboratory, Siberian State Medical University; Professor, Department of Physical Education, Research Institute Tomsk Polytechnic University, Tomsk, kapil@yandex.ru, http://orcid.org/0000-0002-2316-576X

(✉) **Kapilevich Leonid V.,** kapil@yandex.ru

Received 25.07.2024;
approved after peer review 08.08.2024;
accepted 12.09.2024

УДК 616-002.5:616.155.3]-053.2:612.017.1
https://doi.org/10.20538/1682-0363-2024-4-95-104

NETs production and citrullinated histone H3 level in children with tuberculosis

Novikov D.G., Zolotov A.N., Indutny A.V., Mordyk A.V., Kirichenko N.A., Romanova M.A., Ptukhin A.O.

Omsk State Medical University
12, Lenina Str., Omsk, 644099, Russian Federation

ABSTRACT

Aim. To characterize parameters of neutrophil extracellular trap (NET) production in the leukocyte culture and citrullinated histone H3 (citH3) level in peripheral blood to assess the features of NETosis in children with tuberculosis.

Materials and methods. The study included 20 children with active pulmonary tuberculosis (TB group) and 20 clinically healthy children without signs of sensitization to *Mycobacterium tuberculosis* antigens (control group). The ability of neutrophils to form NETs under *ex vivo* exposure to a non-specific immune stimulant and the concentration of citH3 in peripheral blood were investigated.

Results. Neutrophils in children with tuberculosis formed filamentous NETs (*Me* = 21.0 and *Me* = 16.0, respectively; $p = 0.0474$) and cloud-like NETs (*Me* = 10.5 and *Me* = 4.0, respectively; $p = 0.0068$) more frequently than the controls. Filamentous NETs prevailed in both groups. However, cloud-like NETs were registered in all patients in the TB group (100%) and only in 15 of 20 children in the control group ($\chi^2 = 16.01$; $p < 0.0068$). The concentration of citH3 in the blood was 18.9 times higher in the TB group than in the control group (*Me* = 26.5 and *Me* = 1.4, respectively; $p = 0.0041$). A strong positive correlation was found between the citH3 concentration and the generation of filamentous ($r = 0.86$; $p = 0.0137$), but not cloud-like NETs ($r = 0.95$; $p = 0.0008$) in both groups.

Conclusion. The high level of citH3 in the TB group can reflect its NETosis-induced release and be caused by increased NETosis *in vivo*. This may be due to the previously formed potential of neutrophils to generate NETs (a proNETotic phenotype), which is consistent with our observation of an increased ability of isolated neutrophils to form extracellular traps *ex vivo* in children of the TB group.

Keywords: tuberculosis in children, neutrophil extracellular traps (NETs), NETosis-forming ability of neutrophils, citrullinated histone H3, neutrophil ability to form an extracellular trap

Conflict of interest. The authors declare the absence of obvious or potential conflicts of interest related to the publication of this article.

Source of financing. The research was funded by the Russian Science Foundation grant No. 23-25-10043, https://rscf.ru/project/23-25-10043/

Conformity with the principles of ethics. An informed consent was obtained from legal representatives of the study participants. The study was approved by the Ethics Committee at Omsk State Medical University (Protocol No. 5 of 28.04.2023).

For citation: Novikov D.G., Zolotov A.N., Indutny A.V., Mordyk A.V., Kirichenko N.A., Romanova M.A., Ptukhin A.O. NETs production and citrullinated histone H3 level in children with tuberculosis. *Bulletin of Siberian Medicine.* 2024;23(4):95–104. https://doi.org/10.20538/1682-0363-2024-4-95-104.

✉ *Kirichenko Nikolay A.,* honomer_1608@mail.ru

Характеристика продукции нейтрофильных внеклеточных ловушек и концентрации цитруллинированного гистона H3 у детей, больных туберкулезом

Новиков Д.Г., Золотов А.Н., Индутный А.В., Мордык А.В., Кириченко Н.А., Романова М.А., Птухин А.О.

Омский государственный медицинский университет (ОмГМУ)
Россия, 644099, г. Омск, ул. Ленина, 12

РЕЗЮМЕ

Цель исследования: охарактеризовать показатели продукции нейтрофильных внеклеточных ловушек (НВЛ) в культуре лейкоцитов и концентрацию цитруллинированного гистона H3 (citH3) периферической крови для оценки возможных особенностей реализации нетоза у детей, больных туберкулезом.

Материалы и методы. В исследование вошли 20 детей с активным туберкулезом органов дыхания (группа «Туберкулез») и 20 клинически здоровых детей без признаков сенсибилизации к антигенам *Mycobacterium tuberculosis* (группа «Контроль»). Выясняли способность нейтрофилов к формированию НВЛ при воздействии *ex vivo* на них неспецифического антигенного стимулятора и исследовали концентрацию цитруллинированного гистона H3 в периферической крови.

Результаты. Нейтрофилы больных туберкулезом детей чаще, чем детей в группе «Контроль», формировали нитевидные НВЛ (*Me* = 21,0 и *Me* =16,0 соответственно; $p = 0{,}0474$) и облаковидные НВЛ (*Me* = 10,5 и *Me* = 4,0 соответственно; $p = 0{,}0068$). В обеих группах преобладали нитевидные НВЛ. Однако облаковидные НВЛ были отмечены у всех представителей группы «Туберкулез» (100%), а в группе «Контроль» были выявлены только у 15 из 20 обследуемых ($\chi^2 = 16{,}01$; $p < 0{,}0068$). В группе «Туберкулез» медиана концентрации citH3 в крови была в 18,9 раза выше, чем в группе «Контроль» (*Me* = 26,5 и *Me* = 1,4 соответственно; $p = 0{,}0041$). Выявлена сильная положительная корреляционная взаимосвязь между концентрацией citH3 и генерацией нитевидных ($r = 0{,}86$; $p = 0{,}0137$), но необлаковидных форм НВЛ в группе «Туберкулез» и контрольной группе ($r = 0{,}95$; $p = 0{,}0008$).

Заключение. Высокий уровень citH3 в группе «Туберкулез» может отражать его нетоз-индуцированную продукцию и быть следствием возросшей активности данного процесса *in vivo*. Существенную роль в этом может играть ранее сформированная потенциальная готовность нейтрофилов к образованию НВЛ (пронетотический фенотип), что согласуется с нашим наблюдением о возрастании способности к формированию внеклеточных ловушек *ex vivo* изолированных нейтрофилов обследуемых лиц данной группы.

Ключевые слова: туберкулез у детей, нейтрофильные внеклеточные ловушки, нетозобразующая способность нейтрофилов, цитруллинированный гистон H3, способность нейтрофила к формированию внеклеточной ловушки

Конфликт интересов. Авторы декларируют отсутствие явных и потенциальных конфликтов интересов, связанных с публикацией настоящей статьи.

Источник финансирования. Исследование выполнено за счет гранта Российского научного фонда № 23-25-10043, https://rscf.ru/project/23-25-10043/

Соответствие принципам этики. Информированное согласие было получено от законных представителей участников исследования. Исследование одобрено этическим комитетом ОмГМУ (протокол № 5 от 28.04.2023).

Для цитирования: Новиков Д.Г., Золотов А.Н., Индутный А.В., Мордык А.В., Кириченко Н.А., Романова М.А., Птухин А.О. Характеристика продукции нейтрофильных внеклеточных ловушек и концентрации цитруллинированного гистона H3 у детей, больных туберкулезом. *Бюллетень сибирской медицины.* 2024;23(4):95–104. https://doi.org/10.20538/1682-0363-2024-4-95-104.

INTRODUCTION

Mycobacterium tuberculosis infection is accompanied by an increase in the number of Th1 and Th2 lymphocytes, inducing the development of an imbalance of immune responses in patients with pulmonary tuberculosis (TB) [1]. Regulation changes in the immune response are associated with the development of a special cytokine profile [2], stipulating emergency granulopoiesis, which eventually restructures the functional abilities of neutrophils [3].

The formation of neutrophil extracellular traps (NETs) or NETosis, discovered by V. Brinkmann and A. Zychlinsky in 2004, is a mechanism of non-specific protection provided by leukocytes in response to a wide-range of stimuli of both bacterial and non-bacterial origin [4]. NETs are supramolecular structures consisting of decondensed DNA – histone complexes with proteins fixed on their surface, released from neutrophil granules: neutrophil elastase, myeloperoxidase, and other specialized proteins [5]. This NET content contributes to the bactericidal function, which is undoubtedly essential in various infectious diseases, including TB. Impaired NETosis significantly impacts the development of a number of diseases and the risks of their complications [6].

Pronounced NETosis manifestations have been evidently observed in patients with severe forms of TB [7, 8]. Fluorescence microscopy is a routine method for studying NETosis [9]. Various intercalating DNA dyes and fluorescent labeling antibodies are applied to the components of neutrophil leukocytes in the test techniques [9]. It was demonstrated that the process of NETosis in response to antigenic stimuli was accompanied by morphologically different fluorescent microscopic phenomena observed in the sample [10, 11]. At the same time, both the so-called cloud-like and filamentous NET forms were detected, which may reflect different degrees of decondensation of chromatin that formed these forms of NETs. Therefore, the prevalence of a certain NET form (among all NETs observed in a sample) turned out to be associated with a TB course [12]. It is known that the process of chromatin decondensation in NETosis is ensured by histone modification disrupting the non-covalent interaction of histones with DNA.

It has been shown that citrullination of histones is observed in NETosis, including histone H3 with modification of the arginine residues R2, R8, and R17 [4, 13, 14]. Specifically, in neutrophils obtained from adults with TB, an immunofluorescent label to citrullinated histone H3 (citH3) was identified after stimulation with *M. tuberculosis*, whereas no labels were detected in healthy individuals [15]. In adults, citH3 concentration in the blood correlated with the severity of TB and the presence of cavities [8]. It has been demonstrated that citH3 can be determined in the blood serum, also as a marker of NETosis [4]. However, it remains unclear to what extent the citH3 level circulating in the blood can be related to the activity of post-translational enzymatic histone modification in neutrophils in TB patients in NETosis. Taking into consideration the fact that NETosis in children may be accompanied by excessive activation of neutrophils and more pronounced NETosis compared to adults [16], studying the role of NETosis in the infectious process in children with *M. tuberculosis* infection is relevant and significant from the point of view of medicine. No data on citH3 concentration in the peripheral blood in relation to the ability of neutrophils to form NETs in children with TB was found in the available literature.

The aim of the study was to characterize NET production parameters in leukocyte culture and the level of citH3 in the peripheral blood to assess the features of NETosis in children with TB.

MATERIALS AND METHODS

The study included 20 children with active respiratory tuberculosis (TB group) and 20 healthy individuals (control group). The TB group included 14 children diagnosed with primary tuberculous complex (PTC), 3 children with infiltrative pulmonary tuberculosis (IPT), and 3 children with intrathoracic lymph node tuberculosis with bronchopulmonary lesions who were treated at the Specialized Children's Tuberculosis Clinical Hospital, Omsk, in 2022–2023. Inclusion criteria for the TB group were as follows: age of 4–14 years; newly diagnosed active respiratory TB established by the Central Control Commission of the TB Hospital; prescribed chemotherapy for newly diagnosed tuberculosis; an informed consent by the parent (or legal guardian) for the child to be included in the study. Exclusion criteria were concomitant diseases and detected isolated extrapulmonary TB.

The control group included healthy children followed up at the Children's Department of Omsk City Polyclinic No. 10, who, according to the results of the regular annual checkup, had a negative reaction to tuberculin. The controls matched the children from the TB group in terms of gender and age, according

to the copy-pair method. Inclusion criteria for the control group were as follows: a negative reaction to the Mantoux test with 2 TE; no contacts with TB patients; an informed consent signed by the parent (or legal guardian) for the child to participate in the study. Exclusion criteria were immune-associated diseases and acute respiratory diseases within one month preceding the study.

The ability of isolated neutrophils to form NETs was assessed in the control and TB groups according to the method described in the patent [3]. After we isolated the neutrophil culture using Ficoll-Urografin density gradient centrifugation, the ability of neutrophils to form NETs was evaluated. Since specific sensitivity to antigens is atypical for neutrophils, the technique provoking neutrophils to form NETs was applied. Neutrophils were incubated for 30 minutes at 37 °C in a medium containing a non-specific antigenic stimulant (a mixture of *Lactobacillus reuteri*, *L. acidophilius*, *L. rhamnosus* and *Bifidobacterium longum*). Upon completion of the incubation, the number of luminescent-positive objects in the sample was counted using fluorescence microscopy: neutrophils (intact, activated, and hyperactivated), early NETosis cells, and NETs with differentiation of cloud-like and filamentous forms (Fig. 1).

The obtained values were expressed as a percentage of the total number of fluorescent objects (FO) in the sample. In addition, the NET capture coefficient was calculated as the ratio of objects captured by a trap to the total number of NETs. Negative control in studying the ability of a neutrophil to form NETs was carried out by incubating a neutrophil culture with 0.9% NaCl in a volume equal to the volume of the non-specific antigenic stimulant used in the main series of the study. The concentration of citH3 was determined in the peripheral blood serum samples in accordance with the instructions of the manufacturer using the Citrullinated Histone H3 (Clone 11D3) ELISA Kit test system (Cayman Chemical Company, USA).

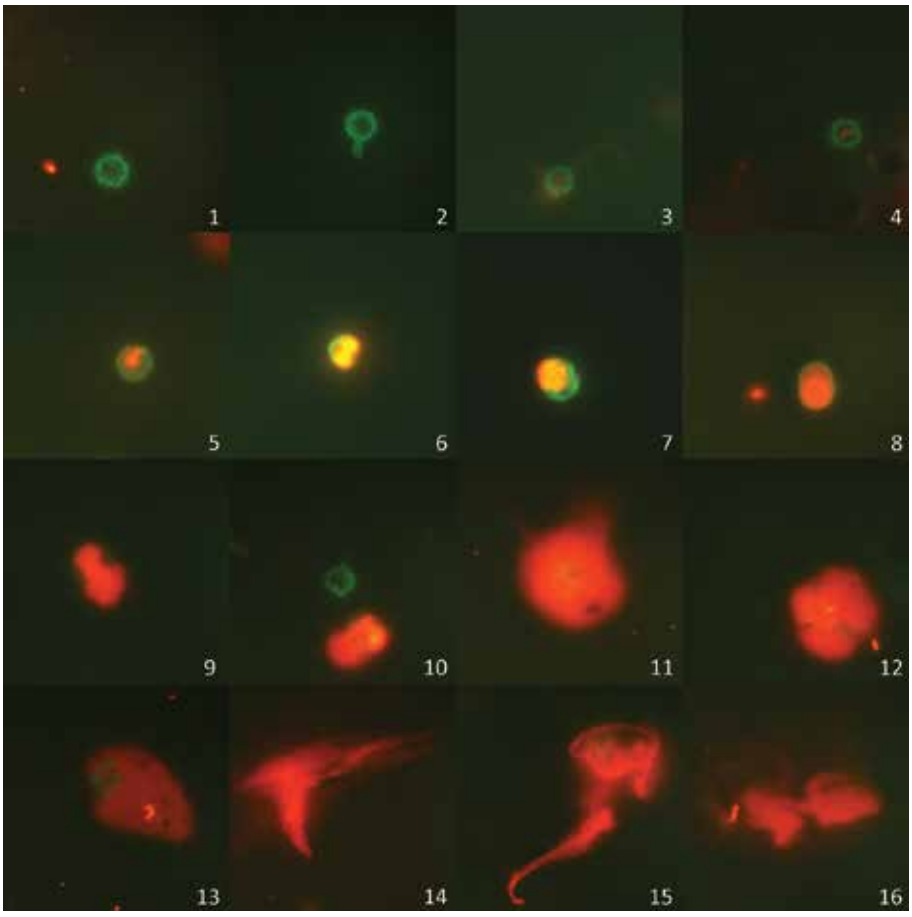

Fig. 1. Micrographs of the objects found in a sample of the isolated fraction of neutrophils: 1, 2 – intact neutrophils; 3, 4 – hypoactivated neutrophils; 5, 6 – activated neutrophils; 7, 8 – hyper-activated neutrophils; 9 – early NETosis cells; 10 – intact neutrophil (top), an early NETosis cell (bottom); 11 – a cloud-like neutrophil extracellular trap; 12, 13 – cloud-like neutrophil extracellular traps with a captured bacterium; 14, 15 – filamentous neutrophil extracellular traps; 16 – a filamentous neutrophil extracellular trap with a captured bacterium. Fluorescence microscopy, ×1,000.

The statistical analysis of the obtained data was carried out using the Statistica 8.0 software. The data distribution in the groups was assessed using the Shapiro – Wilk test. Since the data obtained had a non-normal distribution, the results were represented as the median and the interquartile range (Me (Q_1; Q_3)). The Mann – Whitney U-test was used to calculate the statistical significance of differences for independent samples. The Spearman's rank correlation coefficient was used to measure the association between two variables *ex vivo*, namely neutrophil ability to form NETs and citH3 concentration in the peripheral blood. Pearson's chi-squared test was applied to compare the forms of distribution for individual features of fluorescence microscopy images in the groups. The differences were considered statistically significant at $p < 0.05$.

RESULTS

Neutrophils isolated from the peripheral blood in the TB group were more likely to form NETs during incubation in the presence of th antigenic stimulant (compared to the control group). The number of NETs from all FOs was 31.5 (26.4; 9.6) and 21.1 (19.3; 23.8) in the TB group and the control group, respectively, $p = 0.0087$ (Fig. 2). Neutrophils in the TB group formed predominantly filamentous NETs: 21.0 (19.2; 28.6) compared to the control group 16.0 (15.8; 19.2), $p = 0.0474$ (Fig. 3). Cloud-like NETs (% of all FOs) were detected less often in neutrophil samples in the control group than in the TB group: 4.0 (3.5; 6.2) vs. 10.5 (6.9; 12.3), respectively, $p = 0.0060$.

However, they were not found in neutrophil samples in 5 children of the control group, whereas cloud-like NETs were identified in all patients in the TB group ($\chi^2 = 16.01$; $p < 0.0068$). The NET capture rate (Fig. 4) in the control group was comparable with that in the TB group ($p > 0.05$). No NETs were detected in the negative control.

The median citH3 concentration in the peripheral blood (Fig. 4) was 18.9 times higher in the TB group than in the controls ($p = 0.0041$, the Mann – Whitney U-test). Median values were 1.4 pg / ml (0.9; 1.8) and 26.5 pg / ml (2.7; 33.6) in the control group and in the TB group, respectively.

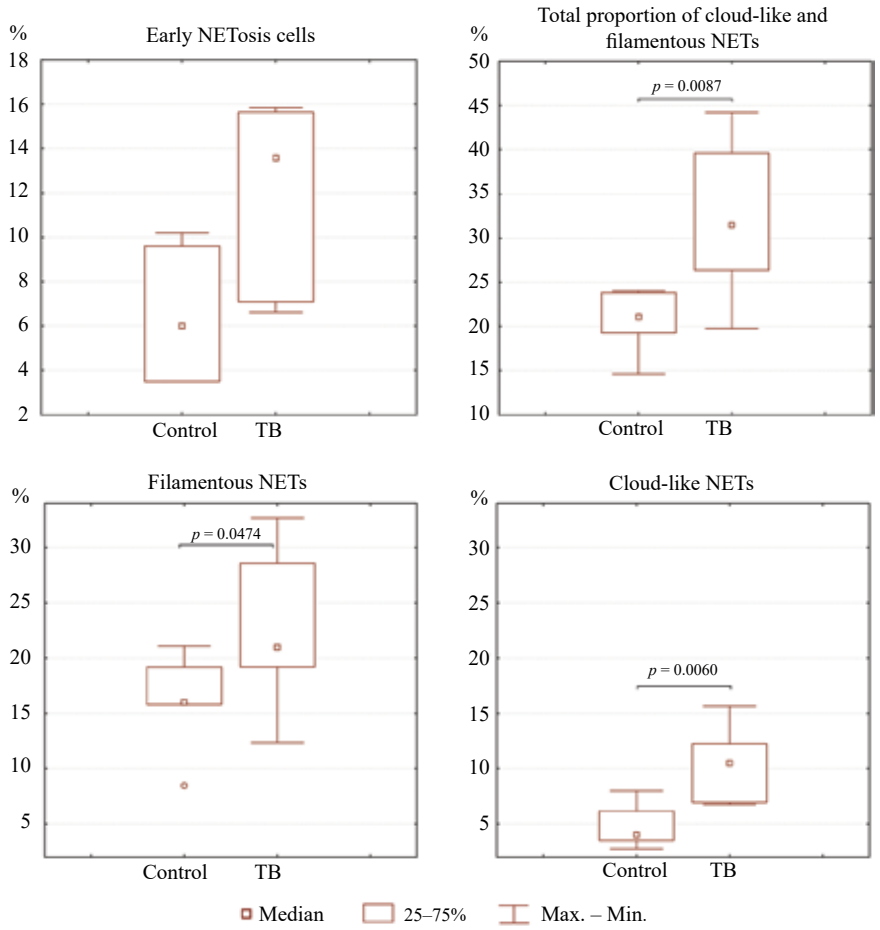

Fig. 2. Fluorescent objects in a sample of isolated neutrophils after stimulation: early NETosis cells, neutrophil extracellular traps

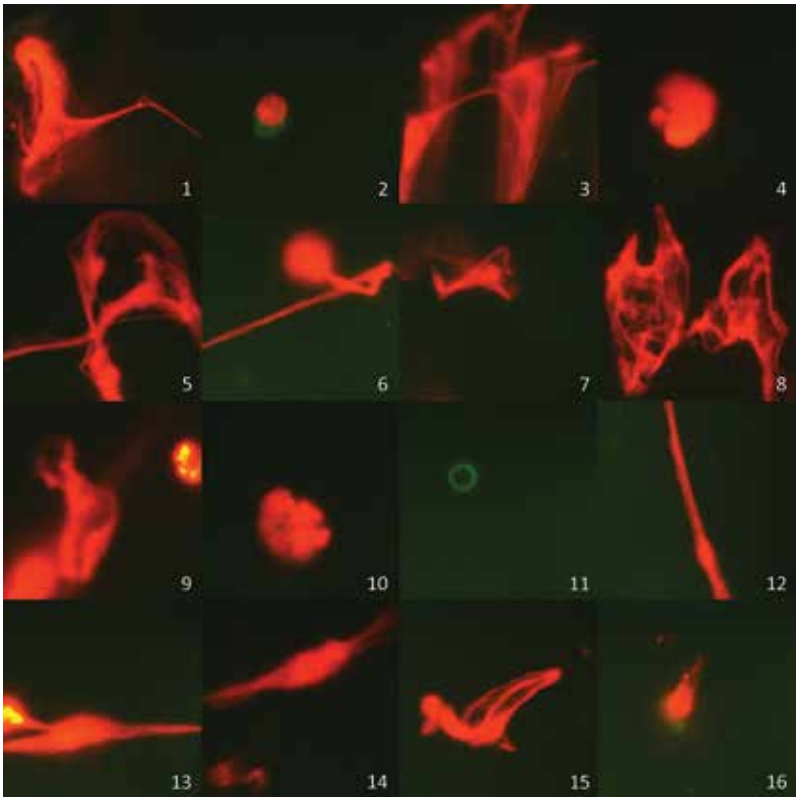

Fig. 3. Examples of fields of view in the sample of isolated neutrophils in children with tuberculosis after exposure to a non-specific antigenic stimulant: filamentous NETs (1, 3, 5–9, 12–15), cloud-like NETs (4, 10), early NETosis cell (16), hyperactivated neutrophil (2), intact neutrophil (11). Fluorescence microscopy, × 1,000

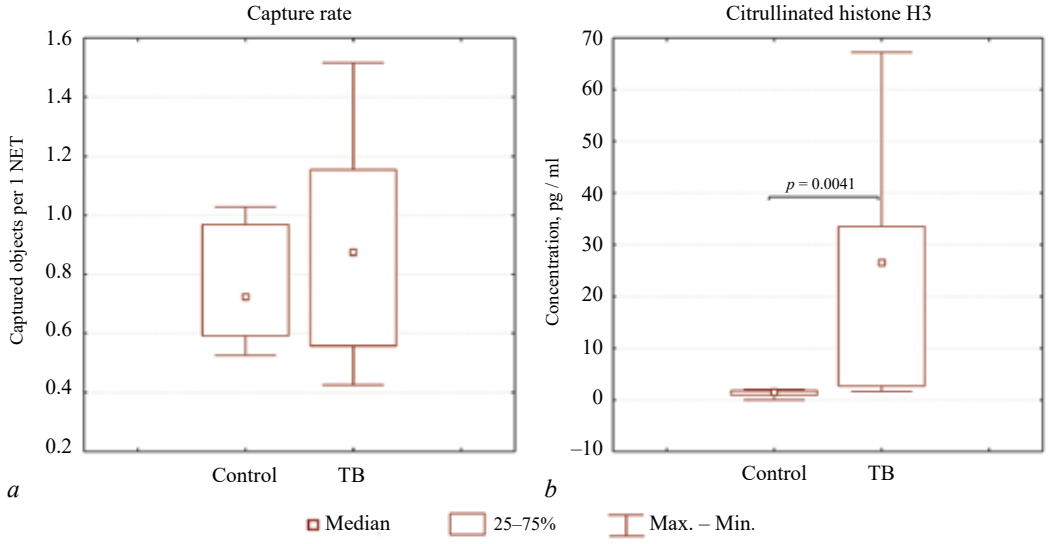

Fig. 4. Capture rate of neutrophil extracellular traps (*a*); citrullinated histone H3 concentration in the peripheral blood (*b*)

After incubation of neutrophils in the presence of the non-specific antigenic stimulant, an expected decrease in the number of intact neutrophils was noted in the sample as a likely consequence of their activation and NETosis. The number of intact neutrophils from the total FO number in the samples of the TB group was 34.6 (26.7; 40.7), while in the control group, this value was significantly higher, 54.0 (46.3; 61.4), p = 0.0040 (the Mann – Whitney U test). Moreover, in the TB group the percentage of hypoactivated neutrophils was slightly smaller than in the control group: 2.6 (1.2; 4.9) vs. 6.0 (4.8; 6.9); p = 0.0295. There were no statistically significant differences between the study groups in terms of the number of activated and hyperactivated neutrophils ($p > 0.05$).

The study of correlations in the control group revealed two strong correlations between the citH3 concentration in the blood and the proportion of

filamentous NETs ($r = 0.95$; $p = 0.0008$) and between citH3 in the blood and the proportion of early NETosis cells ($r = 0.77$; $p = 0.0408$). The study of correlations in the TB group revealed three strong correlations between the citH3 concentration in the blood and the proportion (in %) of filamentous NETs ($r = 0.86$; $p = 0.0137$) and between citH3 in the blood and the proportion of all NETs ($r = 0.89$; $p = 0.0068$). The correlation between citH3 in the blood and the percentage of hyperactivated neutrophils was negative ($r = –0.89$; $p = 0.0068$). No other statistically significant correlations were found between the citH3 concentration in the peripheral blood and the proportion of individual FOs.

DISCUSSION

The diversity of approaches and the lack of a laboratory mainstay in studying NETs lead to ambiguity in the interpretation of research findings. Prominent researchers in this field have failed to reach a consensus on many issues related to NET morphology, mechanisms, the sources of their formation, as well as the regulation of this process [18]. In most publications, the traps were represented by filamentous structures in micrographs obtained using fluorescent dyes to visualize NETs or their components [19]. However, some authors have pointed out that NETs can also take a cloud-like form [11, 18].

Unlike most researchers, Shida Yousefi et al. assume that the appearance of cloud-like structures, consisting predominantly of extracellular DNA, after exposure of neutrophils to certain agents is not the result of NETosis but is due to other forms of cell death associated with cytolysis. Thus, the authors do not classify cloud-like structures as true NETs, whereas they consider filamentous structures as NETs originating from mitochondrial DNA [20, 21]. These authors suppose that the formation of filamentous structures is a normal innate immune response, while the appearance of cloud-like structures is associated with the formation of the so-called vicious circle of inflammation followed by the development of autoimmunity [20, 21]. Regardless of the formation ways and mechanisms of supramolecular cloud-like structures, including nucleoproteins, the opinion expressed by Shida Yousefi et al. is consistent with the results obtained in this study.

A significantly larger number of cloud-like NETs were found in patients with TB compared to the control group, where such NETs were rare. Filamentous NETs were also detected in fairly large numbers in healthy children. Presumably, it is the presence of cloud-like NETs that is associated with the development of the autoimmune reaction observed in TB. Thus, in a number of studies, autoantibodies to various autoantigens were found in patients with TB [22].

The circulation of damage-associated molecular patterns (DAMPs) in the blood is one of the reasons for this response [22]. DAMPs are a rather heterogeneous group of molecules, including histones [23], which also have direct cytotoxicity [24]. Previously, while examining adult patients with TB, it was revealed that a higher level of citH3, whose formation is closely related to NETosis [4, 13, 14], is associated with an increased content of neutrophils in the blood, the presence of cavities in the lungs, and low efficiency of anti-TB treatment [8]. This is consistent with our results that demonstrated a significantly higher level of citH3 in the blood serum of children with TB compared to healthy children. In our previous study, citH3 level in children with TB was significantly higher than in adults with cavities, which was detected using identical test systems in both studies [8]. Probably, at the initial stages of TB, NETosis may play a more crucial role in the development of autoinflammation.

Moreover, in this study, the citH3 level in the blood serum was associated with the formation of filamentous NETs rather than cloud-like ones by peripheral blood leukocytes. At the same time, NETs formed in the site of inflammation may be a source of citH3 in the blood serum. The assessed ability of neutrophils to form NETs describes the pro-NETotic phenotype of neutrophils, which are more likely to form NETs in chronic inflammation [20]. The above correlation can probably be explained by comparing our results with the study by Florence Guillotin et al. [19].

These authors declare the presence of filamentous structures that contain DNA and are recognized by antibodies to myeloperoxidase and citH3 as morphologically similar to vital NETosis observed in fluorescence microscopy [19]. This approach is slightly contradictory because it is based on a set of hypotheses, and it is consistent with the opinion of Shida Yousefi et al. suggesting that the source of filamentous structures is mitochondrial DNA [20, 21]. However, it should be taken into account that mitochondrial DNA does not contain histones [25]. The equivalents of other NETosis types referred to in the article as non-vital NETosis are filamentous structures not containing citH3 [19]. The design of this study did not include the registration of cloud-like

structures. Apparently, suicidal and other NETosis types were simultaneously observed with the vital NETosis. At the same time, in the mentioned study, non-vital NETosis prevailed in the pathology group (pre-eclampsia) in comparison with the control group, and NETosis combined with histone modification prevailed in both groups [19].

In this regard, it is yet to be investigated whether cloud-like structures containing DNA that we observed are a type of suicidal NETosis or another type of cell death. However, they may reflect the process that does not require the regulation of chromatin decondensation mediated by enzymatic modification of histones. The emergence of this phenomenon may reflect the development of an autoimmune component of inflammation. At the same time, an increase in the concentration of citH3 in children with TB can demonstrate the efficacy of the innate immune response and be a normal compensatory adaptation process.

CONCLUSION

A higher level of citH3 was observed in the blood of children with TB compared to healthy controls. In the *ex vivo* study, the relative amount of filamentous and cloud-like NETs was greater in the neutrophil culture exposed to a non-specific antigenic stimulant in children with TB than in a similar experiment with neutrophils of healthy children. It was revealed that the number of filamentous NETs formed *ex vivo* in both groups was positively related to the citH3 level in the blood. However, a similar correlation was not registered between the number of cloud-like NETs and the level of citH3 in the blood. It is likely that the higher level of citH3, an enzymatic modification product, in the blood of children with TB reflects higher activity of NETosis *in vivo*, which may be due to an increased ability of neutrophils to form NETs.

The impact of numerous factors of the immune response in TB probably determines the formation of a unique pro-NETotic neutrophil phenotype. Given the non-specific nature of neutrophils, it can be assumed that in the situation of increased readiness for NETosis, the range of antigenic structures capable of triggering and stimulating NETosis may significantly expand. In particular, the antigens of normal human microbiota, including the antigens of bacterial gut symbionts, can also stimulate NETosis, which is probably indicated by the results of our study.

The data obtained in our study have shown that *in vivo* and *ex vivo* methodological approaches applied for NETosis investigation do not provide equal information content and can complement each other since they describe different aspects of the NETosis phenomena under study. In children with TB, the formation of cloud-like forms of NETs in the culture of peripheral blood neutrophils in response to the stimulation turned out to be notably more common. Researchers consider such NET forms abnormal [21]. Inefficacy of the NETosis reaction in the long-term course of the disease can significantly affect the development of predisposition to autoinflammation and immunopathology. Studying these issues may become the subject of a separate line of research.

REFERENCES

1. Sanina A.E., Serebryakova V.A., Urazova O.I., Gadzhiev A.A. Notch signaling pathway in the development of imbalanced immune responses in patients with disseminated pulmonary tuberculosis. *Bulletin of Siberian Medicine.* 2023;22(4):92–99. (In Russ.). DOI: 10.20538/1682-0363-2023-4-92-99.
2. Rook G.A. Th2 cytokines in susceptibility to tuberculosis. *Curr. Mol. Med.* 2007;7(3):327–337. DOI: 10.2174/156652407780598557.
3. Manz M.G., Boettcher S. Emergency granulopoiesis. *Nat. Rev. Immunol.* 2014;14(5):302–314. DOI: 10.1038/nri3660.
4. Tilley D.O., Abuabed U., Zimny Arndt U., Schmid M., Florian S., Jungblut P.R. et al. Histone H3 clipping is a novel signature of human neutrophil extracellular traps. *Elife.* 2022;11:e68283. DOI: 10.7554/eLife.68283.
5. Kasprzycka W., Homa-Mlak I., Mlak R., Małecka-Massalska T. Direct and indirect methods of evaluating the NETosis process. *J. Pre. Clin. Clin. Res.* 2019;13(1):50–56. DOI: 10.26444/jpccr/105563.
6. Huang J., Hong W., Wan M., Zheng L. Molecular mechanisms and therapeutic target of NETosis in diseases. *Med.Comm. (2020).* 2022;3(3):e162. DOI: 10.1002/mco2.162.
7. Schechter M.C., Buac K., Adekambi T., Cagle S., Celli J., Ray S.M. et al. Neutrophil extracellular trap (NET) levels in human plasma are associated with active TB. *PLoS One.* 2017;12(8):e0182587. DOI: 10.1371/journal.pone.0182587.
8. De Melo M.G.M., Mesquita E.D.D., Oliveira M.M., da Silva-Monteiro C., Silveira A.K.A., Malaquias T.S. et al. Imbalance of NET and Alpha-1-Antitrypsin in Tuberculosis Patients Is Related With Hyper Inflammation and Severe Lung Tissue Damage. *Front. Immunol.* 2019;9:3147. DOI: 10.3389/fimmu.2018.03147.
9. De Buhr N., von Köckritz-Blickwede M. How neutrophil extracellular traps become visible. *J. Immunol. Res.* 2016;2016:4604713. DOI: 10.1155/2016/4604713.

Mordyk A.V., Zolotov A.N., Novikov D.G., Romanova M.A., Kirichenko N.A., Ptuhin A.O. Netosis-forming ability of neutrophils in children with latent tuberculosis infection with the positive test with a tuberculosis recombinant allergen. *Clinical Practice in Pediatrics* . 2023;18(5):7-12. DOI: 10.20953/1817-7646-2023-5-7-12. (In Russ.).

11. Daniel C., Leppkes M., Muñoz L.E., Schley G., Schett G., Herrmann M. Extracellular DNA traps in inflammation, injury and healing. *Nat. Rev. Nephrol.* 2019;15(9):559–575. DOI: 10.1038/s41581-019-0163-2.
12. Mordyk A.V., Zolotov A.N., Novikov D.G., Kirichenko N.A., Pakhtusova P.O., Ptuhin A.O. NETosis-forming ability of neutrophils in patients with limited and disseminated tuberculous lesions. *Tuberculosis and Lung Diseases.* 2023;101(3):78–86. (In Russ.). DOI: 10.58838/2075-1230-2023-101-3-78-86.
13. Wang Y., Li M., Stadler S., Correll S., Li P., Wang D. et al. Histone hypercitrullination mediates chromatin decondensation and neutrophil extracellular trap formation. *J. Cell Biol.* 2009;184(2):205–213. DOI: 10.1083/jcb.200806072.
14. Cuthbert G.L., Daujat S., Snowden A.W., Erdjument-Bromage H., Hagiwara T., Yamada M. et al. Histone deimination antagonizes arginine methylation. *Cell.* 2004;118(5):545–553. DOI: 10.1016/j.cell.2004.08.020.
15. Ong C.W., Elkington P.T., Brilha S., Ugarte-Gil C., Tome-Esteban M.T., Tezera L.B. et al. Neutrophil-derived MMP-8 drives AMPK-dependent matrix destruction in human pulmonary tuberculosis. *PLoS Pathog.* 2015;11(5):e1004917. DOI: 10.1371/journal.ppat.1004917.
16. Appelgren D., Enocsson H., Skogman B.H., Nordberg M., Perander L., Nyman D. et al. Neutrophil extracellular traps (NETs) in the cerebrospinal fluid samples from children and adults with central nervous system infections. *Cells.* 2019;9(1):43. DOI: 10.3390/cells9010043.
17. Novikov D.G., Zolotov A.N., Kirichenko N.A., Mordyk A.V. A method for detecting neutrophilic extracellular traps in a supravitally stained blood sample. Patent for invention No. 2768152. Published on 23.03.2022. Bull. No. 9. (In Russ.).
18. Boeltz S., Amini P., Anders H.J., Andrade F., Bilyy R., Chatfield S. et al. To NET or not to NET:current opinions and state of the science regarding the formation of neutrophil extracellular traps. *Cell Death Differ.* 2019;26(3):395–408. DOI: 10.1038/s41418-018-0261-x.
19. Guillotin F., Fortier M., Portes M., Demattei C., Mousty E., Nouvellon E. et al. Vital NETosis vs. suicidal NETosis during normal pregnancy and preeclampsia. *Front. Cell Dev. Biol.* 2023;10:1099038. DOI: 10.3389/fcell.2022.1099038.
20. Yousefi S., Simon D., Stojkov D., Karsonova A., Karaulov A., Simon H.U. *In vivo* evidence for extracellular DNA trap formation. *Cell Death Dis.* 2020;11(4):300. DOI: 10.1038/s41419-020-2497-x.
21. Yousefi S., Simon H.U. NETosis – Does it really represent nature's "suicide bomber"? *Front. Immunol.* 2016;7:328. DOI: 10.3389/fimmu.2016.00328.
22. Belyaeva I.V., Kosova A.N., Vasiliev A.G. Tuberculosis and autoimmunity. *Pathophysiology.* 2022;29(2):298–318. DOI: 10.3390/pathophysiology29020022.
23. Roh J.S., Sohn D.H. Damage-associated molecular patterns in inflammatory diseases. *Immun. Netw.* 2018;18(4):e27. DOI: 10.4110/in.2018.18.e27.
24. Locke M., Francis R.J., Tsaousi E., Longstaff C. Fibrinogen protects neutrophils from the cytotoxic effects of histones and delays neutrophil extracellular trap formation induced by ionomycin. *Sci. Rep.* 2020;10(1):11694. DOI: 10.1038/s41598-020-68584-0.
25. Alexeyev M., Shokolenko I., Wilson G., LeDoux S. The maintenance of mitochondrial DNA integrity--critical analysis and update. *Cold Spring Harb. Perspect. Biol.* 2013;5(5):a012641. DOI: 10.1101/cshperspect.a012641.

Authors' contribution

Novikov D.G., Zolotov A.N. – conception and design. Ptukhin A.O., Romanova M.A. – selection of the clinical base for analysis, clinical examination of patients. Romanova M.A. – interpretation of the spiral computed tomography results. Zolotov A.N. – conducting fluorescence microscopy. Kirichenko N.A. – pre-analytical stage of the study, conducting fluorescence microscopy. Novikov D.G. – conducting ELISA blood serum research. Novikov D.G., Zolotov A.N. – analysis and interpretation of the data. Indutny A.V. – justification of the manuscript, critical revision of the manuscript for important intellectual content. Mordyk A.V. – final approval of the manuscript for publication.

Authors' information

Novikov Dmitry G. – Cand. Sci. (Med.), Associate Professor, Associate Professor of the Department of Clinical Laboratory Diagnostics of Continuing Professional Education, Head of the Central Research Laboratory, Omsk State Medical University, Omsk, novikov.dm.omsk@gmail.com, http://orcid.org/0000-0002-4339-2222

Zolotov Alexander N. – Cand. Sci. (Med.), Senior Researcher, Central Research Laboratory, Associate Professor of the Department of Pathophysiology, Omsk State Medical University, Omsk, azolotov@mail.ru, http://orcid.org/0000-0002-6775-323X

Indutny Anton V. – Dr. Sci. (Med.), Associate Professor, Head of the Department of Clinical Laboratory Diagnostics of Continuing Professional Education, Omsk State Medical University, Omsk, kld-omsk@mail.ru, http://orcid.org/0000-0003-1951-5824

Mordyk Anna V. – Dr. Sci. (Med.), Professor, Head of the Department of Phthisiology, Pulmonology and Infectious Diseases, Omsk State Medical University, Omsk, amordik@mail.ru, http://orcid.org/0000-0001-6196-7256

Kirichenko Nikolay A. – Junior Researcher, Central Research Laboratory, Omsk State Medical University, Omsk, honomer_1608@mail.ru, http://orcid.org/0000-0002-8411-0973

Romanova Maria A. – Cand. Sci. (Med.), Associate Professor of the Department of Phthisiology, Pulmonology and Infectious Diseases, Omsk State Medical University, Omsk, rmari1@mail.ru, http://orcid.org/0000-0002-1775-607X

Ptukhin Alexander O. – Post-Graduate Student, Department of Phthisiology, Pulmonology and Infectious Diseases, Omsk State Medical University, Omsk, ptuhin.alexandr@mail.ru, http://orcid.org/000-0002-2830-161X

(✉) **Kirichenko Nikolay A.,** honomer_1608@mail.ru

Received 12.03.2024;
approved after peer review 20.03.2024;
accepted 14.05.2024

УДК 616.12-005.4:616.8-008.64]-02:616.8-009.836
https://doi.org/10.20538/1682-0363-2024-4-105-110

Sleep disturbances in patients with comorbid coronary heart disease and depression

Nonka T.G.[1], Lebedeva E.V.[1], Repin A.N.[1], Schastnyy E.D.[2]

[1] *Cardiology Research Institute, Tomsk National Research Medical Center (NRMC), Russian Academy of Sciences 111a, Kievskaya Str., Tomsk, 634014, Russian Federation*

[2] *Mental Health Research Institute, Tomsk National Research Medical Center (NRMC), Russian Academy of Sciences 4, Aleutskaya Str., Tomsk, 634014, Russian Federation*

ABSTRACT

Aim. To study the presence and severity of insomnia in patients with comorbid coronary heart disease (CHD) and depressive disorder (DD).

Materials and methods. The study included 132 patients with CHD (class II–III exertional angina after myocardial infarction experienced more than 6 months ago): 58 patients with DD and 74 patients without depression. The Beck Depression Inventory (BDI) was used to diagnose DD. The diagnosis in all cases was confirmed by a therapist. Sleep disturbances were assessed using the Sheehan Patient-Rated Anxiety Scale (ShAS). The data were presented as $M \pm SD$; n (%); and *Me* [25%; 75%]. The differences were considered significant at $p < 0.05$.

Results. Insomnia in the general group of patients was registered as follows: none or clinically not significant – in 62 patients (54.9%), clinically significant – in 51 patients (45.1%). Night awakenings in the general group of patients were detected as follows: none or clinically not significant – in 66 patients (58.4%), clinically significant – in 47 patients (41.6%). Disturbances in falling asleep and night awakenings were significantly pronounced in patients with CHD with identified DD compared to patients without mental disorders: disturbances in falling asleep – 2 [1; 3] vs. 1 [0; 2] ($p = 0.0001$), night awakenings – 2 [1; 3] vs. 1 [0; 2] ($p = 0.00002$), respectively. In the group of CHD with DD ($n = 58$), 2 people (3.4%) did not complete the scale. Among those who did, 12 patients (21.4%) had no difficulty falling asleep, 9 patients (16.1%) had little difficulty, and 35 patients (62.5%) had clinically significant disturbances. In the group of CHD without DD ($n = 74$), 17 people (23%) did not complete the scale. Among those who did ($n = 57$), 21 patients (36.8%) had no difficulty falling asleep, 20 patients (35.1%) had little difficulty, and 16 patients (28.1%) had clinically significant problems. In patients with comorbid CHD and DD who completed the ShARS ($n = 56$), 7 patients (12.5%) had no night awakenings, 17 patients (30.4%) had few night awakenings, and 32 patients (57.1%) had clinically significant disturbances in maintaining sleep. In the group without DD, among those who completed the ShARS ($n = 57$), 18 patients (31.6%) had no night awakenings, 24 patients (42.1%) had few night awakenings, and 15 patients (26.4%) had clinically significant disturbances in maintaining sleep. Significant differences were noted for all test questions ($p < 0.0005$).

Conclusion. In patients with comorbid CHD and DD, changes in the circadian rhythm are detected in the form of significant disturbances in falling asleep and awakening, which can aggravate the clinical course of CHD and the prognosis of patients with cardiovascular diseases.

Keywords: coronary heart disease, depressive disorders, myocardial infarction, sleep disturbances

Conflict of interest. The authors declare the absence of obvious or potential conflicts of interest related to the publication of this article.

✉ *Nonka Tatiana G.,* tatiananonka@gmail.com

Source of financing. The authors state that they received no funding for the study.

Conformity with the principles of ethics. All patients signed an informed consent to participate in the study. The study was approved by the local Ethics Committee at the Cardiology Research Institute of Tomsk NRMC.

For citation: Nonka T.G., Lebedeva E.V., Repin A.N., Schastnyy E.D. Sleep disturbances in patients with comorbid coronary heart disease and depression. *Bulletin of Siberian Medicine.* 2024;23(4):105–110. https://doi.org/10.20538/1682-0363-2024-4-105-110.

Нарушения сна у больных ишемической болезнью сердца в сочетании с депрессивными расстройствами

Нонка Т.Г.[1], Лебедева Е.В.[1], Репин А.Н.[1], Счастный Е.Д.[2]

[1] Научно-исследовательский институт (НИИ) кардиологии, Томский национальный исследовательский медицинский центр (НИМЦ) Российской академии наук
Россия, 634014, г. Томск, ул. Киевская, 111а

[2] Научно-исследовательский институт (НИИ) психического здоровья, Томский национальный исследовательский медицинский центр (НИМЦ) Российской академии наук
Россия, 634014, г. Томск, ул. Алеутская, 4

РЕЗЮМЕ

Цель. Изучить наличие и выраженность инсомнии у больных ишемической болезнью сердца (ИБС) в сочетании с депрессивными расстройствами (ДР).

Материалы и методы. В исследование включены 132 больных с ИБС (со стенокардией напряжения II–III функциональных классов после перенесенного инфаркта миокарда давностью более 6 мес): 58 пациентов с ДР и 74 пациента без ДР. Для диагностики ДР использовалась шкала депрессии Бека (BDI). Диагноз во всех случаях подтверждался при консультации психиатра-психотерапевта. Нарушения сна оценивались при анализе шкалы Шихана (ShARS). Данные представлены в виде $M \pm SD$; n (%); *Me* [25%; 75%], значимым считалось различие при $p < 0,05$.

Результаты. Нарушение засыпания в общей группе пациентов: нет или клинически не значимы – у 62 пациентов (54,9%), клинически значимые – у 51 пациента (45,1%). Ночные пробуждения в общей группе пациентов: у 66 (58,4%) – нет или клинически незначимые ночные пробуждения, клинически значимые – у 47 (41,6%). Нарушения засыпания и ночные пробуждения были значимо выражены у пациентов ИБС с выявленными ДР в сравнении с больными без расстройств психики: нарушения засыпания 2 [1; 3] vs 1 [0; 2] ($p = 0,0001$), ночные пробуждения 2 [1; 3] vs 1 [0; 2] ($p = 0,00002$) соответственно. В группе ИБС с ДР ($n = 58$) два человека (3,4%) не заполнили шкалу. Среди заполнивших 12 пациентов (21,4%) не имели проблем с засыпанием, 9 (16,1%) – немного, 35 (62,5%) – клинически выраженные нарушения. В группе ИБС без ДР ($n = 74$) 17 человек (23%) не заполнили шкалу. Среди заполнивших ($n = 57$) 21 пациент (36,8%) не имел проблем с засыпанием, 20 (35,1%) имели небольшие нарушения, 16 пациентов (28,1%) имели клинически выраженные нарушения. У больных ИБС в сочетании с ДР и заполнивших ShARS ($n = 56$) 7 (12,5%) не пробуждались ночью, 17 (30,4%) – немного пробуждались, у 32 (57,1%) наблюдались клинически выраженные нарушения поддержания сна. В группе без ДР среди заполнивших шкалу Шихана ($n = 57$) 18 (31,6%) не пробуждались ночью, 24 (42,1%) – немного пробуждались, у 15 (26,4%) отмечались клинически выраженные нарушения поддержания сна. По всем пунктам тестирования отмечены достоверные различия ($p < 0,0005$).

Заключение. У пациентов с хронической коронарной болезнью на фоне ДР выявляются изменения в суточном ритме в виде значительных нарушений засыпания и пробуждений, что может усугубить клиническое течение ИБС и прогноз больных сердечно-сосудистыми заболеваниями.

Ключевые слова: ишемическая болезнь сердца, депрессивные расстройства, инфаркт миокарда, нарушения сна

Конфликт интересов. Авторы декларируют отсутствие явных и потенциальных конфликтов интересов, связанных с публикацией настоящей статьи.

Источник финансирования. Авторы заявляют об отсутствии финансирования при проведении исследования.

Соответствие принципам этики. Информированное согласие было подписано всеми участниками исследования. Исследование одобрено локальным этическим комитетом НИИ кардиологии Томского НИМЦ.

Для цитирования: Нонка Т.Г., Лебедева Е.В., Репин А.Н., Счастный Е.Д. Нарушения сна у больных ишемической болезнью сердца в сочетании с депрессивными расстройствами. *Бюллетень сибирской медицины.* 2024;23(4):105–110. https://doi.org/10.20538/1682-0363-2024-4-105-110.

INTRODUCTION

Every year psycho-emotional stress is increasing worldwide, especially among patients with cardiovascular diseases, as evidenced by large epidemiological studies [1, 2]. Almost 70% of patients with arterial hypertension and coronary heart disease (CHD) are characterized by high stress levels. This means that the incidence of affective disorders in patients with cardiovascular disease is also increasing: in the COMET study, anxiety symptoms were present in 47.2% of outpatient cases, in 25.5% of cases, they were clinically significant; symptoms of depression were found in 42.5% of patients, of which 16.3% of cases were clinically significant [1]. It is important to consider that symptoms of depression had not been previously identified in patients. Subsequently, depressive disorder (DD) is often not diagnosed in a timely manner and can aggravate the course of cardiovascular diseases and affect the prognosis [3, 4].

World Health Organization (WHO) assumes that by 2030, CHD and DD will be the leading causes of disability [5, 6]. Depression is the most powerful risk factor for CHD and a predictor of mortality in this category of patients: DD affects 40% of patients in the post-infarction period, increasing the risk of death by 3–6 times [7]. It is known that cardiovascular catastrophes, in particular myocardial infarctions, most often occur at night and early morning hours [8] and are associated with the activation of the sympathoadrenal system. Healthy sleep plays a major role in the balance between the parasympathetic and sympathetic nervous systems, and sleep disorders (insomnia) prevent a physiological nocturnal decrease in sympathetic activity, which in turn affects many pathogenetic mechanisms of cardiovascular pathology. At the same time, it is known that one of the most common manifestations of DD is sleep disturbances, with the incidence reaching up to 80% [9]. Therefore, there is no doubt in the relevance of studying sleep disturbances in patients with comorbid CHD and DD.

MATERIALS AND METHODS

After signing the informed consent, 132 patients with CHD (class II–III exertional angina after myocardial infarction experienced more than 6 months ago) were included in the study at the Cardiology Department of Cardiology Research Institute (Tomsk): 58 patients with DD (group 1) and 74 patients without depression (group 2). The Beck Depression Inventory (BDI) was used to diagnose and determine the severity of DD (the BDI score of more than 19 was considered as elevated level of depression). In case of elevated depression levels according to BDI, a consultation with a psychiatrist and therapist took place to confirm the diagnosis of DD. We also used the Sheehan Patient-Rated Anxiety Scale (ShARS) to identify sleep disturbances and comorbid DD and anxiety. Sleep disturbances were assessed by analyzing items 30 and 31 of the ShARS. The data were presented as $M \pm SD$; n (%) and Me [25%; 75%]. The differences were considered significant at $p < 0.05$. To test the normality of data distribution, the Shapiro – Wilk test was used. For normally distributed variables, the Student's *t*-test was used, for non-normally distributed variables, the Mann – Whitney test was applied. To analyze qualitative variables, contingency tables and the $\chi 2$ test were used.

RESULTS

The patients did not differ in the main clinical and demographic characteristics. However, in the CHD group with DD, a trend toward more frequent comorbidity of diseases in women was noted: in group 1, 47 men (81%) and 11 women (19%), in group 2 – 68 men (91.9%) and 6 women (8.1%) ($p = 0.06$). The average age in both groups was comparable and

was 55.5 ± 5.9 years vs. 54 ± 7.4 years ($p > 0.05$). After consultation with a psychiatrist, the following disorders were diagnosed: recurrent depressive disorder – in 37.9% of cases, depressive episode – in 27.6% of cases, dysthymia – in 25.9% of cases, bipolar disorder – in 8.6% of cases (Figure). Among depressive episodes, moderately expressed ones prevailed – 92%.

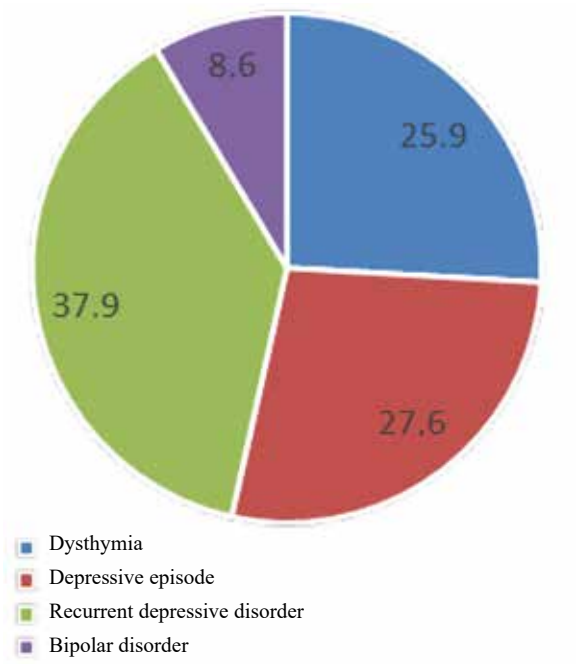

Figure. The diagnosis of depressive disorders in patients with coronary heart disease after previously experienced myocardial infarction

Following the ShARS analysis, high comorbidity with anxiety disorders was noted (53.4%). To study the presence and severity of insomnia, a clinical interview and the ShARS were used (items 30 and 31 (sleep disturbances and night awakenings, respectively)).

Disturbances of falling asleep in the general group of patients were registered as follows: none or clinically not significant – in 62 patients (54.9%), clinically significant – in 51 patients (45.1%). Night awakenings in the general group of patients were registered as follows: none or clinically not significant – in 66 patients (58.4%), clinically significant – in 47 patients (41.6%). Difficulty falling asleep and night awakenings were significantly pronounced in patients with comorbid CHD and DD compared to patients without mental disorders: difficulty falling asleep – 2 [1; 3] vs. 1 [0; 2] ($p = 0.0001$), night awakenings – 2 [1; 3] vs. 1 [0; 2] ($p = 0.00002$), respectively. In the group of CHD with DD ($n = 58$), 2 people (3.4%) did not complete the scale. Among those who did, 12 patients (21.4%) had no difficulty falling asleep, 9 patients (16.1%) had little difficulty, and 35 patients (62.5%) had clinically significant disturbances. In the group of CHD without DD ($n = 74$), 17 people (23%) did not complete the scale. Among those who did ($n = 57$), 21 patients (36.8%) had no difficulty falling asleep, 20 patients (35.1%) had little difficulty, and 16 patients (28.1%) had clinically significant problems. In patients with comorbid CHD and DD who completed the ShARS ($n = 56$), 7 patients (12.5%) had no night awakenings, 17 patients (30.4%) had few night awakenings, and 32 patients (57.1%) had clinically significant disturbances in maintaining sleep. In the group without DD, among those who completed the ShARS ($n = 57$), 18 patients (31.6%) had no night awakenings, 24 patients (42.1%) had few night awakenings, and 15 patients (26.4%) had clinically significant disturbances in maintaining sleep. Significant differences were noted for all test questions ($p < 0.0005$).

DISCUSSION

The relationship between two diseases – CHD and DD – has been studied for years. Data of large studies (Cardiovascular Health Study, MONICA, ENRICHD, INTERHEART, SADHART) prove that depression is a powerful prognostic factor for cardiovascular complications. The relationship between CHD and DD is not accidental, since there are common pathogenetic mechanisms underlying both the diseases and causes of mortality. There are two main mechanisms that cause sudden cardiac death in patients with cardiovascular diseases: increased thrombus formation and impaired cardiac autonomic regulation with the development of severe arrhythmias [10, 11].

It is known that cardiac autonomic regulation is closely related to circadian rhythms and quality of sleep in patients with CHD [12]. Considering the fact that DD is often not diagnosed in a timely manner [1], and sleep disturbances are some of the manifestations and diagnostic criteria of affective disorders, we can always suspect a mental disorder in the context of insomnia and refer to a specialist. In our study, we analyzed sleep disturbances in patients with a history of myocardial infarction in combination with DD. In order to assess insomnia, we used the ShARS. It turned out that there was high comorbidity of DD with anxiety disorders (53.4%), which is consistent with literature data. According to epidemiological studies,

60% of patients with DD have anxiety symptoms [13].

According to our study, sleep disturbances were also found in patients with CHD without mental disorders: approximately every third patient had minor difficulties falling asleep, every fourth patient had significant difficulties falling asleep and maintaining sleep. Apparently at this stage the patient already needs counseling and comprehensive rehabilitation: confidential "doctor-patient" contact for patient awareness about their disease, secondary prevention, healthy lifestyle, maintaining therapy compliance, consultations by a psychologist and therapist to prevent the development of clinically significant signs of anxiety and depression.

With the development of DD in patients with CHD, the severity of sleep disturbances increased significantly: more than half of the patients had severe disturbances of both falling asleep (62.5% of cases) and maintaining sleep throughout the night (57.1% of cases). Given that with sleep disturbances, the resulting stress causes hyperactivation of the sympathoadrenal system and autonomic dysfunction [14], this can contribute to deterioration of the clinical presentation of CHD and cause serious cardiovascular complications. Certainly, the obtained data determine the need for close attention to patients with comorbid CHD and mental disorders, timely screening for DD, and effective correction of the disease with modern antidepressants.

CONCLUSION

Patients with comorbid CHD and DD are characterized by changes in the circadian rhythm in the form of significant disturbances of falling asleep and awakening, which can aggravate the clinical course of CHD and the prognosis of patients with cardiovascular diseases. Identification of sleep disturbances through interviews and the use of psychometric tools will allow to suspect the presence of DD and prescribe antidepressant therapy in a timely manner, improving the clinical presentation of CHD and reducing the risk of developing life-threatening cardiovascular complications.

REFERENCES

1. Pogosova N.V., Sokolova O.Yu., Yufereva Yu.M., Kursakov A.A., Ausheva A.K., Arutyunov A.A. et al. Psychosocial risk factors in patients with the most common cardiovascular diseases, such as hypertension and coronary artery disease (based on the results of the Russian Multicenter COMET Study). *Cardiology.* 2019;59(8):54–63. (In Russ.). DOI: 10.18087/cardio.2019.8.n469.
2. Pogosova N.V., Oganov R.G., Boytsov S.A., Ausheva A.K., Sokolova O.Yu., Kursakov A.A. et al. Psychosocial factors and life quality in coronary heart disease patients: results of the Russian part of the international multicenter study Euroaspire iv. *Cardiovascular Therapy and Prevention*. 2017;16(5):20–26. (In Russ.). DOI: 10.15829/1728-8800-2017-5-20-26.
3. Belialov F.I. Depression, anxiety, and stress in patients with coronary heart disease. *Therapy Archives*. 2017;89(8):104–109. (In Russ.). DOI: 10.17116/terarkh2017898104-109.
4. Nonka T.G., Lebedeva E.V., Repin A.N. Clinical features of coronary artery disease and 5-year survival of patients after myocardial infarction against the background of depressive disorders. *Therapy Archives.* 2024;96(1):17–21. (In Russ.). DOI: 10.26442/00403660.2024.01.202560.
5. Patel H., Mazur W., Williams K.A., Kalra D.K. Myocardial viability-State of the art: Is it still relevant and how to best assess it with imaging? *Trends Cardiovasc. Med*. 2018;28(1):24–37. DOI: 10.1016/j. tcm.2017.07.001.
6. Khandaker G.M., Zuber V., Rees J.M.B., Carvalho L., Mason A.M., Foley C.N. et al. Shared mechanisms between coronary heart disease and depression: findings from a large UK general population-based cohort. *Molecular Psychiatry*. 2020;25(7):1477–1486. DOI: 10.1038/s41380-019-0395-3.
7. Pushkarev G.S., Kuznetsov V.A., Fisher Y.A., Soldatova A.M., Sapozhnikova A.D., Enina T.N. Effect of depressive symptoms on the risk of death from all causes in patients with chronic heart failure who underwent cardiac resynchronization therapy. *Cardiology*. 2019;59(1):5–11. (In Russ.). DOI: 10.18087/cardio.2019.1.10211.
8. Gafarov V.V., Gafarova A.V. World Health Organization Program "Acute Myocardial Infarction Register" as Audit Health Assessment. *Bulletin of NSUEM*. 2015;4:200–222. (In Russ.).
9. Roth T., Roehrs T. Insomnia: Epidemiology, characteristics, and consequences. *Clinical Cornerstone.* 2003;5(3):5–15. DOI: 10.1016/s1098-3597(03)90031-7.
10. Nonka T.G., Lebedeva E.V., Repin A.N. Effects of agomelatine on heart rate variability in patients with coronary artery disease and depression. *Complex Issues of Cardiovascular Diseases*. 2021;10(1):40–49. (In Russ.). DOI: 10.17802/2306-1278-2021-10-1-40-49.
11. Nonka T.G., Lebedeva E.V., Repin A.N. Possibilities of detecting and correcting decreased heart rate variability in patients with coronary artery disease in combination with depressive disorders in a Cardiology Department. *Bulletin of Siberian Medicine*. 2021;20(2):65–70. (In Russ.). DOI: 10.20538/1682-0363-2021-2-65-70.
12. Ibatov A.D. Features of emotional status and autonomic regulation in patients with ischemic heart disease with sleep disorders. *S.S. Korsakov Journal of Neurology and Psychiatry.* 2021;121(1):21–25. (In Russ.). DOI: 10.17116/jnevro202112101121.
13. Salcedo B. The comorbidity of anxiety and depression. National Alliance on Mental Illness. 2018;325–333.
14. Poponina T. M., Gunderina K. I., Poponina Yu. S., Soldatenko M.V. The Effects of agomelatine on heart rate variability in patients with anxiety-depressive disorders who suffered from acute coronary syndrome. *Siberian Medical Journal.* 2018;33(3):36–45. (In Russ.). DOI: 10.29001/2073-8552-2018-33-3-36-45.

Authors' information

Nonka Tatiana G. – Cand. Sci. (Med.), Researcher, Outpatient Cardiology Department, Cardiology Research Institute, Tomsk NRMC, Tomsk, tatiananonka@gmail.com, https://orcid.org/0000-0002-7913-3732

Lebedeva Elena V. – Dr. Sci. (Med.), Researcher, Outpatient Cardiology Department, Cardiology Research Institute, Tomsk NRMC, Tomsk, evl26021971@gmail.com, https://orcid.org/0000-0001-6117-64

Repin Alexey N. – Dr. Sci. (Med.), Professor, Head of the Outpatient Cardiology Department, Cardiology Research Institute, Tomsk NRMC, Tomsk, ran_12@mail.ru, https://orcid.org/0000-0001-7123-0645

Schastnyy Evgeny D. – Dr. Sci. (Med.), Professor, Head of the Affective State Department, Mental Health Research Institute, Tomsk NRMC, Tomsk, evgeny.schastnyy@gmail.com, https://orcid.org/0000-0003-2148-297X

(✉) **Nonka Tatiana G.,** tatiananonka@gmail.com

Received14.06.2024;
approved after peer review 27.06.2024;
accepted 12.09.2024

УДК 615.284.036:616-092.4
https://doi.org/10.20538/1682-0363-2024-4-111-119

A new approach to assessing the efficacy of anthelmintic agents *in vitro*

Perina E.A., Buyko E.E., Kaminskiy I.P., Sobakin D.S., Ufandeev A.A., Kaidash O.A., Ivanov V.V., Udut E.V.

Siberian State Medical University
2, Moscow Trakt, Tomsk, Tomsk, 634050, Russian Federation

ABSTRACT

Aim. To develop a new method to determine the viability of *Opisthorchis felineus in vitro* using the MTS reagent and to evaluate its applicability for analyzing the efficacy of anthelmintic agents in the treatment of opisthorchiasis.

Materials and methods. Golden hamsters were used to create a model of *O. felineus* infection. The animals were infected with metacercariae obtained from fish of the Cyprinidae family. Three months after infection, adult parasites were extracted from the hepatobiliary system. Their viability was assessed using the motility scale and a new method based on the modified MTS test protocol. To account for differences between the size and number of adult parasite cells, the results were normalized with respect to protein content. To evaluate the feasibility of the new approach in the study of pharmacological activity against opisthorchiasis, the viability of adult parasites in the presence of praziquantel was tested.

Results. During incubation of adult flukes in a medium with the addition of the MTS reagent, colored water-soluble formazan was accumulated. Thermal inactivation of parasites significantly decreased the production of this compound. Since the studied adult parasites differed in size and number of cells, the obtained data on their viability were normalized to protein content. The results correlated with the data on parasite viability obtained by the traditional method using the motility scale. Evaluation of praziquantel efficacy at different concentrations using two independent methods (the MTS test and the motility scale) showed that the results of the MTS test were consistent with literature data and comparable with the results obtained using the motility scale.

Conclusion. A new method for *in vitro* evaluation of anti-opisthorchiasis activity of drugs was developed. It is based on the assessment of water-soluble formazan production by adult *O. felineus* flukes in the culture medium using the MTS reagent for screening anti-opisthorchiasis activity of new anthelmintic drugs.

Keywords: trematode infection, *O. felineus*, viability, MTS test, praziquantel, anthelmintic agents, motility

Conflict of interest. The authors declare the absence of obvious or potential conflicts of interest related to the publication of this article.

Source of financing. The study was carried out as part of the state assignment for the provision of public services No. 056-03-2024-063 of 24.01.2024, supplementary agreement No. 056-03-2024-063/3 of 29.08.2024 “Development of a new drug based on a natural complex of phenolic glycosides and arabinogalactanes for the treatment of trematodosis”.

Conformity with the principles of ethics. The study was approved by the Commission for the control over the maintenance and use of laboratory animals of the Center for Preclinical Research of the Central Research Laboratory, Siberian State Medical University (Conclusion No. 1 of 02.09.2024).

For citation: Perina E.A., Buyko E.E., Kaminskiy I.P., Sobakin D.S., Ufandeev A.A., Kaidash O.A., Ivanov V.V., Udut E.V. A new approach to assessing the efficacy of anthelmintic agents *in vitro*. *Bulletin of Siberian Medicine.* 2024;23(4):111–119. https://doi.org/10.20538/1682-0363-2024-4-111-119.

✉ *Perina Ekaterina A.,* catherineperina@gmail.com

Новый подход к оценке эффективности антигельминтных средств *in vitro*

Перина Е.А., Буйко Е.Е., Каминский И.П., Собакин Д.С., Уфандеев А.А., Кайдаш О.А., Иванов В.В., Удут Е.В.

Сибирский государственный медицинский университет (СибГМУ)
Россия, 634050, г. Томск, Московский тракт, 2

РЕЗЮМЕ

Цель. Разработать новый метод определения жизнеспособности описторхов in vitro с использованием MTS-реактива и оценить его применимость для анализа эффективности антигельминтных средств при лечении описторхоза.

Материалы и методы. Для создания модели инвазии *O. felineus* использовались золотистые сирийские хомяки. Животные инфицировались метацеркариями, полученными из рыб семейства карповых. Спустя 3 мес после заражения взрослые особи паразитов (мариты) извлеклись из гепатобилиарной системы. Жизнеспособность марит оценивалась с помощью шкалы подвижности и нового метода, основанного на модификации протокола MTS-теста. Для учета различий между размерами и количеством клеток марит результаты были нормализованы относительно содержания белка. Для оценки возможности применения нового подхода в изучении противоописторхозной фармакологической активности проверена жизнеспособность марит в присутствии празиквантела.

Результаты. При инкубации марит описторхов в среде с добавлением MTS-реактива происходит накопление окрашенного водорастворимого формазана. Термическое инактивирование паразитов значительно снижает продукцию этого соединения. Так как исследуемые мариты различались по размеру и количеству клеток, полученные данные об их жизнеспособности были нормированы на содержание белка. Результаты коррелируют с данными о жизнеспособности паразитов, полученными традиционным методом с использованием шкалы подвижности. Оценка эффективности празиквантела в разных концентрациях с помощью двух независимых методов (MTS-тест и шкала подвижности) показала, что результаты MTS-теста согласуются с литературными данными и сопоставимы с результатами, полученными с использованием шкалы подвижности.

Заключение. Разработан новый метод оценки противоописторхозной активности лекарственных препаратов *in vitro*, основанный на оценке продукции водорастворимого формазана маритами *O. felineus* в среде культивирования с использованием MTS-реагента для скрининга противоописторхозной активности новых антигельминтных препаратов.

Ключевые слова: трематодоз, *O. felineus*, жизнеспособность, MTS-тест, празиквантел, антигельминтные средства, двигательная активность

Конфликт интересов. Авторы декларируют отсутствие явных и потенциальных конфликтов интересов, связанных с публикацией настоящей статьи.

Источник финансирования. Исследование выполнено в рамках реализации государственного задания на оказание государственных услуг (выполнение работ) № 056-03-2024-063 от 24.01.2024, дополнительное соглашение № 056-03-2024-063/3 от 29.08.2024 «Разработка нового лекарственного средства на основе природного комплекса фенолгликозидов и арабиногалактанов для терапии трематодозов».

Соответствие принципам этики. Исследование одобрено комиссией по контролю содержания и использования лабораторных животных центра доклинических исследований центральной научно-исследовательской лаборатории СибГМУ (заключение № 1 от 02.09.2024).

Для цитирования: Перина Е.А., Буйко Е.Е., Каминский И.П., Собакин Д.С., Уфандеев А.А., Кайдаш О.А., Иванов В.В., Удут Е.В. Новый подход к оценке эффективности антигельминтных средств *in vitro*. *Бюллетень сибирской медицины.* 2024;23(4):111–119. https://doi.org/10.20538/1682-0363-2024-4-111-119.

INTRODUCTION

The liver fluke *Opisthorchis felineus* (*O. felineus*) is a member of the triad of epidemiologically important liver fluke species of the Opisthorchiidae family and is the main causative agent of opisthorchiasis in a vast territory, including Russia, Kazakhstan, and a number of European countries [1]. A recent study conducted by O.S. Fedorova et al. (2023) showed that the spread of *O. felineus* infection in the population is closely associated with the development of cholangiocarcinoma [2]. In addition, opisthorchiasis can provoke the development of liver abscesses and pancreatitis [1] Thus, trematode infections are a group of dangerous infectious diseases that pose a significant public health threat [3].

The main approach recommended by WHO to reduce the incidence of opisthorchiasis is to increase the availability of safe and effective drug therapy. To date, praziquantel (PZQ) is the only recommended therapy for opisthorchiasis. The development of new drugs for the treatment of trematode infections is a high priority because of the possibility of liver fluke developing resistance to PZQ [4]. Indeed, *in vitro* studies have confirmed that adult helminth strains exposed continuously to PZQ show increased resistance to the drug [5]. In addition, PZQ has no preventive effect and is ineffective against parasite larvae, which represents a serious gap in the development of mass chemoprophylaxis strategies in regions with high morbidity [6].

Thus, given the limitations of existing preventive and therapeutic approaches, it is necessary to create new therapeutic agents capable of effectively inhibiting the activity of the parasite at all stages of its life cycle.

The assessment of trematode viability plays a key role in the development of new methods for combating these parasites. Currently, the method of assessing parasite motility by visual inspection during microscopy is widely used [7, 8], while scanning electron microscopy to study ultrastructural integrity is less common [8]. The former is a semi-quantitative method requiring a high level of specialist training; the latter requires more effort and involves significant costs.

Currently, a wide range of reagents are used in *in vitro* pharmacological studies to analyze the viability of cultured cells. Among the most common techniques are methods of intravital or postmortem staining followed by spectrophotometry or fluorometry and luminometric analysis [9]. Some articles mention that viability of *Schistosoma mansoni* sporocysts may be assessed by staining with the fluorescent dye propidium iodide [10] or trypan blue [11]. Using 3-(4,5-dimethylthiazol-2-yl)-2,5-diphenyltetrazolium bromide (MTT), widely used in cell culture, is of particular interest as a method to assess parasite viability [7, 12].

However, all the references found refer exclusively to the study of the viability of schistosomiasis pathogens (*Schistosoma mansoni*). There are no data on the application of a protocol using the MTT reagent for opisthorchiasis in the available scientific literature. It is important to note that formazan, formed as a result of MTT molecule reduction by mitochondrial enzymes of living cells, is insoluble in water and forms purple crystals in cells [9]. This means that organic solvents, such as dimethyl sulfoxide (DMSO) or isopropanol, are required to quantify the formed formazan before optical density determination, which complicates the application of this method to multicellular organisms, including Opisthorchis maritas.

The MTT test is a standard method for assessing cell viability and determining cytotoxicity of compounds. When performing it, it is necessary to take into account the duration of incubation and cell seeding density to ensure the accuracy and reproducibility of the results [9]. However, a significant limitation of the MTT test for determining the viability of multicellular organisms is the inability to correctly interpret differences in the size and number of cells, which can lead to distortion of the final data and misinterpretation of the results.

The MTS test based on the use of a modified MTT molecule is a simpler and more reliable assay. This test allows living cells to produce water-soluble stained formazan directly in the culture medium, which simplifies the analysis [9].

The development of a simple and affordable protocol to assess the viability of liver fluke *O. felineus* maritas will facilitate screening of potential therapeutic agents with activity against opisthorchiasis.

The aim of the study was to develop a new method to determine the viability of opisthorchiasis *in vitro* using the MTS reagent and to evaluate its applicability for analyzing the efficacy of anthelmintic agents in the treatment of opisthorchiasis.

MATERIALS AND METHODS

Golden hamsters (*Mesocricetus auratus*) were purchased from the vivarium of the Research Institute of Cytology and Genetics of the Siberian Branch of the Russian Academy of Sciences (Novosibirsk, Russia). The use of animals in this study was approved by

the Committee for the Care and Use of Laboratory Animals of the Center for Preclinical Research of the Central Research Laboratory of Siberian State Medical University (Conclusion No. 1 of 02.09.2024).

Cyprinidae (carp) fish caught in the rivers of the Ob basin in the Tomsk region were used as a source of primary biological material containing Opisthorchis metacercariae. In order to isolate Opisthorchis metacercariae from infected fish, we subjected them to digestion in artificial gastric juice [13, 14].

Three months after infection, the animals were euthanized, and *O. felineus* maritas were extracted from the hepatobiliary tract. After washing in buffer (200 U / ml penicillin – streptomycin in 1×PBS), the maritas were placed in wells of culture plate filled with the culture medium (RPMI 1640, 100 U / ml penicillin – streptomycin, 10 g / l glucose, 2 g / l sodium bicarbonate) at 37 °C in an atmosphere of 5% CO_2 [15]. The viability of Opisthorchis maritas was assessed immediately after the extraction from the bile ducts of infected hamsters and after 24 h of incubation in complete culture medium.

The new proposed method for assessing the viability of adult forms of *O. felineus* includes the use of the MTS reagent and, at the first stages, coincides with previously proposed protocols that include the use of the MTT test [7, 12]. Maritas were placed in eppendorf tubes (1.5 ml) containing 200 µl of phosphate-buffered saline (PBS) and 40 µl of the MTS reagent (Promega, USA) and incubated at 37 °C for 2 hours. The incubation medium was collected and centrifuged at 5,000 rpm for 10 minutes to precipitate eggs of the liver fluke and excretory-secretory products. The supernatant was put into wells of a 96-well plate, and then the optical density of the medium was measured at 492 nm using the Tecan 200 Infinite Pro multifunctional microplate reader (Tecan, Austria). As a negative control, maritas were subjected to heat treatment at 65 °C for 30 min before the test, which is known to cause their death [14].

To compensate for differences in the size and cellularity of the maritas, the optical density values were normalized to the amount of protein. The protein content in adult liver flukes was determined by the bicinchoninic acid assay method using the BCA Protein Assay Kit (Sigma Aldrich, USA) [16]. For this purpose, maritas were homogenized in lysis buffer (0.1% SDS, 0.1M NaOH) followed by ultrasound treatment (Bandelin Sonoplus 2070, Germany). After centrifugation (3,000g for 10 minutes), the protein content was determined in the collected supernatant.

The final viability value was determined as the difference between the optical density of the medium in the experimental wells after the MTS test and the average optical density of the heat-treated samples. The obtained value was normalized to the protein content in each liver fluke.

To evaluate the prospects of using a new approach to study the specific pharmacological activity of anti-opisthorchiasis agents, isolated liver flukes were cultured in the complete medium for 24 h in the presence of PZQ at final concentrations of 0.1, 0.5, 1, and 10 µg / ml. After incubation with PZQ, the viability of Opisthorchis maritas was assessed by two independent methods: the standard semi-quantitative method for assessing parasite motility and a newly developed quantitative method based on the production of water-soluble formazan by live marita cells in the incubation medium using the MTS reagent, taking into account the protein assay content.

Motility of *O. felineus* maritas was assessed visually using a generally accepted motility scale [14, 17]. Qualitative characteristics of motility were described using absolute frequency and the percentage value. Ten maritas were used for each concentration of PZQ. The motility of viable liver flukes was graded on a scale from 0 to 3 ([+++] very active (movement similar to the control flukes); [++] active (reduced motility compared to the control; however, body movements were preserved), [+] reduced viability (only oral sucker movements), and [–] immobility) [17]. Mean parasite motility was calculated for each PZQ concentration and expressed as a percentage relative to the control values.

The experimental data were processed using the GraphPad Prism 8 software (GraphPad Software, USA). All results were presented as the mean and the standard deviation ($M \pm SD$). The nonparametric Kruskal – Wallis and Shapiro – Wilk tests with the Benjamini – Hochberg procedure were used to test the significance of differences between the studied groups. Differences were considered statistically significant at $p < 0.05$ and $p < 0.001$. Normalized non-linear regression analysis was used to calculate the PZQ concentration at which fluke viability decreased by 50% (IC50) after 24 h of incubation.

RESULTS

The results of the experiments showed that incubation of freshly extracted Opisthorchis maritas from the liver of infected hamsters with the addition of the MTS reagent in the culture medium produced

colored water-soluble formazan, and the average value of optical density in the wells was 1.018 ± 0.109 (n = 10) (Fig. 1). It is known that elevated temperature (65 °C for 30 minutes) leads to death of maritas [14]. Indeed, after heat inactivation of maritas, no significant formazan production was observed in the incubation medium under these conditions (Fig. 1). Therefore, in the future, when calculating the viability of maritas using the MTS reagent, this well in the plate was taken as a control sample (blank), to which all the measurements were compared.

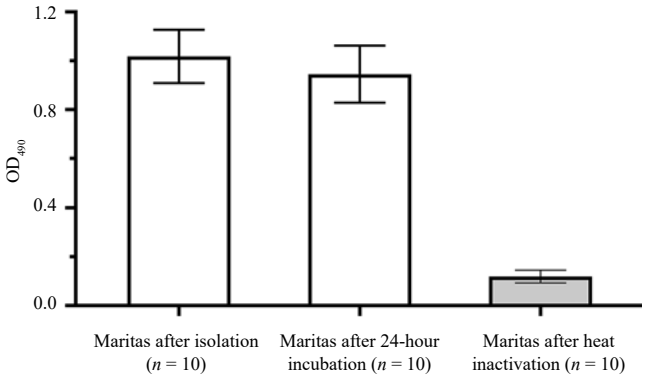

Fig. 1. Production of water-soluble formazan in the marita incubation medium immediately after isolation from the liver bile ducts of infected hamsters, after 24 hours of incubation in a complete culture medium, and after heat inactivation (65 °C, 30 min)

After 24-hour incubation of maritas in the complete culture medium in a CO_2 incubator at 37 °C, the amount of formazan in the medium determined by the MTS test did not differ from the values obtained for freshly incubated mature forms of *O. felineus* (Fig. 1). Firstly, these results confirm the preservation of the viability of Opisthorchis maritas under the indicated culture conditions. Secondly, they indicate that the accumulation of water-soluble formazan in the incubation medium during the MTS test does reflect the viability of maritas.

The process of tetrazolium reduction occurs during oxidative metabolism in the cell mitochondria [9], and the liver flukes isolated from the liver of hamsters differ in size and cellularity. Therefore, the normalization of the formazan amount to the protein content in a marita is a more objective indicator for assessing the viability of flukes.

Indeed, the amount of formazan product formed, expressed in units of optical density after the MTS test, positively correlates with the protein content in *O. felineus* maritas (Fig. 2). Therefore, in further experiments, the obtained data on parasite viability were normalized to the amount of protein.

PZQ is currently one of the most common antiparasitic drugs used to treat diseases, such as opisthorchiasis, clonorchiasis, schistosomiasis, and other trematode infections. In some endemic regions, it is actively used as part of preventive chemotherapy programs against parasitic infections [18, 19]. We studied the effect of PZQ at concentrations of 0.1, 0.5, 1, and 10 μg / ml on the viability of *O. felineus* maritas in the incubation medium using an *in vitro* model. Incubation of maritas for 24 hours with increasing PZQ concentrations in the culture medium (0.1, 0.5, 1, and 10 μg / ml) leads to a dose-dependent decrease in fluke motility up to complete immobilization, as well as a partial change in their color (Table).

Table

Motility of *O. felineus* maritas 24 hours after adding different concentrations of praziquantel (PZQ) to the medium *in vitro*

PZQ concentration, μg / ml	Number of *O. felineus* maritas, % according to the motility scale			
	0	1	2	3
0	0 0	0 0	0 0	10 100
0,1	0 0	9 90	1 10	0 0
0,5	6 60	4 40	0 0	0 0
1	8 80	2 20	0 0	0 0
10	10 100	0 0	0 0	0 0

Note. Motility scale of *O. felineus* maritas: 3 – normal motility; 2 – reduced motility; 1 – very weak motility visible only at microscope magnification of x 20; 0 – absence of motility or death, which is registered when no movement is observed for 2 minutes only at microscope magnification of x 20.

Application of PZQ at a concentration of 0.1 μg / ml in the parasite culture medium leads to paralysis of *O. felineus* muscle tissue, minimizing their motility but preserving their viability during 24 hours of exposure. At a PZQ concentration of 0.5 μg / ml, 40% of *O. felineus* maritas were characterized by very weak motility (1 point on the motility scale), while 60% had no motility. When the PZQ concentration in the incubation medium was increased to 1 μg / ml, 80% of *O. felineus* maritas showed no motility (0 points on the motility scale). At a PZQ concentration of 10 μg / ml, no O. felineus maritas showed motility (Table).

At the same time, a dose-dependent decrease in the production of water-soluble formazan in the incubation medium was observed under the influence of the drug. The percentage of viability of cultured maritas was 63.7, 38.9, 26.5, and 6.4% at PZQ concentrations of 0.1, 0.5, 1, and 10 μg / ml, respectively (the values of formazan production in the incubation medium without the drug were taken as 100%) (Fig. 3). The results correlate with the data obtained by an independent method for assessing the viability of maritas using the motility scale (Table).

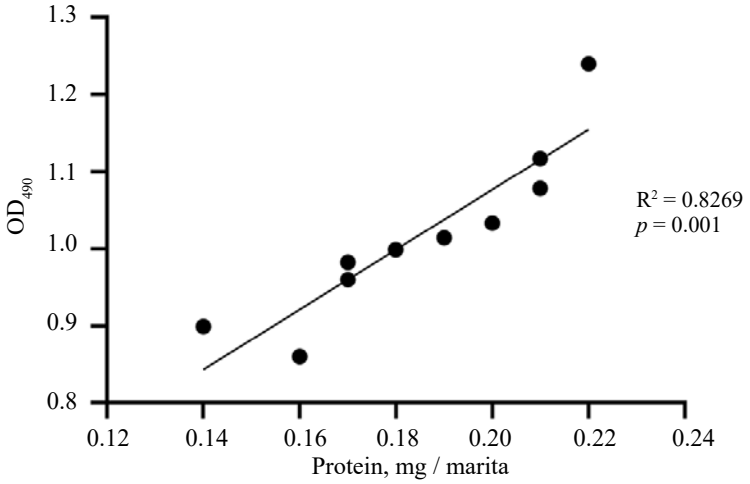

Fig. 2. The relationship between the accumulation of formazan in the marita incubation medium during the MTS test and the protein content in them, $n = 10$

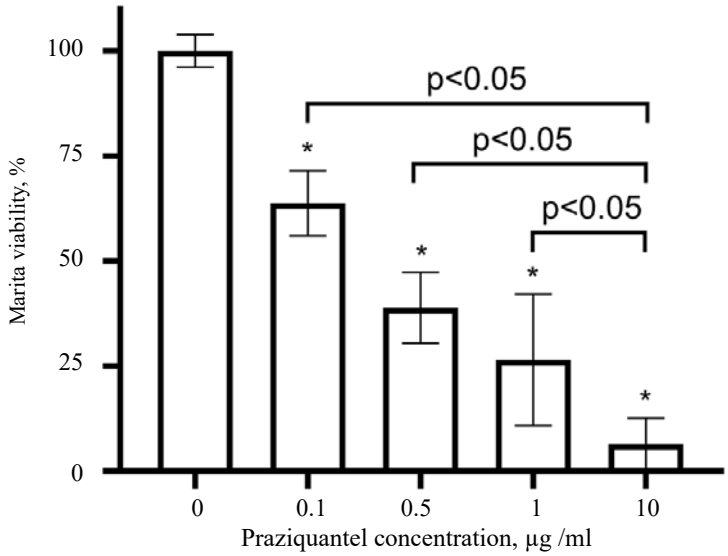

Fig. 3. The effect of different concentrations of praziquantel (μg / ml) on the viability of Opisthorchis maritas during their culture for 24 hours, $n = 10$. * $p < 0.05$ compared to the controls

The IC50 value (concentration causing 50% cell death of marita cells after 24 h of incubation with the drug) was used as an integral index characterizing the anti-opisthorchiasis activity of PZQ.

The nonlinear regression analysis showed that the IC50 value for *O. felineus* maritas was 0.24 μg / ml after 24 hours of incubation with PZQ. Thus, the proposed MTS test approach, which takes into account the protein content in the samples, represents an objective quantitative method for analyzing the viability of *O. felineus* maritas and can be used to evaluate the efficacy of new anthelmintic agents *in vitro*.

DISCUSSION

To date, PZQ remains the only drug of choice for the treatment of opisthorchiasis. Given the potential risk of resistance to PZQ in liver flukes, the development of new drugs for the treatment of trematode infections remains an urgent task and has a high priority [4].

When evaluating the anthelmintic properties of new compounds, it is often necessary to determine the viability of the parasite *in vitro* when it is incubated with different concentrations of the test substance. Currently, the parasite motility scale from 0 to 3 is used to determine the viability of *O. felineus* [14]. This method is not standardized, requires much effort, and depends on the subjective assessment of the researcher.

A more objective approach to assessing trematode viability was first demonstrated in experiments with *Schistosoma mansoni* using the MTT test [19]. This method is most commonly used to estimate the number of viable cells in culture and is based on the ability of mitochondrial and cytoplasmic dehydrogenases of live and metabolically active cells to reduce tetrazolium derivatives, MTT reagent, into water-insoluble formazan, which requires DMSO dye extraction to determine its amount [20]. However, this study does not take into account the differences in cellularity of mature forms of *S. mansoni*, which is an important limitation in interpreting the results.

Recently, a second-generation tetrazolium dye, MTS, has appeared as part of laboratory methods for assessing cell viability [21], which, with the participation of phenazine methasulphate, is reduced in the culture medium to stained water-soluble formazan, which makes it possible to significantly accelerate the analysis and obtain more objective results.

In this study, an attempt was made to develop a screening method to evaluate the *in vitro* anti-opisthorchiasis activity of drugs using the MTS test.

When analyzing the results of the experiments, it was found that during incubation of Opisthorchis maritas in the medium with the addition of the MTS reagent, colored water-soluble formazan accumulates. Heat inactivation of the parasites results in several times lower production of the colored compound. This confirms that the MTS test, traditionally used to assess cell viability in *in vitro* cell culture [22], indeed allows to assess the mitochondrial metabolic activity of cells of multicellular organisms, such as maritas, and thus determine their viability.

Since the investigated maritas differed in size and, consequently, in the number of cells, the data on their viability were normalized to their protein content. Formazan production by the maritas, expressed through their protein content, was consistent with the parasite viability results obtained according to the traditional method using the motility scale [13].

The effect of different PZQ concentrations, the drug of choice for the treatment of opisthorchiasis, on the viability of maritas *in vitro* was also assessed by two independent methods (the MTS test and the use of the motility scale). The data obtained on the viability of maritas using the MTS test were consistent with those obtained using the motility scale. For PZQ, the IC50, defined as the concentration required to kill 50% of the marita cells after 24 hours of incubation with the drug, was calculated to be 0.24 μg / ml. The results obtained are consistent with literature data that the IC50 for PZQ determined using other methods is 0.16 μg / ml for *O. viverrini* 23] and 0.14 μg / ml of *O. felineus* [14].

Thus, we have developed a quantitative method to examine the anti-opisthorchiasis activity of drugs *in vitro*, based on the evaluation of water-soluble formazan production by *O. felineus* maritas in the culture medium using the MTS test, taking into account the protein content in the sample.

CONCLUSION

A new method for *in vitro* evaluation of anti-opisthorchiasis activity of drugs has been developed, based on the assessment of water-soluble formazan production by *O. felineus* maritas in the culture medium using the MTS reagent. The results obtained coincide with the parasite viability indices determined according to the traditional methodology using the motility scale. The normalization of the optical density of the formed formazan to the amount of protein in the parasite is a more objective indicator for expressing the viability of *O. felineus* maritas.

The results of evaluating the efficacy of the drug of choice for the treatment of opisthorchiasis – PZQ – using the MTS test *in vitro* correlate with the published research data, which allows to consider the developed approach as a simple and affordable method for the study of anti-opisthorchiasis activity of new anthelmintic agents.

REFERENCES

1. Pakharukova M.Y., Mordvinov V.A. The liver fluke *Opisthorchis felineus*: biology, epidemiology and carcinogenic

potential. *Transactions of the Royal Society of Tropical Medicine and Hygiene.* 2016;110(1):28–36. DOI: 10.1093/trstmh/trv085.

2. Fedorova O.S., Kovshirina A.E., Kovshirina Y.V., Hattendorf J., Onishchenko S.V., Katanakhova L.L. et al. *Opisthorchis felineus* infection is a risk factor for cholangiocarcinoma in Western Siberia: A hospital-based case-control study. *Clinical Infectious Diseases.* 2023;7(3):e1392–e1398. DOI: 10.1093/cid/ciac497.
3. Khalil R.G., Ibrahim A.M., Bakery H.H. Juglone: "A novel immunomodulatory, antifibrotic, and schistosomicidal agent to ameliorate liver damage in murine schistosomiasis mansoni". *International Immunopharmacology.* 2022;113:109415. DOI: 10.1016/j.intimp.2022.109415.
4. Pakharukova M.Y., Samsonov V.A., Serbina E.A., Mordvinov, V.A. A study of tribendimidine effects *in vitro* and *in vivo* on the liver fluke *Opisthorchis felineus*. *Parasites Vectors.* 2019;12(23):1–6. DOI: 10.1186/s13071-019-3288-z.
5. Harder A. Activation of transient receptor potential channel Sm. (*Schistosoma mansoni*) TRPM PZQ by PZQ, enhanced Ca++ influx, spastic paralysis, and tegumental disrupture-the deadly cascade in parasitic schistosomes, other trematodes, and cestodes. *Parasitology Research.* 2020;119:2371–2382. DOI: 10.1007/s00436-020-06763-8.
6. Spangenberg T. Alternatives to praziquantel for the prevention and control of schistosomiasis. *ACS Infectious Diseases.* 2020;7(5):939–942. DOI: 10.1021/acsinfecdis.0c00542.
7. Detoni M.B., Bortoleti B.T.D.S., Tomiotto-Pellissier F., Concato V.M., Gonçalves M.D., Silva T.F. et al. Biogenic silver nanoparticle exhibits schistosomicidal activity *in vitro* and reduces the parasitic burden in experimental *Schistosomiasis mansoni*. *Microbes and Infection*.2023;25(7):105145. DOI: 10.1016/j.micinf.2023.105145.
8. Rehman L., Ullah R., Rehman A., Khan M.A.H., Beg M.A., Wasim S. et al. Clinostomum complanatum: Anthelmintic potential of curcumin on the infective progenetic metacercarial stage. *Experimental Parasitology.* 2023;249:108514. DOI: 10.1016/j.exppara.2023.108514.
9. Aslantürk Ö.S. *In vitro* cytotoxicity and cell viability assays: principles, advantages, and disadvantages. *Genotoxicity-A Predictable Risk to Our Actual World.* 2018;64–80. DOI: 10.5772/intechopen.71923.
10. Mourão M.M., Dinguirard N., Franco G.R., Yoshino T.P. Role of the endogenous antioxidant system in the protection of *Schistosoma mansoni* primary sporocysts against exogenous oxidative stress. *PLoS Neglected Tropical Diseases*. 2009;3(11):e550. DOI: 10.1371/journal.pntd.0000550.
11. Moné Y., Mitta G., Duval D., Gourbal B.E. E Effect of amphotericin B on the infection success of *Schistosoma mansoni* in *Biomphalaria glabrata. Experimental Parasitology*. 2019;125(2):70–75. DOI: 10.1016/j.exppara.2009.12.024.
12. De Paula R.G., de Magalhães Ornelas A.M., Morais E.R., de Souza Gomes M., de Paula Aguiar D. et al. Proteasome stress responses in *Schistosoma mansoni. Parasitology Research.* 2015;114:1747–1760. DOI: 10.1007/s00436-015-4360-z.
13. Mironov A.N., Bunatyan N.D., Vasiliev A.N. Guidelines for conducting preclinical studies of medicines. M.: Grif and K., 2012: 944 (in Russ.).
14. Pakharukova M.Y., Shilov A.G., Pirozhkova D.S., Katokhin A.V., Mordvinov V.A. The first comprehensive study of praziquantel effects *in vivo* and *in vitro* on European liver fluke *Opisthorchis felineus (Trematoda*). *International Journal of Antimicrobial Agents.* 2015;46(1):94–100. DOI: 10.1016/j.ijantimicag.2015.02.012.
15. Wong Y., Pearson M.S., Fedorova O., Ivanov V., Khmelevskaya E., Tedla B. et al. Secreted and surface proteome and transcriptome of *Opisthorchis felineus. Frontiers in Parasitology.* 2023;1195457. DOI: 10.3389/fpara.2023.1195457.
16. Olson B.J., Markwell J. Assays for determination of protein concentration. *Current Protocols in Pharmacology*. 2007;38(1):A–3A. DOI: 10.1002/0471140864.ps0304s48.
17. Marcos L., Maco V., Terashima A. Triclabendazole for the treatment of human fascioliasis and the threat of treatment failures. *Expert Review of Anti-Infective Therapy.* 2021;19(7):817–823.
18. Olliaro P., Delgado-Romero P., Keiser J. The little we know about the pharmacokinetics and pharmacodynamics of praziquantel (racemate and R-enantiomer). *Journal of Antimicrobial Chemotherapy.* 2014;69(4):863–870. DOI: 10.1093/jac/dkt491.
19. Oliveira M.F., d'Avila J.C., Tempone A.J., Soares J.B., Rumjanek F.D., Ferreira-Pereira A. et al. Inhibition of heme aggregation by chloroquine reduces *Schistosoma mansoni* infection. *Journal of Infectious Diseases*. 2004;190(4):843–852. DOI: 10.1086/422759.
20. Ghasemi M., Turnbull T., Sebastian S., Kempson I. The MTT assay: utility, limitations, pitfalls, and interpretation in bulk and single-cell analysis. *International Journal of Molecular Sciences*. 2021;22(23):12827. DOI: 10.3390/ijms222312827.
21. Stockert J.C., Horobin R.W., Colombo L.L., Blázquez-Castro A. Tetrazolium salts and formazan products in Cell Biology: Viability assessment, fluorescence imaging, and labeling perspectives. *Acta Histochemica.* 2018;120(3):159–167. DOI: 10.1016/j.acthis.2018.02.005.
22. Stone V., Johnston H., Schins R.P. Development of *in vitro* systems for nanotoxicology: methodological considerations. *Critical Reviews in Toxicology.* 2009;39(7):613–626. DOI: 10.1080/10408440903120975.
23. Keiser J., Manneck T., Vargas M. Interactions of mefloquine with praziquantel in the Schistosoma mansoni mouse model and *in vitro. Journal of Antimicrobial Chemotherapy.* 2011;66(8):1791–1797. DOI: 10.1093/jac/dkr178.

Authors' contribution

Perina E.A. – literature analysis, culture of mature forms of liver fluke, determination of viability in vitro. Buyko E.E. – literature analysis, acquisition and interpretation of the experimental data, drafting of the manuscript. Kaminskiy I.P. – reproduction of opisthorchiasis invasion. Sobakin D.S. – acquisition of the experimental data. Ufandeev A.A., Kaidash O.A. – literature analysis, drafting of the manuscript. Ivanov V.V. – conception and design, coordination of the research, drafting of the manuscript, final approval of the manuscript for publication. Udut E.V. – coordination of the research, final approval of the manuscript for publication.

Authors' information

Perina Ekaterina A. – Junior Researcher, Center for Preclinical Research, Central Research Laboratory, Siberian State Medical University, Tomsk, catherineperina@gmail.com, http://orcid.org/0000-0002-4273-8228

Buyko Evgeny E. – Junior Researcher, Center for Preclinical Research, Central Research Laboratory, Siberian State Medical University, Tomsk, buykoevgen@yandex.ru, http://orcid.org/0000-0002-6714-1938

Kaminskiy Ilya P. – Cand. Sci. (Pharmaceut.), Associate Professor, Pharmaceutical Analysis Divisions, Siberian State Medical University, Tomsk, kaminskiy.ip@ssmu.ru, http://orcid.org/0000-0003-4597-1743

Sobakin Danil S. – Laboratory Assistant, Laboratory of Translational Medicine, Siberian State Medical University, Tomsk, sobakin.ds@ssmu.ru, http://orcid.org/0009-0003-1920-2622

Ufandeev Alexander A. – Junior Researcher, Center for Preclinical Research, Central Research Laboratory, Siberian State Medical University, Tomsk, ufandeev@gmail.com, http://orcid.org/0000-0002-3837-1179

Kaidash Olga A. – Cand. Sci. (Biology), Senior Researcher, Center for Preclinical Research, Central Research Laboratory, Siberian State Medical University, Tomsk, kaidash_2011@mail.ru, http://orcid.org/0000-0001-8761-7537

Ivanov Vladimir V. – Cand. Sci. (Biology), Associate Professor, Head of the Center for Preclinical Research, Central Research Laboratory, Siberian State Medical University, Tomsk, ivanovvv1953@gmail.com, http://orcid.org/0000-0003-3326-729X

Udut Elena V. – Dr. Sci. (Med.), Professor of the Russian Academy of Sciences, Head of the Central Research Laboratory, Siberian State Medical University, Tomsk, udut.ev@ssmu.ru, http://orcid.org/0000-0002-61-4782.

(✉) **Perina Ekaterina A.,** catherineperina@gmail.com

Received 24.09.2024;
approved after peer review 03.10.2024;
accepted 04.10.2024

УДК 614.46:616.98:578.834.1]-036.21-02:613
https://doi.org/10.20538/1682-0363-2024-4-120-128

Effects of anti-epidemic (quarantine) measures on people during the COVID-19 pandemic: applying social network analysis to identify the key topics

Pleshkova E.K.[1, 2], Rezanova Z.I.[1]

[1] *National Research Tomsk State University" (NR TSU)*
36, Lenina Av., Tomsk, 634050, Russian Federation

[2] *Siberian State Medical University (SSMU)*
2, Moscow Trakt, Tomsk, 634050, Russian Federation

ABSTRACT

The aim of this study was to examine the public reaction to the implementation of quarantine measures through a personality-oriented discourse.

Materials and methods. Text data were collected from a microblogging platform, resulting in a dataset of 86,750 texts related to the topics of "pandemic" and "quarantine measures". The lexical conceptualization of the pandemic and quarantine measures represented in the texts was analyzed through the lens of a personality-oriented discourse. Text lemmatization was conducted using the "snowball" library. A data feature matrix was then created based on the lemmatized tokens, which included 53 tokens with a frequency of use exceeding 1,300 times. The Social Network Analysis (SNA) method was used to create a keyword co-occurrence network consisting of undirected graphs. This analysis was performed using the free software R version 4.4.1, with the assistance of the Quanteda library, built-in "base" packages, and the gsub function.

Results. The resulting network consisted of 53 key lexemes, which actors used to respond to quarantine measures in the personality-oriented discourse. The central node of the network was "coronavirus", which was used 79,838 times between March 1 and April 30, 2020. The nearest nodes were "test" (used 4,663 times) and "Russia" (used 5,848 times). This network had high centrality, indicating that despite strict restrictive measures, the focus of the general public was on the pandemic itself and its impact on society rather than on the restrictions imposed.

Conclusion. The implementation of these anti-epidemic measures has created a unique sociolinguistic world view, reflecting the interaction between society and the outside world in a time of uncertainty and health risks, affecting the analysis of information and the behavioral strategies chosen by society.

Keywords: coronavirus, personality-oriented discourse, natural language processing, social network analysis, sociolinguistic world view

Conflict of interest. The authors declare the absence of obvious or potential conflicts of interest related to the publication of this article.

Source of financing. The research was funded by the Russian Science Foundation grant (Project No. 23-28-01001).

For citation: Pleshkova E.K., Rezanova Z.I. Effects of anti-epidemic (quarantine) measures on people during the Covid-19 pandemic: applying social network analysis to identify the key topics. *Bulletin of Siberian Medicine.* 2024;23(4):120–128. https://doi.org/10.20538/1682-0363-2024-4-120-128.

✉ *Pleshkova Ekaterina K.,* pleshkova.ek@ssmu.ru

Влияние противоэпидемических (карантинных) мероприятий в условиях пандемии COVID-19 на население: выявление ключевых тематик с помощью социально-сетевого анализа

Плешкова Е.К.[1, 2], Резанова З.И.[1]

[1] *Национальный исследовательский Томский государственный университет (НИ ТГУ)*
634050, г. Томск, пр. Ленина, 36

[2] *Сибирский государственный медицинский университет (СибГМУ)*
634050, г. Томск, Московский тракт, 2

РЕЗЮМЕ

Цель исследования – изучение реакции общества на введение карантинных мер по данным личностно ориентированного дискурса.

Материалы и методы. Произведен сбор текстовых данных на платформе микроблогов. Датасет состоял из 86 750 текстов, объединенных тематикой «пандемия», «карантинные меры». Проведен анализ лексической концептуализации пандемии и карантинных мер в личностно ориентированном дискурсе, репрезентированной в собранных текстах. Выполнена лемматизация на основе библиотеки Snowball, построена матрица datafeature matrix на основе лемматизированных токенов, включавшая 53 токена, частотность употребления которых превышала 1 300 раз. Методом социального-сетевого анализа построена сеть соприсутствия ключевых лексем, состоящая из неориентированных графов. Анализ был выполнен в свободном программном обеспечении R версии 4.4.1 с использованием библиотеки Quanteda, встроенных пакетов base и функции gsub.

Результаты. Получена сеть из 53 ключевых лексем, с помощью которых акторы личностно ориентированного дискурса реагировали на карантинные мероприятия. Ядро сети – узел «коронавирус» употреблено 79 838 раз в период с 1 марта по 30 апреля 2020 г. Ближайшие узлы: «тест» (употреблено 4 663 раза) и «Россия» (употреблено 5 848 раз). Сеть имеет высокую центральность, центральный узел сети «коронавирус» свидетельствует о том, что, несмотря на введение жестких ограничительных мер, население фокусировалось не на введенных ограничениях, а непосредственно на пандемии и ее влиянии на жизнедеятельность общества.

Заключение. Введение противоэпидемических мероприятий сформировало уникальную социолингвистическую картину мира, отражающую взаимодействие общества с внешним миром в условиях неопределенности и риска здоровью, влияющую на анализ информации и выбор поведенческой стратегии обществом.

Ключевые слова: коронавирус, личностно ориентированный дискурс, обработка естественного языка, социально-сетевой анализ, социолингвистическая картина мира

Конфликт интересов. Авторы декларируют отсутствие явных и потенциальных конфликтов интересов, связанных с публикацией настоящей статьи.

Источник финансирования. Исследование выполнено за счет гранта Российского научного фонда (проект № 23-28-01001).

Для цитирования: Плешкова Е.К., Резанова З.И. Влияние противоэпидемических (карантинных) мероприятий в условиях пандемии COVID-19 на население: выявление ключевых тематик с помощью социально-сетевого анализа. *Бюллетень сибирской медицины.* 2024;23(4):120–128. https://doi.org/10.20538/1682-0363-2024-4-120-128.

INTRODUCTION

New challenges have emerged with the advent of a new era. The once-familiar and orderly world, which many believed to be predictable, has been replaced by a volatile and unpredictable VUCA world, which has now evolved into a BANI world: brittle, anxious, nonlinear, and incomprehensible [1]. Each letter of the acronym BANI (brittle, anxious, nonlinear, incomprehensible) defines a new world. The term

was coined in 2020, when society faced a pandemic that brought about radical changes and triggered transformation that affected all aspects of society. The study of the COVID-19 pandemic is not only of interest for researchers in the fields of medicine, biomedicine, and economics, but also for linguists and philologists, as it is crucial to understand how the pandemic has transformed not only society, but also language as a means of expressing collective consciousness [2].

In this article, we will examine how society responded to the implementation of quarantine measures during the COVID-19 pandemic, based on personality-oriented discourse, as this discourse serves to illustrate and shape public opinion [3]. In recent years, the effectiveness of such studies has been enhanced by the use of natural language processing (NLP), computational linguistics, artificial intelligence, and social network analysis (SNA) on large corpora of texts, which allows for structuring information contained in texts. However, the focus of research has primarily been on social networks, with the social media platform X (formerly known as Twitter, which is blocked in the Russian Federation) being the leading platform until recently. By combining mathematical analysis and sociolinguistic analysis of texts, researchers are able to analyze various phenomena, such as the spread of diseases, the growth of protest movements in society, social inequality, the influence of social networks on youth communities, and much more [4]. For instance, Jinghao Wang et al. noted the use of social networks as a means of identifying how the effects of negative temperature dynamics, local air pollution, and natural disasters on individuals are interpreted [5].

Studying the pandemic through the lens of its manifestations in the language, it is important to consider specific stages of its development, particularly the implementation of quarantine measures and a public response to them, which was actively expressed. Researchers have interpreted the quarantine measures introduced in March 2020 in the Russian Federation as the largest psychological or psychosocial experiment, the study of which will continue for a long time in the social sciences using various methods [6].

MATERIALS AND METHODS

Social Network Analysis (SNA) is a method used to study various structures and relationships by applying graph theory to visualize and analyze connections between organizations or individuals in a network [7]. The studied network can be represented by any data, since the method allows for analyzing relationships between actors in a community, events related to a specific topic [8], relationships between scientific publications within a particular organization [9], and connections between lexical units in different types of discourse [10]. Essentially, SNA maps the relationships between different actors, providing a visual representation of how they interact with each other. This allows researchers to identify patterns and assess the strength of connections between network actors.

The analysis was conducted using the free software R version 4.4.1 and the Quanteda library [11], as well as the built-in base package and the gsub function for replacing string sections. In this study, we analyzed the lexical conceptualization of the pandemic and quarantine measures in personality-oriented discourse. At the first stage, the text data was collected from the social media platform X (formerly known as Twitter, which is blocked in the Russian Federation) to form the dataset.

The dataset consisted of 86,750 tweets (short texts) related to the topics of "pandemic" and "quarantine measures", posted between March 1 and April 30, 2020. During the preparation stage, hyperlinks, hashtags, and user tags were removed, as well as punctuation marks and numbers. A corpus of texts was put together based on the dataset, and then it was tokenized. Stop words were removed, and lemmatization was performed based on the Snowball library. A data feature matrix was then created based on the lemmatized tokens. The matrix only included tokens that were mentioned more than 1,300 times. So, the matrix comprised 53 tokens. A feature co-occurrence matrix was then built, including the most frequently occurring words in texts related to the pandemic and quarantine measures. Using this matrix, a feature co-occurrence matrix was created using the textplot_network function. Finally, social network analysis methods were used to study how information about the introduction of quarantine measures was distributed and functioned in personality-oriented discourse.

RESULTS

The analysis resulted in a network of 53 key lexemes that were used at least 1,300 times (Fig. 1). These lexemes were frequently used by actors in personality-oriented discourse to express their attitude towards the introduction of quarantine measures. The resulting network illustrates the lexical landscape of discussions concerning quarantine measures from

March 1 to April 30, 2020. This is a single-core network with high centrality. The network nodes are the most commonly used lexemes related to the pandemic and quarantine measures, while the edges of the graph represent the connections between these lexemes. The weight of the graph edge indicates the strength of the connection between the nodes: the greater the weight, the more frequent the use. This pointed out that these lexemes were frequently used together, thus forming a semantic unity.

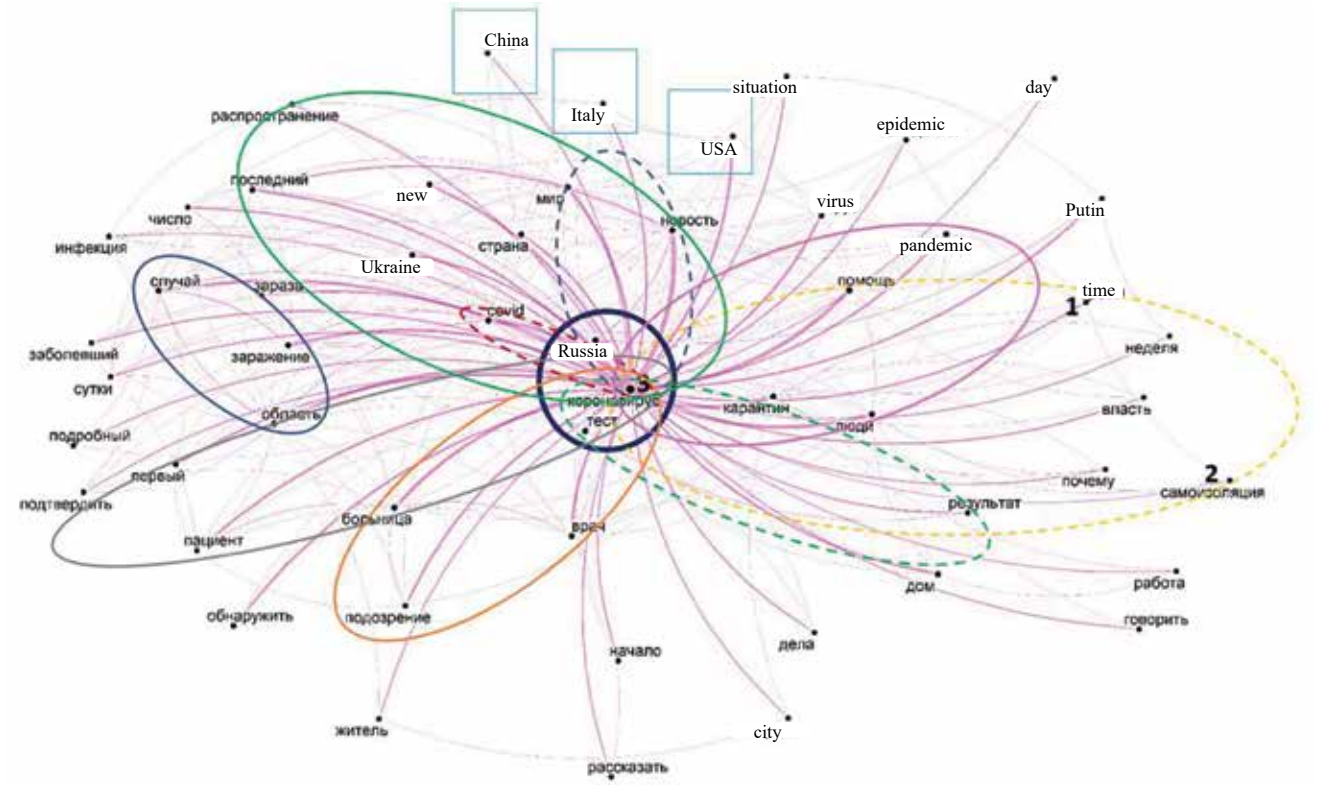

Figure. Network displays the most commonly used lexemes in microblogs collected from the X platform (formerly known as Twitter, blocked in the Russian Federation). These texts were published in response to lockdown measures in March–April 2020. The network consists of 53 key lexemes that were used at least 1,300 times

The core of the network, the most frequently used word, is "coronavirus" which was used 79,838 times in texts and had the highest frequency of use during the period of quarantine measures (March 1 – April 30, 2020). The cluster of key lexemes closest to the network core includes "coronavirus" («коронавирус») (used 79,838 times), "test" («тест») (used 4,663 times), and "Russia" («Россия») (used 5,848 times) and is highlighted by a dark blue circle with a solid line. The nodes "Russia" – "coronavirus", and "test" – "coronavirus" have the smallest geodesic distance in the network, as well as the highest weight of the edges connecting them, indicating frequent co-occurrence of these lexical units. It is likely that in their texts, actors of personality-oriented discourse discussed the incidence (increase in incidence) of the novel coronavirus infection and the availability of diagnostic tests for COVID-19 (e.g. "Today, anyone can take a coronavirus test, even without symptoms" or "What rapid tests for COVID-19 exist?" («Сегодня тест на коронавирус может сдать любой желающий, даже при отсутствии симптомов», «Какие существуют экспресс-тесты на COVID-19?»), etc.).

It is worth noting that in the Russian segment of the social media platform X (formerly known as Twitter blocked in the Russian Federation), people predominantly use the Russian name for the virus, compared to the English name "COVID" (3,970 vs 79,838 uses of the lexeme "coronavirus").

The lexeme "COVID" was often used together with "coronavirus" as seen in the graph (Figure) in the area highlighted by a red dashed line ellipse. A graph with nodes "COVID" and "coronavirus" connected by a high-weight edge confirms the frequent co-occurrence of these lexemes in texts related to the pandemic and quarantine measures. The high edge weight and small

geodesic distance between the nodes also indicate a fairly frequent co-occurrence of these lexical units. Most often, the co-occurrence of "coronavirus" and "COVID" was observed in tweets and hashtags (e.g. "Yes, people wear masks, but the Chinese, even without coronavirus, always wore masks because of the air #covid #coronavirus" (Да, народ ходит в масках, но китайцы даже без короновируса на моей памяти всегда ходили в масках из-за воздуха #covid #coronavirus)). It is worth noting that despite the negative impact of restrictive measures, society still focused on discussing the original source of the problem – the new virus – giving it a predominant role in their discussions within personality-oriented discourse.

The graph shows a cluster of lexemes, including "world" («мир») (3,154 uses), "news" («новость») (3,179 uses), and "coronavirus", highlighted by a blue dashed line ellipse. This suggests that the Russian users on the X platform (formerly known as Twitter, which is blocked in Russia) discussed information from both Russian and international media (represented by the "world" node). This aligns with the findings of international and Russian researchers, who have noted that media discourse is the main source of information about the pandemic, the novel coronavirus infection, and quarantine measures[5, 12, 13]frequent global measurements of affective states to gauge the emotional impacts of pandemic and related policy interventions remain scarce. Using 654 million geotagged social media posts in over 100 countries, covering 74% of world population, coupled with state-of-the-art natural language processing techniques, we develop a global dataset of expressed sentiment indices to track national- and subnational-level affective states on a daily basis. We present two motivating applications using data from the first wave of COVID-19 (from 1 January to 31 May 2020. This connection indicates that society primarily receives information from media discourse rather than other sources, such as business discourse, which may provide unbiased information (orders, regulations, laws, etc.). The graph confirms this statement since its edge connecting the "coronavirus" and "news" nodes has high weight, which indicates a strong connection and a high degree of co-occurrence of these lexemes. This may contribute to the growing infodemic in personality-oriented discourse, as media discourse is not always unbiased.

One of the most discussed topics during the lockdown is visualized in an interesting way. It includes the following nodes: "coronavirus" + "test" + "result" («результат»), which naturally should have formed a semantic unity with high co-occurrence. The resulting network contains this graph, the nodes of which are lexemes "coronavirus" (79,383 uses), "test" (4,663 uses), and "result" (approximately 1,300 uses). However, the nodes "test" and "result" are connected by an edge with very low weight, which suggests that people hardly ever mentioned these lexemes together. Instead, the lexeme "test" was more frequently used with the lexemes "coronavirus" and "result", since the edge connecting it with the former lexeme is of high weight and a small geodesic distance. The edge connecting "test" and "result" has lower weight than that connecting "test" and "coronavirus", but its weight is higher than that connecting the lexemes "result" and "test", with a large geodesic distance between the nodes.

When planning to study the way lockdown is reflected in personality-oriented discourse, we assumed that such units as "restrictions" («ограничения») and "self-isolation" («самоизоляция») would be among the most frequently used and form a large number of combinations (semantic unities). However, the node "restrictions" was not included in our network of 53 most commonly used lexemes. The network contains the node "self-isolation", which is located on the periphery of the network, far from the core node ("coronavirus"). This suggests that "self-isolation" was not a commonly used term in lockdown-related texts. Additionally, the node for "self-isolation" (≥ 1,300 uses) is part of a graph that includes the following nodes: "coronavirus", "time" («время») (≥ 1,300 uses), and "self-isolation". This graph is highlighted by a yellow dotted line ellipse, and the nodes are labeled in the following way: "time" – 1, "self-isolation" – 2, and "coronavirus" – 3. The nodes "time" and "self-isolation" are connected by a weak edge, and the geodesic distance between them is quite large, indicating that these terms were not often used together. It is worth noting that the nodes "time" and "coronavirus" and the nodes "self-isolation" and "coronavirus" also have a low degree of connectivity (with weak edges and a large distance between them).

On the other hand, the graph consisting of the nodes "coronavirus" (used 79,383 times), "help" («помощь») (used 3,923 times), "pandemic" («пандемия») (2,048 times used), and "people" («люди») (3,556 times used) most likely represents a discussion on the topic of medical care provided during the pandemic. The topic related to diagnosing the novel coronavirus

infection among the population by presentation to medical facilities is represented by a cluster of words associated with the "coronavirus" node, which reflects the development of the topic devoted to the pandemic and its impact on social and demographic phenomena. This cluster is highlighted by an orange solid line ellipse and includes the words "coronavirus" (79,383 times used), "suspicion" («подозрение») (2,130 times used), "hospital" («больница») (2,762 times used), and "doctor" («врач») (2,365 times used). It is interesting to note that the edge connecting the nodes "coronavirus" and "hospital" is stronger than the one connecting "coronavirus" and "suspicion", indicating a higher level of connectivity and confirming the joint use of these key lexemes in personality-oriented discourse. The same can be observed with the nodes "coronavirus" and "doctor". This suggests that the actors in personality-oriented discourse discussed the medical community (represented by the node "doctor") and the incidence statistics (represented by the joint use of "coronavirus" and "hospital"), which allows us to identify these clusters in the resulting network.

It is worth noting that the beginning of the pandemic was a frequently discussed topic in personality-oriented discourse, which is evidenced by the presence of a coherent block of co-occurrent terms: "first" («первый») + "patient" («пациент») + "coronavirus". It is obvious that the topic discussed was the first patients with coronavirus, which can be visualized as a graph with the nodes "coronavirus" (79,383 times used), "first" (≥ 1,300 times used), and "patient" (2,029 times used). The cluster is highlighted by a gray solid line ellipse. Additionally, it is worth mentioning that the cluster also includes the node "region" («область») (3,127 times used). This node is part of another cluster, forming a semantic unity with the nodes "case" («случай») (2,602 times used) and "infection" («заражение») (2,418 times used). However, its proximity to the cluster reflecting public attitude towards the beginning of the pandemic suggests that people learning about the first people infected with COVID-19 looked up the statistics of their region. The co-occurrence and high frequency of the key lexemes "region", "case", and "infection" indicate that people actively sought information about the statistics of incidence in their region and expressed their own attitude towards the situation through short text messages. This hypothesis is further supported by the fact that the key lexemes "infection" and "case", which are mentioned with high frequency, form a semantic unity "case of infection" («случай заражения»), which is also frequently mentioned (596 times used) (Table 2). For example, "New cases of COVID-19 infection have been registered in the Kostanay region" («Новые случаи заражения Covid-19 зарегистрированы в Костанайской области»).

The cluster, including the key lexemes "news", "latest" («последний»), and "coronavirus", located at a large geodesic distance from each other, confirms that participants of personality-oriented discourse relied on information obtained from the news when expressing their attitude towards the pandemic and the introduction of restrictive measures. The presence of this cluster in the network, as well as the high frequency of mentions of the key lexeme "news" (3,879 times used) and the phrase "latest news" («последние новости») (822 times used) highlights the close connection of personality-oriented discourse and media discourse. This connection became even more significant during the COVID-19 pandemic, as society was seeking new sources of information to make informed decisions in the face of increasing risks to life and health.

The lexemes "virus" («вирус») (2,245 uses) and "epidemic" («эпидемия») (2,248 uses) formed graphs in the network with the core node "coronavirus", which may indicate that the actors of personality-oriented discourse, as expected, focused on everyday problems and restrictions brought by the pandemic, without discussing the phenomenon of the pandemic as a whole. The absence of connections with the node "virus" may indicate a close connection of personality-oriented discourse and media discourse. People received information from the media and expressed their attitude to the information received, using the terminology specified in media discourse ("coronavirus", and not just "virus" or "disease").

The nodes "China" («Китай») (≥ 1,300 times used), "Italy" («Италия») (≥ 1,300 times used), and "USA" («США») (2,182 times used) indicate that users of the Russian segment of the X platform (formerly known as Twitter, blocked in the Russian Federation) took into account world news when forming their own attitudes towards the new coronavirus pandemic and the introduction of lockdown but were still more focused on the situation in the Russian Federation. This is confirmed by the remoteness of the nodes from the network core, as well as the fact that the nodes are linked to other key lexemes by edges of lower weight, demonstrating a low degree of connectivity of the key lexemes. In addition, the lower interest in foreign

scenarios for the development of the pandemic is confirmed by the frequency of mentions of countries: "China" (≥ 1,300 times used), "Italy" (≥ 1,300 times used), and "USA" (2,182 times used) in comparison with the key lexeme "Russia" (5,848 times used), which ranks second in the frequency of use after the lexeme "coronavirus".

The incoming centrality of the network is estimated by the number of connections included in the node; it can be said that the centrality corresponds to the concept of "popularity". Evaluating the constructed network, we can say that the most popular topic discussed during the period of introduction of quarantine measures was not restrictions but coronavirus, since it is this lexeme that represents the core of the network with the largest number of connections included in it.

In order to estimate the frequency of key lexemes that formed the network and demonstrated the main topics that concerned the population during the lockdown, we used the data feature matrix function in the Quanteda library. We calculated the sum of key lexemes in the columns of the data feature matrix, each row of which is a separate tweet (microblog). The results obtained are shown in Table 1.

Table 1

Numerical expression of nodes located in the network demonstrating key lexemes and their interactions in personality-oriented discourse during the lockdown period

coronavirus	79,838
Russia	5,848
test	4,663
quarantine	4,488
COVID	3,970
help	3,923
news	3,879
people	3,556
world	3,154
region	3,127
home	2,864
hospital	2,762
case	2,602
new	2,484
infection	2,418
doctor	2,365
virus	2,245
Putin	2,207
USA	2,182
suspicion	2,130
pandemic	2,048
patient	2,029

The results presented in Table 1 support the visual representation of personality-oriented discourse (Figure). "Coronavirus" is the most frequently used lexeme, which formed the basis of all combinations expressing the public attitude towards the introduction of quarantine measures and the pandemic. "Russia" is the second most frequently used lexeme, as the analysis was conducted using information from the Russian-speaking segment of the social network. An interesting observation is that the lexeme "pandemic" has one of the lowest frequency rates. It can be assumed that the term "pandemic" is more common for media or business discourse, where the professional medical community expressed their views on the pandemic. In contrast, personality-oriented discourse is characterized by lexemes that reflect the topics concerning the general public during the specified period, such as "coronavirus", "Russia", "quarantine" («карантин»), and "test".

Table 2

The most frequently used phrases in personality-oriented discourse, including key lexemes

Collocation	Number of uses
coronavirus test	3,217
suspected coronavirus	1,883
coronavirus detected	1,136
coronavirus in Russia	1,004
latest news	822
infected with coronavirus	711
coronavirus infection	707
to overcome the coronavirus	599
cases of infection	596
coronavirus analysis	591
coronavirus has been detected	578
coronavirus has been diagnosed	566
the pandemic of coronavirus infection	553
coronavirus testing	550
spread of coronavirus	518
coronavirus news	458

In order to determine the most frequently used semantic units related to quarantine measures between March 1 and April 30, 2020, the textstat_collocations function from the Quanteda library was utilized. The top 20 phrases were extracted. The results are shown in Table 2. This analysis reveals the main topics that were discussed in personality-oriented discourse during the lockdown period from March 1 to April 30, 2020, represented as clusters in the resulting network.

DISCUSSION

The analysis demonstrates that the topic of the novel coronavirus infection, as well as the introduction of quarantine measures, consists of several interconnected key topics. These topics form visually identifiable clusters in the constructed

network, with a high centrality and a core "coronavirus". This confirms the presence of coherent links between the texts studied during the period of March 1 – April 30, 2020, in non-institutional type of discourse. Additionally, the resulting network indicates the integration of discourses in which there was an active discussion of the introduction of quarantine measures in the Russian Federation. The population received information about the pandemic and quarantine measures through media discourse, which formed their perception of the risk to their own health and life, which often led to growing panic due to both information overload and insufficient information. The key term "coronavirus", which forms the core of the network, encompasses discussions on public health, incidence statistics, incidence rates in different regions, the spread of the virus, and measures to contain it. It also includes discussions on measures to help and support the population. The analysis revealed that the key lexemes reflecting the main concepts and concerns of the general public during the pandemic and the introduction of quarantine measures have a sociocultural dependence. They allow us to form a linguistic worldview during this pandemic.

CONCLUSION

This study confirms the presence of a unique set of topics that reflect the sociolinguistic worldview that was shaped by the pandemic and the introduction of quarantine measures. These topics identified through key lexemes not only reveal public attitude towards the pandemic and quarantine measures but also shed light on the evolution of public opinion, sources of information, and factors influencing the interpretation of information. Considering the findings of other researchers studying the pandemic through the lens of sociology, philosophy, and linguistics, we can note a growing trend towards a comprehensive approach to studying the effects of the pandemic on society. This approach involves examining the transformation of society, the reactions and behaviors of the population, and the role of institutional and non-institutional discourses. What makes this study outstanding is its integration of mathematical and sociolinguistic research methods to analyze the complex impact of the pandemic and related measures on the general public. However, it should be noted that this analysis alone cannot provide a complete sociolinguistic worldview of the public response to the pandemic and quarantine measures. To achieve this, it would be beneficial to supplement the existing study with frame analysis and sentiment analysis of texts related to the novel coronavirus infection. Additionally, comparing the representation of the pandemic and quarantine measures across different types of discourse would be an interesting avenue for future research.

REFERENCES

1. Wasserman S., Faust K. Social network analysis: methods and applications (Structural analysis in the social sciences, series number 8). Cambridge University Press; 1994. DOI: 10.1017/CBO9780511815478.
2. Maslova V. A. *Homo lingualis* in culture. Moscow: Gnosis; 2007.320 p. (in Russ.).
3. Zubkova Y. Discourse studies: new results (review of the book: Karasik V.I. Language plasticity of communication). Moscow: Gnosis; 2021.536 p. DOI: 10.18254/S294939000028978-4.
4. Carrington P.J., Scott J., Wasserman S. Models and methods in social network analysis. Cambridge: Cambridge University Press; 2005. DOI: 10.1017/CBO9780511811395.
5. Wang J., Fan Y., Palacios J., Chai Yu., Guetta-Jeanrenaud N., Obradovich N. et al. Global evidence of expressed sentiment alterations during the COVID-19 pandemic. *Nature Human Behaviour*. 2022;3(6):349–358. DOI: 10.1038/s41562-022-01312-y.
6. Pleshkova E. K. Strategies of risk communication in socially significant discourses during the pandemic of a new coronavirus infection: a social network analysis. *Russian Linguistic Bulletin*. 2023;42(6) (in Russ.). DOI: 10.18454/RULB.2023.42.8.
7. Barabási A.-L., Pósfai M. Network science. Camridge: Cambridge University Press; 2016.
8. Borgatti S.P., Everett M.G., Johnson J.C. Analyzing social networks. SAGE Publications Ltd.; 2018.
9. Basarab M.A., Glinskaya E.V., Ivanov I.P., Kolesnikov A.V., Kuzovlev V.I. Study into the structure of the scientific coathorship graph using social network analysis. *Cybersecurity Issues*. 2017;1(19):31–36. (In Russ.). DOI: 10.21681/2311-3456-2017-1-31-36.
10. Rezanova Z.I., Stepanenko A.A. Discoursive variants of thematic modeling of COVID-19 (news media discourse VS social networks). *Tomsk State University Journal of Philology.* 2023;(86):84–101 (in Russ.). DOI: 10.17223/19986645/86/6.
11. Benoit K., Watanabe K., Wang H., Nulty P., Obeng A., Müller S. et al. quanteda: An R package for the quantitative analysis of textual data. *Journal of Open Source Software*. 2018;30(3):774. DOI: 10.21105/joss.00774.
12. Chew C., Eysenbach G. Pandemics in the age of Twitter: content analysis of Tweets during the 2009 H1N1 outbreak. *PloS One*. 2010;11(5). DOI: 10.1371/journal.pone.0014118. DOI: 10.51217/npsyresearch_2023_03_04_08.

Authors' information

Pleshkova Ekaterina K. – Junior Researcher, Laboratory of Linguistic Anthropology, NR TSU, Head of the Department of International Development, Siberian State Medical University, Tomsk, pleshkova.ek@ssmu.ru, https://orcid.org/0000-0002-9075-429X,

Rezanova Zoya I. – Dr. Sci. (Philol.), Professor of the Department of General, Computer and Cognitive Linguistics, NR TSU, Deputy Head of the Laboratory of Anthropological Linguistics, NR TSU, Tomsk, rezanovazi@mail.ru, https://orcid.org/0000-0002-0550-991X

(✉) **Pleshkova Ekaterina K.,** pleshkova.ek@ssmu.ru

Received 23.09.2024;
approved after peer review 01.10.2024;
accepted 04.10.2024

УДК 314.14:616-039.4-053”450*2018/2022”
https://doi.org/10.20538/1682-0363-2024-4-129-135

Analysis of the rate and changes in the incidence of age-related diseases (by medical care uptake) in 2018–2022 (through the example of a municipal hospital in Saint Petersburg)

Saginbaev U.R., Akhmedov T.A., Rukavishnikova S.A., Davydova E.P.

St. Petersburg Institute of Bioregulation and Gerontology
3, Dinamo Av., Saint Petersburg, 197110, Russian Federation

ABSTRACT

The **aim** was to study the rate and changes in the incidence (by uptake) of age-related diseases (ARDs) in 2018–2022 through the example of a municipal hospital in Saint Petersburg.

Materials and methods. The study was carried out on the basis of records and reports for the period of 2018–2022 for the main statistical age groups (adult population (AP), working age population (WAP), persons over working age (POWA)). The incidence was analyzed for the most common ARDs (hypertensive diseases; coronary heart disease; type 2 diabetes mellitus; senile cataract, and glaucoma). The assessment of the incidence rate was carried out both for ARDs in general and for particular diseases.

Results. A long-term observation revealed that the incidence of ARDs has been increasing. In WAP, the rate of the increase in the incidence of ARDs was more pronounced compared to the same indicator in the general population surveyed (16.1 versus 5.4%). Moreover, in the post-COVID period, the incidence rate of a number of ARDs increased. In addition, a regular sequence was found in the manifestation of ARDs: hypertensive diseases, coronary heart disease, type 2 diabetes mellitus, senile cataract, glaucoma.

Conclusion. The incidence rate of age-related diseases has been increasing, which is especially pronounced among WAP. In the post-COVID period, these diseases were found to develop much faster. ARDs are characterized by a sequence of manifestations as patients get older, which in the future will allow to develop clearer approaches to the prevention, diagnosis, and treatment of ARDs depending on the age of the patient.

Keywords: age-related diseases, aging, incidence, post-COVID period, sequence of manifestations

Conflict of interest. The authors declare the absence of obvious or potential conflicts of interest related to the publication of this article.

Source of financing. The authors state that they received no funding for the study.

For citation: Saginbaev U.R., Akhmedov T.A., Rukavishnikova S.A., Davydova E.P. Analysis of the rate and changes in the incidence of age-related diseases (by medical care uptake) in 2018–2022 (through the example of a municipal hospital in Saint Petersburg). *Bulletin of Siberian Medicine.* 2024;23(4):129–135. https://doi.org/10.20538/1682-0363-2024-4-129-135.

✉ *Saginbaev Ural R.,* ural-spb-sag@mail.ru

Анализ уровня и динамики заболеваемости (по обращаемости) возраст-ассоциированной патологией в 2018–2022 гг. (на примере муниципальной поликлиники г. Санкт-Петербурга)

Сагинбаев У.Р., Ахмедов Т.А., Рукавишникова С.А., Давыдова Е.П.

Автономная научная некоммерческая организация высшего образования научно-исследовательский центр (ФННО ВО НИЦ) «Санкт-Петербургский Институт биорегуляции и геронтологии»
Россия, 197110, г. Санкт-Петербург, пр. Динамо, 3

РЕЗЮМЕ

Цель: изучить уровень и динамику заболеваемости (по обращаемости) возраст-ассоциированной патологией (ВАЗ) в 2018–2022 гг. на примере муниципальной поликлиники г. Санкт-Петербурга.

Материалы и методы. Исследование проведено на основе учетно-отчетной документации за период 2018–2022 гг. по основным учетно-статистическим возрастным группам (взрослое население (ВН), лица трудоспособного возраста (ТВ), лица старше трудоспособного возраста (СТВ)). Проводился анализ по наиболее распространенным ВАЗ (болезни, характеризующиеся повышенным кровяным давлением; ишемическая болезнь сердца; сахарный диабет 2-го типа; старческая катаракта и глаукома). Оценка уровня заболеваемости осуществлялась как в целом по ВАЗ, так и по отдельным нозологиям.

Результаты. Многолетняя динамика заболеваемости возраст-ассоциированными заболеваниями характеризовалась восходящей тенденцией. У лиц ТВ темп прироста заболеваемости ВАЗ был более выражен по сравнению с аналогичным показателем в целом у обследованного населения (16,1 против 5,4%). Более того, в постковидном периоде наблюдалось повышение уровня заболеваемости рядом ВАЗ. Кроме того, обнаружена закономерная очередность в манифестации ВАЗ: болезни, характеризующиеся повышенным кровяным давлением, – ишемическая болезнь сердца – сахарный диабет 2-го типа – старческая катаракта – глаукома.

Заключение. Динамика заболеваемости ВАЗ характеризуется восходящей тенденцией, особенно выраженной среди лиц ТВ. В постковидном периоде обнаружено более ускоренное развитие данной категории заболеваний. Для ВАЗ характерна очередность манифестации по мере увеличения возраста, что в перспективе позволит выработать более четкие подходы к профилактике, диагностике и лечению ВАЗ в зависимости от возраста пациента.

Ключевые слова: возраст-ассоциированные заболевания, старение, заболеваемость, постковидный период, очередность манифестации

Конфликт интересов. Авторы декларируют отсутствие явных и потенциальных конфликтов интересов, связанных с публикацией настоящей статьи.

Источник финансирования. Авторы заявляют об отсутствии финансирования при проведении исследования.

Для цитирования: Сагинбаев У.Р., Ахмедов Т.А., Рукавишникова С.А., Давыдова Е.П. Анализ уровня и динамики заболеваемости (по обращаемости) возраст-ассоциированной патологией в 2018–2022 гг. (на примере муниципальной поликлиники г. Санкт-Петербурга). *Бюллетень сибирской медицины.* 2024;23(4):129–135. https://doi.org/10.20538/1682-0363-2024-4-129-135.

INTRODUCTION

From the age of 25–30 years, the probability of developing pathological processes associated with aging begins to increase [1]. Modern researchers note that aging in most cases occurs early, and premature aging has the greatest medical, social, and economic significance as a trigger for the development of age-related diseases [2].

Age-related diseases (ARDs) are a heterogeneous group of pathologies, the likelihood of which increases as the body ages and is characterized by the following features: the predominance of chronic forms; polymorbidity; a decrease in the diversity

of nosological forms; change in the pathogenetic mechanisms of diseases; and, as a result, an atypical course [3]. The most typical representatives of ARDs include hypertension, type 2 diabetes mellitus, senile cataract, primary open-angle glaucoma, Alzheimer's disease, Parkinson's disease, a number of malignant neoplasms, etc.

Atherosclerosis is considered one of the main factors determining the nature of aging and its rate [4]. Moreover, there is an opinion that atherosclerosis is a widespread age-related change in the cardiovascular system and one of the leading pathogenetic links for most ARDs. In turn, atherosclerosis is closely related to arterial hypertension. Undoubtedly, early detection of these pathological processes can reduce (or delay) the likelihood of developing other ARDs and improve the quality of life of older people [5]. The study of patterns in the sequence of development of ARDs and their relationships in order to develop strategies for the prevention and timely diagnosis of age-related conditions is a promising field of research.

The aim of the study was to investigate the level and changes in the incidence (by uptake) of age-related diseases in 2018–2022 through the example of a municipal hospital in Saint Petersburg.

MATERIALS AND METHODS

The study was carried out on the basis of records and reports of a large municipal hospital in Saint Petersburg for the period of 2018–2022. The epidemiological features of ARDs were studied for the main statistical age groups (adult population (AP), working age population (WAP), persons over working age (POWA)). The materials were data from the form of federal statistical observation No. 12 "Information on the number of diseases registered in patients living in the service area of a medical organization". Table 1 shows the number of people registered in order to seek medical care at the polyclinic both on the whole and by individual age groups for the specified study period.

Table 1

Population registered at the polyclinic (number of people) on the whole and by individual age groups in 2018–2022

Year	AP	WAP	POWA
2018	77,259	53,338	23,921
2019	78,361	57,413	20,948
2020	80,457	56,186	24,271
2021	82,748	58,173	24,575
2022	84,126	59,101	25,025

We analyzed the incidence of the most common ARDs: I10–I15 "Hypertensive diseases" (HD), I20–I25 "Coronary heart disease" (CHD), E11 "Type 2 diabetes mellitus" (T2DM), H25 "Senile cataract" (SC), H40 "Glaucoma" (POAG). The assessment of the level and changes in the incidence was carried out both in general for ARDs and for individual diseases.

The conducted study is a comprehensive epidemiological study with time series analysis (the autoregressive moving-average model was used), including the calculation of the incidence (*Yi*), error (*m*), smoothed incidence rate (the autoregressive moving-average model), ranking and trend (*Yt*; the calculation was carried out using the method of least squares). To describe the trend, we calculated the rate of an increase or decrease in the incidence (Rid) as the ratio of an absolute increase or decrease to the previous level of the series. Statistical processing was carried out using the Statistics 20.0 and MS Excel 2010 software.

RESULTS

The assessment of the long-term changes in the incidence of ARDs both among the entire adult population and among the WAP group demonstrated an unambiguous unfavorable upward trend (Fig. 1, 2). In WAP, the rate of the increase in the incidence of ARDs was more pronounced compared to the same parameter in the general population surveyed (16.1 vs 5.4%).

It is worth noting that the incidence rate in the age groups under consideration was characterized by a sharp decrease in 2021 and a significant increase in 2022. This circumstance is probably associated with a decrease in the public uptake of medical care during the COVID-19 pandemic in 2021 and, conversely, a sharp increase in the number of people seeking medical care in 2022, which was more favorable in epidemiological terms. In addition, the increase in the incidence of ARDs in 2022 could be influenced by infection with COVID-19. The number of researchers note the unequivocal impact of COVID-19 on accelerated population aging [6].

ARDs are a heterogeneous group of pathologies, the likelihood of which increases along with aging. Figures 3 and 4 show the long-term changes in the incidence of the diseases (HD, CHD, T2DM, SC, and POAG) among the WAP group. It was established that the incidence of almost all the examined diseases (with the exception of POAG) was characterized by an unfavorable upward trend. The long-term changes in

the incidence of HD were characterized by an increase of 12.2%; for CHD, the increase was 23.0%, and for T2DM and SC, it was 25.3 and 9.3%, respectively. The long-term changes in the POAG incidence were characterized by a slight downtrend with a decline rate of –6.3%.

We calculated the ratio of the incidence of a specific disease in the examined population on the whole to the same parameter in the WAP group (Table 2). It is worth noting that the smaller this ratio, the less pronounced the difference in the incidence rate between different age groups.

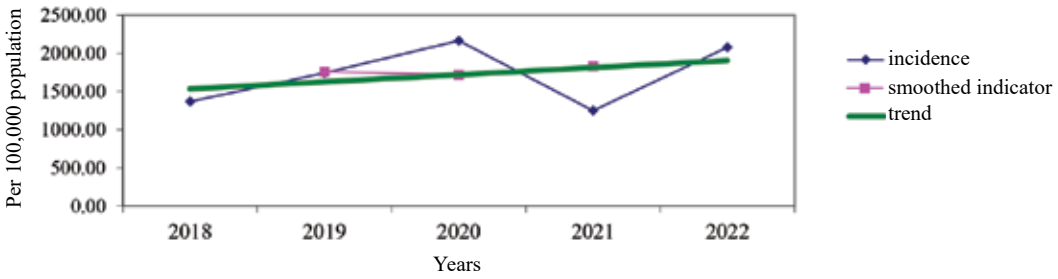

Fig. 1. Long-term changes in the incidence of ARDs in the adult population in 2018–2022

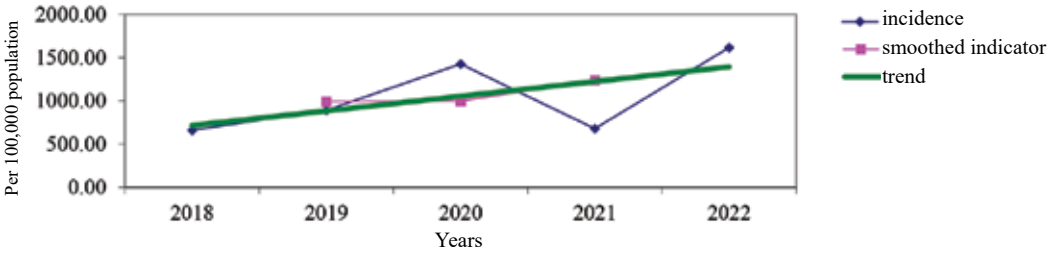

Fig. 2. Long-term changes in the incidence of ARDs in the WAP group in 2018–2022

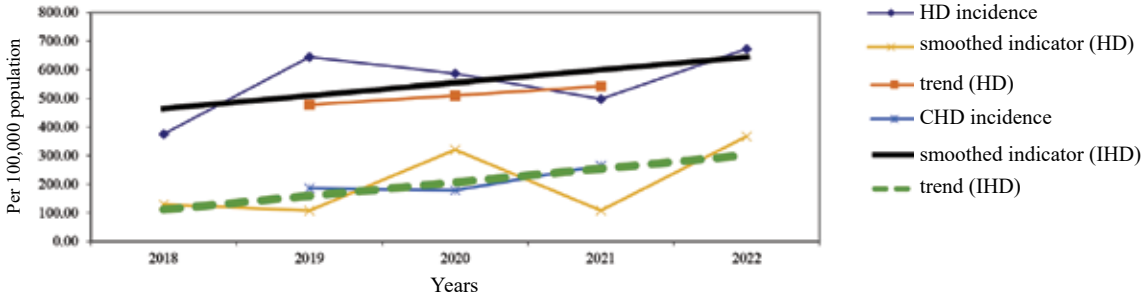

Fig. 3. Long-term changes in the incidence of HD and CHD in the WAP group in 2018–2022

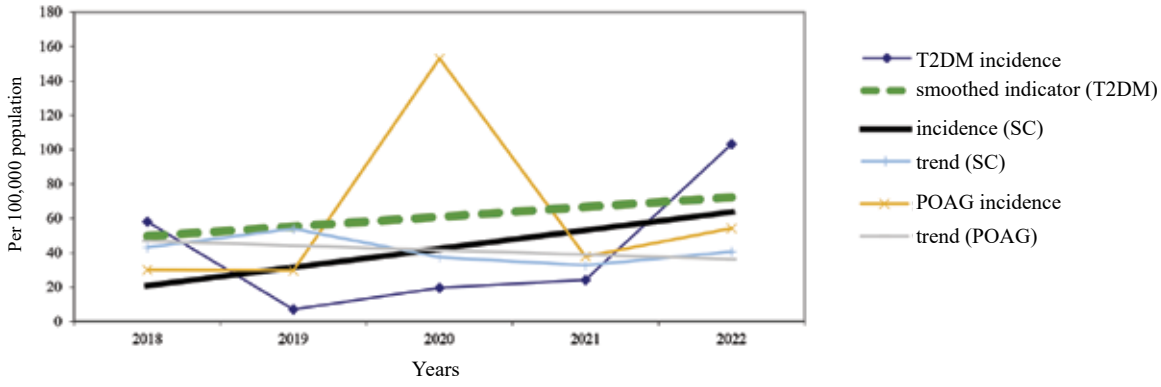

Fig. 4. Long-term changes in the incidence of T2DM, SC, and POAG in the WAP group in 2018–2022

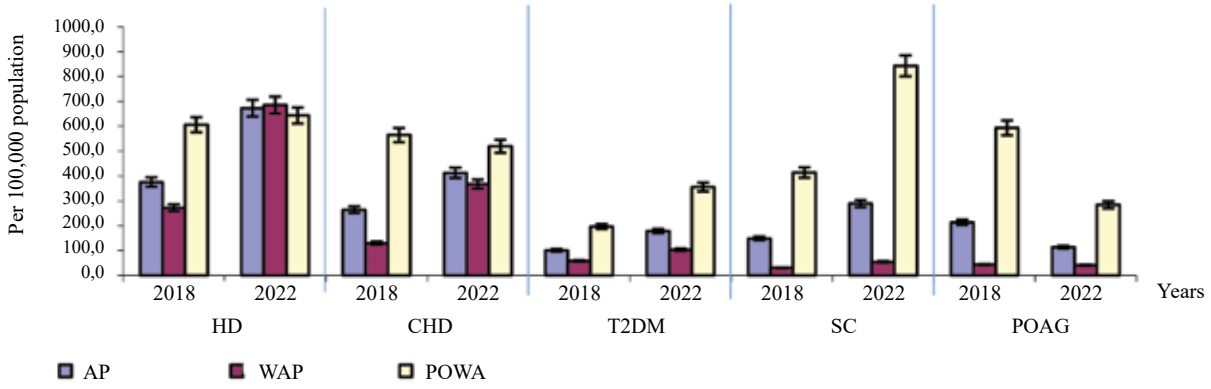

Fig. 5. Incidence rates of individual ARDs in 2018 and 2022

Table 2

Incidence rates of individual ARDs among different age groups in 2018–2022

Year	AP					WAP					Ratio Yi (AP):Yi (WAP)				
	Yi(HD)	Yi(IHD)	Yi(T2DM)	Yi(SC)	Yi(POAG)	Yi(HD)	Yi(IHD)	Yi(T2DM)	Yi(SC)	Yi(POAG)	HD	IHD	T2DM	SC	POAG
2018	375.4	264.1	101.0	148.9	213.6	271.9	129.4	58.1	30.0	43.1	1.4	2.0	1.7	5.0	5.0
2019	644.5	329.3	39.6	188.9	211.8	587	108.0	7	29.6	54.0	1.1	3.0	5.7	6.4	3.9
2020	586.7	377.8	37.3	637.6	149.2	574.9	320.4	19.6	153.1	37.4	1.0	1.2	1.9	4.2	4.0
2021	497.9	201.8	39.9	222.4	85.8	367.9	108.3	24.1	37.8	32.7	1.4	1.9	1.7	5.9	2.6
2022	672.8	412.5	178.3	288.9	112.9	685.3	367.2	103.2	54.1	40.6	1.0	1.1	1.7	5.3	2.8
Median	586.7	329.3	39.9	222.4	149.2	574.9	129.4	24.1	37.8	40.6	1.1	1.9	1.7	5.3	3.9
Rid	8.1	5.3	19.6	10.5	-1.37	12.2	23.0	25.3	9.3	–6.3	–	–	–	–	–

Figure 5 shows the incidence rate of HD, CHD, T2DM, SC, and POAG in persons of different age groups in the pre-COVID (2018) and post-COVID (2022) periods. It was established that the incidence rate of HD in the WAP group in the post-COVID period reached the incidence rate in the POWA group. A similar pattern was characteristic of CHD, T2DM, and SC. On the contrary, in the case of POAG, a decrease in the incidence rate was observed in all age groups considered.

DISCUSSION

The conducted comprehensive research demonstrated the relevance of studying a group of diseases associated with age-related processes. Early manifestation of ARDs from a clinical point of view is identical to the accelerated development of aging processes. Thus, the researchers found that a sharp increase in the incidence of T2DM begins in the age group of 50–54 years [7].

The analysis of the incidence (by uptake) of ARDs showed a moderate growth rate in the adult population on the whole and a pronounced increase in WAP. The revealed pattern corresponds to the trend when ARDs occur in younger people. A similar upward trend was found when assessing the changes in the prevalence of T2DM in the Krasnodar Krai in 2007–2012, with an average long-term level of total incidence of 3,093.7 cases per 100,000 population [8].

According to longitudinal observational studies, the incidence of arterial hypertension in Russia is on average 44% and continues to increase steadily [9]. The median level of incidence of arterial hypertension obtained in our study is slightly higher than its level in Russia (586.7 vs 547.7), which is consistent with the higher prevalence of this pathology in the Northwestern Federal District (8,129.5 cases per 100,000 population) compared to its prevalence in Russia [10].

The assessment of the sequence of pathology development according to the “age-specific morbidity index” (the ratio of the incidence rates in the POWA group to the same parameter in the AP group) clearly demonstrated an earlier manifestation of HD compared to T2DM. To assess the consistency of this index, a similar parameter was calculated for the incidence of certain ARDs in the Russian population according to the latest official statistics [10–12]. The calculation results fully confirmed the data obtained in this study

and corresponded to the following sequence of ARDs: HD – CHD – T2DM – POAG – SC (Table 3). In addition, it should be noted that the calculated index is directly proportional to the degree of association of pathology with older age: the higher the parameter value, the later the disease manifests. This index may be one of the important criteria for classifying pathology as ARD, given that there is debate whether some diseases should belong to this group [13].

Table 3

Ratio of incidence rates (Yi (POWA):Yi (AP)) by particular ARDs in the Russian Federation in 2018

Disease	Ratio
HD	1.32
CHD	1.73
T2DM	1.82
POAG	2.21
SC	2.27

According to the data obtained, among the considered ARDs at the population level, HD develops most early, followed by CHD, T2DM, POAG, and SC. In the future, this pattern will make it possible to develop a strategy for screening premature aging based on targeted early diagnosis of HD and CHD in younger people and T2DM, POAG, and SC in a more mature age. Such a step-by-step concept of secondary prevention of premature aging has a number of advantages: a more rational distribution of time, labor and financial resources; more targeted diagnostic screening increases the efficiency of detection due to optimal provision of the required diagnostic aid.

An increase in the incidence rate was found for the studied group of pathologies in the post-COVID period in all age groups. As noted above, this phenomenon may be associated both with the impact of the coronavirus infection on the accelerated aging and with the fact that the pandemic made people seek medical care in the hospital more often. For a more detailed and comprehensive study of this issue, it is necessary to consider the incidence rate (by uptake) in the post-COVID period over time, as well as to analyze the incidence rates based on the results of medical examinations in the pre- and post-COVID periods.

CONCLUSION

Thus, the incidence rate of age-related diseases is characterized by a continuing upward trend, especially characteristic of the WAP group. This pattern corresponds to the trend when ARDs occur in younger people. In addition, in the post-COVID period, a more accelerated development of such diseases was found. The identified patterns will make it possible to develop clearer approaches to the prevention, diagnosis, and treatment of age-related diseases as a separate group.

REFERENCES

1. Proschaev K.I., Ilnitsky A.N., Zhernakova N.I. The main geriatric syndromes: a textbook. Belgorod, 2012:228 (in Russ.).
2. Xia S., Zhang X., Zheng S., Khanabdali R., Kalionis B., Wu J. al. An update on inflamm-aging: mechanisms, prevention and treatment. *Journal of Immunology Research*. 2016;8:1–12. DOI: 10.1155/2016/8426874.
3. Dartigues J.F., Bourdonnec K. L., Tabue-Teguo M., Le Goff M., Helmer C., Avila-Funes J.A. et al. Co-occurrence of geriatric syndromes and diseases in the general population: assessment of the dimensions of aging. *The Journal of Nutrition, Health, Aging*. 2022;26(1):37–45. DOI: 10.1007/s12603-021-1722-3.
4. Samieri C., Perier M.C., Gaye B., Proust-Lima C., Helmer C., Dartigues J.F. et al. Association of cardiovascular health level in older age with cognitive decline and incident dementia. *JAMA*. 2018;320(7):657–664. DOI: 10.1001/jama.2018.11499.
5. Avila-Funes J.A., Pelletier A., Meillon C., Catheline G., Periot O., Trevino-Frenk I. et al. Vascular cerebral damage in frail older adults: the AMImage study. *The Journals of Gerontology*. 2017;72(7):971–977. DOI: 10.1093/gerona/glw347.
6. Guo X., Franco O.H., Laine J.E. Accelerated ageing in the COVID-19 pandemic: A dilemma for healthy ageing. *Maturitas*. 2022;157: 8–69. DOI: 10.1016/j.maturitas.2021.12.009.
7. Ivanenko A.A., Ushakova O.V. Epidemiology of type 2 diabetes mellitus in Komsomolsk-on-Amur. *Far East Medical Journal*. 2011;3:30–32. (In Russ.).
8. Basinskaya L.A., Komarovskikh E.N., Sakhnov S.N., Zabolotny A.G. The prevalence of diabetes mellitus of the first and second type in the Krasnodar region. *Bulletin Physiology and Pathology of Respiration*. 2013;50:126–129. (In Russ.).
9. Balanova Yu.A., Shalnova S.A., Imaeva A.E., Kapustina A.V., Muromtseva G.A. et al. Prevalence, awareness, treatment and control of arterial hypertension in the Russian Federation (data of the observational study ESSE-RF-2). *Rational Pharmacotherapy in Cardiology*. 2019;15(4):450–466. (In Russ.). DOI: 10.20996/1819-6446-2019-15-4-450-466.
10. Morbidity of the adult population of Russia in 2019. Statistical data. Moscow: Ministry of Health of Russia, 2020:160. (In Russ.).
11. Morbidity of the population over the working age in Russia in 2019. Statistical data. Moscow: Ministry of Health of Russia, 2020:183. (In Russ.).
12. Healthcare in Russia. 2019: Statistical collection. Moscow: Rosstat, 2019:170. (In Russ.).
13. Neudakhin E.V., Moreno I.G. Revisiting the pathogenesis of atherosclerosis and correction of atherogenic disorders in children. *RMJ. Pediatrics*. 2018;9:62–68. (In Russ.).

Authors' information

Saginbaev Ural R.h – Cand. Sci. (Biology), Senior Researcher, Laboratory for Age-related Clinical Pathology, St. Petersburg Institute of Bioregulation and Gerontology, Saint Petersburg, ural-spb-sag@mail.ru, https://orcid.org/0000-0001-9709-1882

Akhmedov Timur A. – Dr. Sci. (Biology), Associate Professor, Leading Researcher, Laboratory for Age-related Clinical Pathology, St. Petersburg Institute of Bioregulation and Gerontology, Saint Petersburg, timaxm@mail.ru, https://orcid.org/0000-0002-3105-4322 ; SPIN code: 5333-0721;

Rukavishnikova Svetlana A. – Dr. Sci. (Biology), Associate Professor, Leading Researcher, Laboratory for Age-related Clinical Pathology, St. Petersburg Institute of Bioregulation and Gerontology, Saint Petersburg, kdb2@yandex.ru, https://orcid.org/0000-0002-3105-4322

Davydova Elena P. – Researcher, Laboratory for Age-related Clinical Pathology, St. Petersburg Institute of Bioregulation and Gerontology, Saint Petersburg, kephala@mail.ru, https://orcid.org/0000-0002-2702-9394

(✉) **Saginbaev Ural R.,** ural-spb-sag@mail.ru

Received 27.10.2023;
approved after peer review 11.03.2024;
accepted 14.05.2024

УДК 616.357:577.175.53:577.2
https://doi.org/10.20538/1682-0363-2024-4-136-144

Studying molecular interactions of synthetic glucocorticoids with TRPM8 by molecular docking

Timkin P.D.[1], Kotelnikov D.D.[2], Timofeev E.A.[1], Naumov D.E.[3], Borodin E.A.[1]

[1] *Amur State Medical Academy*
101, Gorkogo Str., Blagoveshchensk, 675001, Russian Federation

[2] *Far Eastern State Agrarian University*
86, Politekhnicheskaya Str., Blagoveshchensk, 675005, Russian Federation

[3] *Far Eastern Scientific Center for Physiology and Pathology of Respiration*
22, Kalinina Str., Blagoveshchensk, 675011, Russian Federation

ABSTRACT

Aim. To carry out *in silico* screening of interactions of synthetic glucocorticoids with TRPM8.

Materials and methods. Information on the structure of the ligands was obtained from the PubChem chemical database in sdf format. The TRPM8 protein model was downloaded from the AlphaFold Protein Structure Database (AlpahaFold ID: AF-Q7Z2QW). Prediction of molecular cavities and coordinates of their centers was carried out on the PrankWeb web server. Modeling of molecular interactions was carried out using AutoDock (generation of 100 epochs) and MOE (generation of 300 poses) software.

Results. The study revealed that the ligands formed stable complexes with TRPM8, but all of them, except for beclomethasone dipropionate, did not interact with the Tyr745 amino acid residue (the key binding site for channel activation). Thus, it can be assumed that glucocorticoids are most likely inhibitors of this ion channel. Of all glucocorticoids, special attention was paid to prednisolone, flunisolide, and budesonide, since the results of molecular docking of these molecules using AutoDock and MOE showed comparable data.

Conclusion. The results obtained provide an insight into the therapeutic potential of these drugs in terms of their use in the treatment of cold-induced airway hyperresponsiveness and also expand the potential for their personalized use in the treatment of bronchial asthma and COPD.

Keywords: TRPM8, molecular docking, glucocorticoids, *in silico*

Conflict of interest. The authors declare the absence of obvious or potential conflicts of interest related to the publication of this article.

Source of financing. The authors state that they received no funding for the study.

For citation: Timkin P.D., Kotelnikov D.D., Timofeev E.A., Naumov D.E., Borodin E.A Studying molecular interactions of synthetic glucocorticoids with TRPM8 by molecular docking. *Bulletin of Siberian Medicine.* 2024;23(4):136–144. https://doi.org/10.20538/1682-0363-2024-4-136-144.

✉ *Timkin Pavel D.,* timkin.pasha@mail.ru

Исследование молекулярных взаимодействий синтетических глюкокортикоидов с TRPM8 методом молекулярного докинга

Тимкин П.Д.[1], Котельников Д.Д.[2], Тимофеев Э.А.[1], Наумов Д.Е.[3], Бородин Е.А.[1]

[1] *Амурская государственная медицинская академия (ГМА)*
Россия, 675001, Амурская обл., г. Благовещенск, ул. Горького, 101

[2] *Дальневосточный государственный аграрный университет (ГАУ)*
Россия, 675000, Амурская обл., г. Благовещенск, ул. Политехническая, 86

[3] *Дальневосточный научный центр физиологии и патологии дыхания (ДНЦ ФПД)*
Россия, 675011, Амурская обл., г. Благовещенск, ул. Калинина, 22

РЕЗЮМЕ

Цель: осуществление *in silico* скрининга взаимодействий синтетических глюкокортикоидов с TRPM8.

Материалы и методы. Информация о структуре лигандов была получена из базы данных химических соединений PubChem в sdf-формате. Модель белка TRPM8 загружена из базы данных AlphaFold Protein Structure Database (AlpahaFold ID: AF-Q7Z2QW). Предсказание молекулярных полостей и координат их центров осуществлялось на веб-сервере PrankWeb. Моделирование молекулярного взаимодействия проводили с использованием двух программ: AutoDock (генерация 100 эпох) и MOE (генерация 300 поз).

Результаты. В ходе проведения исследования выяснилось, что лиганды образуют стабильные комплексы с TRPM8, но при этом все, кроме беклометазона дипропионата, не взаимодействуют с аминокислотным остатком Tyr745 (ключевой сайт связывания для активации канала). Таким образом, можно полагать, что глюкокортикоиды, вероятнее всего, являются ингибиторами данного ионного канала. Из всех глюкокортикоидов особое внимание было уделено преднизолону, флунизолиду и будесониду, так как результаты молекулярного докинга этих молекул с использованием AutoDock и MOE демонстрируют сопоставимые данные.

Заключение. Полученные результаты позволяют взглянуть на терапевтический потенциал данных препаратов в аспекте их использования при лечении холод-индуцированной гиперреактивности дыхательных путей, а также расширяют потенциал их персонализированного применения в терапии бронхиальной астмы и хронической обструктивной болезни легких.

Ключевые слова: TRPM8, молекулярный докинг, глюкокортикоиды, *in silico*

Конфликт интересов. Авторы декларируют отсутствие явных и потенциальных конфликтов интересов, связанных с публикацией настоящей статьи.

Источник финансирования. Авторы заявляют об отсутствии финансирования при проведении исследования.

Для цитирования: Тимкин П.Д., Котельников Д.Д., Тимофеев Э.А., Наумов Д.Е., Бородин Е.А. Исследование молекулярных взаимодействий синтетических глюкокортикоидов с trpm8 методом молекулярного докинга. *Бюллетень сибирской медицины.* 2024;23(4):136–144. https://doi.org/10.20538/1682-0363-2024-4-136-144.

INTRODUCTION

TRPM8 is an ion channel that provides Ca^{2+} and Na^{+} supply into the cell. This channel is a homotetramer, each subunit of which contains six transmembrane domains (S1–S6) [1].

This channel is known to play an essential role in the sensation of cold. Activation of the channel occurs at certain temperatures (10–28 °C) or under the influence of chemical agents (for example, menthol, icilin) [2-4]. Due to its functional role, TRPM8 is expressed in a subpopulation of primary afferent neurons that innervate cold-hypersensitive tissues, including the skin, oral epithelium, teeth, nasal mucosa, tongue, and cornea. There is also evidence of the presence of this channel in the epithelium of

lung tissue and on leukocytes, including those not in contact with the external environment, which implies the presence of endogenous modulators of TRPM8 activity. The activity of the ion channel is combined with the transcriptional regulation of important immunomodulatory agents interleukin (IL)-6 and IL-8, which are often expressed during inflammation in the respiratory tract [5].

Commonly used drugs to relieve bronchial asthma are synthetic glucocorticoids (GCs), which have an anti-inflammatory effect. The main mechanism of action of GCs is mediated by binding to the cytosolic glucocorticoid receptor. After this, the newly formed complex, which has undergone dimerization, is translocated into the cell nucleus, resulting in the regulation of gene expression. This process is usually called transcriptional activation or transactivation [6, 7].

It is generally accepted that GC hormones do not bind to ion channels of the TRP family, at least there are no experimental data demonstrating this. However, there is evidence of modulation of TRP receptors by some steroid hormones, such as testosterone, estradiol, and androgens [8]. In our previous studies on the search for potential ligands for TRPM8 using *in silico* methods with neural networks, we found that the synthetic GC dexamethasone is a candidate for interaction with the receptor. Data from rigid molecular docking in the region close to amino acid residue Tyr745 demonstrated the hypothetical possibility of complex formation [9]. The Tyr745 residue is the most important in the implementation of the TRPM8 function, since in the native state, it is this residue that forms a hydrogen bond with menthol, resulting in activation of the channel.

All of the above gives a reason to assume the presence of an alternative TRPM8-mediated molecular pathway for the implementation of the effects of GC hormones.

In this study we used budesonide, prednisolone, flunisolide, fluticasone propionate, hydrocortisone, dexamethasone, beclomethasone dipropionate, and triamcinolone acetonide as the most popular synthetic GCs prescribed for the treatment of chronic obstructive pulmonary disease, bronchial asthma, and allergic rhinitis in clinical practice [10–16].

Since molecular docking approaches are promising in the study of drugs, it was decided to focus on a detailed study of the characteristics of GC binding to TRPM8 [17].

The aim of this study was to conduct *in silico* screening of interactions of selected synthetic GCs with TRPM8 by the molecular docking method and to assume a possibility of forming stable complexes to determine potential ligands that act as agonists or antagonists.

MATERIALS AND METHODS

Information about the structure of ligands in sdf format was obtained from the PubChem chemical database (https://pubchem.ncbi.nlm.nih.gov/, access date: 01.10.2023).

The TRPM8 protein model was downloaded from the AlphaFold Protein Structure Database (https://alphafold.ebi.ac.uk/entry/Q7Z2W7, access date: 01.10.2023). Since the full-length structure of the receptor is a homotetramer with a total size of 4.5 thousand amino acid residues, for subsequent structural optimization of the protein and rapid molecular docking, only 1 subunit (PDB: AF-Q7Z2QW) in pdb format was used.

Modeling of intermolecular interactions was carried out using two different programs: AutoDock 4.2 designed to search for a local minimum energy using a genetic algorithm, and MOE 2022.02 (Molecular Operating Environment) [18], which is a complex software consisting of various modules, which allows to conduct full-fledged research in the field of computer-aided drug design of any complexity without using third-party services.

To predict potential molecular cavities and the coordinates of their centers, the PrankWeb web server (https://prankweb.cz/, access date: 01.10.2023) was used [19–21]. These coordinates were selected for the correct orientation of the Grid Box (a three-dimensional lattice within which the search and analysis of interactions between ligands and protein targets occur). Modeling intermolecular interactions with subsequent calculation of the affinity of GCs for TRPM8 was carried out by rigid docking, that is, without changing the conformations of the side chains of amino acid residues in the molecular cavity and the ligand itself. Docking took place according to the standard algorithm with generation in 100 epochs.

The first step before molecular docking is as follows: loading the target protein into the MGLtools working field, removing water molecules, and adjusting the degree of protonation (adding polar hydrogen atoms) to the protein chain at the sites of potential bonds with ligands. Next, the ligand is added in pdbqt format. The second stage is to apply the Grid

Box using the coordinates and dimensions obtained in PrankWeb. The work used a 40 x 40 x 40 Grid Box size: with an interval of 0.375 Å (default size and interval). The third stage is to search for possible conformations of the protein – ligand complex, that is, to perform the docking itself. After docking, a dlg file is created with detailed information about the formed complexes (complex location coordinates, binding energy, RMSD (root mean square deviation of atomic positions). The final stages are the analysis and interpretation of the obtained data [22].

The research software pipeline in MOE was as follows. The first stage involved importing the downloaded protein in pdb format and ligands in sdf format. For convenience, each study was conducted separately. Using the default parameters in the QuickPrep module, primary optimization of the protein was carried out, consisting of its protonation and correction of structural errors (for example, breaks). Next, partial charges were applied in the Partial charges module. The final stage of structural optimization was the implementation of protein energy minimization in the Energy minimization module, General protocol. The protocol parameters were saved by default: forcefields – inherited from the force field settings (described below), cell – no periodicity, constraints – rigid water molecules option is selected, gradient – 0.1 RMS kcal / mol / Å^2. To parameterize atoms and covalent and non-covalent interactions, the Amber14:EHT[1] force field was used, and the behavior of the solvent (water) was modeled by the Generalized Born method.

Before performing molecular docking itself, a search for the binding site was carried out using the Site Finder module with the Solvent option enabled. The experiment used the third binding site found, containing Tyr745, a critical amino acid required for channel activation. The Select Contact Atoms (selects atoms at a distance of 4.5 Å) and Select Residues in SE (selects only residues included in the binding site) options were selected and the Dummies option was executed to overlay dummy atoms, assigning the LP element to hydrophobic atoms and LPA to hydrophilic atoms (having a free pair of electrons) and also optimizing the temperature of the atom.

Molecular docking was carried out according to the General protocol. The Receptor and Solvent Atoms option was selected as the receptor, the binding site was Dummies, the ligand was the loaded ligand molecule (Ligand Atoms). The generation parameters were as follows: Placement – Triangle Matcher (Method), Affinity dG (Score), 300 Poses; Refinement – Induced fit (Method), GBVI/WSA dG (Score), 1 Pose.

A detailed description of the algorithms used for generating conformations and calculating energy before and after structural optimization is not provided in this article. As a result of docking, the most stable conformation with the lowest binding energy was extracted.

To conduct a comparative analysis between the obtained ligand conformations in AutoDock 4.2 and MOE, RMSD was calculated in the LigRMSD web service (https://ligrmsd.appsbio.utalca.cl/, access date: 01.10.2023) [23]. RMSD is a measure of the average distance between atoms (backbone, excluding H atoms) in superimposed molecules. This parameter allows to objectively assess the relative positions of ligands predicted by different methods. Based on the literature data, the threshold RMSD value was chosen to be 3Å [24].

Some of the resulting complexes were visualized using the PyMol visualization software [25] and the built-in Ligand Interactions module to construct 2D maps of interactions of ligands with amino acid residues.

The main task of using the AutoDock and MOE algorithms in our work was to assess the reproducibility of the results of molecular docking carried out by two different methods.

RESULTS

To operate the AutoDock protocol and construct the Grid Box, the coordinates of 8 putative molecular cavities were obtained with probability score values from 0.0003 (corresponding to the lowest quality of the forecast) to 0.497 (for the highest quality of the forecast). The molecular cavity with the highest probability score was selected due to the presence of the Tyr745 residue. This pocket also contains another important residue, Arg1008. According to the PrankWeb prediction, the molecular cavity is formed by amino acid residues numbered: 738, 741, 742, 745, 777, 778, 781, 782, 785, 802, 839, 842, 845, 849, 1004, 1005, 1008, 1013, 1016. The presented results

[1] This force field unites parameters of the Amber ff14SB force field for proteins and nucleic acids and parameters of the Extended Hueckel Theory for simple organic compounds in the MOE 2022.2 software package.

generally correspond to the literature data, with the exception of the absence in the pocket annotation of the Ala1009 residue, which, like Arg1008, acts as a stabilizer for the native ligand – menthol [26].

Due to the lack of a clear distinction between binding sites for agonists and antagonists, it is difficult to select one molecular cavity for the study and draw final conclusions based only on the *in silico* assessment of interactions [27]. Therefore, this study is of a screening nature, that is, it is aimed at selecting potentially suitable ligands for subsequent experiments.

The results of molecular modeling were obtained for each of the GCs (Table 1). For prednisolone, flunisolide, budesonide, beclomethasone dipropionate, and hydrocortisone, the difference in the minimum binding energy obtained by different programs was less than 1 kcal / mol, which, without taking into account chemical bonds, indicates an approximate similarity of the results obtained by the AutoDock and MOE programs, which can be explained by a similar evaluation function.

Table 1

Binding energy of complexes and RMSD of the resulting conformers, kcal / mol

Glucocorticoid	AutoDock	MOE	RMSD (Å)
Prednisolone	–7.25	–7.76	0.83
Flunisolide	–7.76	–8.26	1.62
Budesonide	–8.65	–8.58	2.54
Dexamethasone	–9.35	–7.99	4.68
Fluticasone propionate	–5.31	–7.93	6.64
Hydrocortisone	–7.65	–7.94	6.98
Triamcinolone acetonide	–11.09	–7.92	42.77
Beclomethasone dipropionate	–8.88	–8.76	43.04

Note. Ranked by RMSD, smaller values are better.

For prednisolone, flunisolide, and budesonide, the RMSD was within 3Å, indicating a relatively close relationship between the molecules, despite the use of different approaches to the generation of complexes. The similarity of conformations indicates the reproducibility of the results for GC data when analyzed by two different programs. However, information about the position of molecules is insufficient for a reliable analysis, since both ligands and amino acid residues in different programs are interpreted with different force fields and with different pH, which, in turn, is manifested by different structural interactions of ligands with amino acid residues (Fig.1).

For example, MOE showed the interaction of prednisolone with Arg842, while in AutoDock, this GC interacted with 5 residues: Leu778, Asp781, Glu782, Ile846, and Arg100. Flunisolide and budesonide interacted with almost the same amino acid residues as prednisolone, but in different combinations.

Based on these results, several conclusions can be drawn. The molecular structures of the majority of the selected GCs are very similar and differ in the presence or absence of hydroxyl groups in certain positions. Therefore, firstly, the amino acid residues for the previously mentioned ligands in the binding site are similar, and, secondly, the differences are due to the presence or absence of hydroxyl groups in a certain position, as well as different degrees of protonation. These conclusions are more typical of the results obtained in MOE, since conformational variability of both the binding site and the ligand itself is possible in this program.

The conformation of beclomethasone dipropionate with TRPM8, modeled in MOE, deserves special attention (Fig. 2). This conformation is characterized by two key features despite high RMSD relative to the complex generated in AutoDock. Firstly, interaction occurs with the key amino acid Tyr745 [27] via the H-π (hydrogen) bond. Secondly, this is the lowest binding energy calculated by this software, demonstrating the most stable binding of beclomethasone dipropionate with TRPM8. Interest in the beclomethasone dipropionate – TRPM8 complex in MOE is due to the fact that this is the only conformation where the GC forms a bond with Tyr745. Since molecular docking in AutoDock is rigid, that is, there are no conformational changes in the ligand and binding site, and MOE takes into account this "mobility" in calculations (the Induced Fit protocol was used), these results should be considered as more plausible and potentially suitable for future molecular docking with the assessment of the binding strength of the complex over time and the use of force fields. This need is due to the fact that most molecular docking algorithms take into account only partial charges of the entire ligand molecule, ignoring its individual functional groups, while most GCs have polar solvate groups (propionic, acetonide), which can play a key role in the position of the molecule.

The comparative analysis of AutoDock 4.2 and MOE findings revealed that RMSD values of other ligand positions (fluticasone propionate, hydrocortisone, triamcinolone acetonide, dexamethasone) were significantly higher. This makes it difficult to definitively interpret the resulting interactions for these GCs. So, for these ligands, it would be correct

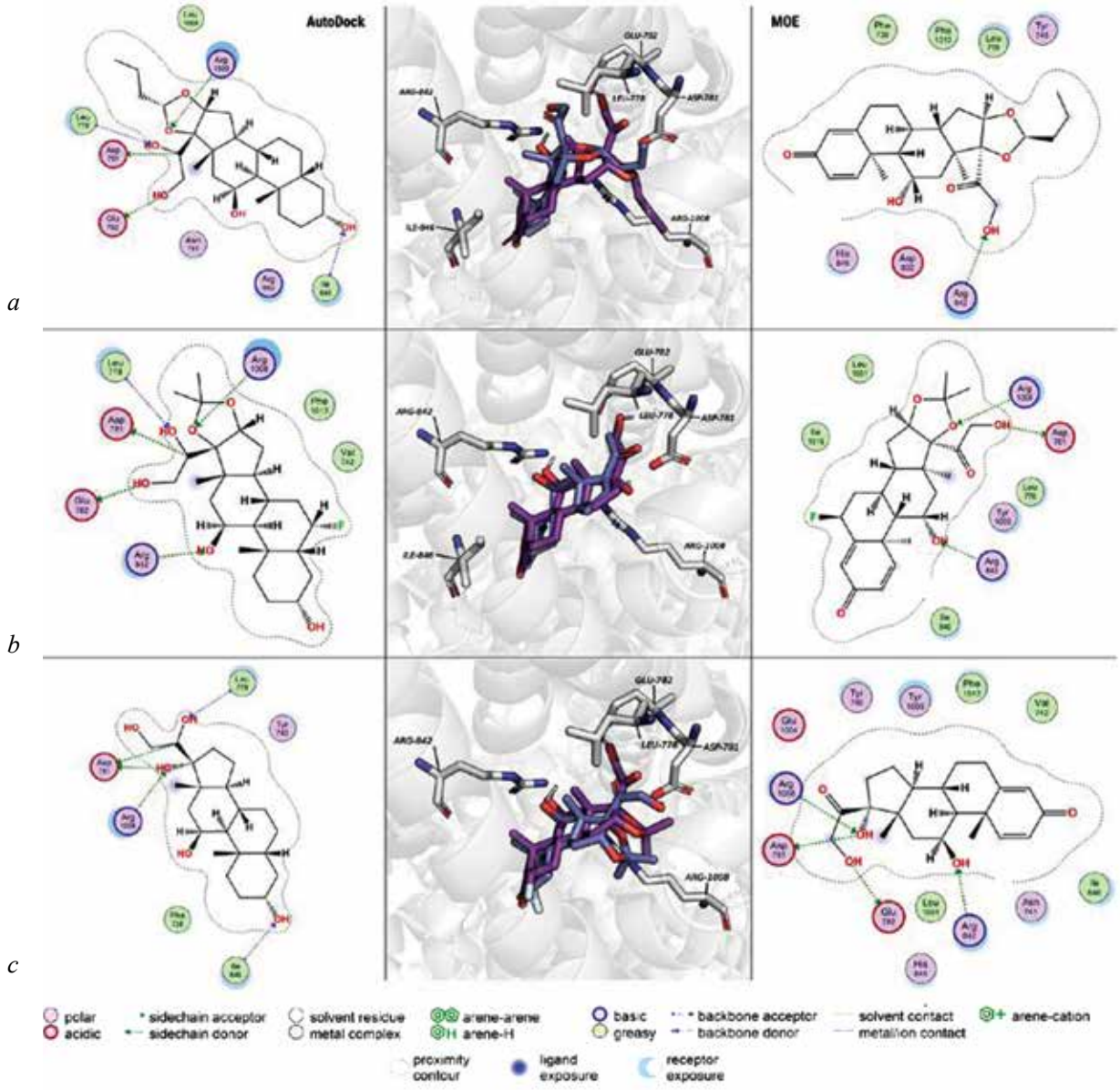

Fig. 1. Position of ligands in the TRPM8 binding site and a 2D map of structural interactions of ligands with site residues: *a* – budesonide, *b* – prednisolone, *c* – flunisolide; on the left – AutoDock, on the right – MOE; blue color marks the positions of molecules obtained in AutoDock 4.2, purple color marks the positions of molecules obtained in MOE

to carry out an additional analysis using *ab initio* methods. The visual analysis of all conformations obtained in AutoDock allow to conclude that the rigid orientation of the GC molecules took place mainly along the steroid ring with minimal deviations relative to each other. As for the conformations modeled in MOE, the differences in them are more significant, which is due to the inclusion of minor differences (functional groups, conformational isomerization of the ligand) in the ligand structures.

The absolute energy values calculated for various conformations, on the one hand, are far from actual values; however, on the other hand, they allow to consider them from a relative point of view and compare the binding energies of different molecules, ranking their degree of affinity relative to each other. Therefore, the series of ligands according to the degree of affinity for TRPM8 (from the greatest to the lowest, from the lowest energy level to the highest) following the results of scoring in AutoDock is as follows: triamcinolone

acetonide, dexamethasone, beclomethasone dipropionate, budesonide, flunisolide, hydrocortisone, prednisolone, and fluticasone propionate. According to the results of scoring in MOE, the ligand series is the following: beclomethasone dipropionate, budesonide, flunisolide, dexamethasone, hydrocortisone, fluticasone propionate, triamcinolone acetonide, and prednisolone. This series shows that beclomethasone, budesonide, flunisolide, hydrocortisone, and fluticasone propionate / prednisolone appear in the same order, which represents a very good correlation of the results (6 out of 8). Based on the series, we are planning to study the effects of synthetic GCs on TRPM8 *in vitro*.

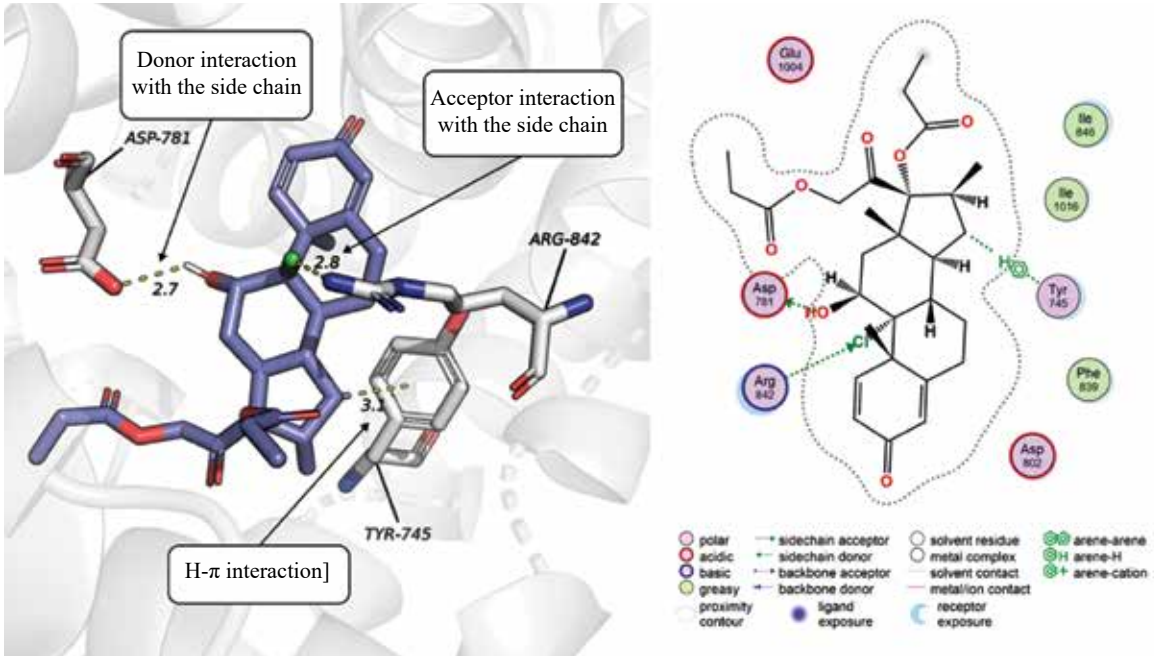

Fig. 2. 3D visualization of the beclomethasone dipropionate – TRPM8 complex, obtained in MOE, with a 2D graph of interactions: the arrows on the left and the yellow dotted line duplicate the interactions shown in the 2D graph; bond length units are given in Angstroms (Å)

DISCUSSION

The conducted study demonstrates general patterns in the molecular interaction of various synthetic GCs with the target, obtained by two different methods. For prednisolone, flunisolide, and budesonide, the RMSD value was less than 2.5Å (±0.1Å), indicating conformational similarities and reproducibility of the results in both AutoDock and MOE. It is worth noting that in the molecular cavity, various amino acid residues served as binding sites, with the exception of Tyr745, which may characterize the antagonistic potential of prednisolone, flunisolide, and budesonide. For GCs, whose conformations differed significantly, the formation of hydrogen bonds with the amino acid residue Tyr745 was also ignored, which is consistent with other results.

An exception to the list of GCs was beclomethasone dipropionate, which ultimately formed a hydrogen bond with Tyr745. The study made it possible to select the most promising GCs suitable for further analysis using molecular dynamics methods, which will make it possible to clarify the stability of GC complexes with TRPM8. A final confirmation of the ability of GCs to not only form complexes with the TRPM8 receptor, but also to inhibit it should be obtained through *in vitro* experiments.

CONCLUSION

Detailed mechanisms of the anti-inflammatory effect of GCs mediated through the TRPM8 ion channel remain a big question for our research group. However, if experimentally confirmed, the possibility of pharmacological modulation of TRPM8 by GCs will allow to optimize approaches to personalized use of GCs and take a different look at the therapeutic potential of these hormones, including their effect in the treatment of chronic obstructive pulmonary disease, respiratory diseases, and cold-induced respiratory diseases.

REFERENCES

1. Bidaux G., Sgobba M., Lemonnier L., Borowiec A.S., Noyer L., Jovanovic S. et al. Functional and modeling studies of the transmembrane region of the TRPM8 channel. *Biophys J.* 2015;109(9):1840–1851. DOI: 10.1016/j.bpj.2015.09.027.
2. Andersen H.H., Olsen R.V., Møller H.G., Eskelund P.W., Gazerani P., Arendt-Nielsen L. A review of topical high-concentration l-menthol as a translational model of cold allodynia and hyperalgesia. *Eur. J. Pain*. 2013;18(3):315–325. DOI: 10.1002/j.1532-2149.2013.00380.x.
3. Diver M.M., Cheng Y., Julius D. Structural insights into TRPM8 inhibition and desensitization. *Science*. 2019;365(6460):1434–1440. DOI: 10.1126/science.aax6672.
4. Key F.M., Abdul-Aziz M.A., Mundry R., Peter B.M., Sekar A., D'Amato M. et al. Human local adaptation of the TRPM8 cold receptor along a latitudinal cline. *PLoS Genet*. 2018;14(5);e1007298. DOI: 10.1371/journal.pgen.1007298.
5. Sabnis A.S., Shadid M., Yost G.S., Reill C.A. Human lung epithelial cells express a functional cold-sensing TRPM8 variant. *Am. J. Respir. Cell Mol. Biol.* 2008;39(4):466–474. DOI: 10.1165/rcmb.2007-0440oc.
6. Sevilla L.M., Jiménez-Panizo A., Alegre-Martí A., Estébanez-Perpiñá E., Caelles C., Pérez P. Glucocorticoid resistance: Interference between the glucocorticoid receptor and the MAPK signalling pathways. *Int. J. Mol. Sci.* 2021;22(18):10049. DOI: 10.3390/ijms221810049.
7. Frank F., Ortlund E.A., Liu X. Structural insights into glucocorticoid receptor function. *Biochem. Soc. Trans.* 2021;49(5):2333–2343. DOI: 10.1042/bst20210419.
8. Méndez-Reséndiz K.A., Enciso-Pablo Ó., González-Ramírez R., Juárez-Contreras R., Rosenbaum T., Morales-Lázaro S.L. Steroids and TRP channels: A close relationship. *Int. J. Mol. Sci.* 2020;21(11):3819. DOI: 10.3390/ijms21113819.
9. Borodin E., Leusova N., Chupalov A., Timkin P., Timofeev E., Kolosov V. et al. The strategy for searching of potential ligands for TRPM8 based on use of deep neural networks and intermolecular docking. *Eur. Respir. J*. 2021;58:PA2383. DOI: 10.1183/13993003.congress-2021.PA2383.
10. Latorre M., Novelli F., Vagaggini B., Braido F., Papi A., Sanduzzi A. et al. Differences in the efficacy and safety among inhaled corticosteroids (ics)/long-acting beta2-agonists (LABA) combinations in the treatment of chronic obstructive pulmonary disease (COPD): Role of ICS. *Pulm. Pharmacol. Ther*. 2015;30:44–50. DOI: 10.1016/j.pupt.2014.10.006.
11. Ramakrishnan S. Prednisolone for COPD exacerbations: Time for a rethink. *ERJ Open Res*. 2023;9(5):00464–2023. DOI: 10.1183/23120541.00464-2023.
12. Melani A.S. Flunisolide for the treatment of asthma. *Expert Rev. Clin Pharmacol.* 2014;7(3):251–258. DOI: 10.1586/17512433.2014.908117.
13. Doymaz S., Ahmed Y.E., Francois D., Pinto R., Gist R., Steinberg M. et al. Methylprednisolone, dexamethasone orhydrocortisone for acute severe pediatric asthma: does itmatter? *J. Asthma*. 2021;59(3):590–596. DOI: 10.1080/ 02770903.2020.1870130.
14. Sellers A.R., Roddy M.R., Darville K.K., Sanchez-Teppa B., McKinley S.D., Sochet A.A. Dexamethasone for pediatric critical asthma: A multicenter descriptive study. *J. Intensive Care Med.* 2022;37(11):1520–1527. DOI: 10.1177/08850666221082540.
15. Kwda A., Gldc P., Baui B., Kasr K., Us H., Wijeratne S. et al. Effect of long term inhaled corticosteroid therapy on adrenal suppression, growth and bone health in children with asthma. *BMC Pediatr*. 2019;19(1):411. DOI: 10.1186/s12887-019-1760-8.
16. Allen D.B. Inhaled corticosteroids and endocrine effects in childhood. Endocrinology and Metabolism *Endocrinol. Meta.b Clin. North. Am.* 2020;49(4):651–665. DOI: 10.1016/j.ecl.2020.07.003.
17. Taldaev A.Kh., Nikitin I.D., Terekhov R.P., Selivanova I.A. Molecular docking: methodological approaches of risk assessment. *Drug Development & Registration*. 2023;12(2):206–210 (in Russ.). DOI: 10.33380/2305-2066-2023-12-2-206-210.
18. Jakubec D., Skoda P., Krivak R., Novotny M., Hoksza D. PrankWeb 3: accelerated ligand-binding site predictions for experimental and modelled protein structures. *Nucleic Acids Res.* 2022;50(W1). DOI: 10.1093/nar/gkac389.
19. Jendele L., Krivak R., Skoda P., Novotny M., Hoksza D. PrankWeb: A web server for ligand binding site prediction and visualization. *Nucleic Acids Res*. 2019;47(W1). DOI: 10.1093/nar/gkz424.
20. Krivák R., Hoksza D. P2Rank: Machine learning based tool for rapid and accurate prediction of ligand binding sites from protein structure. *J. Cheminfor*. 2018;10:39. DOI: 10.1186/s13321-018-0285-8.
21. Morris G.M., Huey R., Lindstrom W., Sanner M.F., Belew R.K., Goodsell D.S. et al. AUTODOCK4 and AutoDockTools4: Automated docking with selective receptor flexibility. *J. Comput. Chem.* 2009;30(16):2785–2791. DOI: 10.1002/jcc.21256.
22. Velázquez-Libera J.L., Durán-Verdugo F., Valdés-Jiménez A., Núñez-Vivanco G., Caballero J. LigRMSD: a web server for automatic structure matching and RMSD calculations among identical and similar compounds in protein-ligand docking. *Bioinformatics*. 2020;36(9):2912–2914. DOI: 10.1093/bioinformatics/btaa018.
23. Castro-Alvarez A., Costa A., Vilarrasa J. The performance of several docking programs at reproducing protein–macrolide-like crystal structures. *Molecules*. 2017;22(1):136. DOI: 10.3390/molecules22010136.
24. Schrödinger L., DeLano W. PyMOL. 2020. URL: http://www.pymol.org/pymol
25. Malkia A., Pertusa M., Fernández-Ballester G., Ferrer-Montiel A., Viana F. Differential role of the menthol-binding residue Y745 in the antagonism of thermally gated TRPM8 channels. *Mol. Pain*. 2009;3(5):62. DOI: 10.1186/1744-8069-5-62.
26. Bertamino A., Ostacolo C., Medina A., Di Sarno V., Lauro G., Ciaglia T. et al. Exploration of TRPM8 binding sites by β-carboline-based antagonists and their in vitro characterization and *in vivo* analgesic activities. *J. Med. Chem.* 2020;3(17):9672–9694. DOI: 10.1021/acs.jmedchem.0c00816.
27. Beccari A.R., Gemei M., Lo Monte M., Menegatti N., Fanton M., Pedretti A. et al. Novel selective, potent naphthyl TRPM8 antagonists identified through a combined ligand- and structure-based virtual screening approach. *Sci. Rep.* 2017;7(1):10999. DOI: 10.1038/s41598-017-11194-0.

Authors' information

Timkin Pavel D. – 1st-year Post-Graduate Student, Department of Chemistry, Amur State Medical Academy, Blagoveshchensk, timkin.pasha@mail.ru, http://orcid.org/0000-0001-6655-1049

Kotelnikov Danil D. – 3rd-year Student, Far Eastern State Agrarian University, Blagoveshchensk, danil.kotelnikov.02@mail.ru, http://orcid.org/0009-0003-5159-5796

Timofeev Eduard A. – 5th-year Student, Amur State Medical Academy, Blagoveshchensk, smileket@inbox.ru, http://orcid.org/0000-0002-3888-2091

Naumov Denis E. – Cand. Sci. (Med.), Head of the Laboratory for Molecular and Translational Research, Far Eastern Scientific Center for Physiology and Pathology of Respiration, Blagoveshchensk, denn1985@bk.ru, http://orcid.org/0000-0003-3921-8755

Borodin Evgeniy A. – Dr. Sci. (Med.), Professor, Department of Chemistry, Amur State Medical Academy, Blagoveshchensk, borodin54@mail.ru, http://orcid.org/0000-0002-0983-4541

(✉) **Timkin Pavel D.,** timkin.pasha@mail.ru

Received 16.01.2024;
approved after peer review 18.04.2024;
accepted 14.05.2024

УДК 616.5-003.93:616-001.4]-089.4:004.356.2
https://doi.org/10.20538/1682-0363-2024-4-145-157

The use of three-dimensional bioprinting for skin regeneration and wound healing (literature review)

Barsuk I.A.[1], Golovko K.P.[1, 2], Alexandrov V.N.[1, 3], Khasanov A.R.[1], Edgeev N.I.[4], Galiullin R.I. [4]

[1] *S.M. Kirov Military Medical Academy*
6, Akademika Lebedeva Str., Saint Petersburg, 194044, Russian Federation

[2] *Saint Petersburg State University*
7–9, Universitetskaya Embankment, Saint Petersburg, 199034, Russian Federation

[3] *Saint Petersburg State Pediatric Medical University*
2, Litovskaya Str., Saint Petersburg, 194100, Russian Federation

[4] *Branch No. 4 of Naval Clinical Hospital No. 1469*
22, Matrosa Ryabinina Str., Murmansk region, Zaozersk, 184310, Russian Federation

ABSTRACT

Three-dimensional (3D) bioprinting is rapidly proliferating across many medical disciplines and is making strides towards manufacturing intricate human organs for clinical application. One of the most promising areas in 3D bioprinting is development of bioinks with certain composition and designed properties.

The aim of this systematic review was to assess current biomedical research evidence regarding the efficacy of 3D bioprinting for skin regeneration and wound healing. A comprehensive search for all applicable original articles was conducted according to pre-established eligibility criteria. The study employed PubMed, Web of Science, Scopus, Medline Ovid, and ScienceDirect databases.

Of the retrieved articles, eighteen satisfied the inclusion criteria, while twenty-three were excluded. A total of 159 animals that had wound defects were considered in all animal-based research. Collagen and gelatin hydrogels were the most commonly employed bioinks. In relation to cellular composition, allogeneic fibroblasts and keratinocytes were predominant. The observation period ranged from one day to six weeks. Complete wound closure was achieved within 2–4 weeks in most animal studies. *In vitro* and *in vivo* animal studies have shown a positive effect of printed bioengineered constructs in accelerating wound healing. Notably, the research where bioprinting was performed directly in the wound *in situ* was of particular interest. Further studies are required to enhance the tissue bioprinting technique to address skin wound healing in animal models. The utilization of standardized parameters may pave the way for human clinical studies.

Keywords: 3D bioprinting, bioinks, biopolymers, wound healing, skin regeneration, wound dressings

Conflict of interest. The authors declare the absence of obvious or potential conflicts of interest related to the publication of this article.

Source of financing. The authors state that they received no funding for the study.

For citation: Barsuk I.A., Golovko K.P., Alexandrov V.N., Khasanov A.R., Edgeev N.I., Galiullin R.I. The use of three-dimensional bioprinting for skin regeneration and wound healing (literature review). *Bulletin of Siberian Medicine.* 2024;23(4):145–157. https://doi.org/10.20538/1682-0363-2024-4-145-157.

✉ *Barsuk Ilya A.,* barsuk20220@gmail.com

Использование трехмерной биопечати для регенерации кожи и заживления ран (обзор литературы)

Барсук И.А.[1], Головко К.П.[1, 2], Александров В.Н.[1, 3], Хасанов А.Р.[1], Едгеев Н.И.[4], Галиуллин Р.И.[4]

[1] Военно-медицинская академия (ВМА) им. С.М. Кирова
Россия, 194044, г. Санкт-Петербург, ул. Академика Лебедева, 6

[2] Санкт-Петербургский государственный университет (СПбГУ)
Россия, 199034, г. Санкт-Петербург, Университетская наб., 7/9

[3] Санкт-Петербургский государственный педиатрический медицинский университет (СПбГПМУ)
Россия, 194100, г. Санкт-Петербург, ул. Литовская, 2

[4] Филиал № 4 1469-го военно-морского клинического госпиталя
Россия, 184310, г. Заозерск, ул. Матроса Рябинина, 22

РЕЗЮМЕ

Трехмерная биопечать в настоящее время применяется в самых разных областях медицины, являясь движущей силой многих медицинских исследований. Эти исследования способствуют продвижению в область персонализированной медицины, включающих печать сложных человеческих органов для их использования в клинической практике. Одним из ведущих направлений в продвижении трехмерной биопечати является разработка биочернил определенного состава с заданными свойствами.

Цель настоящего систематического обзора состоит в анализе данных современных биомедицинских исследований, касающихся оценки эффективности использования трехмерной биопечати для регенерации кожи и заживления ран. Всеобъемлющий поиск всех релевантных оригинальных статей выполнили на основе заранее определенных критериев приемлемости. Поиск проводили с использованием платформ PubMed, Web of Science, Scopus, Medline Ovid и ScienceDirect.

В результате сужения области поиска из 2 256 статей отобрали 18, полностью соответствовавших критериям включения. Во все отобранные исследования было включено 159 животных с раневыми дефектами. В качестве биочернил чаще всего использовали коллагеновые и желатиновые гидрогели. В части клеточного компонента превалировали аллогенные фибробласты и кератиноциты. Период наблюдения колебался от 1 сут до 6 нед. В большинстве включенных исследований на животных полное закрытие раны достигалось через 2–4 нед.

Результаты как *in vitro*, так и *in vivo* показали положительное влияние напечатанных биоинженерных конструкций на ускорение заживления ран. Особый интерес представляет исследование, где биопечать выполняется непосредственно в ране *in situ*.

Проведенное исследование позволяет сделать вывод о необходимости отработки технологии биопечати тканей для лечения кожных ран на животных моделях с использованием стандартизированных параметров, чтобы открыть двери для клинических испытаний на людях.

Ключевые слова: 3D-биопринтинг, биочернила, биополимеры, заживление ран, регенерация кожи, раневые повязки

Конфликт интересов. Авторы декларируют отсутствие явных и потенциальных конфликтов интересов, связанных с публикацией настоящей статьи.

Источник финансирования. Авторы заявляют об отсутствии финансирования при проведении исследования.

Для цитирования: Барсук И.А., Головко К.П., Александров В.Н., Хасанов А.Р., Едгеев Н.И., Галиуллин Р.И. Использование трехмерной биопечати для регенерации кожи и заживления ран (обзор литературы). *Бюллетень сибирской медицины.* 2024;23(4):145–157. https://doi.org/10.20538/1682-0363-2024-4-145-157.

INTRODUCTION

Tissue injury is a significant medical problem, accounting for approximately half of the global annual health care expenditures [1]. Wound healing is a complex multistep process aimed at protecting and regenerating the damaged tissue area [2]. To avoid the development of adverse outcomes, it is essential to provide patient care and utilize appropriate dressings throughout this process. Although traditional wound coverings (e.g., gauze, lint, plasters, and bandages) protect the wound from contamination, these dressings require frequent changing to avoid infection and maceration of neighboring tissues. Additionally, they tend to adhere to the wound, making replacement traumatic and painful [3].

Additive manufacturing technologies offer a method for rapid wound healing, thereby avoiding common complications, such as wound contractures and scar formation [4]. Three-dimensional (3D) bioprinting is one of the emerging adaptive manufacturing technologies aimed at utilizing biocompatible materials, together with living cells and growth factors, to mimic and repair the extracellular matrix of human organs [5]. This approach allows for layer-by-layer printing of flexible hydrogel constructs by converting a digital computer-aided design (CAD) model into complex 3D structures [6].

The characteristics of the product obtained by 3D bioprinting are almost completely determined by the properties of the bioinks used. In this regard, bioinks are a key defining component of 3D bioprinting [7, 8].

In traditional 3D printing, ink is fed to the molding process as a melt at a high temperature (for plastics, ceramics, and alloys). However, such conditions are unacceptable for bioinks, which must meet high biocompatibility requirements to promote cell growth, be mechanically stable, and guarantee shape retention of the printed construct [9]. A number of parameters have a significant impact on high functional integrity of bioinks. These include cell load parameters (e.g. cell type, cell density, and incubation period), physicochemical properties (e.g. shear thinning, viscosity, degree of crosslinking, and gelation time), and printing parameters (e.g. nozzle temperature and diameter, feed rate, and printing duration) [10, 11]. Furthermore, the selection of cell type and source is of paramount importance to prevent immune rejection following implantation. Primary skin cells, including keratinocytes, melanocytes, and fibroblasts, can be properly isolated from donor skin and subsequently co-cultured during skin bioprinting [12, 13].

A variety of natural and synthetic polymeric hydrogels are utilized for bioink production [14]. Hydrogels are a class of cross-linked polymeric substances that are capable of absorbing and retaining a considerable amount of water. They are capable of absorbing water up to 1,000 times their original weight without dissolution [15]. It makes them an optimal choice for encapsulated cells due to their high permeability to oxygen, nutrients, and other water-soluble compounds. The ability of cells within the hydrogel to migrate and bind to each other through the porous network [16] is a key property that has enabled hydrogels to become one of the main materials for 3D bioprinting [17, 18].

Despite the lack of mechanical stability, 90% of the polymers used in bioprinting are derived from natural sources [19]. Natural-based biopolymers exhibit a number of advantages over synthetic biopolymers, due to their high similarity to the composition of the human extracellular matrix. This allows them to mimic the native cell microenvironment, facilitating cell attachment, proliferation, migration, and differentiation [20–22].

Following the widespread adoption of 3D bioprinting in the early part of the last decade, there was a clear need to identify printable biocompatible polymers that would enable the technology to be used in medicine. According to a citation report, the application of 3D bioprinting for wound healing and skin regeneration commenced in 2012, utilizing collagen bioinks. The number of studies in this field reached 12 in 2017 and 19 in 2019, with approximately 70 published studies by mid-2020. The majority of these studies employed natural-based polymers as the primary component of the bioinks.

The use of natural polymers in the manufacture of wound care products has been the subject of debate among researchers. While many of the drawbacks associated with these polymers have been identified and potential solutions proposed, no explicit agreement or decision has been reached.

The objective of this systematic review was to evaluate the efficacy of bioprinting using natural polymer-based bioinks as skin substitutes for skin tissue regeneration and wound healing. In addition to reporting the biological properties of bioprinted constructs in *in vitro* and *in vivo* studies, this review also provides recommendations for the use of such constructs in practice.

This review was conducted in accordance with the Preferred Reporting Items for Systematic Reviews and Meta-Analyses (PRISMA) checklist [18]. To identify relevant digital records from five electronic databases – RINC, PubMed, Web of Science, Scopus, and ScienceDirect – a comprehensive search strategy was employed.

The search query consisted of 18 terms, comprising two sets. The first set included "skin," "skin regeneration," "skin tissue engineering," "wound healing," "wound," "burns," and "wound." The second set included "3D bioprinting," "3D printing," "3D cell printing," "3D printing," "bioprinting," "3D scaffold," and "3D prototyping." This query was aimed at identifying 3D bioprinted skin substitutes as potential wound healing or skin regeneration agents.

The titles and abstracts of all identified records were pre-screened for potentially relevant research. Included entries were further screened by reading full texts to ensure eligibility. To be included, an article had to meet the following criteria: use of natural-based bioinks; actual *in vitro* or *in vivo* study; scaffold obtained by 3D bioprinting; original article written in Russian or English The following criteria were employed to exclude articles: isolated articles that consider the theoretical possibility of using 3D bioprinting; articles that describe synthetic bioinks; articles pertaining to chronic wounds; systematic and descriptive reviews, interpretations, case series, guidelines, and technical reports.

The following data were extracted from the included studies: 1 – information about the study (authors, year of publication, study design, database, and journal name); intervention details (biomaterials and cells used, gelation time, printing temperature, crosslinking materials and techniques, and printing methods); outcome details (rheological, mechanical, and biological characteristics, construct shape accuracy, and wound healing time).

The initial search yielded 4,345 articles, but after removing duplicates, 2,566 articles were selected for review. Following the screening of titles and abstracts, 2,499 records were excluded as they did not meet the inclusion criteria, leaving 18 articles for review. The main parameters identified for evaluation were as follows: study design, bioprinting and polymer crosslinking method, bioink base material, cellular component of bioinks, cell viability level after the printing process, and animals used for the experiment. The study characteristics and results are summarized in Table.

Table

Brief description and results of the selected studies

Study design	Bioinks	Cells / animals used	Conclusion	References
In vitro	Collagen – chitosan blend	NIH 3T3	When printing with inks of varying collagen / chitosan ratios, the optimal ink delivery rate was found to lie between 0.19 µl / s and 0.42 µl / s	[23]
In vitro	CNF/ GelMA	NIH 3T3	The CNF/GelMA scaffolds exhibited no cytotoxicity and demonstrated favorable cytocompatibility with 3T3 mouse fibroblasts	[27]
In vitro	Sulfated and rhamnose-rich XRU	HDFs	*In vitro* testing of the XRU hydrogel with human dermal fibroblasts (HDFs) revealed that the material exhibited high biocompatibility with a high cellular density and the capacity to promote active cell proliferation and attachment	[24]
In vitro	Suspension dSIS	HDFs	The dSIS scaffold developed in the study may be a promising candidate for the treatment of skin defects. Its high precision and high swelling ratio make it an attractive option for this purpose	[28]
In vitro	Viscoll native collagen	NIH 3T3	Viscoll advanced bioink permits the fabrication of intricate geometries without the necessity of chemical or photocrosslinking, thus ensuring the maintenance of the specified shape	[29]

End of table

Study design	Bioinks	Cells / animals used	Conclusion	References
In vitro	Alginate / Gelatin	AECs and WJMSCs	The human AECs demonstrated a superior epithelial cell phenotype, while the WJMSCs exhibited enhanced angiogenic and fibroblastic potential	[30]
In vitro and *in vivo*	BCNFs, SF/ Gelatin	L929 fibroblasts and 12 nude mice	The introduction of bacterial cellulose nanofibers had a minimal impact on the printing parameters of composite bioinks. The obtained data demonstrated that the porous structure exhibited favorable properties for nutrient supply to the forming tissues following *in vivo* implantation	[37]
In vivo	Fibrinogen, thrombin and collagen type I	HDFs, HEK 293 cells, and 36 female nude mice, along with six pigs	The use of three-dimensional *in situ* bioprinting of autologous cells was found to accelerate wound healing by approximately three weeks compared to other treatments	[35]
In vitro	CNF	HDFs	The utilization of a matrix generated through 3D printing, in contrast to 2D frames, facilitated accelerated cell proliferation, a crucial element in the process of rapid wound healing	[31]
In vitro	Sodium alginate / Gelatin	HDFs	The EDC-CaCl2 solution demonstrated enhanced cellular proliferation and was deemed more suitable for use as a dermal replacement	[32]
In vitro	Collagen	NIH 3T3, Vero cell line	The micro- and macropore structure of fibrillar collagen promoted high cell attachment and proliferation at 37 °C	[33]
In vitro and *in vivo*	S-dECM	HDFs, HEK 293 and 8 male BALB/ cA-nu nude mice	The fabricated S-dECM bioink demonstrated no cytotoxicity and exhibited high biocompatibility comparable to native type I collagen. The 3D-printed constructs with S-dECM bioink exhibited accelerated wound closure, neovascularization, and reliable blood flow at the implantation site	[38]
In vitro	Alginate / honey	NIH 3T3	The incorporation of approximately 1–2% honey into the bioprinted alginate resulted in enhanced cell proliferation without a significant impact on printability	[34]
In vitro	Gelatin	HDFs	The growth rate of HDFs was approximately 14% higher in G8–G12 gelatin scaffolds than in G6 gelatin scaffolds. The mechanical properties of the scaffolds are strongly dependent on the pore size	[25]
In vitro and *in vivo*	SS / GelMA	L929 fibroblast lineage, HDFs, HaCaT and 21 female Sprague Dawley rats	The incorporation of silk sericin (SS) into the matrices was demonstrated to facilitate cell growth in HDFs. The study also indicated that SS/GelMA is an appropriate substrate for cell cultures in human keratinocytes (HaCaT), as high cell viability was maintained even after seven days	[39]
In vitro and *in vivo*	G-SF-SO_3-FGF2	HDFs/ 36 male Sprague Dawley rats	The administration of 100 ng / ml FGF2 resulted in a 40% increase in the proliferation rate of the cells in question. The sulfated SF-coated scaffold facilitated cell adhesion, proliferation, and growth. The FGF2 growth factor enhanced re-epithelialization and also stimulated blood vessel formation and the expression of several relevant markers	[40]
In vivo	Gelatin – alginate	40 female mice	The use of gelatin – alginate has been demonstrated to reduce wound bleeding subsequent to implantation. Furthermore, the scaffold has been shown to facilitate granulation tissue maturation and wound healing	[36]
In vitro	Collagen	HDF и HEK 293	The study demonstrated that fibroblasts and keratinocytes can be printed in a sequential, layer-by-layer manner, resulting in dermo- and epidermal-like layers. The 3D printing technique offers a high degree of control over the shape and quality of the resulting engineered skin tissues	[26]

Note. NIH 3T3 – mouse embryonic fibroblast line; CNF – cellulose nanofibrils; GelMA – gelatin methacrylate; XRU – xylorhamno-uronic acid; HDFs – human dermal fibroblasts; dSIS – suspension of decellularized small intestinal submucosa; AECs – amniotic epithelial cells; WJMSCs – Wharton's jelly-derived mesenchymal stromal stem cells; BCNF – bacterial cellulose nanofibers; SF – silk fibroin; EDC –N-ethyl-N'-(3-dimethylaminopropyl)carbodiimide; Vero – cell lines from kidney epithelium taken from an African green monkey; S-dECM – extracellular matrix of cutaneous origin; HEK 293 – cell line derived from human embryonic kidneys; SS – silk sericin; HaCaT – human keratinocyte cell line; G-SF-SO3-FGF2 – gelatin-sulfated silk composite with fibroblast growth factor, 2-sulfonic acid group; CFFs – colony-forming fibroblasts.

DESIGN OF INCLUDED STUDIES

The primary categorization of papers was based on the study design. Twelve studies were conducted *in vitro* [23–34], while two were conducted *in vivo* [35, 36]. Four studies were conducted in both *in vitro* and *in vivo* settings [37–40].

METHODS FOR BIOPRINTING AND POLYMER CROSSLINKING

The extrusion-based bioprinting technique was the most prevalent, with only two studies reporting the use of inkjet bioprinting [26, 35]. Various crosslinking techniques were employed, with only six studies [29, 33, 34, 35, 37, 38] reporting the absence of crosslinking agents. The following methods were utilized:

1. Crosslinking by chemical reagent: Ca2+ [27, 30, 31], CaCl2 [32, 36], 1-ethyl-3-(3-dimethylaminopropyl) carbodiimide (EDC) [28], N-hydroxysuccinimide-1-ethyl-3-(3-dimethylaminopropyl) carbodiimide (EDC-NHS) [23, 25, 32, 40], nebulized sodium bicarbonate (NaHCO3) [26], 1,4-butanediol diglycidyl ether (BDDE) [31].

2. Crosslinking by physical exposure to: UV [24, 27, 39] or cooling [30, 32].

BIOINK BASE MATERIAL

The vast majority of the bioink base materials utilized were a combination of gelatin and collagen hydrogels. While gelatin hydrogel exhibited optimal rheological properties, it demonstrated zero viscosity at temperatures above 27 ± 1 °C [25], and all gelatin studies investigated the use of different crosslinking agents [25, 27, 30, 32, 36, 37, 39, 40]. In contrast, four studies reported the ability to print collagen hydrogel without the need for chemical crosslinking agents [25, 33, 35, 38]. Furthermore, the integration of alginate hydrogel with gelatin [30, 32, 36] or honey [34] has also been reported.

USE OF CELL CULTURES

In general, *in vitro* studies tend to utilize fibroblasts as a cellular component. Among the various types of fibroblasts, human dermal fibroblasts (HDFs) were employed most frequently [24–26, 28, 31, 32, 35, 38–40]. The T3T [23, 27, 29, 33, 34] and L929 [37, 39] mouse fibroblast lines were used in a similar number of studies.

The human epidermal keratinocytes (HEK)/human keratinocyte cell line (HaCaT) was used in four studies [26, 35, 38, 39]. Wharton's jelly-derived mesenchymal stromal stem cells (WJMSC) and amniotic epithelial cells (AECs) were used in one study [30], Vero epithelial cells were also described in one study [33].

CELL VIABILITY RATE AFTER BIOPRINTING

It is believed that high-tech materials based on natural-based polymers exhibit superior biological properties. Of the 16 *in vitro* studies that have been conducted, 13 reported high cell proliferation rates. However, three studies [23, 26, 39] did not demonstrate a significant change in proliferation rates, yet reported high cell viability. Seven studies reported good cell viability [24, 26, 28, 29, 33, 34, 37]. Five studies reported minimal cell viability, with values ranging from 85.07 to 98% [26, 29, 30, 33, 38]. One study reported the appearance of dead cells, indicating low cell viability [28].

Furthermore, 14 studies reported high cell growth rates, and only a decellularized small intestinal submucosa suspension (dSIS) [28] and silk sericin / methacrylate gelatin-based bioink (SS/GelMA) [39] did not promote cell growth. All *in vivo* results were consistent with *in vitro* studies, with the exception of SS/GelMA [39], which demonstrated good healing properties in wounds two weeks after their treatment.

ANIMALS USED FOR THE EXPERIMENT

A total of 159 animals were used in animal studies, with each study including between 8 and 40 animals. Four studies employed mice [35–38], two studies employed rats [39, 40], and one study employed pigs [35].

REVIEW OF INCLUDED STUDIES

The results of 18 *in vitro* cell culture and *in vivo* animal studies indicate that 3D bioprinted natural polymer constructs can promote complete closure of skin wounds. The majority of 3D bioprinted skin substitutes demonstrated the ability to promote cell proliferation, adhesion, and differentiation, and the majority of *in vitro* studies reported high cell viability. Furthermore, all animal studies demonstrated reduction in wound area in animals two weeks after surgery. Nevertheless, it is

important to acknowledge the technical challenges and practical limitations of assessing cell viability *in vitro* and wound dynamics in *in vivo* animal studies. These factors must be taken into account when considering the potential clinical applications of such technologies.

The primary objective of employing 3D bioprinting in the context of wound healing is to facilitate rapid treatment of directly damaged tissues *in situ*. In a study conducted by [35], bioprinting was performed using a combination of fibrinogen and thrombin bioink with type I collagen, comprising cells from the mouse embryonic fibroblast line (HDFs) and human embryonic kidney-derived cell line (HEK 293).

This approach was employed directly on a wound in the back region of mice and pigs. Marker dots were applied around the wound, after which it was scanned with a handheld scanner. Based on the wound scan data, an STL file was generated for the bioprinter, which included information on the planimetry of the points for the movement of the bioprinter nozzle. This is necessary for volumetric filling of the wound during the bioprinting process.

This approach, as demonstrated in the conducted experiment, resulted in significant acceleration of the wound healing process, with an estimated three-week reduction in healing time compared to other treatment methods. The immunohistochemical analysis revealed the presence of HDFs and HEK 293 cells in the dermis and epidermis of the wound at three to six weeks post-surgery, in addition to endogenous cells.

BASIC 3D BIOPRINTING METHOD

As previously stated, the predominant method employed in the reviewed works for 3D bioprinting was extrusion printing, with only two studies utilizing inkjet printing. This pattern is logical, given that extrusion printing is technically the simplest method and allows for the printing of viscous bioinks (30 mPa·s to 6 x 10^7 mPa·s) with high cell density [41, 42]. In comparison to other methods, extrusion printing is associated with several disadvantages. These include a relatively low resolution (2000–1000 μm), potential nozzle clogging, and reduced cell viability at high printing speed, due to increased pressure in the extruder, which can lead to cell membrane damage [41, 43, 44]. Given that optimal printing rates do not lead to cell damage and there is no need for high resolution, coupled with lower equipment costs, extrusion printing remains the method of choice for creating bioengineered constructs for the treatment of skin defects.

MATERIALS FOR BIOINKS

A variety of bioinks have been employed in the studies, including single-component bioinks and composite bioinks comprising multiple components. The materials utilized in the form of hydrogels possess necessary physicochemical properties for printing and exhibit a high degree of similarity to the natural extracellular matrix of the skin, thereby providing them with high biocompatibility [14].

Collagen. Collagen hydrogel has demonstrated the required biodegradation (about 30 days), high shape stability at 37 °C, and excellent micro- and macropore structure that promote cell attachment and proliferation [33]. However, direct 3D bioprinting of collagen is still limited due to physical properties of a collagen solution, which make it poorly suitable for printing, especially when cells or tissue spheroids are incorporated [29]. Notably, despite the limited printing capabilities of pure collagen, most studies have not utilized chemical crosslinking. Instead, various methods have been employed, including mixing with other materials (fibrinogen and thrombin [35], chitosan [23]), using fibrillar collagen [33], using low concentrations of collagen (2–4%) [29], and adjusting the density of bioink by dosing the amount of cell suspension injected [26].

In the same context, the gelation of matrix proteins, such as collagen, is typically initiated by controlling pH, temperature, or both. However, this approach is only valid for thin structures (less than 1 mm) due to the limitations of diffusion or heat transfer in thick structures (1 to 3 mm). Consequently, ungelatinized regions are observed in the printed structure. The utilization of elevated pH or temperature to achieve the aforementioned outcome is not always feasible, as it may result in significant cellular damage within the solution [26].

Gelatin. Gelatin is a denatured form of collagen protein [45]. At low temperatures, gelatin filaments form helical structures, which result in a gel-like form [46]. Gelatin retains the Arg-Gly-Asp sequence and, in contrast to its predecessor, is less immunogenic

and promotes cell adhesion, differentiation, and proliferation [47]. However, pure gelatin solutions exhibit poor mechanical strength and low viscosity at temperatures above 27 ± 1°C, which limits their use in 3D bioprinting.

To overcome this limitation, gelatin is frequently combined with other natural biomaterials, such as alginate [30, 32, 36] and silk fibroin (SF) [37], to enhance its formability. Moreover, gelatin methacrylate (GelMA) is a promising candidate for wound-healing bioinks due to its high heat sensitivity and photocrosslinking ability. GelMA is also known to have good biocompatibility and to promote intercellular interaction and cell migration. Furthermore, the favorable mechanical stability of GelMA after UV crosslinking has been exploited to provide high shape accuracy of composite bioinks, where cellulose nanofibrils [27] and silk sericin [24] were used as the second component.

Alginate. Alginate is a polysaccharide consisting of β-mannuronate and its C-5 epimer α-L-gluronate [48]. It is a popular hydrogel used in bioprinting due to its biocompatibility, the possibility of various crosslinking options, and the ease of use [49]. However, alginate has several limitations. Delayed crosslinking can reduce the shape accuracy of bioprinted constructs, while rapid crosslinking limits the interaction of cells with the material, reducing their further viability.

One study attempted to overcome these limitations by reducing the viscosity of alginate through the addition of honey. It was hypothesized that the inclusion of honey would allow to increase cell viability without altering the printability of the alginate. Even printing with simple alginate solutions was found to have poor shape accuracy. Researchers have attempted to increase the viscosity of alginate or extrude it with chemical crosslinking agents, such as calcium ions (Ca2+) [30].

Skin decellularized extracellular matrix (S-dECM). The extracellular matrix (ECM) is the non-cellular component of a tissue or an organ. It is a network of microenvironments that allows cells to perform their functions. Every tissue has a well-constructed ECM composed of several components that maintain the native structure and promote cell migration. Interestingly, ECM can be obtained with an appropriate protocol and used as a matrix for tissue regeneration [50].

In one of the studies reviewed, the authors successfully decellularized pig skin and generated printable dECM-based bioink from it. In an *in vitro* study, they found that compared to collagen-based bioink, 3D bioprinted skin equivalent using dECM-based bioink promoted dermal stabilization, improved epidermal organization, and provided physiologically important skin functions. Furthermore, dECM-based 3D skin encapsulated endothelial progenitor cells (EPCs) and atypical squamous cells (ASCs) demonstrated the capacity to promote neovascularization and re-epithelialization, which was evidenced by accelerated wound healing *in vivo* [38].

MAIN PARAMETERS OF BIOINKS AFFECTING CELL VIABILITY

The biocompatibility of bioprinting materials has been extensively studied, and a number of factors that may affect cell viability, adhesion, proliferation, migration, and differentiation have been identified. In general, cytotoxicity is the primary criterion to be evaluated when considering a potential material for medical use. The majority of the included studies employed a colorimetric test to assess the metabolic activity of cells (MTT assay), thereby ensuring that there was no cytotoxicity or inflammation caused by chemical interaction between the cell and the material. Notably, only silk sericin / BioVernyl GelMA induced acute inflammation on day 7, which disappeared at the end of the observation period [39].

An additional property of bioinks is the size of pores formed in printed structures during crosslinking of hydrogels or lyophilization of samples. Small pore sizes result in a lack of nutrition and oxygen supply to the cells, which in turn leads to slower cell migration and low viability. The effect of gelatin hydrogel pore size on cell behavior was studied. The study revealed that a pore size of 580 μm led to a 14% increase in the proliferation rate of HDFs after 14 days in comparison to 435-μm pores [25]. Furthermore, the use of natural bioinks offers a favorable intermolecular network. For instance, it is well established that fibrillar collagen possesses an optimal micro- and macropore structure, which has been demonstrated to facilitate robust cell attachment and proliferation, ultimately enhancing cell viability [33].

A crucial aspect of bioinks is the concentration of their primary structural component. This parameter has a profound impact on cell viability, as high concentrations lead to cellular compaction and, consequently, reduction in cell viability. The effect of varying the concentration of Viscoll brand collagen on cell viability was evaluated. The results demonstrated that reduction of the collagen concentration from 4 to 2% led to an increase in cell viability from 87.2 ± 2.1 to 97.2 ± 1.2% ($p < 0.05$) [29].

Another group of authors studied the effect of using a lower-molecular-weight collagen extract on the viability of the mouse embryonic fibroblast cell line (NIH 3T3). Their findings indicated that decreasing the concentration of the extract from 100 to 25% resulted in an increase in cell viability from 85.07 ± 6.73 to 111.31 ± 3.65% ($p < 0.05$) [33]. Another study sought to examine the impact of combining low concentrations of GelMA with cellulose nanofibrils (CNF) on cell proliferation. The results indicated that three days after culture, the number of cells on the CNF/GelMA composite bioink was approximately twice that observed on CNF bioink alone [27].

The density of the cell suspension is another critical factor. As previously described, the use of higher cell counts (greater than 1 million cells per ml) results in reduced cell viability. There is evidence for the use of an inkjet bioprinting system and a study on the effect of using different cell suspension densities and droplet sizes on cell viability. The study demonstrated that cell viability is proportional to cell suspension density and inversely proportional to the space between droplets for both keratinocytes and skin fibroblasts. At very low cell suspension density (0.5 million cells / ml) and large droplet spacing (400 nm), fibroblast viability was moderate (84%). This is likely due to the lack of intercellular communication at relatively low surface coverage. Similarly, at high cell suspension density (5 million cells / ml) and small droplet spacing during printing (400 μm), keratinocyte viability was equal (94%). The highest cell viability rates (98–99%) were achieved using cell suspension density of 1–2 million cells / ml and droplet spacing of 200 nm [26]. In addition, the thickness of the printed structure exerts a significant effect on cell adhesion. The percentage of cell attachment was found to be higher in 3-mm-thick samples than in 2-mm-thick samples. It was demonstrated that a thicker scaffold promoted cell adhesion [31].

Conversely, growth factors, crucial morphogenetic proteins that influence cell activity and guide tissue repair and regeneration, cannot be overlooked [51]. Published data indicate that the addition of 100 ng / ml of fibroblast growth factor (FGF2) to bioink significantly increases the proliferation rate (from ~40 to ~75%), improves the morphology of the construct (approaching the structure of native tissue), and accelerates the assembly of native collagen fibrils responsible for the formation of the ECM of the skin [40]).

THE STRUCTURE AND MECHANICAL PROPERTIES OF THE OBTAINED BIOENGINEERED CONSTRUCTS

Materials utilized for bioprinting should possess acceptable mechanical properties and should not collapse after printing. Additionally, they should have a high swelling coefficient to facilitate moisture and air exchange in the wound area, metabolism, and cell proliferation. According to published literature, human skin exhibits an average modulus of elasticity, with values ranging from 100 to 1,100 kPa [38]. The degree of swelling is inversely proportional to Young's modulus values. Nevertheless, an increase in the fiber spacing of decellularized small intestinal submucosa (dSIS) suspension from 500 to 700 μm has been observed to result in a notable increase in the degree of swelling from 69 to 79% and a simultaneous decrease in the Young's modulus from 26.6 ± 3.8 to 9.7 ± 3.1 kPa ($p < 0.05$) [24]. Similar outcomes were observed in studies that employed a crosslinked solution of cellulose nanofibrils (CNF) [31] and a crosslinked solution of alginate with gelatin [32].

It is essential that the bioinks retain their shape after leaving the tip of the printing nozzle. In general, proper hydrogel viscosity ensures high form accuracy and minimizes the possibility of structural failure after printing [36]. Another important parameter is sheer thinning. Bioinks must have a strictly defined thixotropic effect to avoid nozzle clogging during extrusion and to allow for structural consistency recovery after printing to be ready for the next layer [23, 30, 31]. For instance, collagen

requires approximately one minute to transit to a gel-like state and maintain a solid base for printing the subsequent layer [26]. Additionally, the stiffness of the printed scaffolds has been demonstrated to significantly influence cell proliferation. For instance, as CNF stiffness increased within the range of 3–8 kPa, cell proliferation was accelerated [31].

WOUND CARE IN ANIMAL MODELS

A high rate of wound healing is crucial to avoid prolonged treatment and the formation of hypertrophic scars. The success of using the new material as a wound treatment agent is primarily determined by its high biocompatibility and a lack of cytotoxicity *in vitro*. With further study, the material under consideration should stimulate wound healing and tissue re-epithelialization *in vivo.* The use of bioprinted constructs with the addition of human cell lines has been demonstrated to accelerate wound healing in animal models by approximately three weeks compared to other methods [35].

Implantation of skin constructs with the correct pore size and structure has been shown to significantly influence the nutrition supply and cell growth in the wound area [37]. Uniform and as early as possible application of the printed coating has been shown to maximally reduce the formation of scar tissue in the wound area. It has been demonstrated that the application of a scaffold of gelatin – sulfated silk composite containing fibroblast growth factor (G-SF-SO3-FGF2) to the back of wounded rats resulted in the wound surface becoming smoother after surgery. Furthermore, cross-sectional results indicated that the wound had completely closed, accompanied by the presence of more blood vessels [40]. Furthermore, the histologic examination of a cross-section of the SS/GelMA-treated wound seven days after surgery demonstrated the formation of new collagen accompanied by high fibroblast proliferation, which was comparable to that observed in healthy tissue. This was followed by complete wound closure at week 4 [39].

It is also important to note that the integration of a new tissue or organ into the surrounding tissue or cavity of a bio-object necessitates the presence of an appropriate vascular network. To address this challenge, researchers have employed a range of techniques, including the addition of growth factors that stimulate vascularization [40], the use of a network of interconnected pores with a diameter of 50 to 500 μm and micropores with a diameter of less than 10 μm [33], and the incorporation of skin decellularized extracellular matrix [38].

CONCLUSION

This review presents an analysis of scientific studies conducted *in vitro* on cell cultures and *in vivo* on animals. The aim was to ascertain the possibility of creating a skin substitute using 3D bioprinting. The review first confirms the significant advantages of using extrusion bioprinting with natural-based biopolymers for skin repair and regeneration. The majority of obtained images using this technology demonstrated an excellent ability to mimic the 3D structure of the native skin tissue microenvironment and promote cell adhesion, proliferation, and migration. *In vivo* visualization revealed that the use of a bioprinted construct with well-organized dermal and epidermal layers resulted in complete wound closure four weeks after surgery. Additionally, high significance of different properties of bioinks should be noted, as they greatly impact the acceleration of wound healing.

Despite the limited number of studies conducted, *in situ* bioprinting is one of the most promising advances in skin tissue engineering. It can be utilized by surgeons to efficiently and rapidly print complex organs. However, the main challenge lies in the difficulty of accurately constructing tissue parts. This requires integration of various fields of science, including not only medicine and biology, but also engineering, chemistry, and even IT. In addition, some new polymer crosslinking techniques, such as two-photon crosslinking and UV radiation directed at the nozzle tip, can help improve the speed and accuracy of printing with existing bioinks. Vascularization-prepared scaffolds are of particular interest because they retain their pre-vascularized microstructure after printing and, even when used without cells, are rapidly repopulated with autologous cells due to stimulation of the recipient's regenerative processes.

It is regrettable that the use of 3D bioprinting for wound healing is still being studied in animals. A meta-analysis of the available literature did not identify any randomized human clinical

trials. Another significant issue is that the time of observation and measurement, the cell lines used, the type and number of animals used, the severity and area of the wounds inflicted, and the method of application vary from study to study, contributing to high heterogeneity of results.

REFERENCES

1. Sen C.K. Human wounds and its burden: an updated compendium of estimates. *Adv. Wound Care.* 2019;8(2):39–48. DOI: 10.1089/wound.2019.0946.
2. Beldon P. Basic science of wound healing. *Surgery.* 2010;28(9):409–412. DOI: 10.1016/j.mpsur.2010.05.007
3. Dhivya S., Padma V.V., Santhini E. Wound dressings – a review. *BioMedicine.* 2015;5(4):22. DOI: 10.7603/s40681-015-0022-9.
4. Chouhan D., Dey N., Bhardwaj N., Mandal B.B. Emerging and innovative approaches for wound healing and skin regeneration: status and advances. *Biomaterials.* 2019;216:119267. DOI: 10.1016/j.biomaterials.2019.119267.
5. Ferry P.W. Melchels, Marco A.N. Domingos, Travis J. Klein, Jos Malda, Paulo J. Bartolo, Dietmar W. Hutmacher. Additive manufacturing of tissues and organs. *Prog. Polym. Sci.* 2012;37(8):1079–1104. DOI: 10.1016/j.progpolymsci.2011.11.007.
6. He P., Zhao J., Zhang J., Li B., Gou Z., Gou M., Li X. Bioprinting of skin constructs for wound healing. *Burn. Trauma.* 2018;6:5. DOI: 10.1186/s41038-017-0104-x.
7. Groll J., Burdick J.A., Cho D.W., Derby B. Gelinsky M., Heilshorn S.C., Jüngst T. et al. A definition of bioinks and their distinction from biomaterial inks. *Biofabrication.* 2019;11(1):013001. DOI: 10.1088/1758-5090/aaec52.
8. Cui H., Nowicki M., Fisher J.P., Zhang L.G. 3D bioprinting for organ regeneration. *Advanced Healthcare Materials.* 2017;6(1):1601118. DOI:10.1002/adhm.201601118.
9. Gopinathan J., Noh I. Recent trends in bioinks for 3D printing. *Biomater. Res.* 2018;22:1–15. DOI: 10.1186/s40824-018-0122-1.
10. Panwar A., Tan L.P. Current status of bioinks for micro-extrusion-based 3D bioprinting. *Molecules.* 2016;21(6):685. DOI: 10.3390/molecules21060685.
11. Xia Z., Jin S., Ye K. Tissue and organ 3D bioprinting. *SLAS Technol.* 2018;23(4):301–314. DOI: 10.1177/24726 30318760515.
12. Ng W.L., Wang S., Yeong W.Y., Naing M.W. Skin bioprinting: impending reality or fantasy? *Trends Biotechnol.* 2016;34(9):689–699. DOI: 10.1016/j.tibtech.2016.04.006.
13. Kumar A., Starly B. Large scale industrialized cell expansion: Producing the critical raw material for biofabrication processes. *Biofabrication.* 2015;7(4):44103. DOI: 10.1088/1758-5090/7/4/044103.
14. Griffith L.G., Swartz M.A. Capturing complex 3D tissue physiology in vitro. *Nature Reviews Molecular Cell Biology.* 2006;7(3):211–224. DOI: 10.1038/nrm1858.
15. Ahmed E.M. Hydrogel: preparation, characterization, and applications: A review. *J. Adv. Res*. 2015;6(2):105–121. DOI: 10.1016/j.jare.2013.07.006.
16. Yamamoto M., James D., Li H., Butler J., Rafii S., Rabbany S. Generation of stable co-cultures of vascular cells in a honeycomb alginate scaffold. *Tissue Engineering. Part A*. 2010;16(1):299–308. DOI: 10.1089/ten.TEA.2009.0010.
17. Thomas B.H., Craig Fryman J., Liu K., Mason J. Hydrophilic-hydrophobic hydrogels for cartilage replacement. *Journal of the Mechanical Behavior of Biomedical Materials.* 2009;2(6):588–595. DOI: 10.1016/j.jmbbm.2008.08.001.
18. Zhu J., Marchant R.E. Design properties of hydrogel tissue-engineering scaffolds. *Expert Review of Medical Devices*. 2011;8(5):607–626. DOI: 10.1586/erd.11.27.
19. Montero F.E., Rezende R.A., da Silva J.V., Sabino M.A. Development of a smart bioink for bioprinting applications. *Front. Mech. Eng.* 2019;5(56):1–12. DOI: 10.3389/fmech.2019.00056.
20. Valot L., Martinez J., Mehdi A., Subra G. Chemical insights into bioinks for 3D printing. *Chem. Soc. Rev.* 2019;48(15):4049–4086. DOI: 10.1039/C7CS00718C.
21. Kim J.E., Kim S.H., Jung Y. Current status of three-dimensional printing inks for soft tissue regeneration. *Tissue Eng. Regen. Med.* 2016;13(6):636–646. DOI: 10.1007/s13770-016-0125-8.
22. Liberati A., Altman D.G., Tetzlaff J., Mulrow C., Gøtzsche P.C., Ioannidis J.P. et al. The PRISMA statement for reporting systematic reviews and meta-analyses of studies that evaluate health care interventions: Explanation and elaboration. *J. Clin. Epidemiol.* 2009;62(10):e1–34. DOI: 10.1016/j.jclinepi.2009.06.006.
23. Heidenreich A.C., Pérez-Recalde M., González Wusener A., Hermida É.B. Collagen and chitosan blends for 3D bioprinting: A rheological and printability approach. *Polym. Test.* 2020;82:106297. DOI: 10.1016/j.polymertesting.2019.106297.
24. Xu W., Molino B.Z., Cheng F., Molino P.J., Yue Z., Su D. et al. On low-concentration inks formulated by nanocellulose assisted with gelatin methacrylate (GelMA) for 3D printing toward wound healing application. *ACS Appl. Mater. Interfaces.* 2019;11(9):8838–8848. DOI: 10.1021/acsami.8b21268.
25. Chen X., Yue Z., Winberg P.C., Dinoro J.N., Hayes P., Beirne S., Wallace G.G. Development of rhamnose-rich hydrogels based on sulfated xylorhamno-uronic acid toward wound healing applications. *Biomater. Sci.* 2019;7(8):3497–3509. DOI: 10.1039/C9BM00480G.
26. Shi L., Hu Y., Ullah M.W., Ullah I., Ou H., Zhang W. et al. Cryogenic free-form extrusion bioprinting of decellularized small intestinal submucosa for potential applications in skin tissue engineering. *Biofabrication.* 2019;11(3):035023. DOI: 10.1088/1758-5090/ab15a9.
27. Osidak E.O., Karalkin P.A., Osidak M.S., Parfenov V.A., Sivogrivov D.E., Pereira F.D.A.S. et al. Viscoll collagen solution as a novel bioink for direct 3D bioprinting. *J. Mater. Sci. Mater. Med.* 2019;30(3):31. DOI: 10.1007/s10856-019-6233-y.
28. Liu P., Shen H., Zhi Y., Si J., Shi J., Guo L. et al. 3D bioprinting and in vitro study of bilayered membranous construct with human cells-laden alginate/gelatin composite hydrogels. *Colloids Surfaces B Biointerfaces.* 2019;181:1026–1034. DOI: 10.1016/j.colsurfb.2019.06.069.

29. Huang L., Du X., Fan S., Yang G., Shao H., Li D. et al. Bacterial cellulose nanofibers promote stress and fidelity of 3D-printed silk based hydrogel scaffold with hierarchical pores. *Carbohydr. Polym.* 2019;221:146–156. DOI: 10.1016/j.carbpol.2019.05.080.
30. Albanna M., Binder K.W., Murphy S.V., Kim J., Qasem S.A., Zhao W. et al. *In situ* bioprinting of autologous skin cells accelerates wound healing of extensive excisional full-thickness wounds. *Sci. Rep.* 2019;9(1):1–15. DOI: 10.1038/s41598-018-38366-w.
31. Xu C., Zhang Molino B., Wang X., Cheng F., Xu W., Molino P. et al. 3D printing of nanocellulose hydrogel scaffolds with tunable mechanical strength towards wound healing application. *J. Mater. Chem. B.* 2018;6(43):7066–7075. DOI: 10.1039/C8TB01757C.
32. Shi L., Xiong L., Hu Y., Li W., Chen Z.C., Liu K. et al. Three-dimensional printing alginate/gelatin scaffolds as dermal substitutes for skin tissue engineering. *Polym. Eng. Sci.* 2018;58(10):1782–1790. DOI: 10.1002/pen.24779.
33. Nocera A.D., Comín R., Salvatierra N.A., Cid M.P. Development of 3D printed fibrillar collagen scaffold for tissue engineering. *Biomed. Microdevices.* 2018;20(2):1–13. DOI: 10.1007/s10544-018-0270-z.
34. Kim B.S., Kwon Y.W., Kong J.S., Park G.T., Gao G., Han W. et al. 3D cell printing of *in vitro* stabilized skin model and in vivo pre-vascularized skin patch using tissue-specific extracellular matrix bioink: A step towards advanced skin tissue engineering. *Biomaterials.* 2018;168:38–53. DOI: 10.1016/j.biomaterials.2018.03.040.
35. Datta S., Sarkar R., Vyas V., Bhutoria S., Barui A., Chowdhury A.R. et al. Alginate-honey bioinks with improved cell responses for applications as bioprinted tissue engineered constructs. *J. Mater. Res.* 2018;33:2029–2039. DOI: 10.1557/jmr.2018.202.
36. Dong J.C., Sang J.P., Bon K.G., Young-Jin K., Seok C., Chun-Ho K. Effect of the pore size in a 3D bioprinted gelatin scaffold on fibroblast proliferation. *J. Ind. Eng. Chem.* 2018;67:388–395. DOI: 10.1016/j.jiec.2018.07.013.
37. Chen C.S., Zeng F., Xiao X., Wang Z., Li X.L., Tan R.W. et al. Three-dimensionally printed silk-sericin-based hydrogel scaffold: a promising visualized dressing material for real-time monitoring of wounds. *ACS Appl. Mater. Interfaces.* 2018;10(40):33879–33890. DOI: 10.1021/acsami.8b10072.
38. Xiong S., Zhang X., Lu P., Wu Y., Wang Q., Sun H. et al. A Gelatin-sulfonated silk composite scaffold based on 3D printing technology enhances skin regeneration by stimulating epidermal growth and dermal neovascularization. *Sci. Rep.* 2017;7(1):1–12. DOI: 10.1038/s41598-017-04149-y.
39. Liu J., Chi J., Wang K., Liu X., Gu F. Full-thickness wound healing using 3D bioprinted gelatin-alginate scaffolds in mice: A histopathological study. *Int. J. Clin. Exp. Pathol.* 2016;9:11197–11205.
40. Lee V., Singh G., Trasatti J.P., Bjornsson C., Xu X., Tran T.N. et al. Design and fabrication of human skin by three-dimensional bioprinting. *Tissue Eng. Part C Methods.* 2014;20(6):473–484. DOI: 10.1089/ten.tec.2013.0335.
41. Guillemot F., Mironov V., Nakamura M. Bioprinting is coming of age: report from the international conference on bio printing and bio fabrication in Bordeaux (3B'09). *Biofabrication.* 2010;2(1):010201. DOI: 10.1088/1758-5082/2/1/010201.
42. Peltola S.M., Melchels F.P., Grijpma D.W., Kellomäki M. A review of rapid prototyping techniques for tissue engineering purposes. *Ann. Med.* 2008;40(4):268–280. DOI: 10.1080/07853890701881788.
43. Malda J., Visser J., Melchels F.P., Jüngst T., Hennink W.E., Dhert W.J. et al. 25th anniversary article: Engineering hydrogels for biofabrication. *Advanced materials (Deerfield Beach, Fla.)*. 2013;25(36):5011–5028. DOI: 10.1002/adma.201302042.
44. Chang R., Nam J., Sun W. Effects of dispensing pressure and nozzle diameter on cell survival from solid freeform fabrication-based direct cell writing. *Tissue Eng. Part A*. 2008;14(1):41–48. DOI: 10.1089/ten.a.2007.0004.
45. Gaspar-Pintiliescu A., Stefan L.M., Anton E.D., Berger D., Matei C., Negreanu-Pirjol T. et al. Physicochemical and biological properties of gelatin extracted from marine snail *Rapana venosa. Marine Drugs.* 2019;17(10):589. DOI: 10.3390/md17100589.
46. Chiou B., Avena-Bustillos R.D., Bechtel P.J., Jafri H., Narayan R., Imama S.H. et al. Cold water fish gelatin films: Effects of cross-linking on thermal, mechanical, barrier, and biodegradation properties. *European Polymer Journal*. 2008;44(11):3748–3753. DOI: 10.1016/j.eurpolymj.2008. 08.011.
47. Sakai S., Hirose K., Taguchi K., Ogushi Y., Kawakami K. An injectable, in situ enzymatically gellable, gelatin derivative for drug delivery and tissue engineering. *Biomaterials.* 2009;30(20):3371–3377. DOI: 10.1016/j.biomaterials.2009.03.030.
48. Jung H., Pena-Francesch A., Saadat A., Sebastian A., Kim D.H., Hamilton R.F. et al. Molecular tandem repeat strategy for elucidating mechanical properties of high-strength proteins. *Proceedings of the National Academy of Sciences of the United States of America.* 2016;113(23):6478–6483. DOI: 10.1073/pnas.1521645113.
49. Ozbolat I.T., Hospodiuk M. Current advances and future perspectives in extrusion-based bioprinting. *Biomaterials.* 2016;76:321–343. DOI: 10.1016/j.biomaterials.2015.10.076.
50. Dzobo K., Motaung K.S.C.M., Adesida A. Recent trends in decellularized extracellular matrix bioinks for 3D printing: An updated review. *Int. J. Mol. Sci.* 2019;20(18):4628. DOI: 10.3390/ijms20184628.
51. Mitchell A.C., Briquez P.S., Hubbell J.A., Cochran J.R. Engineering growth factors for regenerative medicine applications. *Acta Biomater.* 2016;30:1–12. DOI: 10.1016/j.actbio.2015.11.007.

Authors' contribution

All authors participated in the conception and design of the study; primary search, analysis and interpretation of the data, critical revision of the manuscript for important intellectual content, and final approval of the article for publication.

Authors' information

Barsuk Ilya A. – Assistant, Research Department (Biomedical Research), Research Center, S.M. Kirov Military Medical Academy, Saint Petersburg, barsuk20220@gmail.com, http://orcid.org/0000-0002-3728-9966

Golovko Konstantin P. – Dr. Sci. (Med.), Associate Professor, Head of the Research Center, S.M. Kirov Military Medical Academy, Saint Petersburg, labws@mail.ru, http://orcid.org/0000-0002-1584-1748

Alexandrov Viktor N. – Dr. Sci. (Med.), Professor, Head of the Research Laboratory (Tissue Engineering), Research Department (Biomedical Research), S.M. Kirov Military Medical Academy, Saint Petersburg, vnaleks9@yandex.ru, http://orcid.org/0009-0001-9229-5293

Khasanov Artur R. – Assistant, Research Department (Biomedical Research), S.M. Kirov Military Medical Academy, Saint Petersburg, khasartrish@yandex.ru, http://orcid.org/0009-0003-0763-7194.

Edgeev Naran I. – Head of the Surgical Department, Branch No. 4 of Naval Clinical Hospital No. 1469, Murmansk region, Zaozersk, luxomjachok@mail.ru, http://orcid.org/ 0009-0006-4989-2523

Galiullin Rinat I. – Senior Resident, Surgical Department, Branch No. 4 of Naval Clinical Hospital No. 1469, Murmansk region, Zaozersk, rinat061989@list.ru, http://orcid.org/0009-0008-6079-956X

(✉) **Barsuk Ilya A.,** barsuk20220@gmail.com

Received 07.11.2023;
approved after peer review 25.03.2024;
accepted 14.05.2024

УДК 616-006-085.277.3:578.7:615.03
https://doi.org/10.20538/1682-0363-2024-4-158-168

Clinical trials on oncolytic viruses

Golovinov I.V.[1], Goncharova A.S.[1], Shulga A.A.[1], Vlasov S.N.[2], Dimitriadi S.N.[1]

[1] *National Medical Research Center for Oncology*
63, 14 Liniya Str., Rostov-on-Don, 344037, Russian Federation

[2] *Rostov State Medical University*
29, Nakhichevanskiy Av., Rostov-on-Don, 344022, Russian Federation

ABSTRACT

Oncolytic viruses (OVs) are a new class of targeted anticancer drugs with unique mechanisms of action. Oncolytic virotherapy has evolved from the use of in vitro-passaged strains (first generation) to genetically engineered viruses with increased selectivity (second generation) and, ultimately, to recombinant OVs expressing a transgene (third generation).

The aim of the review was to analyze and summarize data on the current state of clinical research on OVs.

A PubMed search identified 182 articles from 1997 to 2024 with 154 studies reporting data on 4,850 patients. We found that adenovirus (n = 44) is the most common OV in clinical trials with more than two-thirds (n = 108) using modified or recombinant viral backbones, and granulocyte-macrophage colony-stimulating factor (GM-CSF; n = 40) was the most common transgene. The most common tumors targeted were melanoma (n = 1,997) and gastrointestinal (GI; n = 916) cancers with the most common monotherapy received by intratumoral (n = 3,003) or intravenous (n = 1,318) delivery routes. The most common combination included chemotherapy (n = 54).

Treatment-related adverse events included low-grade constitutional symptoms and local injection site reactions. Measurements of virus shedding were frequently performed, but many studies were limited to blood and tumor tissue analysis, using only polymerase chain reaction (PCR). Although most studies reported antiviral antibody titers (n = 101), only a few reported virus-specific T-cell responses (n = 23). Objective responses were recorded in 458 (9.4%) patients and disease control was achieved in 1,141 (23.5%) patients, although standard reporting criteria were used in only 60.4% of cases.

These data provide an insight into the current state of clinical research on OVs and highlight potential areas requiring further investigation to better define the role of OVs in cancer treatment.

Keywords: oncolytic virus, immunotherapy, virotherapy, clinical research, clinical trials

Conflict of interest. The authors declare the absence of obvious or potential conflicts of interest related to the publication of this article.

Source of financing. The authors state that they received no funding for the study.

For citation: Golovinov I.V., Goncharova A.S., Shulga A.A., Vlasov S.N., Dimitriadi S.N. Clinical trials on oncolytic viruses. *Bulletin of Siberian Medicine.* 2024;23(4):158–168. https://doi.org/10.20538/1682-0363-2024-4-158-168.

✉ *Golovinov Igor V.,* ivgolovinov@yandex.ru

Клинические исследования онколитических вирусов

Головинов И.В.[1], Гончарова А.С.[1], Шульга А.А.[1], Власов С.Н.[2], Димитриади С.Н.[1]

[1] Национальный медицинский исследовательский центр (НМИЦ) онкологии
Россия, 344037, г. Ростов-на-Дону, ул. 14-я Линия, 63

[2] Ростовский государственный медицинский университет (РостГМУ)
Россия, 344022, г. Ростов-на-Дону, пер. Нахичеванский, 29

РЕЗЮМЕ

Онколитические вирусы (ОВ) – это новый класс таргетных противоопухолевых препаратов, обладающих уникальными механизмами действия. Эволюция в области виротерапии прошла от использования штаммов, пассированных *in vitro* (первое поколение), к генно-инженерным вирусам с повышенной селективностью (второе поколение) и, в конечном итоге, к рекомбинантным ОВ, экспрессирующим трансгены (третье поколение).

Цель обзора заключалась в проведении анализа и обобщении данных о текущей ситуации в клинических исследованиях ОВ.

Поиск в PubMed за период с 1997 по 2024 г. выявил 182 статьи, из которых 154 предоставили данные о 4 850 пациентах. Согласно публикациям, аденовирус (n = 44) является наиболее распространенным ОВ в клинических исследованиях, причем более двух третей (n = 108) использовали модифицированные или рекомбинантные вирусные основы с наиболее частым трансгеном в виде гранулоцитарно-макрофагального колониестимулирующего фактора (GM-CSF; n = 40). Среди опухолей в большинстве случаев исследовались меланома (n = 1 997) и рак желудочно-кишечного тракта (ЖКТ; n = 916) с использованием преимущественно монотерапии ОВ через внутриопухолевое (n = 3 003) или внутривенное (n = 1 318) введение. Часто встречающаяся комбинация включала химиотерапию (n = 54).

Нежелательными явлениями, связанными с лечением ОВ, были конституциональные симптомы низкой степени тяжести и местные реакции в месте инъекции. Часто проводили измерения выделения вируса, однако во многих исследованиях ограничивались анализом крови и опухолевой ткани, применяя только полимеразную цепную реакцию. Несмотря на то, что в большинстве работ сообщали о титрах противовирусных антител (n = 101), лишь в некоторых были отмечены вирусспецифические Т-клеточные ответы (n = 23). Объективные ответы (ORR, objective response rate) были зафиксированы у 458 (9,4%) пациентов, а контроль заболевания достигался у 1 141 (23,5%) больного, хотя стандартные критерии отчетности использовались лишь в 60,4% случаев.

Эти данные дают представление о текущем состоянии клинических исследований ОВ и выявляют потенциальные области, требующие дальнейшего изучения для более четкого определения роли ОВ в лечении рака.

Ключевые слова: онколитический вирус, иммунотерапия, виротерапия, клинические исследования, клинические испытания

Конфликт интересов. Авторы декларируют отсутствие явных и потенциальных конфликтов интересов, связанных с публикацией настоящей статьи.

Источник финансирования. Авторы заявляют об отсутствии финансирования при проведении исследования.

Для цитирования: Головинов И.В., Гончарова А.С., Шульга А.А., Власов С.Н., Димитриади С.Н. Клинические исследования онколитических вирусов. *Бюллетень сибирской медицины.* 2024;23(4):158–168. https://doi.org/10.20538/1682-0363-2024-4-158-168.

INTRODUCTION

In the field of cancer treatment, researchers are constantly developing new therapeutic strategies to combat the complex and heterogeneous nature of this serious disease [1, 2]. One innovative approach that is gaining popularity is oncolytic viral therapy, which harnesses the potential of viruses to selectively target and destroy tumor cells while sparing healthy tissue. Oncolytic viral therapy is a promising strategy in the

fight against cancer. It demonstrates multifaceted mechanisms that induce direct tumor lysis, stimulate antitumor immune responses, and improve the effectiveness of conventional treatments [3–5].

Oncolytic viral therapy is based on the use of natural or modified recombinant viruses constructed using genetic engineering methods to infect, replicate, and destroy malignant cells. These viruses are engineered to exploit vulnerabilities and genetic abnormalities present in tumor cells, destroying them while sparing healthy tissue. The selectivity of these viruses against tumor cells is often achieved through genetic modifications that make them unable to replicate in healthy tissues, thereby increasing their safety for clinical use [6].

Prior to conducting studies in humans, it is necessary to evaluate selectivity, cytotoxicity, biodistribution, and replication of the virus in *in vitro* cell lines and animal models [7, 8]. The results obtained from animal models can provide some insight into the response of patients [9].

Over the past few decades, the study of oncolytic viral therapy has progressed from preclinical studies to numerous clinical trials, indicating a transition from theoretical speculation to concrete therapeutic potential. Currently, according to Clinicaltrials.gov, there are 107 ongoing clinical trials, 89 of which are recruiting participants. These trials encompass a variety of cancer types and numerous oncolytic viruses with diverse mechanisms of action and delivery strategies. The results of the studies are crucial in comprehending the safety, efficacy, and challenges related to oncolytic viral therapy as a viable cancer treatment option [10, 11].

The aim of this study was to review the current situation in clinical trials on oncolytic viral therapy.

LITERATURE SEARCH METHODS

A systematic literature search was conducted using the PubMed database with the keywords “oncolytic virus” and “oncolytic viruses”. The search was limited to clinical trials and randomized clinical trials. A total of 182 articles were identified and reviewed, of which 154 contained original reports of clinical trial data using oncolytic viruses.

RESULTS

Oncolytic viruses in clinical trials

The literature search identified 154 clinical trials from 1997 to 2024 that reported on the use of oncolytic viruses (OVs). These studies involved 4,850 patients with various forms of malignant neoplasms (Table). Of the studies conducted, the majority (n = 86; 55.8%) were phase I trials. This suggests that oncolytic virotherapy is a novel approach and indicates that negative results from later-stage studies may not have been published yet, thus hindering complete understanding of the effectiveness of OVs in cancer patients.

We found that out of the total number of studies, 15 (9.7%) were phase I / II trials, 28 (18.2%) were phase II trials, and 20 (13.0%) were clinical trials that were not clearly classified but were mostly early-phase studies or the first clinical trials in humans. Phase III trials accounted for approximately 3% (n = 5) of the selected studies. However, even if a drug successfully completes phase III clinical trials, there is still a risk of failure. For example, on August 2, 2019, Labiotech announced the completion of a phase III clinical trial of Pexa-Vec (JX-594), a genetically modified vaccinia virus expressing *GM-CSF* and lacking the thymidine kinase gene, for the treatment of liver cancer. The interim analysis showed that the efficacy of Pexa-Vec in combination with sorafenib was greater than that of sorafenib alone, but the likelihood of prolonging patient survival was low, so the study was terminated early [12]. Therefore, current literature focuses on early-phase clinical trials.

Table

Patient characteristics in clinical trials of OVs

Characteristics	*n*
Tumor localization	
Brain	377
Breast	156
Gastrointestinal tract	916
Genitourinary system	245
Gynecologic tumors	219
Head and neck	198
Lungs	297
Melanoma	1,997
Sarcoma	148
Other solid tumors	204
Hematologic tumors	93
Delivery method	
Intratumoral	3,003
Intravenous	1,318
Several	122
Other	407
Phase	
I	1,793
I/II	345
II	1,317
III	932
Not specified	463

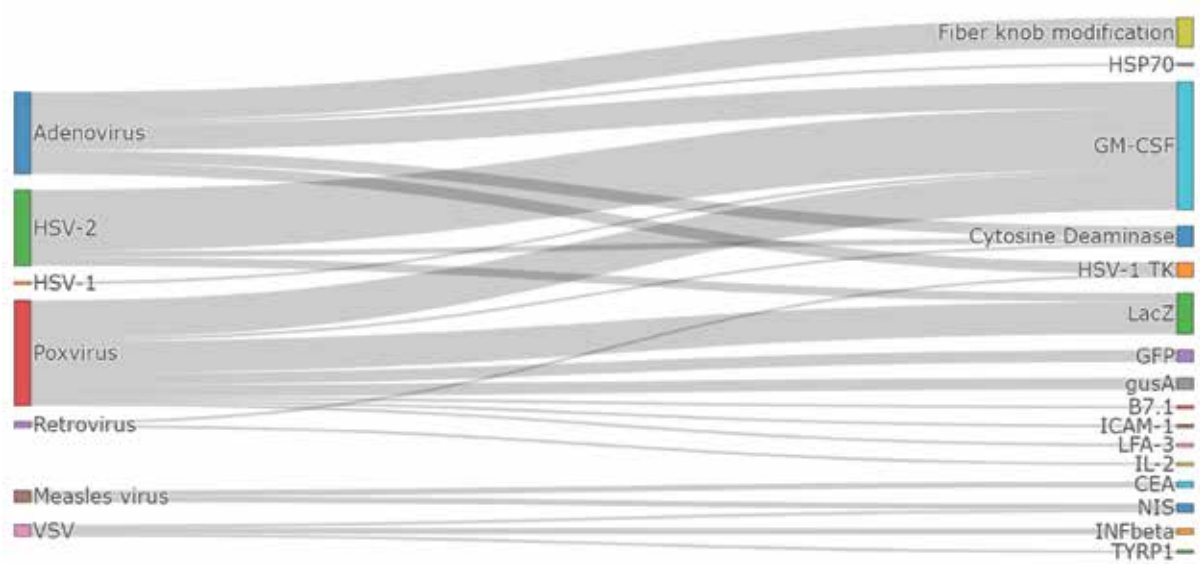

Figure. Transgenes used as a payload for oncolytic viruses

A variety of DNA and RNA viruses can be used as OVs. Most of the clinical trials included in the review used DNA viruses due to the advantages of their larger and more stable genome, which facilitates genetic engineering and the addition of multiple transgenes (Figure) [13]. The most commonly used viruses were adenovirus (n = 44; 28.6%), followed by herpes simplex virus type 1 (HSV-1; n = 37; 24.0%), reovirus (n = 25; 16.2%), and poxviruses (n = 18; 11.7%).

Additionally, six studies (3.9%) utilized Coxsackie virus, while five studies (3.2%) each employed Newcastle disease virus and measles virus. Four studies (2.6%) used parvovirus. Although some clinical trials have mentioned other viruses, such as Seneca Valley virus, Sendai virus, vesicular stomatitis virus (VSV), herpes simplex virus type 2 (HSV-2), retrovirus, and rhinovirus / poliovirus chimera, none of the published studies used more than one type of OVs.

Insertional mutagenesis is a problem that occurs when an exogenous DNA sequence from a virus integrates into the genome of the host organism [14]. This phenomenon can be harmless, but it can also lead to the transformation of host cells and even cause tumorigenesis. The risk of insertional mutagenesis depends on the characteristics of the virus. For instance, RNA viruses without a DNA phase, as well as viruses that replicate in the cytosol, do not pose any risk in this regard. Some viruses, including echoviruses, vaccinia virus, Coxsackie virus, and Newcastle disease virus, are considered safe. Although HSV-1 replicates in the nucleus, it has not been shown to cause insertional mutagenesis [15]. Adenovirus type 5 vectors are also safe due to the episomal nature of DNA [16].

However, retroviruses and lentiviruses are known for their ability to invade the genome of the host cell. Retroviruses are single-stranded RNA viruses that, upon entering the cell cytoplasm, are converted into proviral double-stranded DNA and subsequently translocated into the nucleus. While retroviruses and lentiviruses are popular vectors for gene therapy, the risk of genotoxicity remains a concern [17]. Therefore, it is crucial to thoroughly study the origins of a virus before looking into its development.

Approximately one-third (n = 46) of the clinical studies used wild-type virus, while two-thirds (n = 108) used genetically modified viruses. The modifications primarily consisted of deleting nonessential viral genes to promote selective replication in tumor cells and attenuate viral pathogenicity. In 69 clinical trials, genetic modifications also included the expression of one or more transgenes using 101 recombinant genes (Figure). The most frequently expressed transgene was *GM-CSF* (n = 40; 26.2%). *GM-CSF* stimulates the proliferation, differentiation, and migration of macrophages and dendritic cells, promoting the generation of adaptive immune responses by facilitating the cross-presentation of tumor antigens [18].

The next most commonly expressed transgenes were those used for the selection and identification of recombinant viruses after host infection. The study utilized *LacZ* (n = 16), which encodes bacterial β-galactosidase, and *GUSB* (n = 4), which encodes β-glucuronidase. Additionally, seven viruses were

used, each encoding genes for prodrug enzymes, such as cytosine deaminase (n = 7) and HSV-1 thymidine kinase (n = 7), which convert a nontoxic prodrug into a cytotoxic agent. The transgenes included immune-enhancing genes, such as interleukin-2 (*IL-2*; n = 1), interferon-beta (*IFNβ*; n = 2), lymphocyte function-associated antigen 3 (*LFA-3*; n = 1), costimulatory molecule *B7.1* gene (n = 1), and intercellular adhesion molecule 1 (*ICAM-1*; n = 1) gene.

In addition, several studies have employed different transgenes to monitor viral replication and biodistribution. Specifically, one study utilized heat shock protein 70 (*HSP70*), two studies used the carcinoembryonic antigen (*CEA*) gene, and three studies used sodium iodide symporter (NIS) and the tyrosine kinase-related protein 1 (*TYRP1*) gene. The *NIS* gene has been used to visualize viral biodistribution and replication using CT and sensitize cells to radiation therapy. Finally, ten studies utilized adenoviruses that expressed modified type 5 fibers, which were designed to enhance viral cell entry [19].

The selection of the most suitable virus and transgenes should be based on further biological analysis of tumor cells, host factors, and mechanisms that promote the activation of Th1 and CD8+ effector immune responses in T cells. Studies have shown that intracellular sensors, such as the cGAS-STING complex and Toll-like receptors, play a crucial role in inducing innate immunity by tumor cells [20]. The intracellular sensors used to recognize DNA and RNA viruses are also used for the same purpose in cancer. However, their status in cancer is not yet precisely determined [21].

TYPES OF TUMORS IN CLINICAL TRIALS

Clinical trials on OVs cover a wide range of tumors and focus on a large number of cancer patients (Table). Melanoma and gastrointestinal cancer were the most commonly studied tumors. Melanoma patients accounted for 50 clinical trials with the largest number of patients (n = 1,997), likely due to the relative ease of accessing tumors for local injection. An example of this is a phase III clinical trial of T-VEC, a genetically modified HSV-1-expressing *GM-CSF*, which included 436 melanoma patients [22]. There were 106 clinical trials involving 916 patients with gastrointestinal cancer. Table summarizes various tumor localization targeted in clinical trials, including genitourinary tumors (n = 43), breast and gynecologic cancers (n = 48), sarcomas (n = 27), and head and neck cancers (n = 23).

Based on the number of patients included in clinical trials, melanoma was the most common cancer type, followed by gastrointestinal cancer (n = 916; 18.9%), brain tumors (n = 377; 7.8%), lung cancer (n = 297; 6.1%), genitourinary cancer (n = 245; 5.1%), gynecologic cancer (n = 219; 7.7%), head and neck cancer (n = 198; 4.1%), and breast cancer (n = 156; 3.2%). The study included 204 patients (4.2%) with solid tumors that were not otherwise defined, as well as 93 patients (1.9%) with various hematologic malignancies.

DRUG COMBINATIONS

Of the 154 studies reviewed, 94 (61.0%) clinical trials used OV monotherapy, while 60 (39.0%) studies used OVs in combination with at least one other treatment or anticancer drug. Among the combinations, the most common drugs were cytotoxic chemotherapeutic agents (n = 54; 35.1%) and immune checkpoint inhibitors (n = 16; 10.4%).

Other modalities used in combination OV therapy studies included radiation therapy (n = 9; 5.8%), chemotherapy prodrugs (n = 8; 5.2%), tyrosine kinase inhibitors (n = 2; 1.3%), and immunomodulatory drugs (n = 1; 0.6%). The most common chemotherapy drugs included paclitaxel (n = 9) and cyclophosphamide (n=8), the latter being used in pretreatment chemotherapy to stimulate an antitumor immune response. In addition, gemcitabine was used in six studies. Two studies were unclear about the type of chemotherapy. Eight studies combined OVs with prodrugs, including four studies with the 5-fluorouracil precursor 5-fluorocytosine, three studies with ganciclovir, and one study with valganciclovir. Sixteen studies reported a combination of OVs and immune checkpoint inhibitors. Of these, five studies used ipilimumab and pembrolizumab, two studies evaluated the combination of OVs with bevacizumab, and one study with nivolumab, durvalumab, pucotenlimab, and tremelimumab. Additionally, two studies reported on the combination of OVs and tyrosine kinase inhibitors, specifically bortezomib and erlotinib. Finally, one study used a combination with interleukin-2.

Considering the diversity and heterogeneity of solid tumors, combining OVs with other treatment modalities may enhance their effectiveness. When developing combination therapy, it is crucial to consider drug interactions and the sequence of their use to minimize possible antagonistic effects. Chemotherapy can inhibit DNA synthesis, mitosis, and cell division, and

cause DNA damage. OVs replicate in tumor cells and contribute to the induction of DNA damage. Therefore, combining OVs with chemotherapy may enhance the antitumor effect synergistically [23, 24]. Combination therapy that includes OVs and checkpoint inhibitors is an attractive approach. OVs can attract tumor-infiltrating lymphocytes and stimulate the release of tumor antigens, danger signals, and proinflammatory cytokines, which further increases T cell recruitment and promotes immune cell activation. Viral infection may increase the expression of immune checkpoint molecules, such as CTLA-4 and PD-1, which typically inhibit T cell activation [25–27]. Additionally, the combination of radiation therapy and OVs has a synergistic effect on tumor treatment [28].

In addition to ongoing research that combines OVs with checkpoint inhibitors, viruses are being developed that can produce their own antibodies. For instance, HSV-1, which can express antibodies to PD-1, was developed to treat glioblastoma [29]. Although this construct has only been tested in mouse models so far, it represents a promising example of enhancing OV activity by inserting an antibody gene.

ADMINISTRATION ROUTES

Selecting the optimal route of administration is a controversial issue in the clinical development of OVs. Therefore, we analyzed the routes of administration used in published clinical studies (Table). The most commonly used method was intratumoral injection, which was used in 88 studies (57.1%). OVs are suitable for direct injection into the tumor. However, the number and localization of tumors may restrict the use of this method. Intratumoral injections provide direct tumor access, but the OV may be distributed unevenly within the tumor, reducing its effectiveness.

Intravenous delivery was used in 57 clinical studies (37%). It has the potential to infect metastatic lesions but may be limited by dilution in the blood and clearance from the body. This method avoids challenges of localizing each tumor, but there is a risk of inadequate transmission of the virus to the tumor site, which reduces its effectiveness [30].

Other delivery methods used in the studies included hepatic artery infusion in five studies (3.2%) and intraperitoneal delivery in eight studies (5.2%). Additionally, intravesical injection (n = 3), direct injection into the removed tumor bed (n = 3), convection-enhanced delivery (CED) into the brain tumor bed (n = 2), intradermal injection (n = 2), and infection of tumor cells *ex vivo* (n = 1) were employed. Two studies reported the use of stem cell delivery. No clinical trials using nanovesicle delivery have been reported, although preclinical trials have described such methods [31, 32].

Phase III clinical trials only used intratumoral injections, indicating their primary role in OVs with high commercial potential. This method is safer and ensures that the virus reaches its target directly.

There is interest in discovering new delivery methods that can prevent premature clearance of the virus and improve its biodistribution in tumor sites [33].

According to the Table, the most common delivery routes were intratumoral (n = 3,003; 61.9%) and intravenous (n = 1,318; 27.2%) injections. In the same studies, 122 patients received OVs through multiple routes, mostly combining intravenous with intratumoral administration. Besides, 407 (8.4%) patients received OVs through other routes, as described above.

Intratumoral injections were commonly used for melanoma, prostate cancer, and gliomas [34, 35]. Depending on the tumor localization and accessibility, the virus can be delivered once (for instance, into the glioma cavity during surgery) or several times (as in melanoma) [36].

Intravenous delivery can also take place via peripheral intravenous injection or can be more targeted by hepatic artery infusion for liver metastases [37]. Intravenous administration offers several advantages, including ease of administration, standardized dosage, and the possibility of repeated and prolonged administration [38]. However, the main disadvantage of this method remains the development of neutralizing antibodies and clearance of the virus from the blood.

Biodistribution of the virus depends on the route of administration. Intravenous administration allows the virus to spread through the bloodstream, reaching well-perfused organs, such as the liver, heart, lungs, kidneys, and brain. The spleen is also highly susceptible to circulating particles due to its high blood supply and capillary system. Local administration, on the other hand, results in the virus being mainly concentrated in organs near the injection site [39].

OV SAFETY PROFILE

The reviewed trials primarily assessed the safety of agents used in clinical practice. The adverse events associated with OV treatment were mostly

low-grade constitutional symptoms (CTCAE grade 1–2) and local injection site reactions. Fever was the most frequently reported adverse event, it was noted in 96 studies (grade 1–2 in 80 trials and grade 3–4 in 16 studies). Mild symptoms commonly reported included chills ($n = 83$), nausea and vomiting ($n = 67$), flu-like symptoms ($n = 36$), fatigue ($n = 52$), and pain ($n = 34$). Pain at the injection site was also reported in 43 studies. More severe adverse events (grade 3 or higher) included nausea and vomiting ($n = 12$), pain ($n = 11$), fever ($n = 6$), fatigue ($n = 6$), and flu-like symptoms ($n = 3$).

Clinical trials reported 155 grade 3 and 33 grade 4 adverse events. Many of the events observed were related to disease progression or the effects of other drugs used in combination therapy. The safety profile of OVs appears acceptable, given the large number of early-phase clinical trials that often include late-stage patients. Adverse events were mostly comparable for intratumoral and intravenous administration.

However, there are certain safety issues associated with different administration routes, and risks are present with intra-arterial administration of the agent. Gene therapy can cause a strong immune response, and in rare cases, excessive inflammation can damage organs and lead to death. For instance, in 1999, an 18-year-old patient died after receiving an adenovirus injection into a branch of the hepatic artery. Adenoviral vectors and transgenes were found in all of the patient's organs during autopsy, marking the first report of a death from gene therapy and highlighting its risks and serious side effects. When developing agents for intra-arterial administration, it is crucial to consider their safety and increase the dosage carefully to ensure effectiveness. At present, intravenous OV formulations are primarily used at early clinical stages (phase I and II) and have not yet advanced to phase III.

OV SHEDDING IN CLINICAL TRIALS

Viral shedding from treated patients may pose a risk to the environment and human health. FDA guidelines provide detailed information on viral shedding studies, including clinical trial design, and the collection and analysis of shedding data. The guidelines also note that viral shedding may be dose-dependent, so shedding studies should be performed after phase I when the dosage is well defined [41].

None of the reviewed studies reported transmission of viral infection to family members or healthcare personnel. Out of the 154 studies that were published, 122 (79.2%) assessed viral shedding, while 32 (20.8%) did not.

The presence of the virus in tissues is crucial for delivering the virus to tumor sites and identifying potential shedding sites. Clinical trials on OVs assessed various tissues and fluids, with blood or serum being the most common viral shedding site in 89 (57.8%) studies. Viral shedding in urine was noted in 57 (37.0%) studies and in tumor biopsy specimens – in 41 (26.6%) studies. The next most common was viral shedding in saliva or oral swabs, reported in 28 studies (18.2%), and in sputum samples, reported in 20 studies (13.0%). Other fluids or tissues, including cerebrospinal fluid, peritoneal washings, and injection sites, were collected in 41 studies.

In 122 studies that assessed viral shedding, evidence of the presence of the virus was found. Polymerase chain reaction (PCR) was the most commonly used method for detection in 100 (82.0%) studies. Plaque assays, which measure infectious virus particles, were performed in one study alone and in 21 (17.2%) published studies together with PCR [42].

ANTIVIRAL IMMUNITY IN CLINICAL TRIALS

Antiviral immunity plays a crucial role in clinical trials of oncolytic virotherapy and is a significant correlative biomarker. The presence of neutralizing antibodies is a major obstacle to successful therapy. The agents selected for treatment must be capable of infecting human cells, which has both advantages and disadvantages. One of the primary reasons for limiting the effectiveness of oncolytic virotherapy in humans is their immunity against the virus. Patients may have been previously exposed to or vaccinated against some of the naturally occurring viruses used in OV-based treatment, leading to the formation of neutralizing antibodies [43]. For instance, nearly 90% of people have antibodies against reovirus. The effectiveness of the measles virus, also considered a potential pathogen, is reduced due to the presence of antibodies against it in patients' blood.

Out of the 154 studies analyzed, 101 (65.6%) works measured antiviral antibody titers. Of these, 43 (27.9%) studies assessed neutralizing antibodies, while the remaining studies measured non-neutralizing antibody titers. Virus-specific T cell responses were investigated less frequently and were reported in only 23 (14.9%) clinical studies.

ANTITUMOR ACTIVITY IN CLINICAL TRIALS

Antitumor activity is an important consideration in OV trials, although many of these studies were conducted at early stages of development and were not designed to detect therapeutic responses, which complicates the analysis of clinical endpoints. However, most of them recorded clinical responses. Ninety-three studies (60.4%) used different Response Evaluation Criteria in Solid Tumors (RECIST), including standard RECIST in 74 studies (48.1%), modified RECIST in 12 studies (7.8%), and irRECIST criteria in 7 studies (4.5%). Four additional studies (2.6%) used modified WHO criteria, including the phase III OPTiM T-VEC study. The remaining 57 studies (37%) did not mention specific response criteria.

Out of the 4,850 patients who participated in these studies, the overall objective response rate was 9.4% (n = 458). Complete responses were observed in 3.5% (n = 171) of patients, while partial responses were observed in 5.9% (n = 287) of patients. Additionally, disease stabilization was observed in 14.1% (n = 683) of patients, resulting in disease control in 23.5% (n = 1,141) of patients. It is worth noting that a minor response was recorded in only 0.3% (n = 17) of patients. It is important to note that although the numbers are modest, most of the studies were phase I clinical trials and were not specifically designed to evaluate clinical responses.

CONCLUSION

We conducted a review of clinical experience with OVs over the past two decades. Our analysis provides an overview of different types of OVs used in clinical practice, target tumors, combinations, and the status of ongoing studies. Most clinical trials use large DNA viruses with various modifications, and *GM-CSF* is mainly used as transgenes. Most viruses are administered via intratumoral injection, although there has been an increase in the number of studies using intravenous administration. Monotherapy for osteosarcoma predominates in most studies, and combination therapy most often includes chemotherapy.

Despite the large number of clinical trials conducted, currently only four OVs have received approval for use as a treatment for malignant tumors. The first OV to be approved for the treatment of melanoma was the unmodified picornavirus ECHO-7 (Rigvir) in Latvia in 2004 [44]. In 2005, a modified adenovirus H101 (Oncorine) was registered in China for the treatment of head and neck or esophageal cancer [45]. In 2015, T-VEC (Imlygic) became the first OV to be approved in the United States for the treatment of unresectable advanced melanoma [46]. Subsequently, T-VEC was registered in Europe, Australia, Switzerland, and Israel. The only OV-based drug that has received FDA approval is G47Δ (Delytact), a modified HSV-1 expressing the *E. coli LacZ* gene, which received conditional and time-limited approval in June 2021 in Japan for the treatment of malignant gliomas [47].

Safety concerns for patients and the environment, such as off-target effects, virus mutations, and transmission [48], may be the reason why despite decades of research and numerous clinical trials, only one OV-based drug has been approved. Each time the original virus replicates, there is a high probability of viral evolution, resulting in the proliferation of new viral lineages due to defects in the viral polymerase [49].

The optimal method for administering OVs remains an open question. Developing systemic delivery faces main challenges, such as serum neutralization of the virus and hepatotoxicity. After treatment, individuals may shed live, replicating viruses, increasing the likelihood of transmission to healthy individuals. Due to the high mutation rate of viruses, particularly those containing RNA, there is a risk of infection transmission when they are released into the environment with waste [50].

Based on this, there is a need to conduct additional preclinical trials to better understand the basic biological mechanisms underlying the antitumor activity of OVs. Clinical trials need to standardize methods for assessing viral distribution and implement appropriate biomarkers that will provide information on both antiviral and antitumor immunity. In addition, encouraging publication of research data in this area will help accelerate clinical development and maximize the potential of OVs for the treatment of patients with cancer.

REFERENCES

1. Debela D.T., Muzazu S.G., Heraro K.D., Ndalama M.T., Mesele B.W., Haile D.C. et al. New approaches and procedures for cancer treatment: Current perspectives. *SAGE Open Med*. 2021;9:1–10. DOI: 10.1177/20503121211034366.
2. Kit O.I., Kharagezov D.A., Lazutin Yu.N., Mirzoyan E.A., Milakin A.G., Stateshny O.N., et al. Immunotherapy for epithelial tumors of the thymus. *South Russian Journal of Cancer*.

2023;4(3):56–67. (In Russ.). DOI: 10.37748/2686-9039-2023-4-3-7.
3. Santos Apolonio J., Lima de Souza Gonçalves V., Cordeiro Santos M.L., Silva Luz M., Silva Souza J.V., Rocha Pinheiro S.L. et al. Oncolytic virus therapy in cancer: A current review. *World J. Virol*. 2021;10(5):229–255. DOI: 10.5501/wjv.v10.i5.229.
4. Hemminki O., Dos Santos J.M., Hemminki A. Oncolytic viruses for cancer immunotherapy. *J. Hematol. Oncol*. 2020;13(1):84. DOI: 10.1186/s13045-020-00922-1.
5. Heidbuechel J.P.W., Engeland C.E. Oncolytic viruses encoding bispecific T cell engagers: a blueprint for emerging immunovirotherapies. *J. Hematol. Oncol*. 2021;14(1):63. DOI: 10.1186/s13045-021-01075-5.
6. Cristi F., Gutiérrez T., Hitt M.M., Shmulevitz M. Genetic modifications that expand oncolytic virus potency. *Front. Mol. Biosci*. 2022;9:831091. DOI: 10.3389/fmolb.2022.831091.
7. Silva Lima B., Videira M.A. Toxicology and biodistribution: the clinical value of animal biodistribution studies. *Mol. Ther. Methods Clin. Dev*. 2018;8:183–197. DOI: 10.1016/j.omtm.2018.01.003.
8. Yamaguchi T., Uchida E. Oncolytic virus: regulatory aspects from quality control to clinical studies. *Curr. Cancer Drug Targets*. 2018;18(2):202–208. DOI: 10.2174/1568009617666170222142650.
9. Russell S.J., Peng K.W. Oncolytic virotherapy: a contest between apples and oranges. *Mol. Ther*. 2017;25(5):1107–1116. DOI: 10.1016/j.ymthe.2017.03.026.
10. Li K., Zhao Y., Hu X., Jiao J., Wang W., Yao H. Advances in the clinical development of oncolytic viruses. *Am. J. Transl. Res*. 2022;14(6):4192–4206.
11. Kit O.I., Ignatov S.N., Zlatnik E.Yu., Soldatkina N.V., Rostorguev E.E., Sagakyants A.B., Bondarenko E.S., et al. Oncolytic virotherapy in glioblastoma treatment: progress and challenges in clinical research (literature review). *Siberian Journal of Oncology*. 2020;19(6):133–140. (In Russ.). DOI: 10.21294/1814-4861-2020-19-6-133-140.
12. Abou-Alfa G.K., Galle P.R., Chao Y., Erinjeri J., Heo J., Borad M.J. et al. PHOCUS: A Phase 3, Randomized, Open-Label Study of Sequential Treatment with Pexa-Vec (JX-594) and Sorafenib in Patients with Advanced Hepatocellular Carcinoma. *Liver Cancer*. 2023;1–17. DOI: 10.1159/000533650.
13. Rahman M.M., McFadden G. Oncolytic viruses: newest frontier for cancer immunotherapy. *Cancers (Basel)*. 2021;13(21):5452. DOI: 10.3390/cancers13215452.
14. Aiuti A., Cossu G., de Felipe P., Galli M.C., Narayanan G., Renner M. et al. The committee for advanced therapies' of the European Medicines Agency reflection paper on management of clinical risks deriving from insertional mutagenesis. *Hum. Gene Ther. Clin. Dev*. 2013;24(2):47–54. DOI: 10.1089/humc.2013.119.
15. Kaufman H.L., Kohlhapp F.J., Zloza A. Oncolytic viruses: a new class of immunotherapy drugs. *Nat. Rev. Drug Discov*. 2015;14(9):642–662. DOI: 10.1038/nrd4663.
16. Appaiahgari M.B., Vrati S. Adenoviruses as gene/vaccine delivery vectors: promises and pitfalls. *Expert Opin. Biol. Ther*. 2015;15(3):337–351. DOI: 10.1517/14712598.2015.993374.
17. Sena-Esteves M., Gao G. Introducing genes into mammalian cells: viral vectors. *Cold Spring Harb. Protoc*. 2020;2020(8):095513. DOI: 10.1101/pdb.top095513.
18. Kumar A., Taghi Khani A., Sanchez Ortiz A., Swaminathan S. GM-CSF: a double-edged sword in cancer immunotherapy. *Front. Immunol*. 2022;13:901277. DOI: 10.3389/fimmu.2022.901277.
19. Zhao Y., Liu Z., Li L., Wu J., Zhang H., Zhang H. et al. Oncolytic adenovirus: prospects for cancer immunotherapy. *Front. Microbiol*. 2021;12:707290. DOI: 10.3389/fmicb.2021.707290.
20. Woo S.R., Fuertes M.B., Corrales L., Spranger S., Furdyna M.J., Leung M.Y. et al. STING-dependent cytosolic DNA sensing mediates innate immune recognition of immunogenic tumors. *Immunity*. 2014;41(5):830–842. DOI: 10.1016/j.immuni.2014.10.017.
21. Iurescia S., Fioretti D., Rinaldi M. Targeting cytosolic nucleic acid-sensing pathways for cancer immunotherapies. *Front. Immunol*. 2018;9:711. DOI: 10.3389/fimmu.2018.00711.
22. Andtbacka R.H.I., Collichio F., Harrington K.J., Middleton M.R., Downey G., Öhrling K. et al. Final analyses of OPTiM: a randomized phase III trial of talimogene laherparepvec versus granulocyte-macrophage colony-stimulating factor in unresectable stage III–IV melanoma. *J. Immunother. Cancer*. 2019;7(1):145. DOI: 10.1186/s40425-019-0623-z.
23. Zhang B., Cheng P. Improving antitumor efficacy via combinatorial regimens of oncolytic virotherapy. *Mol. Cancer*. 2020;19(1):158. DOI: 10.1186/s12943-020-01275-6.
24. Soliman H., Hogue D., Han H., Mooney B., Costa R., Lee M.C. et al. Oncolytic T-VEC virotherapy plus neoadjuvant chemotherapy in nonmetastatic triple-negative breast cancer: a phase 2 trial. *Nat. Med*. 2023;29(2):450–457. DOI: 10.1038/s41591-023-02210-0.
25. Ren Y., Miao J.M., Wang Y.Y., Fan Z., Kong X.B., Yang L. et al. Oncolytic viruses combined with immune checkpoint therapy for colorectal cancer is a promising treatment option. *Front. Immunol*. 2022;13:961796. DOI: 10.3389/fimmu.2022.961796.
26. Monge C., Xie C., Myojin Y., Coffman K., Hrones D.M., Wang S. et al. Phase I/II study of PexaVec in combination with immune checkpoint inhibition in refractory metastatic colorectal cancer. *J. Immunother. Cancer*. 2023;11(2):e005640. DOI: 10.1136/jitc-2022-005640.
27. Liu X., Zhang J., Feng K., Wang S., Chen L., Niu S. et al. Efficacy and safety of oncolytic virus combined with chemotherapy or immune checkpoint inhibitors in solid tumor patients: A meta-analysis. *Front. Pharmacol*. 2022;13:1023533. DOI: 10.3389/fphar.2022.1023533.
28. Zhang B., Cheng P. Improving antitumor efficacy via combinatorial regimens of oncolytic virotherapy. *Mol. Cancer*. 2020;19(1):158. DOI: 10.1186/s12943-020-01275-6.
29. Passaro C., Alayo Q., De Laura I., McNulty J., Grauwet K., Ito H. et al. Arming an oncolytic herpes simplex virus type 1 with a single-chain fragment variable antibody against PD-1 for experimental glioblastoma therapy. *Clin. Cancer Res*. 2019;25(1):290–299. DOI: 10.1158/1078-0432.CCR-18-2311.
30. Zhu X., Fan C., Xiong Z., Chen M., Li Z., Tao T. et al. De-

velopment and application of oncolytic viruses as the nemesis of tumor cells. *Front. Microbiol*. 2023;14:1188526. DOI: 10.3389/fmicb.2023.1188526.
31. Ji W., Li L., Zhou S., Qiu L., Qian Z., Zhang H. et al. Combination immunotherapy of oncolytic virus nanovesicles and PD-1 blockade effectively enhances therapeutic effects and boosts antitumour immune response. *J. Drug Target*. 2020;28(9):982–990. DOI: 10.1080/1061186X.2020.1766473.
32. Chen L., Ma Z., Xu C., Xie Y., Ouyang D., Song S., Zhao X. et al. Progress in oncolytic viruses modified with nanomaterials for intravenous application. *Cancer Biol. Med*. 2023;20(11):830–855. DOI: 10.20892/j.issn.2095-3941.2023.0275.
33. Ban W., Guan J., Huang H., He Z., Sun M., Liu F. et al. Emerging systemic delivery strategies of oncolytic viruses: A key step toward cancer immunotherapy. *Nano Res*. 2022;15(5):4137–4153. DOI: 10.1007/s12274-021-4031-6.
34. Fares J., Ahmed A.U., Ulasov I.V., Sonabend A.M., Miska J., Lee-Chang C., Balyasnikova I.V. et al. Neural stem cell delivery of an oncolytic adenovirus in newly diagnosed malignant glioma: a first-in-human, phase 1, dose-escalation trial. *Lancet Oncol*. 2021;22(8):1103–1114. DOI: 10.1016/S1470-2045(21)00245-X.
35. Fujita K., Kato T., Hatano K., Kawashima A., Ujike T., Uemura M. et al. Intratumoral and s.c. injection of inactivated hemagglutinating virus of Japan envelope (GEN0101) in metastatic castration-resistant prostate cancer. *Cancer Sci*. 2020;111(5):1692–1698. DOI: 10.1111/cas.14366.
36. Silk A.W., O'Day S.J., Kaufman H.L., Bryan J., Norrell J.T., Imbergamo C. et al. A phase 1b single-arm trial of intratumoral oncolytic virus V937 in combination with pembrolizumab in patients with advanced melanoma: results from the CAPRA study. *Cancer Immunol. Immunother*. 2023;72(6):1405–1415. DOI: 10.1007/s00262-022-03314-1.
37. Nawrocki S.T., Olea J., Villa Celi C., Dadrastoussi H., Wu K., Tsao-Wei D. et al. Comprehensive Single-Cell Immune Profiling Defines the Patient Multiple Myeloma Microenvironment Following Oncolytic Virus Therapy in a Phase Ib Trial. *Clin. Cancer Res*. 2023;29(24):5087–5103. DOI: 10.1158/1078-0432.CCR-23-0229.
38. Hill C., Carlisle R. Achieving systemic delivery of oncolytic viruses. *Expert Opin. Drug Deliv*. 2019;16(6):607–620. DOI: 10.1080/17425247.2019.1617269.
39. Naumenko V., Van S., Dastidar H., Kim D.S., Kim S.J., Zeng Z. Visualizing oncolytic virus-host interactions in live mice using intravital microscopy. *Mol. Ther. Oncolytics*. 2018;10:14–27. DOI: 10.1016/j.omto.2018.06.001.
40. Bulcha J.T., Wang Y., Ma H., Tai P.W.L., Gao G. Viral vector platforms within the gene therapy landscape. *Signal Transduct. Target Ther*. 2021;6(1):53. DOI: 10.1038/s41392-021-00487-6.
41. Bubela T., Boch R., Viswanathan S. Recommendations for regulating the environmental risk of shedding for gene therapy and oncolytic viruses in Canada. *Front. Med. (Lausanne)*. 2019;6:58. DOI: 10.3389/fmed.2019.00058.
42. Onnockx S., Baldo A., Pauwels K. Oncolytic viruses: an inventory of shedding data from clinical trials and elements for the environmental risk assessment. *Vaccines (Basel)*. 2023;11(9):1448. DOI: 10.3390/vaccines11091448.
43. Berkeley R.A., Steele L.P., Mulder A.A., van den Wollenberg D.J.M., Kottke T.J., Thompson J. et al. Antibody-neutralized reovirus is effective in oncolytic virotherapy. *Cancer Immunol. Res*. 2018;6(10):1161–1173. DOI: 10.1158/2326-6066.CIR-18-0309.
44. Alberts P., Tilgase A., Rasa A., Bandere K., Venskus D. The advent of oncolytic virotherapy in oncology: The Rigvir® story. *Eur. J. Pharmacol*. 2018;837:117–126. DOI: 10.1016/j.ejphar.2018.08.042.
45. Xia Z.J., Chang J.H., Zhang L., Jiang W.Q., Guan Z.Z., Liu J.W. et al. Phase III randomized clinical trial of intratumoral injection of E1B gene-deleted adenovirus (H101) combined with cisplatin-based chemotherapy in treating squamous cell cancer of head and neck or esophagus. *Ai Zheng*. 2004;23(12):1666–1670.
46. Andtbacka R.H., Kaufman H.L., Collichio F., Amatruda T., Senzer N., Chesney J. et al. talimogene laherparepvec improves durable response rate in patients with advanced melanoma. *J. Clin. Oncol*. 2015;33(25):2780–2788. DOI: 10.1200/JCO.2014.58.3377.
47. Frampton J.E. Teserpaturev/G47Δ: first approval. *BioDrugs*. 2022;36(5):667–672. DOI: 10.1007/s40259-022-00553-7.
48. Forbes N.S., Coffin R.S., Deng L., Evgin L., Fiering S., Giacalone M. et al. White paper on microbial anti-cancer therapy and prevention. *J. Immunother. Cancer*. 2018;6(1):78. DOI: 10.1186/s40425-018-0381-3.
49. Lawler S.E., Speranza M.C., Cho C.F., Chiocca E.A. Oncolytic viruses in cancer treatment: a review. *JAMA Oncol*. 2017;3(6):841–849. DOI: 10.1001/jamaoncol.2016.2064.
50. Omole R.K., Oluwatola O., Akere M.T., Eniafe J., Agboluaje E.O., Daramola O.B. et al. Comprehensive assessment on the applications of oncolytic viruses for cancer immunotherapy. *Front. Pharmacol*. 2022;13:1082797. DOI: 10.3389/fphar.2022.1082797.

Authors' contribution

Golovinov I.V., Shulga A.A., Vlasov S.N. – analysis and interpretation of the data. Goncharova A.S., Dimitriadi S.N. – conception and design, final approval of the manuscript for publication.

Authors' information

Golovinov Igor V. – Junior Researcher, Experimental Laboratory Center, National Medical Research Center of Oncology, Rostov-on-Don, ivgolovinov@yandex.ru, https://orcid.org/0000-0003-3011-6904

Goncharova Anna S. – Cand. Sci. (Biology), Head of Experimental Laboratory Center, National Medical Research Center of Oncology, Rostov-on-Don, fateyeva_a_s@list.ru, https://orcid.org/0000-0003-0676-0871

Shulga Anna A. – Junior Researcher, Experimental Laboratory Center, National Medical Research Center of Oncology, Rostov-on-Don, slip.anka96@mail.ru, https://orcid.org/0009-0006-1125-2897

Vlasov Sergei N. – 4th-year Student, Faculty of Medicine and Prevention, Rostov State Medical University, Rostov-on-Don, ser. vl4s0v02@yandex.ru, https://orcid.org/0000-0003-3289-8436

Dimitriadi Sergei N. – Dr. Sci. (Med.), Senior Researcher, Oncourology Department, National Medical Research Center for Oncology, Rostov-on-Don, Dimitriadi.pro@gmail.com, https://orcid.org/0000-0002-2565-1518

(✉) **Golovinov Igor V.,** ivgolovinov@yandex.ru

Received 05.03.2024;
approved after peer review 26.03.2024;
accepted 14.05.2024

УДК 577.112:616-006
https://doi.org/10.20538/1682-0363-2024-4-169-176

Angiogenin: biological role, mechanisms of action, and participation in oncogenesis

Mikhalev D.E., Korotenko S.N., Lomovskikh A.Yu., Baydik O.D.

Siberian State Medical University
2, Moscow Trakt, Tomsk, 634050, Russian Federation

ABSTRACT

Angiogenin is a small polypeptide consisting of 123 amino acids involved in the processes of angiogenesis and tumorigenesis. This protein plays an important role in various physiological and pathological processes through the regulation of cell proliferation, survival, migration, invasion, and differentiation.

The lecture presents data on angiogenin production and interaction with various proteins, describes mechanisms of its action, and shows its biological role in angiogenesis and oncogenesis. The literature search was carried out in the PubMed, Medline, Elibrary, Scopus, The Cochrane Library, and RSCI search engines.

Keywords: angiogenin, angiogenesis, carcinogenesis, biologically active substances

Conflict of interest. The authors declare the absence of obvious or potential conflicts of interest related to the publication of this article.

Source of financing. The authors state that they received no funding for the study.

For citation: Mikhalev D.E., Korotenko S.N., Lomovskikh A.Yu., Baydik O.D. Angiogenin: biological role, mechanisms of action, and participation in oncogenesis. *Bulletin of Siberian Medicine.* 2024;23(4):169–176. https://doi.org/10.20538/1682-0363-2024-4-169-176.

Ангиогенин: биологическая роль, механизмы действия и участие в онкогенезе

Михалев Д.Е., Коротенко С.Н., Ломовских А.Ю., Байдик О.Д.

Сибирский государственный медицинский университет (СибГМУ)
Россия, 634050, г. Томск, Московский тракт, 2

РЕЗЮМЕ

Ангиогенин – небольшой полипептид, состоящий из 123 аминокислот, вовлеченный в процессы ангиогенеза и онкогенеза. Данный белок играет важную роль в различных физиологических и патологических процессах посредством регуляции пролиферации, выживания, миграции, инвазии и дифференцировки клеток.

В лекции представлены данные о получении, взаимодействии ангиогенина с различными белками, приведены механизмы действия, показана биологическая роль в ангиогенезе и онкогенезе. Поиск литературы осуществлялся в поисковых системах PubMed, Medline, Elibrary, Scopus, The Cochrane Library, РИНЦ.

✉ *Mikhalev Dmitry E.,* dm199412@gmail.com

Ключевые слова: ангиогенин, ангиогенез, канцерогенез, биологически активные вещества

Конфликт интересов. Авторы декларируют отсутствие явных и потенциальных конфликтов интересов, связанных с публикацией настоящей статьи.

Источник финансирования. Авторы заявляют об отсутствии финансирования при проведении исследования.

Для цитирования: Михалев Д.Е., Коротенко С.Н., Ломовских А.Ю., Байдик О.Д. Ангиогенин: биологическая роль, механизмы действия и участие в онкогенезе. *Бюллетень сибирской медицины.* 2024;23(4):169–176. https://doi.org/10.20538/1682-0363-2024-4-169-176.

INTRODUCTION

Bioactive substances are essential for our bodies. Since the beginning of the last century, scientists have been trying to experimentally determine which substances are responsible for tissue proliferation. The discovery of growth factors in the late 1970s and early 1980s prompted the scientific community to view tissue repair processes in a new light [1–4]. A separate direction in the study of growth factors has been their influence on carcinogenesis [5, 6]. Some of these factors were first isolated from malignant tumors [7, 8].

Currently, dozens of bioactive substances are known to be involved in the proliferation and migration of various cell types, including angiogenin (ANG) [9–12].

MAIN PART

General information. ANG is a member of the superfamily of ribonucleases (RNase 5) and is a primary protein consisting of 123 amino acids, with a molecular weight of 14.1 kDa. Ten types of ANG have been identified in various mammals and fish, each exhibiting specific biological activities. Evidence suggests that ANG (RNase5) and ribonuclease 4 (RNase4) represent the most ancient forms of ribonucleases, which appeared in the earliest vertebrates as part of a protective antimicrobial system. ANG shares 33% sequence identity and 65% sequence homology with pancreatic ribonuclease (RNase1). A common feature of all ribonucleases is their enzymatic activity toward ribonucleic acid (RNA) [13].

The protein contains three domains, which serve as distinct functional sites of biological activity [14, 15]: (a) cellular receptor binding site: it consists of amino acid residues in the Lys60, Asn68, and Asn109 loop segments, allowing for binding to motor neurons and endothelial cells [14]; (b) nuclear localization sequence (NLS), comprising residues Ile29–Leu35, which facilitate nuclear translocation of ANG [14]; (c) catalytic site: it includes residues His13, Lys40, and His114, which creates the catalytic center (P1), where the phosphodiester bond cleavage occurs [16]. ANG also has a pyrimidine base binding site (B1) and a purine base binding site (B2). Blockage of the B1 site partially explains why ANG reduces ribonucleolytic activity. These structures are responsible for the unique ribonucleolytic activity and diverse biological functions of this protein [15].

Angiogenin production. Since the late 1980s, scientists have been using various types of fungi as producers of heterologous proteins [17]. Recently, the methylotrophic yeast fungus of the *Pichia pastoris* genus has gained popularity as a producer of recombinant proteins. *P. pastoris* offers several advantages over *E. coli*, such as a lack of protein misfolding, a high level of recombinant protein secretion into the extracellular space (which simplifies the purification process), and the ability to perform post-translational modifications of the produced proteins [18].

Currently, a Russian patent has been granted for the synthesis of a recombinant chimeric human ANG protein using *P. pastoris* yeast culture [19].

The role of angiogenin in physiological processes. In healthy individuals, the concentration of ANG in blood plasma ranges from 274 to 496 ng / ml. Changes in ANG levels depend on numerous factors, including gender, age, and body weight. ANG concentrations can fluctuate under various physiological conditions, such as during different phases of the menstrual cycle and pregnancy. Additionally, ANG levels may change due to pathological processes of different etiology. This fact is of great scientific interest and opens new horizons for the early diagnosis of various diseases [20].

At the cellular level, ANG regulates proliferation, migration, invasion, adhesion, and differentiation of cells in various experimental cell models [21, 22].

It has been established that the ANG receptor is absent on the membrane of fused endothelial cells in blood vessels and does not induce ribosome biogenesis [23, 24]. However, high concentrations of ANG in blood vessels stimulate vascular growth and tissue repair in cases where endothelial cells fail to fuse, thereby promoting wound healing when vascular integrity is compromised [25]. Additionally, hemodynamic forces are linked to the cell cycle activity of endothelial cells, which tend to renew very slowly in adult tissues [26]. Thus, plasma ANG may control vascular homeostasis by maintaining the self-renewal of endothelial cells.

Besides stimulating angiogenesis through the activation of vascular endothelial and smooth muscle cells, ANG acts as a trigger in processes, such as tubular structure formation, cell proliferation, invasion, and migration [27].

According to L.M. Cucci et al. (2021), copper plays a significant role in ANG mechanism of action [28]. Copper ions enhance and promote vascular permeability as well as endothelial cell migration and proliferation by interacting with several factors involved in angiogenesis. Copper strengthens the binding of ANG to endothelial cells and affects the intracellular localization of the protein. L.M. Cucci et al. (2021) also suggest that copper can modulate ANG transcription [28].

Copper increases ANG expression in the HUVEC cell line, indicating that an increase in the extracellular copper level during angiogenesis may regulate ANG levels [29].

Mechanisms of action and biological role of angiogenin in angiogenesis. Several mechanisms of ANG action in angiogenesis are known:

1. It exhibits ribonuclease activity.
2. ANG binds to cell receptors.
3. It induces basement membrane degradation.
4. ANG binds to a 170 kDa protein (ANG-binding protein), subsequently transmitting a signal into the cell cytoplasm.
5. ANG translocates to the nucleus of the target cell, enhancing rRNA transcription [27].

Angiogenin-interacting proteins. The first identified ANG-binding protein is human placental ribonuclease inhibitor (RNH1), a leucine-rich protein with a mass of 50 kDa [29]. RNH1 and ANG have extensive binding interfaces, with key contacts involving the catalytic residue Lys-40 of ANG and the C-terminal segment (434–460) of RNH1 [30]. The angiogenic and enzymatic activities of ANG are inhibited by its binding to RNH1 [30]. The interaction between cellular ANG and RNH1 prevents accidental cleavage of cellular RNA. RNH1 has been found to control the subcellular localization of ANG to regulate cell growth and survival [30]. Several proteins interact with ANG, affecting various cellular functions, such as cell proliferation and survival, including follistatin [31], histone H3 [33], four and a half LIM domains 3 (FHL3) [32], and ANG receptor expressed in human endothelial cells [34], or syndecan-4 in astrocytes [35]. ANG also plays a role in apoptosis regulation, interacting with p53 [36], MDM2 [37], heat shock factor 1 (HSF1) [37], and RNH1 [30]. Comprehensive identification of ANG-interacting proteins may help create interaction maps and further clarify its roles and mechanisms.

Under stress conditions, secreted ANG accumulates in the cytoplasm and nucleoli via a receptor-mediated endocytosis mechanism, activating signaling pathways, such as PI3K/AKT, SAPK/JNK, and ERK1/2 in various cells. The interaction between ANG and cell surface complexes can lead to extracellular matrix (ECM) degradation and activation of matrix metalloproteinases (MMPs), supporting cell invasion and migration. Cytoplasmic ANG, under stress, cleaves tRNA to produce tiRNA, which inhibits translation initiation by recruiting eIF4G/A away from uncovered mRNA via interaction with the YB-1 translation silencer. ANG also promotes ubiquitination of p53 by inhibiting p53 phosphorylation at serine-15, allowing for subsequent binding to Mdm2. Furthermore, nuclear ANG enhances mRNA and rRNA transcription under growth conditions.

Cellular angiogenin regulates nucleic acid metabolism

It has been established that secreted ANG accumulates in nucleoli via endocytosis mechanisms and promotes nucleic acid metabolism by facilitating the transcription of 47S pre-rRNA. This occurs through its binding to ABE (ANG-B-indicating element) and UCE (upstream control element) regions on the promoter of ribosomal DNA (rDNA). Secreted ANG increases the number of actively transcribing rDNA units and participates in the assembly of the initiation complex through epigenetic activation, involving promoter methylation and histone modification [38].

Excess ANG in the nucleus has also been linked to mRNA transcription regulation. ANG inhibits the expression of ERRγ by binding to the first exon region of the estrogen-related receptor gamma (ERRγ) [39]. For

genome-wide screening and identification of mRNA regulated by ANG, a chromatin immunoprecipitation analysis was conducted, identifying a total of 699 genes. This analysis revealed that these genes significantly enrich oncogenesis pathways. Given that ANG binds to histone proteins and remodels histone modifications, it likely acts as a chromatin remodeling activator by regulating mRNA transcription.

ANG also plays a crucial role in tRNA metabolism within the cytoplasm. Interestingly, tRNA was the first molecule used for the enzymatic quantification of ANG activity [39]. Recent studies have shown that ANG degrades single-stranded 3'-CCA ends of tRNA or the anticodon loop, producing tiRNA (stress-induced small RNA derived from tRNA) in response to stress (e.g., oxidative, hypoxic, or nutrient deprivation stress) [40–42]. Modification of specific tRNA anticodon loops (such as Val AAC, Gly GCC, and Asp GTC) protects tRNA from ANG-induced cleavage [42]. Additionally, RNH1 may regulate the stress-induced subcellular localization of ANG to control tiRNA production under stress conditions [42].

Angiogenin stimulates basement membrane degradation

In the tumor microenvironment, extracellular ANG can reach the surface of endothelial cells, where it binds to actin and dissociates as a complex known as AngBP [24, 43]. This complex initiates the synthesis of plasmin from plasminogen [44]. ANG-induced changes in the cytoskeleton include: alterations in the physical properties of F-actin and inhibition of G-actin polymerization; activation of the plasminogen / serine protease system and the matrix metalloproteinase (MMP) system, which are driven by the interaction between ANG and surface-bound actin [43, 44].

ANG serves as a bridging molecule, facilitating interactions with proteins, such as uPAR, A2, and the S100-A10 complex, which are essential for plasmin formation and cell migration at the interface of lipid and non-lipid rafts in cell membranes [45, 46]. A peptide has been identified (ANI-E) that inhibits the interaction between ANG and actin, as well as ANG-induced angiogenesis [43]. By activating the fibrinolytic system in cells, ANG at concentrations ≥ 100 ng / cm² enhances endothelial cell migration and invasion. Additionally, ANG promotes the adhesion of various target cells [44]. Thus, ANG contributes to the degradation of the basement membrane and ECM. Furthermore, cytoplasmic ANG optimizes the assembly of stress fibers and the formation of focal adhesions to facilitate cell migration by interacting with β-actin, α-actinin-4, and non-muscle myosin heavy chain 9 [43].

Angiogenin can maintain vascular homeostasis

As previously mentioned, ANG plays a crucial role in both normal angiogenesis and tumor growth by interacting with endothelial and smooth muscle cells. ANG mediates the migration, invasion, and proliferation of these cells, as well as the formation of tubular structures. In addition to these functions, ANG binds to actin in smooth muscle and endothelial cells, initiating proteolytic cascades that produce proteases, including plasmin, which facilitate the degradation of fibronectin and laminin layers in the basement membrane and ECM. This process supports the migration of endothelial cells into the perivascular tissue. Moreover, ANG activates extracellular signal-regulated kinases 1/2 (ERK1/2) and protein kinase B/Akt, which promote cell proliferation and invasion of the basement membrane, further contributing to angiogenesis. The nuclear translocation of ANG is a critical step in angiogenesis, as it enhances the transcription of ribosomal RNA (rRNA) by binding to the CT-rich ANG-binding element (ABE). This, in turn, activates other angiogenic factors that promote the formation of new blood vessels.

Angiogenin in oncogenesis

Tumorigenesis is a multi-step process characterized by genetic and epigenetic changes in tumor cells, as well as the creation of supportive conditions in the tumor microenvironment. It has been shown that ANG influences almost all stages of oncogenesis, including the stimulation of tumor cell proliferation, protection of tumor cells from adverse survival conditions, enhancement of tumor cell migration and invasion, and induction of angiogenesis.

Solid tumor cells, under unfavorable conditions, can reprogram gene expression to adapt to suboptimal conditions, survive, and continue to grow. ANG, as one of the stress-responsive proteins, significantly increases in cell lines of lymphoma, cervical cancer, and human malignant melanoma under hypoxic conditions [47–49]. It has been established that hypoxia-inducible factor-1 (HIF-1), which controls gene expression, is both necessary and sufficient to activate ANG expression in cells exposed to hypoxia [50].

ANG is secreted by tumor cells, promoting the formation of the microenvironment, tumor proliferation, and growth. This protein can constantly move into the nuclei of tumor cells regardless of

their density and contribute to proliferation [22]. Being one of the major angiogenic components of microvesicles (MV), ANG is released by glioblastoma and stimulates tube formation by endothelial cells [51]. Hepatocellular carcinoma cells also secrete ANG, inducing hepatic stellate cells and remodeling the ECM composition [52]. Consequently, ANG facilitates endothelial cell migration to the tumor by degrading the ECM and the basement membrane. Mast cells, accumulating in the tumor stroma, also promote the release of ANG [20]. Another source of ANG is MVs derived from mesenchymal stem cells under hypoxic conditions, whose primary function is the formation of new blood vessels [20]. It has been shown that ANG induces vascular mimicry in HT1080 fibrosarcoma cells, promoting tumor angiogenesis and metastasis through blood vessels [24].

Measuring ANG levels in blood serum is advisable for assessing risk and predicting the progression of various cancers. ANG serum levels vary depending on the cancer stage, type, and treatment. For example, elevated ANG levels in the serum of patients with solid tumors have been associated with poor prognosis [20]. It has been found that during the evolution of prostate epithelial cells from a benign to an invasive phenotype, ANG levels significantly increase [53]. There are ongoing discussions about the use of ANG as a clinical marker for detecting tumor recurrence and evaluating treatment efficacy.

The epithelial-mesenchymal transition (EMT) is a process in which epithelial cells lose their apical-basal polarity, change their phenotype to a mesenchymal state, and exhibit decreased cell – cell adhesion. This leads to increased adhesion to the ECM, acquiring invasive and mesenchymal-like properties. In tissues of squamous cell lung carcinoma, high ANG expression was positively correlated with mesenchymal marker expression and negatively correlated with epithelial markers. Vimentin and TGF-β1 play an important role in the EMT and are key regulators of mesenchymal cell migration. ANG overexpression leads to upregulation of vimentin, TGF-β1, and N-cadherin and downregulation of E-cadherin and β-catenin, indicating that ANG promotes lung cancer invasion and metastasis by inducing the EMT [54].

ANG may also contribute to tumor cell proliferation, invasion, migration, and EMT by cleaving mature tRNAs, forming tiRNAs, which influence cell proliferation, apoptosis, gene expression, post-transcriptional modification, kinase activity, and translation [55].

ANG binds to receptors associated with vascular endothelial cells, promoting tumor angiogenesis. Specific binding of ANG to the receptor tyrosine kinase (RTK) Tie-2 on the surface of endothelial cells leads to phosphorylation and dissociation of perivascular Sertoli cells. This facilitates the formation of vascular structural migration channels, as well as the activation and migration of endothelial cells, vascular remodeling, and the formation of new vascular branches, which in turn increase blood perfusion flow [56]. ANG induces angiogenesis in breast cancer tissue by activating protein kinase B/Akt through binding to its receptor (FHL3) on endothelial cells or by entering cells via endocytosis and undergoing nuclear translocation. Nuclear translocation of ANG is crucial for angiogenesis initiated by other angiogenic factors (e.g., vascular endothelial growth factor (VEGF)). Indeed, if ANG is blocked, these factors may lose their angiogenic function [57].

ANG is capable of regulating the sensitivity of malignant tumors to radiation and chemotherapy. Radiation can destroy blood vessels that supply the tumor with nutrients and oxygen, playing a vital role in cancer elimination [57]. Studies show that a combination of radiation therapy and anti-angiogenic drugs has a synergistic effect, and ANG inhibitors, combined with radiation therapy, hold promise in reducing recurrence rates after tumor radiotherapy and improving survival [58–60]. However, the specific molecular mechanisms behind this effect require further clarification. Research has also shown that ANG plays a role in resistance to radiation therapy (RT). Using a set of RayBio human cytokine antibodies, 297 protein levels were simultaneously investigated, and the conditioned media from HONE1 and HONE1-IR-resistant nasopharyngeal carcinoma cells were analyzed. ANG expression was significantly higher in HONE1-IR cells treated with 4 Gy radiation, which induced radioresistance in nasopharyngeal cancer cells and reduced both recurrence-free and overall survival in nasopharyngeal cancer patients [61].

ANG is a ligand of the epidermal growth factor receptor (EGFR) and can act as a biomarker for predicting sensitivity to the EGFR tyrosine kinase inhibitor erlotinib in patients with pancreatic cancer. In this context, ANG is associated with decreased sensitivity to erlotinib treatment both *in vitro* and *in vivo*. In one patient cohort, high plasma levels of ANG in pancreatic cancer patients were positively correlated with the response to erlotinib treatment. Q93 ANG is necessary for effective EGFR binding

and activation. Activation of the ANG-EGFR axis makes tumors more sensitive to erlotinib treatment, while ANG knockdown reduces sensitivity to erlotinib treatment and sustains colony formation and cell viability [62].

CONCLUSION

ANG is a multifunctional protein with diverse mechanisms of action. On the one hand, it actively participates in cancer initiation and progression by promoting tumor neovascularization and regulating proliferation, invasion, migration, and therapy sensitivity in various cancer types. On the other hand, it acts as a reparative agent with anti-inflammatory properties. The conditions under which ANG wound-healing properties shift to oncogenic ones remain unclear, offering prospects for further research in fundamental oncology.

REFERENCES

1. Wee P., Wang Z. Epidermal growth factor receptor cell proliferation signaling pathways. *Cancers (Basel).* 2017;9(5):52–65. DOI: 10.3390/cancers9050052.
2. Schenck K., Schreurs O., Hayashi K., Helgeland K. The role of nerve growth factor (NGF) and its precursor forms in oral wound healing. *International Journal of Molecular Sciences.* 2017;18(2):386–398. DOI: 10.3390/ijms18020386.
3. Hume R.D., Deshmukh T., Doan T., Shim W.J., Kanagalingam S., Tallapragada V. et al. PDGF-AB reduces myofibroblast differentiation without increasing proliferation after myocardial infarction. *JACC. Basic to Translational Science.* 2023;(8)6:658–674. DOI: 10.1016/j.jacbts.2022.11.006
4. Yamakawa S., Hayashida K. Advances in surgical applications of growth factors for wound healing. *Burns & Trauma.* 2019;7:10–17. DOI: 10.1186/s41038-019-0148-1.
5. Mihaylova Z., Tsikandelova R., Sanimirov P., Gateva N., Mitev V., Ishkitiev N. Role of PDGF-BB in proliferation, differentiation and maintaining stem cell properties of PDL cells in *vitro. Archives of Oral Biology.* 2018;85:1–9. DOI: 10.1016/j.archoralbio.2017.09.019.
6. Heldin C.H., Lennartsson J., Westermark B. Involvement of platelet-derived growth factor ligands and receptors in tumorigenesis. *Journal of Internal Medicine*. 2018;283(1):16–44. DOI: 10.1111/joim.12690.
7. Lyons S.M., Fay M.M., Akiyama Y., Anderson P.J., Ivanov P. RNA biology of angiogenin: current state and perspectives. *RNA Biology.* 2017;14(2):171–178. DOI: 10.1080/15476286.2016.1272746.
8. Lugano R., Ramachandra M., Dimberg A. Tumor angiogenesis: causes, consequences, challenges and opportunities. *Cellular and Molecular Life Sciences.* 2020;77:1745–1770. DOI: 1007/s00018-019-03351-7.
10. Isali I., Al-Sadawi M.A.A., Qureshi A., Khalifa A.O., Agrawal M.K., Shukla S. Growth factors involve in cellular proliferation, differentiation and migration during prostate cancer metastasis. *International Journal of Cell Biology.* 2019;2(1-2):1–13.
11. Fernández-Guarino M., Hernández-Bule M.L., Bacci S. Cellular and molecular processes in wound healing. *Biomedicines.* 2023;11(9):2526–2532. DOI: 10.3390/biomedicines11092526.
12. Yurina N.V., Ageeva T.A., Goryachkin A.M., Varaksin N. Effects of recombinant angiogenin on collagen fiber formation and angiogenesis in the dermis of Wistar rats. *Clinical, Cosmetic and Investigational Dermatology.* 2021;14:187–196. DOI: 10.2147/CCID.S294825.
13. Sultana M.F., Abo H., Kawashima H. Human and mouse angiogenins: emerging insights and potential opportunities. *Frontiers in Microbiology*. 2022;13:1022945. DOI: 10.3389/fmicb.2022.1022945.
14. Marzo T., Ferraro G., Cucci L.M., Pratesi A., Hansson Ö., Satriano C. et al. Oxaliplatin inhibits angiogenin proliferative and cell migration effects in prostate cancer cells. *Journal of Inorganic Biochemistry*. 2021;226:111657. DOI: 10.1016/j.jinorgbio.2021.111657.
15. Naletova I., Cucci L., D'Angeli F., Anfuso C., Magrì A., Mendola D. et al. A tunable nanoplatform of nanogold functionalised with angiogenin peptides for anti-angiogenic therapy of brain tumours. *Cancers (Basel).* 2019;11(9):1322–1350. DOI: 10.3390/cancers11091322.
16. Hoang T.T., Raines R.T. Molecular basis for the autonomous promotion of cell proliferation by angiogenin. *Nucleic Acids Research*. 2017;45(2):818–831. DOI: 10.1093/nar/gkw1192.
17. Kastberg L.L., Barbera A.R., Jensen M.K., Workman C.T. Burden imposed by heterologous protein production in two major industrial yeast cell factories: identifying sources and mitigation strategies. *Frontiers in Fungal Biology.* 2022;3:827704. DOI: 10.3389/ffunb.2022.827704.
18. Mastropietro G., Aw R., Polizzi K.M. Expression of proteins in Pichia pastoris. *Methods in Enzymology*. 2021;660:53–80. DOI: 10.1016/bs.mie.2021.07.004.
19. Purtov A. A., Mamaev A.L. Recombinant plasmid for expression in *Pichia pastoris* yeast gene of chimeric protein of human angiogenin and *Pichia pastoris* yeast strain as a producer of recombinant chimeric protein of human angiogenin. Russian Federation RU 2658758, 2017.10.02 Angiopharm LLC. (In Russ.).
20. Yu D., Cai Y., Zhou W., Sheng J., Xu Z. The Potential of Angiogenin as a Serum Biomarker for Diseases: Systematic Review and Meta-Analysis. *Disease Markers.* 2018;15(2018):1984718. DOI: 10.1155/2018/1984718.
21. Garnett E.R., Raines R.T. Emerging biological functions of ribonuclease 1 and angiogenin. *Critical Reviews in Biochemistry and Molecular Biology.* 2022;57(3):244–260. DOI: 10.1080/10409238.2021.2004577.
22. Mao M., Chen W., Ye D. Research progress on the structure, function, and use of angiogenin in malignant tumours. *Heliyon.* 2024;10(9):e30654. DOI: 10.1016/j.heliyon.2024.e30654.
23. Stillinovic M., Sarangdhar M.A., Andina N., Tardivel A., Greub F., Bambaci G. et al. Ribonuclease inhibitor and angiogenin system regulates cell type-specific global translation. *Science Advances.* 2024;10(22):eadl0320. DOI: 10.1126/sciadv.adl0320.

24. Jinghao S., Zhengping X. Three decades of research on angiogenin: a review and perspective. *Acta Biochimica et Biophysica Sinica*. 2016;48(5):399–410. DOI: 10.1093/abbs/gmv131.
25. Gupta S., Chittoria R.K., Chavan V., Aggarwal A., Reddy L.C., Mohan P.B. et al. Role of burn blister fluid in wound healing. *Journal of Cutaneous and Aesthetic Surgery.* 2021;14(3):370–373. DOI: 10.4103/JCAS.JCAS_90_19.
26. Rajala R. How big is the endothelium? Comment on "Spatial and temporal dynamics of the endothelium". *Journal of Thrombosis and Haemostasis.* 2021;19(10):2634–2635. DOI: 10.1111/jth.15469.
27. Lyons S.M., Fay M.M., Akiyama Y., Anderson P.J., Ivanov P. RNA biology of angiogenin: Current state and perspectives. *RNA Biology.* 2017;14(2):171-178. DOI: 10.1080/15476286.2016.1272746.
28. Cucci L.M., Satriano C., Marzo T., La Mendola D. Angiogenin and copper crossing in wound healing. *International Journal of Molecular Sciences*. 2021;22(19):10704. DOI: 10.3390/ijms221910704.
29. Cong X., Cremer C., Nachreiner T., Barth S., Carloni P. Engineered human angiogenin mutations in the placental ribonuclease inhibitor complex for anticancer therapy: Insights from enhanced sampling simulations. *Protein Science.* 2016;25(8):1451–1460. DOI: 10.1002/pro.2941.
30. Sarangdhar M.A., Allam R. Angiogenin (ANG)-ribonuclease inhibitor (RNH1) system in protein synthesis and disease. *International Journal of Molecular Sciences.* 2021;22(3):1287–1293. DOI: 10.3390/ijms22031287.
31. Janik S., Bekos C., Hacker P., Raunegger T., Schiefer A.I., Müllauer L. et al. Follistatin impacts tumor angiogenesis and outcome in thymic epithelial tumors. *Scientific Reports.* 2019;9(1):17359. DOI: 10.1038/s41598-019-53671-8.
32. Huang Z., Yu C., Yu L., Shu H., Zhu X. The Roles of FHL3 in Cancer. *Frontiers in Oncology*. 2022;12:887828. DOI: 10.3389/fonc.2022.887828.
33. Shi P., Xu J., Cui H. The Recent Research Progress of NF-κB signaling on the proliferation, migration, invasion, immune escape and drug resistance of glioblastoma. *International Journal of Molecular.* 2023;24(12):10337. DOI: 10.3390/ijms241210337.
34. Wang Y.N., Lee H.H., Chou C.K., Yang W.H. Angiogenin/ribonuclease 5 Is an EGFR ligand and a serum biomarker for erlotinib sensitivity in pancreatic cancer. *Cancer Cell.* 2018;33(4):752–769.e8. DOI: 10.1016/j.ccell.2018.02.012.
35. Hoang T.T., Johnson D.A., Raines R.T., Johnson J.A. Angiogenin activates the astrocytic Nrf2/antioxidant-response element pathway and thereby protects murine neurons from oxidative stress. *The Journal of Biological Chemistry*. 2019;294(41):15095–15103. DOI: 10.1074/jbc.RA119.008491.
36. Yeo K.J., Jee J.G., Hwang E., Kim E.H., Jeon Y.H., Cheong H.K. Interaction between human angiogenin and the p53 TAD2 domain and its implication for inhibitor discovery. *FEBS Letters.* 2017;591(23):3916–3925. DOI: 10.1002/1873-3468.12899.
37. Bultman K., Uebersohn A., Dickson K. Angiogenin interacts with heat shock factor 1. *FASEB Journal*. 2015;29:sp880.30. DOI: 10.1096/fasebj.29.1_supplement.880.30.
38. Loveland A.B., Koh C.S., Ganesan R., Jacobson A., Korostelev A.A. Structural mechanism of angiogenin activation by the ribosome. *Nature*. 2024;630(8017):769–776. DOI: 10.1038/s41586-024-07508-8.
39. Su Z., Kuscu C., Malik A., Shibata E., Dutta A. Angiogenin generates specific stress-induced tRNA halves and is not involved in tRF-3-mediated gene silencing. *The Journal of Biological Chemistry*. 2019;294(45):16930-16941. DOI: 10.1074/jbc.RA119.009272.
40. Rashad S., Niizuma K., Tominaga T. tRNA cleavage: a new insight. *Neural Regeneration Research*. 2020;15(1):47–52. DOI: 10.4103/1673-5374.264447.
41. Fu M., Gu J., Wang M., Zhang J., Chen Y., Jiang P. et al. Emerging roles of tRNA-derived fragments in cancer. *Molecular Cancer.* 2023;22(1):30–36. DOI: 10.1186/s12943-023-01739-5.
42. Guzzi N., Bellodi C. Novel insights into the emerging roles of tRNA-derived fragments in mammalian development. *RNA Biology.* 2020;17(8):1214–1222. DOI: 10.1080/15476286.2020.1732694.
43. Weng C., Dong H., Mao J., Lang X., Chen J. characterization and function of the interaction of angiogenin with alpha-actinin 2. *Frontiers in Molecular Biosciences*. 2022;9:837971. DOI: 10.3389/fmolb.2022.837971.
44. Bharadwaj A.G., Holloway R.W., Miller V.A., Waisman D.M. Plasmin and plasminogen system in the tumor microenvironment: implications for cancer diagnosis, prognosis, and therapy. *Cancers (Basel).* 2021;13(8):1838–1845. DOI: 10.3390/cancers13081838.
45. Kushwaha A., Goswami L., Kim B.S. Nanomaterial-based therapy for wound healing. *Nanomaterials (Basel).* 2022;12(4):618–630. DOI: 10.3390/nano12040618.
46. Veith A.P., Henderson K., Spencer A., Sligar A.D., Baker A.B. Therapeutic strategies for enhancing angiogenesis in wound healing. *Advanced Drug Delivery Reviews.* 2019;146:97–125. DOI: 10.1016/j.addr.2018.09.010.
47. Weng C., Dong H., Bai R., Sheng J., Chen G., Ding K. et al. Angiogenin promotes angiogenesis via the endonucleolytic decay of miR-141 in colorectal cancer. *Molecular Therapy. Nucleic Acids.* 2022;27:1010–1022. DOI: 10.1016/j.omtn.2022.01.017.
48. Yang H., Yuan L., Ibaragi S., Li S., Shapiro R., Vanli N. et al. Angiogenin and plexin-B2 axis promotes glioblastoma progression by enhancing invasion, vascular association, proliferation and survival. *British Journal of Cancer*. 2022;127(3):422–435. DOI: 10.1038/s41416-022-01814-6.
49. Mao M., Chen W., Ye D. Research progress on the structure, function, and use of angiogenin in malignant tumours. *Heliyon.* 2024;10(9):e30654. DOI: 10.1016/j.heliyon.2024.e30654.
50. Manuelli V., Pecorari C., Filomeni G., Zito E. Regulation of redox signaling in HIF-1-dependent tumor angiogenesis. *The FEBS Journal*. 2022;289(18):5413–5425. DOI: 10.1111/febs.16110.
51. Marei H.E., Althani A., Afifi N., Hasan A., Caceci T., Cifola I. et al. Glioma extracellular vesicles for precision medicine: prognostic and theragnostic application. *Discover Oncology.* 2022;13(1):49. DOI: 10.1007/s12672-022-00514-0.
52. Bárcena C., Stefanovic M., Tutusaus A., Martinez-Nieto G.A., Martinez L., García-Ruiz C. et al. Angiogenin secretion from

hepatoma cells activates hepatic stellate cells to amplify a self-sustained cycle promoting liver cancer. *Scientific Reports.* 2015;5:7916. DOI: 10.1038/srep07916.
53. González L.O., Eiro N., Fraile M., Beridze N., Escaf A.R., Escaf S. et al. Prostate cancer tumor stroma: responsibility in tumor biology, diagnosis and treatment. *Cancers (Basel).* 2022;14(18):4412. DOI: 10.3390/cancers14184412.
54. Xu L., Yan Y., Xue X., Li C.G., Xu Z.Y., Chen H.Z. Angiogenin elevates the invasive potential of squamous cell lung carcinoma cells through epithelial-mesenchymal transition. *Oncology Reports.* 2016;36(5):2836–2842. DOI: 10.3892/or.2016.5107.
55. Li S., Shi X., Chen M., Xu N. Angiogenin promotes colorectal cancer metastasis via tiRNA production. *International Journal of Cancer*. 2019;145(5):1395–1407. DOI: 10.1002/ijc.32245.
56. Duran C.L., Borriello L., Karagiannis G.S., Entenberg D., Oktay M.H., Condeelis J.S. Targeting Tie2 in the tumor microenvironment: from angiogenesis to dissemination. *Cancers (Basel).* 2021;13(22):5730. DOI: 10.3390/cancers13225730.
57. Li Y., Qu X., Cao B., Yang T., Bao Q., Yue H. et al. Selectively suppressing tumor angiogenesis for targeted breast cancer therapy by genetically engineered phage. *Advanced Materials (Deerfield Beach, Fla.)*. 2020;32(29):e2001260. DOI: 10.1002/adma.202001260.
58. Rani V., Prabhu A. Combining angiogenesis inhibitors with radiation: advances and challenges in cancer treatment. *Current Pharmaceutical Design*. 2021;27(7):919–931. DOI: 10.2174/1381612826666201002145454.
59. Li D., Weng S., Zhong C., Xu D., Yuan Y. Risk of second primary cancers among long-term survivors of breast cancer. *Frontiers in Oncology*. 2019;9:1426–1435. DOI: 10.3389/fonc.2019.01426.
60. Procaccio L., Damuzzo V., Di Sarra F., Russi A., Todino F., Dadduzio, V. et al. Safety and tolerability of anti-angiogenic protein kinase inhibitors and vascular-disrupting agents in cancer: focus on gastrointestinal malignancies. *Drug Safety.* 2019;42(2):159–179. DOI: 10.1007/s40264-018-0776-6.
61. Guo S., Liang Y., Liu L., Chen Q., Wen Y., Liu S. et al. Increased angiogenin expression correlates with radiation resistance and predicts poor survival for patients with nasopharyngeal carcinoma. *Frontiers in Pharmacology*. 2021;12:627935. DOI: 10.3389/fphar.2021.627935.
62. Wang Y.N., Lee H.H., Chou C.K., Yang W.H., Wei Y., Chen C.T. et al. Angiogenin/ribonuclease 5 is an EGFR ligand and a serum biomarker for erlotinib sensitivity in pancreatic cancer. *Cancer Cell*. 2018;33(4):752–769. DOI: 10.1016/j.ccell.2018.02.012.

Authors' information

Mikhalev Dmitry E. – Teaching Assistant, Dentistry Division, Siberian State Medical University, Tomsk, dm199412@gmail.com, https://orcid.org/0000-0002-0647-3576

Korotenko Sergey N. – Teaching Assistant, Dentistry Division, Siberian State Medical University, Tomsk, dr.korotenko@mail.ru. https://orcid.org/0009-0008-7371-318X

Lomovskikh AnastasiaYu. – Student, General Medicine Department, Siberian State Medical University, Tomsk, anastasia17070316@mail.ru, https://orcid.org/0009-0001-7162-1475

Baydik Olga D. – Dr. Sci. (Med.), Professor, Head of the Dentistry Division, Siberian State Medical University, Tomsk, olgabajdik@yandex.ru, https://orcid.org/0000-0002-4748-4175

(✉) **Mikhalev Dmitry E.,** dm199412@gmail.com

Received 01.07.2024;
approved after peer review 09.17.2024;
accepted 12.09.2024

УДК 616.33/.34-092
https://doi.org/10.20538/1682-0363-2024-4-177-186

Markers of gastrointestinal diseases

Ostanko V.L.[1], Kalacheva T.P.[1], Kulumaeva K.A.[1], Li N.A.[2], Beloborodova E.V.[1], Purlik I.L.[1], Kalyuzhina E.V.[1], Brazovskaya N.G.[1], Kalyuzhin V.V.[1]

[1] Siberian State Medical University
2, Moscow Trakt, Tomsk, 634050, Russian Federation

[2] Regional Oncology Center
115, Lenina Av., Tomsk, 634050, Russian Federation

ABSTRACT

The lifestyle of people nowadays and poor diet are factors affecting the increasing incidence of digestive diseases in people all over the world. The search for new methods of early diagnosis of the disease is an urgent issue of modern medicine. In the last decade, much attention has been paid to various biological markers that can be used to assess the risk of disease development, the response to therapy, and the possible development of complications. Biomarkers in clinical medicine can be used as additional tools not only to improve early diagnosis of gastrointestinal diseases but also to assess the effectiveness of therapy.

The aim of this lecture was to analyze and systematize biomarkers in various gastrointestinal diseases.

Keywords: biomarker, atrophic gastritis, inflammatory bowel disease, pancreatic cancer, fecal calprotectin, fatty acid-binding protein, microRNA

Conflict of interest. The authors declare the absence of obvious or potential conflicts of interest related to the publication of this article.

Source of financing. The authors state that they received no funding for the study.

For citation: Ostanko V.L., Kalacheva T.P., Kulumaeva K.A., Li N.A., Beloborodova E.V., Purlik I.L., Kalyuzhina E.V., Brazovskaya N.G., Kalyuzhin V.V. Markers of gastrointestinal diseases. *Bulletin of Siberian Medicine.* 2024;23(4):177–186. https://doi.org/10.20538/1682-0363-2024-4-177-186.

Маркеры заболеваний желудочно-кишечного тракта

Останко В.Л.[1], Калачева Т.П.[1], Кулумаева К.А.[1], Ли Н.А.[2], Белобородова Е.В.[1], Пурлик И.Л.[1], Калюжина Е.В.[1], Бразовская Н.Г.[1], Калюжин В.В.[1]

[1] Сибирский государственный медицинский университет (СибГМУ)
Россия, 634050, г. Томск, Московский тракт, 2

[2] Томский областной онкологический диспансер
Россия, 634050, г. Томск, пр. Ленина, 115

РЕЗЮМЕ

Образ жизни современного человека, неправильное питание – факторы, влияющие на рост заболеваний органов пищеварения у людей во всем мире. Поиск новых методов ранней диагностики болезни – актуальный вопрос современной медицины. В последнее десятилетие большое внимание уделяется различным биологическим маркерам, позволяющим оценивать риск развития заболевания, ответ на терапию и возможное развитие осложнений. Биомаркеры в клинической медицине могут использоваться в качестве

✉ *Kalacheva Tatyana P.,* tatyana-kalachyova@yandex.ru

дополнительных инструментов, способных не только улучшить своевременную диагностику заболеваний желудочно-кишечного тракта, но и оценить эффективность проводимой терапии.

Цель настоящей лекции заключается в анализе и систематизации биомаркеров при различных заболеваниях желудочно-кишечного тракта.

Ключевые слова: биомаркер, атрофия желудка, воспалительные заболевания кишечника, рак поджелудочной железы, фекальный кальпротектин, белок, связывающий жирные кислоты, микроРНК

Конфликт интересов. Авторы декларируют отсутствие явных и потенциальных конфликтов интересов, связанных с публикацией настоящей статьи.

Источник финансирования. Авторы заявляют об отсутствии финансирования при проведении исследования.

Для цитирования: Останко В.Л., Калачева Т.П., Кулумаева К.А., Ли Н.А., Белобородова Е.В., Пурлик И.Л., Калюжина Е.В., Бразовская Н.Г., Калюжин В.В. Маркеры заболеваний желудочно-кишечного тракта. *Бюллетень сибирской медицины.* 2024;23(4):177–186. https://doi.org/10.20538/1682-0363-2024-4-177-186.

INTRODUCTION

Digestive diseases are a socially significant problem as the morbidity and mortality rates are increasing every year. Rosstat data for 2022 reported that the mortality rate from digestive diseases in the Russian Federation is 70.4 per 100,000 population. According to the World Health Organization (WHO), by the mid-21st century, diseases of the digestive system will occupy the leading place in the general morbidity and mortality (https://www.who.int/docs/default-source/gho-documents/world-health-statistic-reports/world-health-statistics-2014.pdf). One of the reasons for this growth lies in the lifestyle of modern man: reduced physical activity, unbalanced diet, bad habits, and stress [1].

The increase in the incidence of digestive diseases among the population has resulted in the situation when doctors have recently been focusing their efforts on identifying the specific features of the disease and using tools to develop a personalized approach, ensuring the choice of the most effective and safest treatment for each patient. The need to improve the approach to an individual patient, taking into account the exact characteristics of their pathological condition or their response to a specific treatment, is a priority goal of personalized medicine [2].

Biomarkers are a key part of the concept of personalized medicine. They are crucial in improving early identification of patients at risk, increasing the accuracy of diagnosis, and facilitating the selection of the best treatment. In addition, biomarkers are essential for understanding the molecular mechanisms underlying diseases and facilitating the identification of potential new therapeutic targets. A biomarker is mainly a serum protein that is found in a particular concentration in various disorders and is also used as an indicator of the response to therapy [3].

Biomarkers have been used in clinical medicine for decades. Back in 2001, the Biomarker Working Group, assembled by the National Institutes of Health (NIH, USA), established the following definition: “A defined characteristic that is measured as an indicator of normal biological processes, pathogenic processes, or responses to an exposure or intervention” [4].

According to the Biomarker Working Group (2001) nomenclature, biomarkers are classified into three types:

– type 0 reflects the natural history of the disease and correlates over time with known clinical indicators;

– type I reflects the effect of therapy, taking into account the mechanism of action of the drug;

– type II includes surrogate endpoints that predict clinical efficacy or harm when using a drug.

The biomarker must meet the criteria of the SMART concept, which means it has to be [5]:

S – specific and sensitive;

M – measurable;

A – available and affordable;

R – responsive and reproducible;

T – timely.

The FDA (Food and Drug Administration) and NIH Biomarker Working Group classifies biomarkers into different types based on their primary clinical application. These types include susceptibility / risk, diagnostic, monitoring, prognostic, predictive, pharmacodynamic/response, and safety (Table 1) [6, 7].

Table

Types of biomarkers based on their primary clinical application [6, 7]

Types of biomarkers	Main features
Diagnostic biomarkers	They play an important role in establishing an accurate diagnosis.
Monitoring biomarkers	This category includes biomarkers measured at different time points to assess the presence and status of disease. Fluctuations in these biomarkers can be used as a tool to assess disease progression or the effectiveness of a therapeutic intervention.
Pharmacodynamic biomarkers	They are used to prove that the effect of the drug on its primary target modifies the progression of the disease.
Predictive biomarkers	They determine the response to therapy and/or drug toxicity.
Prognostic biomarkers	They determine the likelihood of a clinical event, relapse, or disease progression.
Susceptibility/risk	They indicate the potential for disease development in an individual who does not currently have clinically apparent disease. The main difference between this category and prognostic biomarkers is the fact that susceptibility/risk biomarkers are measured in individuals who do not currently have the disease.
Safety	The relevance of these biomarkers consists in predicting toxic side effects caused by drugs, medical interventions, or exposure to environmental agents. Biomarker detection or changes in biomarker levels can reflect toxicity, enabling necessary actions to prevent irreversible damage. These actions may include dose adjustments, treatment interruption, or initiation of specific therapy.

Biomarkers are typically measured in blood, urine, and other tissues [3, 11]. To date, many serum proteins have been evaluated as potential markers for disease diagnosis, but only a few are currently used in clinical practice. When evaluating a biomarker, it is important to compare its level with the clinical pattern and other features [8, 12].

In recent years, an increasing number of studies have aimed at identifying biomarkers that are highly sensitive, highly specific, and minimally invasive. It is important to note that high sensitivity is desirable for biomarkers used in screening, while high specificity is necessary for disease diagnosis [9–11].

BIOMARKERS OF GASTRIC MUCOSAL ATROPHY

Chronic atrophic gastritis and intestinal metaplasia may contribute to the development of dysplasia and adenocarcinoma. Chronic atrophic gastritis is usually asymptomatic for a long time, which makes it difficult to diagnose it early. Studies have demonstrated that the severity of inflammatory and dystrophic mucosal changes does not correlate with the presence and severity of clinical symptoms [13]. Early diagnosis of chronic atrophic gastritis is recommended as a preventive measure, regardless of the presence or absence of dyspepsia symptoms. Researchers are actively seeking screening methods for atrophic gastritis. Determination of pepsinogens and *Helicobacter pylori* (*H. pylori*) infection in serum is considered the optimal method [14].

Pepsinogen I (PG-I) is synthesized by the main gland cells of the gastric mucosa, and its decrease is the first marker of gastric mucosal atrophy. In severe atrophic gastritis, the major cells are lost, leading to a decrease in PG-I, while the level of pepsinogen II (PG-II) remains relatively constant [15]. PG-II is secreted not only by the glands of the fundus but also by the pyloric glands of the antral stomach and Brunner's glands of the proximal duodenum. Therefore, a low serum PG-I level (≤70 ng / ml) and / or a low PG-I / PG-II ratio (≤3.0) indicate the presence of chronic atrophic gastritis and a high risk of gastric cancer [16]. The study by C.B. Conti et al. demonstrated that a reduction in serum pepsinogen levels and a decrease in the PG-I / PG-II ratio are indicative of atrophic changes in the gastric mucosa [17]. The laboratory method has specificity and sensitivity in diagnosing chronic atrophic gastritis of 92.2–97.8% and 15–75%, respectively [18].

Gastrin-17 (G-17) is another biomarker of gastric mucosal atrophy. It is synthesized and released by G cells of the mucous membrane in response to food intake. G-17 stimulates enterochromaffin-like cells (ECL) to secrete histamine, which in turn induces acid release from parietal cells [19]. Disruption of acid-mediated inhibition of gastrin leads to atrophic gastritis, an increased population of ECL, and parietal cells. G-17 is also a proliferative and anti-apoptotic hormone that is thought to play an important role in gastric carcinogenesis. It has been reported that patients with gastric cancer have higher serum G-17 levels than patients without it [20]. Therefore, serum G-17 levels can be used to identify individuals at high risk of gastric cancer.

Another important indicator to consider is *H. pylori*, which is a gram-negative bacterium with 4–8 polar flagella. Although *H. pylori* is not a biomarker as such, the so-called helicobacteriosis has a high prognostic value. In 1994, the International Agency

for Research on Cancer (IARC) expert group classified *H. pylori* as a type 1 carcinogen [21]. The process of gastric carcinogenesis, also known as the Correa's cascade, is a stepwise progression from normal gastric epithelium to chronic non-atrophic gastritis, chronic atrophic gastritis, intestinal metaplasia, dysplasia, and cancer [15]. Many clinical trials in recent years have shown that *H. pylori* infection is associated with a high risk of gastric cancer in patients with atrophic gastritis and intestinal metaplasia [17]. Furthermore, a correlation has been found between a decrease in the prevalence of *H. pylori* in Western Europe, the USA, and Japan and a decrease in the incidence of peptic ulcer disease and gastric cancer [21].

The cag pathogenicity island (cagPAI) and its effector protein, cytotoxin-associated gene A (cagA), are considered virulence factors of *H. pylori*. *H. pylori* strains can be classified as *cag*A-positive or *cag*A-negative based on the presence or absence of the *cagA* gene in their bacterial genome. Literature reports that individuals infected with *cag*A-positive strains are at a greater risk of developing gastric ulcers and cancer than those infected with *cag*A-negative strains of *H. pylori* [22]. In a recent study by K.M. Miernyk et al. involving 263 patients in Alaska, intact cagPAI was detected in 150 (57%) strains of *H. pylori*, which appeared to be associated with the development of more severe gastric pathology. Of the 12 *H. pylori* strains isolated from patients with gastric cancer, 10 (83%) had intact cagPAI [23].

In addition, *H. pylori* secrete vacuolating cytotoxin A (vacA). VacA can alter the permeability of the plasma membrane, destroy mitochondria and endosomes, and affect mitochondrial activity, contributing to apoptosis. It is worth noting that although all *H. pylori* strains possess the *vacA* gene, some bacterial species have mutations in their vacA sequences. Patients infected with strains containing *vacA s1, i1*, or *m1* variants are at an increased risk of developing gastric cancer [24].

BIOMARKERS OF INTESTINAL MUCOSAL DAMAGE

Abnormal gut barrier function plays a central role in the pathogenesis of chronic intestinal inflammation. Tight junctions change, and the frequency of apoptosis events increases. These barrier defects are attributed to the increased activity of proinflammatory cytokines that are highly expressed in the chronically inflamed gut [25]. It is still discussed whether changes in epithelial permeability in patients with inflammatory bowel disease (IBD) play a primary role in the pathogenesis of the disease or whether there is a secondary effect in response to inflammation. IBDs have demonstrated a growing incidence and prevalence since their discovery. Therefore, the search for non-invasive, high-quality, and inexpensive biomarkers of intestinal inflammation activity is becoming increasingly important. Fecal biomarkers are widely recognized as biomarkers of IBD. Fecal markers are a group of substances that are produced in inflammation of the intestinal mucosa. Fecal calprotectin, fatty acid-binding protein (FABP), zonulin, and eosinophil-derived neurotoxin are the most promising markers [26].

Fatty acid-binding proteins (FABP) are a family of transport proteins for fatty acids and other lipophilic substances. These proteins facilitate the transport of fatty acids between extracellular and intracellular membranes. FABPs are classified according to their tissue tropism: adipocyte (A), epidermal (E), cardiac and muscular (H), small intestine (I), liver (L), large intestine (Il), brain (B), and testicular (T) [27].

Intestinal fatty acid-binding protein (I-FABP) is present exclusively in enterocytes throughout the small intestine. This small 15 kDa cytosolic protein rapidly appears in the bloodstream after intestinal epithelial cell damage. I-FABP is expressed in mature enterocytes but not in crypts. The level of I-FABP is quite low under physiological conditions. H. Funaoka et al. determined that the serum concentration of I-FABP in healthy people is 2.0 ng / ml or less [28]. Its amount increases in response to damage to the cell membrane of the small intestinal epithelium [29]. I-FABP circulates in the blood for several hours after tissue damage and is then excreted from the body. I-FABP is measured in serum (or plasma), urine, and coprofiltrate [26]. Several studies have shown that elevated serum or urine I-FABP concentrations are associated with impaired intestinal permeability and may be a marker of early diagnosis of IBD, celiac disease, and ischemic colitis.

The study by M.P. Adriaanse et al. suggests that serum I-FABP is an early marker of gluten-induced enteropathy in patients with celiac disease [30]. Furthermore, it has been studied as a marker of mechanical (strangulation) intestinal obstruction of the small bowel and necrotizing enterocolitis. Thus, the study by M. Schurink et al. demonstrated that I-FABP measured in plasma helps identify patients with necrotizing enterocolitis among preterm infants with non-specific symptoms. Moreover, in patients diagnosed with necrotizing enterocolitis, I-FABP

levels can predict disease complications at early stages. Its highest levels are typically observed within the first 24 hours after the onset of symptoms, and then they gradually decrease [31].

Zonulin, an analogue of cholera toxin, is another biomarker of intestinal mucosal damage. It is synthesized in the liver and intestinal epithelial cells [32]. In 2000, the research group under the supervision of A. Fasano reported the discovery of zonulin, a human protein analogue of Zonula occludens toxin derived from cholera vibrio that regulates paracellular permeability [33]. The chemokine receptor type 3 (CXCR3) is the main regulator of zonulin release in the gut. It is an inflammatory chemokine receptor. The primary function of CXCR3 is to stimulate chemotaxis, cell migration, and adhesion of immune cells. CXCR3 is present in the intestinal lamina and epithelial cells, and its expression is elevated in patients with celiac disease or IBD [34]. Zonulin levels have been found to be elevated in individuals with irritable bowel syndrome, IBD, and necrotizing enterocolitis, which is associated with impaired mucosal barrier function [35]. The degree of change in zonulin concentrations in various biological media (blood, feces) does not always coincide and depends on the form of pathology. For example, in patients with ulcerative colitis, serum zonulin is preferred as a marker of increased intestinal permeability over fecal zonulin. In contrast, fecal zonulin levels are significantly higher than plasma levels in HIV-seropositive patients with gastrointestinal symptoms [36].

Calprotectin is an antimicrobial, immunomodulatory, and antiproliferative protein with a mass of 36 kDa, a member of the S100 protein family. It is found in the membranes of macrophages, in the cytoplasm of neutrophils, in monocytes, and in mucosal epithelial cells. Calprotectin was first described in 1980. It is a heterodimer consisting of S100A8 and S100A9 proteins. Antimicrobial effects of calprotectin are related to its ability to chelate metal ions. Its concentration in feces is approximately six times higher than in plasma [37]. This protein is stable in the external environment and remains the same in feces for up to 7 days. Calprotectin is present in small amounts in the feces of healthy individuals [6].

The level of calprotectin in different tissues of the body is directly proportional to the degree of inflammation. Fecal calprotectin levels are used as one of the diagnostic criteria for IBD. Failure to control inflammatory activity in IBD is associated with both poorer quality of life in patients and worse long-term outcomes (increased risk of colorectal carcinogenesis). Therefore, it is crucial to prevent clinical relapse and maintain remission in the long term [37]. According to the latter concept, clinical remission in patients with IBD should be supported by both biological and endoscopic evidence of the absence of mucosal inflammatory activity. Biological inactivity may be indicated by the absence of inflammatory markers in peripheral blood or feces (calprotectin), whereas mucosal healing is the most appropriate endoscopic goal. Commonly used biomarkers, such as C-reactive protein and erythrocyte sedimentation rate, lack sensitivity and specificity. Fecal calprotectin has a high negative predictive value in ruling out IBD in undiagnosed patients with symptoms and high sensitivity to the diagnosis of the disease [38]. The meta-analysis by T. Rokkas et al. demonstrated that the best sensitivity (90.6%) was achieved for fecal calprotectin levels of 50 μg / g in IBD, whereas the best specificity (78.2%) was found at levels >100 μg / g [39]. Therefore, there is increasing evidence that fecal calprotectin estimation may be useful for monitoring disease activity and response to therapy, as well as for predicting relapse.

Many research groups have focused on microRNAs (miRNAs) over the past 10 years. A significant level of scientific evidence emphasizes the functional role and potential value of small RNA molecules. MicroRNAs are small non-coding RNAs consisting of 18–25 nucleotides. Currently, miRNAs are being investigated as biomarkers for IBD [40]. Firstly, microRNAs are known to be functional molecules that can be dysregulated at early stages of the disease. Secondly, deregulation of microRNAs can cause significant changes in gene expression and contribute to inflammatory and neoplastic diseases. Thirdly, microRNAs are unique molecules with incredible resistance to degradation [41]. Various studies have repeatedly shown that IBD is associated with changes in microRNA expression in the colonic mucosa. In addition to their potential role in monitoring disease activity, whether it is clinical, biochemical, or endoscopic activity [40], microRNAs can also be used as predictors of response to therapy. For example, in an evaluation of patients with severe ulcerative colitis who did not respond to initial corticosteroid therapy, I. Morilla et al. identified 15 microRNAs associated with response to corticosteroids, 6 microRNAs associated with response to infliximab, and 4 microRNAs associated with response to cyclosporine, thus emphasizing the role of microRNA as a predictor of response to therapy in IBD [41].

MARKERS OF LIVER DAMAGE

Among all digestive diseases, liver diseases have been the main cause of death in Russia for many years. About 2 million people die annually of cirrhosis and hepatocellular carcinoma (HCC) worldwide (Global Cancer Statistics 2022).

The main factors in liver damage are alcohol and drugs, infection with hepatitis A, B, C, D, and E, and metabolic disorders. According to the literature reviewed, more than half of patients who abuse alcohol suffer from toxic liver damage and then develop cirrhosis, and 10 years after the beginning of alcohol abuse, they develop HCC [42]. According to WHO, the prevalence of obesity has increased from 4.6% in 1980 to 14.0% in 2020. As a result, the incidence of non-alcoholic fatty liver disease (NAFLD) has also increased. In 2020, the new term metabolic-associated fatty liver disease was introduced [43]. The growth of liver diseases leads to the need to search for new methods of early diagnosis. A number of serum biomarkers can be used to assess the pathological state and disease progression.

The FDA has supported total cytokeratin 18 (K18), glutamate dehydrogenase (GLDH), and microRNA-122 (miR-122) as promising biomarkers for diagnosing liver damage [44]. The study by R.J. Church et al. found a positive correlation between GLDH activity and alanine aminotransferase (ALT) activity. Additionally, K18 and miR-122 levels were positively correlated with ALT activity, indicating a positive association of these biomarkers with cytolytic syndrome [45].

The clinical standard for assessing liver damage is the measurement of serum ALT and aspartate aminotransferase levels. These enzymes are released into the bloodstream due to hepatocyte damage. However, it is important to note that these tests have limitations despite their widespread clinical use. Firstly, the enzymes are not absolutely specific to hepatocytes. Aspartate aminotransferase is expressed in the liver, heart, skeletal muscles, kidneys, brain, pancreas, and lungs. ALT is an intracellular enzyme that is predominantly found in liver and kidney cells and in small amounts in heart and skeletal muscles. Secondly, liver enzymes do not always reflect the severity of the disease [46]. According to the study by H.P. Llewellyn et al., a panel consisting of several biomarkers, including GLDH, K18, and microRNA-122, can differentiate between patients with muscular dystrophies and those with liver pathology. This model has significant advantages over ALT measurement [44].

MiR-122 is the most abundant liver-specific microRNA (accounting for 70% of the total liver microRNA pool) and exists in two mature isoforms: miR-122-3p and miR-122-5p. The deficiency of miR-122 results in inflammation, cholestasis, and, ultimately, liver fibrosis. MiR-122 regulates the synthesis and oxidation pathway of cholesterol and fatty acids and is involved in hepatocyte proliferation and differentiation. In their study, M.I. Kan Changez et al. demonstrated that patients with NAFLD who were obese had higher expression of miR-122-5p in the liver. It should be noted that miR-122 levels in the liver increase during the early stages of NAFLD but gradually decrease as non-alcoholic steatohepatitis (NASH) and fibrosis progress [47].

MARKERS OF PANCREATIC DAMAGE

Pancreatic disease is a serious problem for the healthcare system in the 21st century. Risk factors for pancreatic disease include a high-fat diet, overweight and obesity, as well as alcohol abuse and smoking. Globally, over the past few decades, obesity has been an urgent medical and social problem that has become a non-communicable pandemic [48]. Obesity is a statistically significant risk factor for pancreatic cancer (PCa).

Thus, a 2021 meta-analysis by D. Aune et al. included 10 prospective studies with 1,693,657 participants and showed that a 5 kg / m^2 increase in body mass index was associated with an 18% (95% CI 1.03–1.35) increase in the relative risk of acute pancreatitis, and a 10-cm increase in waist circumference increased the risk by 36% (95% CI 1.29–1.43) [49].

It is important to understand the mechanisms by which obesity affects the onset and progression of pancreatic disease. The main mechanisms are increased inflammation and necrosis due to increased intra- and peripancreatic fat. It has been suggested that, as in pancreatitis, the creation of an inflammatory microenvironment leads to the growth of oncogenically transformed cells, promoting the attraction of immune cells that cause tumor development [48]. Early diagnosis of PCa is difficult because the disease is usually asymptomatic for a long time. This means that it is often detected late, when treatment is already ineffective, leading to poor survival outcomes. Studies are increasingly focusing on the need to find potential

serum biomarkers as additional tests for screening and diagnosis of PCa.

Carbohydrate antigen 19-9 (CA19-9) is a tetrasaccharide expressed on the surface of cancer cells. It is the best known serological biomarker used in the diagnosis of PCa. In 1979, it was first described as a tumor antigen that was recognized by the monoclonal antibody NS19-9 in a colorectal cancer cell line [50]. CA19-9 is the Lewis antigen system expressed exclusively in patients who belong to the Lewis blood group (α-β+) or (α+β-). About 5–10% of the population has a Le (α-β-) phenotype, which lacks the enzyme 1,4-fucosyltransferase required for CA19-9 production. CA19-9 levels are known to be elevated in only 70–80% of patients with PCa. However, a normal CA19-9 level does not exclude PCa [51]. The CA19-9 tumor marker has low specificity for PCa as it is also elevated in other types of cancer, including colorectal, gastric, liver, lung, and ovarian cancers. Various studies have demonstrated that CA19-9 levels can be elevated in benign conditions, such as chronic pancreatitis, pancreatic cysts, biliary obstruction, and cholangitis [52]. The upper range of CA19-9 is more than 37–40 U / ml. It was found that 80–90% of patients with stage III–IV PCa had CA19-9 levels >100 U / ml, while patients with stage I–II tumors had lower CA19-9 values [53].

According to the literature, CA19-9 levels are significantly higher in PCa than in chronic pancreatitis. Therefore, higher threshold values (>100 U / ml) should be used for differential diagnosis of cancer and chronic pancreatitis [54]. In their work, Y. Liang et al. found that patients with PCa have metastasis to lymph nodes when serum CA19-9 levels are ≥ 1,000 U / ml [55].

Finally, let us consider the serum tumor marker CA242, which is a carbohydrate antigen containing sialic acid [56]. Elevated CA242 concentration in blood serum >20 U / ml is found in PCa (sensitivity varies from 41 to 75% and the specificity is 85–95%), whereas in benign diseases the levels of the tumor marker slightly increase [11]. CA242 has advantages over CA19-9, including higher specificity in diagnosing PCa and independence of its level of Lewis antigen expression [57].

CONCLUSION

The biomarkers discussed can be used as additional tools that can not only provide timely recognition of gastrointestinal diseases but also increase the accuracy of assessing the effectiveness of therapy. At the same time, it should be taken into account that the clinical relevance of various studies is generally limited because they focus on individual biomarkers that represent only one of several features within a specific pathological condition. Therefore, one promising approach would be to combine several markers into a multimarker panel to increase their diagnostic and prognostic value, thus improving case management.

REFERENCES

1. Yeganyan R.A., Kushunina D.V., Kalinina A.M. The relevance and efficiency of early detection of digestive diseases during screening of the adult population of Russia. *Russian Journal of Preventive Medicine*. 2017;20(3): 22–27. (In Russ.). DOI: 10.17116/profmed201720322-27.
2. Adamcova M., Šimko F. Multiplex biomarker approach to cardiovascular diseases. *Acta Pharmacologica Sinica*. 2018;39(7):1068–1072. DOI: 10.1038/aps.2018.29.
3. Ranjbar R., Ghasemian M., Maniati M., Khatami S.H., Jamali N., Taheri-Anganeh M. Gastrointestinal disorder biomarkers. *Clinica Chimica Acta*. 2022;530:13–26. DOI: 10.1016/j.cca.2022.02.013.
4. Biomarkers Definitions Working Group. Biomarkers and surrogate endpoints: preferred definitions and conceptual framework. *Clinical Pharmacology and Therapeutics*. 2001;69(3):89–95. DOI: 10.1067/mcp.2001.113989.
5. Sadvakas A.S. Modern concepts of ideal biomarkers in medicine. *Modern Medicine: Current Issues*. 2014;5(31):230–231. (In Russ.).
6. Kozlova I.V., Kudishina M.M., Pakhomova A.L. Biomarkers of inflammatory bowel diseases. *Experimental and Clinical Gastroenterology*. 2018;157(9):4–9. (In Russ.). DOI: 10.31146/1682-8658-ecg-157-9-4-9.
7. FDA-NIH Biomarker Working Group. BEST (Biomarkers, EndpointS, and other Tools) Resource. Silver Spring (MD): Food and Drug Administration (US); 2016. Predictive Biomarker. 2016.URL: https://www.ncbi.nlm.nih.gov/books/NBK402283/ Co-published by National Institutes of Health (US), Bethesda (MD).
8. Fu S., Wu D., Jiang W., Li J., Long J., Jia C. et al. Molecular Biomarkers in Drug-Induced Liver Injury: Challenges and Future Perspectives. *Frontiers in Pharmacology*. 2020;10:1667. DOI: 10.3389/fphar.2019.01667.
9. Baniak N., Senger J.L., Ahmed S., Kanthan S.C., Kanthan R. Gastric biomarkers: a global review. *World Journal of Surgical Oncology*. 2016;14(1):212. DOI: 10.1186/s12957-016-0969-3.
10. Durães C., Almeida G.M., Seruca R., Oliveira C., Carneiro F. Biomarkers for gastric cancer: prognostic, predictive or targets of therapy? *Virchows Archiv*. 2014;464(3):367–378. DOI: 10.1007/s00428-013-1533-y.
11. Varvanina G.G., Lesko K.A., Bordin D.S., Dubtsova E.A., Malykh M.V., Noskova K.K., et al. Blood biomarkers and computed tomography for differential diagnosis of pancreatic cancer and chronic pancreatitis. *Russian Journal of Evidence-Based Gastroenterology*. 2021;10(4):12–21. (In Russ.). DOI: 10.17116/dokgastro20211004112.
12. Konradi A.O. Biomarkers, their types and roles in personalized medicine. *Russian Journal for Personalized Medicine*.

2022;2(3):6–16. (In Russ.). DOI: 10.18705/2782-3806-2022-2-3-6-16.
13. Bakulina N.V., Tikhonov S.V., Lischuk N.B. Chronic gastritis and functional dyspepsia. Unity and struggle of two opposites. *Medical Council*. 2021;(15):164–174. (In Russ.). DOI: 10.21518/2079-701X-2021-15-164-174.
14. Tsukanov V.V., Tonkikh Yu.L., Vasyutin A.V., Peretyatko O.V., Pulikov A.S., Baron I.I. Gastric mucosa structure in patients with different serum pepsinogen levels and ratios. *Medical Council*. 2018;(14):114–117. (In Russ.). DOI: 10.21518/2079-701X-2018-14-114-117.
15. Kornoukhova L.A., Emanuel V.L., Denisov N.L., Nikonov E.L. *Helicobacter pylori* infection: the place of serological and cultural diagnostics in clinical guidelines. *Russian Clinical Laboratory Diagnostics*. 2021;66(8):496–501. (In Russ.). DOI: 10.51620/0869-2084-2021-66-8-496-501.
16. Tu H., Sun L., Dong X., Gong Y., Xu Q., Jing J. et al. A Serological Biopsy Using Five Stomach-Specific Circulating Biomarkers for Gastric Cancer Risk Assessment: A Multi-Phase Study. *The American Journal of Gastroenterology*. 2017;112(5):704–715. DOI: 10.1038/ajg.2017.55.
17. Conti C.B., Agnesi S., Scaravaglio M., Masseria P., Dinelli M.E., Oldani M. et al. Early Gastric Cancer: Update on Prevention, Diagnosis and Treatment. *International Journal of Environmental Research and Public Health*. 2023;20(3):2149. DOI: 10.3390/ijerph20032149.
18. Kuvaev R.O., Kashin C.V., Nikonov E.L., Itoh T., Gotoda T., Gono K. Early stomach cancer: the modern methods for screening, endoscopic diagnostics, and minimally invasive treatment. *Russian Journal of Evidence-Based Gastroenterology*. 2014;3(3):44–51. (In Russ.).
19. Duan S., Rico K., Merchant J.L. Gastrin: from physiology to gastrointestinal malignancies. *Function (Oxford, England)*. 2021;3(1):zqab062. DOI: 10.1093/function/zqab062.
20. Shen H., Xiong K., Wu X., Cheng S., Lou Q., Jin H. et al. The diagnostic alue of serum gastrin-17 and pepsinogen for gastric cancer screening in eastern China. *Gastroenterology Research and Practice*. 2021; 2021: 6894248. DOI: 10.1155/2021/6894248.
21. Bordin D.S., Shengelia M.I., Ivanova V.A., Voinovan I.N. *Helicobacter pylori*: clinical significance and diagnostic principles. *Infectious Diseases: News, Opinions, Training*. 2022;11(1):119–129. (In Russ.). DOI: 10.33029/2305-3496-2022-11-1-119-129.
22. Ansari S., Yamaoka Y. *Helicobacter pylori* virulence factor cytotoxin-associated gene A (CagA)-mediated gastric pathogenicity. *International Journal of Molecular Sciences*. 2020;21(19):7430. DOI: 10.3390/ijms21197430.
23. Miernyk K.M., Bruden D., Rudolph K.M., Hurlburt D.A., Sacco F., McMahon B.J. et al. Presence of cagPAI genes and characterization of vacA s, i and m regions in *Helicobacter pylori* isolated from Alaskans and their association with clinical pathologies. *Journal of Medical Microbiology*. 2020;69(2):218–227. DOI: 10.1099/jmm.0.001123.
24. Muzaheed. *Helicobacter pylori* oncogenicity: mechanism, prevention, and risk factors. *The Scientific World Journal*. 2020;2020:1–10. DOI: 10.1155/2020/3018326.
25. Khavkin A.I., Novikova V.P., Shapovalova N.S. Perspective non-invasive biomarkers: intestinal proteins in the diagnosis for diagnosis and control of intestinal mucosal damage. *Experimental and Clinical Gastroenterology*. 2021;188(4): 155–160. (In Russ.). DOI: 10.31146/1682-8658-ecg-188-4-155-160.
26. Prikhodchenko N.G., Shumatova T.A., Zernova E.S., Ni A.N., Sergeeva E.V. Fecal biomarkers: diagnostic significance and prospects in allergic diseases of the gastrointestinal tract. *Medical Opponent*. 2022;4(20):42-48. (In Russ.).
27. Zvyagin A.A., Bavykina I.A., Nastusheva T.L., Bavykin D.V. Intestinal fatty acid binding protein as the promising marker of small intestine permeability. *Russian Bulletin of Perinatology and Pediatrics*. 2020;65(6):29–33. (In Russ.). DOI: 10.21508/1027-4065-2020-65-6-29-33.
28. Funaoka H., Kanda T., Fujii H. Intestinal fatty acid-binding protein (I-FABP) as a new biomarker for intestinal diseases. *Rinsho Byori the Japanese Journal of Clinical Pathology*. 2010;58(2):162–168.
29. Livzan M.A., Gaus O.V. Fecal zonulin as a biomarker of increased intestinal permeability in patients with irritable bowel syndrome (narrative review and pilot study results). *Russian Journal of Evidence-Based Gastroenterology*. 2021;10(3):47–55. (In Russ.). DOI: 10.17116/dokgastro20211003147.
30. Adriaanse M.P., Leffler D.A., Kelly C.P., Schuppan D., Najarian R.M., Goldsmith J.D. et al. Serum I-FABP detects gluten responsiveness in adult celiac disease patients on a short-term gluten challenge. *The American Journal of Gastroenterology*. 2016;111(7):1014–1022. DOI: 10.1038/ajg.2016.162.
31. Schurink M., Kooi E.M., Hulzebos C.V., Kox R.G., Groen H., Heineman E. et al. Intestinal fatty acid-binding protein as a diagnostic marker for complicated and uncomplicated necrotizing enterocolitis: a prospective cohort study. *PLoS One*. 2015;10(3). DOI: 10.1371/journal.pone.0121336.
32. Veres-Székely A., Szász C., Pap D., Szebeni B., Bokrossy P., Vannay Á. Zonulin as a potential therapeutic target in microbiota-gut-brain axis disorders: encouraging results and emerging questions. *The International Journal of Molecular Sciences*. 2023;24(8):7548. DOI: 10.3390/ijms24087548.
33. Fasano A., Not T., Wang W., Uzzau S., Berti I., Tommasini A. et al. Zonulin, a newly discovered modulator of intestinal permeability, and its expression in coeliac disease. *Lancet.* 2000;355(9214):1518–1519. DOI: 10.1016/S0140-6736(00)02169-3.
34. Haghbin M., Rostami-Nejad M., Forouzesh F., Sadeghi A., Rostami K., Aghamohammadi E. et al. The role of CXCR3 and its ligands CXCL10 and CXCL11 in the pathogenesis of celiac disease. *Medicine (Baltimore)*. 2019;98(25):e15949. DOI: 10.1097/MD.0000000000015949.
35. Rezazadegan M., Soheilipour M., Tarrahi M.J., Amani R. Correlation Between Zinc Nutritional Status with Serum Zonulin and Gastrointestinal Symptoms in Diarrhea-Predominant Irritable Bowel Syndrome: A Case-Control Study. *Digestive Diseases and Sciences*. 2022;67(8):3632–3638. DOI: 10.1007/s10620-021-07368-6.
36. Zhang Y.G., Xia Y., Lu R., Sun J. Inflammation and intestinal leakiness in older HIV+ individuals with fish oil treatment. *Genes & Diseases*. 2018;5(3):220–225. DOI: 10.1016/j.gendis. 2018.07.001.

37. Li J., Xu M., Qian W., Ling F., Chen Y., Li S. et al. Clinical value of fecal calprotectin for evaluating disease activity in patients with Crohn's disease. *Frontiers in Physiology*. 2023;14: 1186665. DOI: 10.3389/fphys.2023.1186665.
38. Ayling R.M., Kok K. Fecal calprotectin. *Advances in Clinical Chemistry*. 2018;87:161–190. DOI: 10.1016/bs.acc.2018.07.005.
39. Rokkas T., Portincasa P., Koutroubakis I.E. Fecal calprotectin in assessing inflammatory bowel disease endoscopic activity: a diagnostic accuracy meta-analysis. *The Journal of Gastrointestinal and Liver Diseases*. 2018;27(3):299–306. DOI: 10.15403/jgld.2014.1121.273.pti.
40. Cordes F., Demmig C., Bokemeyer A., Brückner M., Lenze F., Lenz P. et al. MicroRNA-320a monitors intestinal disease activity in patients with inflammatory bowel disease. *Clinical and Translational Gastroenterology*. 2020;11(3):e00134. DOI: 10.14309/ctg.0000000000000134.
41. Morilla I., Uzzan M., Laharie D., Cazals-Hatem D., Denost Q., Daniel F. et al. Colonic microRNA profiles, identified by a deep learning algorithm, that predict responses to therapy of patients with acute severe ulcerative colitis. *Clinical Gastroenterology and Hepatology*. 2019;17(5):905–913. DOI: 10.1016/j.cgh.2018.08.068.
42. Teschke R. Alcoholic liver disease: alcohol metabolism, cascade of molecular mechanisms, cellular targets, and clinical aspects. *Biomedicines*. 2018;6(4):106. DOI: 10.3390/biomedicines6040106.
43. Zeng M., Chen L., Li Y., Mi Y., Xu L. Problems and challenges associated with renaming non-alcoholic fatty liver disease to metabolic associated fatty liver disease. *Medicine (Baltimore)*. 2023;3(3):105–113. DOI: 10.1097/ID9.0000000000000085.
44. Llewellyn H.P., Vaidya V.S., Wang Z., Peng Q., Hyde C., Potter D. et al. Evaluating the sensitivity and specificity of promising circulating biomarkers to diagnose liver injury in humans. *The Journal of Toxicological Sciences*. 2021;181(1):23–34. DOI: 10.1093/toxsci/kfab003.
45. Church R.J., Kullak-Ublick G.A., Aubrecht J., Bonkovsky H.L., Chalasani N., Fontana R.J. et al. Candidate biomarkers for the diagnosis and prognosis of drug-induced liver injury: An international collaborative effort. *Journal of Hepatology*. 2019;69(2):760–773. DOI: 10.1002/hep.29802.
46. Lehmann-Werman R., Magenheim J., Moss J., Neiman D., Abraham O., Piyanzin S. et al. Monitoring liver damage using hepatocyte-specific methylation markers in cell-free circulating DNA. *JCI Insight*. 2018;3(12):e120687. DOI: 10.1172/jci.insight.120687.
47. Kan Changez M.I., Mubeen M., Zehra M., Samnani I., Abdul Rasool A., Mohan A. et al. Role of microRNA in non-alcoholic fatty liver disease (NAFLD) and non-alcoholic steatohepatitis (NASH): a comprehensive review. *Journal of International Medical Research*. 2023;51(9):3000605231197058. DOI: 10.1177/03000605231197058.
48. Lilly A.C., Astsaturov I., Golemis E.A. Intrapancreatic fat, pancreatitis, and pancreatic cancer. *Cellular and Molecular Life Sciences*. 2023;80(8):206. DOI: 10.1007/s00018-023-04855-z.
49. Aune D., Mahamat-Saleh Y., Norat T., Riboli E. High Body Mass Index and Central Adiposity Is Associated with Increased Risk of Acute Pancreatitis: A Meta-Analysis. *Digestive Diseases and Sciences*. 2021;66(4):1249–1267. DOI: 10.1007/s10620-020-06275-6.
50. O'Neill R.S., Stoita A. Biomarkers in the diagnosis of pancreatic cancer: Are we closer to finding the golden ticket? *World Journal of Gastroenterology*. 2021;27(26):4045–4087. DOI: 10.3748/wjg.v27.i26.4045.
51. Pereira S.P., Oldfield L., Ney A., Hart P.A., Keane M.G., Pandol S.J. et al. Early detection of pancreatic cancer. *The Lancet Gastroenterology and Hepatology*. 2020;5(7):698–710. DOI: 10.1016/S2468-1253(19)30416-9.
52. Binicier O.B., Pakoz Z.B. CA 19-9 levels in patients with acute pancreatitis due to gallstone and metabolic/toxic reasons. *Revista da Associacao Medica Brasileira*. 2019;65(7):965–970. DOI: 10.1590/1806-9282.65.7.965.
53. Lee T., Teng T.Z.J., Shelat V.G. Carbohydrate antigen 19-9-tumor marker: Past, present, and future. *World Journal of Gastrointestinal Surgery*. 2020;12(12):468–490. DOI: 10.4240/wjgs.v12.i12.468.
54. Janga L.S.N., Sambe H.G., Yasir M., Man R.K., Gogikar A., Nanda A. et al. Holistic Understanding of the Role of Carbohydrate Antigen 19-9 in Pancreatic Cancer Screening, Early Diagnosis, and Prognosis: A Systematic Review. *Cureus Journal of Medical Science*. 2023;15(8):e44382. DOI: 10.7759/cureus.44382.
55. Liang Y., Chang S., Guo H., Man Q., Zang F., Gao S. Presence of tumor deposits is an indicator of poor prognosis in patients with pancreatic ductal adenocarcinoma. *The American Journal of Cancer Research*. 2023;13(5):1970–1984.
56. Dong D., Jia L., Zhang L., Ma N., Zhang A., Zhou Y. et al. Periostin and CA242 as potential diagnostic serum biomarkers complementing CA19.9 in detecting pancreatic cancer. *Cancer Science*. 2018;109:2841–2851. DOI: 10.1111/cas.13712.
57. Gu Y.L., Lan C., Pei H., Yang S.N., Liu Y.F., Xiao L.L. Applicative value of sdrum CA19-9, CEA, CA125 and CA242 in diagnosis and prognosis for patients with pancreatic cancer treated by concurrent chemoradiotherapy. *The Asian Pacific Journal of Cancer Prevention*. 2015;16(15):6569–6573. DOI: 10.7314/apjcp.2015.16.15.6569.

Authors' information

Ostanko Valentina L. – Cand. Sci. (Med.), Associate Professor of the Advanced Therapy Division with Rehabilitation, Physiotherapy and Sports Medicine Course, Siberian State Medical University, Tomsk, valentina209@yandex.ru, http://orcid.org/0000-0002-9950-721X

Kalacheva Tatyana P. – Cand. Sci. (Med.), Associate Professor of the General Medical Practice and Outpatient Therapy Division, Siberian State Medical University, Tomsk, tatyana-kalachyova@yandex.ru, http://orcid.org/0000-0002-4292-7723

Kulumaeva Karina A. – Resident, Advanced Therapy Division with Rehabilitation, Physiotherapy and Sports Medicine Course, Siberian State Medical University, Tomsk, karina.kulumaeva12@mail.ru, http://orcid.org/0009-0002-5933-3873

Li Natalia A. – Head of the Endoscopy Unit, Tomsk Regional Oncology Center, Tomsk, nat.an.li@mail.ru, http://orcid.org/0000-0001-5733-8561

Beloborodova Ekaterina V. – Dr. Sci. (Med.), Professor of the Advanced Therapy Division with Rehabilitation, Physiotherapy and Sports Medicine Course, Siberian State Medical University, Tomsk, belobekaterina@yandex.ru, http://orcid.org/0000-0002-8776-5924

Purlik Igor L. – Dr. Sci. (Med.), Professor of the Pathological Anatomy Division, Siberian State Medical University, Tomsk, igor0812@rambler.ru, http://orcid.org/0000-0003-3757-0173

Kalyuzhina Elena V. – Dr. Sci. (Med.), Professor of the Advanced Therapy Division with Rehabilitation, Physiotherapy and Sports Medicine Course, Siberian State Medical University, Tomsk, kalyuzhina.e@mail.ru, http://orcid.org/0000-0002-7978-5327

Brazovskaya Natalia G. – Cand. Sci. (Med.), Associate Professor of the Medical and Biological Cybernetics Division, Siberian State Medical University, Tomsk, brang@mail.ru, http://orcid.org/0000-0002-0706-9735

Kalyuzhin Vadim V. – Dr. Sci. (Med.), Professor, Head of the Advanced Therapy Division with Rehabilitation, Physiotherapy and Sports Medicine Course, Siberian State Medical University, Tomsk, kalyuzhinvv@mail.ru, http://orcid.org/0000-0001-9640-2028

(✉) **Kalacheva Tatyana P.,** tatyana-kalachyova@yandex.ru

Received 02.05.2024;
approved after peer review 15.05.2024;
accepted 13.06.2024

УДК 616.72-002-092
https://doi.org/10.20538/1682-0363-2024-4-187-196

The role of mediators in the formation of leading pathological processes in psoriatic arthritis

Pogonchenkova D.A., Chetvernya L.V., Vasilyeva O.A., Kononova T.E., Poletika V.S., Abramov V.K., Chumakova S.P., Eliseeva L.V., Urazova O.I.

Siberian State Medical University
2, Moscow Trakt, Tomsk, 634050, Russian Federation

ABSTRACT

The lecture analyzes the results of research on the role of humoral and cellular mediators, their interaction, as well as the imbalance of angiogenic factors in psoriatic arthritis. The information is presented with identification of the leading typical pathological processes: inflammation and microcirculation disorders, formed due to the activation of protein cascades and interaction of molecular proinflammatory mediators and angiogenic factors. It is known that the clinical phenotypes of psoriatic arthritis are diverse. A deeper understanding of the pathogenesis and changes in the predominant pathological process can become the basis for the development of a personalized treatment strategy based on the pathogenesis to minimize iatrogenic complications and economic costs, as well as for the introduction of modern diagnostic methods for verification, differentiation, and monitoring of psoriatic arthritis in order to timely correct drug treatment.

Keywords: psoriatic arthritis, inflammation, microcirculation, humoral mediators, C-reactive protein, complement system, bradykinin, eicosanoids, cytokines, angiogenic factors

Conflict of interest. The authors declare the absence of obvious or potential conflicts of interest related to the publication of this article.

Source of financing. The authors state that they received no funding for the study.

For citation: Pogonchenkova D.A., Chetvernya L.V., Vasilyeva O.A., Kononova T.E., Poletika V.S., Abramov V.K., Chumakova S.P., Eliseeva L.V., Urazova O.I. The role of mediators in the formation of leading pathological processes in psoriatic arthritis. *Bulletin of Siberian Medicine.* 2024;23(4):187–196. https://doi.org/10.20538/1682-0363-2024-4-187-196.

Роль медиаторов в формировании ведущих патологических процессов при псориатическом артрите

Погонченкова Д.А., Четверня Л.В., Васильева О.А., Кононова Т.Е., Полетика В.С., Абрамов В.К., Чумакова С.П., Елисеева Л.В., Уразова О.И.

Сибирский государственный медицинский университет (СибГМУ)
Россия, 634050, г. Томск, Московский тракт, 2

РЕЗЮМЕ

В лекции проанализированы результаты исследований, касающихся роли гуморальных и клеточных медиаторов, их взаимодействия, а также дисбаланса ангиогенных факторов при псориатическом артрите. Информация структурирована в соответствии с выделением ведущих типовых патологических процессов: воспаления и нарушений микроциркуляции, формирующихся за счет активации белковых каскадов и

✉ *Pogonchenkova Darya A.,* pogonchenkova.da@ssmu.ru

взаимодействия молекулярных провоспалительных медиаторов и ангиогенных факторов. Известно, что клинические фенотипы псориатического артрита многообразны. Глубокое понимание патогенеза и динамики изменений в преобладании одного патологического процесса над другим может стать основой для разработки персонифицированного патогенетически обоснованного терапевтического подхода с минимизацией ятрогенных осложнений и экономических издержек, а также внедрения современных диагностических методов для верификации, дифференциации и мониторинга активности псориатического артрита с целью своевременной коррекции медикаментозной стратегии.

Ключевые слова: псориатический артрит, воспаление, микроциркуляция, гуморальные медиаторы, С-реактивный белок, система комплемента, брадикинин, эйкозаноиды, цитокины, ангиогенные факторы

Конфликт интересов. Авторы декларируют отсутствие явных и потенциальных конфликтов интересов, связанных с публикацией настоящей статьи.

Источник финансирования. Авторы заявляют об отсутствии финансирования при проведении исследования.

Для цитирования: Погонченкова Д.А., Четверня Л.В., Васильева О.А., Кононова Т.Е., Полетика В.С., Абрамов В.К., Чумакова С.П., Елисеева Л.В., Уразова О.И. Роль медиаторов в формировании ведущих патологических процессов при псориатическом артрите. *Бюллетень сибирской медицины.* 2024;23(4):187–196. https://doi.org/10.20538/1682-0363-2024-4-187-196.

INTRODUCTION

Psoriatic arthritis is an autoimmune, multifactorial, systemic disease associated with psoriasis [1]. The clinical progression of psoriatic arthritis is heterogeneous, ranging from isolated joint involvement (distal interphalangeal arthritis with a relatively benign course or mutilating arthritis, characterized by malignant progression with osteolysis of bone tissue and bone ankylosis) [2, 3] to combinations of articular syndrome with lesions of the axial skeleton (sacroiliitis, spondylitis) [4], musculoskeletal patterns (enthesitis, dactylitis, tenosynovitis) [5–7], or extraskeletal extra-articular manifestations (anterior uveitis, chorioretinitis, nonspecific colitis, etc.) [8, 9]. Despite the generally accepted terminology, in the scientific literature one can come across the synonym "psoriatic disease", which emphasizes the systemic nature of this pathology [10].

Lack of specific laboratory markers and pathognomonic symptoms of psoriatic arthritis can make the diagnosis difficult to establish. The diagnosis is confirmed if the clinical, test, and radiological signs match with the CASPAR (Classification of Psoriatic Arthritis) classification criteria. It should be noted that the CASPAR criteria have significant limitations in the differential diagnosis of early arthritis [11].

Difficulties may arise in patients without manifestations of skin psoriasis or with a symmetric rheumatoid-like subtype of psoriatic arthritis, as well as in individuals with mono- or oligoarthritis, with positive rheumatoid factor (RF) test and / or anti-cyclic-citrullinated peptide (CCP) antibody and minimal skin manifestations, which often causes misdiagnosis [12]. Additionally, the DAPSA (Disease Activity index for Psoriatic Arthritis) activity scales used in real clinical practice often evoke reasonable criticism for their limited reproducibility and low prognostic sensitivity [13]. Diagnostic and therapeutic approaches for psoriatic arthritis require reevaluation, taking into consideration modern fundamental knowledge in the field of proteomics and molecular cell biology.

Accordingly, the aim of this lecture was to summarize and systematize relevant data on the role of key humoral and cellular mediators and their interaction during the initiation of the inflammatory process and microcirculatory disorders in psoriatic arthritis.

HUMORAL INFLAMMATORY MEDIATORS IN PSORIATIC ARTHRITIS

Currently, a large amount of scientific data indicates that, in addition to general patterns, the inflammatory process in psoriatic arthritis has specific characteristics related to the mediators, which justifies the isolation of this disease into an independent nosological unit. The clinical phenotypes of psoriatic arthritis depend on the multitudinous and cross-inducible expression of mediators, the order of mediator network formation, the duration and location (systemic or limited to a topographic location) of the mediator-induced effect, and the degree of the imbalance of proinflammatory and anti-inflammatory regulators [14, 15].

C-reactive protein (CRP) is a mediator of the acute phase of inflammation and a leading marker

of choice in assessing the activity of psoriatic arthritis [16]. CRP activates early components of the complement system via the classical pathway while inhibiting the alternative pathway, preventing the formation of the membrane attack complex (MAC) [17, 18]. The functions of CRP are not limited to humoral effects, as it is involved in the formation of the humoral-cellular proinflammatory networks. By interacting with the Fcγ receptor on the membranes of myeloid cells, CRP modulates the production of interleukin (IL) 1® and tumor necrosis factor (TNF) α. In addition, CRP stimulates the synthesis of reactive oxygen species [19].

The role of CRP in the pathogenesis of psoriatic arthritis requires clarification. The studies whose results have been implemented in clinical practice compared the levels of total and high-sensitivity CRP with the activity of the inflammatory process, without considering the influence of different peptide isoforms. It should be noted that CRP isoforms may exhibit opposite biological effects [20, 21]. For example, monomeric CRP (mCRP) can accumulate in tissues and enhance local inflammation, whereas the native isoform of CRP (nCRP) mostly remains within the systemic circulation [22]. The accumulation of mCRP in the cells of the synovial membrane was demonstrated in the model of rheumatoid arthritis [23], while no similar studies have been carried out focusing on psoriatic arthritis. Native isoform of CRP also opsonizes apoptotic cells, triggering their phagocytosis [24].

The complement system is crucial in initiating and maintaining inflammation in psoriatic arthritis [25]. Displaying an additive effect with other mediators, the complement system participates in forming a molecular basis for the clinical manifestation of the disease. An increased concentration of the components C3 and C4 in the blood and C3 in the synovial fluid triggers the activation of phagocytes in the vascular bed and stimulation of effector cells incorporated into the synovial membrane. The recruitment of innate and adaptive immune cells from the bloodstream into target organs is realized with the assistance of light chain fragments C3a and C4a, which act as chemoattractants and display kinin-like activity [26].

Fragments C3b attach to the surface of the synovial membranes, representing opsonized targets to effector cells [28]. According to the classical model of inflammation, the complex formed by C5b-C9, when integrated into cell membranes, forms a channel for hydrogen ions, sodium ions, and water to flow into target cells [27]. However, the degree of involvement of this mechanism in psoriatic arthritis is not fully understood. While the proteins of the C5b-C9 complex present in a liquid medium lack the capacity for lysis, an increase in their concentration positively correlates with the activity of psoriatic arthritis and may represent an indirect indicator of tissue destruction [28]. It is evident that the complement system in psoriatic arthritis has lost its biologically determined protective function. The components C3, C4, and C5b-C9 do not have selective histological affinity [27].

Certainly, the complement system is involved in the initiation of acute inflammation at the onset of the disease, maintaining and enhancing local inflammatory process during periods of exacerbation, potentiating the mechanisms leading to the alteration of articular tissues. The production of humoral mediators can be a precursor of comorbidity, with a high probability of complications whose etiology will not be related to psoriatic arthritis. An increase in C3 levels in the bloodstream in the context of psoriatic arthritis represents a synergistic cardiometabolic effect, which contributes to an increase in cardiovascular risk [29–31].

To date, the role of the kallikrein – kinin system in the pathogenesis of psoriatic arthritis has not been sufficiently studied. Several studies have explored the correlation between the progression of cutaneous psoriasis, the levels of bradykinin, and the overexpression of B1 and B2-kinin receptors [32, 33]. Vasoactive amines, in particular bradykinin, regulate the diameter and permeability of the microvasculature. They also stimulate the migration of T lymphocytes and neutrophils, enhancing the inflammatory process. Thus, the blockade of bradykinin receptors is able to reduce the activity of psoriasis [34].

Moreover, bradykinin acts as an inducer of the inflammatory pain, which is the leading clinical symptom of psoriatic arthritis [35–37]. Despite the common nature of the autoimmune process in cutaneous psoriasis and arthritis, and a high theoretical probability of a similar role of bradykinin receptors and ligands, it is still too early to extrapolate the available data due to the lack of objective evidence for receptor overexpression in articular tissues, tendons, or entheses. At the same time, it would be unwise to ignore the role of the kallikrein – kinin system in the pathogenesis of psoriatic arthritis. An increase in the level of kallikreins in the synovial fluid and blood was demonstrated in rheumatoid arthritis, which is also characterized by inflammatory arthralgia [38–40].

According to the literature, psoriatic arthritis is associated with dysregulation of the hemostatic system, characterized by an imbalance in procoagulant factors. This includes the activation of Hageman factor, an imbalance of plasminogen activator-1 inhibitor (PAI-1) and tissue plasminogen activator (t-PA), decreased levels of natural anticoagulants (proteins C and S, antithrombin III), and elevated fibrinogen and D-dimer levels in the blood [41–44].

CELLULAR MEDIATORS OF INFLAMMATION IN PSORIATIC ARTHRITIS

Lipid and protein cellular mediators are key signaling molecules in the initiation of an autoimmune inflammatory process. In patients with psoriatic arthritis, there is an increase in the plasma levels of lipid mediators (endocannabinoids and certain eicosanoids), which are produced as a result of lipid peroxidation within cell membranes and the metabolism of arachidonic acid [45, 46].

Free 4-hydroxynonenal (4-HNE) is a secondary messenger and a reactive biomarker associated with lipid peroxidation. The effector potential of free 4-HNE depends on its concentration. Through its capacity to modulate the expression of specific receptors on the membranes of immunocompetent cells, free 4-HNE effectively neutralizes the effects of endocannabinoids, stimulates the selection of lymphocytes with a proinflammatory phenotype, and participates in the activation of intracellular enzyme systems that trigger apoptosis of injured cells [47].

Prostaglandin E_2 is a lipid mediator with pronounced pyrogenic activity. This eicosanoid has a kinin-like effect, modulates dilation of the microvasculature, and, while lacking a direct affinity for pain receptors (nociceptors), indirectly leads to hyperalgesia by causing hypersensitization to bradykinin [48–50]. In the context of the inflammatory process, 8-Isoprostaglandin F_{2a} (8-isoPGF_{2a}) acts as a signaling molecule activating TNFα synthesis [51].

Hepoxilin B3 (HXB3) is a bioactive substance that promotes exudation by increasing the permeability of the vascular wall. It interacts with TrpV1 and TRPA1 receptors, inducing the inflammatory pain in psoriatic arthritis [52].

Eicosanoids, possessing ty for PPARδ receptors, suppress antioxidant protection of cells (by inhibiting the production of superoxide dismutase and heme oxygenase), provoking oxidative stress, which leads to the chronification of the disease [46]. When discussing the role of eicosanoids in the onset and progression of psoriatic arthritis, it should be emphasized that, in addition to the overproduction of proinflammatory signaling molecules, the imbalance of proinflammatory and anti-inflammatory lipid mediators plays a significant role in the pathogenesis of the disease. A decrease in resolvins, which deactivate arachidonic acid derivatives, has been demonstrated [45]. The deficiency of resolvins inhibits the feedback mechanisms, leading to overproduction of proinflammatory cytokines and thromboxanes, an increase in platelet aggregation and leukocyte chemotaxis, stimulation of neoangiogenesis in inflamed tissues, and accumulation of superoxide anion radicals, which contributes to the local resorption of periarticular bone tissue [53].

Protein cellular mediators (cytokines) are molecules whose main function is to organize intercellular crosstalk [54]. The leading role in the pathogenesis of psoriatic arthritis is attributed to cytokines that stimulate the recruitment of immune cells into tissues to initiate and maintain the inflammatory process. The trigger for cross-overproduction of IL-1, IL-6, and IL-8 in psoriatic arthritis is the interaction between the soluble form of TNFα and the CD120b receptor on cells of mesenchymal origin.

Notably, TNFα should be considered a mediator, which is a regulator and an effector at the same time. During the onset of the disease, high concentrations of TNFα trigger activation of intracellular signaling, resulting in cells producing TNFα and forming a vicious circle of cytokine overproduction. At the molecular and cellular level, the mechanisms responsible for self-limitation of the TNFα production fail to eliminate it effectively, preventing the remission of the disease and reconvalescence at the body level. It is important to note that the inflammatory response depends on the concentration of TNFα [55–57]. In psoriatic arthritis, overproduction of proinflammatory cytokines IL-1β and IL-6 can result in a self-sustaining pathological process if constitutive expression of TNFα is present [58]. The IL-23/IL-17A axis is another example of cross cytokine expression. Acting as a ligand, IL-23 modulates the activation of T-helper lymphocytes (Th) type 17 that synthesize IL-17A, as well as IL-21, IL-22, and TNFα [59].

Similarly, IL-1β activates signaling pathways that are responsible for the overproduction of IL-17A or IL-36. The proinflammatory potential of IL-36 has been observed in skin psoriasis. According to a number of studies, IL-36 can maintain inflammation in psoriatic arthritis as a regulator of cross-inflammatory

expression [60]. IL-17A activates transcription factors and kinases, mediates cross-inducible secretion of IL-1, IL-6, TNFα, and chemokines, and modulates the expression of TNFα receptor type 2 [61].

On the one hand, the ability of cytokines to duplicate each other's biological functions ensures the maintenance of the pathological process and justifies the status of psoriatic arthritis as a chronic disease [54]. On the other hand, the diversity of the effector potential of each individual mediator and the absence of a strictly determined structure of the mediator network per unit of time underlie the heterogeneous phenotype of the disease.

As previously mentioned, TNFα realizes its proinflammatory potential in a concentration-dependent manner, polarizes monocytes and macrophages, and enhances their migration, stimulates Th1-lymphocytes, and mediates Th17-cells, aggravates the course of arthritis, and participates in the pathogenesis of joint erosion [54, 66–68].

IL-6, a pyrogen and a cytokine with a pronounced systemic effect, stimulates the production of acute-phase proteins (CRP, fibrinogen) by hepatocytes, polarizes the maturation of macrophages towards the proinflammatory M1-phenotype, and activates the STAT3-mediated signal transduction pathway in inflammatory cells [54, 62–64]. IL-23 induces the formation of psoriatic plaques, tendonitis, and enthesitis but exerts a protective effect towards the intestinal mucosa at physiological concentrations.

IL-17A realizes its proinflammatory potential in cooperation with other cytokines (TNFα, IL-1, and IL-6), links factors of innate and adaptive immunity, promotes recruitment of Th17 cells, innate lymphoid cells (ILC) 3, and neutrophils, increases the procoagulant potential of the blood, and participates in the initiation and maintenance of cutaneous manifestations of psoriasis, enthesitis, and tendonitis [65].

IL-36α produced by B lymphocytes and plasmocytes promotes the proliferation of synovial fibroblasts and stimulates the production of IL-6 and IL-8, which enhance local inflammation [60, 69–71].

Microcirculatory disorders in psoriatic arthritis: the role of lipid and cellular mediators

True inflammatory hyperemia of tissues, which arises due to impaired rheological properties of blood and changes in the vascular wall and perivascular tissues, as well as exudation, are the crucial components of the pathogenesis of psoriatic arthritis. The activity of the disease and the presence of a particular complex of symptoms depend on the spectrum of signaling molecules that modulate the effects of immunocompetent cells, perivascular cells, and microvasculature.

In psoriatic arthritis, the severity of exudation depends on the permeability of venules and capillaries. Humoral mediators with a direct effect on blood vessels include bradykinin and proteins of the complement system, C3a and C5a, which can modulate the contraction of endotheliocytes [72, 73]. CRP can potentially affect the permeability of the vascular wall as well. It has been shown that the mCRP isoform induces the expansion of microcirculatory vessels by activating local overproduction of nitric oxide. The nCRP isoform has the opposite effect, provoking vasoconstriction and leukocyte adhesion [22]. At present, there is no comprehensive understanding of the relationship between the variability of the level of individual CRP isoforms in the blood and synovial fluid and the activity of psoriatic arthritis.

Cellular mediators can influence the architecture of the microvasculature, increasing exudation through cell-mediated damage to the vascular wall or defective cellular contact between pericytes and endothelial cells. Psoriatic arthritis is characterized by an increase in the number of immature vessels. TNFα and IL-1 can trigger cross-expression of angiogenic factors, such as vascular endothelial growth factor (VEGF). In turn, IL-17 stimulates the recruitment of endothelial cells during the formation of new vessels [74, 75].

Angiogenic factors in the pathogenesis of microcirculation disorders in psoriatic arthritis

In psoriatic arthritis, an imbalance of angiogenic mediators stimulates the development of microangiopathies with specific signs. The synovial membrane is characterized by the presence of elongated, bushy, and tortuous capillaries, is hypervascularized due to an increase in the number of functioning capillaries, accompanied by neoangiogenesis and impaired rheological properties of blood due to the aggregation of blood cells [76, 77]. Microangiopathy of the nail bed in patients with psoriatic arthritis is manifested by the presence of avascular zones, hemorrhages, the appearance of giant capillaries, and an increase in the number of tortuous and twisted capillaries. A number of researchers note a decrease in the linear density of capillaries, while other authors describe an increase in the density of capillaries [78–80]. Dermal microangiopathy occurs prior to the clinical manifestation of cutaneous psoriasis and is characterized by capillary dilation

and increased endothelial permeability, leading to exudation and edema [81, 82]. Important angiogenic factors include VEGF, platelet-derived growth factor (PDGF), angiopoietin, and transforming growth factor (TGF) β.

VEGF has regenerative potential, being a key factor in the process of neoangiogenesis. In psoriatic arthritis, a local increase in VEGF expression is detected in the synovial membrane of the joint [83–85]. However, the data on the diagnostic and prognostic significance of an increase in the concentration of VEGF in the blood plasma of patients with psoriatic arthritis remains inconclusive.

PDGF is a growth factor that ensures the migration of pericytes to the area of vascular sprouts [85]. Angiopoietin, another growth factor, is overexpressed in the synovial membrane, while its isoform, Ang2, plays the key biological role. In inflammation, Ang2 enters the bloodstream via endothelial cells, increases the permeability of the vascular wall, and stimulates the recruitment of endothelial cells into new tissue niches, promoting neoangiogenesis. It should be noted that the proangiogenic potential of angiopoietin is realized in the presence of VEGF [86, 87].

TGFβ is also highly expressed within the synovial membrane, especially in patients with erosive psoriatic arthritis [88]. TGFβ regulates the composition and quantity of the vascular matrix by preserving and stimulating neoangiogenesis [89].

CONCLUSION

At the current stage, research of psoriatic arthritis is markedly focused on the role of individual cytokines, which does not allow for formulating a generalized model of pathogenesis that would reflect the mechanisms of interaction between humoral and cellular mediators. In addition, there is no clear understanding of the hierarchy of various mediators of different origins and their combinations within the pathogenesis of psoriatic arthritis, with relation to the activity of the disease and its clinical phenotype. The priority is to determine the dominant pathological process during the evolution of the disease in a particular patient. Absolute reciprocal relationship between inflammation and microcirculation disorders has not been proven. Given the generally accepted paradigm in which tissue inflammation is the primary event, the hypothesis that microcirculation disorders can be the initiating process in the pathogenesis may seem revolutionary. Evidently, the contribution of vascular bed pathology to the development of psoriatic arthritis has not yet been sufficiently studied and is a promising area of research.

It is important to acknowledge that incomplete understanding of the pathogenesis of psoriatic arthritis renders the practical application of therapeutic modalities based on genetic engineering purely empirical. Given the pleiotropic potential of most cytokines, this strategy is comparable to the use of antibiotics without determining microbial susceptibility [90], which discredits the concept of translational medicine and the principles of a rational personalized approach, increasing the burden of non-targeted economic costs in the healthcare system.

REFERENCES

1. Cigolini C., Fattorini F., Gentileschi S., Terenzi R., Carli L. Psoriatic arthritis: one year in review 2022. *Clin. Exp. Rheumatol*. 2022;40(9):1611–1619. DOI: 10.55563/clinexprheumatol/x3sfxe.
2. Antony A.S., Allard A., Rambojun A., Lovell C.R., Shaddick G., Robinson G. et al. Psoriatic Nail Dystrophy Is Associated with Erosive Disease in the Distal Interphalangeal Joints in Psoriatic Arthritis: A Retrospective Cohort Study. *J. Rheumatol*. 2019;46(9):1097–1102. DOI: 10.3899/jrheum.180796.
3. Mistegård J., Gudbjornsson B., Lindqvist U., Laasonen L., Ejstrup L., Ståhle M. et al. Comorbidities in a Cohort of 66 Patients With Psoriatic Arthritis Mutilans-Results From the Nordic PAM Study. *Front. Med. (Lausanne)*. 2021;8:629741. DOI: 10.3389/fmed.2021.629741.
4. Poddubnyy D., Jadon D.R., Van den Bosch F., Mease P.J., Gladman D.D. Axial involvement in psoriatic arthritis: An update for rheumatologists. *Semin. Arthritis. Rheum*. 2021;51(4):880–887. DOI: 10.1016/j.semarthrit.2021.06.006.
5. Araujo E.G., Schett G. Enthesitis in psoriatic arthritis (Part 1): pathophysiology. *Rheumatology (Oxford)*. 2020;59(Suppl. 1):i10–i14. DOI: 10.1093/rheumatology/keaa039.
6. Girolimetto N., Giovannini I., Crepaldi G., De Marco G., Tinazzi I., Possemato N. et al. Psoriatic dactylitis: current perspectives and new insights in ultrasonography and magnetic resonance imaging. *J. Clin. Med*. 2021;10(12):2604. DOI: 10.3390/jcm10122604.
7. Sudoł-Szopińska I., Pracoń G. Diagnostic imaging of psoriatic arthritis. Part II: magnetic resonance imaging and ultrasonography. *J. Ultrason*. 2016;16(65):163–174. DOI: 10.15557/JoU.2016.0018.
8. De Vicente Delmás A., Sanchez-Bilbao L., Calvo-Río V., Martínez-López D., Herrero-Morant A., Galíndez-Agirregoikoa E. et al. Uveitis in psoriatic arthritis: study of 406 patients in a single university center and literature review. *RMD Open*. 2023;9(1):e002781. DOI: 10.1136/rmdopen-2022-002781.
9. Li Y., Guo J., Cao Z., Wu J. Causal Association Between Inflammatory Bowel Disease and Psoriasis: A Two-Sample Bidirectional Mendelian Randomization Study. *Front. Immunol*. 2022;13:916645. DOI: 10.3389/fimmu.2022.916645.
10. Kim W.B., Jerome D., Yeung J. Diagnosis and management of psoriasis. *Can. Fam. Physician.* 2017;63(4):278–285.

11. Taylor W., Gladman D., Helliwell P., Marchesoni A., Mease P., Mielants H. Classification criteria for psoriatic arthritis: development of new criteria from a large international study. *Arthritis Rheum*. 2006;54(8):2665–2673. DOI: 10.1002/art.21972.
12. Dai L.Y., Gong D.D., Zhao J.X. Clinical characteristics of psoriatic arthritis with positive rheumatoid factor or anti-cyclic citrullinated peptide antibody. *Beijing Da Xue Bao Yi Xue Ban.* 2019;51(6):1008–1013. DOI: 10.19723/j.issn.1671-167X.2019.06.005.
13. Gialouri C.G., Fragoulis G.E. Disease activity indices in psoriatic arthritis: current and evolving concepts. *Clin. Rheumatol*. 2021;40(11):4427–4435. DOI: 10.1007/s10067-021-05774-9.
14. Roe K. An inflammation classification system using cytokine parameters. *Scand. J. Immunol*. 2021;93(2):e12970. DOI: 10.1111/sji.12970.
15. Chereshnev V.A., Gusev E.Iu., Zotova N.V. Fundamental and applied aspects of systemic inflammation in terms of a physiological and typical pathological process. *Ross. Fiziol. Zh. Im. I.M. Sechenova.* 2010;96(7):696–707 (in Russ.).
16. Gialouri C.G., Evangelatos G., Pappa M., Karamanakos A., Iliopoulos A., Tektonidou M.G. et al. Normal C-reactive protein in active psoriatic arthritis: results from real-world clinical practice. *Ther. Adv. Musculoskelet. Dis*. 2022;14:1–8. DOI: 10.1177/1759720X221122417.
17. Singh S.K., Ngwa D.N., Agrawal A. Complement activation by c-reactive protein is critical for protection of mice against pneumococcal infection. *Front. Immunol*. 2020;11:1812. DOI: 10.3389/fimmu.2020.01812.
18. Chirco K.R., Potempa L.A. C-reactive protein as a mediator of complement activation and inflammatory signaling in age-related macular degeneration. *Front. Immunol*. 2018;9:539. DOI: 10.3389/fimmu.2018.00539.
19. Ryu J., Lee C.W., Shin J.A., Park C.S., Kim J.J., Park S.J. et al. FcgammaRIIa mediates C-reactive protein-induced inflammatory responses of human vascular smooth muscle cells by activating NADPH oxidase 4. *Cardiovasc. Res*. 2007;75(3):555–565. DOI: 10.1016/j.cardiores.2007.04.027.
20. Wu Y., Potempa L.A., El Kebir D., Filep J.G. C-reactive protein and inflammation: conformational changes affect function. *Biol. Chem*. 2015;396(11):1181–1197. DOI: 10.1515/hsz-2015-0149.
21. Ji S.R., Wu Y., Zhu L., Potempa L.A., Sheng F.L., Lu W. et al. Cell membranes and liposomes dissociate C-reactive protein (CRP) to form a new, biologically active structural intermediate: mCRP(m). *FASEB J*. 2007;21(1):284–294. DOI: 10.1096/fj.06-6722com.
22. Sproston N.R., Ashworth J.J. Role of C-reactive protein at sites of inflammation and infection. *Front. Immunol*. 2018;9:754. DOI: 10.3389/fimmu.2018.00754.
23. Kim K.W., Kim B.M., Moon H.W., Lee S.H., Kim H.R. Role of C-reactive protein in osteoclastogenesis in rheumatoid arthritis. *Arthritis. Res. Ther.* 2015;17(1):41. DOI: 10.1186/s13075-015-0563-z.
24. Gershov D., Kim S., Brot N., Elkon K.B. C-Reactive protein binds to apoptotic cells, protects the cells from assembly of the terminal complement components, and sustains an antiinflammatory innate immune response: implications for systemic autoimmunity. *J. Exp. Med*. 2000;192(9):1353–1364. DOI: 10.1084/jem.192.9.1353.
25. Chimenti M.S., Perricone C., Graceffa D., Di Muzio G., Ballanti E., Guarino M.D. et al. Complement system in psoriatic arthritis: a useful marker in response prediction and monitoring of anti-TNF treatment. *Clin. Exp. Rheumatol.* 2012;30(1):23–30.
26. Coss S.L., Zhou D., Chua G.T., Aziz R.A., Hoffman R.P., Wu Y.L. et al. The complement system and human autoimmune diseases. *J. Autoimmun.* 2023;137:102979. DOI: 10.1016/j.jaut.2022.102979.
27. Cavalli S., Lonati P.A., Gerosa M., Caporali R., Cimaz R., Chighizola C.B. Beyond systemic lupus erythematosus and anti-phospholipid syndrome: the relevance of complement from pathogenesis to pregnancy outcome in other systemic rheumatologic diseases. *Front. Pharmacol*. 2022;13:841785. DOI: 10.3389/fphar.2022.841785.
28. Pouw R.B., Ricklin D. Tipping the balance: intricate roles of the complement system in disease and therapy. *Semin. Immunopathol*. 2021;43(6):757–771. DOI: 10.1007/s00281-021-00892-7.
29. Nurmohamed M.T., Heslinga M., Kitas G.D. Cardiovascular comorbidity in rheumatic diseases. *Nat. Rev. Rheumatol*. 2015;11(12):693–704. DOI: 10.1038/nrrheum.2015.112.
30. Engström G., Hedblad B., Janzon L., Lindgärde F. Complement C3 and C4 in plasma and incidence of myocardial infarction and stroke: a population-based cohort study. *Eur. J. Cardiovasc. Prev. Rehabil*. 2007;14(3):392–397. DOI: 10.1097/01.hjr.0000244582.30421.b2.
31. Arias de la Rosa I., Font P., Escudero-Contreras A., López-Montilla M.D., Pérez-Sánchez C., Ábalos-Aguilera MC. et al. Complement component 3 as biomarker of disease activity and cardiometabolic risk factor in rheumatoid arthritis and spondyloarthritis. *Ther. Adv. Chronic. Dis*. 2020;11:1–12. DOI: 10.1177/2040622320965067.
32. Soley B.S., Silva L.M., Mendes D.A.G.B., Báfica A., Pesquero J.B., Bader M. et al. B1 and B2 kinin receptor blockade improves psoriasis-like disease. *Br. J. Pharmacol*. 2020;177(15):3535–3551. DOI: 10.1111/bph.15077.
33. Golias Ch., Charalabopoulos A., Stagikas D., Charalabopoulos K., Batistatou A. The kinin system-bradykinin: biological effects and clinical implications. Multiple role of the kinin system-bradykinin. *Hippokratia*. 2007;11(3):124–128.
34. Costa-Neto C.M., Dillenburg-Pilla P., Heinrich T.A., Parreiras-e-Silva L.T., Pereira M.G., Reis R.I. et al. Participation of kallikrein-kinin system in different pathologies. *Int. Immunopharmacol*. 2008;8(2):135–142. DOI: 10.1016/j.intimp.2007.08.003.
35. Choi S.I., Hwang S.W. Depolarizing effectors of bradykinin signaling in nociceptor excitation in pain perception. *Biomol. Ther. (Seoul).* 2018;26(3):255–267. DOI: 10.4062/biomolther.2017.127.
36. Ramjeeawon A., Choy E. Neuropathic-like pain in psoriatic arthritis: evidence of abnormal pain processing. *Clin. Rheumatol*. 2019;38(11):3153–3159. DOI: 10.1007/s10067-019-04656-5.
37. Grinnell-Merrick L.L., Lydon E.J., Mixon A.M., Saalfeld W. Evaluating Inflammatory Versus Mechanical Back Pain in Individuals with Psoriatic Arthritis: A Review of the Literature.

Rheumatol. Ther. 2020;7(4):667–684. DOI: 10.1007/s40744-020-00234-3.
38. Cassim B., Shaw O.M., Mazur M., Misso N.L., Naran A., Langlands D.R. et al. Kallikreins, kininogens and kinin receptors on circulating and synovial fluid neutrophils: role in kinin generation in rheumatoid arthritis. *Rheumatology (Oxford).* 2009;48(5):490–496. DOI: 10.1093/rheumatology/kep016.
39. Tan D.B.A., Tedja C., Kuster L., Raymond W.D., Harsanyi A., Chowalloor P.V. et al. The relationship between clinical phenotype and kallikrein-kinin bioregulation in different forms of arthritis. *BMC Musculoskelet. Disord*. 2023;24(1):396. DOI: 10.1186/s12891-023-06388-9.
40. Tsou P.S., Lu C., Gurrea-Rubio M., Muraoka S., Campbell P.L., Wu Q. et al. Soluble CD13 induces inflammatory arthritis by activating the bradykinin receptor B1. *J. Clin. Invest*. 2022;132(11):e151827. DOI: 10.1172/JCI151827.
41. Di Minno M.N., Iervolino S., Peluso R., Di Minno A., Ambrosino P., Scarpa R. Hemostatic and fibrinolytic changes are related to inflammatory conditions in patients with psoriatic arthritis-effect of different treatments. *J. Rheumatol*. 2014;41(4):714–722. DOI: 10.3899/jrheum.130850.
42. Visser M.J.E., Venter C., Roberts T.J., Tarr G., Pretorius E. Psoriatic disease is associated with systemic inflammation, endothelial activation, and altered haemostatic function. *Sci. Rep*. 2021;11(1):13043. DOI: 10.1038/s41598-021-90684-8.
43. Ogdie A., Kay McGill N., Shin D.B., Takeshita J., Jon Love T., Noe M.H. et al. Risk of venous thromboembolism in patients with psoriatic arthritis, psoriasis and rheumatoid arthritis: a general population-based cohort study. *Eur. Heart J*. 2018;39(39):3608–3614. DOI: 10.1093/eurheartj/ehx145.
44. Nohawica M., Nowak-Terpilowska A., Adamska K., Wyganowska-Swiatkowska M. Simulated *in vitro* hypoxic conditions from psoriatic arthritis cartilage change plasminogen activating system urokinase and serpine functionality. *Adv. Dermatol. Alergol*. 2022;39(5):944–952. DOI: 10.5114/ada.2022.113405.
45. Coras R., Kavanaugh A., Boyd T., Huynh Q., Pedersen B., Armando A.M. et al. Pro- and anti-inflammatory eicosanoids in psoriatic arthritis. *Metabolomics*. 2019;15(4):65. DOI: 10.1007/s11306-019-1527-0.
46. Wójcik P., Biernacki M., Wroński A., Łuczaj W., Waeg G., Žarković N. et al. Altered lipid metabolism in blood mononuclear cells of psoriatic patients indicates differential changes in psoriasis vulgaris and psoriatic arthritis. *Int. J. Mol. Sci*. 2019;20(17):4249. DOI: 10.3390/ijms20174249.
47. Łuczaj W., Gęgotek A., Skrzydlewska E. Antioxidants and HNE in redox homeostasis. *Free Radic. Biol. Med*. 2017;111:87–101. DOI: 10.1016/j.freeradbiomed.2016.11.033.
48. Cheng H., Huang H., Guo Z., Chang Y., Li Z. Role of prostaglandin E2 in tissue repair and regeneration. *Theranostics*. 2021;11(18):8836–8854. DOI: 10.7150/thno.63396.
49. Samuels J.S., Holland L., López M., Meyers K., Cumbie W.G., McClain A. et al. Prostaglandin E2 and IL-23 interconnects STAT3 and RoRγ pathways to initiate Th17 $CD4^+$ T-cell development during rheumatoid arthritis. *Inflamm. Res*. 2018;67(7):589–596. DOI: 10.1007/s00011-018-1153-8.
50. Diao G., Huang J., Zheng X., Sun X., Tian M., Han J. et al. Prostaglandin E2 serves a dual role in regulating the migration of dendritic cells. *Int. J. Mol. Med*. 2021;47(1):207–218. DOI: 10.3892/ijmm.2020.4801.
51. Timmermann M., Högger P. Oxidative stress and 8-iso-prostaglandin F(2alpha) induce ectodomain shedding of CD163 and release of tumor necrosis factor-alpha from human monocytes. *Free Radic. Biol. Med*. 2005;39(1):98–107. DOI: 10.1016/j.freeradbiomed.2005.02.031.
52. Antón R., Camacho M., Puig L., Vila L. Hepoxilin B3 and its enzymatically formed derivative trioxilin B3 are incorporated into phospholipids in psoriatic lesions. *J. Invest. Dermatol.* 2002;118(1):139–146. DOI: 10.1046/j.0022-202x.2001.01593.x.
53. Arnardottir H.H., Dalli J., Norling L.V., Colas R.A., Perretti M., Serhan C.N. Resolvin D3 Is Dysregulated in Arthritis and Reduces Arthritic Inflammation. *J. Immunol*. 2016;197(6):2362–2368. DOI: 10.4049/jimmunol.1502268.
54. Rea I.M., Gibson D.S., McGilligan V., McNerlan S.E., Alexander H.D., Ross O.A. Age and age-related diseases: role of inflammation triggers and cytokines. *Front. Immunol*. 2018;9:586. DOI: 10.3389/fimmu.2018.00586.
55. Faustman D.L., Davis M. TNF Receptor 2 and disease: autoimmunity and regenerative medicine. *Front. Immunol.* 2013;4:478. DOI: 10.3389/fimmu.2013.00478.
56. Fitzgerald O., Winchester R. Psoriatic arthritis: from pathogenesis to therapy. *Arthritis. Res. Ther*. 2009;11(1):214. DOI: 10.1186/ar2580.
57. Merola J.F., Espinoza LR., Fleischmann R. Distinguishing rheumatoid arthritis from psoriatic arthritis. *RMD Open*. 2018;4(2):e000656. DOI: 10.1136/rmdopen-2018-000656.
58. Lee B.W., Moon S.J. Inflammatory cytokines in psoriatic arthritis: understanding pathogenesis and implications for treatment. *Int. J. Mol. Sci*. 2023;24(14):11662. DOI: 10.3390/ijms241411662.
59. Fragoulis G.E., Siebert S. The role of IL-23 and the use of IL-23 inhibitors in psoriatic arthritis. *Musculoskeletal Care*. 2022;20(Suppl. 1):S12–S21. DOI: 10.1002/msc.1694.
60. Iznardo H., Puig L. Exploring the role of IL-36 cytokines as a new target in psoriatic disease. *Int. J. Mol. Sci*. 2021;22(9):4344. DOI: 10.3390/ijms22094344.
62. Aggarwal B.B. Signalling pathways of the TNF superfamily: a double-edged sword. *Nat. Rev. Immunol*. 2003;3(9):745–756. DOI 10.1038/nri1184.
63. Bodmer J.L., Schneider P., Tschopp J. The molecular architecture of the TNF superfamily. *Trends Biochem. Sci*. 2002;27(1):19–26. DOI: 10.1016/s0968-0004(01)01995-8.
64. Brenner D., Blaser H., Mak T.W. Regulation of tumour necrosis factor signalling: live or let die. *Nat. Rev. Immunol*. 2015;15(6):362–374. DOI: 10.1038/nri3834.
61. Blauvelt A., Chiricozzi A. The immunologic role of IL-17 in psoriasis and psoriatic arthritis pathogenesis. *Clin. Rev. Allergy. Immunol*. 2018;55(3):379–390. DOI: 10.1007/s12016-018-8702-3.
65. Boras E., Slevin M., Alexander M.Y., Aljohi A., Gilmore W., Ashworth J. et al. Monomeric C-reactive protein and Notch-3 co-operatively increase angiogenesis through PI3K signaling pathway. *Cytokine*. 2014;69(2):165–179. DOI: 10.1016/j.cyto.2014.05.027.
66. Narazaki, M. The two-faced cytokine IL-6 in host defense and

diseases. *Int. J. Mol. Sci*. 2018;19(11):3528. DOI 10.3390/ijms19113528.
67. Rose-John S. Interleukin-6 family cytokines. *Cold. Spring. Harb. Perspect. Biol.* 2018;10(2):a028415. DOI 10.1101/cshperspect.a028415.
68. Blauvelt A., Chiricozzi A. The immunologic role of IL-17 in psoriasis and psoriatic arthritis pathogenesis. *Clin. Rev. Allergy. Immunol*. 2018;55(3):379–390. DOI: 10.1007/s12016-018-8702-3.
69. Boutet M.A., Nerviani A., Pitzalis C. IL-36, IL-37, and IL-38 Cytokines in Skin and Joint Inflammation: A Comprehensive Review of Their Therapeutic Potential. *Int. J. Mol. Sci*. 2019;20(6):1257. DOI: 10.3390/ijms20061257.
70. Bettiol A., Fagni F., Mattioli I., Bagni G., Vitiello G., Grassi A. et al. Serum interleukin-36 α as a candidate biomarker to distinguish behçet's syndrome and psoriatic arthritis. *Int. J. Mol. Sci*. 2023;24(10):8817. DOI: 10.3390/ijms24108817.
71. Wang C., Hu J., Shi J. Role of interleukin-36 in inflammatory joint diseases. *Zhejiang Da XueXue Bao Yi Xue Ban*. 2023;52(2):249–259. DOI: 10.3724/zdxbyxb-2023-0034.
72. Kaplan A.P., Joseph K. Pathogenic mechanisms of bradykinin mediated diseases: dysregulation of an innate inflammatory pathway. *Adv. Immunol*. 2014;121:41–89. DOI: 10.1016/B978-0-12-800100-4.00002-7.
73. Oncul S., Afshar-Kharghan V. The interaction between the complement system and hemostatic factors. *Curr. Opin. Hematol*. 2020;27(5):341–352. DOI: 10.1097/MOH.0000000000000605.
74. Risau W. Mechanisms of angiogenesis. *Nature*. 1997;386(6626):671–674. DOI: 10.1038/386671a0.
75. Cantatore F.P., Maruotti N., Corrado A., Ribatti D. Angiogenesis dysregulation in psoriatic arthritis: molecular mechanisms. *Biomed. Res. Int*. 2017;2017:5312813. DOI: 10.1155/2017/5312813.
76. Espinoza L.R., Vasey F.B., Espinoza C.G., Bocanegra T.S., Germain B.F. Vascular changes in psoriatic synovium. A light and electron microscopic study. *Arthritis Rheum*. 1982;25(6):677–684. DOI: 10.1002/art.1780250611.
77. Tenazinha C., Barros R., Fonseca J.E., Vieira-Sousa E. Histopathology of Psoriatic Arthritis Synovium-A Narrative Review. *Front. Med (Lausanne).* 2022;9:860813. DOI: 10.3389/fmed.2022.860813.
78. Lazar L.T., Guldberg-Møller J., Lazar B.T., Mogensen M. Nailfold capillaroscopy as diagnostic test in patients with psoriasis and psoriatic arthritis: A systematic review. *Microvasc. Res*. 2023;147:104476. DOI: 10.1016/j.mvr.2023.104476.
79. Anghel D., Sîrbu C.A., Petrache O.G., Opriș-Belinski D., Negru M.M., Bojincă V.C. et al. Nailfold videocapillaroscopy in patients with rheumatoid arthritis and psoriatic arthropathy on ANTI-TNF-ALPHA therapy. *Diagnostics (Basel).* 2023;13(12):2079. DOI: 10.3390/diagnostics13122079.
80. Guldberg-Møller J., Henriksen M., Ellegaard K., Haedersdal M., Lazar L.T., Kristensen L.E. et al. Novel application of optical coherence tomography and capillaroscopy in psoriatic arthritis in relationship to psoriasis and hand osteoarthritis. *Rheumatol. Adv. Pract*. 2021;5(3):rkab065. DOI: 10.1093/rap/rkab065.
81. Sivasankari M., Arora S., Vasdev V., Mary E.M. Nailfold capillaroscopy in psoriasis. *Med. J. Armed. Forces India*. 2021;77(1):75–81. DOI: 10.1016/j.mjafi.2020.01.013.
82. Li W., Man X.Y., Chen J.Q., Zhou J., Cai S.Q., Zheng M. Targeting VEGF/VEGFR in the treatment of psoriasis. *Discov. Med*. 2014;18(98):97–104.
83. Fearon U., Reece R., Smith J., Emery P., Veale D.J. Synovial cytokine and growth factor regulation of MMPs/TIMPs: implications for erosions and angiogenesis in early rheumatoid and psoriatic arthritis patients. *Ann. N. Y. Acad. Sci.* 1999;878:619–621. DOI: 10.1111/j.1749-6632.1999.tb07743.
84. Yamamoto T. Angiogenic and inflammatory properties of psoriatic arthritis. *ISRN Dermatology.* 2013;2013:2017. DOI: 10.1155/2013/630620.630620.
85. Ballara S.C., Miotla J.M., Paleolog E.M. New vessels, new approaches: angiogenesis as a therapeutic target in musculoskeletal disorders. *Int. J. Exp. Pathol*. 1999;80(5):235–250. DOI: 10.1046/j.1365-2613.1999.00129.x.
86. Parikh S.M. The angiopoietin-tie2 signaling axis in systemic inflammation. *J. Am. Soc. Nephrol*. 2017;28(7):1973–1982. DOI: 10.1681/ASN.2017010069.
87. Moss A. The angiopoietin:Tie 2 interaction: a potential target for future therapies in human vascular disease. *Cytokine Growth Factor Rev*. 2013;24(6):579–592. DOI: 10.1016/j.cytogfr.2013.05.009.
88. Pinto Tasende J.A., Fernandez-Moreno M., Vazquez-Mosquera M.E., Fernandez-Lopez J.C., Oreiro-Villar N., De Toro Santos F.J. et al. Increased synovial immunohistochemistry reactivity of TGF-β1 in erosive peripheral psoriatic arthritis. *BMC Musculoskelet. Disord.* 2023;24(1):246. DOI: 10.1186/s12891-023-06339-4.
89. Wang J., Xiang H., Lu Y., Wu T. Role and clinical significance of TGFβ1 and TGFβR1 in malignant tumors (Review). *Int. J. Mol. Med*. 2021;47(4):55. DOI: 10.3892/ijmm.2021.4888.
90. Walger P. Rational use of antibiotics. *Internist. (Berl.).* 2016;57(6):551–568. DOI: 10.1007/s00108-016-0071-5.

Authors' information

Pogonchenkova Daria A.– Cand. Sci. (Med.), Head of the Rheumatology Unit, Medical Center "Professor", Siberian State Medical University, Tomsk, pogonchenkova.da@ssmu.ru, http://orcid.org/0000-0002-5903-3662

Chetvernya Lada V. – Rheumatologist, Medical Center "Professor", Siberian State Medical University, Tomsk, chetvernya.lv@ssmu.ru, http://orcid.org/0009-0003-0436-5349

Vasilyeva Olga A. – Cand. Sci. (Med.), Associate Professor of the Pathological Physiology Division, Associate Professor of the Biochemistry and Molecular Biology Division with Clinical Laboratory Diagnostics Course, Siberian State Medical University, Tomsk, vasileva.oa@ssmu.ru, http://orcid.org/0000-0002-2882-4533;

Kononova Tatyana E. – Cand. Sci. (Med.), Associate Professor, Pathological Physiology Division, Siberian State Medical University, Tomsk, kononova.te@ssmu.ru, http://orcid.org/0000-0001-8457-9440

Poletika Vadim S. – Cand. Sci. (Med.), Associate Professor, Pathological Physiology Division, Siberian State Medical University, Tomsk, vpoletika@yandex.ru, http://orcid.org/0000-0002-2005-305X

Abramov Vitaly K. – Laboratory Assistant, Pathological Physiology Division, Siberian State Medical University, Tomsk, abramoff.vk@yandex.ru, http://orcid.org/0000-0002-7991-9786;

Chumakova Svetlana P. – Dr. Sci. (Med.), Associate Professor, Professor of the Pathological Physiology Division, Siberian State Medical University, Tomsk, chumakova.sp@ssmu.ru, http://orcid.org/0000-0003-3468-6154

Eliseeva Larisa V. – Cand. Sci. (Med.), Head of the Rheumatology Unit, Assistant of the Intermediate-Level Therapy Division with Clinical Pharmacology Course, Siberian State Medical University, Tomsk, eliseeva.lv@ssmu.ru, http://orcid.org/0000-0001-9089-3321

Urazova Olga I. – Dr. Sci. (Med.), Professor, Corresponding Member of the RAS, Head of the Pathological Physiology Division, Siberian State Medical University, Tomsk, urazova.oi@ssmu.ru, http://orcid.org/0000-0002-9457-8879

(✉) **Pogonchenkova Darya A.,** pogonchenkova.da@ssmu.ru

Received 02.05.2024;
approved after peer review 15.05.2024;
accepted 13.06.2024

УДК 616.248-053.2-02:579.61
https://doi.org/10.20538/1682-0363-2024-4-197-204

The importance of biodiversity of human microbiota and environment in the susceptibility to the development of bronchial asthma in children

Sokolova T.S., Malchuk V.N., Nogai A.A., Fedorova O.S., Ogorodova L.M.

Siberian State Medical University
2, Moscow Trakt, Tomsk, 634050, Russian Federation

ABSTRACT

Bronchial asthma (BA) remains one of the most common chronic respiratory diseases in childhood. BA develops with a combination of genetic predisposition and environmental factors. Epidemiological data on the development of BA emphasize the role of early-life microbiota in the formation of immune responses and susceptibility to the development of BA. In recent years, enough data has been accumulated to suggest that an imbalance in intestinal and airway microbiota during early life may predispose a child to the development of BA. In turn, the biodiversity of the environment influences the colonization of various biotopes in the human body by microorganisms. The study of the mechanisms of interaction between microbiota communities of the environment and humans will pave the way for the development of new strategies for the prevention of BA.

The aim of this review was to analyze current research aimed at assessing the importance of biodiversity of human microbiota and environment in the susceptibility to the development of BA in children.

Keywords: bronchial asthma, children, intestinal microbiota, airway microbiota, environmental microbiota

Conflict of interest. The authors declare the absence of obvious or potential conflicts of interest related to the publication of this article.

Source of financing. The study was funded by the Russian Science Foundation grant (“The role of microbiota in parasite–host interactions and its metabolic potential as a tool for bronchial asthma control”, agreement dated 01.08.22, No. 22-75-00078).

For citation: Sokolova T.S., Malchuk V. N., Nogai A.A., Fedorova O.S., Ogorodova L.M. The importance of biodiversity of human microbiota and environment in the susceptibility to the development of bronchial asthma in children. *Bulletin of Siberian Medicine.* 2024;23(4):197–204. https://doi.org/10.20538/1682-0363-2024-4-197-204.

Значение биоразнообразия микробиоты человека и окружающей среды в подверженности развитию бронхиальной астмы у детей

Соколова Т.С., Мальчук В.Н., Ногай А.А., Федорова О.С., Огородова Л.М.

Сибирский государственный медицинский университет (СибГМУ)
Россия, 634050, г. Томск, Московский тракт, 2

РЕЗЮМЕ

Бронхиальная астма (БА) остается одним из наиболее распространенных хронических заболеваний дыхательных путей в детском возрасте. Развитие БА реализуется при сочетании генетической

✉ *Sokolova Tatyana S.,* sokolova.ts@ssmu.ru

предрасположенности и воздействия факторов внешней среды. Эпидемиологические данные, касающиеся развития БА, подчеркивают важность воздействия микробиоты в раннем возрасте в формировании иммунных реакций и подверженности развитию БА. В последние годы накоплено достаточно данных, позволяющих предположить, что дисбаланс микробиоты кишечника и дыхательных путей в раннем возрасте может предрасполагать ребенка к развитию астмы. В свою очередь, биоразнообразие окружающей среды оказывает влияние на колонизацию микроорганизмами различных биотопов организма человека. Исследование механизмов взаимодействия микробиотических сообществ окружающей среды и человека откроет перспективу для разработки новых стратегий профилактики астмы.

Цель настоящего обзора – провести анализ современных исследований, направленных на оценку значения биоразнообразия микробиоты человека и окружающей среды в подверженности развитию бронхиальной астмы у детей.

Ключевые слова: бронхиальная астма, дети, кишечная микробиота, микробиота дыхательных путей, микробиота окружающей среды

Конфликт интересов. Авторы декларируют отсутствие явных и потенциальных конфликтов интересов, связанных с публикацией настоящей статьи.

Источник финансирования. Исследование выполнено при поддержке Российского научного фонда (грант «Микробиота в системе “паразит – хозяин” и ее метаболический потенциал как инструмент управления бронхиальной астмой»; договор от 01.08.22, № 22-75-00078).

Для цитирования: Соколова Т.С., Мальчук В.Н., Ногай А.А., Федорова О.С., Огородова Л.М. Значение биоразнообразия микробиоты человека и окружающей среды в подверженности развитию бронхиальной астмы у детей. *Бюллетень сибирской медицины.* 2024;23(4):197–204. https://doi.org/10.20538/1682-0363-2024-4-197-204.

INTRODUCTION

Asthma is one of the most common chronic respiratory diseases, affecting up to 10% of children and adolescents [1]. Asthma develops through a combination of genetic predisposition to atopy and bronchial hyperreactivity and exposure to environmental factors[1]. Recent data suggest a possible link between the high prevalence of asthma and a decrease in exposure to microbes as a result of changes in dietary habits. This includes a decrease in dietary fiber intake and an increase in fat intake, improved hygiene, irrational use of antibacterial drugs, and other factors [2, 3]. Currently, there is more and more information on changes in the composition of human microbiota in various diseases and its role in the pathogenesis of various disorders, including asthma [4]. Epidemiological and experimental data demonstrate the importance of exposure to microbial factors at an early age in the formation of immune responses [5–7].

According to modern research, there are several hypotheses that explain the relationship between the prevalence of allergic diseases and environmental changes that have occurred in recent decades (such as urbanization, improved housing conditions, and changes in the diet) and a decrease in environmental biodiversity [3, 8, 9] Epidemiological studies show that reduced exposure to environmental bacteria in early life (e.g., cesarean birth, infant formula feeding, living in an urban environment, in small families, and with limited contact with various animals) is associated with an increased risk of developing allergies and asthma later in life [3, 8–10]. Conversely, a reduced risk of developing asthma is observed in children living in rural areas, as well as in large families with older children. This is probably due to the child’s exposure to a wide range of microorganisms and their metabolites [11]

Experimental and clinical studies aimed at studying the characteristics of the microbiota in asthma described the intestinal and airway microbiota. The formation of the microbiota is affected by many internal and external factors. One of the striking examples of the environment affecting the development of asthma is the “farm effect” [12]. Many epidemiological studies have shown that living on a farm in early life is associated with a reduced risk of asthma in children [12–15].

The aim of this review was to analyze current research focused on assessing the importance of biodiversity of human microbiota and the

environment in the susceptibility to the development of bronchial asthma in children.

MATERIALS AND METHODS

We analyzed scientific publications of clinical studies aimed at assessing the biodiversity of the microbiota of airway, intestine, and environment in the development of asthma in children.

The search was conducted using the PubMed search engine (https://pubmed.ncbi.nlm.nih.gov/) and the Elibrary scientific electronic library (https://www.elibrary.ru/). The review presents original articles published from April 1, 2014 to April 1, 2024.

Initially, we searched for publications devoted to the study of the intestinal and/or airway and/or environmental microbiota in asthma in children from birth to 18 years of age. The search was conducted with the following keywords in English and Russian: asthma microbiota gut or microbiota airway or microbiota environment or microbiota household, asthma, children, intestinal microbiota, airway microbiota, environmental microbiota. We examined the summaries of 7,708 articles selected in the initial search.

Then we analyzed the summaries of 907 publications, excluding reviews, case-control studies, and works that did not contain data on the intestinal and/or airway and/or environmental microbiota in asthma in children.

The analysis included 19 publications that met the following inclusion criteria: a study of the intestinal and/or airway and/or environmental microbiota (microbiota of household dust samples) using sequencing in children without asthma symptoms at the time of inclusion in the study, followed by an assessment of the association with the development of asthma, and a complete description of the study design.

THE IMPORTANCE OF AIRWAY MICROBIOTA IN THE DEVELOPMENT OF ASTHMA IN CHILDREN

It is currently known that the respiratory mucosa in healthy individuals is colonized by bacterial communities specific to this biotope [16]. Studies have shown that the composition of the airway microbiota differs in healthy children and patients with asthma, and differences in the microbiota in different asthma phenotypes have been established [17].

Multiple studies have demonstrated that changes in the microbiota in early childhood are crucial for the development of asthma later in life [18–23]. However, the results of the studies are contradictory due to differences in the techniques for collecting the studied biospecimens, methods, and time points, which makes it difficult to generalize the results. As a result of the analysis of publications, we selected 6 prospective studies that analyzed the association of the airway microbiota in infants with the development of asthma later in life [18–23]. Most studies used samples taken from the nasopharynx to study the microbiota, and two studies reported airway aspirates as the studied biospecimens [18, 19]. Three studies reported on the assessment of alpha and beta diversity of the microbiota [18, 20, 21].

However, only one study found an association with the development of asthma of a higher alpha diversity index and a difference in beta diversity compared to children who did not have asthma symptoms at the age of 6 [18]. This study also demonstrated an increase in Veillonella and Prevotella in infants aged 1 month who later developed asthma [18].

Two studies have shown that higher relative abundance of Streptococcus in the nasal microbiota of infants is associated with the development of asthma [22, 23].

Another study showed that the abundance of Staphylococcus bacteria in the nasopharynx in the first 6 months of life is associated with recurrent wheezing in the first 3 years of life and the development of asthma at an older age [19]. Also, two studies demonstrated the association of Haemophilus with the risk of developing asthma [19,21]. Several studies have noted changes in the number of bacteria belonging to the Moraxella genus, but the data are contradictory [19, 21]. A prospective cohort study also confirmed the association of Streptococcus pneumoniae, Haemophilus influenzae, and Moraxella catarrhalis with the development of asthma [20].

It should be noted that in children suffering from asthma, an increase in the Moraxella and Streptococcus w genera was noted in samples of the lower airway microbiota (analysis of sputum and exhaled air condensate) [24, 25].

THE IMPORTANCE OF INTESTINAL MICROBIOTA IN THE DEVELOPMENT OF ASTHMA IN CHILDREN

The intestinal microbiota is one of the most important factors determining human health and is currently considered as a system responsible for regulating the metabolic and immune homeostasis of the body [26]. Intestinal microbiota and its metabolites play an important role in the development of local and systemic immune responses [27]. Changes in the intestinal microbial composition can have a significant impact on respiratory diseases, such as asthma, by shaping microbial communities and modulating the metabolic and immune response. This concept is called the gut – lung axis [4, 28].

The development of the intestinal microbiome in early life is influenced by many environmental factors, such as living in a microbial-rich environment (e.g., on a farm or with frequent contact with livestock and pets) or dietary diversity, the preventive value of which in relation to the development of asthma in childhood has been shown in studies [29, 30]. Early life exposure and colonization by certain microbes are thought to be important for intestine development, immune cell maturation, and resistance to pathogens [31].

The taxonomic richness of the intestinal microbiota is thought to determine its resistance to various effects, including pathogen colonization, while low diversity of bacterial communities is associated with pathological conditions [32. The studies included in the review noted a decrease in alpha diversity in stool samples of infants who later developed asthma compared to healthy children [32, 33].

In a prospective study, G. Galazzo et al. showed that the *Lachnobacterium, Lachnospira*, and *Dialister* genera were significantly decreased in the intestinal microbiome of infants who developed asthma by school age compared to healthy children [34]. The analysis of the taxonomic composition of the microbiota showed that a high risk of developing asthma is associated with a decrease in genera such as *Faecalibacterium, Bifidobacterium, Roseburia, Alistipes, Ruminococcus,* and *Dialister* and a higher content of Veillonella [35, 36]. Similar results were obtained by scientists from the USA: the abundance of Veillonella in the intestine was associated with episodes of wheezing, while no association was found between wheezing and beta diversity [37].

However, in a cohort study conducted in Canada involving more than 300 children, the risk of developing asthma was associated with a decrease in the relative abundance of bacteria of the *Veillonella* genus [38]. Another study also showed an association of a decrease in the Bifidobacterium, Faecalibacterium, and Akkermansia genera with a high risk of developing asthma [39]. Several studies have described an association between a decrease in the relative abundance of the *Roseburia*, *Ruminococcus, Faecalibacterium*, and *Lachnospira* genera with an increased risk of developing this pathology [12, 33–35].

Despite the multifaceted and heterogeneous nature of the studies, taken together, these data confirm the importance of the composition of the intestinal microbiota in early life with susceptibility to the development of asthma in children.

THE IMPORTANCE OF ENVIRONMENTAL MICROBIOTA IN THE DEVELOPMENT OF ASTHMA IN CHILDREN

The microbiota of different biotopes is formed mainly during the first year of life and continues to develop until adulthood. The types of delivery and feeding affect the colonization with microorganisms in early life [22, 38]. Studies have shown that the type of delivery (vaginal or cesarean birth) and the environment in the first 6 months of life are of great importance for the formation of a stable microbiota of the respiratory and intestinal organs, which determines the state of health in older age [22, 38].

According to the meta-analysis, children delivered by cesarean section have a higher risk of developing bronchial asthma and allergic rhinitis compared to children born vaginally [40]. However, another study showed that the microbiota of infants is determined to a greater extent by maternal factors and does not depend on the mode of delivery [41]. Probably, the risk of developing allergic diseases is also associated with the influence of conditions that determine the mode of delivery in favor of cesarean section. Epidemiological studies have shown that contact with older siblings or attending preschool in the first two years of life prevents developing

allergies, which is associated with an increase in the taxonomic diversity of the microbiota [11, 42].

It has also been shown that children living on farms are less susceptible to allergic diseases [2, 13, 14, 43, 44]. The results of a cohort study in Denmark showed that an increased risk of developing asthma was recorded in adolescents who lived in moldy and damp houses at an early age. In contrast, adolescents who lived in farmhouses and had contact with domestic animals were less likely to suffer from asthma by the age of 18 [45].

These factors are thought to affect the development of the immune system in childhood by shaping a taxonomically rich microbiota of diverse biotopes [14, 32]. Experimental and clinical studies have shown that inhaled dust particles can carry a complex mixture of microbes and their metabolites that influence susceptibility to asthma development through their effects on airway immune responses [14, 46]. The study also demonstrated the relationship between fungal and bacterial communities at home and the airway microbiota in early life [47]. The review of publications over the past 10 years identified six studies assessing indoor microbiota using molecular genetic methods and its association with asthma development [14, 43, 48–51]

A prospective cohort study showed that microorganisms associated with the rural environment in infant crib dust samples were associated with a lower risk of developing asthma and allergic rhinitis at the age of 6 years [48]. Low bacterial diversity was found in the microbiota collected from crib dust samples from children who later developed asthma [48]. Another study showed differences in beta diversity, increased *Lactococcus* and *Streptococcus*, and decreased *Sphingomonas* in house dust samples from homes of patients with asthma compared to homes of participants without asthma [49]. Among high-risk urban children, higher levels of indoor allergens in infancy were associated with a lower risk of developing asthma at age 7 [50]. In addition, studies of the farm environment and asthma risk have shown that the number of *Streptococcaceae* in the dust microbiota is higher in homes not located in rural areas, which is associated with the risk of developing asthma [43].

However, studies of dust microbiota in the homes of patients diagnosed with asthma demonstrate an association of high microbial biodiversity with uncontrolled asthma. Thus, a study conducted in the USA reported a positive association between bacterial abundance at home and asthma severity in children [52].

Diverse composition of indoor microbiota affects the colonization of the intestine and airways by microorganisms, promoting the development of immune tolerance [13, 53]. Exposure to environmental microbial communities in early life is associated with the risk of developing asthma in children, and these results can serve as guidelines for the development of asthma prevention strategies.

CONCLUSION

Thus, the analysis of modern studies demonstrates the important role of diversity and composition of human microbiota and the environment in the development of asthma in children. Summarizing the research results, we can conclude that the period from birth to 12 months is the ideal time for epigenetic changes associated with environmental exposure and susceptibility to asthma. Further research is needed to study the pathogenetic mechanisms of interaction between microbial communities and the human immune system. New studies will provide the basis for the development of new technologies for asthma management.

REFERENCES

1. Reddel H.K., Bacharier L.B., Bateman E.D., Brightling C.E., Brusselle G.G., Buhl R. et al. Global initiative for asthma strategy 2021: executive summary and rationale for key changes. *Am. J. Respir. Crit .Care Med*. 2022;205(1):17–35. DOI: 10.1164/rccm.202109-2205PP.
2. Haahtela T., Laatikainen T., Alenius H., Auvinen P., Fyhrquist N., Hanski I. et al. Hunt for the origin of allergy – comparing the Finnish and Russian Karelia. *Clin. Exp. Allergy*. 2015; 45(5):891–901. DOI: 10.1111/cea.12527.
3. Haahtela T., Holgate S., Pawankar R., Akdis C.A., Benjaponpitak S., Caraballo L. et al. The biodiversity hypothesis and allergic disease: world allergy organization position statement. *World Allergy Organ J.* 2013;6(1):3. DOI: 10.1186/1939-4551-6-3.
4. Dang A.T., Marsland B.J. Microbes, metabolites, and the gut-lung axis. *Mucosal Immunol.* 2019;12(4):843–850. DOI: 10.1038/s41385-019-0160-6.
5. Smulders T., Van Der Schee M.P., Maitland-Van Der Zee A.H., Dikkers F.G., Van Drunen C.M. Influence of the gut and airway microbiome on asthma development and disease. *Pediatr. Allergy Immunol.* 2024;35(3):e14095. DOI: 10.1111/pai.14095.
6. Olszak T., An D., Zeissig S., Vera M.P., Richter J., Franke A.

et al. Microbial exposure during early life has persistent effects on natural killer T cell function. *Science*. 2012;336(6080):489–493. DOI: 10.1126/science.1219328.
7. Lynch S.V., Wood R.A., Boushey H., Bacharier L.B., Bloomberg G.R., Kattan M. et al. Effects of early-life exposure to allergens and bacteria on recurrent wheeze and atopy in urban children. *J. Allergy Clin. Immunol*. 2014;134(3):593–601. e12. DOI: 10.1016/j.jaci.2014.04.018.
8. Strachan D.P. Hay fever, hygiene, and household size. *BMJ*. 1989;299(6710):1259–1260. DOI: 10.1136/bmj.299.6710.1259.
9. Rook G.A., Lowry C.A., Raison C.L. Microbial 'Old Friends', immunoregulation and stress resilience. *Evol. Med. Public Health*. 2013;2013(1):46–64. DOI: 10.1093/emph/eot004.
10. Stokholm J., Thorsen J., Chawes B.L., Schjørring S., Krogfelt K.A., Bønnelykke K. et al. Cesarean section changes neonatal gut colonization. *J. Allergy Clin. Immunol.* 2016;138(3):881–889.e2. DOI: 10.1016/j.jaci.2016.01.028.
11. Christensen E.D., Hjelmsø M.H., Thorsen J., Shah S., Redgwell T., Poulsen C.E. et al. The developing airway and gut microbiota in early life is influenced by age of older siblings. *Microbiome.* 2022;10(1):106. DOI: 10.1186/s40168-022-01305-z.
12. Depner M., Taft D.H., Kirjavainen P.V., Kalanetra K.M., Karvonen A.M., Peschel S. et al. Maturation of the gut microbiome during the first year of life contributes to the protective farm effect on childhood asthma. *Nat. Med*. 2020;26(11):1766–1775. DOI: 10.1038/s41591-020-1095-x.
13. Von Mutius E., Vercelli D. Farm living: effects on childhood asthma and allergy. *Nat. Rev. Immunol*. 2010;10(12):861–868. DOI: 10.1038/nri2871.
14. Stein M.M., Hrusch C.L., Gozdz J., Igartua C., Pivniouk V., Murray S.E. et al. Innate immunity and asthma risk in amish and hutterite farm children. *N. Engl. J. Med*. 2016; 375(5):411–421. DOI: 10.1056/NEJMoa1508749.
15. Strieker S., Weinmann T., Gerlich J., von Mutius E., Nowak D., Radon K. et al. Farm living and allergic rhinitis from childhood to young adulthood: Prospective results of the GABRIEL study. *J. Allergy Clin. Immunol.* 2022;150(5):1209–1215. e2. DOI: 10.1016/j.jaci.2022.05.027.
16. Bassis C.M., Erb-Downward J.R., Dickson R.P., Freeman C.M., Schmidt T.M., Young V.B. et al. Analysis of the upper respiratory tract microbiotas as the source of the lung and gastric microbiotas in healthy individuals. *mBio*. 2015;6(2):e00037. DOI: 10.1128/mBio.00037-15.
17. Hilty M., Burke C., Pedro H., Cardenas P., Bush A., Bossley C. et al. Disordered microbial communities in asthmatic airways. *PLoS One*. 2010;5(1):e8578. DOI: 10.1371/journal.pone.0008578.
18. Thorsen J., Rasmussen M.A., Waage J., Mortensen M., Brejnrod A., Bønnelykke K. et al. Infant airway microbiota and topical immune perturbations in the origins of childhood asthma. Nat Commun. 2019 Nov 1; 10(1):5001. DOI: 10.1038/s41467-019-12989-7.
19. Tang H.H.F., Lang A., Teo S.M., Judd L.M., Gangnon R., Evans M.D. et al. Developmental patterns in the nasopharyngeal microbiome during infancy are associated with asthma risk. J *Allergy Clin. Immunol.* 2021;47(5):1683–1691. DOI: 10.1016/j.jaci.2020.10.009.
20. Thorsen J., Li X.J., Peng S., Sunde R.B., Shah S.A., Bhattacharyya M. et al. The airway microbiota of neonates colonized with asthma-associated pathogenic bacteria. *Nat. Commun*. 2023;14(1):6668. DOI: 10.1038/s41467-023-42309-z.
21. Toivonen L., Karppinen S., Schuez-Havupalo L., Waris M., He Q., Hoffman K.L. et al. Longitudinal changes in early nasal microbiota and the risk of childhood asthma. *Pediatrics.* 2020;146(4):e20200421. DOI: 10.1542/peds.2020-0421.
22. Teo S.M., Mok D., Pham K., Kusel M., Serralha M., Troy N. et al. The infant nasopharyngeal microbiome impacts severity of lower respiratory infection and risk of asthma development. *Cell Host Microbe*. 2015;17(5):704–715. DOI: 10.1016/j.chom.2015.03.008.
23. Zhu Z., Camargo C.A. Jr., Raita Y., Freishtat R.J., Fujiogi M., Hahn A. et al. Nasopharyngeal airway dual-transcriptome of infants with severe bronchiolitis and risk of childhood asthma: A multicenter prospective study. *J. Allergy Clin. Immunol*. 2022;150(4):806–816. DOI: 10.1016/j.jaci.2022.04.017.
24. Bataineh M.T., Hamoudi R.A., Dash N.R., Ramakrishnan R.K., Almasalmeh M.A., Sharif H.A. et al. Altered respiratory microbiota composition and functionality associated with asthma early in life. *BMC Infect. Dis*. 2020;20(1):697. DOI: 10.1186/s12879-020-05427-3.
25. Bar K., Żebrowska P., Łaczmański Ł., Sozańska B. Airway bacterial biodiversity in exhaled breath condensates of asthmatic children-does it differ from the healthy ones? *J. Clin. Med.* 2022;11(22):6774. DOI: 10.3390/jcm11226774.
26. Weinstock G.M. Genomic approaches to studying the human microbiota. *Nature*. 2012;489(7415):250–256. DOI: 10.1038/nature11553.
27. Enaud R., Prevel R., Ciarlo E., Beaufils F., Wieërs G., Guery B. et al. The gut-lung axis in health and respiratory diseases: a place for inter-organ and inter-kingdom crosstalks. *Front. Cell Infect. Microbiol*. 2020;10:9. DOI: 10.3389/fcimb.2020.00009.
28. Wypych T.P., Wickramasinghe L.C., Marsland B.J. The influence of the microbiome on respiratory health. *Nat. Immunol.* 2019;20(10):1279–1290. DOI: 10.1038/s41590-019-0451-9.
29. Zhong C., Guo J., Tan T., Wang H., Lin L., Gao D. et al. Increased food diversity in the first year of life is inversely associated with allergic outcomes in the second year. *Pediatr. Allergy Immunol*. 2022;33(1):e13707. DOI: 10.1111/pai.13707.
30. Frei R., Ferstl R., Roduit C., Ziegler M., Schiavi E., Barcik W. et al. Exposure to nonmicrobial N-glycolylneuraminic acid protects farmers' children against airway inflammation and colitis. *J. Allergy Clin. Immunol*. 2018;141(1):382–390.e7. DOI: 10.1016/j.jaci.2017.04.051.
31. Rook G.A., Adams V., Hunt J., Palmer R., Martinelli R., Brunet L.R. Mycobacteria and other environmental organisms as immunomodulators for immunoregulatory disorders. *Springer Semin. Immunopathol*. 2004;25(3-4):237–255. DOI: 10.1007/s00281-003-0148-9.
32. Abrahamsson T.R., Jakobsson H.E., Andersson A.F., Björkstén B., Engstrand L., Jenmalm M.C. Low gut microbiota diversity in early infancy precedes asthma at school age. *Clin. Exp. Allergy*. 2014;44(6):842–850. DOI: 10.1111/cea.12253.
33. Patrick D.M., Sbihi H., Dai D.L.Y., Al Mamun A., Ras-

ali D., Rose C. et al. Decreasing antibiotic use, the gut microbiota, and asthma incidence in children: evidence from population-based and prospective cohort studies. *Lancet Respir. Med.* 2020;8(11):1094–1105. DOI: 10.1016/S2213-2600(20)30052-7.
34. Galazzo G., van Best N., Bervoets L., Dapaah I.O., Savelkoul P.H., Hornef M.W. et al. Development of the microbiota and associations with birth mode, diet, and atopic disorders in a longitudinal analysis of stool samples, collected from infancy through early childhood. *Gastroenterology.* 2020;158(6):1584-1596. DOI: 10.1053/j.gastro.2020.01.024.
35. Stokholm J., Blaser M.J., Thorsen J., Rasmussen M.A., Waage J., Vinding R.K. et al. Maturation of the gut microbiome and risk of asthma in childhood. *Nat. Commun*. 2018;9(1):141. DOI: 10.1038/s41467-017-02573-2.
36. Chiu C.Y., Cheng M.L., Chiang M.H., Kuo Y.L., Tsai M.H., Chiu C.C. et al. Gut microbial-derived butyrate is inversely associated with IgE responses to allergens in childhood asthma. *Pediatr. Allergy Immunol*. 2019;30(7):689–697. DOI: 10.1111/pai.13096.
37. Lee-Sarwar K., Dedrick S., Momeni B., Kelly R.S., Zeiger R.S., O'Connor G.T. et al. Association of the gut microbiome and metabolome with wheeze frequency in childhood asthma. *J. Allergy Clin. Immunol.* 2022;150(2):325–336. DOI: 10.1016/j.jaci.2022.02.005.
38. Arrieta M.C., Stiemsma L.T., Dimitriu P.A., Thorson L., Russell S., Yurist-Doutsch S. et al. Early infancy microbial and metabolic alterations affect risk of childhood asthma. *Sci. Transl. Med*. 2015;7(307):307ra152. DOI: 10.1126/scitranslmed.aab2271.
39. Fujimura K.E., Sitarik A.R., Havstad S., Lin D.L, Levan S., Fadrosh D. et al. Neonatal gut microbiota associates with childhood multisensitized atopy and T cell differentiation. *Nat. Med.* 2016; 22(10):1187–1191. DOI: 10.1038/nm.4176.
40. Thavagnanam S., Fleming J., Bromley A., Shields M.D., Cardwell C.R. A meta-analysis of the association between Caesarean section and childhood asthma. *Clin. Exp. Allergy.* 2008;38(4):629–633. DOI: 10.1111/j.1365-2222.2007.02780.x.
41. Chu D.M., Ma J., Prince A.L., Antony K.M., Seferovic M.D., Aagaard K.M. Maturation of the infant microbiome community structure and function across multiple body sites and in relation to mode of delivery. *Nat. Med*. 2017;23(3):314–326. DOI: 10.1038/nm.4272.
42. Laursen M.F., Zachariassen G., Bahl M.I., Bergström A., Høst A., Michaelsen K.F. et al. Having older siblings is associated with gut microbiota development during early childhood. *BMC Microbiol*. 201515:154. DOI: 10.1186/s12866-015-0477-6.
43. Kirjavainen P.V., Karvonen A.M., Adams R.I., Täubel M., Roponen M., Tuoresmäki P. et al. Farm-like indoor microbiota in non-farm homes protects children from asthma development. *Nat. Med.* 2019;25(7):1089–1095. DOI: 10.1038/s41591-019-0469-4.
44. Ege M.J., Mayer M., Normand A.C., Genuneit J., Cookson W.O., Braun-Fahrländer C. et al. Exposure to environmental microorganisms and childhood asthma. *N. Engl. J. Med*. 2011;364(8):701–709. DOI: 10.1056/NEJMoa1007302.
45. Keller A., Groot J., Clippet-Jensen C., Pinot de Moira A., Pedersen M., Sigsgaard T. et al. Exposure to different residential indoor characteristics during childhood and asthma in adolescence: a latent class analysis of the Danish National Birth Cohort. *Eur. J. Epidemiol.* 2024;39(1):51–65. DOI: 10.1007/s10654-023-01051-y.
46. Schuijs M.J., Willart M.A., Vergote K., Gras D., Deswarte K., Ege M.J. et al. Farm dust and endotoxin protect against allergy through A20 induction in lung epithelial cells. *Science.* 20154;349(6252):11061110. DOI: 10.1126/science.aac6623.
47. Gupta S., Hjelmsø M.H., Lehtimäki J., Li X., Mortensen M.S., Russel J. et al. et al. Environmental shaping of the bacterial and fungal community in infant bed dust and correlations with the airway microbiota. *Microbiome.* 2020;8(1):115. DOI: 10.1186/s40168-020-00895-w.
48. Lehtimäki J., Gupta S., Hjelmsø M., Shah S., Thorsen J., Rasmussen M.A. et al. Fungi and bacteria in the beds of rural and urban infants correlate with later risk of atopic diseases. *Clin. Exp. Allergy*. 2023;53(12):1268–1278. DOI: 10.1111/cea.14414.
49. Karvonen A.M., Kirjavainen P.V., Täubel M., Jayaprakash B., Adams R.I., Sordillo J.E. et al. Indoor bacterial microbiota and development of asthma by 10.5 years of age. *J. Allergy Clin. Immunol.* 2019;144(5):1402–1410. DOI: 10.1016/j.jaci.2019.07.035.
50. O'Connor G.T., Lynch S.V., Bloomberg G.R., Kattan M., Wood R.A., Gergen P.J. et al. Early-life home environment and risk of asthma among inner-city children. *J. Allergy Clin. Immunol.* 2018;141(4):1468–1475. DOI: 10.1016/j.jaci.2017.06.040.
51. Dannemiller K.C., Mendell M.J., Macher J.M., Kumagai K., Bradman A., Holland N. et al. Next-generation DNA sequencing reveals that low fungal diversity in house dust is associated with childhood asthma development. *Indoor Air*. 2014;24(3):236–247. DOI: 10.1111/ina.12072.
52. Dannemiller K.C., Gent J.F., Leaderer B.P., Peccia J. Indoor microbial communities: Influence on asthma severity in atopic and nonatopic children. *J. Allergy Clin. Immunol.* 2016;138(1):76–83.e1. DOI: 10.1016/j.jaci.2015.11.027.
53. Von Mutius E., Smits H.H. Primary prevention of asthma: from risk and protective factors to targeted strategies for prevention. *Lancet.* 2020;396(10254):854–866. DOI: 10.1016/S0140-6736(20)31861-4.

Authors' information

Sokolova Tatyana S. – Cand. Sci. (Med.), Associate Professor of the Intermediate-Level Pediatrics Division with a Pediatric Diseases Course of the General Medicine Department, Siberian State Medical University, Tomsk, sokolova.ts@ssmu.ru, 0000-0002-1085-0733

Malchuk Victoria N. – Post-Graduate Student, Intermediate-Level Pediatrics Division with a Pediatric Diseases Course of the General Medicine Department, Siberian State Medical University, Tomsk, malchuk.viktoriya@mail.ru, 0000-0003-0083-3398

Nogai Anita A. – 6th-year Student, Department of Pediatrics, Siberian State Medical University, Tomsk, anita_2000vip@mail.ru, 0009-0002-473 5-9099

Fedorova Olga S. – Dr. Sci. (Med.), Head of the Intermediate-Level Pediatrics Division with a Pediatric Diseases Course of the General Medicine Department, Siberian State Medical University, Tomsk, olga.sergeevna.fedorova@gmail.com, 0000-0002-7130-9609

Ogorodova Lyudmila M. – Dr. Sci. (Med.), Corresponding member of RAS, Professor of the Intermediate-Level Pediatrics Division with a Pediatric Diseases Course of the General Medicine Department, Siberian State Medical University, Tomsk kaf.fak.ped@ssmu.ru, 0000-0002-2962-1076.

(✉) **Sokolova Tatyana S.,** sokolova.ts@ssmu.ru

Received 02.05.2024;
approved after peer review 15.05.2024;
accepted 13.06.2024

H

J

K

L

M

N

P

R

S

T

U

V

Y

Z

Издательский дом Сибирского государственного медицинского университета представляет серию книг

«Наследие томской медицины»

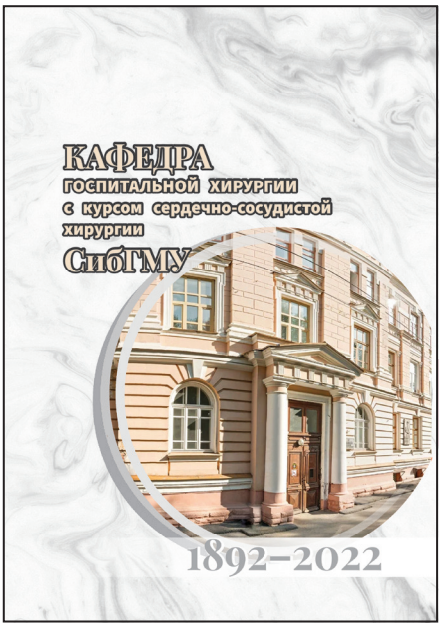

Книга посвящена 130-летнему юбилею кафедры госпитальной хирургии СибГМУ. Приведены биографические данные 79 сотрудников клиники и кафедры госпитальной хирургии в период с 1892 по 2022 г. Им предшествует подробная статья, характеризующая основные научно-практические достижения коллектива на каждом историческом отрезке. В издании упомянуты не только выдающиеся хирурги, звезды мировой величины, но и рядовые профессора, доценты, ассистенты, врачи-ординаторы, многие из которых связали с кафедрой и клиникой всю свою трудовую биографию. При изложении материала наряду с традиционными источниками информации использованы автобиографические документы, данные из семейных архивов, производственные характеристики нередко с сохранением авторского стиля.

Это позволяет полнее ощутить атмосферу в обществе и рабочем коллективе в разные годы существования клиники. Текстовая информация сопровождена богатым иллюстративным материалом, многие фотографии опубликованы впервые.

Издание предназначено для хирургов, студентов старших курсов врачебных факультетов, специалистов по истории медицины.

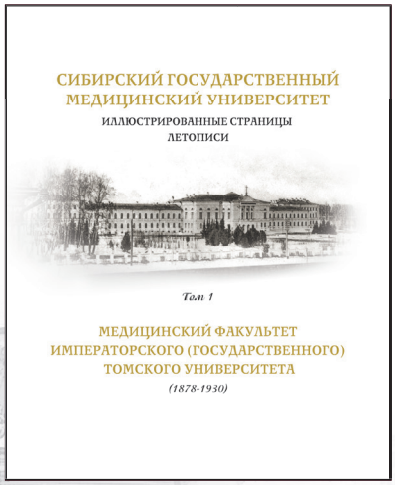

Трёхтомная иллюстрированная летопись одного из старейших и наиболее авторитетных медицинских вузов России – Сибирского (Томского) государственного медицинского университета является по сути первой серьёзной попыткой осветить более чем 140-летнюю историю этого прославленного университета.Особенностью издания является его богатейший иллюстративный материал, включающий более четырёх тысяч фотографий (в том числе ранее практически неизвестных), и никогда не публиковавшиеся до этого крайне любопытные и интересные факты о жизни университета, его студентов и профессоров, воспоминания и рассказы выпускников и преподавателей вуза. Для самого широкого круга читателей, интересующихся историей российских университетов, отечественного высшего медицинского образования и науки, развитием клинических и научно-медицинских школ, здравоохранения, историей Томска, Сибири, России…

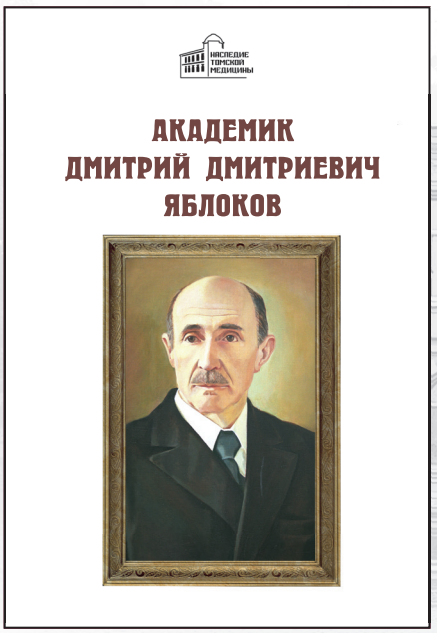

В книге представлены биография и обзор научной, педагогической и общественной деятельности выдающегося ученого, терапевта, клинициста, академика АМН СССР, Героя Социалистического труда, лауреата Сталинской премии Дмитрия Дмитриевича Яблокова (1896-1993).

Для врачей, студентов, всех интересующихся историей медицины.

bulletin.ssmu.ru

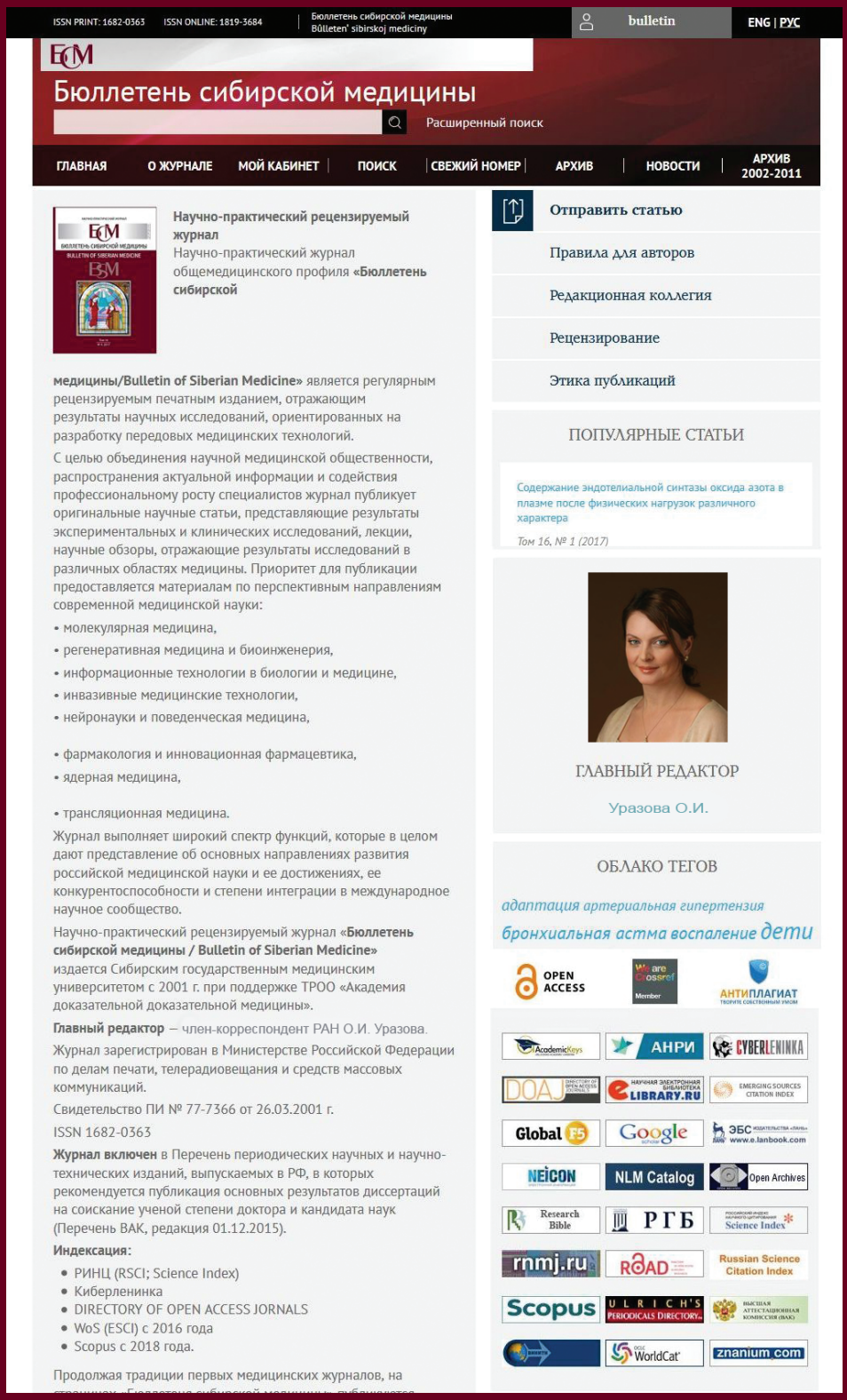

ISSN 1682-0363 (print)
ISSN 1819-3684 (online)
БЮЛЛЕТЕНЬ СИБИРСКОЙ МЕДИЦИНЫ
2024. Т. 23. № 4. 1–208